

Towards a higher international standard - *World Journal of Gastroenterology* will be published semimonthly in 2004

Lian-Sheng Ma, Bo-Rong Pan, Jing-Yun Ma, Jia-Yu Xu, Xie-Ning Wu, Xian-Lin Wang, Han-Ming Lu, Harry Hua-Xiang Xia, Hong-Xiang Liu, Jian-Zhong Zhang, Qin Su, Shi-Yan Ren, Li Zhu, Li-Hong Zhu, You-Yong Lu

Lian-Sheng Ma, Bo-Rong Pan, Jing-Yun Ma, Jia-Yu Xu, Xie-Ning Wu, Xian-Lin Wang, Han-Ming Lu, Harry Hua-Xiang Xia, Hong-Xiang Liu, Jian-Zhong Zhang, Qin Su, Shi-Yan Ren, Li Zhu, Li-Hong Zhu, You-Yong Lu, The WJG Press, PO Box 2345, Beijing 100023, China

Correspondence to: Lian-Sheng Ma, M.D., The WJG Press, PO Box 2345, Beijing 100023, China. wjg@wjgnet.com
Telephone: +86-10-85381901 **Fax:** +86-10-85381893
Received: 2003-12-10 **Accepted:** 2003-12-11

Ma LS, Pan BR, Ma JY, Xu JY, Wu XN, Wang XL, Lu HM, Xia HHX, Liu HX, Zhang JZ, Su Q, Ren SY, Zhu L, Zhu LH, Lu YY. Towards a higher international standard - *World Journal of Gastroenterology* will be published semimonthly in 2004. *World J Gastroenterol* 2004; 10(1): 1-4

<http://www.wjgnet.com/1007-9327/10/1.asp>

INTRODUCTION

World Journal of Gastroenterology (WJG) is an international academic journal in digestology published in China. The WJG was established in 1995 under the name of *China National Journal of New Gastroenterology*, and adapted its present title in 1998. The WJG (ISSN 1007-9327), now published monthly by the WJG Press, is a 210×297 mm-sized journal with 256 pages in each issue. The Journal is distributed by the Beijing Newspaper and Periodical Subscription and Distribution Bureau (Postal Issuance Code 82-261). In response to continuing growth in both basic and clinical studies on digestive diseases and the increasing demands for the international exchange in science and technology, the WJG journal will be published twice monthly from January 2004, with 160 pages in each issue. The publication dates are on the 1st and 15th of each month.

MISSION

The WJG seeks to publish high-quality, original and innovative papers and short communications on basic and clinical studies in gastroenterology and hepatology. The editors accept manuscripts that report important findings in esophageal cancer, gastric cancer, liver cancer, intestinal cancer, viral hepatitis, *Helicobacter pylori* infection, as well as Chinese medicine and integrated Chinese and Western medicine in the treatment of digestive diseases. The Journal gives a higher priority to review articles that are based mainly on the own work of the authors. Thus, the WJG establishes itself as a window for the international academic exchange, and provides a bridge to the world for local medical researchers and professionals.

EDITORIAL BOARDS

The WJG Editorial Board consists of 179 members, representing a team of worldwide experts in gastroenterology and hepatology. They are from 53 countries including: Albania (1), Algeria (1), Argentina (2), Austria (1), Belarus (1), Belgium (1), Brazil (1),

Bulgaria (1), Canada (1), China (41), Costa Rica (1), Croatia (1), Denmark (1), Egypt (1), Finland (1), France (2), Germany (7), Greece (1), Hungary (2), Iceland (1), India (2), Iran (1), Ireland (2), Israel (2), Italy (2), Japan (4), Latvia (1), Lithuania (1), Macedonia (1), Malaysia (2), Monaco (1), Netherlands (3), New Zealand (1), Pakistan (1), Philippines (1), Poland (2), Portugal (1), Romania (1), Russia (3), Singapore (1), Slovakia (1), Slovenia (2), South Africa (1), South Korea (2), Spain (1), Sri Lanka (1), Sweden (2), Switzerland (2), Thailand (1), Turkey (1), United Kingdom (6), United States (56), and Yugoslavia (1).

The WJG has a group of young and middle-aged experts who have made outstanding achievements in both medical research and clinical practice. The duties of WJG editorial members are to evaluate the originality, innovation, scientific standards and readability of the papers, provide constructive comments, suggestions and advice for further revision and improve English writing for papers written by non-English speaking authors. Acceptance of a submitted paper is based on the overall assessment of the title, introduction, materials and methods, findings, and discussion sections, and whether the paper reflects a high standard of clinical or basic study on digestive diseases. There has been a considerable variation in the quality of papers submitted to the journal over the past years. Major problems include the scientific standards and readability. To overcome these problems and improve the quality of the journal, the WJG has established its evaluation criteria.

EVALUATION

According to the evaluation of editorial members, submitted papers are classified as "high priority", "ready for publication", "publication after revision", "re-evaluation after revision" and "rejection". To ensure the academic standards of published papers, WJG defines the following evaluation criteria:

Title should accurately reflect the scientific nature of the study, and should be concise and innovative.

Abstract should clearly present the research background and objectives, the materials and methods, the findings (including important data) and the conclusion. The innovative and focal points of study should be consistent with the objectives, the materials and methods, the findings (including important data), and the conclusion.

Introduction should include research objectives and other study related matters.

Materials and methods should include material characteristics, e.g., randomization of large samples, safety and efficiency, double-blind and double-simulation, comparisons between multi-center parallel control groups in contrast to clinical experiments, special cases, and cell or tissue samples. Test methods and techniques should be standard, innovative, or systematic. Improved or innovative methods should be repeatable and verifiable by others. The design of comparative studies should be rational and reliable, and statistical methods should be appropriate.

Results should have a well-defined scientific conclusion based on the experimental evidence. Attention should be paid to the

sample size and statistical analysis when evaluating a clinical study. **Discussion** should include logistic and systematic theoretical analyses and valuable scientific conclusions.

Bibliography Studies quoted should be proper and sufficient, especially for the latest literature.

General evaluation The originality, scientific standard, innovation and readability of the paper should reflect the advances in clinical and basic studies in gastroenterology and hepatology.

EDITING

Excellent papers as assessed by the editorial board may be published without revision. The authors will be advised to revise their papers according to the comments/suggestions made by the editorial members and in consistent with the journal format. The revised papers will be subjected to the first and second language processing. Format-revised papers will then be put into layout. Thereafter, laid out draft will be sent to the editor-in-charge for the proofreading and finally for printing once there are no grammatical and spelling mistakes. In order to ensure the editing quality of published papers, WJG defines the following editorial criteria.

Title should be concise and unique. The following words should be avoided: evaluation, study, analysis, observation, investigation, exploration, the article “the” and abbreviations that are not commonly used. For further information, please refer to “*Writing English Title for Scientific Papers*” <http://www.wjgnet.com/1009-3079/new/26.asp>.

Abstract should be in a structural format. Objectives should be directly pointed to the topic, e.g. “To investigate the...”. A summary of the background or current development in the topic may be provided. Methods (including materials) and findings (including important data) should be stated in the past tense, and conclusion should be stated in the present tense. Personal address and voice should be natural, avoiding using “the dangling participles”. First sentence of the abstract should not be a repetition of the title, it should be more specific. For further information, please see “*Writing English Abstract for Scientific Papers*” <http://www.wjgnet.com/1009-3079/new/25.asp>.

Text (1) *Short sentences*: Short sentences are preferred. As much as possible, multiple subordinate clauses should be avoided. The spelling and tenses should be correct, and tenses should be consistent. The past tense should be generally used in the Methods and Results sections. In the Discussion, the past tense should be used when a specific study is cited and present tense should be used when a conclusive statement is made based on previous studies. Tenses used in the main and subordinate clauses should be consistent with the tenses and implications of the paragraph. For Chinese authors, the Chinese version of the paper should be referred to in order to accurately express the original meanings. When using the participial phrases to express the adverb and attribute, attention should be paid to the proper voice usage for proper correspondence. Word comparisons should be consistent, and the same term should be used to refer to the same thing. Basic data and their percentages should be checked during editing. Editing checks should include accurate use of symbols and Latin terms (singular and plural forms). (2) *Numerals*: Numerals appearing at the beginning of the sentence should be stated in words, e.g. Sixteen cases...or A total number of 16 cases. No Arabic numerals, e.g. 16 cases, 100 patients, should be used to start a sentence. (3) *Abbreviations*: When an *abbreviation is used* for the first time in the text, the entire term should be spelt out, followed by the *abbreviation* in parenthesis. (4) *Italics*: The following should be italicized: Latin terms of bacteria, virus, plants and animals, statistical symbols, genetic symbols, END for endonucleases (first three characters), measurement

symbols, Latin terms, e.g. *in vivo*, *in situ*, *et al*, and titles of publications stated in the bibliography. (5) *Graphs*: The same graph should be used only once, data expressed in graphs should not be expressed in table again, or *vice versa*. Data shown in tables and graphs should be the same as those in the text. Annotation of the graph or table data should be stated in the present tense, e.g. the data are shown in Table 1. Graphs and tables should be included in the body text, first letter of the notation/definition should be capitalized, the rest should be in small letters.

References should be indicated in the order appeared in the text. Authors and titles should be consistent with those shown in the first page of the paper. The same is true for journals, year, volume number, pages (beginning and last pages), and PMID codes.

Others (1) The manuscript should be printed in double-space. (2) Formal language should be used. Informal and non-standard abbreviations or contractions, e.g., isn't, aren't, hasn't, hadn't, haven't, don't, can't, wouldn't, a lot of, a bit, too (also), thru (through), exam (examination), lab (laboratory), *etc.* should be avoided. (3) Methods and results should be objectively presented, statements should be simple and unexaggerated. Emotional or advertising promotional terms should be avoided. (4) The verb form is preferable, the gerund or noun form of verb should be avoided. (5) Proper use of articles is required, countable nouns should be expressed in the plural form as much as possible. (6) A prepositional phrase or a hyphen should be used to break off a noun phrase, and a long series of adjectives or nouns to modify nouns should be avoided. (7) As much as possible, sentences begin with important facts, not with phrases or subordinate clauses. (8) When referring to the work or research outcome of other investigators, the authors should state full name of the investigators, in the case of more than two investigators, the term “*et al*” should be used. For further information, please see “*Writing Scientific Paper in English*” <http://www.wjgnet.com/1009-3079/new/31.asp>.

COLUMNS

WJG consists of the following columns.

Review papers come from experts who are specialized in the fields.

Special topics include esophageal cancer, gastric cancer, liver cancer, viral hepatitis, Chinese medicine, integrated Chinese and Western medicine, and pioneering papers with Chinese characteristics or first-class international standards.

Basic research Studies should have complete experiment data, high academic values, and innovative and original findings.

Clinical research Studies should demonstrate randomization of large samples, safety and efficiency, double-blind and double-simulation, comparison between multi-center control groups and clinical experiments.

Brief reports should present innovative and original phase outcomes.

Case reports should have some instructional significance to clinical practitioners.

MANUSCRIPT MANAGEMENT

In an effort to speed up the computerization and electronization of WJG manuscript management, improve the journal quality, standardize editing procedures, and increase the work efficiency, the WJG Publishing Manuscript Management System was successfully established on April 15, 2003. It enables the automation and electronization of submission registration, submission acknowledgment, preliminary evaluation, second evaluation, evaluation results, final decision, acceptance/rejection notification, editing processing, data

exchange, and Internet submission inquiry. Authors can follow-up the status of their submitted papers at the WJG website, by typing in user name (first author's name) and password (manuscript number). Information regarding serial number, journal name, title, author, date of receipt, editing date, acceptance/rejection date, official invoice number, date of publication, issue (volume) and pages will be provided.

PUBLICATION FREQUENCY

From January 2004, the journal will be published twice monthly. Thus, the submission-publication lag period is expected to be controlled as short as between 1 to 4 months. This journal has been included in the famous international search systems such as the Science Citation Index-Expanded and *Index Medicus*/MEDLINE, in the hope of demonstrating the world leading position of Chinese researchers in gastroenterology. For instance, the paper "Different approaches to caudate lobectomy with "curettag and aspiration" technique using a special instrument PMID: A report of 76 cases" written by Shu-You Peng, Jiang-Tao Li, Yi-Ping Mou, Ying-Bin Liu, Yu-Lian Wu, He-Qing Fang, Li-Ping Cao, Li Chen, Xiu-Jun Cai, Cheng-Hong Peng, Department of Surgery, 2nd Affiliated Hospital, School of Medicine, Zhejiang University and published in volume 10 of 2003 is of international standards. The submission-publication lag time of this paper was only 45 days.

TYPESETTING AND PRINTING

The WJG uses a uniform font and format from the top margin of book, column, title, author, position of authors, fund and grants, contact address, e-mail address, telephone numbers, fax numbers, date of receipt, acceptance date, abstract, reference format, class 1 heading font, class 2 heading font, graph, chart, to references. No subsequent papers are followed after the end of each paper, thus, papers can be used in the abstract database, ASP, SML, or PDF format. WJG uses the PageMaker publishing software, hence files can be automatically converted to ASP, XML or PDF format.

The printing films for WJG are imported films. Heidelberg color printing is used for the monochrome and color printing. In addition, the three-sided knife is used for trimming. Actual printing work is contracted by the Beijing KH Printing Company. The printing service covers the full-length production work from filming, design drafting, pre-binding sample, to full delivery to the magazine office for approval. Printing follows after every aspect has been approved.

ELECTRONIC VERSION

WJG website (<http://www.wjgnet.com/1007-9327/index.asp>) went online on April 15, 2003, and as of December 21, 2003, the site has been visited 678 857 times. The electronic version of the WJG has the following seven columns.

Journal introduces Editorial Board, Board member briefs, indexing services by which the WJG is abstracted, and current impact factor.

Published gives information about the publisher, copyright and subscription.

Submission includes instructions to authors and details for preparing review, original manuscript, brief report and case report.

News lists journals indexed in *Index Medicus* (IM) and impact factors by Journal Citation Reports (JCR).

Submission search allows authors to enter user name and password to obtain full information (up to 28 features) on their submissions.

E-journal allows search for current and previous issues (1995-2003). The WJG E-journal offers options such as HTM or PDF

files, abstracts, related studies, citation frequency, visiting times, download counts, and comments.

Reference links WJG proofreads the entire reference and first page to ensure accuracy of the author, title, year, volume, page number, and PMID. Reference is also linked with the PubMed and <http://www.wjgnet.com/1007-9327/index.asp> abstracts and documents for citation accuracy, thus providing readers with an access to the citation material and abstract.

CIRCULATION

In 2003, 973 WJG journals were circulated, that is 168 local post office subscriptions within 27 Chinese administrative regions, 105 international subscriptions from 56 countries and regions, and 700 complimentary issues mailed to the investigators in charge of National Project No. 973 and No. 863, as well as the project coordinators of China National Natural Science Foundation. We are providing with complimentary copies of the e-journal to the members of the American College of Gastroenterology, the American Association for the Study of Liver Diseases, and the American Association for Cancer Research, hoping that more international experts in gastroenterology read the papers published in the WJG. Currently, circulation volume of the e-journal has reached 21 200 copies.

SUBMISSION SOURCES AND GRANT STATUS FOR PUBLISHED PAPERS

The upgrade of our national scientific research standards has gradually increased the quality of scientific papers. A higher growth rate was noticed in the volume of papers coming from the famous universities, research facilities (especially laboratories with excellent scientific records), subject groups and scientists. During the period from April 01 to October 01, 2003, we received a total of 618 papers: 501 (81.06%) from China, and 117 (18.93%) from the overseas. A total of 521 papers (21 reviews, 27 esophageal cancer, 54 gastric cancer, 65 liver cancer, 39 intestinal cancer, 46 viral hepatitis, 20 *Helicobacter pylori*, 115 basic studies, 62 clinical studies, 62 brief reports, 8 case reports, and 2 letters from readers) were published in issues 1 to 10 in 2003, 450 (86.37%) were from Chinese institutions, and 71 (13.62%) from the overseas. There were 2 949 authors with 14.41% being from the overseas. The authors were from 34 nations and regions including Argentina, Australia, Pakistan, Brazil, Belgium, Poland, Denmark, Germany, France, Finland, Korea, the Netherlands, Canada, Croatia, United States, South Africa, Yugoslavia, Japan, Sweden, Switzerland, Saudi Arabia, Thailand, Turkey, Spain, Greece, Singapore, Hungary, Iran, Italy, India, United Kingdom, the Mainland of China, Taiwan and Hong Kong. Grant-funded papers accounted for 292 (56.04%) of the published papers. Grant-funded case study papers accounted for 440 (84.45%) papers, which were composed of 25 (4.79%) international grant-funded, 180 (34.54%) National Project No. 973 and No. 863, and National Science Council funded, and 235 (45.10%) government (ministry or provincial office) funded papers. In 2002, the WJG published 226 papers from 26 regions, 93.36% from China, and 6.63% from the overseas, and 60.61% were grant-funded papers. In 2001, the WJG published 173 papers from 20 regions and 112 institutions, 35% were from the overseas and 55% were grant-funded. In 2000, the WJG published 205 papers, and 50% were grant-funded. In 1999, the WJG published 144 papers from 20 regions and 100 institutions, 23% were from overseas and 50% were grant-funded. In 1998, the WJG published 183 papers from 11 regions, 9.84% were from the overseas and 59.56% were grant-funded.

VISITING NUMBER AND DOWNLOAD COUNT

The WJG started producing dynamic web pages from issues 4 to 9 in 2003 e-journal. Visiting number and download count of the papers were recorded. A total of 322 papers were published from issues 4 to 9, and 265 (82.29%) papers were visited and downloaded. During the period from April 13 to October 13, 2003, these 265 papers were visited 35 745 times, or an average of 134.89 times per paper. The highest visiting number was 1 918 and the lowest one was 11. Of these papers 131 (49.43%) had visiting times exceeding 100, 123 (46.41%) had 30-99 times and 11 (4.15%) had 11-29 times. The highest download count was 1 087 and the lowest was 10. For instance, in the review paper "RNA interference: Antiviral weapon and beyond. World J Gastroenterol 2003; 9(8): 1657-1661" written by Quan-Chu Wang, Qing-He Nie, Zhi-Hua Feng, The Center of Diagnosis and Treatment for Infectious Diseases of Chinese PLA, Tangdu Hospital, Fourth Military Medical University was visited 1 918 times and downloaded 1 087 times.

IMPACT FACTORS

Impact factor is an international journal evaluation index. It is a general quantification index reflecting the importance of a journal. Usually a greater impact factor would mean that a journal has a greater academic impact and effect. The total journal citation frequency refers to the total number that the entire paper content of a journal has been abstracted from the time the issue was published in the yearly statistics. It is a highly objective and practical evaluation index capable of showing the usage and degree of attention paid to the journal, as well as its effects and status in the science community. In the Journal Citation Reports (JCR) of the Institute for Scientific Information (ISI), the impact factor of the WJG in 2002 was rated 2.532 with a citation frequency of 1 535, which was ranked thirteenth among 45 journals in the international gastroenterology and liver disease fields, and ranked 797th among the 5 876 international science journals registered in the SCI. The impact factor of the WJG in 2001 and 2000 was 1.445 and 0.993, respectively, with a citation frequency of 722 and 327, respectively. The complete electronic version (ASP, PDF) of the papers published since 1998 has been linked to the PubMed digest, hence worldwide readers can have a free access to the papers published in the WJG using the PubMed search engine. Authors of the journal are thus given worldwide and immediate exposure. As a result, the impact factor of the journal has shown an annual growth, and more importantly, the international influence of the journal continues to expand.

AWARDS FOR PUBLISHED PAPERS

A total of 15 papers won the National, Ministerial, or Provincial Science and Technology Progress Awards during the 1998-

2002 period. For example, the paper "Pharmacokinetics of traditional Chinese syndrome and recipe: A hypothesis and its verification (I). World J Gastroenterol 2000; 6(3): 384-391" written by Huang X, Ren P, Wen AD, Wang LL, Zhang L, Gao F, won the second prize of the National Science & Technology Progress Award.

COLLECTIONS OF INTERNATIONAL SEARCH SYSTEMS

Science Citation Index®-Expanded (SCI-E) of the ISI is a comprehensive search engine that collects over 5 876 authoritative scientific journals from different parts of the world. It has a stringent journal selection standard, and is an internationally recognized principal scientific statistics and evaluation engine, thus making it an important citation in the assessment of the value of a journal and the academic standards of its papers. The special citing and cited relations between the author-to-author and paper-to-paper for SCI-E make SCI-E become the most authoritative assessment system for scientific research results internationally. The frequency of scientific journals and papers that are collected or cited by SCI-E in one country or region, will be considered as an index of assessing the scientific research standards for that country or region. Since 1998, the WJG has been successively collected by (SCI-E, Research Alert®, Current Contents/Clinical Medicine®, Journal Citation Reports®, Clinical Medicine Citation Index®), *Index Medicus*/MEDLINE (US), Chemical Abstracts, CA (US), EMBASE/Excerpta Medica, EM (Netherlands), Abstract Journals, AJ (Russia).

HONORS

The WJG is nationally recognized as a core journal in national natural science and an outstanding journal in science and technology, with an honor of the 2nd National Journal Award, and was listed as one of the 100 most important journals in China. In 2001, it was selected into the China Journal Square consisting of "200" journals. It was awarded a specific project grant for the key academic journals by the National Natural Science Foundation in 2002 (project grant no.: 30224801).

Overall, the WJG has already developed to a value-oriented (quality and quantity) journal and functions pursuant to the international standard requirements. In addition, the journal has also completed the management marketation from manuscript submission to publication. Fair and scientific evaluation is applied to make acceptance/rejection decision for each paper submitted. In terms of academic standards and editorial quality, the WJG aims to become one of the best international journals. With the strong support of the authorities, authors, readers, the entire editorial board and the community, the WJG will become one of the most influential international academic journals of its field.

Edited by Xia HHX, Liu HX and Wang XL

Primary gastric lymphoma

Ahmad M. Al-Akwaa, Neelam Siddiqui, Ibrahim A. Al-Mofleh

Ahmad M. Al-Akwaa, Neelam Siddiqui, Ibrahim A. Al-Mofleh, Gastroenterology Division, Neelam Siddiqui, Oncology Division, Department of Medicine, College of Medicine and King Khalid University Hospital, King Saud University, Riyadh, Saudi Arabia

Correspondence to: Professor Ibrahim A. Al-Mofleh, MD, Department of Medicine, Gastroenterology Division (59), College of Medicine & KKHU, P. O. Box 2925, Riyadh 11461, Saudi Arabia. iamofleh@yahoo.com

Telephone: +966-1-4671215 **Fax:** +966-1-4671217

Received: 2003-08-08 **Accepted:** 2003-10-08

Abstract

AIM: The purpose of this review is to describe the various aspects of primary gastric lymphoma and the treatment options currently available.

METHODS: After a systematic search of Pubmed, Medscape and MDconsult, we reviewed and retrieved literature regarding gastric lymphoma.

RESULTS: Primary gastric lymphoma is rare however, the incidence of this malignancy is increasing. Chronic gastritis secondary to *Helicobacter pylori* (*H pylori*) infection has been considered a major predisposing factor for MALT lymphoma. Immune histochemical marker studies and molecular biology utilizing polymerase chain reaction have facilitated appropriate diagnosis and abolished the need for diagnostic surgical resection. Advances in imaging techniques including Magnetic Resonance Imaging (MRI) and Endoscopic Ultrasonography (EUS) have helped evaluation of tumor extension and invasion. The clinical course and prognosis of this disease is dependent on histopathological sub-type and stage at the time of diagnosis. Controversy remains regarding the best treatment for early stages of this disease. Chemotherapy, surgery and combination have been studied and shared almost comparable results with survival rate of 70-90%. However, chemotherapy possesses the advantage of preserving gastric anatomy. Radiotherapy alone has been tried and showed good results. Stage III E, IVE disease treatment is solely by chemotherapy and surgical resection has been a remote consideration.

CONCLUSION: We conclude that methods of diagnosis and staging of the primary gastric lymphoma have dramatically improved. The modalities of treatment are many and probably chemotherapy is superior because of high success rate, preservation of stomach and tolerable complications.

Al-Akwaa AM, Siddiqui N, Al-Mofleh IA. Primary gastric lymphoma. *World J Gastroenterol* 2004; 10(1): 5-11
<http://www.wjgnet.com/1007-9327/10/5.asp>

INTRODUCTION

Primary gastric lymphoma is a rare tumor, accounting for less than 5% of primary gastric neoplasms^[1-5]. However it is the most common extranodal lymphoma, representing 4-20% of all extranodal lymphomas^[6,7]. In the Middle East, stomach is the most common gastrointestinal site, with an incidence rate

similar to that reported in the western literature^[8-11]. However Turkish and Indian series suggested that intestinal lymphomas have been more predominant than gastric lymphoma in those regions^[12,13].

Gastric lymphomas are prevalent in patients aged more than 50 years, however it still has been reported in the second decade of life^[14,15]. Reported median age is 60-65 years and males are 2-3 times more affected than females^[16-18]. Recently, several studies have shown an increase in the incidence among HIV infected and AIDS patients, affecting increasingly younger age groups^[19-21].

PATHOLOGY

Malignant lymphomas affect the stomach as a primary tumor or as part of more wide spread disease process. Stomach is the most common site with secondary lymphoma^[22,23]. Generally lymphomas are considered as "primary" in the gastrointestinal tract when the initial symptoms of the disease are in the abdomen indicating a disturbance of the gastrointestinal function, or when the bulk of the disease is in the stomach.

Most gastric lymphomas are thought to arise in the mucosa or submucosa from the so-called mucosa-associated lymphoid tissues (MALT), which usually develop after chronic inflammation induced by *H pylori* infection^[23-26]. Histologically and immunohistochemically MALT lymphomas are of the B-cell non-Hodgkins type (NHLs) and share many features in common, therefore they are denoted as malignant lymphomas of MALT. The association between *H pylori* chronic gastritis and MALT lymphoma has been confirmed in large population based studies where immunological evidence of *H pylori* infection has been shown to be more in patients with gastric lymphomas than in matched controls^[24-26]. Other forms of gastric lymphomas are non-MALT type, although many may be initially MALT tumors. Rare tumors may be T cell in origin^[27-30].

The histological classification may vary from low to high grade. Grading has been classified into low, intermediate and high grade. Other terminology of primary and secondary high-grade lymphomas has been adopted^[24]. In the histology of secondary high-grade lymphomas, there is evidence of low-grade component. Various systems (Rappaport, Working formulation and Modified Kiel) have frequently been utilized for histological classification, Combination of two or three classification systems have also been commonly used^[17,23,30,31].

A majority of primary gastric lymphomas are histologically of the diffuse histiocytic or large cell type^[15,32,33]. Reports from Saudi Arabia have shown a predominance of diffuse large B-cell type^[14,33]. Gastric maltoma represents up to one half of primary gastric lymphoma. In the last few years, the Revised European American Lymphoma (REAL) classification of lymphoid neoplasms has been widely used with the advantage of high reproducibility and clinical relevance (Tables 1,2)^[32,34].

Microscopically, low-grade lymphomas may not easily be distinguished from pseudolymphomas, a term used to describe the lymphocytic infiltration of the gastric mucosa, which may occur with chronic gastritis and peptic ulceration. Pseudolymphomas may mimic clinically and endoscopically gastric adenocarcinomas or lymphomas. Pathologists can differentiate between pseudolymphomas and lymphomas based on several histological characteristics which indicate malignant

changes, like prominent lymphoepithelial lesions (lymphoid infiltration of glands or crypts with partial destruction), Dutcher bodies and moderate cytologic atypia^[35]. In cases which can not be diagnosed with histological differentiation, immunohistochemical marker studies or molecular biology utilizing polymerase chain reaction (PCR) may facilitate establishing an accurate diagnosis^[36,37]. However, recent studies have indicated that the great majority of pseudolymphomas are in fact true lymphomas of low-grade malignancy using markers of clonality, and this term preferably has to be abandoned^[37].

Table 1 The REAL classification of non-Hodgkin's Lymphomas

B-cell lymphomas	
Precursor B-cell lymphomas:	B-lymphoblastic
Mature B-cell lymphomas:	B-cell CLL/small lymphocytic
	Follicular
	Marginal-zone-nodal
	Extranodal marginal-zone (MALT)
	Splenic marginal-zone
	Lymphoplasmacytic
	Mantle-cell
	Diffuse large B-cell
	Primary mediastinal large B-cell
	Burkitt's like
	Burkitt's
T-cell lymphomas	
Precursor T-cell lymphomas:	T-lymphoblastic
Mature T-cell lymphomas:	Mycosis fungoides/sezary syndrome
	Peripheral T-cell (many subtypes)
	Anaplastic large T/null cell
	Adult T-cell leukemia/lymphoma

Table 2 Histologic classification of gastrointestinal lymphomas

B-cell	
Mucosa-associated lymphoid tissue (MALT)-type (extranodal marginal-zone lymphoma):	Low-grade
	High-grade, with or without a low-grade component
Immunoproliferative small intestinal disease (IPSID):	Low-grade
	High-grade, with or without a low-grade component
Lymphomatous polyposis (mantle-cell lymphoma)	
Burkitt's and Burkitt's-like	
Other types of low- or high-grade lymphoma corresponding to lymph node equivalents	
T-cell	
Enteropathy-associated T-cell lymphoma (EATCL)	
Other types not associated with enteropathy	

Macroscopically, gastric lymphomas may appear as ulcerated (single, multiple or diffuse), polypoid, granulonodular or infiltrative lesions^[13,24,33]. Ulcerative type alone or combined with other lesions has been the most frequent endoscopic presentation of primary tumors. The lesion may vary from fine nodularity or normally looking mucosa to very advanced large fungating ulcerated mass^[13]. Endoscopically, the differentiation between lymphomas and adenocarcinomas may not be easy, however early lymphomas tend to produce larger tumors than adenocarcinomas and may be multifocal as well^[15]. Gastric lymphomas involve more frequently the antrum and corpus^[33]. In a series, 46% of lesions are located at gastric body^[24]. Entire

gastric involvement has also been reported^[18,24]. In advanced diseases tumors may spread to extraintestinal sites like central nervous system, bone, liver, kidneys, ovary and lungs^[24].

CLINICAL PRESENTATION

The initial symptoms of upper abdominal pain and early satiety may be vague and nonspecific, leading to a delayed establishment of diagnosis up to several years^[39]. Symptoms and signs may mimic that of other abdominal pathologies including peptic ulcer disease, gall bladder, pancreatic or functional disorders as well as other gastric neoplasms^[15]. Other common symptoms included weight loss, nausea, vomiting, abdominal fullness and indigestion^[30,31,33]. Weakness, night sweat, jaundice, fever and dysphagia occur less frequently^[13,23,30]. Many patients came down late with advanced disease and complications may develop before diagnosis^[38]. Twenty to thirty percent may present with bleeding in the form of hematemesis or melena while, gastric obstruction and perforation are less common^[37,38]. Physical examination could be normal in 55%-60%^[30]. Common signs include epigastric tenderness and palpable mass. The tenderness is encountered in 20%-35% and masses in 17%-25%^[15,23,31]. Other uncommon findings included fever, hepatomegaly, splenomegaly, jaundice and lymphadenopathy. In one series, lymphadenopathy is found in 12%^[24,30,31]. Signs of malnutrition may also appear in advanced disease^[39].

DIAGNOSIS

Clinical presentation and radiological features are often nonspecific. Esophagogastroduodenoscopy (EGD) and biopsy are primary methods for diagnosis^[15,40]. The diagnosis of low-grade MALT lymphoma by forceps biopsy is often difficult in early disease and repeated endoscopies and biopsies may be required before final diagnosis is achieved^[25].

Multiple and step biopsies are required because endoscopic findings may vary from subtle mucosal changes to gross lesions. These may include mucosal edema, friability, patchy redness, irregular patchy gray or whitish granularity, contact bleeding, superficial irregular erosions and ulcerations^[33]. Repeated endoscopic biopsies are mandatory in case of clinical suspicion and negative or inconclusive histology. Furthermore, endoscopic mucosal resection enhances the histological yield^[41]. Occasionally, rapid diagnosis by endoscopy can be made by detection of monoclonality in immunoglobulin heavy chain rearrangement of the lymphoproliferative disease by PCR^[42]. It is recommended that biopsy specimens should undergo histological, immunohistochemical and genotyping studies to make the diagnosis.

Radiological examinations can help establish diagnosis and determine the extent of the lesions. Gastric wall thickening, atypical ulcer deformities, obstruction and mass effect are enhanced features suggestive, but not specific for gastric lymphoma^[30,31,38]. CT scan of the abdomen can identify the gastric wall thickening or mass lesions in 85% of cases. Sometimes it may show typical imaging features of more homogenous and pronounced mural thickening that can help differentiate lymphomas from adenocarcinomas^[42,43]. On CT scan, three quarters of cases of low grade MALT lymphomas may present with infiltrative form and polypoid form in the remainder. Lymphadenopathy is detected in only 50%^[43]. Conventional sonographic examination can be of value in identification of gastrointestinal involvement as well as abdominal lymph node enlargement in lymphoma staging. The MRI features include irregularly thickened mucosal folds, irregular submucosal infiltration, annular constricting lesion, exophytic tumor growth, mesenteric masses and mesenteric/retroperitoneal lymphadenopathy^[44]. EUS is a valuable

technique in assessing the extent and invasion of the lesion. By EUS, infiltrative carcinomas tend to show a vertical growth in the gastric wall, while lymphomas tend to show mainly a horizontal extension^[45,46]. It is highly accurate in determining the depth of lymphomatous infiltration and the presence of perigastric lymph nodes, thus providing additional information for therapeutic planning. It can differentiate between lymphomas and carcinomas in early stages, but in advanced stages both have similar appearances. With the development of the above diagnostic methods, open surgery is rarely needed to confirm the diagnosis.

STAGING

After establishing the diagnosis of primary gastric lymphoma, staging is essential for planning treatment. It is also important to rule out systemic lymphoma with secondary involvement of the stomach. The staging process starts with endoscopy and step biopsy to rule out microscopic infiltration of nearby structures like the duodenum. Chest radiography may show gross lesions in the lungs and mediastinum. CT scan of chest, abdomen and pelvis permits assessment of nodal involvement above and below the diaphragm, and extension of the tumor outside the stomach. EUS may be employed for accurate estimation of both the depth of invasion and involvement of regional lymph nodes^[45,46]. It is superior to CT scan in false negative cases. Bone marrow examination helps determine presence or absence of tumor spread. Indirect laryngoscopy is also helpful for excluding Waldeyer's ring involvement, which is reported to be associated with gastric lymphoma^[32].

Table 3 Staging classification according to Musshoff's criteria

Stage	Definition
IE	Lymphoma limited to the stomach
IIE ₁	Involvement of stomach and contiguous lymph nodes
IIE ₂	Involvement of stomach and noncontiguous subdiaphragmatic lymph nodes
III	Involvement of stomach and lymph nodes on both sides of diaphragm
IV	Hematogenous spread (stomach and one or more extralymphatic organs or tissues)

The following subscripts may be added E=extranodal, S=splenic, A=asymptomatic, B=symptomatic.

Table 4 Modified Blackledge staging system for gastrointestinal lymphomas

Stage I	Tumor confined to gastrointestinal tract without serosal penetration: Single primary site Multiple, non-contiguous lesions
Stage II	Tumor extending into abdomen from primary site: Nodal involvement II ₁ Local (gastric/mesenteric) II ₂ Distant (para-aortic/paracaval)
Stage II_E	Penetration of serosa to involve adjacent 'structures': Enumerate actual site of involvement, e.g. stage II _E (pancreas), stage II _E (large intestine), stage II _E (post-abdominal wall) Perforation/peritonitis
Stage IV	Disseminated extranodal involvement or a gastrointestinal-tract lesion with supradiaphragmatic nodal involvement

Various staging systems have been used. The Ann Arbor staging for primary lymphomas has been modified by

Musshoff, and utilized by several authors for staging gastric lymphomas (Table 3)^[18,47,48]. Several alternative staging systems have been proposed, and the revised version of the Blackledge staging system has been recommended for general use (Table 4)^[49,34]. Several authors have suggested that such staging modification may be of prognostic significance^[50,51,53].

TREATMENT

The modalities of treatment for gastric lymphomas have been a controversial subject, and the best regimen has not been standardized. However, options of treatment depend on the histologic classification and stage of the disease. Some centers adopt surgery alone, while others advocate non-surgical treatment with radiation, chemotherapy or both.

SURGERY

Traditionally, aggressive surgical resection has been the main stay of treatment because it can collect definitive tissues for pathologic examination, allow exploration of the abdomen, reduce tumor burden and obviate the concern that gastric hemorrhage or perforation would complicate medical treatment of lymphomas. More recently, radical gastrectomy is disputed and considered unnecessary. Lesser procedures are now accepted where resection of the gross disease and involved lymph nodes will provide adequate results^[39,52,53]. Several reports have shown a superior outcome when surgical resection is undertaken in the early stages of the disease with a 5-year survival rate of 80%-93%^[54,55].

Kazaya *et al* advocated wide resection of early gastric tumor and extensive lymph node dissection^[15]. Other authors also found surgery alone to be an adequate treatment for stage IE or pure MALT lymphomas with a survival rate of >95%, provided staging is performed after radical gastrectomy^[56]. In a large series of patients treated according to *H pylori* status, tumor grade and stage, surgical resection remained the treatment of choice in patients with stage IIE, low-grade lymphoma and non-responders of stage IE treated by eradication for *H pylori*, however the author advised further studies to compare surgical with conservative treatment^[57].

A prospective study from France, has found that in stages IE and IIE, the complete response, survival rate and disease free survival rates were similar to those who underwent complete resection, partial or no surgery prior to administration of chemotherapy. The survival rates of 60% with surgery alone compared to 85% if adjuvant chemotherapy was given, were reported^[40]. In a retrospective study of 92 patients from Italy in different stages who underwent surgical resection when it was feasible, the ten-year actuarial survival rates were 100% and 80% for stage IE and IIE respectively compared with 21% and 0 for stage IIIIE and IVE^[58].

Surgical resection with clear margins is advised in order to maximize the chance of cure^[39,55,59]. On the contrary, other reports have found no difference in survival, whether the margin of resection was clear or not, as long as post-operative chemotherapy had been given^[60,61].

The mortality and morbidity related to surgery were similar if not more than those related to non-surgical treatment for stage I and II. Therefore, aggressive surgery is not indicated due to increased morbidity which is outweighing the benefit gained in terms of survival^[60-62] and gastrointestinal organ preservation may provide substantial advantage for the quality of life in these patients^[39]. Resectability rates ranged from 60%-88%, and the 5-year survival ranged from 50%-87%^[55,60]. Debulking of advanced disease was associated with the high morbidity and mortality and low response rates of 6%-40%^[63]. Operative mortality was between 3%-25% with higher rates

for palliative procedures which were performed for symptomatic relief, removal of tumor mass and avoidance of hemorrhage or perforation related to other mode of therapy^[63]. In a prospective study of 208 patients, there was no difference in therapeutic outcome in surgically or conservatively treated patients, even after complete resection, the authors concluded that surgery favored by most authors in treatment of primary gastric lymphoma should be reassessed^[64].

CHEMOTHERAPY

The effect of chemotherapy alone as a sole treatment for gastric lymphomas is still debatable. The needs behind trying chemotherapy were the considerable morbidity and mortality associated with resection^[63]. Stomach conservation, and avoidance of postoperative complications such as myocardial infarction, gastrointestinal bleeding, enterocutaneous fistula and malabsorption syndrome were important factors that obviated the choice of chemotherapy. Initial trial in a small number of patients in stage I E and II E has shown excellent results by combination of chemotherapy and radiotherapy with a survival rate of 70% and few complications^[52]. Salvgnol *et al* reported a survival rate of 71% in patients treated by chemotherapy^[55]. Another recent study on aggressive gastrointestinal lymphoma found primary chemotherapy with or without radiotherapy useful and induced a complete response in 81% of patients, with fewer complications compared with surgery including less risk of perforation or bleeding^[65]. Other reports showed no apparent difference in survival between patients treated by chemotherapy or surgery and chemotherapy with survival rates of 67% and 60%, respectively. There has been no report of serious adverse effects such as bleeding or perforation in chemotherapy-treated patients of intermediate and high grade non-Hodgkin lymphomas^[60]. In a report from Italy, 17 patients with resectable large cell lymphoma treated primarily by chemotherapy with or without consolidation radiotherapy, only two failed in the first line therapy and 15 were free of disease at 6 years^[66]. Consolidation radiotherapy might improve the efficacy of chemotherapy. None of the patients experienced acute treatment related morbidity or mortality from local complications^[68]. In three recent trials with variable chemotherapy regimens, the survival rates of 82%-88% in stage IE and IIE, high grade lymphoma with only few and manageable complications were found^[65,67,68].

In other series, chemotherapy alone compared with surgical resection alone, has shown no significant difference in the matter of survival. The overall 2-year survival was 67% and 81%^[69-71].

In patients with comorbid factors and increased risk of surgery-related morbidity and mortality, chemotherapy offered an effective or equally effective mode of treatment to surgical resection 57% vs 58%^[71].

The fear of chemotherapy-related complications, for instance, bleeding and perforation, has been disputed, and less significant compared with surgical resection^[65,67-69]. Some authors reported the incidence of chemotherapy-related bleeding between zero and three percent and no perforation^[60,72]. Therefore, chemotherapy has been suggested and adopted as a primary mode of treatment. Combined chemotherapy comprising cyclophosphamide, doxorubicin, vincristine and prednisolone (CHOP), has been the preferable and the most effective regimen for all tumor stages^[31,65]. Several other regimens have also been used with almost similar efficacy and comparable toxicity^[75]. While cyclophosphamide, vincristine and prednisolone (COP) were adopted for low grade lymphomas, high grade tumors were treated with doxorubicin, teniposide, cyclophosphamide and prednisolone (AVmCP). The latter two regimens combined with surgical resection have shown the survival rates of 80% and 100%, respectively^[73].

COMBINED THERAPY

Multimodal therapy, combining resection with chemotherapy and occasionally radiotherapy have been commonly and widely accepted in many centers. It has significantly improved the 5-year survival^[10,27,55,59,60,74]. Combination of radical surgery followed by chemotherapy has been associated with a significantly improved outcome in comparison with chemotherapy alone^[73]. Lin *et al* have compared surgery, surgery with adjuvant chemotherapy and chemotherapy alone and found the 5-year survival rates of 57%, 76% and 58% compared with 0% in the untreated group. They recommended surgery when feasible with adjuvant chemotherapy as the mainstay of treatment for gastric lymphoma^[71]. A Chinese study has suggested that chemotherapy plays a role in improving survival rates post-surgical resection^[53]. A prospective study from France in 1990 reported a 100% survival in patients with high-grade tumors who underwent resection and adjuvant chemotherapy. A recent series has shown the superiority of combined surgery and chemotherapy to single mode with survival rates between 86%-94% for stages IE and IIE^[53,59,66]. In these series the survival rates were higher for those who had complete resection, resection was the most important variable and major determinant of prolonged complete remission^[59,60]. Survival was higher in low-grade lymphomas, although the initial response might be superior in high grade lymphomas^[59]. Combined radical surgery and chemotherapy depending on the histologic grading were also associated with prolonged remission^[73].

Resection of the tumor with clear margins is thought to have a better prognosis than with diseased margins^[52,74,75]. However, other authors have found insignificant difference between the two procedures as long as post-operative chemotherapy was administered, and the extent of the disease at time of surgery, full thickness disease and lymph node involvement were important determining factors^[39].

On the contrary, other studies reported no significant difference in outcome in groups treated with single or combined mode of treatment^[57,62,70,72].

The stage and histologic grade of the disease play a role in the selection of the treatment modality, in addition to the comorbid disease and age of the patients.

Early stages of the disease regardless of the histological grade may be controlled by chemotherapy or chemotherapy and radiotherapy with the advantage of gastric conservation and avoidance of post-operative mortality and morbidity^[54,62,65-67,69,74]. On the other hand, surgery is advocated as the first option with adequate control of the disease^[57-59, 61], and occasionally with the necessity of wide resection and extensive lymph node dissection^[15,78], however, adjuvant chemotherapy is indicated to control the local and distant disease if any^[75,78].

In advanced stages of gastric lymphoma (stage IIIE, IVE) the behaviour of the tumor has the same manner as other advanced non-Hodgkin lymphomas, therefore combined chemotherapy is considered the treatment of choice for locally advanced or disseminated aggressive disease. In a prospective study of 700 patients with aggressive lymphoma treated with intensive chemotherapy, no difference in outcome was observed between patients with an advanced aggressive nodal lymphoma and the subset of patients (15%) in which the lymphoma was deemed to occur in the gastrointestinal tract^[40].

MALT lymphomas have aroused special interest because regression of the tumor has been reported after *H pylori* eradication. Standardization of therapy is not yet available and is still a subject of controversies. The initial results were shown in five of six patients with low grade MALT lymphomas who had regression of the tumor after eradication of *H pylori*^[77]. Thiede and associates studied a total of 120 patients with early gastric MALT lymphomas treated with amoxicillin and

omeprazole, a complete remission rate of 81% was achieved with partial response in 9%^[78]. Zucca and colleagues, in a large multinational cooperative study, treated 233 patients with antibiotics and randomized them to observation alone or maintenance with chlorambucil. Complete remission was documented in 62% and partial response in 12% with a 6-month median time to lymphoma regression. At a 40-month follow-up, a total of 15 (13%) cases had relapse^[79]. Manfred reported regression of reactive lymphoid infiltrates after *H pylori* eradication, without endoscopic or histological regression in MALT lymphomas^[26]. It is not yet known which stages of MALT lymphomas respond to *H pylori* eradication. Although it seems that eradication therapy is an adequate option of treatment taking into consideration the utility of endosonography in determining the invasion of the disease^[80].

Surgical resection, radiotherapy or chemotherapy and their combination have proven to be effective treatment modalities. Radiotherapy was tried as a local form of treatment in a small number of patients, resulting in a survival rate of 93%. Surgery, radiotherapy and antibiotics were compared and similar results were found^[81].

Radiotherapy

In most instances, radiotherapy is used as an adjuvant to surgery, chemotherapy or both. It has rarely been tried as a single mode of therapy^[31,81]. However, limited trials have suggested that radiotherapy can be utilized as a primary mode of treatment with reasonable outcome^[78,81].

Radiotherapy has been studied in comparison with other treatment modalities for stage IE and IIE with comparable outcome of 80%-89% survival^[13,31,68]. Higher survival rates (93%) have been reported in early stages of MALT lymphomas not responding to antibiotics^[83]. Radiation was used post-operatively in high- and low-grade lymphomas, for any residual tumors in stages I and II to improve the disease free survival^[9,57]. Combined chemotherapy might improve the chance of stomach conservation which may approach 100%^[72]. Total gastrectomy has not improved the survival in patients in whom radiotherapy has been utilized as the primary mode of therapy with a survival rate of 84%. Contradictory studies have found the combined radiotherapy with either resection or chemotherapy to be of no significant difference in both modalities with a survival rate of 82%-88%^[9,68,81].

PROGNOSIS

The prognostic factors in early stages were evaluated and defined in several studies. Good prognosis was associated with low grade disease, age below 65 years, free surgical margins in cases of resection, and achievement of initial complete remission^[49,50,53]. In advanced diseases, good prognosis was found in low-grade histology, initial complete response, and in general the prognosis is the same as non-gastrointestinal lymphoma^[50]. The grade of the disease also plays an important role in prognosis with better survival in low-grade disease rather than primary or secondary high-grade taking into consideration the stage^[17]. Five-year survival rates were reported to be 91% for low-grade, 73% for secondary high-grade and 56% for primary high-grade tumors^[17]. Debulking of the disease has not significantly altered the prognosis^[50,53,61,64].

CONCLUSION

Due to the rarity of primary gastric lymphoma, many aspects of this neoplasm are still controversial. The incidence of the disease is increasing and HIV-infected people are more vulnerable. Universally, gastric lymphoma is the commonest gastrointestinal lymphoma except in a few countries where

small intestinal lymphoma has been reported to be more common. On many occasions, patients present late, however with the availability of sophisticated diagnostic tools, the diagnosis can be made early and the classification and staging can be assessed accurately. The REAL classification despite being complex, has met a general agreement among pathologists and facilitated reproducibility. Most of the gastric lymphomas are primarily MALT type in origin. The best treatment for primary gastric lymphoma has not yet been exactly identified. It seems that for advanced disease, i.e., stage III and IV, combined chemotherapy and radiotherapy is superior since surgery is associated with failure of complete resection and significant morbidity and mortality. Most recent reports have advocated conservative treatment for early stages IE and IIE with the advantage of stomach conservation. On the other hand, many centers are still considering tumor resection as a better option. *H pylori* eradication with close observation has been considered adequate to treat early MALT lymphoma. Randomized trials are still needed to clarify whether conservative, surgical or combined treatment is more appropriate for treatment of localized gastric lymphoma.

REFERENCES

- 1 **Loehr WJ**, Mujahed Z, Zahn FD, Gray GR, Thorbjarnarson B. Primary lymphoma of the gastrointestinal tract: a review of 100 cases. *Ann Surg* 1969; **170**: 232-238
- 2 **Sandler RS**. Has primary gastric lymphoma become more common? *J Clin Gastroenterol* 1984; **6**: 101-107
- 3 **Aozasa K**, Tsujimoto M, Inoue A, Nakagawa K, Hanai J, Nosaka J. Primary gastrointestinal lymphoma. A clinicopathologic study of 102 patients. *Oncology* 1985; **42**: 97-103
- 4 **Laajam MA**, Al Mofleh IA, Al Faleh FZ, Al Aska AI, Jessen K, Hussain J, Al Rashed RS. Upper Gastrointestinal Endoscopy in Saudi Arabia: Analysis of 6386 procedures. *Quarterly J Med* 1988; **249**: 21-25
- 5 **Al Mofleh IA**. Endoscopic features of primary upper gastrointestinal lymphoma. *J Clin Gastroenterol* 1994; **19**: 69-74
- 6 **Aisenberg AC**. Coherent view of non-Hodgkin's lymphoma. *J Clin Oncol* 1995; **13**: 2656-2675
- 7 **ReMine SG**. Abdominal lymphoma. Role of surgery. *Surg Clin North Am* 1985; **65**: 301-313
- 8 **Salem P**, Anaissie E, Allam C, Geha S, Hashimi L, Ibrahim N, Jabbour J, Habboubi N, Khalyf M. Non-Hodgkin's lymphomas in the Middle East. A study of 417 patients with emphasis on special features. *Cancer* 1986; **58**: 1162-1166
- 9 **Almasri NM**, Al Abbadi M, Rewaily E, Abulkhalil A, Tarawneh MS. Primary gastrointestinal lymphomas in Jordan are similar to those in Western countries. *Mod Pathology* 1997; **10**: 137-141
- 10 **Gray GM**, Rosenberg SA, Cooper AD, Gregory PB, Stein DT, Herzenberg H. Lymphomas involving the gastrointestinal tract. *Gastroenterology* 1982; **82**: 143-152
- 11 **Willich NA**, Reinartz G, Horst EJ, Delker G, Reers B, Hiddemann W, Tiemann M, Parwaresch R, Grothaus-Pinke B, Kocik J, Koch P. Operative and conservative management of primary gastric lymphoma: interim results of a German multicenter study. *Int J Radiat Oncol Biol Phys* 2000; **46**: 895-901
- 12 **Dincol D**, Icli F, Erekel S, Gunel N, Karaoguz H, Demirkazik A. Primary gastrointestinal lymphomas in Turkey: A retrospective analysis of clinical features and results of treatment. *J Surg Oncol* 1992; **51**: 270-273
- 13 **Chandran RR**, Raj EH, Chaturvedi HK. Primary gastrointestinal lymphoma: 30 year experience at the cancer institute, Madras, India. *J Surg Oncol* 1995; **60**: 41-49
- 14 **Kyriacou C**, Loewen RD, Gibbon K, Hafeez M, Stuart AE, Whorton G, Al-Faleh FZ, Al-Mofleh I, Jessen K, Mass RE, El-Saghir N, Al-Khudairy N, Rifai MM, Qteishat W. Pathology and clinical features of gastro-intestinal lymphoma in Saudi Arabia. *Scottish Med J* 1991; **36**: 68-74
- 15 **Kitamura K**, Yamaguchi T, Okamoto K, Ichikawa D, Hoshima M, Taniguchi H, Takahashi T. Early gastric lymphoma; a clinicopathologic study of ten patients, literature review, and compari-

- son with early gastric adenocarcinoma. *Cancer* 1996; **77**: 850-857
- 16 **Shimm DS**, Dosoretz DE, Anderson T, Linggood RM, Harris NL, Wang CC. Primary gastric lymphoma; an analysis with emphasis on prognostic factors and radiation therapy. *Cancer* 1983; **52**: 2044-2048
 - 17 **Cogliatti SB**, Schmid U, Schumacher URS, Eckert F, Hansmann ML, Hedderich J, Takahashi H, Lennert K. Primary B-cell gastric lymphoma: A clinicopathological study of 145 patients. *Gastroenterology* 1991; **101**: 1159-1170
 - 18 **Weingrad DN**, Decosse JJ, Sherlock P, Straus D, Lieberman PH, Filippa DA. Primary gastrointestinal lymphoma: A 30-year review. *Cancer* 1982; **49**: 1258-1265
 - 19 **Hayes J**, Dunn E. Has the incidence of primary gastric lymphoma increased? *Cancer* 1989; **63**: 2073-2076
 - 20 **Powitz F**, Bogner JR, Sandor P, Zietz C, Goebel FD, Zoller WG. Gastrointestinal lymphomas in patients with AIDS. *Z Gastroenterol* 1997; **35**: 179-185
 - 21 **Imrie KR**, Sawka CA, Kutas G, Brandwein J, Warner E, Burkes R, Quirt I, McGeer A, Shepherd FA. HIV-associated lymphoma of the gastrointestinal tract: The University of Toronto AIDS-Lymphoma Study Group experience. *Leuklymphoma* 1995; **16**: 343-349
 - 22 **Dragosics B**, Bauer P, Radzskiewicz T. Primary gastrointestinal non-Hodgkin's lymphoma. A retrospective clinicopathological study of 150 cases. *Cancer* 1985; **55**: 1060-1073
 - 23 **Radzskiewicz T**, Dragosics B, Bauer P. Gastrointestinal malignant lymphomas of the mucosa-associated lymphoid tissue: Factors relevant to prognosis. *Gastroenterology* 1992; **102**: 1628-1638
 - 24 **Parsonnet J**, Hansen S, Rodriguez L, Gelb AB, Warnke RA, Jellum E, Orentreich N, Vogelman JH, Friedman GD. *Helicobacter pylori* infection and gastric lymphoma. *N Engl J Med* 1994; **330**: 1267-1271
 - 25 **Stolte M**. *Helicobacter pylori* gastritis and gastric MALT-lymphoma. *Lancet* 1992; **339**: 745-746
 - 26 **Isaacson P**, Wright DH. Extranodal malignant lymphoma arising from mucosa associated lymphoid tissue. *Cancer* 1984; **53**: 2515-2524
 - 27 **Muller AF**, Maloney A, Jenkins D, Dowling F, Smith P, Bessell EM, Toghil PJ. Primary gastric lymphoma in clinical practice 1973-1992. *Gut* 1995; **36**: 679-683
 - 28 **Kanavaros P**, Lavergne A, Galian A, Houdart R, Bernard JF. Primary gastric peripheral T-cell malignant lymphoma with helper/inducer phenotype. First case with a complete histological, ultrastructural, and immunochemical study. *Cancer* 1988; **61**: 1602-1610
 - 29 **Moubayed P**, Kaiserling E, Stein H. T-cell lymphoma of the stomach, morphologic and immunological studies characterizing two cases of T-cell lymphoma. *Virchows Arch A Pathol Anat Histopathol* 1987; **411**: 523-529
 - 30 **Brooks JJ**, Enterline HT. Primary gastric lymphomas: a clinicopathologic study of 58 cases with long-term follow-up and literature review. *Cancer* 1983; **51**: 701-711
 - 31 **Sutherland AG**, Kennedy M, Anderson DN, Park KGM, Keenan RA, Davidson AI. Gastric lymphoma in Grampian region: presentation, treatment and outcome. *J R Coll Surg Edinb* 1996; **41**: 143-147
 - 32 **Harris NL**, Jaffe ES, Stein H, Banks PM, Chan JK, Cleary ML, Delsol G, De Wolf-Peters C, Falini B, Gatter KC. A revised European-American classification of lymphoid neoplasms: a proposal from the international lymphoma study group. *Blood* 1994; **84**: 1361-1392
 - 33 **El Saghir NS**, Jessen K, Al-Mofleh IA, Ajarim DS, Fawzy E, Al-Faleh FZ, Dahaba N, Qteishat W. Primary gastrointestinal lymphoma in the Middle East: Analysis of 23 cases from Riyadh, Saudi Arabia. *Saudi Med J* 1990; **11**: 95-98
 - 34 **Armitage JO**, Cavalli F, Longo DL. Text atlas of lymphomas, 1sted. London. *Martin Dunitz Ltd* 1999; **2**: 133-152
 - 35 **Wotherspoon AC**, Ortiz-Hidalgo C, Falzon MR, Isaacson PG. *Helicobacter pylori*-associated gastritis and primary B-cell gastric lymphoma. *Lancet* 1991; **338**: 1175-1176
 - 36 **Ono H**, Kondo H, Saito D, Yoshida S, Shiroa K, Yamaguchi H, Yokota T, Hosokawa K, Fukuda H, Hayashi S. Rapid diagnosis of gastric malignant lymphoma from biopsy specimens: Detection of immunoglobulin heavy chain reaction. *Jpn J Cancer Res* 1993; **84**: 813-817
 - 37 **Isaacson PG**. Recent developments in our understanding of gastric lymphomas. *Am J Surg Pathol* 1996; **20**(Suppl 1): S1-S7
 - 38 **Al-Mofleh IA**. Complications of primary upper gastrointestinal lymphoma. *Ann Saudi Med* 1992; **12**: 297-299
 - 39 **Rackner VL**, Thirlby RC, Ryan JA. Role of surgery in multimodality therapy for gastrointestinal lymphoma. *Am J Surg* 1991; **161**: 570-575
 - 40 **Salles G**, Herbrecht R, Tilly H, Berger F, Brousse N, Gisselbrecht C, Coiffier B. Aggressive primary gastrointestinal lymphomas: review of 91 patients treated with LNH-84 regimen. *Am J Med* 1991; **90**: 77-84
 - 41 **Suekane H**, Iida M, Kuwano Y, Kohroggi N, Yao T, Iwashita A, Fujishima M. Diagnosis of primary early gastric lymphoma. Usefulness of endoscopic mucosal resection for histologic evaluation. *Cancer* 1993; **71**: 1207-1213
 - 42 **Park SH**, Han JK, Kim TK, Lee JW, Kim SH, Kim YI, Choi BI, Yeon KM, Han MC. Unusual gastric tumors: radiologic-pathologic correlation. *Radiographics* 1999; **19**: 1435-1446
 - 43 **Brown JA**, Carson BW, Gascayne RD, Cooperberg PL, Connors JM, Mason AC. Low grade gastric MALT lymphoma: radiographic findings. *Clin Radiol* 2000; **55**: 384-389
 - 44 **Chou CK**, Chen LT, Sheu RS, Yang CW, Wang ML, Jaw TS, Liu GC. MRI manifestations of gastrointestinal lymphoma. *Abdom Imaging* 1994; **19**: 495-500
 - 45 **Yucl C**, Ozdemir H, Isik S. Role of endosonography in the evaluation of gastric malignancy. *J Ultrasound Med* 1999; **18**: 283-288
 - 46 **Caletti G**, Fusaroli P, Togliani T, Bocus P, Roda E. Endosonography in gastric lymphoma and large gastric folds. *Eur J Ultrasound* 2000; **11**: 31-40
 - 47 **Musshoff K**. Clinical staging classification of non-Hodgkin's lymphomas. *Strahlentherapie* 1977; **153**: 218-221
 - 48 **Carbone PP**, Kaplan HS, Musshoff K, Smithes DW, Tubiana M. Report of the committee on Hodgkin disease staging procedures. *Cancer Res* 1971; **31**: 1860-1861
 - 49 **Rohatiner A**, d' Amore F, Coiffier B, Crowther D, Gospodarowicz M, Isaacson P, Lister TA, Norton A, Salem P, Shipp M. Report on a workshop convened to discuss the pathological and staging of GI tract lymphomas. *Ann Oncol* 1994; **5**: 397-400
 - 50 **Azab MB**, Henry-Amar M, Rougier P, Bognel C, Theodore C, Carde P, Lasser P, Cosset JM, Caillou B, Oroz JP, Marcel H. Prognostic factors in primary gastrointestinal non-Hodgkin lymphoma. *Cancer* 1989; **64**: 1208-1217
 - 51 **Weingrad DN**, Decosse JJ, Sherlock P, Straus D, Lieberman PH, Filippa DA. Primary gastrointestinal lymphoma: a 30-year review. *Cancer* 1982; **49**: 1258-1265
 - 52 **Maor MH**, Velasquez WS, Fuller LM, Silvermintz KB. Stomach conservation in stage IE and IIE gastric non-Hodgkin's lymphoma. *J Clin Oncol* 1990; **8**: 266-271
 - 53 **Liang R**, Todd D, Chan TK, Chiu E, Lie A, Kwong YL, Choy D, Ho FC. Prognostic factors for primary gastrointestinal lymphoma. *Hematol Oncol* 1995; **13**: 153-163
 - 54 **Fung CY**, Grossbard ML, Linggood RM, Younger J, Flieder A, Harris NL, Graeme-Cook F. Mucosa-associated lymphoid tissue lymphoma of the stomach: long term outcome after local treatment. *Cancer* 1999; **85**: 9-17
 - 55 **Salvagno L**, Soraru M, Busetto M, Puccetti C, Sava C, Endrizzi L, Giusto M, Aversa S, Chiarion Sileni V, Polico R, Bianco A, Rupolo M, Nitti D, Doglioni C, Lise M. Gastric non-Hodgkin's lymphoma: analysis of 252 patients from a multicenter study. *Tumori* 1999; **85**: 113-121
 - 56 **Kodera Y**, Yamamura Y, Nakamura S, Shimizu Y, Torii A, Hirai T, Yasui K, Morimoto T, Kato T, Kito T. The role of radical gastrectomy with systematic lymphadenectomy for the diagnosis and treatment of primary gastric lymphoma. *Ann Surg* 1998; **227**: 45-50
 - 57 **Fischbach W**, Dragosics B, Kolve-Goebler ME, Ohmann C, Greiner A, Yang Q, Bohm S, Verreet P, Horstmann O, Busch M, Duhmke E, Muller-Hermelink HK, Wilms K, Allingers S, Bauer P, Bauer S, Bender A, Brandstatter G, Chott A, Dittrich C, Erhart K, Eysselt D, Ellersdorfer H, Ferlitsch A, Fridrik MA, Gartner A, Hausmaninger M, Hinterberger W, Hugel K, Ilsinger P, Jonaus K, Judmaier G, Karner J, Kerstan E, Knoflach P, Lenz K, Kandutsch A, Lobmeyer M, Michlmeier H, Mach H, Marosi C, Ohlinger W, Oprean H, Pointer H, Pont J, Salabon H, Samec HJ, Ulsperger A, Wimmer A, Wewalka F. Primary gastric B-cell lymphoma: results of a prospective multicenter study. *Gastroenterology* 2000; **119**: 1191-1202
 - 58 **Lucandri G**, Stipa F, Mingazzini PL, Ferri M, Sapienza P, Stipa S.

- The role of surgery in the treatment of primary gastric lymphoma. *Anticancer Res* 1998; **18**: 2089-2094
- 59 **Vaillant JC**, Ruskone-Fourmestraux A, Aegerter P, Gayet B, Rambaud JC, Valleur P, Parc R. Management and long-term results of surgery for localized gastric lymphomas. *Am J Surg* 2000; **179**: 216-222
- 60 **Popescu RA**, Wotherspoon AC, Cunningham D, Norman A, Prendiville J, Hill ME. Surgery plus chemotherapy or chemotherapy alone for primary intermediate and high-grade gastric non-Hodgkin's lymphoma: The Royal Marsden Hospital experience. *Eur J Cancer* 1999; **35**: 928-934
- 61 **Ong CL**, Ti TK, Rauff A. Primary gastric lymphoma. *Singapore Med J* 1993; **34**: 442-444
- 62 **Cooper DI**, Doria R, Salloum E. Primary gastrointestinal lymphomas. *Gastroenterologist* 1996; **4**: 54-64
- 63 **Law MM**, Willimas SB, Wong JH. Role of surgery in the management of primary lymphoma of the gastrointestinal tract. *J Surg Oncol* 1996; **61**: 199-204
- 64 **Koch P**, del Valle F, Berdel WE, Willich NA, Reers B, Hiddemann W, Grothaus-Pinke B, Reinartz G, Brockmann J, Temmensfeld A, Schmitz R, Rube C, Probst A, Jaenke G, Bodenstern H, Junker A, Pott C, Schultz J, Heinecke A, Parwaresch R, Tiemann M. Primary gastrointestinal non-Hodgkin's lymphoma: II. Combined surgical and conservative or conservative management only in localized gastric lymphoma - results of the prospective German multicenter study. The German Multicenter Study Group on GIT-NHL. *J Clin Oncol* 2001; **19**: 3874-3883
- 65 **Raderer M**, Valencak J, Osterreicher C, Drach J, Hejna M, Kornek G, Scheithauer W, Brodowicz ZT, Chott A, Dragosics B. Chemotherapy for the treatment of patients with primary high grade gastric B-cell lymphoma of modified Ann Arbor stages IE and IIE. *Cancer* 2000; **88**: 1979-1985
- 66 **Tondini C**, Balzarotti M, Santoro A, Zanini M, Fornier M, Giardini R, Di Felice G, Bozzetti F, Bonadonna G. Initial chemotherapy of primary resectable large-cell lymphoma of the stomach. *Ann Oncol* 1997; **8**: 497-499
- 67 **Liu HT**, Hsu C, Chen CL, Chiang IP, Chen LT, Chen YC, Cheng AL. Chemotherapy alone versus surgery followed by chemotherapy for stage I/II large-cell lymphoma of the stomach. *Am J Hematol* 2000; **64**: 175-179
- 68 **Ferreri AJ**, Cordio S, Paro S, Ponzoni M, Freschi M, Veglia F, Villa E. Therapeutic management of stage I-II high-grade primary gastric lymphomas. *Oncology* 1999; **56**: 274-282
- 69 **Thieblemont C**, Dumontet C, Bouafia F, Hequet O, Arnaud P, Espinouse D, Felman P, Berger F, Salles G, Coiffier B. Outcome in relation to treatment mortalities in 38 patients with localized gastric lymphoma: A retrospective study of patients treated during 1976-2001. *Leuk Lymphoma* 2003; **44**: 257-262
- 70 **Au E**, Ang PT, Tan P, Sng I, Fong CM, Chua EJ, Ong YW. Gastrointestinal lymphoma-a review of 54 patients in Singapore. *Ann Acad Med Singapore* 1997; **26**: 758-761
- 71 **Lin KM**, Penney DG, Mahmoud A, Chae W, Kolachalam RB, Young SC. Advantage of surgery and adjuvant chemotherapy in the treatment of primary gastrointestinal lymphoma. *J Surg Oncol* 1997; **64**: 237-241
- 72 **Ferreri AJ**, Cordio S, Ponzoni M, Villa E. Non-surgical treatment with primary chemotherapy, with and without radiation therapy of stage I-II high-grade lymphoma. *Leuk Lymphoma* 1999; **33**: 531-541
- 73 **Ruskone-Fourmestraux A**, Aegerter P, Delmer A, Brousse N, Galian A, Rambaud JC. Primary digestive tract lymphoma: a prospective multicentric study of 91 patients. *Gastroenterology* 1993; **105**: 1662-1671
- 74 **Thirlby RC**. Gastrointestinal lymphoma: a surgical perspective. *Oncology (Huntingt)* 1993; **7**: 29-32,34
- 75 **Thomas CR Jr**, Share R. Gastrointestinal lymphoma. *Med Pediatr Oncol* 1991; **19**: 48-60
- 76 **Tedeschi L**, Romanelli A, Dallavalle G, Tavani E, Arnoldi E, Vinci M, Mortara G, Bedoni P, Labianca R, Luporini G. Stages I and II non-Hodgkin's lymphoma of the gastrointestinal tract. Retrospective analysis of 79 patients and review of the literature. *J Clin Gastroenterol* 1994; **18**: 99-104
- 77 **Wotherspoon AC**, Doglioni C, Diss TC, Pan L, Moschini A, de Boni M, Isaacson PG. Regression of primary low-grade B-cell gastric lymphoma of mucosa-associated lymphoid tissue type after eradication of *Helicobacter pylori*. *Lancet* 1993; **342**: 575-577
- 78 **Pinotti G**, Zucca E, Roggero E, Pascarella A, Bertoni F, Savio A, Savio E, Capella C, Pedrinis E, Saletti P, Morandi E, Santandrea G, Cavalli F. Clinical features, treatment and outcome in a series of 93 patients with low-grade gastric MALT lymphoma. *Leuk Lymphoma* 1997; **26**: 527-537
- 79 **Bertoni F**, Conconi A, Capella C, Motta T, Giardini R, Ponzoni M, Pedrinis E, Novero D, Rinaldi P, Cazzaniga G, Biondi A, Wotherspoon A, Hancock BW, Smith P, Souhami R, Cotter FE, Cavalli F, Zucca E. International extranodal lymphoma study group: United Kingdom lymphoma group. Molecular follow-up in gastric mucosa-associated lymphoid tissue lymphoma: early analysis of the LY03 cooperative trial. *Blood* 2002; **99**: 2541-2544
- 80 **Fischbach W**. Primary gastric lymphoma of MALT: considerations of pathogenesis, diagnosis and therapy. *Can J Gastroenterol* 2000; **14**(Suppl D): 44D-50D
- 81 **Kocher M**, Muller RP, Ross D, Hoederath A, Sack H. Radiotherapy for treatment of localized non-Hodgkin's lymphoma. *Radiother Oncol* 1997; **42**: 37-41

Safety of interferon b treatment for chronic HCV hepatitis

D Festi, L Sandri, G Mazzella, E Roda, T Sacco, T Staniscia, S Capodicasa, A Vestito, A Colecchia

D Festi, L Sandri, G Mazzella, E Roda, A Colecchia, Department of Internal Medicine and Gastroenterology, University of Bologna, Bologna, Italy

T Sacco, T Staniscia, S Capodicasa, A Vestito, Department of Medicine and Aging, University G.d' Annunzio, Chieti, Italy

Correspondence to: Davide Festi, MD Dipartimento di Medicina Interna e Gastroenterologia, Policlinico S.Orsola-Malpighi, Via Massarenti 9, 40126 Bologna, Italy. festi@med.unibo.it

Telephone: +39-051-6364123 **Fax:** +39-051-6364123

Received: 2003-07-12 **Accepted:** 2003-10-23

Abstract

Hepatitis C is a major cause of liver-related morbidity and mortality worldwide. In fact, chronic hepatitis C is considered as one of the primary causes of chronic liver disease, cirrhosis and hepatocellular carcinoma, and is the most common reason for liver transplantation. The primary objectives for the treatment of HCV-related chronic hepatitis is to eradicate infection and prevent progression of the disease. The treatment has evolved from the use of α -interferon (IFN α) alone to the combination of IFN α plus ribavirin, with a significant improvement in the overall efficacy, and to the newer PEG-IFNs which have further increased the virological response, used either alone or in combination with ribavirin. Despite these positive results, in terms of efficacy, concerns are related to the safety and adverse events. Many patients must reduce the dose of PEG-IFN or ribavirin, others must stop the treatment and a variable percentage of subjects are not suitable owing to intolerance toward drugs. IFN β represents a potential therapeutic alternative for the treatment of chronic viral hepatitis and in some countries it plays an important role in therapeutic protocols. Aim of the present paper was to review available data on the safety of IFN β treatment in HCV-related chronic hepatitis.

The rates of treatment discontinuation and/or dose modification due to the appearance of severe side effects during IFN β are generally low and in several clinical studies no requirements for treatment discontinuation and/or dose modifications have been reported. The most frequent side effects experienced during IFN β treatment are flu-like syndromes, fever, fatigue and injection-site reactions. No differences in terms of side-effect frequency and severity between responders and non-responders have been reported. A more recent study, performed to compare IFN β alone or in combination with ribavirin, confirmed the good safety profile of both treatments. Similar trends of adverse event frequency have been observed in subpopulations such as patients with genotype-1b HCV hepatitis unresponsive to IFN α treatment or with HCV-related cirrhosis and patients with acute viral hepatitis. If further studies will confirm the efficacy of combined IFN β and ribavirin treatment, this regimen could represent a safe and alternative therapeutic option in selected patients.

Festi D, Sandri L, Mazzella G, Roda E, Sacco T, Staniscia T, Capodicasa S, Vestito A, Colecchia A. Safety of interferon β treatment for chronic HCV hepatitis. *World J Gastroenterol* 2004; 10(1): 12-16

<http://www.wjgnet.com/1007-9327/10/12.asp>

INTRODUCTION

Hepatitis C is a major cause of liver-related morbidity and mortality worldwide and represents a significant public health problem^[1]. In fact, chronic hepatitis C is considered as one of the primary causes of chronic liver disease, cirrhosis and hepatocellular carcinoma, and is the most common reason for liver transplantation^[2]. Based on the increased knowledge surrounding the natural history of the disease, the primary objectives for the treatment of hepatitis C virus (HCV)-related chronic hepatitis are to eradicate infection and prevent progression to cirrhosis and thereby preventing complications associated with end-stage liver disease^[3,4]. The treatment of HCV has evolved from the use of a single agent - mainly interferon alpha (IFN α) to the combination of IFN α and ribavirin treatment. Combination therapy can significantly improve the overall treatment efficacy compared to monotherapy (i.e., from 10%-15% of sustained viral clearance to 30%-40%) and now represents the standard treatment for chronic hepatitis.

Recently, new IFN preparations, such as pegylated IFNs (PEG-IFNs), have been introduced in clinical practice. Results obtained from large, multicenter studies of combined PEG-IFN and ribavirin treatment have shown a further increase in treatment efficacy. In fact, HCV infection was eradicated in 47%-54% of patients treated with PEG-IFN α -2b^[5]. Similar results have been found with PEG-IFN α -2a treatment^[6]. However, despite these positive results, several clinical problems remain. Of primary significance is the large number of patients treated with PEG-IFN (both α -2a and α -2b) and ribavirin who discontinue treatment due to the occurrence of adverse events associated with therapy. In fact, it has been reported that 34%-42% of patients treated with PEG-IFN α -2b (high and low doses, respectively) required dose reductions due to the appearance of adverse events and 13% stopped treatment for safety reasons^[5]. In another trial concerning the efficacy of PEG-IFN α -2a, dose modifications due to adverse events were required in 8% of patients and treatment discontinuation was required in 19%^[6]. In a pivotal trial of IFN α -2b and ribavirin performed by McHutchison *et al.*^[7], dose reductions due to adverse events were needed in 13% and 17% of patients treated for 24 and 48 weeks, respectively. Treatment discontinuation rates were 8% and 21% in patients treated for 24 and 48 weeks, respectively. Furthermore, it has been recently documented that, due primarily to safety issues, the number of HCV patients eligible for current treatments and the rate of treatment completion were much lower in clinical practice than in clinical trials^[8]. These concerns are particularly relevant considering that the primary goals of HCV treatment are viral eradication and the slowing of disease progression^[9,10].

Since IFNs are a family of glycoproteins with a broad range of antiviral effects, IFN beta (IFN β) represents a potential therapeutic alternative for the treatment of chronic viral hepatitis. In fact, in some countries, mainly in Japan, IFN β already plays a central role in therapeutic protocols. Differences have been reported between the physicochemical, biological and pharmacological properties of IFN α and IFN β ^[11,12]. Three forms of human IFN β are available:^[13] 1) Natural human IFN β (nIFN β) which is produced using human fibroblasts and is currently used in Japan for the treatment of chronic hepatitis C. 2) Recombinant human IFN β -1a (rhIFN β -1a), which is

procured from mammalian cells and is identical to IFN β that occurs naturally in humans. 3) *Escherichia coli*-produced recombinant human IFN β (IFN β -1b) which contains an altered amino acid sequence with a serine substitution for the cysteine at position 17. rhIFN β -1a appears to have advantages over the other two formulations and, in particular, is less immunogenic and more potent^[14]. The aim of the present paper was to review available data on the safety of IFN β for the treatment of chronic hepatitis C. Since IFN β has been widely used for the treatment of multiple sclerosis (MS), studies referring to the safety of IFN β in MS are reviewed briefly before discussing the results of this treatment in HCV-related chronic hepatitis.

IFN β in multiple sclerosis

Recombinant IFN β is currently the gold standard for the treatment of relapsing-remitting MS (RRMS). In MS, IFN β treatment lasts several years and regimens require high doses and frequent administration. Therefore, safety data on IFN β therapy recorded in MS studies and clinical practice could be useful for providing an overview of the drug's safety characteristics.

In the PRISMS (prevention of relapses and disability by interferon beta-1a subcutaneously in multiple sclerosis) study^[15], 560 patients with RRMS received 2.2 μ g or 4.4 μ g IFN β or placebo subcutaneously (s c) thrice weekly (t.i.w.) for 2 years (PRISMS-2) and then, the subjects completing treatment ($n=503$) or study ($n=533$) were re-randomized to receive either 2.2 μ g or 4.4 μ g IFN β s c, t.i.w., for an additional 2 years (PRISMS-4)^[16]. The adverse events reported during the PRISMS-4 study were similar to those observed in the PRISMS-2 trial and, in general, most adverse events were mild. During the 4-year period of observation, the most frequent events reported were injection-site inflammation, flu-like symptoms, headache and fatigue, with similar rates in both active treatment groups. In the 2.2- and 4.4 μ g groups, respectively, less frequent adverse events included laboratory abnormalities such as lymphopenia (27% and 35%), elevated ALT levels (24% and 30%), elevated AST levels (11% and 20%) and thrombocytopenia (3% and 8%). All cases of thrombocytopenia were mild and only one patient over the 4 years (in the 4.4 μ g group) stopped treatment due to lymphopenia. In two other patients, treatment was discontinued as a result of elevated liver enzymes. In the SPECTRIMS (secondary progressive efficacy trial of rebif [interferon beta-1a] in multiple sclerosis) study^[17] conducted in secondary progressive MS (SPMS) patients using a treatment schedule similar to that used in the PRISMS-2 study, the type, frequency and severity of adverse events with IFN β -1a were similar to those reported in the PRISMS study. Overall, IFN β -1a was well tolerated. Of the 618 patients enrolled, 3 receiving placebo, 8 receiving 2.2 μ g IFN β -1a and 7 receiving 4.4 μ g IFN β -1a discontinued treatment permanently. In general, liver function test abnormalities were mild or moderate and either resolved with treatment interruption or no treatment modification whatsoever. The recent EVIDENCE (The evidence for interferon dose-response: European North American comparative efficacy) study^[18] compared the safety and efficacy of IFN β -1a, 4.4 μ g, s c, t.i.w., to IFN β -1b, 3.0 μ g, once weekly by intramuscular (i m) injection, in 677 patients with RRMS over 24 weeks. The most common adverse events recorded were injection-site disorders, flu-like symptoms, headaches, rhinitis and fatigue. The higher frequency of injection-site disorders in the IFN β -1a group was related to the more frequent administration of this agent. However, injection-site disorders were mild and no skin necrosis was observed in over 20 000 s c injections. Hepatic and hematologic laboratory abnormalities were also more common on IFN β -1a but again, these abnormalities were generally mild and responsive to dose

reductions (if required). In both treatment groups, severe laboratory abnormalities were rare (<1%).

IFN β pharmacokinetics

IFN β can be administered intravenously (i v), intramuscularly (i m) and subcutaneously (s c). Pharmacokinetic and pharmacodynamic studies^[19-21] have shown that the extent and duration of the clinical and biologic effects of IFN β are independent of the route of administration. Furthermore, studies evaluating the most efficacious IFN β dosing regimen^[22-25] have shown that, in general, the highest doses have the greatest efficacy. However, these higher doses are also associated with a greater incidence of side effects (see below).

Evaluation of IFN β safety

Similar to the adverse events associated with IFN α therapy^[26,27], the side effects of IFN β can be separated into different categories, namely: a) common side effects (these range from mild-to-severe in nature and do not require dose modification), b) mild-to-moderate side effects which occur less frequently (i.e., less than 10% of treated patients) and may or may not require dose modification, and c) severe or life-threatening side effects. Thus far, no severe or life-threatening side effects have been reported with IFN β use. Clinical IFN β data are based on the results of clinical studies involving 1096 patients^[23-25,28-52]. Studies have been performed on treatment-naïve patients as well as patients who did not respond to previous treatment (generally with IFN α), two other studies were performed in special populations (i.e., cirrhotic patients and patients with renal failure)^[46,54].

Discontinuation and dose modification during IFN β treatment

The rates of treatment discontinuation and/or dose modification due to the appearance of severe side effects during IFN β are generally low (Table 1). Furthermore, several clinical studies reported no requirements for treatment discontinuation and/or dose modifications. Kiyosawa *et al*^[28] found that in naïve patients treated with i v IFN β , dose modifications due to leukocyte counts below $1 \times 10^9/L$ were required in only 4.2% of patients (1 of 12 patients). In a study by Villa *et al*^[29] 5.3% of patients (1 of 19) did not complete the trial. Reasons for discontinuation were not specified. A comparison study of i v recombinant IFN β and IFN α -2b plus ribavirin in patients who did not respond to previous IFN α treatment found that 12% of patients in the IFN α -2b plus ribavirin group (12 of 100) withdrew from treatment due to side effects such as flu-like symptoms. In the IFN β group, the corresponding frequency was 9% (9 of 100 patients)^[30].

Table 1 Frequency of treatment discontinuation and dose modifications during therapy with IFN β

	Number of cases	References
Discontinuation		
Adverse events	14	25,28,29,30
Laboratory abnormalities	2	31
Dose modifications		
Adverse events	-	
Laboratory abnormalities	1	43

In a comparative study of two different doses (9 MU and 12 MU) of rhIFN β produced using Chinese hamster ovaries, Habersetzer *et al*^[25] observed a treatment discontinuation rate of 18.2% (2 of 11 patients in the lower dose group) in naïve patients due to the occurrence of side effects such as mild depression and cutaneous ulcers at the injection site. A treatment discontinuation rate of 18.2% (2 of 11 patients) was also found in a study^[31] comparing the effects of different IFN β

administration regimens (i v 6 MU once daily versus 3 MU twice daily), two patients who discontinued treatment were using IFN β twice daily. Liver enzyme alterations (serum ALT/AST levels >700 IU/l) and severe proteinuria (urinary protein excretion >40 g/L and serum albumin level <30 g/L) were the causes of discontinuation. In conclusion, the frequency of treatment discontinuation and dose modifications that occur during IFN β therapy is low.

Frequency of side effects during IFN β treatment

The frequency of side effects experienced during IFN β treatment is reported in Table 2.

Table 2 Frequency of side effects with IFN β therapy

Side effects	Frequency (range) (%)	References
Flu-like syndrome	10-100	25,30,32,33,35, 36, 37, 39, 46
Fever	67-100	28,43,40
Fatigue	16-74	24, 33, 39,46
Local reactions (at the injection site)	43-76	25,34, 37
Headaches	8-47	33, 39, 46
Malaise	50	39
Arthro-myalgias	21-42	39,40,46
Weight loss	6-42	39,40
Gastrointestinal symptoms	20-26	25,37, 38
Anxiety, insomnia, irritability	10-25	32, 39, 38
Depression	10-21	25, 38,46
Alopecia	8-16	33, 39
Proteinuria	46-73	22, 51
Reduced platelet count	13-44	22, 32,51
Reduced white-cell count	13-20	32,38

Flu-like syndromes, fever, fatigue and injection-site reactions are the most frequently observed side effects of IFN β therapy. No differences in terms of the frequency and severity of side effects between therapeutic responders and non-responders have been reported. In order to better evaluate the clinical significance of these side effects, results have been analysed with reference to the type of study.

Clinical studies evaluating the safety of IFN β

In a study of 8 naïve patients, Chemello *et al*^[32] found that treatment with i v natural human fibroblast IFN β was well tolerated, the predominant side effect was a mild form of a flu-like syndrome, which lasted between 3 and 23 days after the initiation of therapy. No hematologic toxicity was observed and reductions in white-blood-cell and platelet counts occurred in only one patient. A low side-effect rate was also observed in a study of 90 naïve patients treated with i m IFN β for 6 months^[33]. In fact, mild flu-like syndromes appeared in less than 10% of treated patients and asthenia in 16% of patients. The frequency of other side effects was less than 10%. The same investigators^[34] obtained similar results in another study of naïve patients treated with s c IFN β . A good safety profile with mild, transient flu-like syndromes as the predominant side effect was documented in two Italian studies^[35,36] performed in patients previously unresponsive to IFN α and subsequently treated with i v IFN β . Pellicano *et al*^[37] treated 30 patients who did not respond to a standard course of IFN α therapy with rhIFN β -1a (12 MU s.c., t.i.w.) for 3 months. The observed rate of flu-like symptoms, inflammation at the injection site, abdominal symptoms and psychiatric disturbances were 63%, 43%, 26% and 13%, respectively.

Clinical studies comparing different doses of IFN β

In a study of 92 naïve patients, Fesce *et al*^[24] compared two

different doses of i m natural human fibroblast IFN β : 3 MU and 6 MU t.i.w. for 12 months. Compared to the low-dose group, an increased frequency of flu-like syndromes (17% vs 9%), weakness (73% vs 57%), headache (48% vs 30%) and irritability (23% vs 11%) was documented in the high-dose group. However, these differences were not statistically significant. Habersetzer *et al*^[25] compared two different doses of recombinant IFN β -1a administered s c for 24 weeks in 21 naïve patients: 9 MU t.i.w. and 12 MU t.i.w. No differences were found between the two groups with regards to individual side effects. In a study aimed at comparing i v IFN β 3 MU twice daily vs 6 MU once daily in genotype-1b HCV-infected patients with high virus titres^[23], side effects were found to be more prevalent in the 3-MU group, particularly proteinuria (56% vs 30%) and thrombocytopenia (44% vs 20%).

Clinical studies comparing the safety of IFN β to IFN α

Several studies comparing the safety of IFN β and IFN α have been performed^[29,30,38-42].

Frosi *et al*^[38] compared IFN α and IFN β in 20 naïve patients treated for 6 months and did not observe any significant differences between the two treatment groups in terms of the frequency of adverse events. In another study^[39], flu-like syndromes and hair loss were less frequent in the IFN β group (16% and 16%, respectively) compared to the IFN α group (86% and 57%, respectively), the frequency of other adverse events were similar between the two groups. Cecere *et al*^[40] evaluated the efficacy and tolerability of the following types of IFN in 150 patients: lymphoblastoid IFN α , leukocytic IFN α and natural IFN β . The frequency of side effects was lower in the IFN β group than in the other treatment groups. In the IFN β , the frequency of lymphoblastoid IFN α and leukocytic IFN α , respectively, fever was present in 66.8%, 83.9% and 73.4%, the frequency of bone and muscle pains in 33%, 72.5% and 46.3%, fatigue in 21%, 52% and 31%, and the frequency of weight loss in 6%, 21% and 15%. Barbaro *et al*^[30] found no significant differences in the rates of side effects and treatment discontinuation between IFN β -treated and recombinant IFN α -2b plus ribavirin-treated patients ($n=200$) who were non-responders to previous IFN α -2b therapy.

Clinical studies evaluating combination therapy (IFN β plus ribavirin)

Kakumu *et al*^[43] compared the efficacy of ribavirin alone, IFN β alone and combined ribavirin/IFN β therapy. The combined therapy was found to significantly reduce red-blood-cell count and hemoglobin concentrations. A significant reduction in white-blood-cell count was documented in the IFN β and combined treatment groups. Despite these findings, all enrolled patients completed the study. More recently, a multicenter, randomised and controlled study has been performed^[44] to compare rhIFN β alone or in combination with ribavirin. One hundred and two naïve patients with chronic hepatitis C were randomized to receive either rhIFN β -1a alone (6 MU, s c, everyday) or in combination with ribavirin for 6 weeks. All patients in the IFN β -alone group completed the study, while 3 of 51 patients in the combined treatment group stopped therapy due to adverse events. Overall, both treatment regimens were well tolerated, hematological and hematochemical parameters remained unchanged by the end of the study period (except for a significant decrease in hemoglobin levels in the combined treatment group).

Clinical studies in sub-populations of patients

Vezzoli *et al*^[45] evaluated the efficacy and safety of IFN β in 10 patients with genotype-1b HCV hepatitis who were

unresponsive to a previous cycle of IFN α treatment, no reference to side effects was reported. Bernardinello *et al*^[46] examined the safety and tolerability of natural i m IFN β in 61 patients with HCV-related cirrhosis and found that the treatment was well tolerated, the most frequent side effects were fatigue (24%), irritability or depression (21%), arthromyalgias (21%), headache (21%) and flu-like symptoms (16%). The frequency of these adverse events are similar to those found in chronic hepatitis patients without cirrhosis using IFN β . Interestingly, in this study, the probability of developing clinically significant liver-related events during the follow-up period was not significantly different in untreated *versus* treated patients (the cumulative probability of decompensation at 60 months was 24% in treated patients and 35% in untreated ones). Although a recent Cochrane review^[47] states that there is no definitive conclusion about the safety of IFN β in acute hepatitis, IFN β has been used in patients with acute hepatitis without causing significant side effects^[48-50]. Takano *et al*^[49] studied the effects of six different IFN β treatment schedules in 97 patients with acute non-A, non-B hepatitis. The authors did not report data regarding the safety of IFN β , however, all enrolled patients completed the study. A pharmacokinetic study^[54] has been performed in patients with end-stage renal failure, i v infusion of natural human IFN β was found to be safe.

CONCLUSION

HCV infection is a major health problem and efforts have been made to identify drugs able to eradicate the disease and, thereby reducing HCV-related morbidity and mortality. According to recent consensus conference reports^[55,56], treatment of IFN α in combination with ribavirin represents the standard therapy for HCV-related chronic hepatitis. However, the use of high treatment doses for long periods, which is often required in subgroups of patients (i.e., those with genotype 1 disease) to reach acceptable levels of efficacy, increases the risk of side effects and as a result, can reduce patient compliance to treatment. In these cases, the search for further treatment strategies could be useful. IFN β has been proposed as a possible therapy for chronic hepatitis. Studies examining the use of IFN β in hepatitis originated in Japan^[57] but, in recent years, studies have also been performed in Europe^[25,29,30,32-38,40,44-46,53]. According to the available data, the treatment of chronic hepatitis C with IFN β is associated with a good safety and tolerability profile. In fact, in most clinical studies, the frequency of side effects is lower, or at least similar, to that reported with IFN α therapy. Furthermore, the rate of dropouts in controlled clinical studies as well as the need for dose reductions or treatment discontinuation are very low. IFN β has also been shown to be well tolerated and has an excellent safety profile in special patient populations, such as those with acute hepatitis^[48-50], cirrhosis^[46], and renal insufficiency^[54].

The goals of treatment strategies for HCV-related chronic hepatitis are to eradicate HCV infection and to reduce disease progression. The availability of different therapeutic choices is critical in achieving these goals, particularly in patients unresponsive to a standard course of antiviral therapy. Due to its good safety profile, IFN β may represent a possible second-line therapy if additional clinical studies can confirm this drug's efficacy, mainly in combination with ribavirin.

The eradication of HCV and the prevention or slowing of disease progression are clinical challenges that require a careful cost/benefit analysis. In order to expand the population of patients eligible for therapy and to treat subjects who cannot tolerate first-line treatments, new therapeutic options should be evaluated. If further studies will confirm the efficacy of combined IFN β and ribavirin treatment, this regimen can represent a safe, alternative therapeutic option.

REFERENCES

- 1 **Ray Kim W.** The burden of hepatitis C in the United States. *Hepatology* 2002; **36**: S30-S34
- 2 **Alberti A,** Chemello L, Benvegna', L. Natural history of hepatitis C. *J Hepatol* 1999; **31** (Suppl 1): 17-24
- 3 **Alberti A,** Benvegna' L. Management of hepatitis C. *J Hepatol* 2003; **38**: S104-S118
- 4 **Mazzella G,** Accogli E, Sottili S, Festi D, Orsini M, Salzetta A, Novelli V, Cipolla A, Fabbri C, Pezzoli A, Roda E. Alpha interferon may prevent hepatocellular carcinoma in HCV-related liver cirrhosis. *J Hepatol* 1996; **24**: 141-147
- 5 **Manns MP,** McHutchinson JG, Gordon SC, Rustgi VK, Shiffman M, Reindollar R, Goodman ZD, Koury K, Ling M, Albrecht JK. Peginterferon alfa-2b plus ribavirin compared with interferon alfa-2b plus ribavirin for initial treatment of chronic hepatitis C: a randomized trial. *Lancet* 2001; **358**: 958-965
- 6 **Zeuzem S,** Feinman SV, Rasenack J, Heathcote EJ, Lai MY, Gane E, O' Grady J, Reichen J, Diago M, Lin A, Hoffman J, Brunda MJ. Peginterferon alfa-2a in patients with chronic hepatitis C. *N Engl J Med* 2000; **343**: 1666-1672
- 7 **McHutchinson JG,** Gordon SC, Schiff ER, Shiffmann ML, Lee WM, Rustgi VK, Goodman ZD, Ling MH, Cort S, Albrecht JK. Interferon alfa-2b alone or in combination with ribavirin as initial treatment for chronic hepatitis. Hepatitis Interventional Therapy Group. *N Engl J Med* 1998; **339**: 1485-1492
- 8 **Falck-Ytter Y,** Kale H, Mullen K, Sarbah S, Sorescu L, McCullough A. Surprisingly small effect of antiviral treatment in patients with hepatitis C. *Ann Intern Med* 2002 **136**: 288-292
- 9 **Poynard T,** McHutchinson J, Davis GL, Esteban-Mur R, Goodman Z, Bedossa P, Albrecht J. Impact of interferon alfa-2b and ribavirin on progression of liver fibrosis in patients with chronic hepatitis C. *Hepatology* 2000; **32**: 1131-1137
- 10 **Yoshida H,** Arakawa Y, Sata M, Nishiguchi S, Yano M, Fujiyama S, Yamada G, Yokosuka O, Shiratori Y, Omata M. Interferon therapy prolonged life expectancy among chronic hepatitis C patients. *Gastroenterology* 2002; **123**: 483-491
- 11 **Petska S,** Langer JA, Zoon KC, Samuel CE. Interferons and their actions. *Ann Rev Biochem* 1987; **56**: 727-777
- 12 **Bocci V.** Physicochemical and biological properties of interferons and their potential uses in drug delivery systems. *Crit Rev Drug Carrier Syst* 1992; **9**: 91-133
- 13 **Alam JJ.** Interferon- β treatment of human disease. *Curr Opin Biotechnol* 1995; **6**: 688-691
- 14 **Salmon P,** Le Cottonnec JY, Galazka A, Abdul-Ahad A, Darragh A. Pharmacokinetics and pharmacodynamics of recombinant human interferon- β in healthy male volunteers. *J Interferon Cytokine Res* 1996; **16**: 759-764
- 15 **PRISMS Study Group.** Randomized double-blind placebo-controlled study of interferon-beta-1a in relapsing/remitting multiple sclerosis. *Lancet* 1998; **352**: 1498-1504
- 16 **PRISMS Study Group.** PRISMS-4: long-term efficacy of interferon-beta-1a in relapsing MS. *Neurology* 2001; **56**: 1628-1636
- 17 **SPECTRIMS Study Group.** Randomized controlled trial of interferon-beta-1a in secondary progressive MS. *Neurology* 2001; **56**: 1496-1504
- 18 **Panitch H,** Goodin DS, Francis G, Chang P, Coyle PK, O' Connor P, Monaghan E, Li D, Weinshenker B. Randomized, comparative study of interferon beta-1a treatment regimens in MS: The EVIDENCE Trial. *Neurology* 2002; **59**: 1496-1506
- 19 **Munafa A,** Trincharad-Lugan I, Nguyen TXQ, Buraglio M. Comparative pharmacokinetics and pharmacodynamics of recombinant human interferon beta-1a after intramuscular and subcutaneous administration. *Eur J Neurol* 1998; **5**: 187-193
- 20 **Matsuyama S,** Henmi S, Ichihara N, Sone S, Kikuchi T, Ariga T, Taguchi F. Protective effects of murine recombinant interferon b administered by intravenous, intramuscular or subcutaneous route on mouse hepatitis virus infection. *Antiviral Res* 2000; **47**: 131-137
- 21 **Scagnolari C,** Bellomi F, Turriziani O, Bagnato F, Tomassini V, Lavalpe V, Ruggieri M, Bruschi F, Meucci G, Dicuonzo G, Antonelli G. Neutralizing and binding antibodies to IFN-beta: relative frequency in relapsing-remitting multiple sclerosis patients treated with different IFN β preparations. *J Interferon Cytokine Res* 2002; **22**: 207-213

- 22 **Shiratori Y**, Perelson AS, Weinberger L, Imazeki F, Yokosuka O, Nakata R, Ihori M, Hirota K, Ono N, Motojima T, Nishigaki M, Omata M. Different turnover rate of hepatitis C virus clearance by different treatment regimens using interferon-beta. *J Hepatol* 2000; **33**: 313-322
- 23 **Suzuki F**, Chayama K, Tsubota A, Akuta N, Someya T, Kobayashi M, Suzuki Y, Saitoh S, Arase Y, Ikeda K, Kumada H. Twice-daily administration of interferon-beta for chronic hepatitis C is not superior to a once-daily regimen. *J Gastroenterol* 2001; **36**: 242-247
- 24 **Fesce E**, Airolidi A, Mondazzi L, Maggi G, Gubertini G, Bernasconi G, Del Poggio P, Bozzetti F, Ideo G. Intramuscular beta interferon for chronic hepatitis C: is it worth trying? *Ital J Gastroenterol Hepatol* 1998; **30**: 185-188
- 25 **Habersetzer F**, Boyer N, Marcellin P, Bailly F, Ahmed SN, Alam J, Benhamou JP, Trepo C. A pilot study of recombinant interferon beta-1a for the treatment of chronic hepatitis C. *Liver* 2000; **20**: 437-441
- 26 **Dusheiko G**. Side effects of alpha interferon in chronic hepatitis C. *Hepatology* 1997; **26**: 112S-121S
- 27 **Fried MW**. Side effects of therapy of hepatitis C and their management. *Hepatology* 2002; **36**: 237S-244S
- 28 **Kiyosawa K**, Sodeyama T, Nakano Y, Yoda H, Tanaka E, Hayata T, Tsuchiya K, Yousuf M, Furuta S. Treatment of chronic non-A non-B hepatitis with human interferon beta: a preliminary study. *Antiviral Res* 1989; **12**: 151-161
- 29 **Villa E**, Trande P, Grottola A, Buttafoco P, Rebecchi AM, Stroffolini T, Callea F, Merighi A, Camellini L, Zoboli P, Cosenza R, Miglioli L, Loria P, Iori R, Carulli N, Manenti F. Alpha but not beta interferon is useful in chronic active hepatitis due to hepatitis C virus. A prospective, double-blind, randomized study. *Dig Dis Sci* 1996; **41**: 1241-1247
- 30 **Barbaro G**, Di Lorenzo G, Soldini M, Giancaspro G, Pellicelli A, Grisorio B, Barbarini G. Intravenous recombinant interferon-beta versus interferon-alpha-2b and ribavirin in combination for short-term treatment of chronic hepatitis C patients not responding to interferon-alpha. *Scand J Gastroenterol* 1999; **34**: 928-933
- 31 **Shiratori Y**, Nakata R, Shimizu N, Katada H, Hisamitsu S, Yasuda E, Matsumura M, Narita T, Kawada K, Omata M. High viral eradication with a daily 12-week natural interferon β treatment regimen in chronic hepatitis C patients with low viral load. *Dig Dis Sci* 2000; **45**: 2414-2421
- 32 **Chemello L**, Silvestri E, Cavalletto L, Bernardinello E, Pontisso P, Belassi F, Alberti A. Pilot study on the efficacy of intravenous natural b interferon therapy in Italian patients with chronic hepatitis C and relation to the HCV genotype. *Int Hepat Comm* 1995; **3**: 237-243
- 33 **Castro A**, Suarez D, Inglada L, Carballo E, Dominguez A, Diago M, Such J, Del Olmo JA, Perez-Mota A, Pedreira J, Quiroga JA, Carreno V. Multicenter randomized, controlled study of intramuscular administration of interferon β for the treatment of chronic hepatitis C. *J Interferon Cytokine Res* 1997; **17**: 27-30
- 34 **Castro A**, Carballo E, Dominguez A, Diago M, Suarez D, Quiroga JA, Carreno V. Tolerance and efficacy of subcutaneous interferon β administered for treatment of chronic hepatitis C. *J Interferon Cytokine Res* 1997; **17**: 65-67
- 35 **Mazzoran L**, Grassi G, Giacca M, Gerini U, Baracetti S, Fannicanelles M, Zorat F, Pozzato G. Pilot study on the safety and efficacy of intravenous natural beta-interferon therapy in patients with chronic hepatitis C unresponsive to alpha-interferon. *Ital J Gastroenterol Hepatol* 1997; **29**: 338-342
- 36 **Montalto G**, Tripi S, Cartabellotta A, Fulco M, Soresi M, Di Gaetano G, Carroccio A, Levvero M. Intravenous natural β interferon in white patients with chronic hepatitis C who are nonresponders to a interferon. *Am J Gastroenterol* 1998; **93**: 950-953
- 37 **Pellicano R**, Palmas F, Cariti G, Tappero G, Boero M, Tabone M, Suriani R, Pontisso P, Pitaro M, Rizzetto M. Re-treatment with interferon-beta of patients with chronic hepatitis C virus infection. *Eur J Gastroenterol Hepatol* 2002; **14**: 1377-1382
- 38 **Frosi A**, Sgorbati C, Bosio Bestetti M, Lodeville D, Vezzoli S, Vezzoli F. Interferon a and b in chronic hepatitis C: efficacy and tolerability. *Clin Drug Invest* 1995; **9**: 226-231
- 39 **Perez R**, Pravia R, Artimez ML, Giganto F, Rodriguez M, Lombrana JL, Rodrigo L. Clinical efficacy of intramuscular human interferon b vs interferon-a2 for the treatment of chronic hepatitis C. *J Viral Hepatitis* 1995; **2**: 103-106
- 40 **Cecere A**, Romano C, Caiazzo R, Lucariello A, Tancredi L, Gattoni A. Lymphoblastoid a interferon, leukocytic α -IFN and natural β -IFN in the treatment of chronic hepatitis C: a clinical comparison of 150 cases. *Hepato Res* 1999; **15**: 225-237
- 41 **Furusyo N**, Hayashi J, Ohmiya M, Sawayama Y, Kawakami Y, Ariyama I, Kinukawa N, Kashiwagi S. Differences between interferon-a and -b treatment for patients with chronic hepatitis C virus infection. *Dig Dis Sci* 1999; **44**: 608-617
- 42 **Asahina Y**, Izumi N, Uchihara M, Noguchi O, Tsuchiya K, Hamano K, Kanazawa N, Itakura J, Miyake S, Sakai T. A potent antiviral effect on hepatitis C viral dynamics in serum and peripheral blood mononuclear cells during combination therapy with high-dose daily interferon alfa plus ribavirin and intravenous twice-daily treatment with interferon beta. *Hepatology* 2001; **34**: 377-384
- 43 **Kakumu S**, Yoshioka K, Wakita T, Ishikawa T, Takayanagi M, Higashi Y. A pilot study of ribavirin and interferon beta for the treatment of chronic hepatitis C. A pilot study of ribavirin and interferon beta for the treatment of chronic hepatitis C. *Gastroenterology* 1993; **105**: 507-512
- 44 **Rizzetto M**, Alberti A, Craxi A, Ideo G, Demelia L, Pitaro M, Picciotto A. for the IBIS Study Group. Open, multicenter, randomized, controlled trial to compare safety and efficacy of r-hIFN beta 1a alone or in combination with ribavirin in HCV naïve patients. *Dig Liver Dis* 2003; **35** (Suppl 1): A14
- 45 **Vezzoli M**, Girola S, Fossati G, Mazzucchelli I, Gritti D, Mazzone A. Beta-interferon therapy of chronic hepatitis HCV+, 1b genotype. *Recenti Prog Med* 1998; **89**: 235-240
- 46 **Bernardinello E**, Cavalletto L, Chemello L, Mezzocollini I, Donada C, Benvegno L, Merkel C, Gatta A, Alberti A. Long-term clinical outcome after β -interferon therapy in cirrhotic patients with chronic hepatitis C. *Hepatogastroenterol* 1999; **46**: 3216-3222
- 47 **Poynard T**, Regimbeau C, Myers RP, Thevenot T, Leroy V, Mathurin P, Opolon P, Zarski JP. Interferon for acute hepatitis C. *Cochrane Database Syst Rev* 2002; **1**: CD000369
- 48 **Omata M**, Uokosuka O, Takano S. Resolution of acute C hepatitis after therapy with natural beta interferon. *Lancet* 1991; **338**: 914-915
- 49 **Takano S**, Satomura Y, Omata M. Effects of interferon beta on non-A, non-B acute hepatitis: a prospective, randomized, controlled-dose study. *Gastroenterology* 1994; **107**: 805-811
- 50 **Oketani M**, Higashi T, Yamasaki N, Shinmyozu K, Osame M, Arima T. Complete response to twice-a-day interferon-beta with standard interferon-alpha therapy in acute hepatitis C after a needle-stick. *J Clin Gastroenterol* 1999; **28**: 49-51
- 51 **Fukutomi T**, Fukutomi M, Iwao M, Watanabe H, Tanabe Y, Hiroshige K, Kinukawa N, Nakamura M, Nawata H. Predictors of the efficacy of intravenous natural interferon-beta treatment in chronic hepatitis C. *Med Sci Monit* 2000; **6**: 692-698
- 52 **Fujiwara K**, Mochida S, Matsuo S. Randomized control trial of interferon-beta injections at 12-h intervals as a therapy for chronic hepatitis C. *Hepatology Res* 1998; **12**: 240-251
- 53 **Barbarini G**, Calderon W, Bottari G. Beta-interferon therapy of chronic C hepatitis in 85 patients: results after one year of treatment. *Med J Infect Paras Dis* 1994; **9**: 25-28
- 54 **Nakayama H**, Shiotani S, Akiyama S, Gotoh H, Tani M, Akine Y. Pharmacokinetic study of human beta-interferon in patients with end-stage renal failure. *Clin Nephrol* 2001; **56**: 382-386
- 55 **Anonymous**. EASL International Consensus Conference on Hepatitis C. *J Hepatol* 1999; **31** (Suppl 1): 1-264
- 56 **Anonymous**. National Institute of Health Consensus Development Conference: Management of Hepatitis C: 2002. *Hepatology* 2002; **36** (Suppl 1): S1-S252
- 57 **Kobayashi Y**, Watanabe S, Konishi M, Yokoi M, Kakehashi R, Kaito M, Kondo M, Hayashi Y, Jomori T, Suzuki S. Quantitation and typing of serum hepatitis C virus RNA in patients with chronic hepatitis C treated with interferon-beta. *Hepatology* 1993; **18**: 1319-1325

Differences in proximal (cardia) versus distal (antral) gastric carcinogenesis via retinoblastoma pathway

Christian Gulmann, Helen Hegarty, Antoinette Grace, Mary Leader, Stephen Patchett, Elaine Kay

Christian Gulmann, Helen Hegarty, Antoinette Grace, Mary Leader, Elaine Kay, Department of Pathology, Beaumont Hospital and Royal College of Surgeons in Ireland, Dublin, Ireland

Stephen Patchett, Department of Gastroenterology, Beaumont Hospital, Dublin, Ireland

Supported by The Research Committee of the Royal College of Surgeons in Ireland

Correspondence to: Christian Gulmann, Department of Pathology, Royal College of Surgeons in Ireland, Beaumont Hospital, Dublin 9, Ireland. cgulmann@rcsi.ie

Telephone: +353-1-809 3701 **Fax:** +353-1-809 3720

Received: 2003-08-11 **Accepted:** 2003-10-25

Abstract

AIM: Disruption of cell cycle regulation is a critical event in carcinogenesis, and alteration of the retinoblastoma (pRb) tumour suppressor pathway is frequent. The aim of this study was to compare alterations in this pathway in proximal and distal gastric carcinogenesis in an effort to explain the observed striking epidemiological differences.

METHODS: Immunohistochemistry was performed to investigate expression of p16 and pRb in the following groups of both proximal (cardia) and distal (antral) tissue samples: (a) biopsies showing normal mucosa, (b) biopsies showing intestinal metaplasia and, (c) gastric cancer resection specimens including uninvolved mucosa and tumour.

RESULTS: In the antrum there were highly significant trends for increased p16 expression with concomitant (and in the group of carcinomas inversely proportional) decreased pRb expression from normal mucosa to intestinal metaplasia to uninvolved mucosa (from cancer resections) to carcinoma. In the cardia, there were no differences in p16 expression between the various types of tissue samples whereas pRb expression was higher in normal mucosa compared with intestinal metaplasia and tissue from cancer resections.

CONCLUSION: Alterations in the pRb pathway appear to play a more significant role in distal gastric carcinogenesis. It may be an early event in the former location since the trend towards p16 overexpression with concomitant pRb underexpression was seen as early as between normal mucosa and intestinal metaplasia. Importantly, the marked differences in expression of pRb and p16 between the cardia and antrum strongly support the hypothesis that tumours of the two locations are genetically different which may account for some of the observed epidemiological differences.

Gulmann C, Hegarty H, Grace A, Leader M, Patchett S, Kay E. Differences in proximal (cardia) versus distal (antral) gastric carcinogenesis via retinoblastoma pathway. *World J Gastroenterol* 2004; 10(1): 17-21

<http://www.wjgnet.com/1007-9327/10/17.asp>

INTRODUCTION

In the last decades the pattern of incidence of gastric cancer in the Western world has changed. Distal (corpus and antrum) cancers have decreased slightly whereas proximal (cardia/gastro-oesophageal) cancers have increased more than any other cancer^[1,2]. The tumours are morphologically indistinguishable and intestinal metaplasia (IM) appears to be an important step in carcinogenesis in both sites^[3,4]. The observed epidemiological differences are likely to be due to differences in the genetic pathways of carcinogenesis. However, so far they are poorly evaluated^[4-6].

Abnormal regulation of the cell cycle is a feature of many neoplasms^[7]. Regulation of the G1/S checkpoint is critical and is controlled by the retinoblastoma protein (pRb). Phosphorylated pRb releases E2F transcription factors which activate genes involved in DNA synthesis and cause G1/S transition. Phosphorylation of pRb is stimulated by the cyclin dependent kinase (CDK) 4-cyclin D complex. p16 specifically binds CDK4 which displaces it from cyclin D and thus acts to maintain pRb in an underphosphorylated state which causes G1 arrest^[8]. Disruption of this so-called 'Rb pathway' is a critical event in many tumours. It is resulted from primary inactivation of Rb function, by overexpression of CDKs, or through loss of p16^[7] which has a similar effect of G1/S progression. Several studies have shown a reciprocal expression of p16 and pRb^[9,10]. The role of the pRb pathway in gastric carcinogenesis is the subject of many papers. In distal gastric cancers it may be that disruption of p16 is an early event^[11] and a recent immunohistochemical study^[12] has shown a progressive decrease in expression from gastritis to atrophy and dysplasia. Less information is available on the role of pRb expression.

The aim of the present study was to compare the role of the pRb pathway in proximal and distal gastric cancers. p16 and pRb immunoexpression was investigated in the following groups of both proximal (cardia) and distal (antral) tissue samples: (a) biopsies showing normal mucosa, (b) biopsies showing intestinal metaplasia and, (c) gastric cancer resection specimens including uninvolved mucosa and tumour.

MATERIALS AND METHODS

Patient and specimen data

Six groups were included in this cross sectional study on archival, paraffin embedded tissues. The material was retrieved from the files in Beaumont Hospital, Dublin, Ireland and the local ethics committee approved the study. Tissue samples from the gastric cardia included endoscopic biopsies showing histologically normal mucosa ($n=56$) or IM ($n=49$) and material from gastric cancer resection specimens ($n=39$). Non-involved mucosa as well as tumour were investigated in the latter specimens. Tissue samples from the gastric antrum included the same groups: Normal ($n=52$), IM ($n=50$) as well as non-involved mucosa and tumour from cancer resections ($n=78$). All patients were Caucasians. Clinical details are shown in Table 1.

Endoscopic biopsy material was obtained from patients who had presented to the endoscopy service with a variety of upper gastrointestinal symptoms. Biopsies of the cardia were

Table 1 Clinical data

	Proximal			Distal		
	Biopsies normal	Biopsies IM	Cancer resections	Biopsies normal	Biopsies IM	Cancer resections
Number of subjects	56	49	39	52	50	78
Gender[F/M]	28/28	22/27	13/26	30/22	29/21	34/44
Age, years	50 (16)	58 (16) _A	67 (11) _B	52 (18)	59 (14) _C	69 (10) _D
Mean and (SD)						
Tumour type			30 Intestinal 9 Diffuse			42 Intestinal 36 Diffuse
TNM-stage, mean and (SD)			T 3.1 (0.6) N 1.0 (0.8)			T 3.0 (1.1) N 1.0 (0.8)

There was a significant stepwise increase in patient age between patients with biopsies showing normal mucosa to patients with biopsies showing IM to patients with gastric cancer resections in both proximal and distal locations. A-D, $P < 0.0001$. SD=Standard deviation.

only included when clearly labelled as such on the original request form without any endoscopic suspicion of Barrett's oesophagus or any prior or subsequent oesophageal biopsies showing Barrett's metaplasia. The distinction between proximal and distal gastric cancers was made on the basis of the clinical data as well as macroscopic description of the resection specimens on the pathology report. A case was labelled as proximal gastric cancer if it straddled the gastro-oesophageal junction with approximately equal amounts in the oesophagus and stomach and no histological evidence of Barrett's mucosa in the oesophagus. Distal gastric cancers were labelled as such when the tumour was clinically, macroscopically and histologically (i.e. at no point adjacent to squamous mucosa) confined to the more distal stomach. Tumours were classified according to the Lauren classification^[13] as diffuse or intestinal.

Methods

Initially, 4 μ m sections were cut from all blocks and stained with haematoxylin and eosin. Tissue microarrays (TMAs) were constructed^[14]. The technique involves taking cylindrical core biopsies from 'donor' blocks with subsequent precise arraying into a new 'recipient' paraffin block using a precision instrument (Beecher Instruments, Silver Spring, MD, USA)^[14,15]. Two different types of TMAs were constructed. Endoscopic biopsy fragments from wax blocks were arrayed using 2 mm punches. This size punch covers most endoscopic fragments in toto and all individual fragments from a donor wax block were sampled in separate cores (in this study 1-8 cores per donor block). Therefore, all the tissue from an original donor block containing endoscopic biopsy material was arrayed into the TMA block. Each 'biopsy-TMA' could hold up to 40 2 mm cores (i.e. up to 40 donor blocks depending on numbers of tissue fragments per original donor block). In the cancer resection specimens a different type of TMA was constructed due to the large size of tissue pieces in each block. The whole-section glass-slides were evaluated and areas of tumour as well as uninvolved mucosa were marked on the glass slides and identified in the corresponding wax blocks. Four 0.6 mm core biopsies were taken from each area. In 31 cases tumour and uninvolved mucosa were not present in the same wax block and two separate blocks were used. In this fashion, a total of 8 cores were taken per case (4 from tumour and 4 from uninvolved mucosa) with 35-40 cases (a total of 280-320 cores) fitted on to each TMA-block. Using TMAs the total number of TMA-blocks constructed was twenty-one.

Immunohistochemistry

Monoclonal mouse antibodies directed against p16 (1:100. Clone G175-405, PharMingen, USA) and pRb (1:300. Clone M7131, DAKO, Denmark) were used. Immunostaining was

performed using standard procedures. Heat mediated antigen retrieval using a pressure cooker was required to unmask the antigen sites. Antibody binding was detected using the Vectastain universal elite ABC-peroxidase kit (Vector Laboratories Inc., Burlingame, CA, USA). The positive p16 control was a case of severe uterine cervical dysplasia which strongly expressed p16 in dysplastic foci. The positive control for pRb was a multi-tissue block including tonsil.

Immunohistochemical interpretation

p16 Positive staining was defined as nuclear staining whereas cytoplasmic staining was considered non-specific and ignored. Extent was scored semi-quantitatively as negative (0) if <5% of cells stained, 1 if 5-25% of cells stained, 2 if 26-50% of cells stained and 3 if >50% cells stained. In cancer resections the average score was calculated from each of the four 0.6 mm TMA cores of either carcinoma or non-involved mucosa. The average score of each of the four decided the overall positivity/negativity.

pRb Nuclear staining was considered positive. Extent was scored semi-quantitatively as negative (0) if <5% of cells stained, 1 if 5-25% of cells stained, 2 if 26-50% of cells stained and 3 if >50% cells stained. In cancer resections the average score was calculated from each of the four 0.6 mm TMA cores of either carcinoma or non-involved mucosa. The average score of each of the four decided the overall positivity/negativity.

Statistical analysis

Statistical significance was defined as $P < 0.05$. Chi-square test was used for comparison between groups. Logistic regression analysis on the actual numbers of positive cases was used to test trends between tissue types within the proximal and distal groups.

RESULTS

Comparisons of p16 expression between different histological subsets within proximal and distal locations

In mucosa from biopsies (i.e. not associated with carcinoma) with and without intestinal metaplasia there was a low level of expression in both proximal and distal locations, mainly within the neck regions of the glands and absent in superficial epithelium. In distal tissue samples there was a statistically significant stepwise increase from normal mucosa to intestinal metaplasia to non-involved mucosa from cancer resections to carcinoma ($P < 0.0001$, Table 2). In proximal tissue samples no such trend was noted and there were no differences between the different tissue samples (Figure 4). No differences in p16 expression were noted between tumour types in either of the two locations and there were no correlations between p16 expression and stage of tumour or any clinical parameters.



Figure 1 Antral biopsy showing focal intestinal metaplasia. This composite figure shows the H&E appearance, negative p16 staining (with some positive inflammatory cells in the background) and positive pRb staining limited to the neck region of the glands. Original magnification 200 \times .

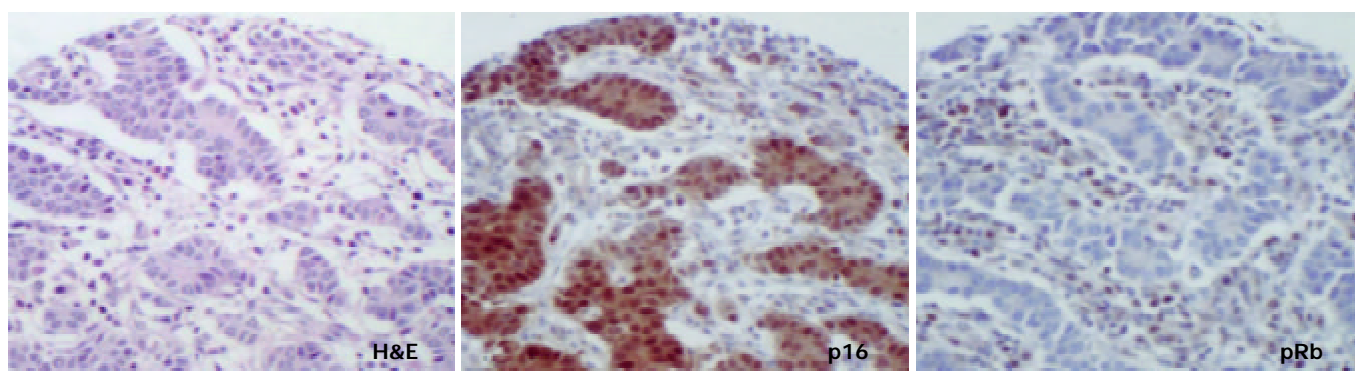


Figure 2 Gastric antral carcinoma of intestinal type. The same 0.6 mm TMA core is shown stained with H&E, p16 and pRb. The latter is negative whereas p16 shows strong nuclear and cytoplasmic staining. The cytoplasmic staining was ignored for the scoring. Original magnification 200 \times .

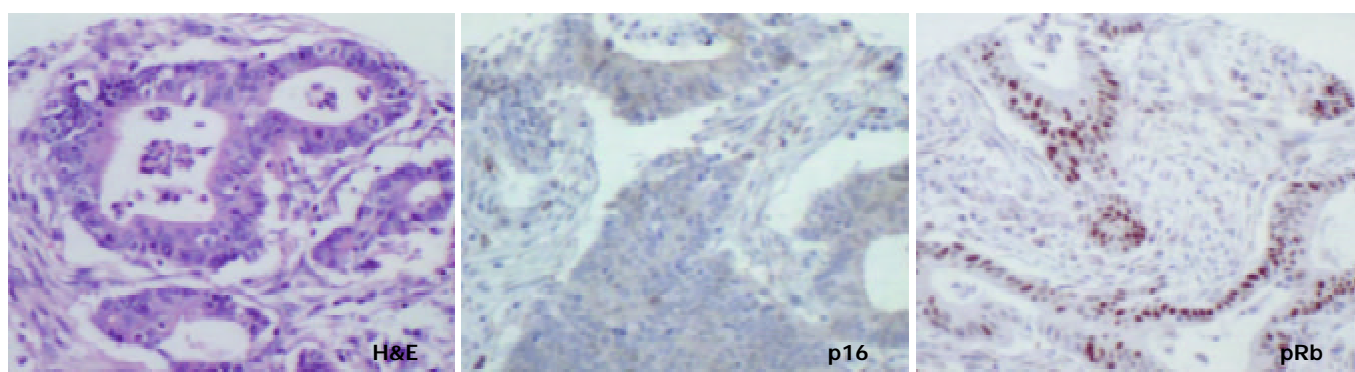


Figure 3 Gastric antral carcinoma of intestinal type. The same 0.6 mm TMA core is shown stained with H&E, p16 and pRb. The latter shows strong and crisp nuclear staining whereas p16 is negative. Original magnification 200 \times .

Table 2 Percentage of cases staining for and extent scores of p16 and pRb

	Proximal				Distal			
	Biopsies normal	Biopsies IM	Resections UM	Resections cancer	Biopsies normal	Biopsies IM	Resections UM	Resections cancer
Number and (%) of cases positive for p16	12 (21%)	13 (27%)	8 (21%)	13 (33%)	4 (8%)	13 (26%)	37 (47%)	42 (54%)
Mean (and SD) of extent scores for p16	0.21 (0.41)	0.27 (0.45)	0.23 (0.48)	0.41 (0.68)	0.077 (0.27)	0.26 (0.44)	0.49 (0.53)	0.69 (0.79)
Number and (%) of cases positive for pRb	52 (93%)	37 (76%)	31 (80%)	30 (77%)	46 (88%)	35 (70%)	51 (65%)	38 (49%)
Mean (and SD) of extent scores for pRb	0.41 (0.5)	0.34 (0.48)	0.33 (0.48)	0.5 (0.51)	0.42 (0.5)	0.24 (0.43)	0.17 (0.38)	0.28 (0.45)

SD: Standard deviation. UM: Uninvolved mucosa from cancer resections.

Comparisons of pRb expression between different histological subsets within proximal and distal locations

pRb was highly expressed in normal epithelium and intestinal metaplasia, mainly in the more proliferative areas, i.e. the neck region within the glandular epithelium. In both proximal and distal stomach there was a statistically significant trend for decreased pRb expression from normal mucosa to intestinal metaplasia to non-involved mucosa from cancer resections to carcinoma. It was more pronounced in the distal tissue samples ($P < 0.0001$) than in the proximal tissue samples ($P = 0.035$) and in the latter location it was mainly a function of the high expression in normal mucosa compared with the other histological subsets which showed very similar expression rates (Figure 5). No differences in pRb expression were noted between tumour types in the two locations and there were no correlations between pRb expression and stage of tumour or any clinical parameters.

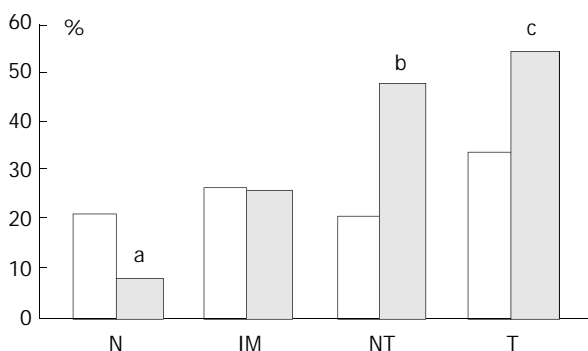


Figure 4 Graph showing percentage of p16 positive cases as pairs of proximal (empty columns, left hand sides) and distal (black columns, right hand sides) tissue samples. N: Biopsies showing normal mucosa, IM: Biopsies showing intestinal metaplasia, NT: Non-involved mucosa from gastric cancer resection specimens, T: Tumour from gastric cancer resection specimens. There was a significant stepwise increase in expression from normal mucosa → intestinal metaplasia → non-involved mucosa from cancer resections → carcinoma in the distal stomach only. ^aThere was a significantly lower p16 expression in distal normal mucosa than in proximal normal mucosa, $P = 0.0045$. ^b and ^c: There was a significantly higher p16 expression in both non-involved as well as carcinoma from cancer resections from distal compared with proximal stomach, ^b $P = 0.0048$ and ^c $P = 0.036$.

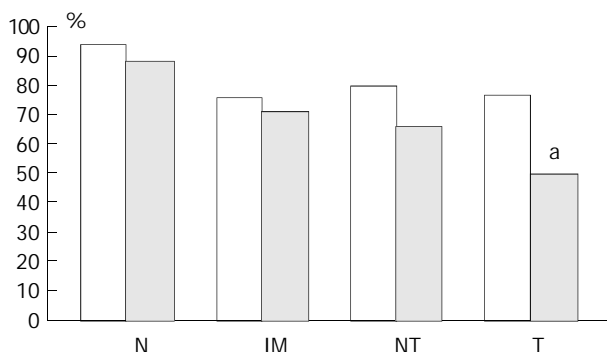


Figure 5 Graph showing percentage of pRb positive cases as pairs of proximal (empty columns, left hand side) and distal (black columns, right hand side) tissue samples. N: Biopsies showing normal mucosa, IM: Biopsies showing intestinal metaplasia, NT: Non-involved mucosa from gastric cancer resection specimens, T: Tumour from gastric cancer resection specimens. There was a significant stepwise decrease in expression from normal mucosa → intestinal metaplasia → non-involved mucosa from cancer resections → carcinoma in both the

distal and proximal stomach although in the latter location it was most likely due to the high expression in normal mucosa compared with the other types of tissues. ^aThere was a significantly lower pRb expression in distal than in proximal carcinomas, $P = 0.0047$.

Comparison of p16 and pRb expressions between similar histological subsets in proximal versus distal location

In cancer resection specimens there was a significantly lower expression of p16 in proximal than distal location, both in uninvolved mucosa ($P = 0.0048$) and carcinoma ($P = 0.0036$) whereas the opposite was seen in normal mucosa ($P = 0.0045$) (Figure 4). pRb expression was significantly higher in proximal carcinomas ($P = 0.0047$) (Figure 5).

Correlations between pRb and p16

In distal carcinomas there was a significantly negative association between expressions of the two molecules ($P = 0.043$) (Table 3).

Table 3 p16 versus pRb staining in distal gastric carcinomas

		pRb	
		+	-
p16	+	16	26
	-	22	14

This distribution was significant, $P = 0.043$.

DISCUSSION

Disruption of cell cycle regulation is a critical event in carcinogenesis. Alteration of the retinoblastoma (pRb) tumour suppressor pathway, which controls the G1/S checkpoint, is a common event in many neoplasms and typically implicates abnormal expression of both pRb and p16 although other molecules may be involved.

The current study aimed to compare alterations in this pathway in proximal and distal gastric carcinogenesis in an effort to explain the observed epidemiological differences between the two sites. Immunohistochemistry was performed to investigate expression of p16 and pRb in various histological stages from normal mucosa to carcinoma in both proximal (cardia) and distal (antral) tissue samples.

The results of this study showed highly significant trends for increase in p16 expression with a concomitant decrease in pRb expression in distal tissue samples from normal mucosa to intestinal metaplasia to uninvolved mucosa from cancer resections to carcinoma. This suggests that the pRb pathway plays a definite role in distal gastric carcinogenesis. It may be an early event since the trend towards p16 overexpression and pRb underexpression was seen even between normal mucosa and intestinal metaplasia. In the proximal stomach no differences in p16 expression were seen between the various stages whereas pRb expression decreased slightly from normal mucosa to carcinoma. This seemed to be mainly an effect of a higher expression of pRb in normal mucosa compared with any of the other tissue samples. Furthermore, the trend for decreasing pRb was not matched by an increase in p16 expression and there was no inverse relationship between the two molecules in the group of carcinomas. Taken together this argues against the pRb pathway as important in proximal gastric carcinogenesis.

Other studies on (distal) gastric carcinogenesis have shown a similar p16 'overexpression' in gastric carcinomas^[16,17] with weak staining in non-involved mucosa. However, a recent immunohistochemical study found a progressive p16 decrease and a pRb increase from gastritis to dysplasia^[12] in samples from the cardia. This is surprising in view of the *opposite* trend

in distal gastric samples seen here and also by others^[17]. The reason for this discrepancy is uncertain. In the above-mentioned study patients were from an area in China with a high incidence of gastric carcinoma and compared with the current study, different entities (chronic gastritis, dysplasia) were investigated. Also, racial differences may play a role since all the patients in this study were Caucasians.

A study on p16 expression in normal tissues^[18] showed some staining in gastric antral glands. The following scenario is therefore likely: p16 is expressed with a low frequency in the normal state, which may be related to a relatively low proliferative status. In support of this is the limited expression in glandular (proliferative area) rather than surface epithelium (quiescent area) seen here and also noted by others^[17,18]. In tumours there may be loss of negative feedback through decrease in pRb expression which causes p16 overexpression and other studies have also shown an inverse relationship between expression of the two molecules^[9,10]. The current study showed mainly cases of distal gastric cancer resections with gain of p16 expression in cancers compared with non-involved mucosa. However, loss of p16 expression in cancers compared with uninvolved mucosa was also seen in some cases and it is entirely possible that, whereas most cancers lose pRb function/expression, some preferentially lose p16 expression.

This study did not entirely rule out a role for the pRb pathway in proximal gastric carcinogenesis since other molecules participate in this complex cell cycle control mechanism. It is unlikely, however, since altered expression of p16 and pRb would be expected if abnormal feedback from other molecules in this pathway existed.

In conclusion this study strongly suggests that alterations in the pRb pathway are significant in distal, but not proximal, gastric carcinogenesis. In the former location it may be an early event. Importantly, this study therefore supports the hypothesis that tumours of the two locations are genetically different which may account for some of the observed epidemiological differences.

ACKNOWLEDGEMENTS

Mr. Ronan Conroy is thanked for his help with the statistical analysis.

REFERENCES

- 1 **Blot WJ**, Devesa SS, Kneller RW, Fraumeni JF Jr. Rising incidence of adenocarcinoma of the esophagus and gastric cardia. *JAMA* 1991; **265**: 1287-1289
- 2 **Devesa SS**, Blot WJ, Fraumeni JF Jr. Changing patterns in the incidence of esophageal and gastric carcinoma in the United States. *Cancer* 1998; **83**: 2049-2053

- 3 **Jass JR**. Role of intestinal metaplasia in the histogenesis of gastric carcinoma. *J Clin Pathol* 1980; **33**: 801-810
- 4 **Ruol A**, Parenti A, Zaninotto G, Merigliano S, Costantini M, Cagol M, Alfieri R, Bonavina L, Peracchia A, Ancona E. Intestinal metaplasia is the probable common precursor of adenocarcinoma in Barrett esophagus and adenocarcinoma of the gastric cardia. *Cancer* 2000; **88**: 2520-2528
- 5 **Morales TG**, Camargo E, Bhattacharyya A, Sampliner RE. Long-term follow-up of intestinal metaplasia of the gastric cardia. *Am J Gastroenterol* 2000; **95**: 1677-1680
- 6 **Sipponen P**. Intestinal metaplasia and gastric carcinoma. *Ann Clin Res* 1981; **13**: 139-143
- 7 **Sherr CJ**. The Pezcoller lecture: cancer cell cycles revisited. *Cancer Res* 2000; **60**: 3689-3695
- 8 **Liggett WH Jr**, Sidransky D. Role of the p16 tumor suppressor gene in cancer. *J Clin Oncol* 1998; **16**: 1197-1206
- 9 **Yang G**, Zhang Z, Liao J, Seril D, Wang L, Goldstein S, Yang CS. Immunohistochemical studies on Waf1p21, p16, pRb and p53 in human esophageal carcinomas and neighboring epithelia from a high-risk area in northern China. *Int J Cancer* 1997; **72**: 746-751
- 10 **Lee WA**, Woo DK, Kim YI, Kim WH. p53, p16 and Rb expression in adenocarcinoma and squamous cell carcinomas of the stomach. *Pathol Res Pract* 1999; **195**: 747-752
- 11 **Jang TJ**, Kim DI, Shin YM, Chang HK, Yang CH. p16(INK4a) Promoter hypermethylation of non-tumorous tissue adjacent to gastric cancer is correlated with glandular atrophy and chronic inflammation. *Int J Cancer* 2001; **93**: 629-634
- 12 **Zhou Y**, Gao SS, Li YX, Fan ZM, Zhao X, Qi YJ, Wei JP, Zou JX, Liu G, Jiao LH, Bai YM, Wang LD. Tumor suppressor gene p16 and Rb expression in gastric cardia precancerous lesions from subjects at a high incidence area in northern China. *World J Gastroenterol* 2002; **8**: 423-425
- 13 **Lauren P**. The two histologic main types of gastric carcinoma: diffuse and so-called intestinal-type carcinoma. *APMIS* 1965; **64**: 31-49
- 14 **Kononen J**, Bubendorf L, Kallioniemi A, Barlund M, Schraml P, Leighton S, Torhorst J, Mihatsch MJ, Sauter G, Kallioniemi OP. Tissue microarrays for high-throughput molecular profiling of tumor specimens. *Nat Med* 1998; **4**: 844-847
- 15 **Moch H**, Kononen T, Kallioniemi OP, Sauter G. Tissue microarrays: what will they bring to molecular and anatomic pathology? *Adv Anat Pathol* 2001; **8**: 14-20
- 16 **Rocco A**, Schandl L, Nardone G, Tulassay Z, Staibano S, Malfertheiner P, Ebert MP. Loss of expression of tumor suppressor p16(INK4) protein in human primary gastric cancer is related to the grade of differentiation. *Dig Dis* 2002; **20**: 102-105
- 17 **Tsujie M**, Yamamoto H, Tomita N, Sugita Y, Ohue M, Sakita I, Tamaki Y, Sekimoto M, Doki Y, Inoue M, Matsuura N, Monden T, Shiozaki H, Monden M. Expression of tumor suppressor gene p16(INK4) products in primary gastric cancer. *Oncology* 2000; **58**: 126-136
- 18 **Nielsen GP**, Stemmer-Rachamimov AO, Shaw J, Roy JE, Koh J, Louis DN. Immunohistochemical survey of p16INK4A expression in normal human adult and infant tissues. *Lab Invest* 1999; **79**: 1137-1143

Edited by Wang XL

Effect of NF- κ B, survivin, Bcl-2 and Caspase3 on apoptosis of gastric cancer cells induced by tumor necrosis factor related apoptosis inducing ligand

Liu-Qin Yang, Dian-Chun Fang, Rong-Quan Wang, Shi-Ming Yang

Liu-Qin Yang, Dian-Chun Fang, Rong-Quan Wang, Shi-Ming Yang, Department of Gastroenterology, Southwest Hospital, Third Military Medical University, Chongqing 400038, China

Supported by the Scientific Research Foundation of Chinese PLA, during the 10th-Five-Year Plan Period, No. 01MA172

Correspondence to: Dian-Chun Fang, M.D., Ph.D. Southwest Hospital, Third Military Medical University, Chongqing 400038, China. fangdianchun@hotmail.com

Telephone: +86-23-68754624 or +86-23-68754124

Fax: +86-23-68754124

Received: 2003-05-11 **Accepted:** 2003-08-16

Abstract

AIM: To study the effect of NF- κ B, survivin, Bcl-2 and Caspase3 on tumor necrosis factors related apoptosis inducing ligand (TRAIL) induced apoptosis of gastric cancer cells.

METHODS: Gastric cancer cells of SGC-7901, MKN28, MKN45 and AGS lines were cultured in PRMI-1640 medium and the apoptosis rates of the cells of 4 lines were observed after treatment of tumor necrosis factors related apoptosis inducing ligand (TRAIL) with a flow cytometer. The expression of NF- κ B, survivin, Bcl-2 and Caspase3 in gastric cancer cells of 4 lines was analyzed with Western blot.

RESULTS: After the gastric cancer cells were exposed to TRAIL 300 ng/ml for 24 hours, the apoptosis rate was 36.05%, 20.27%, 16.50% and 11.80% in MKN28, MKN45, AGS and SGC-7901 cells respectively. Western blot revealed that the expressions of NF- κ B and survivin were lower in MKN28 cells than in MKN45, AGS and SGC-7901 cells. In contrast, the expression of Caspase3 was higher in MKN28 cells than in MKN45, AGS and SGC-7901 cells.

CONCLUSION: There is a selectivity of TRAIL potency to induce apoptosis in gastric cancer cells of different cell lines. The anticancer potency of TRAIL is associated with the decreased expression of NF- κ B and survivin and increased expression of Caspase3 of gastric cancer cells.

Yang LQ, Fang DC, Wang RQ, Yang SM. Effect of NF- κ B, survivin, Bcl-2 and Caspase3 on apoptosis of gastric cancer cells induced by tumor necrosis factor related apoptosis inducing ligand. *World J Gastroenterol* 2004; 10(1): 22-25

<http://www.wjgnet.com/1007-9327/10/22.asp>

INTRODUCTION

Tumor necrosis factors related apoptosis inducing ligand (TRAIL) is one of the members of TNF family. TRAIL, also known as APO-2L^[1,2], is highly homologous to FasL. TRAIL is capable of inducing apoptosis of many kinds of cancer cells but nontoxic to normal cells^[3-13]. It has been found that cells of different cancers and even different types of cells of a cancer

exhibit significantly different sensitivity to TRAIL^[14-17].

Nuclear transcript factor (NF- κ B), survivin and Bcl-2 are apoptosis inhibitors and play a key role in the mechanism of anti-apoptosis of tumors^[18-29]. If the activity of these factors is suppressed, tumor cells can undergo apoptosis and stop growing^[30,31]. Various modulation elements of cell apoptosis exert their action through Caspase enzyme system. Among them, Caspase 3 (also known as CPP32, YAMA, or apopain) is probably the one that so far best correlates with apoptosis^[32,33]. Furthermore, Caspase 3 expression could be detected in several human malignancies such as non-small cell lung carcinoma^[34], esophageal squamous cell carcinoma^[35] and gastric cancer^[36]. The inhibition of cell apoptosis is closely related to the onset, development and sensitivity to chemotherapy of malignant tumors. Consequently, we studied the relationship of the sensitivity of the cells of 4 gastric cancer cell lines to TRAIL with the expression of NF- κ B, survivin, Bcl-2 and Caspase3 in order to clarify why and how gastric cancer cells were resistant to TRAIL.

MATERIALS AND METHODS

SGC-7901 line of gastric cancer cells was preserved in our laboratory. MKN28, MKN45 and AGS cell lines were donated by our colleagues of the Fourth Military Medical University. NC membrane and mouse antihuman survivin monoclonal antibody were bought from Santa Cruz Biotech Company. Mouse antihuman NF- κ B (p65) monoclonal antibody, mouse antihuman Bcl-2 monoclonal antibody, mouse antihuman Caspase3 monoclonal antibody and peroxidase-conjugated rabbit anti-mouse IgG were from the Zhongshan Company in Beijing, and ECL chemofluorescent agent kit was from DingguoBiotech Center in Beijing. TRAIL protein was prepared by ourselves^[37].

Gastric cancer cells of SGC-7901, MKN28, MKN45 and AGS lines were incubated in PRMI-1640 medium and 10% inactivated calf serum. Penicillin and streptomycin were added to a final concentration of 100 u/ml. Generation transition of the cells was achieved every 3 to 5 days through the adoption of 0.25% pancreatic enzyme and 0.02% EDTA.

Gastric cancer cells in the logarithmic proliferation stage were studied. The culture medium of every cell line was distributed into 5 bottles (100 ml in each). TRAIL was added to the 5 bottles of every cell line with a final concentration of 0 ng/ml, 50 ng/ml, 100 ng/ml, 200 ng/ml and 300 ng/ml respectively. All the bottles were incubated under 37 °C, 5%CO₂ and saturated humidity for 24 hours.

The apoptosis rate of gastric cancer cells was determined with a flow cytometer. All the cells were collected, digested and washed twice in PBS, and the floating cells were precipitated with 0.1 ml PBS. After the cells were fixed in 70% precooled ethanol for 24 hours, they were stained with PI and examined.

Western blot was used to determine the expression of NF- κ B, survivin, Bcl-2 and Caspase3. The gastric cancer cells were

ruptured with lysozyme and protein concentration of cells was measured with Lowry method. The protein concentration was unified with PBS. In order to denature the protein, the samples were heated with middle molecular weight protein Marker to 100 °C for 3 minutes. The protein, after being separated with SDS-PAGE electrophoresis, was transferred to a piece of nitrocellulose membrane with moisture transfer technique at 100v for 2 hours. The membrane was stained with ponceau-S to confirm whether the protein transfer was successful. Five percent of defat milk powder-PBS solution was used to block the unspecific antibody binding site for one hour. Then the membrane was washed 3 times in PBS-T solution, 15 minutes each time. Monoclonal antibody solution (1:1 000) of mouse antihuman NF- κ B, survivin, Bcl-2 and Caspase3 was incubated with the membrane for 1 hour respectively. Again, each piece of membrane was washed 3 times in PBS-T solution, 15 minutes each time. Then, all the membranes were incubated with rabbit antimouse IgG solution (1:1 000) for one hour. The membranes were washed 3 times in PBS-T solution, 15 minutes each time. Eventually, the membranes were incubated with chemofluorescent agent for 5 minutes, and then were exposed to X-ray films in a dark room. The X-ray films were developed and examined.

SPSS statistic soft package was used to undergo single factor Chi square analysis and *t* test. $P < 0.05$ was considered as significant.

RESULTS

TRAIL exerted a considerable apoptosis-inducing effect on the 4 line gastric cancer cells and the effect was in a dosage dependent manner. Figure 1 shows that the gastric cancer cells of the 4 lines had a different sensitivity to TRAIL. After the action of 300 ng/ml TRAIL for 24 hours, the apoptosis rate was 36.05% in MKN28, 20.27% in MKN45, 16.50% in AGS and 11.80% in SGC-7901 lines. The apoptosis rate was significantly higher in MKN28 than in other 3 kinds of cells ($P < 0.05$), but there was no significant difference among the other 3 lines of gastric cancer cells. SGC-7901 cells were resistant to TRAIL.

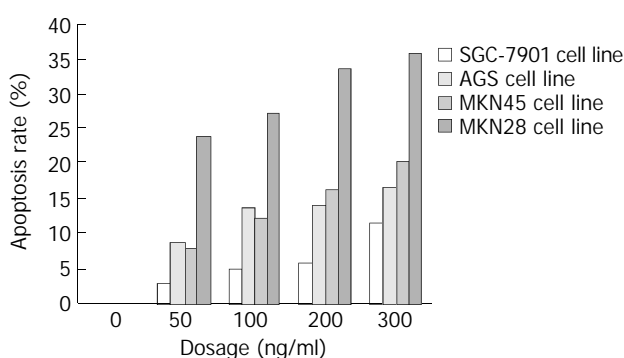


Figure 1 Changes of apoptosis rate in 4 gastric cancer cell lines after 24 hours action of different dosage of TRAIL.

The expression of NF- κ B (p65) in the 4 lines of gastric cancer cells is shown in Figure 2. NF- κ B expression was lower in MKN28 than in SGC-7901 cells, but no significant difference was found between MKN45 and AGS cells.

Before administration of TRAIL, Western blot revealed that the expression of survivin was significantly lower in MKN28 than in SGC-7901 cells, and no significant difference was found between MKN45 and AGS cells (Figure 3).

Before administration of TRAIL, Western blot revealed that the expression of Bcl-2 had no significant difference in the 4 line gastric cancer cells (Figure 4).

Before administration of TRAIL, Western blot showed that the expression of Caspase 3 was lower in SGC-7901 and highest in MKN28 cells. The expression in AGS and MKN45 cells was in the middle range (Figure 5).

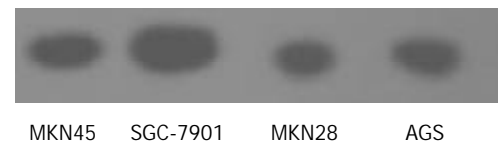


Figure 2 Expression of NF- κ B in 4 lines of gastric cancer cells.

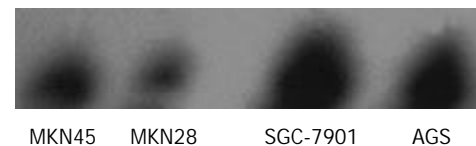


Figure 3 Expression of survivin in 4 lines of gastric cancer cells.

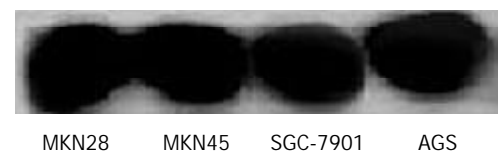


Figure 4 Expression of Bcl-2 in 4 lines of gastric cancer cells.

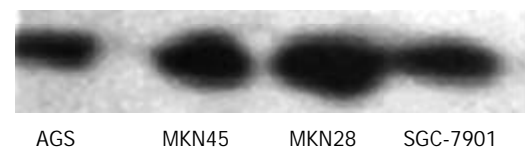


Figure 5 Expression of Caspase 3 in 4 lines of gastric cancer cells.

DISCUSSION

TRAIL is a recently discovered apoptosis inducing molecule. It has aroused great interest in the medical circle because it can selectively induce cancer cells, transform cells and virus-infected cells to undergo apoptosis with no toxicity to normal cells. In this study, anticancer effect of TRAIL on the 4 lines of gastric cancer cells was observed. We found that TRAIL exerted a certain degree of apoptosis inducing action on the gastric cancer cells and the action potency was dosage dependent. Twenty-four hours after administration of 300 ng/ml TRAIL, the apoptosis rate was 36.05% in MKN28, 20.27% in MKN45, 16.50% in AGS and 11.80% in SGC-7901 cells. This implies that the sensitivity to apoptosis inducing action of TRAIL varied among the 4 lines of gastric cancer cells.

Apoptosis is a cellular suicidal action. This process is under the combined modulation of apoptosis promoting factors including p53, Fas and others and apoptosis inhibiting factors including Bcl-2, CIAP, survivin and others. Survivin is an inhibitor of apoptosis protein (IAP), which has been found to be crucial for mitosis and cell cycle progression^[38]. Survivin could act directly on Caspases and mainly suppress the activity of Caspase 3 and Caspase 7^[39]. Disruption of survivin-microtubule interactions could result in loss of survivin's anti-apoptosis function and increase caspase-3 activity, a mechanism involved in cell death during mitosis^[40]. In addition, it has been found that deficiency of survivin in transgenic mice could exacerbate Fas-induced apoptosis via mitochondrial pathways^[41]. In the present study, we found that the difference of sensitivity to TRAIL among the 4 lines of gastric cancer

cells was related to the expression of survivin and Caspase of the cells. SGC-7901 cells with high expression of survivin and low expression of Caspase 3 were resistant to TRAIL, but MKN28 cells with low expression of survivin and high expression of Caspase 3 were sensitive to TRAIL. So, the determination of the expression level of survivin and Caspase 3 in gastric cancer cells is helpful to determine whether the cells are sensitive to TRAIL. To suppress the expression of survivin and increase the expression of Caspase 3 could strengthen the sensitivity of gastric cancer cells to TRAIL^[42].

The transcription factor NF- κ B is a key regulator of immune responses and inflammation operating through the induction of numerous genes, including those coding for cytokines, chemokines and adhesion molecules^[43-45]. NF- κ B suppresses apoptosis by inducing expression of a number of genes whose products inhibit apoptosis, including inhibitors of apoptosis (IAPs), Caspase 8-FADD-like IL-1 β -converting enzyme (Caspase 8-FLICE) inhibitory protein (cFLIP), A1 (also known as Bfl1), TNF receptor associated factor 1 (TRAF1) and TRAF2. These anti-apoptotic proteins have been found to work in a coordinated fashion to block apoptosis at multiple steps along the apoptotic cascade or to regulate other pro- or anti-apoptotic pathways^[46]. NF- κ B could also regulate the expression of several members of the Bcl-2 family^[47]. In this study, we found that the sensitivity of the 4 line gastric cancer cells to TRAIL was related to the expression of NF- κ B. SGC-7901 cells showed a relatively high expression of NF- κ B and were resistant to TRAIL. On the contrary, MKN28 cells with a low expression of NF- κ B were sensitive to TRAIL. It is considered that suppression of the expression of NF- κ B in gastric cancer cells can increase their sensitivity to TRAIL.

Bcl-2 is a proto-oncogene and can suppress apoptosis. Bcl-2 has been found to be closely related to the onset and drug resistance of many kinds of malignant tumors^[48-52]. Previous studies have confirmed that overexpression of Bcl-2 in the cells of various malignant tumors could result in resistance against cell apoptosis induced by chemotherapeutic agents such as cisplatin^[53,54] and arsenic trioxide^[55]. If Bcl-2 expression is suppressed, tumors are impelled to undergo apoptosis. We found that the sensitivity difference among the 4 lines of gastric cancer cells was not related with Bcl-2 expression, but the sensitivity difference to TRAIL did occur among them. This finding was in agreement with the recently published data on breast cancer^[56].

To sum up, TRAIL possesses the characteristics of selectively inducing apoptosis of tumor cells. TRAIL-resistant tumor cells may be related to the expression of apoptosis-inhibitor survivin and NF- κ B. Suppression of the expression of survivin and NF- κ B, and reinforcement of Caspase 3 expression would increase the sensitivity of gastric cancer cells to TRAIL. Further study is imperative to clarify the mechanism of the apoptosis-inducing action of TRAIL.

REFERENCES

- Pitti RM**, Marsters SA, Ruppert S, Donahue CJ, Moore A, Ashkenazi A. Induction of apoptosis by Apo-2 ligand, a new member of the tumor necrosis factor cytokine family. *J Biol Chem* 1996; **271**: 12687-12690
- LeBlanc HN**, Ashkenazi A. Apo2L/TRAIL and its death and decoy receptors. *Cell Death Differ* 2003; **10**: 66-75
- Walczak H**, Miller RE, Ariail K, Gliniak B, Griffith TS, Kubin M, Chin W, Jones J, Woodward A, Le T, Smith C, Smolak P, Goodwin RG, Rauch CT, Schuh JC, Lynch DH. Tumoricidal activity of tumor necrosis factor-related apoptosis-inducing ligand *in vivo*. *Nat Med* 1999; **5**: 157-163
- Silvestris F**, Cafforio P, Tucci M, Dammacco F. Negative regulation of erythroblast maturation by Fas-L(+)/TRAIL(+) highly malignant plasma cells: a major pathogenetic mechanism of anemia in multiple myeloma. *Blood* 2002; **99**: 1305-1313
- Odoux C**, Albers A, Amoscato AA, Lotze MT, Wong MK. TRAIL, FasL and a blocking anti-DR5 antibody augment paclitaxel-induced apoptosis in human non-small-cell lung cancer. *Int J Cancer* 2002; **97**: 458-465
- Seki N**, Hayakawa Y, Brooks AD, Wine J, Wiltout RH, Yagita H, Tanner JE, Smyth MJ, Sayers TJ. Tumor necrosis factor-related apoptosis-inducing ligand-mediated apoptosis is an important endogenous mechanism for resistance to liver metastases in murine renal cancer. *Cancer Res* 2003; **63**: 207-213
- Kim DM**, Koo SY, Jeon K, Kim MH, Lee J, Hong CY, Jeong S. Rapid induction of apoptosis by combination of flavopiridol and tumor necrosis factor (TNF)-alpha or TNF-related apoptosis-inducing ligand in human cancer cell lines. *Cancer Res* 2003; **63**: 621-626
- Smyth MJ**, Takeda K, Hayakawa Y, Peschon JJ, van den Brink MR, Yagita H. Nature's TRAIL-on a path to cancer immunotherapy. *Immunity* 2003; **18**: 1-6
- Guillemet J**, Saint-Laurent N, Rochaix P, Cuvillier O, Levade T, Schally AV, Pradayrol L, Buscail L, Susini C, Bousquet C. Somatostatin receptor subtype 2 sensitizes human pancreatic cancer cells to death ligand-induced apoptosis. *Proc Natl Acad Sci U S A* 2003; **100**: 155-160
- Naka T**, Sugamura K, Hylander BL, Widmer MB, Rustum YM, Repasky EA. Effects of tumor necrosis factor-related apoptosis-inducing ligand alone and in combination with chemotherapeutic agents on patients' colon tumors grown in SCID mice. *Cancer Res* 2002; **62**: 5800-5806
- Wajant H**, Pfizenmaier K, Scheurich P. TNF-related apoptosis inducing ligand (TRAIL) and its receptors in tumor surveillance and cancer therapy. *Apoptosis* 2002; **7**: 449-459
- Inoue H**, Shiraki K, Yamanaka T, Ohmori S, Sakai T, Deguchi M, Okano H, Murata K, Sugimoto K, Nakano T. Functional expression of tumor necrosis factor-related apoptosis-inducing ligand in human colonic adenocarcinoma cells. *Lab Invest* 2002; **82**: 1111-1119
- Wei XC**, Wang XJ, Chen K, Zhang L, Liang Y, Lin XL. Killing effect of TNF-related apoptosis inducing ligand regulated by tetracycline on gastric cancer cell line NCI-N87. *World J Gastroenterol* 2001; **7**: 559-562
- MacFarlane M**, Harper N, Snowden RT, Dyer MJ, Barnett GA, Pringle JH, Cohen GM. Mechanisms of resistance to TRAIL-induced apoptosis in primary B cell chronic lymphocytic leukaemia. *Oncogene* 2002; **21**: 6809-6818
- Held J**, Schulze-Osthoff K. Potential and caveats of TRAIL in cancer therapy. *Drug Resist Updat* 2001; **4**: 243-252
- de Almodovar CR**, Ruiz-Ruiz C, Munoz-Pinedo C, Robledo G, Lopez-Rivas A. The differential sensitivity of Bcl-2-overexpressing human breast tumor cells to TRAIL or doxorubicin-induced apoptosis is dependent on Bcl-2 protein levels. *Oncogene* 2001; **20**: 7128-7133
- Ibrahim SM**, Ringel J, Schmidt C, Ringel B, Muller P, Koczan D, Thiesen HJ, Lohr M. Pancreatic adenocarcinoma cell lines show variable susceptibility to TRAIL-mediated cell death. *Pancreas* 2001; **23**: 72-79
- Ohshima K**, Sugihara M, Haraoka S, Suzumiya J, Kanda M, Kawasaki C, Shimazaki K, Kikuchi M. Possible immortalization of Hodgkin and Reed-Sternberg cells: telomerase expression, lengthening of telomere, and inhibition of apoptosis by NF-kappaB expression. *Leuk Lymphoma* 2001; **41**: 367-376
- Wall NR**, O'Connor DS, Plescia J, Pommier Y, Altieri DC. Suppression of survivin phosphorylation on Thr34 by flavopiridol enhances tumor cell apoptosis. *Cancer Res* 2003; **63**: 230-235
- Hussein MR**, Haemel AK, Wood GS. Apoptosis and melanoma: molecular mechanisms. *J Pathol* 2003; **199**: 275-288
- Kim IK**, Jung YK, Noh DY, Song YS, Choi CH, Oh BH, Masuda ES, Jung YK. Functional screening of genes suppressing TRAIL-induced apoptosis: distinct inhibitory activities of Bcl-X(L) and Bcl-2. *Br J Cancer* 2003; **88**: 910-917
- Fulda S**, Meyer E, Debatin KM. Inhibition of TRAIL-induced apoptosis by Bcl-2 overexpression. *Oncogene* 2002; **21**: 2283-2294
- Zhou HB**, Zhu JR. Paclitaxel induces apoptosis in human gastric carcinoma cells. *World J Gastroenterol* 2003; **9**: 442-445
- Guo XZ**, Shao XD, Liu MP, Xu JH, Ren LN, Zhao JJ, Li HY, Wang D. Effect of bax, bcl-2 and bcl-xL on regulating apoptosis in tis-

- sues of normal liver and hepatocellular carcinoma. *World J Gastroenterol* 2002; **8**: 1059-1062
- 25 **Li HL**, Chen DD, Li XH, Zhang HW, Lü YQ, Ye CL, Ren XD. Changes of NF- κ B, p53, Bcl-2 and caspase in apoptosis induced by JTE-522 in human gastric adenocarcinoma cell line AGS cells: role of reactive oxygen species. *World J Gastroenterol* 2002; **8**: 431-435
- 26 **Xu AG**, Li SG, Liu JH, Gan AH. Function of apoptosis and expression of the proteins Bcl-2, p53 and C-myc in the development of gastric cancer. *World J Gastroenterol* 2001; **7**: 403-406
- 27 **Wang LD**, Zhou Q, Wei JP, Yang WC, Zhao X, Wang LX, Zou JX, Gao SS, Li YX, Yang CS. Apoptosis and its relationship with cell proliferation, p53, Waf1p21, bcl-2 and c-myc in esophageal carcinogenesis studied with a high-risk population in northern China. *World J Gastroenterol* 1998; **4**: 287-293
- 28 **Liu HF**, Liu WW, Fang DC, Men RP. Expression of bcl-2 protein in gastric carcinoma and its significance. *World J Gastroenterol* 1998; **4**: 228-230
- 29 **Zhou HB**, Yan Y, Sun YN, Zhu JR. Resveratrol induces apoptosis in human esophageal carcinoma cells. *World J Gastroenterol* 2003; **9**: 408-411
- 30 **Dalen H**, Neuzil J. alpha-Tocopheryl succinate sensitises a T lymphoma cell line to TRAIL-induced apoptosis by suppressing NF-kappa B activation. *Br J Cancer* 2003; **88**: 153-158
- 31 **Biswas DK**, Martin KJ, McAlister C, Cruz AP, Graner E, Dai SC, Pardee AB. Apoptosis Caused by Chemotherapeutic Inhibition of Nuclear Factor-kappaB Activation. *Cancer Res* 2003; **63**: 290-295
- 32 **Nicholson DW**, Ali A, Thornberry NA, Vaillancourt JP, Ding CK, Gallant M, Gareau Y, Griffin PR, Labelle M, Lazebnik YA. Identification and inhibition of the ICE/ CED-3 protease necessary for mammalian apoptosis. *Nature* 1995; **376**: 37-43
- 33 **Fernandes-Alnemri T**, Litwack G, Alnemri ES. CPP32, a novel human apoptotic protein with homology to Caenorhabditis elegans cell death protein Ced-3 and mammalian interleukin-1 beta-converting enzyme. *J Biol Chem* 1994; **269**: 30761-30764
- 34 **Tormanen-Napankangas U**, Soini Y, Kahlos K, Kinnula V, Paakko P. Expression of caspases-3, -6 and -8 and their relation to apoptosis in non-small cell lung carcinoma. *Int J Cancer* 2001; **93**: 192-198
- 35 **Hsia JY**, Chen CY, Chen JT, Hsu CP, Shai SE, Yang SS, Chuang CY, Wang PY, Miaw J. Prognostic significance of caspase-3 expression in primary resected esophageal squamous cell carcinoma. *Eur J Surg Oncol* 2003; **29**: 44-48
- 36 **Kania J**, Konturek SJ, Marlicz K, Hahn EG, Konturek PC. Expression of survivin and caspase-3 in gastric cancer. *Dig Dis Sci* 2003; **48**: 266-271
- 37 **Li XA**, Fang DC, Yang SM, Luo YH. The expression, purification and anticancer activity of TRAIL. *Acta Acad Med Milit Tert* 2002; **23**: 1058-1060
- 38 **Suzuki A**, Hayashida M, Ito T, Kawano H, Nakano T, Miura M, Akahane K, Shiraki K. Survivin initiates cell cycle entry by the competitive interaction with Cdk4/p16(INK4a) and Cdk2/cyclin E complex activation. *Oncogene* 2000; **19**: 3225-3234
- 39 **Shin S**, Sung BJ, Cho YS, Kim HJ, Ha NC, Hwang JI, Chung CW, Jung YK, Oh BH. An anti-apoptotic protein human survivin is a direct inhibitor of caspase-3 and -7. *Biochemistry* 2001; **40**: 1117-1123
- 40 **Li F**, Ambrosini G, Chu EY, Plescia J, Tognin S, Marchisio PC, Altieri DC. Control of apoptosis and mitotic spindle checkpoint by survivin. *Nature* 1998; **396**: 580-584
- 41 **Conway EM**, Pollefeyt S, Steiner-Mosonyi M. Deficiency of survivin in transgenic mice exacerbates Fas-induced apoptosis via mitochondrial pathways. *Gastroenterology* 2002; **123**: 619-631
- 42 **Wall NR**, O' Connor DS, Plescia J, Pommier Y, Altieri DC. Suppression of survivin phosphorylation on Thr34 by flavopiridol enhances tumor cell apoptosis. *Cancer Res* 2003; **63**: 230-235
- 43 **Gong JP**, Liu CA, Wu CX, Li SW, Shi YJ, Li XH. Nuclear factor kB activity in patients with acute severe cholangitis. *World J Gastroenterol* 2002; **8**: 346-349
- 44 **Rossi A**, Kapahi P, Natoli G, Takahashi T, Chen Y, Karin M, Santoro MG. Anti-inflammatory cyclopentenone prostaglandins are direct inhibitors of IkappaB kinase. *Nature* 2000; **403**: 103-108
- 45 **Ghosh S**, Karin M. Missing pieces in the NF-kB puzzle. *Cell* 2002; **109** (Suppl): S81-S96
- 46 **Lin A**, Karin M. NF-kappaB in cancer: a marked target. *Semin Cancer Biol* 2003; **13**: 107-114
- 47 **Wang CY**, Guttridge DC, Mayo MW. NF-kappaB induces expression of the Bcl-2 homologue A1/Bfl-1 to preferentially suppress chemotherapy-induced apoptosis. *Mol Cell Biol* 1999; **19**: 5923-5929
- 48 **Sosic D**, Richardson JA, Yu K. Twist regulates cytokine gene expression through a negative feedback loop that represses NF-kappaB activity. *Cell* 2003; **112**: 169-180
- 49 **Zhou HB**, Zhu JR. Paclitaxel induces apoptosis in human gastric carcinoma cells. *World J Gastroenterol* 2003; **9**: 442-445
- 50 **Liu JR**, Chen BQ, Yang YM, Wang XL, Xue YB, Zheng YM, Liu RH. Effect of apoptosis on gastric adenocarcinoma cell line SGC-7901 induced by cis-9, trans-11-conjugated linoleic acid. *World J Gastroenterol* 2002; **8**: 999-1004
- 51 **Zhao AG**, Zhao HL, Jin XJ, Yang JK, Tang LD. Effects of Chinese Jianpi herbs on cell apoptosis and related gene expression in human gastric cancer grafted onto nude mice. *World J Gastroenterol* 2002; **8**: 792-796
- 52 **Wu YL**, Sun B, Zhang XJ, Wang SN, He HY, Qiao MM, Zhong J, Xu JY. Growth inhibition and apoptosis induction of Sulindac on Human gastric cancer cells. *World J Gastroenterol* 2001; **7**: 796-800
- 53 **Siervo-Sassi RR**, Marrangoni AM, Feng X, Naoumova N, Winans M, Edwards RP, Lokshin A. Physiological and molecular effects of Apo2L/TRAIL and cisplatin in ovarian carcinoma cell lines. *Cancer Lett* 2003; **190**: 61-72
- 54 **Rudin CM**, Yang Z, Schumaker LM, VanderWeele DJ, Newkirk K, Egorin MJ, Zuhowski EG, Cullen KJ. Inhibition of glutathione synthesis reverses Bcl-2-mediated cisplatin resistance. *Cancer Res* 2003; **63**: 312-318
- 55 **Xu HY**, Yang YL, Gao YY, Wu QL, Gao GQ. Effect of arsenic trioxide on human hepatoma cell line BEL-7402 cultured *in vitro*. *World J Gastroenterol* 2000; **6**: 681-687
- 56 **Kim IK**, Jung YK, Noh DY, Song YS, Choi CH, Oh BH, Masuda ES, Jung YK. Functional screening of genes suppressing TRAIL-induced apoptosis: distinct inhibitory activities of Bcl-X(L) and Bcl-2. *Br J Cancer* 2003; **88**: 910-917

Edited by Xu JY and Wang XL

Construction and identification of recombinant vectors carrying herpes simplex virus thymidine kinase and cytokine genes expressed in gastric carcinoma cell line SGC7901

Jian-Hua Zhang, Ming-Xi Wan, Jia-Ying Yuan, Bo-Rong Pan

Jian-Hua Zhang, Ming-Xi Wan, Department of Biomedical Engineering, School of Life Science and Technology, Xi'an Jiaotong University, 28 West Xianning Road, Xi'an 710049, Shaanxi Province, China

Jia-Ying Yuan, Department of Ultrasonic Diagnosis, Xijing Hospital, Fourth Military Medical University, 127 West Changle Road, Xi'an 710033, Shaanxi Province, China

Bo-Rong Pan, Department of Oncology, Xijing Hospital, Fourth Military Medical University, 127 West Changle Road, Xi'an 710033, Shaanxi Province, China

Supported by Doctoral Foundation of Xi'an Jiaotong University, No.69925101 and National Natural Science Foundation of China, No.30270404

Correspondence to: Dr. Ming-Xi Wan, Department of Biomedical Engineering, School of Life Science and Technology, Xi'an Jiaotong University, 28 West Xianning Road, Xi'an 710049, Shaanxi Province, China. wanmingxi@yahoo.com.cn

Telephone: +86-29-2667924

Received: 2002-12-07 **Accepted:** 2003-03-18

Abstract

AIM: To construct and identify the recombinant vectors carrying herpes simplex virus thymidine kinase (HSV-TK) and tumor necrosis factor alpha (TNF- α) or interleukin-2 (IL-2) genes expressed in gastric carcinoma cell line SGC7901.

METHODS: The fragments of HSV-TK, internal ribosome entry sites (IRES) and TNF- α or IL-2 genes were inserted in a TK-IRES-TNF- α or TK-IRES-IL-2 order into pEGFP-N₃ and pLXSN to generate the therapeutic vectors pEGFP-TT, pEGFP-TI, pL(TT)SN and pL(TI)SN respectively, which were structurally confirmed by the digestion analysis of restriction endonuclease. The former two plasmids were used for the transient expression of recombinant proteins in the target cells while pL(TT)SN and pL(TI)SN were transfected into SGC7901 cells by lipofectamine for the stable expression of objective genes through G418 selection. The protein products expressed transiently and stably in SGC7901 cells by the constructed vectors were confirmed by fluorescent microscopy and Western blot respectively.

RESULTS: The inserted fragments in all constructed plasmids were structurally confirmed to be consistent with that of the published data. In the transient expression, both pEGFP-TT and pEGFP-TI were shown expressed in nearly 50% of the transfected SGC7901 cells. Similarly, the G418 selected vectors PL(TT)SN and PL(TI)SN were confirmed to be successful in the stable expression of the objective proteins in the target cells.

CONCLUSION: The constructed recombinant vectors in the present study that can express the suicide gene TK in combination with cytokines genes may serve as the potential tools to perform more effective investigations in future for the gene therapy of gastric carcinoma.

Zhang JH, Wan MX, Yuan JY, Pan BR. Construction and identification of recombinant vectors carrying herpes simplex virus thymidine kinase and cytokine genes expressed in gastric carcinoma cell line SGC7901. *World J Gastroenterol* 2004; 10(1): 26-30

<http://www.wjgnet.com/1007-9327/10/26.asp>

INTRODUCTION

Gastric cancer is one of the most common malignancies both in China and abroad^[1-7]. Despite the improvements in surgical techniques, radiation and chemotherapeutic regimens, the disease remains a great challenge. Most patients still die finally of their disease, even after apparent "curative resection". In recent years, the promising conception of gene therapy has been advocated in a hope to deal with the malignant diseases more effectively. One of the landmark discoveries for this therapeutic strategy is the transfer of suicide genes, such as HSV-TK, into the tumor cells, which has been shown to exert antitumor efficacy on a variety of cancer cells^[8-11]. The expressed HSV-TK/ganciclovir (GCV) system can not only inhibit the DNA synthesis of the target cells but also produce a bystander effect against tumors^[12-16]. However, these effects have been found to be unstable in some of the transfected cells, which may result in a decreased efficiency in the treatment of malignancies. The use of tissue-specific vectors to deliver genes and combination of TK with cytokine genes may improve the efficacy of the antitumor effects^[17-20]. In the present study, therefore, we tried to construct and identify the recombinant vectors containing HSV-TK, IRES in combination with cytokine genes, TNF- α or IL-2, in an attempt to establish more effective recombinants for the gene therapy of gastric malignancies.

MATERIALS AND METHODS

Materials

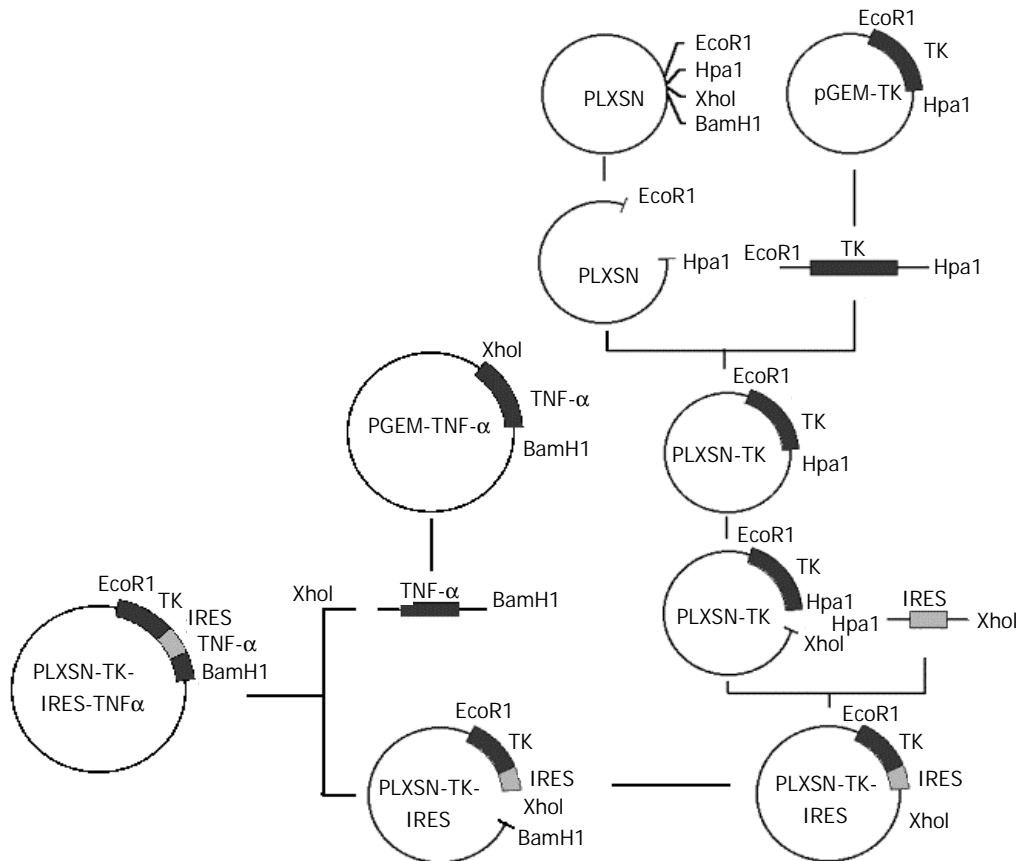
Reagents Restriction enzymes (*EcoR* I, *Hpa* I, *Xho* I and *Bam*HI), T₄ DNA ligase and *Taq* DNA polymerase were purchased from Gibco Co., USA. Lipofectamine was supplied by Boeringer Mannheim Co., Mannheim, Germany. Monoclonal antibodies of mouse anti-IL-2 and anti-TNF- α proteins and horseradish peroxidase-conjugated antimouse immunoglobulin were purchased from Zhongshan Co., Shanghai, China.

PCR primers The primer sequences used in the study were designed according to that of the individual genes (Table 1) with the modification of adding the recognition site sequences for the corresponding restriction enzymes (*EcoR* I, *Hpa* I, *Xho* I and *Bam*HI), and synthesized by Shanghai GeneCore Bio Technologies Co.

Plasmids and cell lines Plasmid pBluescript-TK was provided by Shanghai Institute of Biochemistry. pIRZA1neo with 585 bp IRES sequence^[21,22] was purchased from Invitrogen Co., USA. The plasmid PT₇-TNF- α , pEGFP-N₃ carrying green fluorescent protein (GFP) gene, pGEM-T-Easy vector and *E.coli* JM109 were provided by Orthopedic Oncology Institute of PLA,

Table 1 Primer sequences of amplified genes

Genes	Primer sequences	Fragment length
TK	Forward: 5' -GC GAA TTC ATG GCT TCG TAC CCC TGC CAT C-3' Reverse: 5' -GC GTT AAC TTA AGC CTC CCC CAT CTC CCG G-3'	1 128 bp
IL-2	Forward: 5' -GC CTC GAG ATG TAC AGG ATG CAA CTC CTG-3' Reverse: 5' -GC GGA TTC TTA AGT CAG TGT TGA GAT GAT GC-3'	456 bp
TNF- α	Forward: 5' -GC CTC GAG ATG GTC AGA TCA TCT TCT CGA AC -3' Reverse: 5' -GC GGA TCC TTA CAG GGC AAT GAT CCC AAA -G-3'	474 bp
IRES	Forward: 5' -GC GTT AAC AAT TCC GCC CCT CTC CCT CCC CC-3' Reverse: 5' -GC CTC GAG AAT AGT AGC ACA AAA AGT TTC C-3'	585 bp

**Figure 1** Diagram of the construction of the expression vector PL(TT)SN.

Xi'an, China. The retroviral expressing vector pLXSN was provided by Dr. Yu Bing from Fourth Military Medical University, Xi'an, China. IL-2 cDNA was made from human peripheral blood by RT-PCR.

The gastric carcinoma cell line SGC7901 was provided by Shanghai Institute of Biochemistry. Virus packaging cell PA317 and NIH3T3 cell lines were provided by Dr. Yu Bing. Cells were maintained in RPMI 1640 medium supplemented with 10% FBS (Hangzhou, Sijiqing Biotech Company), 2 mM L-glutamine, 100 units/ml penicillin and 100 μ g/ml streptomycin. The PA317 was used as the packaging cell and the NIH 3T3 cells were used to assay the virus titre. The cell cultures were maintained at 37 °C in a humidified atmosphere with 5% CO₂.

Methods

Construction of the recombinant vectors The recombinant vectors were constructed with routine molecular cloning techniques^[23-25]. The DNA fragments of HSV-TK, IRES, TNF- α and IL-2 were obtained by PCR amplification with specific primers from their corresponding templates. For the transient

expression of the recombinant genes, the fragments of HSV-TK, IRES, TNF- α and the fragments of HSV-TK, IRES, IL-2 were cloned into pEGFP-N₃ to generate pEGFP-TT and pEGFP-TI respectively. Similarly, those fragments were separately inserted into pLXSN to generate plasmid PL (TT)SN and PL (TI)SN as shown in Figure 1 for the selection of the stable expression vectors. The structure of all these constructed vectors was confirmed by the digestion analysis of restriction endonuclease.

Transient expression The transient expression of recombinants was performed according to the literature^[26]. The constructed vectors pEGFP-TT and pEGFP-TI, and the control plasmid were transfected into SGC7901 cells with a routine protocol by lipofectamine. Twenty hours after the transfection, cells were harvested and the expressed marker protein GFP fused with the objective genes were detected under a fluorescent microscope.

Stable expression The plasmids pL(TT)SN, pL(TI)SN and pL(TK)SN were transfected respectively into PA317 cells with lipofectamine (Gibco) according to the manufacturer's

instruction. After 48 h of transfection, G418 (Promega) was added to the culture media at a concentration of $500 \text{ mg} \cdot \text{L}^{-1}$ to select G418-resistant colonies. After 2-weeks' culture with the changing of the G418-containing media every 3 days, the supernatant of G418-resistant colony was collected and diluted to different concentrations to infect NIH3T3 cells, which was further undergone the G418 selection for 2w when the G418-resistant NIH3T3 colonies were counted for the determination of viral titre. The viral titer of pL(TT)SN, pL(TI)SN, pL(TK)SN and empty plasmid pLXSN were $5 \times 10^8 \text{ CFU/L}$, $6 \times 10^8 \text{ CFU/L}$, $1 \times 10^9 \text{ CFU/L}$ and $1 \times 10^9 \text{ CFU/L}$ respectively.

For the stable expression of recombinants, a total number of 5×10^5 SGC7901 cells were incubated in a 6-well plate for 24 h, then rinsed with serum-free RPMI 1640 medium twice and incubated with 100 μl supermatant of G418-resistant PA317 colony for 3 h. After 4-weeks' cultivation, the G418-resistant colonies designated as SGC/TK-TNF- α , SGC/TK-IL-2, SGC/TK and SGC/0 respectively were used to confirm the objective gene expression by Western blot analysis.

Western blotting analysis The SGC/TT and SGC/TI cells were incubated respectively in the six-well plates at a density of 2.5×10^5 cells/well for 24 h, followed by a further cultivation of 48 h with the culture medium replaced with 1 ml of serum-free RPMI 1640. Then the serum-free medium was totally collected, concentrated in a microconcentrator to 20 μl and subjected to electrophoresis on a $120 \text{ g} \cdot \text{L}^{-1}$ SDS/PAGE gel. Proteins were transferred to a nitrocellulose membrane and incubated overnight in 50 $\text{ml} \cdot \text{L}^{-1}$ fat free milk in PBS at 4°C . After washed in $10 \text{ ml} \cdot \text{L}^{-1}$ fat free milk, the membrane was incubated with monoclonal antibody of mouse anti-rhIL-2 or anti-TNF- α , followed by incubation with horseradish peroxidase-conjugated antimouse immunoglobulin. Proteins were detected by using the ECL kit according to the manufacturer's protocol (Amersham).

RESULTS

Identification of constructed vectors

The segment analysis by restriction endonuclease digestion confirmed that the inserted gene sequences in all of the constructed plasmids were structurally consistent with that of the published data. The inserted fragments in pEGFP-TI and pEGFP-TT were identified as shown in Figure 2.

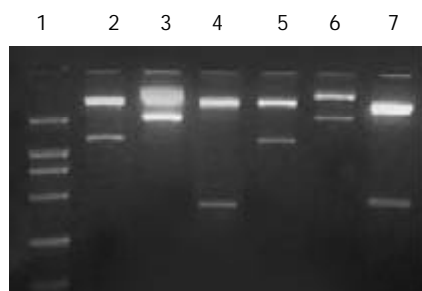


Figure 2 Segment analyses of pEGFP-TI and pEGFP-TT by restriction endonuclease digestion. Lane 1: DNA marker (from top to bottom: 1 543, 994, 697, 515 and 337 bp); Lane 2: pEGFP-TI/*EcoRI* and *HpaI* (TK gene 128 bp); Lane 3: pEGFP-TI/*EcoRI* and *XhoI* (TK+IRES 1.71kb); Lane 4: pEGFP-TI/*XhoI* and *BamHI* (IL-2 gene 456 bp); Lane 5: pEGFP-TT/*EcoRI* and *HpaI* (TK gene 128 bp); Lane 6: pEGFP-TT/*EcoRI* and *XhoI* (TK+IRES 1.71 kb); Lane 7: pEGFP-TT/*XhoI* and *BamHI* (TNF- α gene 474 bp).

Transient expressions of GFP-TT and GFP-TI protein

Twenty hours after the transfection, the GFP fluorescence was detected under fluorescent microscope in nearly 50% of the

total cells transfected with pEGFP-TT or pEGFP-TI. The fluorescence was gradually increased with time and peaked at 72 h, which indicated that the TK-IRES-IL-2 and TK-IRES-TNF- α were transiently expressed in SGC7901 cells (Figure 3 A and B).

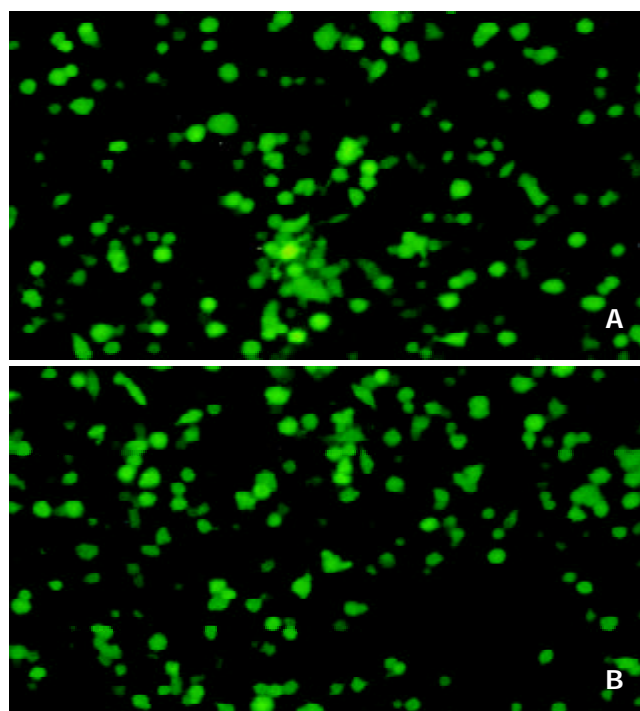


Figure 3 Transient expression of the recombinant genes in SGC7901 cells. A: Transient expression of pEGFP-TT in SGC7901 cells $\times 100$. B: Transient expression of pEGFP-TI in SGC7901 cells $\times 100$.

Expressions of stable transfectants

The stable expression of recombinant proteins in SGC7901 cells was confirmed by Western blotting, in which two distinct bands of 15ku and 17ku were observed on the nitrocellulose membrane, corresponding to the fragment sizes of IL-2 and TNF- α respectively (Figure 4).

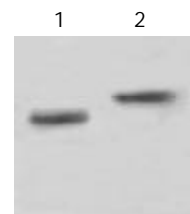


Figure 4 Stably expressed recombinant protein in transduced SGC7901 cells confirmed by Western blot. Lane 1: IL-2 (15ku) expressed in SGC/TI cells; Lane 2: TNF- α (17ku) expressed in SGC/TT cells.

DISCUSSION

Gene therapy has become a promising strategy for the treatment of gastric cancer^[27-31], in which the transfer of suicide genes into tumor cells has emerged as an attractive modality for the selective elimination of cancer cells^[14-16,30,31]. The suicide genes encode non-mammalian enzymes that can convert nontoxic prodrugs into cellular toxic metabolites. The most widely used suicide gene is the HSV-TK/ganciclovir (GCV) system that can convert prodrug GCV into GCV monophosphate. The latter is further phosphorylated by cellular kinase to form GCV

triphosphate, a toxic substance that can inhibit cellular DNA synthesis and lead to cell death. Besides, the “bystander effect” induced by TK gene can also enhance the tumor-killing capacity of the HSV-TK/GCV system^[16-20,32]. Because of the antitumor properties exerted by certain cytokines such as IL-2 and TNF- α , it is believed that the gene therapy combining cytokine with TK suicide gene would be more beneficial and effective for the treatment of cancers, which has been strongly supported by some of the recently published literatures^[33]. However, there are fewer reports of this therapeutic strategy applied to the antitumor study of gastric malignancy.

Construction of a bicistronic retroviral vector with an internal ribosome entry site (IRES)^[34,35] allows the simultaneous expression of two genes from a single transcript, which has been demonstrated to be efficient. However, the expressive levels of the objective protein are found lower in some circumstance. Five different genes, including human IL-2, IL-4, granulocyte macrophage stimulating factor, HSV-TK and hepatitis C virus core gene, have been tested using the modified vector for the gene transfer^[36,37]. The new bicistronic vector, modified by abolishing the functional viral gag initiation codon and keeping it before the 5' end to the first initiation codon of the transduced gene, has made the protein expression greatly increased compared with the original vector. As the RNA levels and splicing patterns of these two vectors remain similar, the improvement was most likely at the translation level. Thus, the incorporation of the internal ribosome entry site sequence into a proper location of the retroviral vector for gene therapy represents a promising strategy to facilitate the simultaneous and efficient expression of several genes from the same promoter^[21, 22].

In the present study, we employed the strategy to construct our expression vectors, in which the IRES gene was cloned in TK-IRES-TNF- α or TK-IRES-IL-2 order and the recombinants were constructed in combination with TK and cytokine genes. In the transient expression, the constructed vectors pEGFP-TT and pEGFP-TI were shown to be effectively expressed *in vitro* as demonstrated by the appearance of the fusing fluorescent protein GFP^[26,38] in nearly 50% of the transfected SGC7901 cells. Similarly, in the experiment of stable expression, the G418 selected vectors PL(TT)SN and PL(TD)SN were also confirmed to be successful in both of the transfection into the target cells and the expression of the objective proteins. All of these results indicate that the expressive vectors constructed in the present study may serve as the potential tools to perform more effective investigations for the gene therapy of gastric carcinoma in future. Further studies are therefore needed to elucidate and characterize the antitumor effects of these constructed vectors on the transfected SGC7901 cells.

REFERENCES

- Xu CT**, Huang LT, Pan BR. Current gene therapy for stomach carcinoma. *World J Gastroenterol* 2001; **7**: 752-759
- Song ZJ**, Gong P, Wu YE. Relationship between the expression of iNOS, VEGF, tumor angiogenesis and gastric cancer. *World J Gastroenterol* 2002; **8**: 591-595
- Tao HQ**, Zou SC. Effect of preoperative regional artery chemotherapy on proliferation and apoptosis of gastric carcinoma cells. *World J Gastroenterol* 2002; **8**: 451-454
- Han Y**, Han ZY, Zhou XM, Shi R, Zheng Y, Shi YQ, Miao JY, Pan BR, Fan DM. Expression and function of classical protein kinase C isoenzymes in gastric cancer cell line and its drug-resistant sublines. *World J Gastroenterol* 2002; **8**: 441-445
- Wang X**, Lan M, Shi YQ, Lu J, Zhong YX, Wu HP, Zai HH, Ding J, Wu KC, Pan BR, Jin JP, Fan DM. Differential display of vincristine-resistance-related genes in gastric cancer SGC7901 cell. *World J Gastroenterol* 2002; **8**: 54-59
- Shen LZ**, Wu WX, Xu DH, Zheng ZC, Liu XY, Ding Q, Hua YB, Yao K. Specific CEA-producing colorectal carcinoma cell killing with recombinant adenoviral vector containing cytosine deaminase gene. *World J Gastroenterol* 2002; **8**: 270-275
- Thomas AL**, Steward WP. Recent advances in the nonsurgical treatment of upper gastrointestinal tract tumors. *Expert Rev Anticancer Ther* 2001; **1**: 258-268
- Narita M**, Bahar R, Hatano M, Kang MM, Tokuhisa T, Goto S, Saisho H, Sakiyama S, Tagawa M. Tissue-specific expression of a suicide gene for selective killing of neuroblastoma cells using a promoter region of the NCX gene. *Cancer Gene Ther* 2001; **8**: 997-1002
- Van Dillen IJ**, Mulder NH, Vaalburg W, de Vries EF, Hospers GA. Influence of the bystander effect on HSV-tk/GCV gene therapy. A review. *Curr Gene Ther* 2002; **2**: 307-322
- Nowak AK**, Lake RA, Kindler HL, Robinson BW. New approaches for mesothelioma: biologics, vaccines, gene therapy, and other novel agents. *Semin Oncol* 2002; **29**: 82-96
- Qiao J**, Doubrovin M, Sauter BV, Huang Y, Guo ZS, Balatoni J, Akhurst T, Blasberg RG, Tjuvahev JG, Chen SH, Woo SL. Tumor-specific transcriptional targeting of suicide gene therapy. *Gene Ther* 2002; **9**: 168-175
- Engelmann C**, Heslan JM, Fabre M, Lagarde JP, Klatzmann D, Panis Y. Importance, mechanisms and limitations of the distant bystander effect in cancer gene therapy of experimental liver tumors. *Cancer Lett* 2002; **179**: 59-69
- Adachi Y**, Matsubara S, Muramatsu T, Curiel DT, Reynolds PN. Midkine promoter-based adenoviral suicide gene therapy to midkine-positive pediatric tumor. *J Pediatr Surg* 2002; **37**: 588-592
- Pulkkanen KJ**, Laukkanen JM, Fuxe J, Kettunen MI, Rehn M, Kannasto JM, Parkkinen JJ, Kauppinen RA, pettersson RF, Yla-Herttuala S. The combination of HSV-tk and endostatin gene therapy eradicates orthotopic human renal cell carcinomas in nude mice. *Cancer Gene Ther* 2002; **9**: 908-916
- Floeth FW**, Shand N, Bohar H, Prisack HB, Felsberg J, Neuen-Jacob E, Aulich A, Burger KJ, Bock WJ, Weber F. Local inflammation and devascularization-*in vivo* mechanisms of the “bystander effect” in VPC-mediated HSV-Tk/GCV gene therapy for human malignant glioma. *Cancer Gene Ther* 2001; **8**: 843-851
- Warren P**, Song W, Holle E, Holmes L, Wei Y, Li J, Wagner T, Yu X. Combined HSV-TK/GCV and secondary lymphoid tissue chemokine gene therapy inhibits tumor growth and elicits potent antitumor CTL response in tumor-bearing mice. *Anticancer Res* 2002; **22**: 599-604
- Guan J**, Ma L, Wei L. Characteristics of ovarian cancer cells transduced by the bicistronic retroviral vector containing GM-CSF and HSV-TK genes. *Chin Med J* 2001; **114**: 147-151
- Hall SJ**, Canfield SE, Yan Y, Hassen W, Selleck WA, Chen SH. A novel bystander effect involving tumor cell-derived Fas and FasL interactions following Ad.HSV-tk and Ad.mIL-12 gene therapies in experimental prostate cancer. *Gene Ther* 2002; **9**: 511-517
- Boucher PD**, Ostruszka LJ, Murphy PJ, Shewach DS. Hydroxyurea significantly enhances tumor growth delay *in vivo* with herpes simplex virus thymidine kinase/ganciclovir gene therapy. *Gene Ther* 2002; **9**: 1023-1030
- Hayashi K**, Hayashi T, Sun HD, Takeda Y. Contribution of a combination of ponidicin and acyclovir/ganciclovir to the anti-tumor efficacy of the herpes simplex virus thymidine kinase gene therapy system. *Hum Gene Ther* 2002; **10**: 415-423
- Ulrich-Vinther M**, Carmidy EE, Goater JJ, S balle K, O' Keefe RJ, Schwarz EM. Recombinant adeno-associated virus-mediated osteoprotegerin gene therapy inhibits wear debris-induced osteolysis. *J Bone Joint Surg Am* 2002; **84A**: 1405-1412
- Wong ET**, Ngoi SM, Lee CG. Improved co-expression of multiple genes in vectors containing internal ribosome entry sites (IRESes) from human genes. *Gene Ther* 2002; **9**: 337-344
- Cao MM**, Pan W, Chen QL, Ma ZC, Ni ZJ, Wu XL, Wu WB, Pan X, Cao GW, Qi ZT. Construction of the eukaryotic expression vector expressing the fusion protein of human endostatin protein and IL3 signal peptide. *Shijie Huaren Xiaohua Zazhi* 2001; **9**: 43-46
- Pan X**, Ke CW, Pan W, Wu WB, Zhang B, He X, Cao GW, Qi ZT. Construction of eukaryotic expression vector carrying IFN- β gene under control of human HBV promoter. *Shijie Huaren Xiaohua Zazhi* 2000; **8**: 520-523

- 25 **Zhang J**, Liu YF, Yang SJ, Sun ZW, Qiao Q, Zhang SZ. Construction and expression of mouse/humanized scFv and their fusion to humanized mutant TNF α against hepatocellular carcinoma. *Shijie Huaren Xiaohua Zazhi* 2000; **8**: 616-620
- 26 **Cheng H**, Liu YF, Zhang HZ, Shen WA, Zhang SZ. Construction and expression of anti-HCC immunotoxin of sFv-TNF- α and GFP fusion proteins. *Shijie Huaren Xiaohua Zazhi* 2001; **9**: 640-644
- 27 **Chen JP**, Lin C, Xu CP, Zhang XY, Wu M. The therapeutic effects of recombinant adenovirus RA538 on human gastric carcinoma cells *in vitro* and *in vivo*. *World J Gastroenterol* 2000; **6**: 855-860
- 28 **Feng RH**, Zhu ZG, Li JF, Liu BY, Yan M, Yin HR, Lin YZ. Inhibition of human telomerase in MKN-45 cell line by antisense hTR expression vector induces cell apoptosis and growth arrest. *World J Gastroenterol* 2002; **8**: 436-440
- 29 **Yu ZC**, Ding J, Pan BR, Fan DM, Zhang XY. Expression and bio-activity identification of soluble MG₇ scFv. *World J Gastroenterol* 2002; **8**: 99-102
- 30 **Guo SY**, Gu QL, Liu BY, Zhu ZG, Yin HR, Lin YZ. Experimental study on the treatment of gastric cancer by TK gene combined with mIL-2 gene. *Shijie Huaren Xiaohua Zazhi* 2000; **8**: 974-978
- 31 **Huang H**, Wang A. The adenovirus-mediated HSV-TK/GCV suicide gene system in the treatment of tongue carcinoma cell line. *Zhonghua Kouqiang Yiyue Zazhi* 2001; **36**: 457-460
- 32 **Gao G**, Huang T, Chen S. *In vitro* and *in vivo* bystander effect of adenovirus-mediated transfer of the herpes simplex virus thymidine kinase gene. *Zhonghua Waike Zazhi* 2002; **40**: 301-303
- 33 **Majumdar AS**, Zolotorey A, Samuel S, Tran K, Vertin B, Hall-Meier M, Antoni BA, Adeline E, Philip M, Philip R. Efficacy of herpes simplex virus thymidine kinase in combination with cytokine gene therapy in an experimental metastatic breast cancer model. *Cancer Gene Ther* 2000; **7**: 1086-1099
- 34 **Kobayashi T**, Kida Y, Kaneko T, Pastan I, Kobayashi K. Efficient ablation by immunotoxin-mediated cell targeting of the cell types that express human interleukin-2 receptor depending on the internal ribosome entry site. *J Gene Med* 2001; **3**: 505-510
- 35 **Royal RE**, Kershaw MH, Reeves ME, Wang G, Daly T, Treisman J, Lam J, Hwu P. Increased functional expression of transgene in primary human lymphocytes using retroviral vectors modified with IRES and splicing motifs. *Gene Ther* 2002; **9**: 1085-1092
- 36 **Wang SI**, Mukhtar H. A high-efficiency translational control element with potential for cancer gene therapy. *Int J Oncol* 2002; **20**: 1269-1274
- 37 **Qiao J**, Roy V, Girard MH, Caruso M. High translation efficiency is mediated by the encephalomyocarditis virus internal ribosomal entry sites if the natural sequence surrounding the eleventh AUG is retained. *Hum Gene Ther* 2002; **13**: 881-887
- 38 **Zhang X**, Wu J, Li X, Fu L, Gao D, Bai H, Liu X. Effects of recombinant human bone morphogenic protein-2 and hyaluronic acid on invasion of brain glioma *in vivo*. *Zhonghua Yixue Zazhi* 2002; **82**: 90-93

Edited by Zhu LH

Does surgical resection of hepatocellular carcinoma accelerate cancer dissemination?

I-Shyan Sheen, Kuo-Shyang Jeng, Shou-Chuan Shih, Po-Chuan Wang, Wen-Hsiung Chang, Horng-Yuan Wang, Li-Rung Shyung, Shee-Chan Lin, Chin-Roa Kao, Yi-Chun Tsai, Tsu-Yen Wu

I-Shyan Sheen, Divisions of Hepatogastroenterology, Chang Gung Memorial Hospital, Taipei, Taiwan, China

Kuo-Shyang Jeng, Departments of Surgery, Mackay Memorial Hospital, Taipei, Taiwan, China

Shou-Chuan Shih, Po-Chuan Wang, Wen-Hsiung Chang, Horng-Yuan Wang, Li-Rung Shyung, Shee-Chan Lin, Chin-Roa Kao, Department of Internal Medicine, Mackay Memorial Hospital, Taipei, Taiwan, China

Yi-Chun Tsai, Tsu-Yen Wu, Medical Research, Mackay Memorial Hospital, Taipei, Taiwan, China

Kuo-Shyang Jeng, Mackay Junior School of Nursing, Taipei, Taiwan, China

Supported by the grants from the Department of Health, National Science Council, Executive Yuan, Taiwan (Dr. Jeng) (NSC 86-2314-B-95-001)

Correspondence to: Kuo-Shyang Jeng, M.D., F.A.C.S. Department of Surgery, Mackay Memorial Hospital, No. 92, Sec 2, Chung-San North Road, Taipei, Taiwan, China. issheen.jks@msa.hinet.net

Telephone: +886-2-25433535 **Fax:** +886-2-27065704

Received: 2003-08-30 **Accepted:** 2003-10-01

Abstract

AIM: This study was to investigate whether surgery could increase cancer dissemination and postoperative recurrence in patients with hepatocellular carcinoma (HCC) by detection of human α -fetoprotein messenger RNA (hAFP mRNA). hAFP mRNA in the peripheral blood of patients with HCC has been considered as a surrogate marker for circulating tumor cells.

METHODS: Eighty-one consecutive patients who underwent curative resection for HCC entered this prospective cohort study. We examined hAFP mRNA from the peripheral blood obtained preoperatively, perioperatively, and postoperatively to correlate the prognosis after curative resections from HCC patients and from the control subjects. Detection of hAFP mRNA by reverse transcriptase and polymerase chain reaction amplification (RT-PCR) was performed with primers specifically. The relations between the clinical variables (age, sex, associated liver cirrhosis, hepatitis B virus infection, hepatitis C virus infection, serum α -fetoprotein and Child-Pugh class), the histological variables (size, capsule, vascular permeation, grade of differentiation, and daughter nodules), hAFP mRNA in peripheral blood of 3 different sessions, and postoperative course (recurrence, and recurrence related death) were analysed.

RESULTS: No hAFP mRNA was detected in control group subjects. Twenty-two (27%), 24 (30%) and 19 (23%) of 81 HCC patients had hAFP mRNA positivity in the preoperative, perioperative and postoperative peripheral blood. The preoperative presence did not influence the risk of HCC recurrence (55% vs 41%, $P=0.280$). In contrast, patients with postoperative presence had a significantly higher recurrence (90% vs 31%, $P<0.001$; odds ratio 19.2; 95% confidence interval: 4.0-91.7). In the multivariate analysis by COX proportional hazards model, postoperative positivity

had a significant influence on recurrence ($P=0.067$) and recurrence related mortality ($P=0.017$). Whereas, the perioperative positivity of hAFP mRNA did not increase HCC recurrence (58% vs.39%, $P=0.093$). The correlation between perioperative hAFP mRNA positivity and recurrence related mortality had no statistical significance ($P=0.836$).

CONCLUSION: From our study, perioperative detection of hAFP mRNA in peripheral blood of patients has no clinical relevance and significant role in the prediction of HCC recurrence. Surgical resection itself may not accelerate cancer dissemination and does not increase postoperative recurrence significantly either.

Sheen IS, Jeng KS, Shih SC, Wang PC, Chang WH, Wang HY, Shyung LR, Lin SC, Kao CR, Tsai YC, Wu TY. Does surgical resection of hepatocellular carcinoma accelerate cancer dissemination? *World J Gastroenterol* 2004; 10(1): 31-36
<http://www.wjgnet.com/1007-9327/10/31.asp>

INTRODUCTION

Hepatocellular carcinoma (HCC) is the leading malignancy with a poor prognosis in areas of high hepatitis B and C prevalence^[1-4]. After curative resections of HCC, a large proportion of patients develop tumor recurrence within the first 3 years. Whether intraoperative manipulation contributes to cancer dissemination remains a debating subject.

How to detect these disseminated cancer cells in the perioperative period is a problem. The isolation and identification of tumor cells in a small blood sample by conventional methods is very difficult because the number of malignant cells in the circulation may be extremely small^[5-8]. Recently, it has become possible and sensitive to identify tumor-specific gene transcripts (messenger RNA/circular DNA) by means of polymerase chain reaction (PCR). With the use of PCR-based method which permits detection of 1 tumor cell among 10^7 normal peripheral, mononuclear blood cells, the blood-borne dispersion of tumor cells during surgical manipulation has been reported in humans with prostatic carcinoma, melanoma, breast carcinoma and pancreatic carcinoma^[9-12].

For detecting HCC cells in circulation, reverse transcriptase (RT) PCR targeting human α -fetoprotein (hAFP) messenger RNA (mRNA) or human albumin mRNA has been proposed^[13-22]. Lack of the specificity of albumin mRNA has been emphasized^[21,22]. Human AFP mRNA has been accepted as a liver specific and cancer-specific marker^[23,24]. Many clinical studies have suggested that hAFP mRNA in peripheral blood can be used as a surrogate marker of circulating HCC cells and as a prognostic indicator in patients treated with ethanol injection and/or arterial embolization^[18].

In an attempt to elucidate whether surgical resection of HCC accelerated cancer dissemination, we designed this prospective study.

MATERIALS AND METHODS

Study population

From August 1995 to July 1999, 81 consecutive patients [42 men and 39 women, with a mean age of 52 ± 13 years (range: 16 to 79 years)] with HCC undergoing curative hepatic resection at Mackay Memorial Hospital, Taipei, Taiwan, China, were enrolled in this prospective study (Table 1). Patients who had previously or simultaneously other malignant disorders, and who had previously received hepatectomy, intraoperative blood transfusion, preoperative and postoperative hepatic arterial chemoembolization (TACE) or neoadjuvant ethanol injection were all excluded.

Table 1 Demographic data including clinical and tumor variables of patients with HCC undergoing curative resection ($n=81$)

Variables	No. of patients (%)
Age (mean, years)	52 ± 13
Male	42 (52)
Cirrhosis	56 (69)
Child- Pugh' s class A	70 (86)
HBsAg (+)	62 (77)
Anti-HCV (+)	31 (38)
Serum AFP <20 ng/ml	29 (36)
20-10 ³ ng/ml	29 (36)
>10 ³ ng/ml	23 (28)
Size of HCC < 3 cm	25 (30)
3-10 cm	28 (35)
> 10 cm	28 (35)
Complete capsule	28 (35)
Daughter nodules	32 (40)
Vascular permeation	37 (46)
Edmondson-Steiner' s grade I	6 (7)
grade II	36 (44)
grade III	26 (32)
grade IV	13 (16)

AFP: serum alpha fetoprotein, HBsAg(+): positive hepatitis B surface antigen, Anti-HCV(+): positive hepatitis C virus antibody, Edmondson and Steiner grade: differentiation grades I, II, III, and IV.

The hepatectomy procedure was selected according to the patient' s liver function and cancer location. Prior to resection, intraoperative ultrasonography to scan the entire hepatic field was performed in every patient. Surgery was defined as curative when all gross lesions were removed with an over 1 cm free resection margin which was proven tumor-free histologically. The surgical procedures included 62 major resections (6 extended right lobectomies, 18 right lobectomies, 14 left lobectomies, and 24 double segmentectomies) and 19 minor resections (11 segmentectomies, 5 subsegmentectomies, and 3 wedge resections).

Peripheral blood samples for detection of hAFP mRNA were obtained from all study patients from forearm one day prior to surgery (preoperation), immediately (i.e., within 12 hours) after liver resection (perioperation), and 90 days after surgery (postoperation) from all 81 patients.

After discharge, all the patients were followed up at our outpatient clinic and received regular clinical assessments to detect tumor recurrence including periodic abdominal ultrasonography (every 2-3 months during the first 5 years, then every 4-6 months thereafter), and serum AFP and liver biochemistry (every 2 months during the first 2 years, then every 4 months during the following 3 years, and every 6 months thereafter). Abdominal computed tomography scans (CT) were also done (every 6 months during the first 5 years, then every year). Hepatic arteriography was obtained if there was a suspicion of cancer recurrence from ultrasonography or

CT scan, or serum AFP. Chest X ray to detect pulmonary metastasis was done every 6 months. Bone scan to detect osseous metastasis was undertaken every 6 months. Detection of tumor on any imaging studies was defined as "clinical recurrence".

Parameters analyzed for recurrence included sex (male vs. female), age, the presence of liver cirrhosis, Child-Pugh class of liver functional reserve (A vs. B), hepatitis B virus infection (hepatitis B surface antigen), hepatitis C virus infection (anti-hepatitis C virus antibody), serum AFP level (<20 ng/ml vs. 20-1 000 ng/ml vs. >1 000 ng/ml), tumor size (<3 cm vs. 3-10 cm vs. >10 cm), tumor encapsulation (complete vs. incomplete or absent), presence of daughter nodules, and vascular permeation (including vascular invasion and/or tumor thrombi, in either the portal vein or hepatic vein), and cell differentiation (Edmondson and Steiner grades I, II, III and IV)(Table1).

A control group included 30 healthy volunteers without liver disease and 20 patients with chronic liver disease without evidence of HCC. They also received hAFP mRNA detection from peripheral blood.

Detection of hAFP mRNA

We used human hepatocytes to determine the sensitivity of the assay. Using tetradecyltrimethyl- ammonium bromide, nucleated cells were isolated from peripheral blood. Total RNA was extracted from cryopreserved liver tissues. The sequences of the sense primers were 5' -ACT GAA TCC AGA ACA CTG CAT AG-3' (external-sense) and 5' -TGC AGT CAA TGC ATC TTT CAC CA-3' (internal-sense) and those of the antisense primers 5' -TGG AAT AGC TTC CAT ATT GGA TTC- 3' (external-antisense) and 5' -AAG TGG CTT CTT GAA CAA ACT GG- 3' (internal-antisense). The sizes of the amplified products of hAFP mRNA were 176 and 101 base pairs by external and internal primer pairs, respectively.

A Hep G2 (hepatoblastoma) cell line served as positive control for hAFP mRNA expression. For negative controls, we used EDTA treated water (filtered and vaporized). With cDNA derived from Hep G2, specific bands for hAFP (101 bp) were observed. In contrast, the cell lines that served as negative controls did not yield these bands. It was also impossible to detect free RNA extracted from 5 ml aliquots of control blood, in which Hep G2 cells were suspended. The sensitivity of our assay, determined in a dilution experiment using freshly isolated human hepatocytes (10^5 to 10^1) in 1 ml whole blood before RNA extraction, was approximately 1 hepatocyte for every 10^5 peripheral mononuclear cells.

Ethylendiamine tetraacetic acid (EDTA)-treated whole blood was centrifuged and the plasma fraction was removed. The cellular fraction was enriched for mononuclear cells (MNC) or possible tumor cells according to the method described by Oppenheim. Total cellular RNA was then extracted with PUREscript RNA isolation kits TRI-Zol (Life Technologies Inc., Gaithersburg, USA), from 5 μ g of which cDNA was synthesized. The reverse transcription reaction solution contained 6 μ l of 5 \times first strand buffer, 10 mM dithiothreitol, 125 mM each of dCTP, dATP, dGTP and dTTP, 0.3 μ g of random hexamers, and 200 units of superscriptase II moloney murine leukemia virus reverse transcriptase (Life Technologies Inc.). The RNA solution was incubated at 95 $^{\circ}$ C for 10 minutes, quickly chilled on ice, then mixed with the reverse transcription reaction solution (total volume 20 μ l), and incubated at 37 $^{\circ}$ C for 60 minutes. The first PCR reaction solution contained 5 μ l of the synthesized cDNA solution, 10 μ l of 10X polymerase reaction buffer, 500 μ M each of dCTP, dATP, dGTP and dTTP, 15 pmol of each external primer (EX-sense and EX-antisense), 4 units of Thermus Brockiamus Prozyme DNA polymerase (PROtech Technology Ent. Co., Ltd. Taipei, Taiwan, China), and water. The PCR cycles were: denaturing at 94 $^{\circ}$ C for 1 minute, annealing at 52 $^{\circ}$ C for 1 minute,

and primer extension at 72 °C for 1 minute. The cycles were repeated 40 times. The PCR product was reamplified with internal primers for nested PCR to obtain a higher sensitivity. The first and second PCR components were the same, but for the primer pairs (IN-sense and IN-antisense), the final product was electrophoresed on 2 % agarose gel and stained with ethidium bromide for the specific band of 101 base pairs.

Statistical analysis

A statistical software (SPSS for Windows, version 8.0, Chicago, Illinois) was used, with Student's *t*-test for continuous variables, χ^2 test or Fisher's exact test for categorical variables. Stepwise logistic regression and COX proportional hazards model were used for multivariate stepwise analysis to identify independently significant factors in predicting recurrence and mortality. A *P* value <0.05 was defined as significant.

RESULTS

No hAFP mRNA was detected in peripheral blood of all patients in control group

In patients with HCC, hAFP mRNA in peripheral blood was detected in 27% (22/81), 30% (24/81), and 23% (19/81) preoperatively, perioperatively and postoperatively, respectively. According to hAFP mRNA status, we classified patients into 8 groups. For example, in group 1, hAFP mRNA was consistently positive preoperatively, perioperatively, and postoperatively; in group 2, positive preoperatively and perioperatively but negative postoperatively; and in group 8, consistently negative preoperatively, perioperatively, and postoperatively, *etc* (Table 2).

Thirty-six patients (44.4%) had clinically detectable recurrence during the follow-up period (median 3 years, range 2-5 years), of whom 25 died. The presence of hAFP mRNA preoperatively did not correlate with the risk of recurrence (55% *vs.* 41%, *P*=0.280) and recurrence related mortality (*P*=0.7283) (Tables 3 and 4). In contrast, patients with postoperative hAFP mRNA had a significantly higher recurrence rate (90% *vs.* 31%, *P*<0.001), with an odds ratio of 19.2 (95% confidence interval [CI]: 4.0-91.7), which was also significantly associated with recurrence related mortality (*P*=0.017) (in the multivariate analysis by COX proportional hazards model) (Tables 3 and 4). The presence of hAFP mRNA perioperatively did not significantly correlate with the risk of recurrence (58% *vs.* 39%, *P*=0.093) and the recurrence related mortality (*P*=0.836) (Tables 3 and 4).

On multivariate analysis, the significant predictors of recurrence included vascular premeation (*P*=0.023), grade of cellular differentiation (*P*=0.007) and postoperative hAFP mRNA positivity (*P*<0.001 by univariate; *P*=0.067 by multivariate, weak significance) (Table 3). The significant parameters correlating with mortality after recurrence consisted of grade of cellular differentiation (*P*=0.057, weak significance) and postoperative hAFP mRNA (*P*=0.017) (Table 4).

Table 3 Predictors of HCC recurrence

Variables	<i>P</i> values	
	UV	MV
Sex	0.274	-
Age	0.842	-
Liver cirrhosis	0.019	-
HBsAg (+)	0.505	-
Anti-HCV (+)	0.622	-
Serum AFP	<0.001	-
Child-Pugh class	0.087	-
Size (<3 cm, >10 cm)	0.140	-
Capsule	<0.001	n.s.
Daughter nodules	<0.001	n.s.
Vascular permeation	<0.001	0.023
Edmondson Steiner grade	<0.001	0.007
Preoperative hAFP mRNA(+)	0.280	-
Preoperative hAFP mRNA(+)	0.093	-
Postoperative hAFP mRNA(+)	<0.001	0.067

UV: univariate analysis, MV: multivariate analysis, AFP: serum alpha fetoprotein, HBsAg(+): positive hepatitis B surface antigen, Anti-HCV(+): positive hepatitis C virus antibody, Edmondson and Steiner grade: differentiation grades I, II *vs.* III, IV, n.s.: not significant.

Table 4 Correlation between variables and recurrence related mortality

Variables	<i>P</i> values	
	UV	MV
Sex	0.815	-
Age	0.930	-
Liver cirrhosis	0.039	n.s.
HBsAg (+)	0.835	-
Anti-HCV (+)	0.548	-
Serum AFP	<0.000	-
Child-Pugh class	0.092	-
Size (<3 cm, >10 cm)	0.274	-
Capsule	0.004	n.s.
Daughter nodules	0.004	n.s.
Vascular permeation	<0.001	n.s.
Edmondson Steiner grade	<0.001	0.057
Preoperative hAFP mRNA (+)	0.728	-
Perioperative hAFP mRNA (+)	0.835	-
Postoperative hAFP mRNA (+)	<0.001	0.017

UV: univariate analysis, MV: multivariate analysis, AFP: serum alpha fetoprotein, HBsAg (+): positive hepatitis B surface antigen, Anti-HCV(+): positive hepatitis C virus antibody, Edmondson Steiner grade: differentiation grades I, II *vs.* III, IV, n.s. :not significant.

Table 2 Correlation among timing of blood sample collection and circulating tumor cell status and postoperative recurrence

Group	Preoperation (baseline)	Perioperation (within 12 hours after surgery)	Postoperation (90 days after surgery)	Number of patients	Patient number of recurrence (%)
1.	Positive	Positive	Positive	9	8 (88.9)
2.	Positive	Positive	Negative	3	2 (66.7)
3.	Positive	Negative	Positive	2	2 (100)
4.	Positive	Negative	Negative	8	0 (0)
5.	Negative	Positive	Positive	5	4 (80)
6.	Negative	Positive	Negative	7	0 (0)
7.	Negative	Negative	Positive	3	3 (100)
8.	Negative	Negative	Negative	44	17 (38.6)
Overall				81	36 (44.4)

DISCUSSION

Surgical dissemination of tumor cells has been observed in various solid cancers and manipulation *per se* has been regarded as the main cause. According to Nishizaki, using inoculation of VX2 carcinoma into rabbit liver, manual manipulation of a tumor might well enhance metastasis^[25]. According to Liotta, tumor massage resulted in at least a 10-fold rise over the initial concentration of tumor cells, as well as a higher proportion of large clumps^[26]. Yamanaka *et al.* demonstrated a large quantity of HCC cells in the portal vein during hepatic resection^[27]. In our series, 30% of patients had the presence of hAFP mRNA perioperatively. The detection rate seemed higher than that of preoperation (27%), and postoperation (23%), but the difference had no statistical significance among them. In addition, this increase did not correlate with postresection recurrence. Further more, from individual group point of view, we found the alteration from preoperative negativity to perioperative positivity in groups 5 and 6 (Table 2). Whereas the postoperative recurrence varied greatly (80% vs 0%) between them. Statistically, perioperative detection did not contribute to cancer dissemination (Table 3).

The interpretation of detection of hAFP mRNA remains controversial. From our study, among 3 different sessions of blood sampling, only postoperative detection of hAFP mRNA correlated significantly with postresection recurrence related mortality. We proposed that some possible factors contributed to the different significance among the three different blood sampling times.

The detection before surgery may be attributed to the cells released spontaneously from primary tumor *in situ*. HCC tissue is surrounded by a vascular space analogous to the hepatic sinusoids. Because of this anatomic structure, tumor cells might easily be released into the sinusoids spontaneously. Thereafter, they might migrate into the portal or hepatic vein and finally enter the systemic circulation. However, from our study, these preoperative circulating HCC cells had no prognostic significance.

Molecular methods now permit us to detect a small number of cancer cells in the blood by use of RT-PCR targeting a cell-specific gene. Studies in animal models have indicated that at least 10^4 circulating tumor cells are required for metastasis to develop. To date, however, the absolute number of cells required for metastasis in the human circulation is unclear and even if cancer cells are detected in the circulation, their potential to develop metastatic foci is unknown. When malignant cells were released into the circulation, a variety of host and tumor cell factors could determine their distribution and fate^[28-33]. Most circulating HCC cells may rapidly die in the blood by various host immune and non-immune defenses, and are destroyed by mechanical forces, including turbulence and the trauma associated with vascular adhesion and transcapillary passage, or lysed by lymphocytes, monocytes, and natural killer (NK) cells. Some tumor cells are nonspecifically trapped or specifically arrested in the first capillary bed encountered. Circulating tumor cells trapped in a given location could then recirculate and arrest at other locations, then grow into tumor colonies^[29-33].

Okuda *et al.*^[34] and Komeda *et al.*^[14] could not detect any hAFP gene transcripts in patients with liver metastases or in healthy persons. Ijichi *et al.* considered this RT-PCR assay targeting hAFP mRNA as a sensitive and specific method for detecting HCC cells in the circulation *in vivo* and *in vitro* experiments, and no positivity was found in any healthy controls^[35]. From our study, hAFP mRNA could not be detected from all the 50 controls. However, some authors suggested that AFP gene was not hepatoma-specific, but rather a liver-specific marker^[13,15,17,18,36,37].

Surgery itself may increase the release of liver cells, not only HCC cells but also normal hepatocytes. Both kinds of cells may contribute to the positivity of hAFP mRNA. According to Louha M, not only liver surgery but also nonsurgical invasive managements such as needle liver biopsy or intervention therapies such as TACE, chemotherapy and ethanol ablation therapy, the increased shedding of either HCC cells or normal hepatocytes into circulation might contribute to the increase of detection rate of hAFP mRNA^[38]. This was also the reason why we excluded those who had received these intervention therapies from the current study.

It has become a fact that RT-PCR based tests lose its specificity for HCC cell detection when they are performed on samples obtained immediately after surgical or nonsurgical invasive procedures. This pitfall may also account for the gap between the frequency of cell detection after surgery and the expected tumor recurrence rate. A consensus existed that hAFP mRNA might not be regarded as specific markers of HCC cells if blood samples were taken during liver surgery^[39].

Secondly, the different site of blood sampling might contribute to the discrepancy. Central venous blood in Kienle's study was drawn before it passed through any capillary bed, with only a short distance after leaving the liver, the cells expressing hAFP might not undergo apoptosis or were not filtered out in capillary beds, therefore possibly accounting for the high detection rate (46%) during surgery^[37]. Another factor influencing the detection of hAFP mRNA in intraoperative central venous blood samples might be by a "dilution effect" following intraoperative blood transfusion^[37]. This was the reason why we excluded those receiving transfusion from our study.

Thirdly, the different blood sampling time might contribute to the discrepancy. Similarly, from the literature, in intraoperative detection of other tumors, this factor also existed. Brown *et al.* sampled blood at the time of maximum tumor manipulation and postoperative 24 hours in those with breast cancer^[11]. Eschwege P obtained blood samples 5 minutes after prostate carcinoma removal^[9]. Warr RP obtained blood samples at 2 different sessions and 24 hours postoperatively in those with malignant melanoma^[10]. According to Hayashi N, the blood samples were obtained through a catheter in the portal vein before, during, and after manipulation of colorectal cancer^[40].

Lemoni obtained peripheral blood samples at two different intervals: the first, during the exploratory phase and the second, after hepatectomy was completed^[41]. Witzigmann obtained blood samples before and during the operation (after mobilization of the liver), and on the second postoperative day^[39]. Louha obtained peripheral blood samples before treatment, 1 hour and 24 hours after percutaneous ethanol injection or TACE treatment^[38]. Witzigmann obtained blood samples on the second day after TACE^[39].

Louha found unexpectedly that liver cells began spreading at an early stage during surgery, i.e., after liver mobilization and rotation, before liver parenchyma transection. This was probably related to the sponge-like structure of the liver and to the stretching and compression of the organ during liver mobilization^[42]. Surgery-related liver cell spreading also occurred more frequently, compared with that induced by needle liver biopsy. This difference of cell number was probably related to the different degree of manipulation on the liver between resection and biopsy.

In the present study, we selected the sampling time within the first 12 hours after hepatectomy because of two reasons. First, the so-called "maximal manipulation" during surgery was usually difficult to define. The degrees of manipulation among the mobilization of the liver, or the division of important vessels and ducts of the segment or lobe, and the dissection of

hepatic parenchyma, were difficult to quantitate. In addition, the detailed procedure among individual patients varied. Second, we believed that within 12 hours after resection, the released cells, if present, might still remain. Funaki, Okuda, and Ijichi thought destruction of circulating HCC cells transiently liberated during surgery needed 7 days^[15,34,35].

From prognostic point of view, in literature, whether the shedding of cancer cells during intraoperative manipulation contributed to cancer dissemination and postoperative recurrence has remained debatable^[33].

Witzigmann^[39] and Lemonie^[41] did not find any correlation between postresection recurrence of HCC and the presence of hAFP mRNA irrespective of whether it was measured before, during, or after surgery. Lemonie mentioned that his result concurred with other experimental and clinical data, suggesting that release of abnormal cells in the circulation, either spontaneously or secondary to surgical manipulation, was an intermittent and transient phenomenon^[41]. Okuda found that most patients whose hAFP mRNA was not detected in peripheral blood perioperatively were diagnosed as free of intrahepatic recurrence or distant metastasis within 9 months after the operation^[34].

In contrast, Ijichi *et al.* suggested that surgical dissemination might actually cause HCC recurrence within a short period^[35]. The fact that alteration from negative to positive hAFP mRNA throughout the perioperative time might indicate a high risk of recurrence has been emphasized by Okuda^[34]. Funaki *et al.* reported that hAFP mRNA positive 2-3 days after the operation might be thought of as a high risk indicator of recurrence^[15]. Ferris found HCC recurred in 28% of patients with HCC after orthotopic liver transplantation^[43]. Ferris inferred that circulating HCC cells were present in the peripheral blood even after removal of the diseased liver, and that these residual tumor cells formed intra- and extra-hepatic metastatic foci after transplantation. To decrease cancer dissemination, we suggest that forceful mobilization or manipulation of the liver has to be avoided.

In addition, some studies have proposed anesthesia and unrelated surgery promote the spread of malignant disease^[44]. It is another challenging issue whether surgery *per se*, or general anesthesia *per se*, or both, may change the immune system of the host perioperatively and increase the opportunity of postoperative cancer spread.

Based on Salo's animal studies, during an operation, operative trauma was generally considered to have a greater role than anaesthesia in altering immune responses. The immune responses to major surgery, and operative complications resulting in massive mediator release might place the patient at risk^[44].

Recent investigations have suggested that general anesthesia may cause an unregulated activation of the process of apoptosis leading to lymphocytopenia and immune suppression resulting in different response in B-lymphocytes (but not in T-lymphocytes), natural killer cell activity or antibody-dependent cellular cytotoxicity 3-4 days after surgery^[44,45]. The true trigger mechanisms are still unclear. However, lymphocytopenia was not found in our patients, and it might not have significant contribution to recurrence. The association between transfusion-induced immunosuppression and poorer prognosis in patients with cancer has also been mentioned^[46]. It was also the reason why we excluded those receiving intraoperative transfusion from this study.

The postoperative presence of circulating HCC cells may therefore represent surviving malignancy that can continue the metastatic process. The possible explanations are as follows. A proportion of cancer cells released from the resected tumor (s) survive in the circulation for a long time without being destroyed, or the presence of unresected occult metastases are undetectable at the time of surgery, or a newly developing

malignant focus is too small to be detected by conventional follow-up studies.

Perioperative detection of hAFP mRNA has no relevant and significant role in the prediction of prognosis. We suggest surgical resection itself accelerate cancer dissemination and does not increase postoperative recurrence significantly either.

REFERENCES

- Anonymous.** Primary liver cancer in Japan. Clinicopathologic features and results of surgical treatment. Liver Cancer Study Group of Japan. *Ann Surg* 1990; **211**: 277-287
- Lee CS, Hwang LY, Beasley RP, Hsu HC, Lee HS, Lin TY.** Prognostic significance of histologic findings in resected small hepatocellular carcinoma. *Acta Chir Scand* 1988; **154**: 199-203
- Lai EC, Ng IO, Ng MM, Lok AS, Tam PC, Fan ST, Choi TK, Wong J.** Long term results of resection for large hepatocellular carcinoma: A multivariate analysis of clinicopathological features. *Hepatology* 1990; **11**: 815-818
- Jeng KS, Chen BF, Lin HJ.** En bloc resection for extensive hepatocellular carcinoma: Is it advisable? *World J Surg* 1994; **18**: 834-839
- Goldblatt SA, Nadel EM.** Cancer cells in the circulating blood: a critical review. *Acta Cytol* 1965; **305**: 6-20
- Glaves D.** Correlation between circulation cancer cells and incidence of metastases. *Br J Cancer* 1983; **48**: 665-673
- Fidler IJ.** The biology of human cancer metastasis. 7th Jan Waldenstrom lecture. *Acta Oncol* 1991; **30**: 668-675
- Raper SR.** Answering questions on a microscopic scale: the detection of circulation cancer cells. *Surgery* 1999; **126**: 827-828
- Eschwege P, Dumas F, Blanchet P, Le Maire V, Benoit G, Jardin A, Lacour B, Loric S.** Haematogenous dissemination of poststatic epithelium cells during radical prostatectomy. *Lancet* 1995; **346**: 1528-1530
- Warr RP, Zebedee Z, Kenealy J, Rigby H, Kemshead JT.** Detection of melanoma seeding during surgical procedures - an RT-PCR based model. *Eur J Surg Oncol* 2002; **28**: 832-837
- Brown DC, Purushotham AD, Birnie GD, George WD.** Detection of intraoperative tumor cell dissemination in patients with breast cancer by use of reverse transcription and polymerase chain reaction. *Surgery* 1995; **117**: 96-101
- Miyazono F, Takao S, Natsugoe S, Uchikura K, Kijima F, Aridome K, Shinchi H, Aikou T.** Molecular detection of circulating cancer cells during surgery in patients with biliary-pancreatic cancer. *Am J Surg* 1999; **77**: 475-479
- Matsumura M, Niwa Y, Hikiba Y, Okano K, Kato N, Shiina S, Shirator Y, Omata M.** Sensitive assay for detection of hepatocellular carcinoma associated gene transcription (Alpha-fetoprotein mRNA) in blood. *Biol and Biophys Communi* 1995; **2**: 813-815
- Komeda T, Fukuda Y, Sando T, Kita R, Furudawa M, Nishida N, Amenomri M, Nakao K.** Sensitive detection of circulating hepatocellular carcinoma cells in peripheral venous blood. *Cancer* 1995; **75**: 2214-2219
- Funaki NO, Tanaka J, Seto S, Kasamatsu T, Kaido T, Imamura M.** Hematogenous spreading of hepatocellular carcinoma cells: possible participation in recurrence in the liver. *Hepatology* 1997; **25**: 564-568
- Jiang SY, Shyu RY, Huang MF, Tang HS, Young TH, Roffler SR, Chiou YS, Yeh MY.** Detection of alphafetoprotein-expressing cells in the blood of patients with hepatoma and hepatitis. *Br J Cancer* 1997; **75**: 928-933
- Wong IHN, Lau WY, Leung T, Johnson PJ.** Quantitative comparison of alpha-fetoprotein and albumin mRNA levels in hepatocellular carcinoma/adenoma, non-tumor liver and blood: implications in cancer detection and monitoring. *Cancer Lett* 2000; **156**: 141-149
- Matsumura M, Niwa Y, Kato N, Komatsu Y, Shiina S, Kawabe T, Kawase T, Toyoshima H, Ihori M, Shiratori Y.** Detection of α -fetoprotein mRNA, an indicator of hematogenous spreading hepatocellular carcinoma, in the hepatocellular carcinoma, in the circulation: A possible predictor of metastatic hepatocellular carcinoma. *Hepatology* 1994; **20**: 1418-1425
- Barbu V, Bonnand AM, Hillaire S, Coste T, Chazouilleres O, Gugenheim J, Boucher E, Poupon R, Poupon RE.** Circulating al-

- bumin messenger RNA in hepatocellular carcinoma: results of a multicenter prospective study. *Hepatology* 1997; **26**: 1171-1175
- 20 **Hillaire S**, Barbu V, Boucher E, Moukhtar M, Poipon R. Albumin messenger RNA as a marker of circulating hepatocytes in hepatocellular carcinoma. *Gastroenterology* 1994; **106**: 239-242
- 21 **Chou HC**, Sheu JC, Huang GT, Wang JT, Chen DS. Albumin messenger RNA is not specific for circulating hepatoma cells. *Gastroenterology* 1994; **2**: 630
- 22 **Muller C**, Petermann D, Pfeffel F, Osterreicher C, Fugger R. Lack of specificity of albumin-mRNA-positive cells as a marker of circulating hepatoma cells. *Hepatology* 1997; **25**: 896-899
- 23 **Niwa Y**, Matsumura M, Shiratori Y, Imamura M, Kato N, Shiina S, Okudaira T, Ikeda Y, Inoue T, Omata M. Quantitation of α -fetoprotein and albumin messenger RNAs in human hepatocellular carcinoma. *Hepatology* 1996; **23**: 1384-1392
- 24 **Di Bisceglie AM**, Dusheiko GM, Paterson AC, Alexander J, Shouval D, Lee CS, Beasley RP, Kew MC. Detection of alphafetoprotein messenger RNA in human hepatocellular carcinoma and hepatoblastoma tissue. *Br J Cancer* 1986; **54**: 779-785
- 25 **Nishizaki T**, Matsumata T, Kanematsu T, Yasunaga C, Sugimachi K. Surgical manipulation of VX2 carcinoma in the rabbit liver evokes enhancement of metastases. *J Surg Res* 1990; **49**: 92-97
- 26 **Liotta LA**, Kleinerman J, Saidel GM. Quantitative relationships of intravascular tumor cells, tumor vessels and pulmonary metastasis following tumor implantation. *Cancer Res* 1974; **34**: 997-1004
- 27 **Yamanaka N**, Okamoto E, Fujihara S, Kato T, Fujimoto J, Oriyama T, Mitsunobu M, Toyosaka A, Uematsu K, Yamamoto K. Do the tumor cells of hepatocellular carcinomas dislodge into the portal venous stream during hepatic resection? *Cancer* 1992; **70**: 2263-2267
- 28 **Hermanek P**, Hutter RVP, Sobin LH, Wittekind C. International Union Against Cancer. Classification of isolated tumor cells and micrometastasis. *Cancer* 1999; **86**: 2668-2673
- 29 **Glaves D**. Metastasis: reticuloendothelial system and organ retention of disseminated malignant cells. *Int J Cancer* 1980; **26**: 115-122
- 30 **Fidler I**, Gersten D, Riggs C. Relationship of host immune status to tumor cell arrest, distribution, and survival in experimental metastasis. *Cancer* 1977; **40**: 46-55
- 31 **Mayhew E**, Glaves D. Quantitation of tumorigenic disseminating and arrested cancer cells. *Br J Cancer* 1984; **50**: 159-166
- 32 **Romsdahl MM**, Mcgrath RG, Hoppe E, McGrew EA. Experimental model for the study of tumor cells in the blood. *Acta Cytol* 1965; **9**: 141-145
- 33 **Mori M**, Mimori K, Ueo H, Karimine N, Barnard GF, Sugimachi K, Akiyoshi T. Molecular detection of circulating solid carcinoma cells in the peripheral blood: the concept of early systemic disease. *Int J Cancer* 1996; **68**: 739-743
- 34 **Okuda N**, Nakao A, Takeda S, Oshima K, Kanazumi N, Nonami T, Kurokawa T, Takagi H. Clinical significance of alpha-fetoprotein mRNA during perioperative period in HCC. *Hepatogastroenterology* 1999; **46**: 381-386
- 35 **Ijichi M**, Takayama T, Matsumura M, Shiratori Y, Omata M, Makuuchi M. alpha-Fetoprotein mRNA in the circulation as a predictor of postsurgical recurrence of hepatocellular carcinoma: a prospective study. *Hepatology* 2002; **35**: 853-860
- 36 **Ishikawa T**, Kashiwagi H, Iwakami Y, Hirai M, Kawamura T, Aiyoshi Y, Yashiro T, Ami Y, Uchida K, Miwa M. Expression of alpha-fetoprotein and prostate-specific antigen genes in several tissues and detection of mRNAs in normal circulating blood by reverse transcriptase-polymerase chain reaction. *Jpn J Clin Oncol* 1998; **28**: 723-728
- 37 **Kienle P**, Weitz J, Klaes R, Koch M, Benner A, Lehnert T, Herfarth C, von Knebel Doeberitz M. Detection of isolated disseminated tumor cells in bone marrow and blood samples of patients with hepatocellular carcinoma. *Arch Surg* 2000; **135**: 213-218
- 38 **Louha M**, Poussin K, Ganne N, Zylberberg H, Nalpas B, Nicolet J, Capron F, Soubrane O, Vons C, Pol S, Beaugrand M, Berthelot P, Franco D, Trinchet JC, Brechot C, Paterlini P. Spontaneous and iatrogenic spreading of liver-derived cells into peripheral blood of patients with primary liver cancer. *Hepatology* 1997; **26**: 43-50
- 39 **Witzigmann H**, Geibler F, Benedix F, Thiery J, Uhlmann D, Tannapfel A, Wittekind C, Hauss J. Prospective evaluation of circulating hepatocytes by α -fetoprotein messenger RNA in patients with hepatocellular carcinoma. *Surgery* 2002; **131**: 34-43
- 40 **Hayashi N**, Egami H, Kai M, Kurusu Y, Takano S, Ogawa M. No-touch isolation technique reduces intraoperative shedding of tumor cells into the portal vein during resection of colorectal cancer. *Surgery* 1999; **125**: 369-374
- 41 **Lemonie A**, Bricon TL, Salvucci M, Azoulay D, Pham P, Raccuia J, Bismuth H, Debuire B. Prospective evaluation of circulating hepatocytes by alpha-fetoprotein mRNA in humans during liver surgery. *Ann Surg* 1997; **226**: 43-50
- 42 **Louha M**, Nicolet J, Zylberberg H, Sabile A, Vons C, Vona G, Poussin K, Tournebize M, Capron F, Pol S, Franco D, Lacour B, Brechot C, Paterlini-Brechot P. Liver resection and needle liver biopsy cause hematogenous dissemination of liver cells. *Hepatology* 1999; **29**: 879-882
- 43 **Ferris JV**, Baron RL, Marsh JW, Oliver JH, Carr BI, Dodd III GD. Recurrent hepatocellular carcinoma after liver transplantation: spectrum of CT findings and recurrence patterns. *Radiology* 1996; **198**: 233-238
- 44 **Salo M**. Effects of anaesthesia and surgery on the immune response. *Acta Anaesthesiol Scand* 1992; **36**: 201-220
- 45 **Delogu G**, Mortti S, Famularo G, Marce;ono S, Santini G, Antonucci A, Marandola M, Signore L. Mitochondria perturbations and oxidant stress in lymphocytes from patients undergoing surgery and general anesthesia. *Arch Surg* 2001; **136**: 1190-1196
- 46 **Yamamoto J**, Kosuge T, Takayama T, Shimada K, Yamasaki S, Ozaki H, Yamaguchi N, Mizuno S, Makuuchi M. Perioperative blood transfusion promotes recurrence of hepatocellular carcinoma after hepatectomy. *Surgery* 1994; **115**: 303-309

Effects of *Ginkgo biloba* extract on cell proliferation and cytotoxicity in human hepatocellular carcinoma cells

Jane CJ Chao, Chia Chou Chu

Jane CJ Chao, Chia Chou Chu, School of Nutrition and Health Sciences, Taipei Medical University, Taipei 110, Taiwan, China

Supported by Taipei Medical University, No. TMU90-Y05-A112

Correspondence to: Jane CJ Chao, School of Nutrition and Health Sciences, Taipei Medical University, Taipei 110, Taiwan, China. chenju@tmu.edu.tw

Telephone: +86-2-2736-1661 #6551~6556 Ext. 117

Fax: +886-2-2737-3112

Received: 2003-08-23 **Accepted:** 2003-10-12

Abstract

AIM: To study the effect of *Ginkgo biloba* extract (EGb 761) containing 22-27% flavonoids (ginkgo-flavone glycosides) and 5-7% terpenoids (ginkgolides and bilobalides) on cell proliferation and cytotoxicity in human hepatocellular carcinoma (HCC) cells.

METHODS: Human HCC cell lines (HepG2 and Hep3B) were incubated with various concentrations (0-1 000 mg/L) of EGb 761 solution. After 24 h incubation, cell proliferation and cytotoxicity were determined by 3-(4,5-dimethylthiazol-2-yl)-5-(3-carboxymethoxyphenyl)-2-(4-sulfophenyl)-2H-tetrazolium (MTS) assay and lactate dehydrogenase (LDH) release, respectively. After 48 h incubation, the expression of proliferating cell nuclear antigen (PCNA) and p53 protein was measured by Western blotting.

RESULTS: The results showed that EGb 761 (50-1 000 mg/L) significantly suppressed cell proliferation and increased LDH release ($P < 0.05$) in HepG2 and Hep3B cells compared with the control group. The cell proliferation of HepG2 and Hep3B cells treated with EGb 761 (1 000 mg/L) was 45% and 39% of the control group ($P < 0.05$), respectively. LDH release of HepG2 cells without and with EGb 761 (1 000 mg/L) treatment was 6.7% and 37.7%, respectively, and that of Hep3B cells without and with EGb 761 (1 000 mg/L) treatment was 7.2% and 40.3%, respectively. The expression of PCNA and p53 protein in HepG2 cells treated with EGb 761 (1 000 mg/L) was 85% and 174% of the control group, respectively.

CONCLUSION: *Ginkgo biloba* extract significantly can suppress proliferation and increase cytotoxicity in HepG2 and Hep3B cells. Additionally, *Ginkgo biloba* extract can decrease PCNA and increase p53 expression in HepG2 cells.

Chao JCJ, Chu CC. Effects of *Ginkgo biloba* extract on cell proliferation and cytotoxicity in human hepatocellular carcinoma cells. *World J Gastroenterol* 2004; 10(1): 37-41
<http://www.wjgnet.com/1007-9327/10/37.asp>

INTRODUCTION

Extract from the leaves of *Ginkgo biloba* (maidenhair tree) has been used therapeutically in China and Western countries for centuries. The liquid extract was made from dried leaves with an extraction ratio of 1:50^[1]. Standard *Ginkgo biloba*

extract, EGb 761 (commercial name), contains 22-27% flavonoids (ginkgo-flavone glycosides) and 5-7% terpenoids (ginkgolides and bilobalides), which are the most important active substances in the extract. The most important flavonoids are glycosides of kaempferol, quercetin, and isorhamnetin with glucose or rhamnose. Ginkgolides, not found in any other living species and only present in *Ginkgo biloba* extract, can be divided into types A, B, C, and a very small quantity of J, which are only different in the number and position of hydroxyl groups.

Ginkgo biloba extract has been mentioned in the traditional Chinese pharmacopoeia, and used for the treatment of asthma and bronchitis^[1]. *Ginkgo biloba* extract is well known for its antioxidant property, which may result from its ability to scavenge free radicals^[2], and to neutralize ferryl ion-induced peroxidation^[3]. Several studies have reported that the antioxidant activity of *Ginkgo biloba* extract could be helpful in the prevention and therapy of diseases and degenerative processes associated with oxidative stress^[4-8]. However, there have been very limited studies on the anti-proliferative activity of *Ginkgo biloba* extract. Ginkgetin or isoginkgetin, a biflavonoid from *Ginkgo biloba* extract, at 10 $\mu\text{mol/L}$ showed a suppressive activity against lymphocyte proliferation induced by concanavalin A (ConA) or lipopolysaccharides (LPS)^[9]. Additionally, Su *et al.*^[10] found that ginkgetin selectively inhibited the proliferation of human ovarian carcinoma OVCAR-3 cells via the induction of apoptosis in a dose-dependent manner. So far, no study has investigated the effect of *Ginkgo biloba* extract on hepatocellular carcinoma (HCC), which is the most common malignant tumor occurred in men in Taiwan. It is reasonably hypothesized that *Ginkgo biloba* extract may be helpful for the therapy of HCC through regulating cell proliferation and/or cell death. Therefore, the purpose of this study was to investigate the cytotoxic effect of *Ginkgo biloba* extract on HCC.

MATERIALS AND METHODS

Cell culture and treatments

Human hepatocellular carcinoma cell lines, HepG2 (BCRC No. 60025) and Hep3B2.1-7 (Hep3B, BCRC No. 60434) were purchased from the Bioresources Collection and Research Center (BCRC) of the Food Industry Research and Development Institute (Hsinchu, Taiwan). Cells were grown in 900 mL/L minimum essential medium (MEM, GIBCO™, Invitrogen Corp., Carlsbad, CA) containing 100 mL/L fetal bovine serum (GIBCO™) at 37 °C in a humidified atmosphere of 950 mL/L air and 50 mL/L CO₂. Prior to addition of the treatment, the cells were grown to 80-90% confluency and synchronized by incubating in the basal medium (100% MEM) for 24 h. The cells were then incubated with various concentrations (0-1 000 mg/L) of standard *Ginkgo biloba* extract solution (EGb 761, Cerenin®, Dr. Willmar Schwabe GmbH and Co., Karlsruhe, Germany) for 24 or 48 h. *Ginkgo biloba* extract contained 22-27% flavonoids and 5-7% terpenoids in 10 mL/L ethanol and 10 mL/L sorbitol solution. Cells without addition of *Ginkgo biloba* extract as the control group were incubated with 10 mL/L ethanol and 10 mL/L sorbitol solution. The cells and medium were collected. Protein contents in cells and medium were

measured by the modified method of Lowry *et al.*^[11] using a Bio-Rad DC protein kit (Bio-Rad Laboratories, Hercules, CA).

Cell proliferation assay

Cell viability was colorimetrically determined at 490 nm using a commercial proliferation assay kit (CellTiter 96[®] AQ_{ueous}, Promega Corp., Madison, WI). After incubation with various concentrations of EGb 761 for 24 h, the cells ($n=8$) in a 96-well plate were incubated with 333 mg/L 3-(4,5-dimethylthiazol-2-yl)-5-(3-carboxymethoxyphenyl)-2-(4-sulfophenyl)-2H-tetrazolium (MTS) and 25 μ mol/L phenazine methosulfate solution for 3 h at 37 °C in a humidified, 50 mL/L CO₂ atmosphere^[12]. The absorbance of soluble formazan produced by cellular reduction of MTS was measured at 490 nm using an ELISA reader (Multiskan RC, Labsystems, Helsinki, Finland).

Cell cytotoxicity assay

Lactate dehydrogenase (LDH) release from cells was determined as an index of cytotoxicity or necrosis. The quantity of LDH released by the cells into the medium was measured by the decrease in the absorbance at 340 nm for NADH disappearance within 5 min^[13]. After incubation with various concentrations of EGb 761 for 24 h, the cell culture supernatant and medium (100 μ L) were mixed with 900 μ L of modified Krebs-Henseleit buffer (118 mmol/L NaCl, 4.8 mmol/L KCl, 1 mmol/L KH₂PO₄, 24 mmol/L NaHCO₃, 3 mmol/L CaCl₂, 0.8 mmol/L MgPO₄, pH 7.4), 0.2 mmol/L NADH, 1.36 mmol/L sodium pyruvate, and 20 mg/L bovine serum albumin (BSA). Percentage of LDH release ($n=3$) was equal to LDH activity in medium divided by that in both cell culture supernatant and medium $\times 100\%$.

Analysis of proliferating cell nuclear antigen (PCNA) and p53 protein

After incubation with various concentrations of EGb 761 for 48 h, cell suspension (15 μ g and 50 μ g protein for PCNA and p53) pooled from 6 independent experiments ($n=6$) was mixed with an equal volume of 2 \times SDS-PAGE sample buffer (0.125 mol/L Tris-HCl, pH 6.8/40 mg/L SDS/200 mL/L glycerol/100 mL/L 2-mercaptoethanol)^[14], denatured at 100 °C for 3 min, and applied to SDS-PAGE (Bio-Rad Mini-PROTEAN 3 Cell, Bio-Rad Laboratories). Proteins were separated by 12.5% resolving gel, with 4% stacking gel in the running buffer (25 mmol/L Tris, pH 8.3/192 mmol/L glycine/1 mg/L SDS) at 100 V for 1.5 h. After that, the proteins were transferred onto nitrocellulose membrane (0.45 μ m) using a semi-dry transfer unit (Hoefer Semiphor TE 70, Amersham Biosciences Corp., San Francisco, CA) in Towbin buffer (25 mmol/L Tris/192 mmol/L glycine/1.3 mmol/L SDS/100 mL/L methanol) at 200 mA for 1.5 h^[15]. The membrane was washed briefly with PBS, and incubated with a blocking buffer (50 mg/L skim milk/1 mL/L Tween-20 in PBS) for 1 h. Then the membrane was incubated with 0.4 mg/L mouse anti-human PCNA (PC-10, 0.2 mg/L), p53 (DO-1, 0.4 mg/L), or α -tubulin (TU-02, 1 mg/L) mAb (Santa Cruz Biotechnology, Inc., Santa Cruz, CA) at room temperature for 1 h. Alpha-tubulin was as an internal control. The membrane was washed 3 times with the wash buffer (1 mL/L Tween-20 in PBS), and incubated with 0.2 mg/L goat anti-mouse IgG-horseradish peroxidase conjugate (Santa Cruz Biotechnology, Inc.) for 1.5 h. The blot was washed 3 times again with the wash buffer, incubated with luminol reagent (Santa Cruz Biotechnology, Inc.) for 1 min, and exposed to an X-ray film (Eastman Kodak Co., Rochester, NY) for 5-10 s. The bands were quantitated by an image analysis system (Gel analysis system, EverGene Biotechnology, Taipei, Taiwan) and Phoretix 1D Lite software (version 4.0, Phoretix International Ltd., Newcastle upon Tyne, UK).

Statistical analysis

Data are expressed as $\bar{x} \pm s$. Data were analyzed by one-way ANOVA to determine the treatment effect using SAS (version 8.2, SAS Institute Inc., Cary, NC). Fisher's least significant difference test was used to make *post-hoc* comparisons if the treatment effect was demonstrated. Differences were considered significant when $P < 0.05$.

RESULTS

Cell proliferation assay

After 24 h incubation, EGb 761 (25-1 000 mg/L) significantly inhibited cell growth ($P < 0.05$) in HepG2 cells compared with the control group in a dose-dependent manner determined by MTS assay (Figure 1). EGb 761 at 750 and 1 000 mg/L inhibited cell growth to 50% and 45% of the control, respectively, in HepG2 cells. Similarly, EGb 761 (50-1 000 mg/L) dose-dependently inhibited cell growth ($P < 0.05$) in Hep3B cells compared with the control group. EGb 761 at 750 and 1 000 mg/L inhibited cell growth to 48% and 39% of the control, respectively, in Hep3B cells.

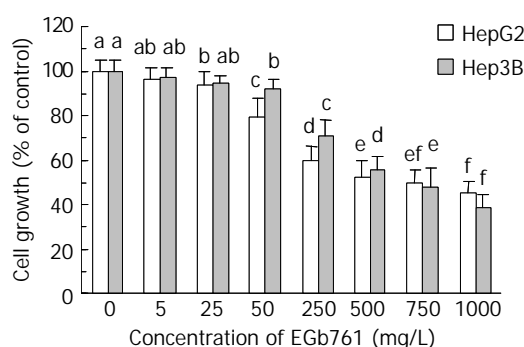


Figure 1 Effects of EGb 761 on cell growth in HepG2 and Hep3B cells measured by MTS assay. Data are expressed as $\bar{x} \pm s$ ($n=8$). Values not sharing the same letter differed significantly ($P < 0.05$) in the same cell line by Fisher's least significant difference test.

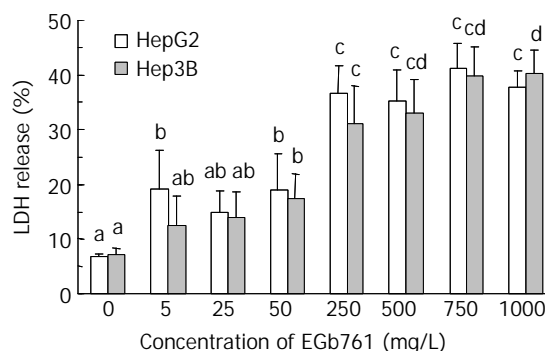


Figure 2 Effects of EGb 761 on cell cytotoxicity in HepG2 and Hep3B cells determined by lactate dehydrogenase (LDH) release. Data are expressed as $\bar{x} \pm s$ ($n=3$). Values not sharing the same letter differed significantly ($P < 0.05$) in the same cell line by Fisher's least significant difference test.

Cell cytotoxicity assay

Cell cytotoxicity was directly measured by LDH release. After 24 h incubation, EGb 761 (50-1 000 mg/L) significantly increased cell cytotoxicity ($P < 0.05$) in both HepG2 and Hep3B cells compared with the control group (6.7% and 7.2% in HepG2 and Hep3B cells) (Figure 2). EGb 761 at a dose of 250 mg/L significantly increased LDH release to 36.6% and 31.2% ($P < 0.05$), respectively, in HepG2 and Hep3B cells compared with EGb 761 at a dose of 50 mg/L (18.9% and

17.5% in HepG2 and Hep3B cells). However, EGb 761 at the dose of 250-1 000 mg/L did not dose-dependently increase cell cytotoxicity in both HepG2 (35.2-41.3% LDH release) and Hep3B (31.2-40.3% LDH release) cells.

Analysis of proliferating cell nuclear antigen (PCNA) and p53 protein

After 48 h incubation with EGb 761, the expression of PCNA and p53 protein in HepG2 cells was analyzed by SDS-PAGE and Western blotting. EGb 761 at the dose of 500, 750, and 1 000 mg/L decreased PCNA expression to 90%, 84%, and 85% of the control, respectively (Figure 3). However, EGb 761 at the dose of 500, 750, and 1 000 mg/L increased p53 expression to 135%, 152%, and 174% of the control, respectively (Figure 4).

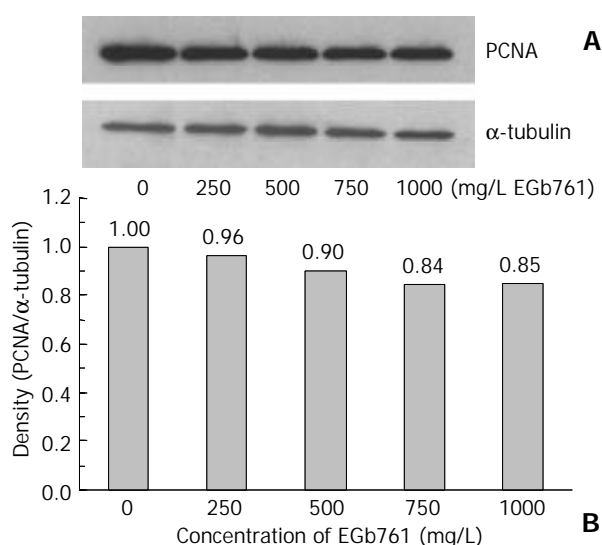


Figure 3 Expression of proliferating cell nuclear antigen (PCNA) with the molecular weight of 36 kDa which was visualized by Western blotting (A) and quantitated by an image analysis system (B) after HepG2 cells were incubated with 0-1 000 mg/L EGb 761 for 48 h. Samples were pooled from 6 independent experiments ($n = 6$). Alpha-tubulin (55 kDa) was as an internal control.

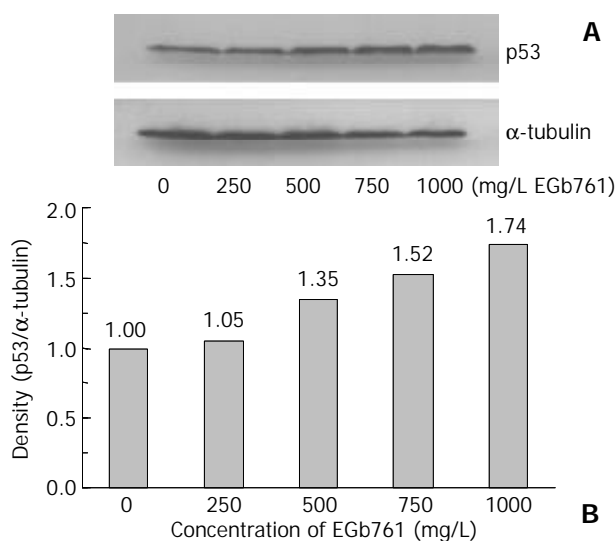


Figure 4 Expression of p53 protein with the molecular weight of 53 kDa which was visualized by Western blotting (A) and quantitated by an image analysis system (B) after HepG2 cells were incubated with 0-1 000 mg/L EGb 761 for 48 h. Samples were pooled from 6 independent experiments ($n=6$). Alpha-tubulin (55 kDa) was as an internal control.

DISCUSSION

Ginkgo biloba extract (EGb 761) at the dose of 50-1 000 mg/L significantly decreased cell proliferation measured by MTS assay in a dose-dependent manner in both HepG2 and Hep3B cells with 50% inhibition at approximately 750 mg/L. Similarly, EGb 761 and ginkgolide B were found to inhibit cell proliferation in highly aggressive human breast cancer MDA-231 cells in a dose-dependent manner^[16]. Another *Ginkgo biloba* extract, IPS200 devoid of proanthocyanidins, at 200 mg/L decreased cell proliferation of Hep3B cells^[17]. EGb 761 also showed an inhibitory effect on cell proliferation of cultured vascular smooth muscle cells in a dose-dependent pattern *in vitro* and significantly decreased the percentage of proliferating cells in the balloon-injured abdominal aorta of cholesterol-fed rabbits *in vivo*^[18]. Additionally, EGb 761 given orally at 50 or 100 mg/kg·d or superoxide dismutase injected intravenously at 15 000 U/kg·d inhibited preretinal proliferation in pigmented rabbits, suggesting that antioxidants might efficiently prevent preretinal proliferation^[19]. The biflavonoids of *Ginkgo biloba* extract, ginkgetin and isoginkgetin at 10 μmol/L, inhibited lymphocyte proliferation induced by Con A or LPS^[9]. Ginkgetin was also found to dose-dependently inhibit the growth of human ovarian adenocarcinoma OVCAR-3 cells with 50% inhibition at 1.8 mg/L^[20]. Quercetin, an important flavonoid of *Ginkgo biloba* extract, significantly inhibited cell proliferation of HCC cell lines BEL-7402, HuH-7, and HLE with a peak inhibition at 50 μmol/L^[21]. The inhibitory effect of EGb 761 on cell proliferation may be attributed to its antioxidation capacity, however, other constituents of EGb 761 may contribute to its cytotoxic action. Recently, *Ginkgo biloba* extract has been reported to affect gene expression related to cell growth^[17]. EGb 761 dramatically reduced, in a consistent manner, the expression of α-fetoprotein in Hep3B cells using fluorescence and membrane DNA microarrays, in which protein is present at very low concentration in adults but is increased in hepatoma patients. Moreover, IPS200 inhibited 40-50% mRNA levels of peripheral-type benzodiazepine receptor, positively correlated with cell proliferation and metastasis in MDA-231, Hep3B, and U87 (human glioblastoma) cells using quantitative RT-PCR and Northern blot analysis. In contrast to our study, a previous study demonstrated that the components of *Ginkgo biloba* extract, such as quercetin, kaempferol, sciadopitysin, ginkgetin, and isoginkgetin, enhanced cell proliferation of normal human skin fibroblasts *in vitro*^[22]. The various effects of *Ginkgo biloba* extract on cell proliferation may result from different cell lines, cell morphology (normal vs malignant), and the dosage of *Ginkgo biloba* extract or the individual constituents.

Besides the inhibitory effect of EGb 761 on cell proliferation, EGb 761 at higher doses (50-1 000 mg/L) significantly increased cytotoxicity determined by LDH release in both HepG2 and Hep3B cells. However, the cytotoxic effect of EGb 761 reached the plateau at the dose over 250 mg/L. The cytotoxic effect of EGb 761 could be attributed to necrosis and/or apoptosis. Our result revealed increased LDH release as an index of necrosis in EGb 761-treated cells, indicating that EGb 761 could enhance necrosis. Although we did not directly measure apoptosis, the expression of p53 protein, as an inducer of apoptosis in human HCC cells^[23], was increased in EGb 761-treated groups. There may exist the possibility that apoptosis contributes to the cytotoxic effect of EGb 761. The cytotoxic activity of EGb 761 has been suspected to derive from ginkgolic acids^[24,25] and ginkgetin^[10] through their induction of apoptosis. Ginkgolic acids restricted in EGb 761 at less than 5 μg/g have been recognized as hazardous compounds with suspected cytotoxic, allergenic, mutagenic, and carcinogenic properties^[24,25]. Ginkgolic acids caused death

of cultured chick embryonic neurons in a dose-dependent manner, and ginkgolide acid-induced death showed both signs of apoptosis and necrosis possibly via the mediation of protein phosphatase 2C^[24]. Additionally, increased apoptotic cells from 6% (control) to nearly 80% were found in human keratinocyte cell line HaCaT incubated with ginkgolide acids at the concentration of more than 30 mg/L, which was primarily regulated by transformation of mitochondria probably induced by uncoupling of oxidative phosphorylation^[25]. Ginkgetin (5 mg/L) increased intracellular levels of hydrogen peroxide and induced apoptosis in OVCAR-3 cells, which was mediated mainly through the activation of caspase (s) by the generation of hydrogen peroxide perhaps through autooxidation of ginkgetin^[10]. However, some constituents of EGb 761 have been reported to possess anti-apoptotic capacity^[26,27]. EGb 761 (100 mg/L), ginkgolide J (100 μmol/L), and ginkgolide B (10 μmol/L) reduced apoptosis from 74% in staurosporine-induced apoptotic chick embryonic neurons to 24%, 62%, and 31%, respectively^[26]. Furthermore, EGb 761 (100 mg/L) and bilobalide (100 μmol/L) rescued rat neurons from apoptosis induced by serum deprivation. A previous study also found that the total flavonoids of EGb 761, two pure flavonoid components (rutin and quercetin), and a mixture of flavonoids and terpenes protected cerebellar granule cells from oxidative stress and apoptosis induced by hydroxyl radicals^[27]. However, total terpenes of EGb 761 neither protected against apoptosis nor had a synergistic effect, suggesting that terpenes did not scavenge hydroxyl radicals directly to suppress apoptosis. The apoptosis-stimulatory and anti-apoptotic properties of EGb 761 might depend on the target cells, the dosage, and its constituents.

Both cell proliferation and apoptosis were involved in HCC^[27]. The expression of PCNA and p53 proteins has been regarded as cell proliferation and apoptosis biomarkers, respectively, for the malignant phenotype of HCC, and was associated with prognosis and therapeutic outcome^[28-31]. Cell proliferation was increased as HCC progressed to become more poorly differentiated^[29,30]. Apoptotic HCC cancer cells were consistently negative for PCNA, and p53-positive cancer cells showed apoptosis^[28]. Consistent with the result of MTS assay that EGb 761 suppressed cell proliferation of HCC cells, EGb 761 at the dose of 500-1 000 mg/L decreased the expression of PCNA by 10-16%. Additionally, the expression of p53 protein, measured in HepG2 cells expressing endogenous p53, while not in Hep3B cells lacking endogenous p53 expression^[32], was increased by 35-74% in EGb 761-treated groups (500-1 000 mg/L). It suggested that EGb 761 might be potentially useful for the prevention of HCC progression. *Ginkgo biloba* extract or its constituent has been considered as an anti-cancer agent. A previous study showed that EGb 761 ameliorated the deleterious effects on the forestomach and liver in mice with benzo(a)pyrene-induced gastric carcinoma^[33]. Furthermore, combined quercetin and a recombinant adenovirus vector expressing human p53, granulocyte-macrophage colony-stimulating factor (GM-CSF), and B7-1 (CD80) genes, as a combined anti-cancer agent, synergistically inhibited cell proliferation and induced apoptosis of HCC cells^[21].

In conclusion, *Ginkgo biloba* extract at the concentration above 50 mg/L can significantly suppress cell proliferation and increase cell cytotoxicity in human hepatocellular carcinoma cell lines. Additionally, *Ginkgo biloba* extract can decrease PCNA and increase p53 protein expression in HepG2 cells, suggesting that *Ginkgo biloba* extract may regulate not only cell proliferation but also apoptosis of HCC cells. Therefore, *Ginkgo biloba* extract may have therapeutic potential for HCC.

REFERENCES

- Kleijnen J**, Knipschild P. *Ginkgo biloba*. *Lancet* 1992; **340**: 1136-1139
- Gardès-Albert M**, Ferradini C, Sekaki A, Droy-Lefaix MT. Oxygen-centered free radicals and their interactions with EGb 761 or CP 202. In: Ferradini C, Droy-Lefaix MT, Christen Y, eds. *Advances in Ginkgo biloba extract research: Ginkgo biloba extract (EGb 761) as a free-radical scavenger*. New York: Elsevier Science 1993: 1-11
- Deby C**, Deby-Dupont G, Dister M, Pincemail J. Efficiency of *Ginkgo biloba* Extract (EGb 761) in neutralizing ferryl ion-induced peroxidations: therapeutic implication. In: Ferradini C, Droy-Lefaix MT, Christen Y, eds. *Advances in Ginkgo biloba extract research: Ginkgo biloba extract (EGb 761) as a free-radical scavenger*. New York: Elsevier Science 1993: 13-26
- Tosaki A**, Droy-Lefaix MT. Effects of free-radical scavengers, superoxide dismutase, catalase and *Ginkgo biloba* extract (EGb 761) on reperfusion-induced arrhythmias in isolated hearts. In: Ferradini C, Droy-Lefaix MT, Christen Y, eds. *Advances in Ginkgo biloba extract research: Ginkgo biloba extract (EGb 761) as a free-radical scavenger*. New York: Elsevier Science 1993: 141-152
- Šrám RJ**, Binková B, Stejskalová J, Topinka J. Effect of EGb 761 on lipid peroxidation, DNA repair and antioxidant activity. In: Ferradini C, Droy-Lefaix MT, Christen Y, eds. *Advances in Ginkgo biloba extract research: Ginkgo biloba extract (EGb 761) as a free-radical scavenger*. New York: Elsevier Science 1993: 27-38
- Szabo ME**, Droy-Lefaix MT, Doly M. Reduction of reperfusion-induced ionic imbalance by superoxide dismutase, vitamin E and *Ginkgo biloba* extract 761 in spontaneously hypertensive rat retina. In: Ferradini C, Droy-Lefaix MT, Christen Y, eds. *Advances in Ginkgo biloba extract research: Ginkgo biloba extract (EGb 761) as a free-radical scavenger*. New York: Elsevier Science 1993: 93-106
- Oken BS**, Storzbach DM, Kaye JA. The efficacy of *Ginkgo biloba* extract on cognitive function in Alzheimer disease. *Arch Neurol* 1998; **55**: 1409-1415
- Onen A**, Deveci E, Inaloz SS, Isik B, Kilinc M. Histopathological assessment of the prophylactic effect of *ginkgo-biloba* extract on intestinal ischemia-reperfusion injury. *Acta Gastroenterol Belg* 1999; **62**: 386-389
- Lee SJ**, Choi JH, Son KH, Chang HW, Kang SS, Kim HP. Suppression of mouse lymphocyte proliferation in vitro by naturally-occurring biflavonoids. *Life Sci* 1995; **57**: 551-558
- Su Y**, Sun CM, Chuang HH, Chang PT. Studies on the cytotoxic mechanisms of ginkgetin in a human ovarian adenocarcinoma cell line. *Naunyn Schmiedebergs Arch Pharmacol* 2000; **362**: 82-90
- Lowry OH**, Rosebrough NJ, Farr A, Randall RJ. Protein measurement with the Folin phenol reagent. *J Biol Chem* 1951; **193**: 265-275
- Dunigan DD**, Waters SB, Owen TC. Aqueous soluble tetrazolium/formazan MTS as an indicator of NADH- and NADPH-dependent dehydrogenase activity. *Biotechniques* 1995; **19**: 640-649
- Arechabala B**, Coiffard C, Rivalland P, Coiffard LJ, de Roeck-Holtzauer Y. Comparison of cytotoxicity of various surfactants tested on normal human fibroblast cultures using the neutral red test, MTT assay and LDH release. *J Appl Toxicol* 1999; **19**: 163-165
- Laemmli UK**. Cleavage of structural proteins during the assembly of the head of bacteriophage T4. *Nature* 1970; **227**: 680-685
- Towbin H**, Staehelin T, Gordon J. Electrophoretic transfer of proteins from polyacrylamide gels to nitrocellulose sheets: procedure and some applications. *Proc Natl Acad Sci U S A* 1979; **76**: 4350-4354
- Papadopoulos V**, Kapsis A, Li H, Amri H, Hardwick M, Culty M, Kasprzyk PG, Carlson M, Moreau JP, Drieu K. Drug-induced inhibition of the peripheral-type benzodiazepine receptor expression and cell proliferation in human breast cancer cells. *Anticancer Res* 2000; **20**: 2835-2847
- Li W**, Pretner E, Shen L, Drieu K, Papadopoulos V. Common gene targets of *Ginkgo biloba* extract (EGb 761) in human tumor cells: relation to cell growth. *Cell Mol Biol* 2002; **48**: 655-662
- Lin SJ**, Yang TH, Chen YH, Chen JW, Kwok CF, Shiao MS, Chen YL. Effects of *Ginkgo biloba* extract on the proliferation of vascular smooth muscle cells *in vitro* and on intimal thickening and interleukin-1beta expression after balloon injury in cholesterol-fed rabbits *in vivo*. *J Cell Biochem* 2002; **85**: 572-582
- Baudouin C**, Ettaiche M, Imbert F, Droy-Lefaix MT, Gastaud P, Lapalus P. Inhibition of preretinal proliferation by free radical scavengers in an experimental model of tractional retinal detachment. *Exp Eye Res* 1994; **59**: 697-706
- Sun CM**, Syu WJ, Huang YT, Chen CC, Ou JC. Selective cyto-

- toxicity of ginkgetin from *Selaginella moellendorffii*. *J Nat Prod* 1997; **60**: 382-384
- 21 **Shi M**, Wang FS, Wu ZZ. Synergetic anticancer effect of combined quercetin and recombinant adenoviral vector expressing human wild-type p53, GM-CSF and B7-1 genes on hepatocellular carcinoma cells *in vitro*. *World J Gastroenterol* 2003; **9**: 73-78
- 22 **Kim SJ**, Lim MH, Chun IK, Won YH. Effects of flavonoids of *Ginkgo biloba* on proliferation of human skin fibroblast. *Skin Pharmacol* 1997; **10**: 200-205
- 23 **Lee KH**, Kim KC, Jung YJ, Ham YH, Jang JJ, Kwon H, Sung YC, Kim SH, Han SK, Kim CM. Induction of apoptosis in p53-deficient human hepatoma cell line by wild-type p53 gene transduction: inhibition by antioxidant. *Mol Cells* 2001; **12**: 17-24
- 24 **Ahlemeyer B**, Selke D, Schaper C, Klumpp S, Krieglstein J. Ginkgolic acids induce neuronal death and activate protein phosphatase type-2C. *Eur J Pharmacol* 2001; **430**: 1-7
- 25 **Hecker H**, Johannisson R, Koch E, Siegers CP. *In vitro* evaluation of the cytotoxic potential of alkylphenols from *Ginkgo biloba* L. *Toxicology* 2002; **177**: 167-177
- 26 **Ahlemeyer B**, Mowes A, Krieglstein J. Inhibition of serum deprivation- and staurosporine-induced neuronal apoptosis by *Ginkgo biloba* extract and some of its constituents. *Eur J Pharmacol* 1999; **367**: 423-430
- 27 **Chen C**, Wei T, Gao Z, Zhao B, Hou J, Xu H, Xin W, Packer L. Different effects of the constituents of EGb 761 on apoptosis in rat cerebellar granule cells induced by hydroxyl radicals. *Biochem Mol Biol Int* 1999; **47**: 397-405
- 28 **Terada T**, Nakanuma Y. Expression of apoptosis, proliferating cell nuclear antigen, and apoptosis-related antigens (bcl-2, c-myc, Fas, Lewis(y) and p53) in human cholangiocarcinomas and hepatocellular carcinomas. *Pathol Int* 1996; **46**: 764-770
- 29 **Mise K**, Tashiro S, Yogita S, Wada D, Harada M, Fukuda Y, Miyake H, Isikawa M, Izumi K, Sano N. Assessment of the biological malignancy of hepatocellular carcinoma: relationship to clinicopathological factors and prognosis. *Clin Cancer Res* 1998; **4**: 1475-1482
- 30 **Nakano A**, Watanabe N, Nishizaki Y, Takashimizu S, Matsuzaki S. Immunohistochemical studies on the expression of P-glycoprotein and p53 in relation to histological differentiation and cell proliferation in hepatocellular carcinoma. *Hepatol Res* 2003; **25**: 158-165
- 31 **Qin LX**, Tang ZY. The prognostic molecular markers in hepatocellular carcinoma. *World J Gastroenterol* 2002; **8**: 385-392
- 32 **Lee KH**, Kim KC, Jung YJ, Ham YH, Jang JJ, Kwon H, Sung YC, Kim SH, Han SK, Kim CM. Induction of apoptosis in p53-deficient human hepatoma cell line by wild-type p53 gene transduction: inhibition by antioxidant. *Mol Cells* 2001; **12**: 17-24
- 33 **Agha AM**, El-Fattah AA, Al-Zuhair HH, Al-Rikabi AC. Chemopreventive effect of *Ginkgo biloba* extract against benzo(a)pyrene-induced forestomach carcinogenesis in mice: amelioration of doxorubicin cardiotoxicity. *J Exp Clin Cancer Res* 2001; **20**: 39-50

Edited by Zhu LH and Wang XL

Increased nociceptin/orphanin FQ plasma levels in hepatocellular carcinoma

Ferenc Szalay, Mónika B Hantos, Andrea Horvath, Peter L. Lakatos, Aniko Folhoffer, Kinga Dunkel, Dalma Hegedus, Kornélia Tekes

Ferenc Szalay, Andrea Horvath, Peter L. Lakatos, Aniko Folhoffer, Kinga Dunkel, Dalma Hegedus, 1st Department of Medicine of Semmelweis University, Budapest, Hungary

Kornélia Tekes, Department of Pharmacodynamics of Semmelweis University, Budapest, Hungary

Mónika B Hantos, Neurochemical Research Unit of Hungarian Academy of Sciences, Budapest, Hungary

Correspondence to: Professor Ferenc Szalay, MD., PhD, 1st Department of Medicine Semmelweis University, Koranyi S u. 2/A, Budapest, H-1083 Hungary. szalay@bell.sote.hu

Telephone: +36-1-210 1007 **Fax:** +36-1-210 1007

Received: 2003-10-08 **Accepted:** 2003-11-16

Abstract

AIM: The heptadecapeptide nociceptin alias orphanin FQ is the endogenous agonist of opioid receptor-like 1 receptor. It is involved in modulation of pain and cognition. High blood level was reported in patients with acute and chronic pain, and in Wilson disease. An accidental observation led us to investigate nociceptin in hepatocellular carcinoma.

METHODS: Plasma nociceptin level was measured by radioimmunoassay, aprotinin was used as protease inhibitor. Hepatocellular carcinoma was diagnosed by laboratory, ultrasound, other imaging, and confirmed by fine needle biopsy. Results were compared to healthy controls and patients with other chronic liver diseases.

RESULTS: Although nociceptin levels were elevated in patients with Wilson disease (14.0 ± 2.7 pg/mL, $n=26$), primary biliary cirrhosis (12.1 ± 3.2 pg/mL, $n=21$) and liver cirrhosis (12.8 ± 4.0 pg/mL, $n=15$) compared to the healthy controls (9.2 ± 1.8 pg/mL, $n=29$, $P < 0.001$ for each), in patients with hepatocellular carcinoma a ten-fold increase was found (105.9 ± 14.4 pg/mL, $n=29$, $P < 0.0001$). High plasma levels were found in each hepatocellular carcinoma patient including those with normal alpha fetoprotein and those with pain (104.9 ± 14.9 pg/mL, $n=12$) and without (107.7 ± 14.5 pg/mL, $n=6$).

CONCLUSION: A very high nociceptin plasma level seems to be an indicator for hepatocellular carcinoma. Further research is needed to clarify the mechanism and clinical significance of this novel finding.

Szalay F, Hantos MB, Horvath A, Lakatos PL, Folhoffer A, Dunkel K, Hegedus D, Tekes K. Increased nociceptin/orphanin FQ plasma levels in hepatocellular carcinoma. *World J Gastroenterol* 2004; 10(1): 42-45

<http://www.wjgnet.com/1007-9327/10/42.asp>

INTRODUCTION

The heptadecapeptide nociceptin (N/OFQ), alias orphanin FQ, is the endogenous agonist ligand of a G-protein-coupled,

naloxon insensitive opioid receptor-like 1 receptor (ORL1), recently named as NOP^[1]. Although N/OFQ is structurally related to opioid peptides, especially to dynorphin A, it does not interact with μ , δ and κ receptors. The nociceptin/NOP system represents a new peptide-based signalling pathway. Nociceptin is involved in a number of pharmacological actions in the central nervous system (CNS), including modulation of pain and cognition. However, numerous studies investigating the functional role of nociceptin in physiology have failed to provide coherent view, and its exact physiological role remains to be determined^[2,3]. Although N/OFQ is produced by some brain structure and peripheral neurons, it is present in the liquor and blood^[4], and recent data prove that nociceptin transcripts are expressed in human immune cells as well^[5]. NOP mRNA is expressed not only in nervous system, but in immune cells and other organs including the liver^[6-8]. High nociceptin blood level was shown in patients with acute and chronic pains^[9], and Wilson disease^[10].

An accidental observation led us to investigate plasma nociceptin level in patients with hepatocellular carcinoma (HCC). While measuring plasma nociceptin in patients with Wilson disease, we noticed that in one patient the nociceptin level was extremely high compared both with the controls and other Wilson patients. This patient had liver cirrhosis and primary hepatocellular carcinoma without any pain. This observation prompted us to study N/OFQ in patients with hepatocellular carcinoma and other liver diseases. Striking differences were found.

MATERIALS AND METHODS

Patients

Plasma nociceptin level was measured in 26 patients with Wilson disease (aged from 14-55 years, 11 with hepatic, and 15 with neurological symptoms, each D-penicillamine treated), 21 patients with primary biliary cirrhosis (age ranged from 36-72 years; each woman with AMA M2 positive, histologically proven and treated with ursodeoxycholic acid; mean disease duration: 9.4 years), 18 patients with chronic hepatitis (14 HCV positive, 1 HBV positive and 3 autoimmune, each proved by liver biopsy), 15 patients with liver cirrhosis (9 alcoholic, 6 HCV positive), and 18 patients with primary hepatocellular carcinoma (8 with alcoholic cirrhosis, 6 HCV cirrhosis, 1 HBV cirrhosis, 1 Wilson disease, 1 PBC, and 1 patient without any underlying liver disease) from the Hepatological Unit, the 1st Department of Medicine, the Semmelweis University, Budapest. The diagnosis of HCC was based on clinical laboratory tests, US, CT, MRI findings and was confirmed by fine needle aspiration cytology, and histology, in which 3 cases underwent surgery, and one case by autopsy. Serum alpha fetoprotein (AFP) was elevated in 11 out of 18 HCC patients. The size of the tumour ranged from 2.5 cm to 12 cm in diameter. It was smaller than 5 cm in 5 patients, and larger than 5 cm in 13 patients. No metastasis was found outside the liver. In the HCC group 12 patients had temporary pain treated with non-opioid analgetics and 6

patients were without any pain.

Two scoring systems were used for characterisation of patients with HCC. The distribution of patients according to the Barcelona Clinic Liver Cancer (BCLC) classification^[11], which includes the performance status, single or multifocal appearance of the tumor, vascular invasion, portal hypertension, Okuda stage and Child-Pugh classification: Stage A1 ($n=5$), stage A4 ($n=6$), stage B ($n=3$) and stage D ($n=4$). Ranking of patients according to the Cancer of the Liver Italian Program group (CLIP) criteria^[12,13], which includes Child-Pugh stage, tumor morphology and extent, presence of portal vein thrombosis and serum level of alpha fetoprotein: CLIP 0 ($n=2$), CLIP 1 ($n=5$), CLIP 2 ($n=5$), CLIP 3 ($n=4$), CLIP 4 ($n=1$), CLIP 5 ($n=1$). Demographics, clinical data and ranking of HCC patients according to the BCLC and CLIP classification are shown in Table 1.

Twenty-nine healthy persons including blood donors and members of the medical staff served as control group. The study was approved by the Local Regional Committee of Science and Research Ethics. Written informed consent was obtained.

Methods

Blood drawn from fasting subjects between 08:00 and 10:00 AM was collected in vacutainer tubes containing K-EDTA as anticoagulant. Aprotinin was added immediately as protease inhibitor. Plasma samples were stored at minus 80 °C. Nociceptin was measured by radioimmunoassay (¹²⁵I-Nociceptin kit, Phoenix Pharmaceuticals, Phoenix, CA, USA) with minimum sensitivity of 1 pg/mL, as described before^[9]. Comparison of the plasma N/OFQ concentration in groups was made using Mann-Whitney U Test. Correlation between N/OFQ level and liver function test results was evaluated by Spearman RO correlation.

RESULTS

Results are shown in Figure 1. Although nociceptin levels were elevated in patients with Wilson disease (14.0 ± 2.7 pg/mL), in patients with PBC (12.1 ± 3.2 pg/mL) and liver cirrhosis (12.8 ± 4.0 pg/mL) compared to the healthy controls (9.2 ± 1.8

pg/mL, $P<0.001$ for each), more than ten-fold higher values were found (105.9 ± 14.4 pg/mL, $P<0.0001$) in patients with HCC. In patients with chronic hepatitis the N/OFQ level was 10.2 ± 3.6 , but the difference was not significant compared to the healthy controls. The clinical data, chemical laboratory findings, AFP and N/OFQ levels of patients with HCC are individually indicated in Table 1.

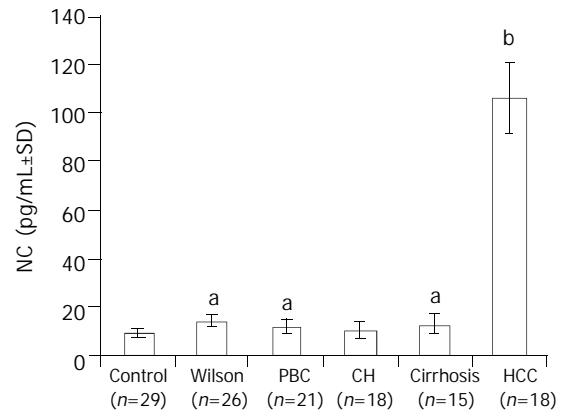


Figure 1 Plasma nociceptin level (pg/mL±SD) in healthy controls (Control) and in patients with Wilson disease (Wilson), primary biliary cirrhosis (PBC), chronic hepatitis (CH), cirrhosis and hepatocellular carcinoma (HCC). * $P<0.001$ vs control, ^b $P<0.0001$ vs control and each other group.

We did not find any correlation between nociceptin level and liver chemical laboratory tests including AFP in any group of patients with liver disease. Nociceptin was elevated in each HCC patient including those with normal AFP. The N/OFQ level did not show correlation with the presence and severity of the pain. High levels were found in subgroups of patients with pain (104.9 ± 14.9 pg/mL, $n=12$) and without pain (107.7 ± 14.5 pg/mL, $n=6$). There was no difference in nociceptin level between groups with tumor size smaller than 5 cm and larger than 5 cm (109.4 ± 16.5 , $n=5$ and 115.2 ± 12.7 , $n=13$,

Table 1 Profile of patients with HCC and plasma N/OFQ levels

	Age y	Gender	Aetiology	AFP (ng/mL)	Tumor size in UH	Uni- nod.	Multi- nod.	BCLC st.cl.	CLIP cl.	Bi (mg/dL)	ALP (U/L)	GGT (U/L)	Ascites	C-P	N/OFQ (pg/mL)
1	80	M	Alcoholic	937	15×11 cm	+		A 4	3	1.72	306	102	-	A	108.39
2	64	M	Alcoholic	1 385.9	5×7×6 cm	+		A 1	1	1.92	242	107	-	A	95.02
3	60	M	Alcoholic	89	5 -15 mm and 3 cm		+	B	2	1.07	2 169	1 000	-	B	96.05
4	62	M	Alcoholic	91	1-1.5 cm and 3.5 cm		+	B	2	1.12	2 038	995	-	B	104.17
5	80	M	Alcoholic	937	15×11 cm	+		A 1	3	1.71	306	102	-	A	111.59
6	70	M	Alcoholic	459	7×6 cm	+		A 1	2	0.78	192	68	-	A	111.51
7	59	M	Alcoholic	7.7	23 mm	+		D	2	8.32	44.3	97	-	C	128
8	66	M	Alcoholic	2	1.5 cm	+		A 1	0	1.25	192	24	-	A	81.6
9	48	F	HCV	15	6×6 cm	+		A 4	1	5.75	1 766	253	-	B	90.41
10	66	M	HCV	171	two, 2×2 cm lesion		+	A 4	1	2.55	460	232	-	A	89.81
11	76	M	HCV	9	6×7 cm + 5×4 cm		+	D	4	13.91	834	276	+	C	114.65
12	78	M	HCV	350	5×6 cm	+		A 1	0	0.68	270	37	-	A	114.7
13	48	F	HCV	13	21×20 mm and 16×21 mm		+	B	1	1.36	474	1 060	-	A	128
14	81	M	HCV	1 050	8×10 cm	+		A 4	3	3	569	517	-	A	98.31
15	66	M	HBV	6	4×4.5 cm	+		D	2	3.35	442	199	+	C	106.03
16	45	F	WD	5	60×46 mm	+		A 4	1	0.42	910	212	+	B	128
17	68	F	PBC	3 480	11×7.5 cm	+		D	5	4.79	1 856	960	+	C	172.2
18	32	F	Unknown	1 050	100×85×180 mm	+		A 4	3	0.34	233	24	-	-	85.5

AFP=alpha fetoprotein, BCLC st. cl.=Barcelona Clinic Liver Cancer (BCLC) staging classification, CLIP cl.=Cancer of the Liver Italian Program Group (CLIP) scoring system, Bi=Serum total bilirubin, ALP=alkaline phosphatase, GGT=gamma glutamyl transferase, C-P=Child-Pugh score, N/OFQ=nociceptin/orphanin FQ.

respectively) or between single nodular and multinodular HCC groups, and even symptomatic or asymptomatic tumors. No difference was found in the N/OFQ level between any subgroup of patients with different BCLC and CLIP score values.

Repeated nociceptin measurements were done in one patient before and after non-surgical ablation treatment of HCC. The high nociceptin level did not decrease significantly at least within 10 days following ethanol injection treatment of the tumor, since values were 116 pg/mL before, and 110, 108, 112, 103 pg/mL after treatment at 1, 3, 7, and 10 days, respectively.

However, progressive and significant elevation in plasma nociceptin level parallel with the increase of AFP was observed in a PBC patient with HCC during the follow up. This 67 year old patient was monitored and treated with ursodeoxycholic acid throughout 18 years when her liver tumor was detected by yearly regular ultrasound check up. Fine needle aspiration cytology proved HCC, and she died within two years. Nociceptin was measured in blood samples collected from other reason. The AFP level was normal throughout the years, but elevated at the time of the diagnosis of HCC (426 ng/mL) and rose up to 3 480 ng/mL. The plasma nociceptin (10.6 pg/mL) was within the normal range (9.2 ± 1.8 pg/mL) in the tumor free stage, ten-fold higher (103.7 pg/mL) when the tumor was diagnosed and reached 172.2 pg/mL before the death. Sixteen-fold higher nociceptin content was measured in the tumor tissue (0.16 pg/mg) compared to the tumor-free liver tissue sample (0.01 pg/mg) taken during the autopsy. Detailed presentation of this case is published in this issue of World Journal of Gastroenterology (Horvath *et al* World J Gastroenterol 2004; 10: 152-154)

DISCUSSION

Shortly after cloning of the three known opioid receptors a fourth member of the subfamily of G protein-coupled receptors was identified. In a search for additional opioid receptor subtypes, a sequence of an opioid-like receptor, termed ORL1 was found, which, however, did not bind any of the known natural opioid ligands. Therefore ORL1 represented an "orphan" receptor. Later two working groups simultaneously reported the isolation of the natural ligand for ORL1, a 17 aminoacid polypeptide and named it orphanin FQ or nociceptin^[14,15].

Anatomic studies have revealed high levels of expression of N/OFQ messenger RNS in brain structures involved in sensory, emotional and cognitive processing. Like all other neuropeptides, the heptadecapeptid N/OFQ is synthesized as a part of a larger precursor named prepro-nociceptin, a 176 aminoacid polypeptide in human, from which N/OFQ and nocistatin are cleaved in brain cells and peripheral neurons^[16,17]. Although nociceptin is present in the brain, the liquor and blood, human immune cells and polymorphonuclear cells, the gastrointestinal tract and other organs, there are no data on N/OFQ or its receptor in malignant diseases with exception of human neuroblastoma cell lines^[18,19]. This is the first report focusing on nociceptin in hepatocellular carcinoma and other liver diseases.

The novel finding of this study is the striking elevation in plasma N/OFQ level in patients with hepatocellular carcinoma. Although nociceptin was elevated in patients with Wilson disease, primary biliary cirrhosis and liver cirrhosis, very high levels over ten-fold increase compared with healthy controls was found in HCC. Since nociceptin level was extremely high in each patient with HCC, and the difference among HCC patients and groups of patients with other liver diseases was highly significant ($P < 0.0001$), the very high plasma level of nociceptin seems to be an indicator for HCC. It is remarkable that nociceptin level was very high in even those patients with normal level of alpha-fetoprotein^[20]. The size of HCC is an

important element of prognostic assessment^[21]. However, nociceptin level was equally very high in patients with tumor size smaller and larger than 5 cm in diameter.

Further research is needed to clarify the mechanism and clinical significance of the highly elevated nociceptin level in HCC. Increased production or decreased catabolism of nociceptin may be the cause of elevation in plasma level. It is to be determined whether the tumor produces nociceptin or it gives signal for brain cells or peripheral neurons to increase the secretion of N/OFQ. We had the opportunity to determine the tissue nociceptin content in one PBC patient with HCC. Although more than 15-fold higher nociceptin content was measured in the carcinoma tissue than in the tumor-free liver tissue samples taken during autopsy, it did not necessarily mean that nociceptin was produced by the tumor. It is also possible that the tumor simply accumulates nociceptin via binding it by NOP receptors. This possibility could be supported by the fact that ORL1/NOP receptor mRNA has been detected in the liver^[22], although no study is yet available on nociceptin or its receptor mRNA expression in hepatocellular carcinoma tissue.

Nociceptin is involved in the processing of pain signals, and it modulates the pain perception^[23,24]. However, we did not find difference in N/OFQ level between patients with pain and without. There was no correlation between the plasma N/OFQ level and the severity of pain.

Whether a very high plasma N/OFQ level is a specific marker of HCC should be investigated and subjected to further study. Since nociceptin transcripts are expressed in immune cells^[5], it has also been shown that polymorphonuclear cells express nociceptin receptors and N/OFQ stimulates neutrophil chemotaxis and recruitment^[25]. The high nociceptin level could also be an indicator of altered reaction of the body including immunological, cytokine and other mechanisms. The bacterial endotoxin (LPS) and proinflammatory cytokines including TNF-alpha, commonly increased in malignancies, induce N/OFQ mRNAs in astrocytes. It may suggest a role for nociceptin in neural-glia communication and in inflammatory responses^[26].

In humans, the N/OFQ gene has been mapped to the chromosomal location 8p21^[27]. Transcription of this gene was shown to be enhanced by cytokines, neurotrophic factors^[26], also by estrogen^[28]. This cAMP-dependent transcription could be blocked by glucocorticoids^[19]. Our patients in this study have not received glucocorticoid treatment, and only one PBC patient used transdermal estrogen hormone replacement for osteoporosis prevention.

Elevated N/OFQ level might partly represent a compensatory mechanism in the nociceptin/NOP system to modulate pain perception in the central nervous system. That mechanism might explain why some patients with a very high plasma N/OFQ level did not have any pain despite advanced stage of the malignant liver tumor. It is remarkable that nociceptin in HCC patients was 3-fold higher than the highest values reported in patients with chronic pain without malignant diseases^[19]. We believe that our results could stimulate further investigation.

REFERENCES

- 1 **Calo' G**, Rizzi A, Bigoni R, Guerrini R, Salvadori S, Regoli D. Pharmacological profile of nociceptin/orphanin FQ receptors. *Clin Exp Pharmacol Physiol* 2002; **29**: 223-228
- 2 **Terenius L**, Sandin J, Sakurada T. Nociceptin/orphanin FQ metabolism and bioactive metabolites. *Peptides* 2000; **21**: 919
- 3 **Heinricher MM**. Orphanin FQ/nociceptin: from neural circuitry to behavior. *Life Sci* 2003; **73**: 813-822
- 4 **Brooks H**, Elton CD, Smart D, Rowbotham DJ, McKnight AT, Lambert DG. Identification of nociceptin in human cerebrospinal fluid: comparison of level in pain and non-pain states. *Pain* 1998; **78**: 71-73

- 5 **Arjomand J**, Cole S, Evans C. Novel orphanin FQ/nociceptin transcripts are expressed in human immune cells. *J Neuroimmunol* 2002; **130**: 100
- 6 **Peluso J**, Gaveriaux-Ruff C, Matthes HW, Filliol D, Kieffer BL. Orphanin FQ/nociceptin binds functionally coupled ORL1 receptors on human immune cell lines and alters peripheral blood mononuclear cell proliferation. *Brain Res Bull* 2001; **54**: 655-660
- 7 **Peluso J**, LaForge KS, Matthes HW, Kreek MJ, Kieffer BL, Gaveriaux-Ruff C. Distribution of nociceptin/orphanin FQ receptor transcript in human central nervous system and immune cells. *J Neuroimmunol* 1998; **81**: 184-192
- 8 **Reinscheid RK**, Nothacker HP, Civelli O. The orphanin FQ/nociceptin gene: structure, tissue distribution of expression and functional implications obtained from knockout mice. *Peptides* 2000; **21**: 901-906
- 9 **Ko MH**, Kim YH, Woo RS, Kim KW. Quantitative analysis of nociceptin in blood of patients with acute and chronic pain. *Neuroreport* 2002; **13**: 1631-1633
- 10 **Hantos MB**, Szalay F, Lakatos PL, Hegedüs D, Firneisz G, Reiczigel J, Torok T, Tekes K. Elevated plasma nociceptin level in patients with Wilson disease. *Brain Research Bulletin* 2002; **58**:311-313
- 11 **Llovet JM**, Bru C, Bruix J. Prognosis of hepatocellular carcinoma: the BCLC staging classification. *Semin Liver Dis* 1999; **19**: 329-337
- 12 **The Cancer of the Liver Italian Program (CLIP) Investigators.** A new prognostic system for hepatocellular carcinoma: a retrospective study of 435 patients. *Hepatology* 1998; **28**: 751-755
- 13 **Zhao WH**, Ma ZM, Zhou XR, Feng YZ, Fang BS. Prediction of recurrence and prognosis in patients with hepatocellular carcinoma after resection by use of CLIP score. *World J Gastroenterol* 2002; **8**: 237-242
- 14 **Reinscheid RK**, Nothacker HP, Bourson A, Ardati A, Henningsen RA, Bunzow JR, Grandy DK, Langen H, Monsma FJ Jr, Civelli O. Orphanin FQ: a neuropeptide that activates an opioidlike G protein-coupled receptor. *Science* 1995; **270**: 792-794
- 15 **Meunier JC**, Mollereau C, Toll L, Suandeu C, Moisan C, Alvineire P, Butour JL, Guillemot JC, Ferrara P, Monserrat B. Isolation and structure of the endogenous agonist of opioid receptor-like ORL-1 receptor. *Nature* 1995; **377**: 532-535
- 16 **Okuda-Ashitaka E**, Ito S. Nocistatin: a novel neuropeptide encoded by the gene for the nociceptin/orphanin FQ precursor. *Peptides* 2000; **21**: 1101-1109
- 17 **Okuda-Ashitaka E**, Minami T, Tachibana S, Yoshihara Y, Nishiuchi Y, Kimura T, Ito S. Nocistatin, a peptide that blocks nociceptin action in pain transmission. *Nature* 1998; **392**: 286-289
- 18 **Spampinato S**, Di Toro R, Qusem AR. Nociceptin-induced internalization of the ORL1 receptor in human neuroblastoma cells. *Neuroreport* 2001; **12**: 3159-3163
- 19 **Sirianni MJ**, Fujimoto KI, Nelson CS, Pellegrino MJ, Allen RG. Cyclic AMP analogs induce synthesis, processing and secretion of prepro nociceptin/orphanin FQ-derived peptides by NS20Y neuroblastoma cells. *DNA Cell Biol* 1999; **18**: 51-58
- 20 **Qin LX**, Tang ZY. The prognostic significance of clinical and pathological features in hepatocellular carcinoma. *World J Gastroenterol* 2002; **8**: 193-199
- 21 **Bruix J**, Llovet JM. Prognostic assessment and evaluation of the benefits of treatment. *J Clin Gastroenterol* 2002; **35**(Suppl 2): S138-142
- 22 **Wang JB**, Johnson PS, Imai Y, Persico AM, Ozenberger BA, Eppler CM, Uhl GR. cDNA cloning of an orphan opiate receptor gene family member and its splice variant. *FEBS Lett* 1994; **348**: 75-79
- 23 **Inoue M**, Kawashima T, Takeshima H, Calo G, Inoue A, Nakata Y, Ueda H. *In vivo* pain-inhibitory role of nociceptin/orphanin FQ in spinal cord. *J Pharmacol Exp Ther* 2003; **305**: 495-501
- 24 **Meunier JC**. Utilizing functional genomics to identify new pain treatments: the example of nociceptin. *Am J Pharmacog* 2003; **3**: 117-130
- 25 **Serhan CN**, Fierro IM, Chiang N, Pouliot M. Cutting edge: Nociceptin stimulates neutrophil chemotaxis and recruitment: inhibition by aspirin-triggered-15-epi-lipoxin A₄. *J Immunol* 2001; **166**: 3650-3654
- 26 **Buzas B**, Symes AJ, Cox BM. Regulation of nociceptin/orphanin FQ gene expression by neuroipoietic cytokines and neurotrophic factors in neurons and astrocytes. *J Neurochem* 1999; **72**: 556-563
- 27 **Mollereau C**, Simons MJ, Soularue P, Liners F, Vassart G, Meunier JC, Parmentier M. Structure, tissue distribution and chromosomal localization of the prepronociceptin gene. *Proc Natl Acad Sci U S A* 1996; **93**: 8666-8670
- 28 **Xie GX**, Ito E, Maruyama K, Suzuki Y, Sugano S, Sharma M, Pietruck C, Palmer PP. The promoter region of the human prepronociceptin gene and its regulation by cyclic AMP and steroid hormones. *Gene* 1999; **238**: 427-436

Edited by Zhang JZ

Potential role of p53 mutation in chemical hepatocarcinogenesis of rats

Wei-Guo Deng, Yan Fu, Yu-Lin Li, Toshihiro Sugiyama

Wei-Guo Deng, Department of Nutrition and Food Hygiene, School of Public Health, Jilin University, Changchun 130021, Jilin Province, China

Yan Fu, Department of Obstetrics and Gynecology, First Hospital, Jilin University, Department of Pathology, School of Preclinical Medicine, Jilin University, Changchun 130021, Jilin Province, China

Yu-Lin Li, Department of Pathology, School of Preclinical Medicine, Jilin University, Changchun 130021, Jilin Province, China

Toshihiro Sugiyama, Department of Biochemistry, Akita University School of Medicine, 1-1-1 Hondo, Akita, 010-8543, Japan

Supported by Jilin University Excellent Young Teacher Foundation, No. 2001033

Correspondence to: Dr. Yan Fu, Department of Obstetrics and Gynecology, First Hospital, Jilin University, 1 Xinmin Street, Changchun 130021, Jilin Province, China

Telephone: +86-431-5612482

Received: 2003-06-05 **Accepted:** 2003-08-16

Abstract

AIM: Inactivation of p53 gene is one of the most frequent genetic alterations in carcinogenesis. The mutation status of p53 gene was analyzed, in order to understand the effect of p53 mutation on chemical hepatocarcinogenesis of rats.

METHODS: During hepatocarcinogenesis of rats induced by 3'-methyl-4-dimethylaminoazobenzene (3'-Me-DAB), prehepatocarcinoma and hepatocarcinoma foci were collected by laser capture microdissection (LCM), and quantitatively analyzed for levels of p53 mRNA by LightCycler™ real-time RT-PCR and for mutations in p53 gene exons 5-8 by direct sequencing.

RESULTS: Samples consisting of 44 precancerous foci and 24 cancerous foci were collected by LCM. A quantitative analysis of p53 mRNA showed that p53 mRNA peaked at an early stage (week 6) in the prehepatocarcinoma lesion, more than ten times that of adjacent normal tissue, and gradually decreased from week 6 to week 24. The expression of p53 mRNA in adjacent normal tissue was significantly lower than that in prehepatocarcinoma. Similar to prehepatocarcinoma, p53 mRNA in cancer was markedly higher than that in adjacent normal tissue at week 12, and was closer to normal at week 24. Direct p53 gene sequencing showed that 35.3% (24/68) (9 precancer, 15 cancer) LCM samples exhibited point mutations, 20.5% of prehepatocarcinoma LCM samples presented missense mutations at exon 6/7 or/and 8, and was markedly lower than 62.5% of hepatocarcinoma ones ($P < 0.01$). Mutation of p53 gene formed the mutant hot spots at 5 codons. Positive immunostaining for p53 protein could be seen in prehepatocarcinoma and hepatocarcinoma foci at 24 weeks.

CONCLUSION: p53 gene mutation is present in initial chemical hepatocarcinogenesis, and the mutation of p53 gene induced by 3'-Me-DAB is an important factor of hepatocarcinogenesis.

Deng WG, Fu Y, Li YL, Sugiyama T. Potential role of p53 mutation in chemical hepatocarcinogenesis of rats. *World J Gastroenterol* 2004; 10(1): 46-52

<http://www.wjgnet.com/1007-9327/10/46.asp>

INTRODUCTION

Abnormalities of some tumor suppressor genes and oncogenes play important roles in the development and progression of hepatoma^[1,2]. Gene abnormalities in precancerous liver lesions (adenomatous hyperplasia and atypical adenomatous hyperplasia) and early hepatocellular carcinoma have been reported^[3-5]. p53 tumor suppressor protein plays an important role in preventing malignant development, and p53 function is lost or compromised in most human cancers^[6-8]. One of the principal functions of p53 is to inhibit cell growth, and p53 shows a strong cell cycle arrest and apoptotic activities^[9,10]. As a result, cell proliferation is suppressed and/or programmed cell death is induced^[11,12]. In cells with DNA injury, p53 can stop the cell cycle through p21 protein and then promote DNA repair. When DNA is seriously damaged, p53 can induce the cell to undergo programmed cell death to maintain the stability of genome and cells. Loss of p53 function activates oncogenes and inactivates cancer suppressor genes, playing an essential role in multistage carcinogenesis^[13,14]. Some study has shown that mutation and loss of p53 gene are closely related to the conversion of adenoma to early colorectal cancer, and so are those in liver^[15]. When cancer cell differentiation is low and the tumor becomes large, p53 gene mutation frequently arises in hepatocarcinoma, making p53 gene most closely concerned with the progress of hepatocarcinoma^[16]. It is not yet clear which of these gene alterations is responsible for hepatocarcinogenesis, especially in a prehepatocarcinoma lesion.

3'-methyl-4-dimethylaminoazobenzene (3'-Me-DAB) could produce prehepatocarcinomatous lesions (altered focus and neoplastic nodules) in rats. Our study showed that mutation of p53 gene, in precancerous and cancerous foci of the F344 rat liver induced by 3'-Me-DAB, was successfully detected by integrating LCM, LightCycler RT-PCR with direct sequencing.

MATERIALS AND METHODS

Animals

Thirty-nine male F344 rats at 10 weeks of age were kept in a room with a 12h light and dark cycle and maintained at 22 °C. They were provided with a diet containing 0.06% 3'-Me-DAB^[17] and tap water *ad libitum* for 6 weeks, 12 weeks, and 24 weeks, respectively. After the last day of each experimental period, the animals were anesthetized with ether and hepatectomized. The cavum thoracis and abdominal cavity were opened immediately with a sterilized scalpel, and part of the liver was quickly dissected out, placed in a cryomold, covered with Tissue-Tek O. C. T compound before being frozen in liquid nitrogen, and preserved at -80 °C until use. The remaining liver was perfused with 30% PBS-buffered sucrose before being removed and fixed in 10% neutral formalin, and then embedded in paraffin.

LCM of sample

The liver preserved at -80°C was sequentially sliced into twenty $10\ \mu\text{m}$ thick sections, in a cryostat, which were mounted on clean microscope slides. The sections were stored at -80°C . Of the 10 successive slide sections, three were stained chemically with H&E and immunohistochemically with glutathione *S* transferase placenta (GST-P) and AFP polyclonal antibody using Elite ABC kit (Funakoshi Co. Ltd., Tokyo, Japan). Prehepatocarcinoma and hepatocarcinoma foci were diagnosed by Pathologists and their positions were identified on the slides. Other slide sections underwent quick H&E staining based on the LCM manufacturer's protocols, and were then cleaned in xylene for over 1 min. Once air-dried, slides were ready for LCM. Based on the position of GST-P (+) or AFP (+) foci from immunostained slide sections and the cancer pathology on the H&E section, a LCM cap was placed over the target area of the slide section^[18,19]. Target foci in the same position as GST-P (+) or AFP (+) foci were then microdissected.

Extraction of DNA of LCM samples

After microdissection, the LCM cap was inserted into an Eppendorf tube containing $50\ \mu\text{l}$ of digestion buffer of 0.04% proteinase K, 10 mM Tris-HCl pH 8.0, 1 mM EDTA, and 1% Tween-20. The tube was then placed upside down overnight at 37°C . Following ethanol precipitation, DNA was extracted by the phenol/chloroform/isopropanol method and used directly as a template for PCR.

Extraction of total RNA of LCM samples

After laser transfer, the LCM cap was gently placed on the Eppendorf tube containing $200\ \mu\text{l}$ of reaction mixture. The tube was inverted back and shaken several times for over two minutes to digest the tissue on the cap. The digestive solution was removed from the Eppendorf tube and placed into a 1.5 ml sturdy tube, extraction and purification of total RNA were conducted according to conventional methods. The pellet of total RNA was then resuspended in H_2O , and stored at -80°C .

Primers for RT-PCR, direct sequencing of p53

We designed upstream PCR primers P1, P2, and P3 in the region corresponding to introns 4, 5, and 7 (Figure 1 and Table 1). They were used in combination with downstream primers P4, P5, and P6 within the region corresponding to introns 5, 7 and 8 of p53 gene (Figure 1 and Table 1), to specifically amplify exons 5, 6/7, and 8 of the functional p53 gene without p53 pseudo-gene. The primers Pmu and Pmd for RT-PCR were located on exons 7 and 8 (Figure 1 and Table 1).

Quantitative analysis of mRNA

RNAs extracted from prehepatocarcinoma and hepatocarcinoma foci captured by LCM were reverse-transcribed into first strand cDNA at 42°C for 50 min and at 99°C for 5 min using Oligo-dT-adaptor-primer of an RNA PCR kit (Takara, Co. Ltd., Japan) as the primer. A $1\ \mu\text{l}$ aliquot of first-strand cDNA or H_2O (as a negative control) was put into LightCycler capillary, together with $1\ \mu\text{l}$ of 20 pM primer (Table 1) for target DNA and $18\ \mu\text{l}$ of mixture of LightCycler-DNA Master SYBR Green I mixture. Various concentrations of standard sample cDNA were also used to construct a standard curve. After instantaneous centrifugation, capillaries were loaded onto a LightCycler instrument. Quantitative analysis of mRNA was conducted under PCR conditions in Table 1. The standard curve was shown as a straight line of linear regression with cycle number *versus* log-concentration of standard samples. This standard curve, in turn, was used to estimate the concentration of each sample. Since the expression of β -actin mRNA is constant in all types of cells, it was used to calibrate the original concentration of mRNA, i.e., the concentration unit of mRNA in tissue was defined as the ratio of target mRNA copies *versus* β -actin mRNA copies^[20].

Mutation screening of p53 exons 5, 6/7, and 8

DNAs from the same LCM samples were amplified by PCR under the conditions in Table 1. PCR products were refined by a Microcon-100 kit (Takara, Co. Ltd., Japan). The sense strand

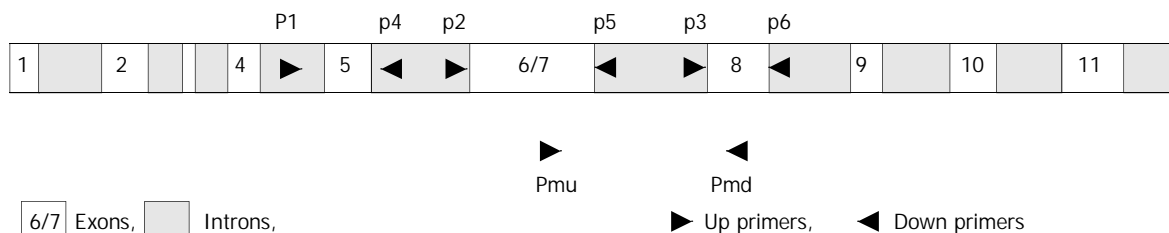


Figure 1 Strategy of primers. To avoid p53 pseudogene co-amplification, the upstream PCR primers P1, P2, and P3 in the region corresponding to introns 4, 5, and 7 were used in combination with downstream primers P4, P5, and P6 within the region corresponding to introns 5, 7, and 8 of p53 gene. Primers Pmu and Pmd for RT-PCR located in exons 7 and 8, respectively.

Table 1 Primer sequences and PCR conditions used in sequencing DNA of p53 gene and RT-PCR

Exons	Primer	Primer sequences of p53	Conditions
5	P1	GACCTTTGATTCTTTCTCCTCTCC	94°C , 3 min (94°C , 30 sec; 56°C , 30 sec; 72°C , 30 sec) $\times 30$
	P4	GGGAGACCCTGGACAACCAG	
6/7	P2	GCCTCTGACTTATTCTTGCTC	94°C , 3 min (94°C , 30 sec; 56°C , 30 sec; 72°C , 30 sec) $\times 30$
	P5	CCCAACCTGGCACACAGCTTC	
8	P3	CTGTGCCTCCTCTTGTCCTCCG	94°C , 3 min (94°C , 30 sec; 56°C , 30 sec; 72°C , 30 sec) $\times 30$
	P6	CCACCTTCTTTGTCTCTGCCTG	
P53 mRNA	Pu	GTCGGCTCCGACTATAACCACTATC	95°C , 2 min (95°C , 0 sec; 56°C , 5 sec; 72°C , 11 sec) $\times 30$
	Pd	CTCTCTTTGCACTCCCTGGGGG	
GST-P mRNA	Pu	ATCGTCCACGCAGCTTTGA	95°C , 2 min (95°C , 0 sec; 57°C , 5 sec; 72°C , 13 sec) $\times 30$
	Pd	AGCCTCCTTCTGGTCTTTC	
β -actin mRNA	Pu	ACCACCATGTACCCAGGCAT	95°C , 2 min (95°C , 0 sec; 56°C , 5 sec; 72°C , 10 sec) $\times 30$
	Pd	CCGGACTCATCGTACTCCTG	

of PCR products was sequenced using a cycler sequencing ready reaction kit (ABI, Perkin-Elmer Corp., USA) and analyzed on an ABI Prism™ 310 genetic analyzer (ABI, Perkin-Elmer Corp., USA).

Immunohistochemical staining

Immunohistochemical staining was conducted using the avidin-biotin-peroxidase complex technique (Vectastain Elite ABC Kit, Funakoshi Co. Ltd., Tokyo, Japan)^[21]. Paraffin-embedded or frozen rat liver specimens were sectioned at 5 μm and placed on a pre-cleaned glass microscope slide. After deparaffination and blocking of endogenous biotin activity, the sections were incubated with primary antibodies (anti-GST-P IgG diluted at 1:500, anti-AFP IgG diluted at 1:200 (polyclonal antibody) and anti-p53 monoclonal antibody Ab1 (Oncogene Science, Inc., USA) diluted at 1:100) for 90 min at 30 °C, then incubated with biotinylated anti-rabbit (for polyclonal antibody) or anti-mouse (for monoclonal antibody) secondary antibody for 30 min at 30 °C. The slides were incubated for 30 min with avidin-peroxidase conjugates. Finally, the sections were reacted with 3' 3-diaminobenzidine tetrahydrochloride and hydrogen peroxide for 3 min followed by counter-staining with hematoxylin. For a negative control, pre-immune serum instead of primary antibody was used.

Statistical methods

Student-*t* test was used to identify the differences of mRNA concentration in normal tissue, precancerous and cancerous foci.

RESULTS

Hepatocarcinogenesis

Prehepatocarcinoma foci could be found in all (13) the livers of rats treated with 3'-Me-DAB for 12 weeks, which were intensely stained by GST-P (Figure 2, B). By H&E staining, the size of prehepatocarcinoma cells was similar to that of normal hepatocytes, but the cytoplasm of precancer cells

was clearer. Under low power magnification, the edge of prehepatocarcinoma focus was distinct and bright (Figure 2, A). Hepatocarcinoma foci were seen in 6 liver sections. By H&E staining, the sizes of nuclei were different, the cytoplasm was a little basophilic and a lot of fat vesicles were present in cytoplasm of hepatocarcinoma cells (Figure 2, C). Immunohistochemically staining for AFP was intensive in hepatocarcinoma foci. At week 24 (Figure 2, D), all (13) the livers exhibited hepatocarcinoma foci and some showed prehepatocarcinoma foci simultaneously. The diameter of precancerous foci was 0.5 mm-1.0 mm at week 6, 1.2 mm-1.5 mm at week 12 and >2.5 mm at week 23. Forty-four precancerous and 24 cancerous samples were obtained for DNA sequencing analysis and quantitative analysis of p53 mRNA.

Expression of p53 and GST-P mRNA

The time course of p53 gene expression showed that the mRNA levels peaked at week 6 in prehepatocarcinoma foci and at week 12 in hepatocarcinoma foci, although they declined significantly by week 24 ($P < 0.01$, Figure 3). The relative concentration of p53 mRNA in adjacent normal tissue remained significantly lower than in prehepatocarcinoma and hepatocarcinoma foci. In hepatocarcinoma foci, the relative concentration of p53 mRNA was 10 *odd* times higher than in adjacent normal tissue at week 6 of the experiment ($P = 5.6 \times 10^{-9}$) and 4 times as high at week 12 ($P = 4.8 \times 10^{-9}$). p53 mRNA concentration was also significantly higher in cancer than in adjacent normal tissue at week 12 ($P = 0.028$). However, at week 24, p53 mRNA of both prehepatocarcinoma and hepatocarcinoma foci was obviously elevated. Relative p53 mRNA concentration was the highest in prehepatocarcinoma foci and the lowest in adjacent normal tissue among the three tissues examined (Figure 3).

Moreover, the expression of GST-P mRNA was low in adjacent normal tissue from week 6 to week 24, and was significantly higher in prehepatocarcinoma foci than in adjacent normal tissue and hepatocarcinoma foci ($P < 0.001$),

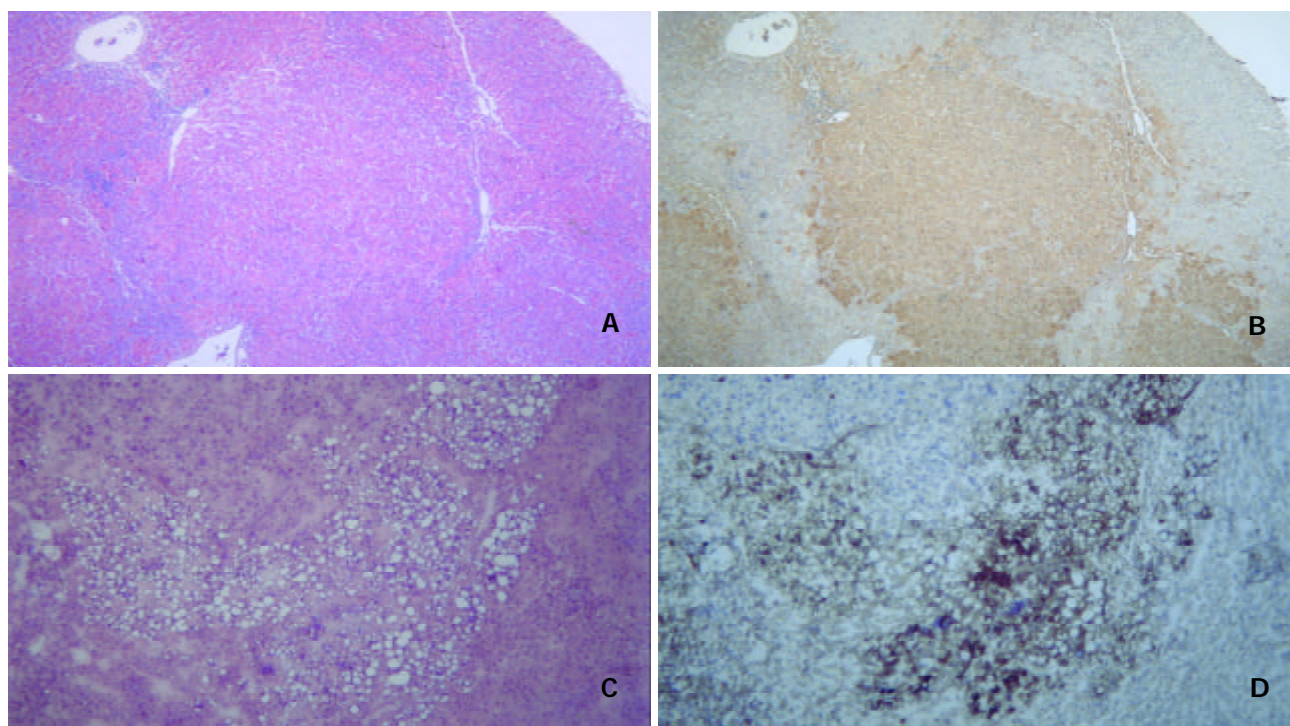


Figure 2 Hepatocarcinogenesis. A: Prehepatocarcinoma foci were stained by H&E, morphology of prehepatocarcinoma cells was similar to that of normal hepatocytes, and the edge of prehepatocarcinoma focus was distinct and bright. B: Prehepatocarcinoma focus was as intensely stained by GST-P as A. C: Hepatocarcinoma foci by H&E staining showed a lot of foam cells. D: Immunohistochemical staining for AFP was intensive in hepatocarcinoma foci.

and higher in hepatocarcinoma foci than in adjacent normal tissue (Figure 4).

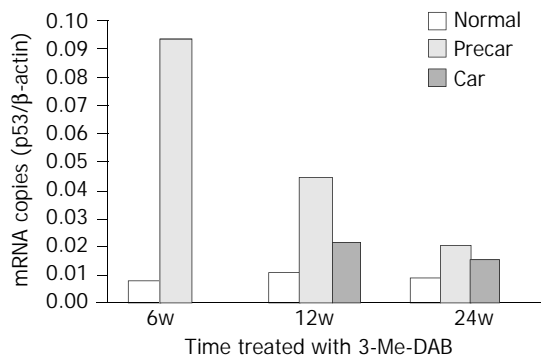


Figure 3 Quantitative analysis of p53 mRNA. After rats were treated with 3'-Me-DAB for 6, 12 and 24 weeks, the expressions of p53 mRNA were markedly higher in prehepatocarcinoma than in hepatocarcinoma and adjacent normal tissue, $P < 0.001$. The time course of p53 mRNA showed that mRNA levels peaked at week 6, and gradually decreased to minimum at week 24. Normal=adjacent normal tissue, Precar=prehepatocarcinoma, Car=hepatocarcinoma.

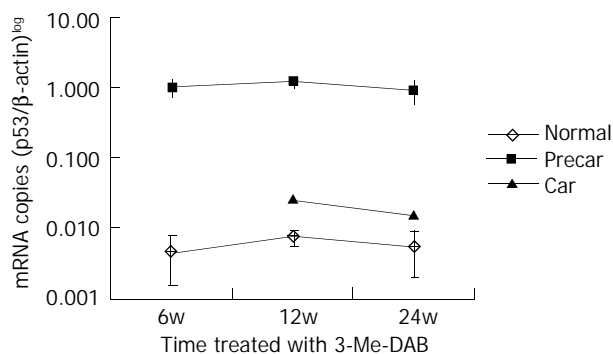


Figure 4 Quantitative analysis of GST-P mRNA. After rats were treated with 3'-Me-DAB for 6, 12 and 24 weeks, the expressions of GST-P mRNA were markedly higher in prehepatocarcinoma than that in hepatocarcinoma and adjacent normal tissue, $P < 0.001$, and also higher in hepatocarcinoma than that in adjacent normal tissue, $P < 0.001$. GST-P mRNA levels were expressed on a logarithmic scale. Normal=adjacent normal tissue, Precar=prehepatocarcinoma, Car=hepatocarcinoma.

Direct sequencing analysis of p53 mutation

Direct sequencing analysis of genomic DNA from 24 LCM samples showed 39 mutations at 18 codons of exons 6/7 and 8 in p53 gene (Figure 5, A, C, E). Of these 39 mutations, 10 transition mutations (1 A:T→G:C, 9 G:C→A:T) (Figure 5, A,C) and 29 transversion mutations (9 G:C→C:G, 9 G:C→T:A, 5 C:G→A:T, 2 C:G→G:C, 2 A:T→C:G, 1 T:A→A:T and 1 A:T→T:A) (Figure 5, E) were identified. A base inserting mutation following the first base substitution, G→TA, in codon 283 of exon 7 resulted in a putative substitution "end" for glutamic acid in p53 protein. Interestingly, four LCM samples had triple mutations and eight LCM samples had double mutations in exons 6/7 or/and 8 simultaneously. One LCM sample with triple mutations and 3 with double mutations were prehepatocarcinoma foci, and 3 other samples with triple mutations and 5 with double mutations were hepatocarcinoma foci.

In brief, 24/68 (35.3%) of LCM samples had mutations of p53 gene. No mutation in exon 5 was found by direct sequencing.

Incidence of p53 gene mutation in hepatocarcinogenesis

20.5% precancerous foci samples expressed point mutation or

inserting mutation in exons 6/7 and 8, and the incidence of mutation was markedly higher than that of cancerous samples ($\chi^2=12.02$, $P < 0.01$). At 12 weeks, the incidence of mutation was significantly higher in hepatocarcinoma samples than in prehepatocarcinoma samples, $P=0.034$ by Fisher's exact probabilities (Figure 6). At 24 weeks, the incidence of mutation was not different between prehepatocarcinoma and hepatocarcinoma foci samples.

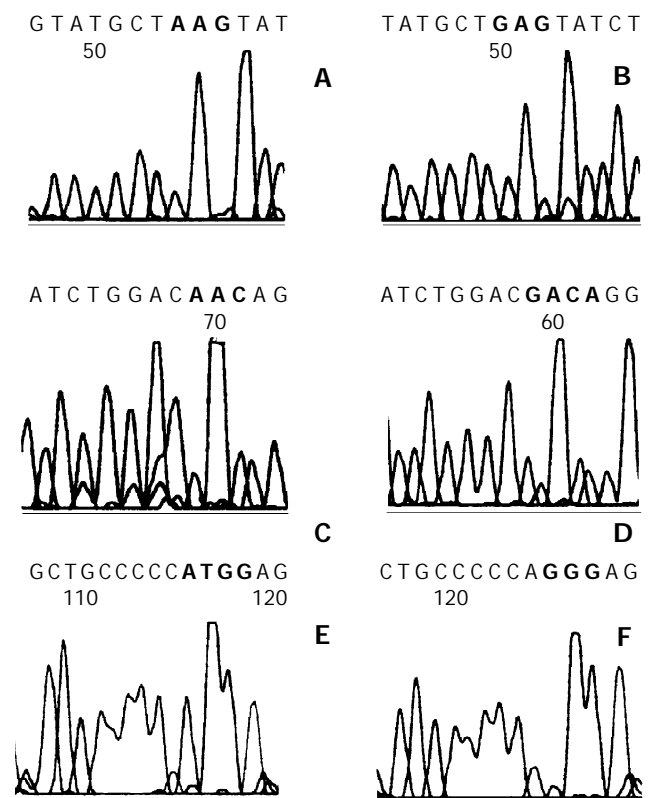


Figure 5 Direct sequencing of p53 exons 6/7 and 8. A: GAG to AAG transition mutation (red box) at codon 202 of exon 6/7 was seen in prehepatocarcinoma foci at 6 weeks. C: Four hepatocarcinoma foci with GAC to AAC transition mutation (red box) at codon 206 formed one of the mutation hot spots. E: GGG to CTG transversion mutation (red box) at codon 300 of exon 8 in hepatocarcinoma foci. B, D and F were normal sequence.

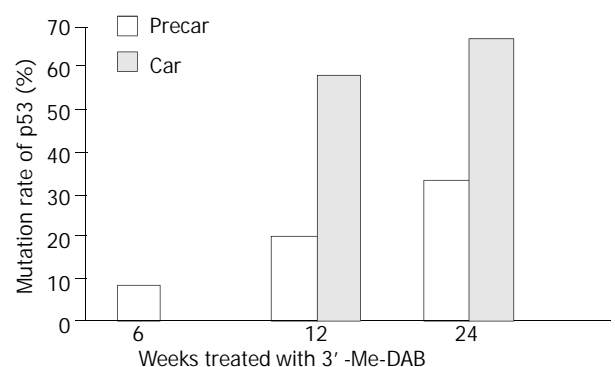


Figure 6 Mutation ratio of p53 exons 6/7 and 8 in prehepatocarcinoma (precar) and hepatocarcinoma foci (car).

Hot spot of mutation

Among the 34 mutation codons of p53 exons 6/7 and 8, 9 were at codon 233, 5 at codons 278 and 279, respectively, 4 at codon 206 (Figure 5,C), and 3 mutations were at codon 112. These mutational codons formed the mutational hot spots of precancerous and cancerous foci in this study, and were located in highly conservative DNA binding domain of p53 protein.

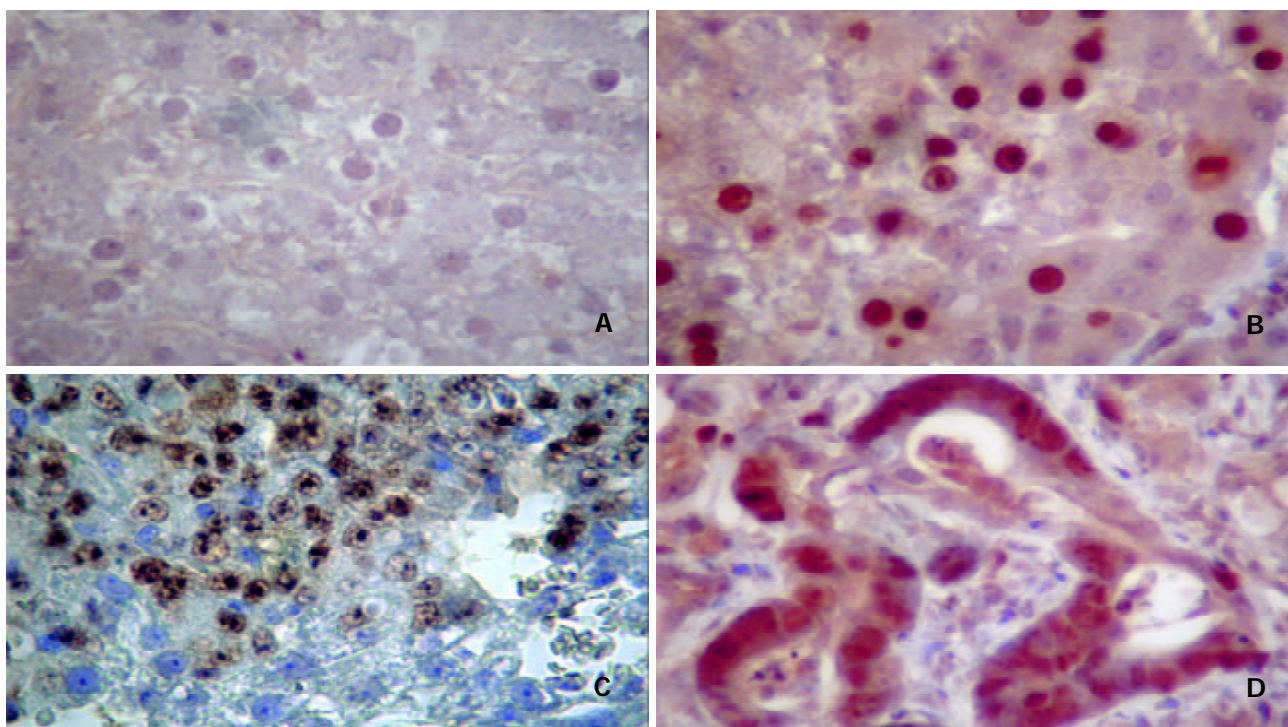


Figure 7 Mutant p53 protein expressions in prehepatocancer and hepatocancer. A: Normal tissue. B: Nuclei of prehepatocarcinoma cells immunostained by anti-p53 Ab1. C: Nuclei of hepatocellular carcinoma cells stained by anti-p53 Ab1. D: Nuclei of adenohepatoma cells stained by anti-p53 Ab1. Enlarged nuclei intensely stained for Ab1 were seen in cells. Original magnification 400 \times .

Expression of p53 protein in cells

As shown in Figure 7, paraffin-embedded or frozen liver sections from rats treated with 3'-Me-DAB for 24 weeks exhibited intensive immunostaining of p53 protein in at least 30% cells of prehepatocarcinoma (Figure 7B) and hepatocarcinoma foci (Figure 7, C, D). Staining was predominantly limited to enlarged nuclei with intensive staining for the anti-p53 antibody. In contrast, no liver sections from rats treated with 3'-Me-DAB for 6 or 12 weeks demonstrated immunostaining for p53 protein (Figure 7, A).

DISCUSSION

Researchers are used to studying human tumors by obtaining human hepatocarcinoma tissue after hepatectomy, but it is difficult to obtain pre-hepatocarcinoma foci in cases without clinical symptoms. We and other investigators were therefore constrained to using rats as the animal model for assessing the effects of p53 gene mutations on hepatocarcinogenesis^[22,23]. It has been found that rat p53 gene differs from human p53 gene, in that it processes pseudogenes in its genome^[24,25]. Pitfalls associated with p53 pseudogene co-amplification from genomic DNA could be avoided, however, by designing PCR primers based on the intron sequence^[24,26].

Carcinogenesis is a complex process characterized by the cumulative activation of various oncogenes and the inactivation of suppressor genes. About 30-40% of human hepatocarcinomas and 20-60% of rat experimental tumors demonstrated mutations of p53 gene^[2,27-30]. Chemically induced rat liver cancer proceeds through multiple, distinct initiation-promotion-progression stages and mutation of the suppressor p53 gene has been found in relatively early preneoplastic lesions in the rat liver.

We used quantification of p53 mRNA expression to detect genetic alterations at RNA level in the present study. The results showed that in precancerous foci of the rat liver, p53 mRNA rose quickly and peaked at week 6 of 3'-Me-DAB treatment. It then gradually decreased from week 12 and fell to a minimum

at week 24 of the experiment. Similar results were also seen in cancer foci. The time course of mRNA expression differed from that of p53 protein accumulation in nuclei. GST-P is one of the detoxification enzymes involved in the metabolism of 3'-Me-DAB as well as other carcinogens and plays a protective role during chemical hepatocarcinogenesis. It is considered as an early marker of preneoplastic lesion. When GST-P played a protective role, mRNA transcript increased coincidentally with positive GST-P immunostaining in prehepatocarcinoma foci of the rats at all experimental time points tested (data not shown). GST-P overexpression was not consistent with an aberration in p53 protein expression^[31].

In this paper, 20.5% of precancerous foci occurring after week 6, week 12, and week 24 exhibited missense mutations of p53 exons 6/7 or/and 8, with double or triple codon mutations found in the same sample by direct sequencing. Of the hepatocarcinoma foci, 58.3% and 66.7% had mutations in p53 gene at week 12 and week 24 of 3'-Me-DAB treatment, respectively. Mutations were distributed widely throughout exons 6/7 and 8, but not in exon 5. p53 mutation rate increased from week 6 to week 24, suggesting that p53 gene mutation is closely associated with hepatocarcinoma development and progression. It is possible that p53 mutation ran through the initiative, intermediate, and late stages of hepatocarcinogenesis, and was not an event occurring only at the advanced stage of liver cancer. Therefore, mutant p53 molecules have been thought to have some unique properties that are important in carcinogenesis in rats^[32].

A tetramer of p53 molecules has been assembled through carboxyterminal oligomerization domains. This allows the central domains to interact directly with a consensus DNA element. As a consequence, aminoterminal transactivation domains could interact with basal transcription factors, resulting in increased gene expression^[33,34]. Among the 39 mutation codons of p53 exons 6/7 and 8, 9 were at codon 233, 5 at codons 278 and 279, respectively, 4 at codon 206, and 3 mutations were at codon 212. These mutational codons formed

mutational hot spots of precancerous and cancerous foci in this study, and were located in the highly conservative DNA binding domain of p53 protein^[35].

Over 90% of mutations are missensed, causing the substitution of amino acids. It has been found that mutation hot spots were dispersed in three exons of p53 gene, and three hotspots fell within two evolutionarily highly conserved regions^[35,36], suggesting no single spot is responsible for maintaining p53 tumor suppressor function. In fact, a certain oncogenic agent could act on only one or more spots of the p53 gene DNA sequence. The effect of the hotspots is yet uncertain, because a certain oncogenic agent has made different mutational hotspots of p53 gene in different species^[37-40] and tissues^[28,39,40].

Amino acid residues 278 and 279 of the p53 protein have been found to be located in helix H₂ of loop-sheet-helix fitting in the major groove of DNA, allowing them to contact edges of the bases, and to play a central role in DNA recognition^[41], so mutation occurring in this area may cause p53 to lose its growth regulation.

Positive immunostaining of p53 was only found in sections of LCM samples treated with 3'-Me-DAB for 24 weeks, not in those treated for 6 or 12 weeks, demonstrating that p53 protein accumulates relatively late during hepatocarcinogenesis. Positive immunostaining of p53 was consistent with the increased half-life of mutant p53 protein compared to wild-type p53^[35,42,43]. As the half-life of wild-type p53 protein is short, it is usually too difficult to detect it in normal tissue with Western blotting or immunohistochemical staining. Mutant p53 protein could competitively inhibit the function of wild p53 protein, promoting hyperplasia of cells and leading to tumor development^[44,45]. A few studies have reported that accumulation of p53 protein in nuclei in late chemical hepatocarcinogenesis was not synchronized with the increased expression of p53 mRNA^[28,46,47]. The rise of p53 mRNA markedly preceded the rise of the expression quantity of p53 protein^[19,48].

We showed that mutation of p53 gene occurred in early precancerous and cancerous foci of F344 rats treated with 3'-Me-DAB and mutation increased progressively from week 6 to week 24, but the expression of p53 mRNA decreased progressively from week 6 to week 24. The detection of p53 gene mutation may benefit the early diagnosis of tumors^[49], and also may aid in understanding the mechanism behind hepatocarcinogenesis.

REFERENCES

- Teeguarden JG**, Newton MA, Dragan YP, Pitot HC. Genome-wide loss of heterozygosity analysis of chemically induced rat hepatocellular carcinomas reveals elevated frequency of allelic imbalances on chromosomes 1, 6, 8, 11, 15, 17, and 20. *Mol Carcinog* 2000; **28**: 51-61
- De Miglio MR**, Muroi MR, Simile MM, Viridis P, Asara G, Frau M, Calvisi DF, Seddaiu MA, Pascale RM, Feo F. Frequent loss of heterozygosity at the Hcr1 (hepatocarcinogenesis resistance) locus on chromosome 10 in primary hepatocellular carcinomas from LFF1 rat strain. *Hepatology* 2001; **33**: 1110-1117
- Kishimoto Y**, Shiota G, Kamisaki Y, Wada K, Nakamoto K, Yamawaki M, Kotani M, Itoh T, Kawasaki H. Loss of the tumor suppressor p53 gene at the liver cirrhosis stage in Japanese patients with hepatocellular carcinoma. *Oncology* 1997; **54**: 304-310
- Ashida K**, Kishimoto Y, Nakamoto K, Wada K, Shiota G, Hirooka Y, Kamisaki Y, Itoh T, Kawasaki H. Loss of heterozygosity of the retinoblastoma gene in liver cirrhosis accompanying hepatocellular carcinoma. *J Cancer Res Clin Oncol* 1997; **123**: 489-495
- Lu JP**, Mao JQ, Li MS, LU SL, Hu XQ, Zhu SN, Nomura S. *In situ* detection of TGF betas, TGF beta receptor II mRNA and telomerase activity in rat cholangiocarcinogenesis. *World J Gastroenterol* 2003; **9**: 590-594
- Ryan KM**, Phillips AC, Vousden KH. Regulation and function of the p53 tumor suppressor protein. *Curr Opin Cell Biol* 2001; **13**: 332-337
- Miller DP**, Liu G, De Vivo I, Lynch TJ, Wain JC, Su L, Christiani DC. Combinations of the variant genotypes of GSTP1, GSTM1, and p53 are associated with an increased lung cancer risk. *Cancer Res* 2002; **62**: 2819-2823
- Campling B**, El-Deiry W. Clinical Implication of p53 Mutation in Lung Cancer. *Mol Biotechnol* 2003; **24**: 141-156
- Vousden KH**. p53: death star. *Cell* 2000; **103**: 691-694
- Wilson DR**. Viral-mediated gene transfer for cancer treatment. *Curr Pharm Biotechnol* 2002; **3**: 151-164
- Vousden KH**. Switching from life to death: The Miz-ing link between Myc and p53. *Cancer Cell* 2002; **2**: 351-352
- Vousden KH**. Activation of the p53 tumor suppressor protein. *Biochim Biophys Acta* 2002; **1602**: 47-59
- Harris CC**. p53: at the crossroads of molecular carcinogenesis and risk assessment. *Science* 1993; **262**: 1980-1981
- Livingstone LR**, White A, Sprouse J, Livanos E, Jacks T, Tlsty TD. Altered cell cycle arrest and gene amplification potential accompany loss of wild-type p53. *Cell* 1992; **70**: 923-935
- Fearon ER**, Vogelstein B. A genetic model for colorectal tumorigenesis. *Cell* 1990; **61**: 759-767
- Oda T**, Tsuda H, Scarpa A, Sakamoto M, Hirohashi S. p53 gene mutation spectrum in hepatocellular carcinoma. *Cancer Res* 1992; **52**: 6358-6364
- Sugioka Y**, Fujii-Kuriyama Y, Kitagawa T, Muramatsu M. Changes in polypeptide pattern of rat liver cells during chemical hepatocarcinogenesis. *Cancer Res* 1985; **45**: 365-378
- Bonner RF**, Emmert-Buck M, Cole K, Pohida T, Chuaqui R, Goldstein S, Liotta LA. Laser capture microdissection: molecular analysis of tissue. *Science* 1997; **278**: 1481-1483
- Fu Y**, Deng WG, Li YL, Sugiyama T. Quantitative analysis of p53 and related genes mRNA in rat hepatocarcinogenesis induced by 3'-Me-DAB. *Ai Zheng* 2003; **22**: 35-41
- Wittwer CT**, Ririe KM, Andrew RV, David DA, Gundry RA, Balis, UJ. The LightCycler: a microvolume multisample fluorimeter with rapid temperature control. *Biotechniques* 1997; **22**: 176-181
- Lehman TA**, Haffty BG, Carbone CJ, Bishop LR, Gumbs AA, Krishnan S, Shields PG, Modali R, Turner BC. Elevated frequency and functional activity of a specific germ-line p53 intron mutation in familial breast cancer. *Cancer Res* 2000; **60**: 1062-1069
- Fukuda I**, Ogawa K. Alternatively-spliced p53 mRNA in the FAA-HTC1 rat hepatoma cell line without the splice site mutations. *Cell Struct Funct* 1992; **17**: 427-432
- Ohgaki H**, Hard GC, Hirota N, Maekawa A, Takahashi M, Kleihues P. Selective mutation of codons 204 and 213 of the p53 gene in rat tumors induced by alkylating N-nitroso compounds. *Cancer Res* 1992; **52**: 2995-2998
- Weghorst CM**, Buzard GS, Calvert RJ, Hulla JE, Rice JM. Cloning and sequence of a processed p53 pseudogene from rat: a potential source of false 'mutations' in PCR fragments of tumor DNA. *Gene* 1995; **166**: 317-322
- Lin Y**, Chan SH. Cloning and characterization of two processed p53 pseudogenes from the rat genome. *Gene* 1995; **156**: 183-189
- Hulla JE**, Schneider RP. Structure of the rat p53 tumor suppressor gene. *Nucleic Acids Res* 1993; **21**: 713-717
- Masui T**, Nakanishi H, Inada K, Imai T, Mizoguchi Y, Yada H, Futakuchi M, Shirai T, Tatematsu M. Highly metastatic hepatocellular carcinomas induced in male F344 rats treated with N-nitrosomorpholine in combination with other hepatocarcinogens show a high incidence of p53 gene mutations along with altered mRNA expression of tumor-related genes. *Cancer Lett* 1997; **112**: 33-45
- Bressac B**, Kew M, Wands J, Ozturk M. Selective G to T mutations of p53 gene in hepatocellular carcinoma from southern Africa. *Nature* 1991; **350**: 429-431
- Volkman M**, Hofmann WJ, Muller M, Rath U, Otto G, Zentgraf H, Galle PR. p53 overexpression is frequent in European hepatocellular carcinoma and largely independent of the codon 249 hot spot mutation. *Oncogene* 1994; **9**: 195-204
- Vancutsem PM**, Lazarus P, Williams GM. Frequent and specific mutations of the rat p53 gene in hepatocarcinomas induced by tamoxifen. *Cancer Res* 1994; **54**: 3864-3867

- 31 **Liu YP**, Lin Y, Ng ML. Immunochemical and genetic analysis of the p53 gene in liver preneoplastic nodules from aflatoxin-induced rats in one year. *Ann Acad Med Singapore* 1996; **25**: 31-36
- 32 **Haas MJ**, Pitot HC. Characterization of rare p53 mutants from carcinogen-treated albumin-simian virus 40 T-antigen transgenic rats. *Mol Carcinog* 1998; **21**: 128-134
- 33 **Vousden KH**, Lu X. Live or let die: the cell's response to p53. *Nat Rev Cancer* 2002; **2**: 594-604
- 34 **Vogelstein B**, Lane D, Levine AJ. Surfing the p53 network. *Nature* 2000; **408**: 307-310
- 35 **Hollstein M**, Sidransky D, Vogelstein B, Harris CC. p53 mutations in human cancers. *Science* 1991; **253**: 49-53
- 36 **Tam AS**, Foley JF, Devereux TR, Maronpot RR, Massey TE. High frequency and heterogeneous distribution of p53 mutations in aflatoxin B1-induced mouse lung tumors. *Cancer Res* 1999; **59**:3634-3640
- 37 **Denissenko MF**, Koudriakova TB, Smith L, O'Connor TR, Riggs AC, Pfeifer GP. The p53 codon 249 mutational hotspot in hepatocellular carcinoma is not related to selective formation or persistence of aflatoxin B1 adducts. *Oncogene* 1998; **17**: 3007-3014
- 38 **Hulla JE**, Chen ZY, Eaton DL. Aflatoxin B1-induced rat hepatic hyperplastic nodules do not exhibit a site-specific mutation within the p53 gene. *Cancer Res* 1993; **53**: 9-11
- 39 **Hsu IC**, Metcalf RA, Sun T, Welsh JA, Wang NJ, Harris CC. Mutational hotspot in the p53 gene in human hepatocellular carcinomas. *Nature* 1991; **350**: 427-428
- 40 **Makino H**, Ishizaka Y, Tsujimoto A, Nakamura T, Onda M, Sugimura T, Nagao M. Rat p53 gene mutations in primary zymbal gland tumors induced by 2-Amino-3-methylimidazo [4,5-f] quinoline, a food mutagen. *Proc Natl Acad Sci U S A* 1992; **89**: 4850-4854
- 41 **Cho Y**, Gorina S, Jeffrey PD, Pavletich NP. Crystal structure of a p53 tumor suppressor-DNA complex: understanding tumorigenic mutations. *Science* 1994; **265**: 346-355
- 42 **Oren M**, Maltzman W, Levine AJ. Post-translational regulation of the 54K cellular tumor antigen in normal and transformed cells. *Mol Cell Biol* 1981; **1**: 101-110
- 43 **Sturzbecher HW**, Chumakov P, Welch WJ, Jenkins JR. Mutant p53 proteins bind hsp 72/73 cellular heat shock-related proteins in SV40-transformed monkey cells. *Oncogene* 1987; **1**: 201-211
- 44 **Milner J**, Medcalf EA. Cotranslation of activated mutant p53 with wild type drives the wild-type p53 protein into the mutant conformation. *Cell* 1991; **65**: 765-774
- 45 **Michalovitz D**, Halevy O, Oren M. p53 mutations: Gains or losses? *J Cell Biochem* 1991; **45**: 22-29
- 46 **Hsu HC**, Tseng HJ, Lai PL, Lee PH, Peng SY. Expression of p53 gene in 184 unifocal hepatocellular carcinomas: association with tumor growth and invasiveness. *Cancer Res* 1993; **53**: 4691-4694
- 47 **Ng IO**, Srivastava G, Chung LP, Tsang SW, Ng MM. Overexpression and point mutations of p53 tumor suppressor gene in hepatocellular carcinomas in Hong Kong Chinese people. *Cancer* 1994; **74**: 30-37
- 48 **Mosner J**, Mummenbrauer T, Bauer C, Sczakiel G, Grosse F, Deppert W. Negative feedback regulation of wild-type p53 biosynthesis. *EMBO J* 1995; **14**: 4442-4449
- 49 **Ono K**, Tanaka T, Tsunoda T, Kitahara O, Kihara C, Okamoto A, Ochiai K, Takagi T, Nakamura Y. Identification by cDNA microarray of genes involved in ovarian carcinogenesis. *Cancer Res* 2000; **60**: 5007-5011

Edited by Zhu LH and Wang XL

Superantigen-SEA gene modified tumor vaccine for hepatocellular carcinoma: An *in vitro* study

Shao-Ying Lu, Yan-Fang Sui, Zeng-Shan Li, Jing Ye, Hai-Long Dong, Ping Qu, Xiu-Min Zhang, Wen-Yong Wang, Yu-Song Li

Shao-Ying Lu, Yan-Fang Sui, Zeng-Shan Li, Jing-Ye, Hai-Long Dong, Ping-Qu, Xiu-Min Zhang, Wen-Yong Wang, Yu-Song Li, Department of Pathology, Fourth Military Medical University, Xi'an 710032, Shaanxi Province, China

Shao-Ying Lu, Ph.D. Candidate of Xi'an Jiaotong University
Supported by National Natural Science Foundation of China, No. 30271474 and No. 39770827

Correspondence to: Professor Yan-Fang Sui, Department of Pathology, Fourth Military Medical University, Xi'an 710032, China. suiyanf@fmmu.edu.cn

Telephone: +86-29-3374541-211 **Fax:** +86-29-3374597

Received: 2003-05-13 **Accepted:** 2003-06-12

Abstract

AIM: To construct an eukaryotic superantigen gene expression vector containing the recombinant gene of SEA and CD80 molecule transmembrane region (CD80TM), and to express staphylococcus enterotoxin A (SEA) on the membrane of hepatocellular carcinoma (HCC) cell to form a superantigen gene modified tumor vaccine for HCC.

METHODS: SEA and linker-CD80TM gene were amplified through PCR from plasmid containing cDNA of SEA and CD80. Gene fragments were then subcloned into the multiple cloning sites of retroviral vector pLXSN. Recombinant plasmid was transferred into HepG2 cells mediated with lipofectamine, positive clones were selected in culture medium containing G418. RT-PCR and indirect immunofluorescence studies confirmed that SEA was expressed specifically on HCC cell membrane. INF- γ -ELISPOT study demonstrated that SEA protein was expressed on the membrane of HCC cells. Cytotoxicity of HepG2-SEA primed CTLs (SEA-T) was analyzed by ^{51}Cr release assay. T cells cultured with rhIL-2 (IL-2-T) were used as control.

RESULTS: Restriction digestion and sequence analyses confirmed the correctness of length, position and orientation of inserted fusion genes. SEA was expressed on the surface of HepG2 cells, HepG2-SEA had strong stimulating effect on production of HepG2 specific CTL ($P < 0.001$). SEA-T had enhanced cytotoxicity to HepG2 cells ($P < 0.05$).

CONCLUSION: Tumor cell membrane expressed superantigen can be used to reinforce the immune effect of tumor cell vaccine for HCC, which provides a new method of the enhanced active immunotherapy for HCC.

Lu SY, Sui YF, Li ZS, Ye J, Dong HL, Qu P, Zhang XM, Wang WY, Li YS. Superantigen-SEA gene modified tumor vaccine for hepatocellular carcinoma: An *in vitro* study. *World J Gastroenterol* 2004; 10(1): 53-57

<http://www.wjgnet.com/1007-9327/10/53.asp>

INTRODUCTION

Autologous and allogeneic tumor cells have been used as tumor

vaccines in clinic for a long time^[1,2]. The tumor cell-based vaccines possess the entire relevant tumor antigens recognized by the immune system and can be produced even without knowing the gene sequence of specific antigens. To identify the tumor specific antigen is time consuming, only few tumor specific antigens have been identified until now. But tumor cell-based immunization could not always elicit anti-tumor responses in sufficient magnitude to cause regression of established tumors due to scarcity of stimulatory surface molecules such as MHC-I, MHC-II or CD80^[3].

Superantigens are a family of bacterial and viral proteins that bind to MHC class II molecules as unprocessed proteins and activate a large number of T cells bearing T cell receptor variable region beta chain (TCR V β)^[4,5]. These T cells proliferate, and secrete cytokines (e.g. IFN- γ , TNF- α , IL-2, and IL-12), induce strong cytolytic activity, and mediate tumor regression^[6-12]. SEA is an important member of superantigen family. Anchoring SEA onto MHC-II negative tumor cells through monoclonal antibody has been demonstrated to direct T cell-mediated cytotoxicity against these tumors^[13,14]. Other studies suggested that artificially anchoring a recombinant superantigen-transmembrane region chimera (SAG-TM) onto a tumor cell surface could substitute for the effect of MHC-II presentation^[15].

In the present study we sought to construct an eukaryotic expression vector containing recombinant gene of SEA and transmembrane region sequence of CD80 molecule (CD80TM). Recombinant gene was transfected into HCC cells, chimera protein (SEA-CD80TM) was expressed on the membrane of living cells. SEA gene modified cells were irradiated and used as a superantigen enhanced tumor cell-based vaccine for HCC, which was capable of inducing antitumor immunity *in vitro*.

MATERIALS AND METHODS

Reagents

EX Taq DNA polymerase, T4 DNA ligation kit Ver.2.0, and restriction endonuclease were obtained from TakaRa Biotechnology (Dalian). DNA isolation and purification kit was purchased from Shanghai ShunHua Biotechnology. LipofectamineTM 2000 were from Invitrogen. IPTG, X-gal, DNA maker and FITC labeled sheep anti mouse IgG were from Sino-American Biotechnology. Dulbecco's modified Eagle media, Trizol and G418 were from GibcoBRL. Access RT-PCR system was from Promega. Human INF- γ ELISPOT assay kit was from Diaclone, Recombinant human interleukin-2 (rhIL-2) and BD TriTESTTM antibody CD4 FITC/ CD8 PE/ CD3 PerCP were from BD Biosciences. Mouse anti-SEA monoclonal antibody was provided by the Department of Immunology, Fourth Military Medical University, P. R. China.

Plasmids

PBluescript II KS (+) plasmids containing cDNA of SEA and CD80 were constructed by Li *et al*^[16]. Retroviral vector pLXSN was preserved in our laboratory.

Cell culture

Human HCC cell lines HepG2 and SMMC-7721 were cultured

in DMEM containing 10% heat-inactivated fetal calf serum, 100 units/ml penicillin, 100 µg/ml streptomycin, 0.292 mg/ml glutamine. The cell lines were incubated in a humidified 5% CO₂ incubator at 37 °C.

Polymerase chain reaction (PCR) and vector construction

The primers used for cloning SEA (774 bp) and CD80TM (147 bp) were as follows. SEA, forward: GCGAATTCGCATGAAAAAACAGCATTAC, reverse: CGGGATCCACTTGTATATAAATATATATCAAT. CD80TM, forward1: GGTGGCTCTGGCGGTGGCGGATCGGATAACCTGCTCCCATCC, forward2: CGGGATCCGGTGGAGGCGGTTTCAGGCGGAGGTGGCTCTGGCGGT, reverse: CCGCTCGAGTTATACAGGGCGTACT. Linker (GGGSGGGSGGGSGGG) was introduced into the upstream of CD80TM using two forward primers. PCR was performed in a 50 µl reaction system consisting of 1 µM each primer, 200 µM each dNTP, 5 µL 10×polymerase reaction buffer, and 1.25U EX Taq DNA polymerase with 1 µL SEA or CD80 gene vector. Samples were heated to 94 °C for 5 min followed by 30 cycles at 94 °C for 30 s, at 50 °C for 50 s, and at 68 °C for 1 min. The final extension was done at 72 °C for 7 min. Then 10 µl of each PCR product was electrophoresed on 1 % agarose gel containing 0.5 µg/mL EB, and PCR products were then purified from agarose gel according to the protocol of DNA purification kit. DNA fragments of SEA (S) and linker-CD80TM (LC) were subcloned into pBluescript II ks(+). The positive clones were selected from the transfected DH5α by the method described by Sambrook *et al*^[17]. The constructed plasmids (designated as ks-S, ks-LC) were identified by restriction enzyme analysis. DNA sequences were verified in DNA sequencing core facility in Bioasia Biotechnology (Shanghai, China). Gene fragments were cut with *EcoRI-BamHI*, *BamHI-XhoI*, and inserted into the *EcoRI-XhoI* site of pLXSN to construct SAg gene expression vector pLXSN-SLC. The recombinant gene was verified by digestion with restriction endonuclease (Figure 1).

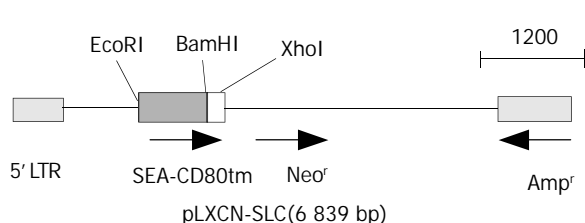


Figure 1 Gene map of expression vector.

In vitro transfection of pLXSN-SLC

pLXSN-SLC was transfected into HepG2 cells using Lipofectamine™ 2000 reagent according to the manufacturer's instructions. Briefly, 2×10⁵ HepG2 cells were seeded into 12-well culture plates and cultured for 18 hours until 90% to 95% confluence of the cells, transfection was performed with 1 µg of DNA per dish. Forty eight h after transfection, cells were passaged at 1:4 dilution into a fresh medium. The next day, G418 400 µg/mL was added into culture medium for the screening of stably transfected cells. The cells were then grown in G418 culture medium for 4 weeks and cloned by limiting dilution. Mock cell line transfected with empty pLXSN vector was selected in G418, and used as control (HepG2-pLXSN).

Detection of SEA expression in transfected cells

Expression of SEA in screened monoclonal cells was detected by RT-PCR. Total RNA was extracted from the tumor cells (HepG2 cells and SEA gene transfected or mock transfected HepG2 cells) using Trizol reagent. RNA (1.5 µg) was used to

synthesize cDNA in 20 µl reaction mixtures following standard protocol of Access RT-PCR system. PCR was carried out with 5 µl of RT products in 50 µl PCR reaction buffer containing *Tfi* polymerase, 1 mM MgCl₂, annealing temperature was 50 °C. SEA cDNA was used as positive control in PCR. Indirect immunofluorescence was performed to locate the expressed SEA. Briefly, 2×10⁵ SEA transfected HepG2 cells (HepG2-SEA) were plated into 12-well culture plates. At the bottom of each well a sterilized coverslip was placed in advance. HepG2 cells were plated as control. When the plated cells were 95-100% confluence, the coverslips were washed twice in cold PBS (0.01M) and fixed with 4% paraformaldehyde for 30 min at room temperature. Cells were stained following the standard protocol of indirect immunofluorescence. First antibody was 1:100 diluted mouse anti-SEA monoclonal antibody in PBS, irrelevant sheep anti-mouse IgG was used as control. Second antibody was 1:500 diluted FITC labeled sheep anti-mouse IgG in 0.1% Evans blue. Coverslips were then mounted directly onto a glass slide with a tiny drop of 50% glycerol in PBS (9.1 mM Na₂HPO₄/1.7 mM NaH₂PO₄/50 mM NaCl, pH 7.4). Fluorescent images were captured at 490 nm using a Nikon Eclipse E1000 microscope attached to a MicroMax camera (Princeton Instruments, Trenton, NJ).

Preparation of T cell lines

Human peripheral blood mononuclear cells (PBMC) were isolated from healthy volunteers by routine density centrifugation, and stimulated with HepG2-SEA to establish SEA-reactive T-cell line (SEA-T). The T cell line was stimulated repeatedly by exposure to irradiated (4 000 rad) HepG2-SEA and rhIL-2 (200 U/mL) in complete medium for 2 weeks, and then stored in frozen. These cells were thawed 1 week before use. T-cell lines stimulated by HepG2-pLXSN (pLXSN-T), HepG2 (HepG2-T) or just maintained with rhIL-2 (IL-2-T) were also prepared and used as control. Cell phenotypes of T cell lines were analyzed using BD TriTEST™ antibody by FACS.

Elispot assay

PVDF 96-well plates were incubated with 100 µl of 70% ethanol for 10 min at room temperature, and washed three times in 100 µl of PBS. Capture antibody was added and incubated at 4 °C overnight. After washed in 100 µl of PBS, each well was added 100 µl of 2% skimmed dry milk in PBS, and incubated for 2 hours at room temperature. Wells were emptied and tapped on absorbent paper, 5×10⁴ effector cells (including SEA-T, pLXSN-T, HepG2-T, IL-2-T) and 1×10⁴ target cells (irradiated HepG2) were seeded to each well and incubated for 20 h in RPMI-1640 medium without IL-2 and serum. Plates were then washed and incubated with detection antibody in PBS-1% BSA for 1 hour and 30 min at 37 °C, and with streptavidin-alkaline phosphatase for 1 h at 37 °C. After washed, substrate (5-bromo-4-chloro-3-indolyl phosphate/nitroblue tetrazolium) was added and incubated for 5-20 min. After the final washing, dark-violet spots on plate membranes were counted under microscope.

Cytotoxicity of HepG2-SEA stimulated T cell line

Cytotoxicity was measured in a standard 4-hour ⁵¹Cr-release assay and expressed in formula: (%) specific lysis = 100 × (experimental - background cpm / maximal background cpm). Target cells (HepG2, SMMC-7721) were labeled for 2 hours with Na₂⁵¹CrO₄ (⁵¹Cr, New England Nuclear, Boston, MA), 250 µCi/1×10⁶ cells. The cells were then washed twice and 5×10³ cells per well were seeded in triplicate in v-bottomed microtiter plates. Effector cells (SEA-T, HepG2-T and IL-2-T) were added at an effector-to-target (E:T) cell ratio of 40:1, 25:1, 10:1, 5:1 and 3:1, respectively. The plates were incubated

at 37 °C and 5% CO₂ for 4 h, supernatants were collected, and the released ⁵¹Cr was measured with a gamma counter (LKB-Wallac 1 282; Stockholm, Sweden). Spontaneous release was estimated by incubation of target cells in medium alone, and maximum release by resuspending the wells with 0.1% Tween 20. Spontaneous release was typically less than 30% of maximum release.

Statistical analysis

All experiments were performed in triplicate, data were presented as the mean ± SD and analyzed using Student's *t* test.

RESULTS

Insertion of SEA and linker-CD80TM into MCS of pLXSN

PCR products were subcloned into a pBluescript II ks (+) vector. DNA sequencing confirmed the correct sequence of both fragments. SEA gene was cloned into the *EcoR* I/*Xho* I site of pLXSN with linker-CD80TM. Recombinant gene SEA-linker-CD80TM was 1.0 kb with *EcoR* I and *Xho* I restriction site on each side, the size of pLXSN was 5.9 kb. Expressing vector pLXSN-SLC was digested by *EcoR* I/*Xho* I, 1.0 kb and 5.9 kb DNA fragments were appeared as expected (Figure 2).

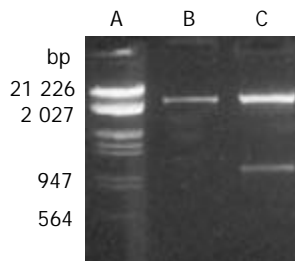


Figure 2 Enzyme digestion analysis of expression vector. A. Lambda DNA (*EcoR*I, *Hind*III); B. pLXSN (*EcoR*I, *xho*I); C. pLXSN-SLC (*EcoR*I, *xho*I).

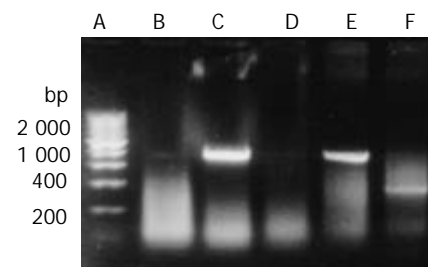


Figure 3 RT-PCR detected the transcription of SEA gene. A. 200 bp DNA marker; B. HepG2; C. HepG2 transfected with pLXSN-SLC; D. HepG2 transfected with pLXSN; E. Positive control; F. β -actin (RNA of C).

SEA expressed on the membrane of HepG2

HepG2 was transfected with plasmid pLXSN-SLC and empty pLXSN vector, respectively. The expression of SEA was detected in HepG2 cells transfected with pLXSN-SLC only by RT-PCR (Figure 3). Indirect immunofluorescence test confirmed that most of the expressed SEA appeared to be located on the HepG2 cells membrane (Figure 4). SEA expression was detected in 5-10 percent of cells screened with G418. Irradiated HepG2-SEA cells were used as T cell stimulator in following experiments.

Increased HepG2 reactive T cells with HepG2-SEA

Interferon- γ (IFN- γ) ELISPOT assay was used to detect the

specificity of HepG2 CD8⁺ T cells quantitatively. Cells tested included unstimulated PBMC (IL-2-T) and polyclonal T-lymphocyte lines stimulated by HepG2-SEA, HepG2-pLXSN or HepG2. After a short term of culture *in vitro*, the percentage of positive cells was more than 90% for CD3⁺, 80% to 90% for CD8⁺, and 5% to 10% for CD4⁺ (Figure 5). The number of HepG2 reactive CTL in the SEA-T cell line was much higher than that of HepG2-T (155.67±7.22 vs 38.03±8.18, *t*=18.67, *P*<0.0001), pLXSN-T (39.50±6.26, *t*=21.06, *P*<0.0001) or IL-2-T (32.00±4.26, *t*=25.56, *P*<0.0001) (Figure 6). Both the size and density of spots in SEA-T group were greater than those of controls (data not shown). The difference of spot number between HepG2-T and IL-2-T cell lines was not significant (*t*=-1.13, *P*=0.321).

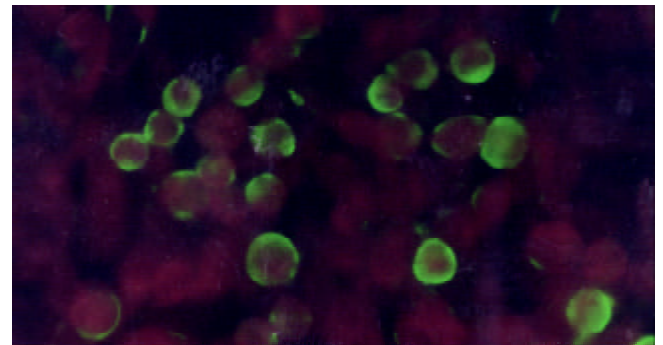


Figure 4 SEA expressed on the membrane of HepG2 (indirect immunofluorescence). HepG2-SEA cells were stained according to the standard protocol of indirect immunofluorescence. First antibody is mouse anti-SEA IgG and second antibody is FITC labeled sheep anti-mouse IgG diluted in 0.1% evan blue. Positive signal is green while the background is red. SEA was located on the membrane of HepG2. Untransfected HepG2 cells did not express SEA (data not show).

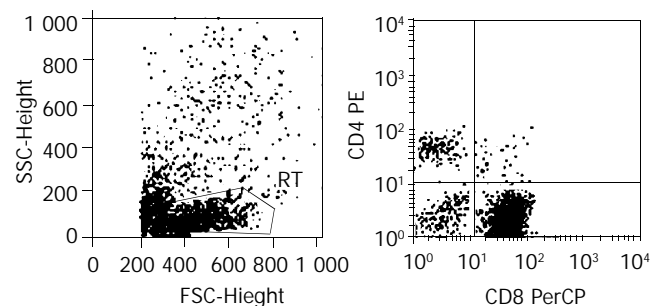


Figure 5 Lymphocyte phenotype analysis. 1×10^5 SEA-T cells were stained with BD TriTEST™ antibody CD4 FITC/CD8 PE/CD3 PerCP, and assayed by FACS. CD3⁺90.75%, CD8⁺84.46%, CD4⁺6.29%.

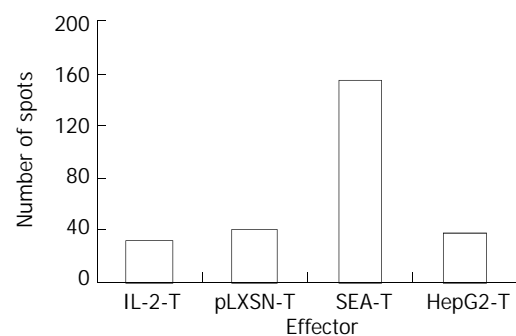


Figure 6 HepG2-SEA increased the number of hepG2 specific CTL in T lymphocyte line. Each bar represents average of spots in triplicate wells.

Enhanced cytotoxicity elicited by membrane expressed SEA

Cytotoxicity of the SEA-T effector cell line against HepG2, and SMMC-7721 target cells was measured (Figure 7). HepG2-T and IL-2-T cells were used as control. In contrast, SEA-T was highly efficient in directing specific lysis of HepG2 cells when compared with HepG2-T ($51.55 \pm 5.051\%$ vs 33.16 ± 4.54 , $t=4.47$, $P=0.011$). The two T cell lines had effective cytotoxicity to SMMC-7721 cells.

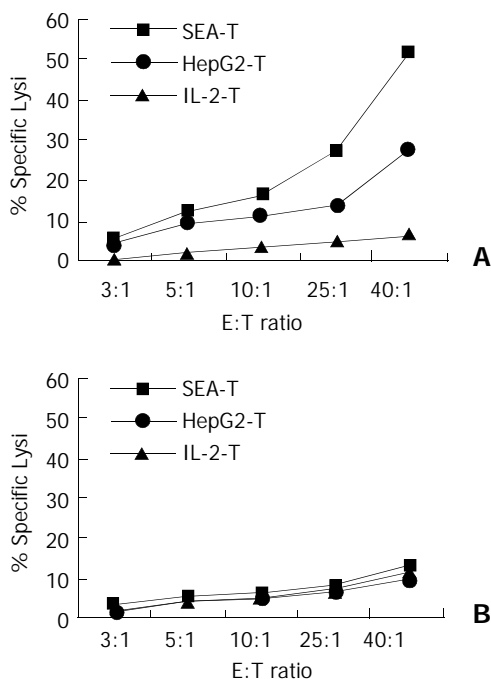


Figure 7 Membrane expressed SEA enhanced specific lysis on autologous tumor cells. Cytotoxicity was measured in a standard 4-hour ^{51}Cr -release assay. Target cells (HepG2, SMMC-7721) were seeded in triplicate in v-bottomed microtiter plates at a concentration of 5×10^3 cells per well. Effector cells were added at an effector-to-target (E:T) cell ratio of 40:1, 25:1, 10:1, 5:1 and 3:1 respectively. A: SEA-T was highly efficient in directing specific lysis of HepG2 cells (squares), HepG2-T has moderate cytotoxicity on HepG2 (cross) cells ($P < 0.001$). B: None of T cell line has killing effect on SMMC-7721 cells.

DISCUSSION

T cells have been found to possess various potent antitumor effects through releasing cytotoxic effector molecules such as perforin or growth-suppressive cytokines IFN- γ and TNF- α ^[18-21]. However, the frequency of tumor-specific T cells could be generally too low and insufficient to interfere with progressive tumor growth. The goal of this experiment was to examine the possibility of developing a new experimental vaccine from irradiated HepG2 cells that were transfected to express superantigen-SEA on membrane (designed as HepG2-SEA) to augment cellular and humoral anti-tumor immune responses. Superantigen is the most effective T cell activator. Upon stimulation by superantigens, naïve T cells could respond and then become quickly anergized and/or deleted, while mature T cells could not become anergized^[22-24]. Characteristics of superantigens can thus be exploited to enhance specific antigen responses. Because superantigens can cause anergy and/or deletion of potentially competing naïve T cells bearing the same V β element (s), thus there is less “competition” for cytokines and the desired specific immune response can be amplified.

HCC cells do not induce an effective immunological rejection process because of their weak antigenicity, the abnormal expression of MHC molecules as well as the

deletion or deficiency of costimulatory molecules. In the present study, the expressed superantigen-SEA on the membrane of HepG2 cells was confirmed by RT-PCR and indirect immunofluorescence assays. When HepG2-SEA cells were used as a vaccine, two stimulating signals would present to T cells simultaneously, one was SEA, the other was tumor-associated antigens expressed on the surface of HepG2 cells, which facilitated the occurrence of specific anti-tumor immune reaction.

IFN- γ ELISPOT (enzyme-linked immunospot) assay was used for the quantitative detection of HepG2-specific CD8⁺ T cells. This technique could detect T cells that secrete a given cytokine (e.g., IFN- γ) in response to an antigenic stimulation^[25]. The size and density of spots represented the quantity of IFN- γ secreted by single CTL^[18]. The results showed that the number of HepG2 cell specific CTLs in repeatedly stimulated T cell line (SEA-T) with new vaccines was significantly increased than that of HepG2 cell-based vaccines ($P < 0.001$). Cytotoxic assay demonstrated that SEA-T was highly efficient in directing specific lysis of HepG2 cells other than SMMC-7721 cells. When compared with HepG2-T, the difference induced by new vaccines had statistical significance ($P=0.011$). So we conclude that tumor cell membrane expressed SEA can stimulate the proliferation of tumor specific CTL and enhance the specific lysis on autologous tumor cells.

This superantigen modified tumor cell-based vaccine has an advantage over ordinary tumor cell-based vaccines in three aspects. First, this vaccine could make up for the disadvantage of low-level expression of class II MHC molecule on the surface of most tumor cells^[26]. It has been found that T cell activation by SEA superantigen could occur in the absence or presence of MHC class II^[14,27-29], and artificially anchoring a superantigen onto a cell surface through transmembrane protein could substitute for MHC-II presentation^[15]. Second, although most immunotherapeutic strategies have focused on activating tumor-specific CD8⁺ T cells, optimal antitumor activity could be achieved if both CD4⁺ and CD8⁺ tumor specific T cells were induced^[30,31]. Likewise, if tumor immunity plays a role in limiting the recurrence of primary tumor or the future onset of metastatic diseases, then CD4⁺ and CD8⁺ immunological memory should be optimized. Both CD4⁺ and CD8⁺ T cells can be activated by bacterial superantigens. Third, superantigens could preferentially direct cytotoxicity against MHC-II-positive cells^[32-34], *in vivo* administration of intact superantigens in sufficiently therapeutic amount could produce unwanted cytotoxicity to normal cells. Anchoring of superantigen and other TM fusion proteins on the surface of tumor cells would offer a novel strategy for the use of superantigens as immunostimulatory molecules. This method can confine the effect of SEA within the tumor, thus decreasing the side effects of treatment.

As presented above, irradiated HepG2-SEA cells could be used as an effective tumor cell-based vaccine *in vitro*. The superantigen enhanced vaccine is superior to tumor cell alone on the prime of tumor cell specific T cells, which provides a new strategy for the addition of superantigen as immunostimulatory molecules in tumor therapy. *In vivo* studies are currently under way to evaluate the effectiveness of these superantigen based vaccines for cancer therapy.

REFERENCES

- 1 Teshima T, Mach N, Hill GR, Pan L, Gillessen S, Dranoff G, Ferrara JL. Tumor cell vaccine elicits potent antitumor immunity after allogeneic T-cell-depleted bone marrow transplantation. *Cancer Res* 2001; **61**: 162-171
- 2 Nelson WG, Simons JW, Mikhak B, Chang JF, DeMarzo AM, Carducci MA, Kim M, Weber CE, Baccala AA, Goeman MA, Clift

- SM, Ando DG, Levitsky HI, Cohen LK, Sanda MG, Mulligan RC, Partin AW, Carter HB, Piantadosi S, Marshall FF. Cancer cells engineered to secrete granulocyte-macrophage colony-stimulating factor using *ex vivo* gene transfer as vaccines for the treatment of genitourinary malignancies. *Cancer Chemother Pharmacol* 2000; **46**(Suppl): S67-S72
- 3 **Antonia SJ**, Seigne J, Diaz J, Muro-Cacho C, Extermann M, Farmelo MJ, Friberg M, Alsarraj M, Mahany JJ, Pow-Sang J, Cantor A, Janssen W. Phase I trial of a B7-1 (CD80) gene modified autologous tumor cell vaccine in combination with systemic interleukin-2 in patients with metastatic renal cell carcinoma. *J Urol* 2002; **167**: 1995-2000
 - 4 **Marrack P**, Kappler J. The staphylococcal enterotoxins and their relatives. *Science* 1990; **248**: 705-711
 - 5 **Fraser JD**. High-affinity binding of staphylococcal enterotoxins A and B to HLA-DR. *Nature* 1989; **339**: 221-223
 - 6 **Kotzin BL**, Leung DY, Kappler J, Marrack P. Superantigens and their potential role in human disease. *Adv Immunol* 1993; **54**: 99-166
 - 7 **Leung DY**, Gately M, Trumble A, Ferguson-Darnell B, Schlievert PM, Picker LJ. Bacterial superantigens induce T cell expression of the skin-selective homing receptor, the cutaneous lymphocyte-associated antigen, via stimulation of interleukin 12 production. *J Exp Med* 1995; **181**: 747-753
 - 8 **Sriskandan S**, Evans TJ, Cohen J. Bacterial superantigen-induced human lymphocyte responses are nitric oxide dependent and mediated by IL-12 and IFN- γ . *J Immunol* 1996; **156**: 2430-2435
 - 9 **Lando PA**, Hedlund G, Dohlsten M, Kalland T. Bacterial superantigens as anti-tumour agents: induction of tumour cytotoxicity in human lymphocytes by staphylococcal enterotoxin A. *Cancer Immunol Immunother* 1991; **33**: 231-237
 - 10 **Ochi A**, Migita K, Xu J, Siminovitch K. *In vivo* tumor immunotherapy by a bacterial superantigen. *J Immunol* 1993; **151**: 3180-3186
 - 11 **Dow SW**, Elmslie RE, Willson AP, Roche L, Gorman C, Potter TA. *In vivo* tumor transfection with superantigen plus cytokine genes induces tumor regression and prolongs survival in dogs with malignant melanoma. *J Clin Invest* 1998; **101**: 2406-2414
 - 12 **Shu S**, Krinock RA, Matsumura T, Sussman JJ, Fox BA, Chang AE, Terman DS. Stimulation of tumor-draining lymph node cells with superantigenic staphylococcal toxins leads to the generation of tumor-specific effector T cells. *J Immunol* 1994; **152**: 1277-1288
 - 13 **Wang Q**, Yu H, Zhang L, Ju D, Pan J, Xia D, Yao H, Zhang W, Wang J, Cao X. Adenovirus-mediated intratumoral lymphotactin gene transfer potentiates the antibody-targeted superantigen therapy of cancer. *J Mol Med* 2002; **80**: 585-594
 - 14 **Ihle J**, Holzer U, Krull F, Dohlsten M, Kalland T, Niethammer D, Dannecker GE. Antibody-targeted superantigens induce lysis of major histocompatibility complex class II-negative T-cell leukemia lines. *Cancer Res* 1995; **55**: 623-628
 - 15 **Wahlsten JL**, Mills CD, Ramakrishnan S. Antitumor response elicited by a superantigen-transmembrane sequence fusion protein anchored onto tumor cells. *J Immunol* 1998; **161**: 6761-6767
 - 16 **Li Z**, Sui Y, Jiang Y, Lei Z, Shang J, Zheng Y. Reconstruction of SEA-B7.1 double signals on human hepatocellular carcinoma cells and analysis of its immunological effect. *Biochem Biophys Res Commun* 2001; **288**: 454-461
 - 17 **Sambrook J**, Fritsch EF, Maniatis T. Molecular Cloning: A Laboratory Manual, 2nd ed. *New York: Cold Spring Harbor Laboratory Press* 1989
 - 18 **Clay TM**, Hobeika AC, Mosca PJ, Lysterly HK, Morse MA. Assays for monitoring cellular immune responses to active immunotherapy of cancer. *Clin Cancer Res* 2001; **7**: 1127-1135
 - 19 **Street SE**, Cretney E, Smyth MJ. Perforin and interferon- γ activities independently control tumor initiation, growth, and metastasis. *Blood* 2001; **97**: 192-197
 - 20 **Masson D**, Tschopp J. Isolation of a lytic, pore-forming protein (perforin) from cytolytic T-lymphocytes. *J Biol Chem* 1985; **260**: 9069
 - 21 **Merger M**, Viney JL, Borojevic R, Steele-Norwood D, Zhou P, Clark DA, Riddell R, Maric R, Podack ER, Croitoru K. Defining the roles of perforin, Fas/FasL, and tumour necrosis factor alpha in T cell induced mucosal damage in the mouse intestine. *Gut* 2002; **51**: 155-163
 - 22 **Stohl W**, Elliott JE, Lynch DH, Kiener PA. CD95 (Fas)-based, superantigen-dependent, CD4+ T cell-mediated down-regulation of human *in vitro* immunoglobulin responses. *J Immunol* 1998; **160**: 5231-5238
 - 23 **Torres BA**, Perrin GQ, Mujtaba MG, Subramaniam PS, Anderson AK, Johnson HM. Superantigen enhancement of specific immunity: antibody production and signaling pathways. *J Immunol* 2002; **169**: 2907-2914
 - 24 **Mahlknecht U**, Herter M, Hoffmann MK, Niethammer D. The toxic shock syndrome toxin-1 induces anergy in human T cells *in vivo*. *Hum Immunol* 1996; **45**: 42-45
 - 25 **Herr W**, Schneider J, Lohse AW, Meyer zum Buschenfelde KH, Wolfel T. Detection and quantification of blood-derived CD8+ T lymphocytes secreting tumor necrosis factor alpha in response to HLA-A2.1-binding melanoma and viral peptide antigens. *J Immunol Methods* 1996; **191**: 131-142
 - 26 **Baskar S**. Gene-modified tumor cells as cellular vaccine. *Cancer Immunol Immunother* 1996; **43**: 165-173
 - 27 **Gidlof C**, Dohlsten M, Lando P, Kalland T, Sundstrom C, Totterman TH. A superantigen-antibody fusion protein for t-cell immunotherapy of human B-lineage malignancies. *Blood* 1997; **89**: 2089-2097
 - 28 **Lando PA**, Dohlsten M, Hedlund G, Akerblom E, Kalland T. T cell killing of human colon carcinomas by monoclonal-antibody-targeted superantigens. *Cancer Immunol Immunother* 1993; **36**: 223-228
 - 29 **Holzer U**, Bethge W, Krull F, Ihle J, Handgretinger R, Reisfeld RA, Dohlsten M, Kalland T, Niethammer D, Dannecker GE. Superantigen-staphylococcal-enterotoxin-A-dependent and antibody-targeted lysis of GD2-positive neuroblastoma cells. *Cancer Immunol Immunother* 1995; **41**: 129-136
 - 30 **Mortara L**, Gras-Masse H, Rommens C, Venet A, Guillet JG, Bourgault-Villada I. Type 1 CD4+ T-cell help is required for induction of antipeptide multispecific cytotoxic T lymphocytes by a lipopeptidic vaccine in rhesus macaques. *J Virol* 1999; **73**: 4447-4451
 - 31 **Yu Z**, Restifo NP. Cancer vaccines: progress reveals new complexities. *J Clin Invest* 2002; **110**: 289-294
 - 32 **Torres BA**, Kominsky S, Perrin GQ, Hobeika AC, Johnson HM. Superantigens: the good, the bad, and the ugly. *Exp Biol Med* 2001; **226**: 164-176
 - 33 **Herrmann T**, Maryanski JL, Romero P, Fleischer B, MacDonald HR. Activation of MHC class I-restricted CD8+ CTL by microbial T cell mitogens. Dependence upon MHC class II expression of the target cells and V beta usage of the responder T cells. *J Immunol* 1990; **144**: 1181-1186
 - 34 **Hansson J**, Ohlsson L, Persson R, Andersson G, Ilback NG, Litton MJ, Kalland T, Dohlsten M. Genetically engineered superantigens as tolerable antitumor agents. *Proc Natl Acad Sci U S A* 1997; **94**: 2489-2494

CT-guided percutaneous ethanol injection with disposable curved needle for treatment of malignant liver neoplasms and their metastases in retroperitoneal lymph nodes

Chang-Jing Zuo, Pei-Jun Wang, Cheng-Wei Shao, Min-Jie Wang, Jian-Ming Tian, Yi Xiao, Fang-Yuan Ren, Xi-Yan Hao, Min Yuan

Chang-Jing Zuo, Pei-Jun Wang, Cheng-Wei Shao, Min-Jie Wang, Jian-Ming Tian, Yi Xiao, Fang-Yuan Ren, Xi-Yan Hao, Min Yuan, Department of Radiology, Changhai Hospital, Second Military Medical University, Shanghai 200433, China

Supported by the National Natural Science Foundation of China, No. 30070233

Correspondence to: Chang-Jing Zuo, Department of Radiology, Changhai Hospital, the Second Military Medical University, Shanghai 200433, China. baobao66@sh163.net

Telephone: +86-21-25070575

Received: 2003-05-10 **Accepted:** 2003-06-12

Abstract

AIM: To explore the feasibility of computed tomography (CT)-guided percutaneous ethanol injection (PEI) using a disposable curved needle for treatment of malignant liver neoplasms and their metastases in retroperitoneal lymph nodes.

METHODS: CT-guided PEI was conducted using a disposable curved needle in 26 malignant liver tumors smaller than 5 cm in diameter and 5 lymph node metastases of liver cancer in the retroperitoneal space. The disposable curved needle was composed of a straight trocar (21G) and stylet, a disposable curved tip (25 G) and a fine stylet. For the tumors found in deep sites and difficult to reach, or for hepatic masses inaccessible to the injection using a straight needle because of portal vein and bile ducts, the straight trocar was used at first to reach the side of the tumor. Then, the disposable curved needle was used via the trocar. When the needle reached the tumor center, appropriate amount of ethanol was injected. For relatively large malignant liver tumors, multi-point injection was carried out for a better distribution of the ethanol injected throughout the masses. The curved needle was also used for treatment of the metastasis in retroperitoneal lymph nodes blocked by blood vessels and inaccessible by the straight needle.

RESULTS: All of the 26 liver tumors received 2 or more times of successful PEI, through which ethanol was distributed throughout the whole tumor mass. Effect of the treatment was monitored by contrast-enhanced multi-phase CT and magnetic resonance imaging (MRI) examinations three months later. Of the 18 lesions whose diameters were smaller than 3 cm, the necrotic change across the whole mass and that in most areas were observed in 15 and 3 tumors, respectively. Among the 8 tumors sizing up to 5 cm, 5 were completely necrotic and 3 largely necrotic. Levels of tumor seromarkers were significantly reduced in some of the cases. In 5 patients with metastases of liver cancer in retroperitoneal lymph nodes who received 1 to 3 times of PEI, all the foci treated were completely necrotic and smaller demonstrated by dynamic contrast-enhanced CT or MRI 3 months later.

CONCLUSION: CT-guided PEI using a disposable curved needle is effective, time-saving and convenient, providing an alternative therapy for the treatment of malignant liver tumors and their retroperitoneal lymph node metastases.

Zuo CJ, Wang PJ, Shao CW, Wang MJ, Tian JM, Xiao Y, Ren FY, Hao XY, Yuan M. CT-guided percutaneous ethanol injection with disposable curved needle for treatment of malignant liver neoplasms and their metastases in retroperitoneal lymph nodes. *World J Gastroenterol* 2004; 10(1): 58-61
<http://www.wjgnet.com/1007-9327/10/58.asp>

INTRODUCTION

Percutaneous ethanol injection (PEI) is a common procedure for the treatment of malignant liver neoplasms. But in the treatment of small or deep foci with CT-guided PEI, repeated punctures are necessary for the needle tip to reach an appropriate position. This may result in prolongation of the operation time and an increase of the risk for complications. This article reported our recent experience in PEI treatment of liver tumors using a disposable curved needle.

MATERIALS AND METHODS

Clinical data

Thirty-one patients (22 males, 9 females; 37 to 72 years old, mean 48.9 years) were included in this study. Of them, 19 had primary liver cancer and 7 had metastatic liver tumors, including a single focus in 15 patients and multiple foci (\geq two tumors) in 11 patients. Twenty-six foci in 26 patients were treated by PEI using a disposable curved needle, including 18 smaller than 3 cm in diameter and 8 sizing from 3 cm to 5 cm. Metastases in retroperitoneal lymph nodes were found in 5 patients, with a single node involved in 3, 2 nodes in one and 3 nodes in the other. All of the five patients received PEI treatment, one lesion for each. Every patient was informed of possible complications and the consent was obtained before operation. The procedure was approved by the Ethics Commission of the hospital.

Instruments

PQ 5000 V helical CT machine (Picker International INC, Cleveland, Ohio, USA) was used to guide the puncture. The disposable curved needle set (DCHNS, COOK, Bloomington, USA) is composed of a tip (25 G), a fine stylet, a straight trocar (21 G) and a trocar stylet. Volume Zoom multi-slice helical CT scanner (Siemens AG, Forchheim, Germany) and Symphony 1.5T MRI machine (Siemens AG, Munchen, Germany) were used to evaluate the post-operative lesions.

Procedures

The location, morphology and size of the focus were determined by enhanced CT or MRI. Prothrombin time, blood

routine, liver function and tumor markers were evaluated. The patients were fasted for four hours and notified of precautions before the procedure. Sedatives were administered for patients with mental stress.

An appropriate posture was selected and the skin surface was marked. The focal area was scanned by 5-10 mm thickness to determine the optimal puncture point, angle and depth. Local sterilization, draping and local anesthesia with 2% lidocaine were conducted. The patients were advised to hold breath at rest, when the needle was inserted into the focus according to the preplanned angle. The needle was adjusted under CT guidance in case of any deviation. The disposable curved needle was used in the following cases: 1) foci too small in size or too deep in location for the straight needle, 2) the way to the tumor center blocked by the portal vessel or bile duct, 3) large foci with multiple-site injections of ethanol by one puncture. When the straight trocar of the disposable curved needle reached the proximity of the tumor, stylet was withdrawn and the 25 G curved needle was inserted. The needle tip was 90° to the needle body in a natural state. When the tip traveled out of the trocar, it was bent by its own elasticity. The next step was to direct the tip to the focus and insert into it the tumor. Then, the stylet was removed and ethanol was injected. For the larger foci, the trocar was inserted, through which ethanol was injected from superficial to deeper areas. After that, the flexible needle was inserted, through which ethanol was injected into the areas around the trocar. Before injecting ethanol, a test withdrawal was done to make sure that the needle was not misled to the blood vessel or biliary duct. Ethanol injection should be sufficient to diffuse to all or most parts of the tumor. The total volume of ethanol injected each time should not exceed 40 ml. As absolute alcohol is of low density, it could be mixed with a small amount of contrast medium to increase its density so that the diffusion of ethanol could be more visible. A small amount of the anesthetic was administered while the needle was being withdrawn. When the needle was removed, a check-up was necessary to see whether the ethanol was well distributed within the tumor, whether there was ethanol reflux, or whether passage of the needle through the pulmonary region caused pneumothorax.

Postoperative treatment included fluid replacement, analgesic and liver protection therapies, and re-examination of liver function and tumor markers. A second treatment was given at an interval of 5 to 7 days.

Outcome evaluation

Multi-slice helical CT scan or contrast-enhanced MRI was done three months after PEI to evaluate the outcome by the necrotic area of the foci, changes of the tumor marker level and clinical manifestations.

RESULTS

All of the 26 tumors received 2 or more times of CT-guided PEI. Single-point or multi-point injections were performed for foci smaller than 3 cm, and multi-point injections for all of the foci larger than 3 cm in diameter. The ethanol distribution was found to cover the whole tumor areas in all these 26 cases (Figures 1-4). CT or MRI images showed that, of the 18 foci smaller than 3 cm, 15 were completely necrotic (Figure 5) and the remaining three were mostly necrotic. Of the 8 foci larger than 3 cm, 5 were completely necrotic and the other three were mostly necrotic. In four patients who were found to have residue nodules, CT-guided PEI was performed again, and AFP level declined markedly and the symptoms improved in some of these patients. Apart from abdominal pain of varying degrees during the procedure, no other severe complication was observed.

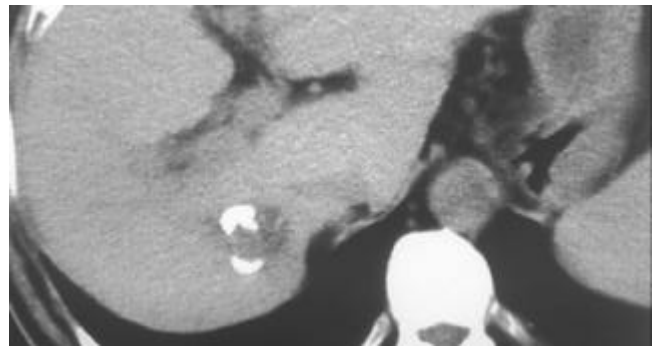


Figure 1 A tumor in the right lobe of liver (2.2 cm×2.0 cm). A small amount of high-density iodipin could be seen in some areas of the tumor receiving TACE.

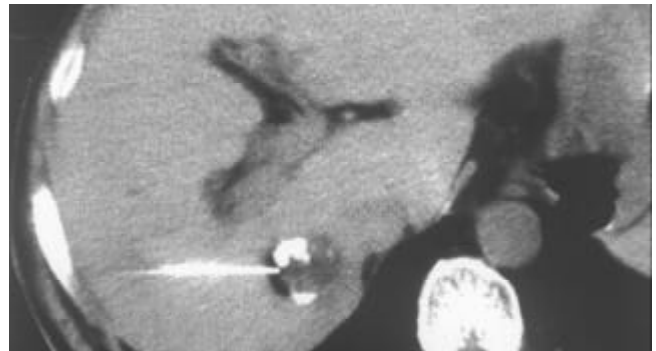


Figure 2 When a deeply embedded tumor is difficult for a straight needle to reach the appropriate point within it, a straight trocar (21G) is used to reach the tumor side.

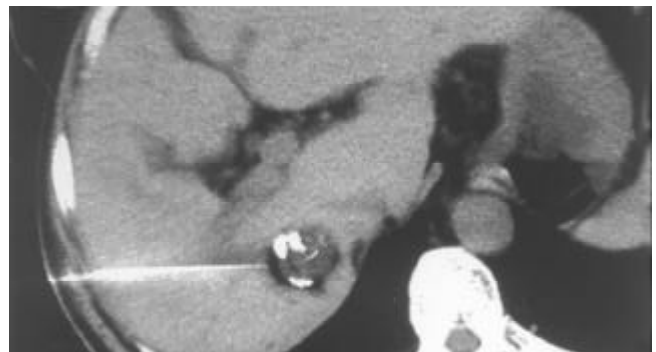


Figure 3 Insertion of the 25-G disposable curved needle into the tumor through the straight trocar. The tip position is adjusted to the target by changing the direction of the curved needle. Ethanol can be injected at multiple points within the tumor by changing the direction of the curved needle.

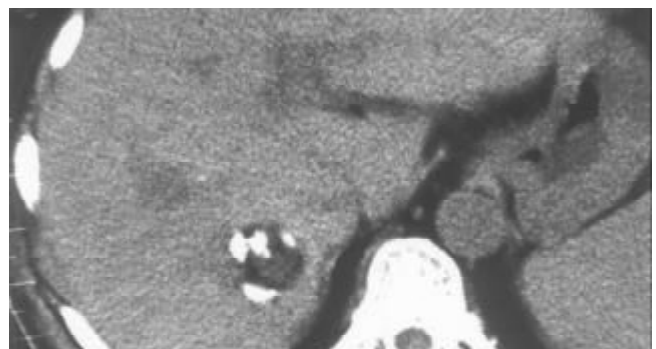


Figure 4 Distribution of ethanol in the whole tumor.

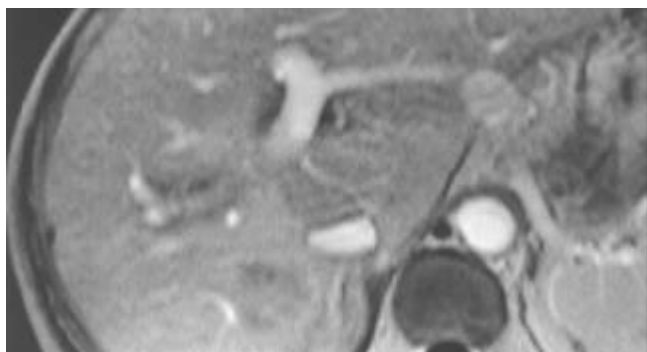


Figure 5 A complete necrotic change of the tumor found at enhanced MRI check-up three months after the PEI.

DISCUSSION

The common treatments for malignant liver tumors include surgery, transcatheter arterial chemoembolization (TACE), PEI, radiofrequency thermal ablation, microwave coagulation, laser thermal ablation therapy^[1-4]. Although surgery is the most radical treatment, it is not indicative for patients with severe cirrhosis or in cases where tumors are very close to the major vessels. Surgery was not usually preferable if there were multiple foci within the liver^[5]. TACE is a good alternative, but it causes severe damage to the liver. The outcome of TACE is usually poor for tumors with insufficient blood supply. PEI is a better alternative approach for treatment of malignant liver tumors, as it has proved to be effective and to cause minimal trauma^[6-10]. According to Ryu *et al.*, PEI was the choice of treatment for clinical stage II patients with tumors smaller than 3 cm. For clinical stage I patients with such small tumors, selective PEI or surgical resection should be considered^[11]. In these cases, the outcomes of PEI and surgery were similar but better than TACE. Therefore, PEI should be selected according to the conditions of individual patients^[12]. Combination of PEI and TACE and other treatment was sometimes used to achieve optimal outcomes^[13-18]. Moreover, PEI is more convenient and safer than radiofrequency thermal ablation and microwave coagulation therapy. PEI has become a preferable approach for lesions adjacent to main biliary ducts or to intestinal loops and for well-differentiated hepatocellular carcinoma^[19-21].

Chemotherapy, radiotherapy and surgery have become the routine treatments for retroperitoneal metastases of liver cancer and other malignant tumors^[22-28], but some of the lesions are not sensitive to radiotherapy and chemotherapy. In addition, radiotherapy and chemotherapy are more traumatic and expensive. Dissection of metastatic lymph nodes usually results in more traumas and complications. Some patients whose general conditions are poor can not tolerate chemotherapy, radiotherapy or surgery. While CT-guided PEI is more effective for the treatment of lymph node metastases in the retroperitoneal space and abdominal cavity with less trauma and lower cost. Following CT-guided PEI, appropriate chemotherapy and radiotherapy still can be considered.

Clear visualization of tumor location and ethanol distribution during CT-guided PEI for malignant liver tumors makes it possible to inject sufficient ethanol for a better outcome. It is especially suitable for foci that could be clearly detected on ultrasound^[29]. For the CT-guided PEI, it is a key step to insert the needle accurately into the target. Using the needle with a disposable curved tip, it is convenient to reach the foci and to avoid disadvantages of routine PEI procedure. What you need to do is to insert the trocar to the edge of the tumor and the disposable curved needle tip into the tumor through the trocar. It saves time and reduces complications. The disposable curved

tip can easily reach a deeply embedded tumor and avoid possible damages to the surrounding vessels or bile ducts. For tumors larger than 3 cm, multiple injections are necessary. By the procedure described here, a straight trocar is used at first to inject ethanol, and then the disposable curved needle tip is inserted through the trocar to inject ethanol into areas that the straight trocar cannot reach, so that ethanol can diffuse to the whole tumor. Retroperitoneal lymph nodes are usually deep and adjacent to abdominal aorta and inferior vena cava, PEI is usually done under CT guidance because CT guidance is accurate and the distribution of ethanol within the metastatic lymph node can be clearly visualized. The disposable curved needle can be used for metastatic lymph nodes in way to which is blocked by vessels. For larger metastatic lymph nodes, multiple-site injections of ethanol by one puncture can be done using a disposable curved needle and the procedure is more convenient than that using a routine straight needle.

As we know, this is the first report describing the use of a disposable curved puncture needle in CT-guided PEI for malignant liver tumors and retroperitoneal lymph node metastases. This procedure could also be used in CT-guided acetic acid injection for liver tumors^[30,31], ethanol injection for adrenal tumors^[32], and thymus ethanol injection for myasthenia gravis^[33].

REFERENCES

- 1 **Goldberg SN**, Ahmed M. Minimally invasive image-guided therapies for hepatocellular carcinoma. *J Clin Gastroenterol* 2002; **35**(5 Suppl 2): S115-129
- 2 **Livraghi T**. Radiofrequency ablation, PEIT, and TACE for hepatocellular carcinoma. *J Hepatobiliary Pancreat Surg* 2003; **10**: 67-76
- 3 **Seki T**, Tamai T, Nakagawa T, Imamura M, Nishimura A, Yamashiki N, Ikeda K, Inoue K. Combination therapy with transcatheter arterial chemoembolization and percutaneous microwave coagulation therapy for hepatocellular carcinoma. *Cancer* 2000; **89**: 1245-1251
- 4 **Pacella CM**, Bizzarri G, Cecconi P, Caspani B, Magnolfi F, Bianchini A, Anelli V, Pacella S, Rossi Z. Hepatocellular carcinoma: long-term results of combined treatment with laser thermal ablation and transcatheter arterial chemoembolization. *Radiology* 2001; **219**: 669-678
- 5 **Lau WY**, Leung TW, Yu SC, Ho SK. Percutaneous local ablative therapy for hepatocellular carcinoma: a review and look into the future. *Ann Surg* 2003; **237**: 171-179
- 6 **Livraghi T**. Percutaneous ethanol injection in the treatment of hepatocellular carcinoma in cirrhosis. *Hepato-gastroenterology* 2001; **48**: 20-24
- 7 **Livraghi T**, Giorgio A, Marin G, Salmi A, de Sio I, Bolondi L, Pompili M, Brunello F, Lazzaroni S, Torzilli G. Hepatocellular carcinoma and cirrhosis in 746 patients: long-term results of percutaneous ethanol injection. *Radiology* 1995; **197**: 101-108
- 8 **Lin SM**, Lin DY, Lin CJ. Percutaneous ethanol injection therapy in 47 cirrhotic patients with hepatocellular carcinoma 5 cm or less: a long-term result. *Int J Clin Pract* 1999; **53**: 257-262
- 9 **Livraghi T**, Benedini V, Lazzaroni S, Meloni F, Torzilli G, Vettori C. Long term results of single session percutaneous ethanol injection in patients with large hepatocellular carcinoma. *Cancer* 1998; **83**: 48-57
- 10 **Takayasu K**, Muramatsu Y, Asai S, Muramatsu Y, Kobayashi T. CT fluoroscopy-assisted needle puncture and ethanol injection for hepatocellular carcinoma: a preliminary study. *Am J Roentgenol* 1999; **173**: 1219-1224
- 11 **Ryu M**, Shimamura Y, Kinoshita T, Konishi M, Kawano N, Iwasaki M, Furuse J, Yoshino M, Moriyama N, Sugita M. Therapeutic results of resection, transcatheter arterial embolization and percutaneous transhepatic ethanol injection in 3225 patients with hepatocellular carcinoma: a retrospective multicenter study. *Jpn J Clin Oncol* 1997; **27**: 251-257
- 12 **Ueno S**, Tanabe G, Nuruki K, Oketani M, Komorizono Y, Hokotate H, Fukukura Y, Baba Y, Imamura Y, Aikou T. Prognosis of hepatocellular carcinoma associated with Child class B and

- C cirrhosis in relation to treatment: a multivariate analysis of 411 patients at a single center. *J Hepatobiliary Pancreat Surg* 2002; **9**: 469-477
- 13 **Tanaka K**, Nakamura S, Numata K, Kondo M, Morita K, Kitamura T, Saito S, Kiba T, Okazaki H, Sekihara H. The long term efficacy of combined transcatheter arterial embolization and percutaneous ethanol injection in the treatment of patients with large hepatocellular carcinoma and cirrhosis. *Cancer* 1998; **82**: 78-85
- 14 **Kirchhoff T**, Chavan A, Galanski M. Transarterial chemoembolization and percutaneous ethanol injection therapy in patients with hepatocellular carcinoma. *Eur J Gastroenterol Hepatol* 1998; **10**: 907-909
- 15 **Lencioni R**, Paolicchi A, Moretti M, Pinto F, Armillotta N, Di Giulio M, Cicorelli A, Donati F, Cioni D, Bartolozzi C. Combined transcatheter arterial chemoembolization and percutaneous ethanol injection for the treatment of large hepatocellular carcinoma: local therapeutic effect and long-term survival rate. *Eur Radiol* 1998; **8**: 439-444
- 16 **Koda M**, Murawaki Y, Mitsuda A, Oyama K, Okamoto K, Idobe Y, Suou T, Kawasaki H. Combination therapy with transcatheter arterial chemoembolization and percutaneous ethanol injection compared with percutaneous ethanol injection alone for patients with small hepatocellular carcinoma: a randomized control study. *Cancer* 2001; **92**: 1516-1524
- 17 **Kamada K**, Kitamoto M, Aikata H, Kawakami Y, Kono H, Imamura M, Nakanishi T, Chayama K. Combination of transcatheter arterial chemoembolization using cisplatin-lipiodol suspension and percutaneous ethanol injection for treatment of advanced small hepatocellular carcinoma. *Am J Surg* 2002; **184**: 284-290
- 18 **Guo WJ**, Yu EX, Liu LM, Li J, Chen Z, Lin JH, Meng ZQ, Feng Y. Comparison between chemoembolization combined with radiotherapy and chemoembolization alone for large hepatocellular carcinoma. *World J Gastroenterol* 2003; **9**: 1697-1701
- 19 **Livraghi T**, Goldberg SN, Lazzaroni S, Meloni F, Solbiati L, Gazelle GS. Small hepatocellular carcinoma: treatment with radiofrequency ablation versus ethanol injection. *Radiology* 1999; **210**: 655-661
- 20 **Livraghi T**, Lazzaroni S, Meloni F. Radiofrequency thermal ablation of hepatocellular carcinoma. *Eur J Ultrasound* 2001; **13**: 159-166
- 21 **Horigome H**, Nomura T, Saso K, Itoh M. Standards for selecting percutaneous ethanol injection therapy or percutaneous microwave coagulation therapy for solitary small hepatocellular carcinoma: consideration of local recurrence. *Am J Gastroenterol* 1999; **94**: 1914-1917
- 22 **Uenishi T**, Hirohashi K, Tanaka H, Yamamoto T, Kubo S, Kinoshita H. A surgically treated case of hepatocellular carcinoma with extensive lymph node metastases. *Hepatogastroenterology* 2000; **47**: 1714-1716
- 23 **Uenishi T**, Hirohashi K, Shuto T, Kubo S, Tanaka H, Sakata C, Ikebe T, Kinoshita H. The clinical significance of lymph node metastases in patients undergoing surgery for hepatocellular carcinoma. *Surg Today* 2000; **30**: 892-895
- 24 **Mosharafa AA**, Foster RS, Leibovich BC, Bihrl R, Johnson C, Donohue JP. Is post-chemotherapy resection of seminomatous elements associated with higher acute morbidity? *J Urol* 2003; **169**: 2126-2128
- 25 **Foster R**, Bihrl R. Current status of retroperitoneal lymph node dissection and testicular cancer: when to operate. *Cancer Control* 2002; **9**: 277-283
- 26 **Hendry WF**, Norman AR, Dearnaley DP, Fisher C, Nicholls J, Huddart RA, Horwich A. Metastatic nonseminomatous germ cell tumors of the testis: results of elective and salvage surgery for patients with residual retroperitoneal masses. *Cancer* 2002; **94**: 1668-1676
- 27 **Steyerberg EW**, Marshall PB, Keizer HJ, Habbema JD. Resection of small, residual retroperitoneal masses after chemotherapy for nonseminomatous testicular cancer: a decision analysis. *Cancer* 1999; **85**: 1331-1341
- 28 **Hermans BP**, Foster RS, Bihrl R, Little S, Sandler A, Einhorn LH, Donohue JP. Is retroperitoneal lymph node dissection necessary for adult paratesticular rhabdomyosarcoma? *J Urol* 1998; **160**(6 Pt 1): 2074-2077
- 29 **Lee MJ**, Mueller PR, Dawson SL, Gazelle SG, Hahn PF, Goldberg MA, Boland GW. Percutaneous ethanol injection for the treatment of hepatic tumors: indications, mechanism of action, technique, and efficacy. *Am J Roentgenol* 1995; **164**: 215-220
- 30 **Ohnishi K**, Yoshioka H, Ito S, Fujiwara K. Prospective randomized controlled trial comparing percutaneous acetic acid injection and percutaneous ethanol injection for small hepatocellular carcinoma. *Hepatology* 1998; **27**: 67-72
- 31 **Arrive L**, Rosmorduc O, Dahan H, Fartoux L, Monnier-Cholley L, Lewin M, Poupon R, Tubiana JM. Percutaneous acetic acid injection for hepatocellular carcinoma: using CT fluoroscopy to evaluate distribution of acetic acid mixed with an iodinated contrast agent. *Am J Roentgenol* 2003; **180**: 159-162
- 32 **Wang P**, Zuo C, Qian Z, Tian J, Ren F, Zhou D. Computerized tomography guided percutaneous ethanol injection for the treatment of hyperfunctioning pheochromocytoma. *J Urol* 2003; **170**(4Pt1): 1132-1134
- 33 **Wang P**, Zuo C, Tian J, Qian Z, Ren F, Shao C, Wang M, Lu T. CT-guided percutaneous ethanol injection of the thymus for treatment of myasthenia gravis. *Am J Roentgenol* 2003; **181**: 721-724

Edited by Su Q and Wang XL

Cooperative inhibitory effects of antisense oligonucleotide of cell adhesion molecules and cimetidine on cancer cell adhesion

Nan-Hong Tang, Yan-Ling Chen, Xiao-Qian Wang, Xiu-Jin Li, Feng-Zhi Yin, Xiao-Zhong Wang

Nan-Hong Tang, Yan-Ling Chen, Xiao-Qian Wang, Xiu-Jin Li, Feng-Zhi Yin, Hepato-Biliary Surgery Institute of Fujian Province, Union Hospital, Fujian Medical University, Fuzhou 350001, Fujian Province, China

Xiao-Zhong Wang, Gastroenterology Department, Union Hospital, Fujian Medical University, Fuzhou 350001, Fujian Province, China
Supported by the Foundation of Education Committee of Fujian Province, No. K99054

Correspondence to: Nan-Hong Tang, Hepato-Biliary Surgery Institute of Fujian Province, Union Hospital, 29 Xinquan Road, Fuzhou 350001, Fujian Province, China. fztjh@sina.com

Telephone: +86-591-3357896 Ext. 8373

Received: 2003-06-05 **Accepted:** 2003-08-16

Abstract

AIM: To explore the cooperative effects of antisense oligonucleotide (ASON) of cell adhesion molecules and cimetidine on the expression of E-selectin and ICAM-1 in endothelial cells and their adhesion to tumor cells.

METHODS: After treatment of endothelial cells with ASON and/or cimetidine and induction with TNF- α , the protein and mRNA changes of E-selectin and ICAM-1 in endothelial cells were examined by flow cytometry and RT-PCR, respectively. The adhesion rates of endothelial cells to tumor cells were measured by cell adhesion experiment.

RESULTS: In comparison with TNF- α inducing group, lipo-ASON and lipo-ASON/cimetidine could significantly decrease the protein and mRNA levels of E-selectin and ICAM-1 in endothelial cells, and lipo-ASON/cimetidine had most significant inhibitory effect on E-selectin expression (from $36.37 \pm 1.56\%$ to $14.23 \pm 1.07\%$, $P < 0.001$). Meanwhile, cimetidine alone could inhibit the expression of E-selectin ($36.37 \pm 1.56\%$ vs $27.2 \pm 1.31\%$, $P < 0.001$), but not ICAM-1 ($69.34 \pm 2.50\%$ vs $68.07 \pm 2.10\%$, $P > 0.05$) and the two kinds of mRNA, either. Compared with TNF- α inducing group, the rate of adhesion was markedly decreased in lipo-E-selectin ASON and lipo-E-selectin ASON/cimetidine treated groups ($P < 0.05$), and lipo-E-selectin ASON/cimetidine worked better than lipo-E-selectin ASON alone except for HepG2/ECV304 group ($P < 0.05$). However, the decrease of adhesion was not significant in lipo-ICAM-1 ASON and lipo-ICAM-1 ASON/cimetidine treated groups except for HepG2/ECV304 group ($P > 0.05$).

CONCLUSION: These data demonstrate that ASON in combination with cimetidine *in vitro* can significantly reduce the adhesion between endothelial cells and hepatic or colorectal cancer cells, which is stronger than ASON or cimetidine alone. This study provides some useful proofs for gene therapy of antiadhesion.

Tang NH, Chen YL, Wang XQ, Li XJ, Yin FZ, Wang XZ. Cooperative inhibitory effects of antisense oligonucleotide of cell adhesion molecules and cimetidine on cancer cell adhesion. *World J Gastroenterol* 2004; 10(1): 62-66

<http://www.wjgnet.com/1007-9327/10/62.asp>

INTRODUCTION

Previous researches have shown that recurrence and metastasis of cancer are closely related to the adhesion between tumor cells and endothelial cells. A variety of cell adhesion molecules (CAM) induced by cytokines such as IL- β and TNF- α released by tumor cells, promote the adhesion. Therefore, how to inhibit the adhesion is worth of study.

Antisense oligonucleotide (ASON) technique is a new alternative of gene therapy. ASOs are short synthetic oligonucleotides (10 to 25 bases in length) designed to hybridize to RNA (sense strand) that encodes the protein of interest. On binding to an mRNA, the oligonucleotide may inhibit the expression of target protein by multiple mechanisms^[1,2], exhibiting an important significance in antiviral and cancer treatment researches^[3,4]. Phosphorothioate oligonucleotides have a sulfur substituting for one of the nonbridging oxygens in the phosphate backbone, markedly enhancing the stability against cellular and serum nucleases^[5,6]. E-selectin, an early expressed CAM, and intercellular adhesion molecule-1 (ICAM-1), a late expressed CAM, are important proteins that mediate cell adhesion. Relevant studies on antiinflammation or antiadhesion using ASON have aroused increasing attention^[7-9].

Cimetidine, a kind of H₂R antagonist, has been shown to improve the survival of patients with colorectal cancer, melanoma, and renal cell cancer. Other H₂R antagonists including ranitidine and famotidine did not have such an effect^[10,11], indicating that cimetidine may exert its effect by enhancing the host immune response against tumor cells^[12] or by blocking the cell growth-promoting activity of histamine^[13], but not directly via histamine antagonism.

The key of anti-metastatic therapy lies in the complete inhibition of metastasis, because even if one metastatic colony is formed in an organ, it may result in death of the host eventually. Combined treatment may be an effective way to reach the goal. On the basis of previous work, we investigated the combined inhibitory effects of E-selectin or ICAM-1 ASON and cimetidine on tumor cell adhesion to provide data for further animal experiment and potential clinical application.

MATERIALS AND METHODS

Materials

Human endothelial cell line ECV304, hepatic cancer cell lines HepG2 and BEL7404 and colorectal cancer cell line Ls-174-t were purchased from the Cellular Biology Institute of Chinese Academy of Sciences and grown in DF medium (DMEM: Ham's F12=3:1) containing 100 mL · L⁻¹ fetal calf serum, penicillin 1 × 10⁵ U · L⁻¹ and streptomycin 100 mg · L⁻¹. Transfection kit TransFast™ liposome, Taq enzyme, RT-PCR kit and marker were from Promega. Mouse anti-human ICAM-1 mAb and E-selectin mAb were from Lab Vision. RNA extract (Trizol) was purchased from GIBCO BRL. Human recombinant TNF- α was purchased from Jingmei Biological Engineering Co., Shenzhen. ³H-TdR was purchased from the Atomic Energy Institute of Shanghai. Cimetidine was the product of Smithkline d Beecham Pharmaceutical Co., Germany.

ASON and primers

As previously described^[14,15], phosphorothioate oligoribonucleotides of ICAM-1, E-selectin and control ASON were synthesized by Sheng Gong Bio-Engineering Company, Shanghai. The sequences of ICAM-1, E-selectin and control ASON, and the primers for ICAM-1, E-selectin and β -actin are shown in Table 1.

Table 1 Sequences of ASON and primers

Name	Sequence	Length
ASON		
E-selectin	5'-TTCCCCAGATGCACCTGTTT-3'	
ICAM-1	5'-CCCCACCACTTCCCCTC-3'	
Control primer	5'-GCCGAGTCCATGTCGTACGC-3'	
E-selectin	Forward: 5'-AAAATGTTCAAGCCTGGCAGTTCC-3' Reverse: 5'-GTGGTGATGGGTGTTGCGGTTTCA-3'	509 bp
ICAM-1	Forward: 5'-CACAAGCCACGCCTCCCTGAACCTA-3' Reverse: 5'-TGTGGCCCTTTGTGTTTGTATGCTA-3'	458 bp
β -actin	Forward: 5'-CTGTCTGGCGGCACCACCAT-3' Reverse: 5'-GCAACTAAGTCATAGTCCGC-3'	250 bp

Methods

Preparation of lipo-ASON In order to improve the efficiency of ASON uptake of cells and prevent degradation in cultured cells and human serum, we used a commercial liposome that was comprised of synthetic cationic lipid and neutral lipid. It enhanced ASON's biofunction by improving its merging with cell membrane of eukaryotic cells and entering cell plasma to combine with mRNA^[16]. At a lower final concentration of 1/10 the nude ASON, lipo-ASON worked more effectively on inhibition in our previous report. According to the manufacturer's protocol of TransFast™ liposome, 200 μ l of serum-free medium per well should contain 3.6 μ l (1.5 μ g) ASON and 4.4 μ l liposome. So 10 minutes before the experiment, ASON was first mixed with serum-free medium, then liposome was added to make lipo-ASON medium (1 μ mol/L) at room temperature.

Treatment of endothelial cells A total of 5×10^4 ECV304 endothelial cells (3 to 6 generations) per well were put into a 24-well plate and incubated at 37 °C in 5 mL/L CO₂ humidified atmosphere for 48 hours, when cells grew to a confluence of 80%. E-selectin and ICAM-1 were divided into 5 groups according to the following different treatments, respectively. Group I (Basal): Treatment with TNF- α without lipo-ASON or cimetidine, and the cultivation time was identical to the other groups. Group II (TNF- α): After cultivation for 48 hours, the supernatants were discarded, endothelial cells were washed with PBS and replaced with 200 μ l of serum-free medium. Group III (cimetidine): After cultivation for 24 hours, 200 μ l of serum-free medium containing cimetidine (10^{-8} M) was added and cultured for another 24 hours, then the supernatants were discarded, cells were washed with PBS and replaced with 200 μ l of serum-free medium. Group IV (lipo-ASON): After cultivation for 48 hours, the supernatants were discarded, cells were washed with PBS and replaced with 200 μ l of serum-free medium containing lipo-ASON. Group V (lipo-ASON/cimetidine): After cultivation for 24 hours, 200 μ l of serum-free medium containing cimetidine (10^{-8} M) was added and cultured for another 24 hours, then the supernatants were discarded, cells were washed with PBS and replaced with 200 μ l of serum-free medium containing lipo-ASON.

Groups II to V were cultured for 4 hours at 37 °C. For E-selectin expression groups, the supernatants were discarded, 200 μ l medium containing 5 ng TNF- α was added and continuously cultured for 4 hours at 37 °C. For ICAM-1 expression groups, the supernatants were discarded, 200 μ l

medium was added and continuously cultured for 4 hours at 37 °C, then 5 ng TNF- α was added and cultured for 16 hours. **Flow cytometry** Endothelial cells, treated with ASON or cimetidine and TNF- α as described above, were removed from the plate by brief trypsinization with 0.25% trypsin. Cells were washed with DME plus 10% FCS, stained with primary mAb (2 μ g/ μ l) diluted in D-PBS containing 2% BSA and 0.2% sodium azide, followed by fluorescein-conjugated goat anti-mouse IgG. Each step was performed at 4 °C. Cells were analyzed by flow cytometry using a Brite HSFACScan (BID-RAD, US).

RT-PCR 2.5×10^5 of ECV304 endothelial cells per well were placed into a 6-well plate and then performed as described above. Total cellular RNAs were extracted and quantitated by a spectrophotometer. 2 μ g of RNA was used to perform reverse transcription as recommended by the supplier. E-selectin gene was amplified 30 cycles by half-quantitation under the following conditions: denaturation at 94 °C for 5 min followed by 94 °C for 30 s, at 64 °C for 45 s and at 72 °C for 45 s, then extension at 72 °C for 7 min. ICAM-1 gene was amplified 30 cycles by half-quantitation under the following conditions: denaturation at 94 °C for 5 min followed by 94 °C for 30 s, at 60 °C for 45 s and at 72 °C for 45 s, then extension at 72 °C for 7 minutes. For analysis, 10 μ l of the amplified product was tested in 20 g/L agarose gel with ethidium bromide staining, then photographed and scan-analysed. The ratio of average integrated density value (IDV) of E-selectin and ICAM-1 to IDV of β -actin was expressed as the relative intensity of E-selectin and ICAM-1, respectively.

Monolayer cell adhesion assays 1×10^4 ECV304 endothelial cells per well were placed into a 96-well plate and then performed as described above. Human hepatic cancer cell lines HepG2 and BEL7404 and colorectal cancer cell line Ls-174-t were subcultured for 24 hours, then incubated with medium containing ³H-TdR (9 μ Ci/ml) for 12 hours at 37 °C. The three kinds of cells (2.5×10^5) were added to ECV304 monolayer in a final volume of 0.1 ml respectively, and incubated for 1 h at 37 °C. Nonadherent cells were removed from the plate by gentle washing with warm PBS. By brief trypsinization with 0.25% trypsin, the adherent cells were removed onto a piece of fiberglass paper (49#), washed with 5% trichloroacetic acid and dried at 80 °C. The number of adherent cells was determined by measuring flash value using a flash-detecting device (Tri-Carb 2300TR, Packard Co Lit).

Statistics analysis

Data were presented with $\bar{x} \pm s$, statistical analysis was performed using ANOVA. Differences were judged to be statistically significant when the *P* value was less than 0.05.

RESULTS

Effect of ASON and/or cimetidine on expression of E-selectin and ICAM-1

Using cytofluorometry, we examined the effect of lipo-ASON or cimetidine on the level of E-selectin and ICAM-1 protein in ECV304 cells stimulated by TNF- α (Figure 1). Maximum expression of E-selectin or ICAM-1 was observed in TNF- α inducing group with no other treatments. Compared with TNF- α inducing group, the expression of E-selectin in all treated groups was differently decreased ($P < 0.001$), most markedly in lipo-ASON/cimetidine treated group ($P < 0.001$, vs lipo-ASON alone group), showing that lipo-ASON in combination with cimetidine had a better inhibitory effect. Similarly, the expression of ICAM-1 in lipo-ASON and lipo-ASON/cimetidine treated groups decreased significantly ($P < 0.001$), but the change of ICAM-1 expression in cimetidine treated group was not significant ($P = 0.296$), suggesting that cimetidine did not affect ICAM-1 expression in endothelial cells.

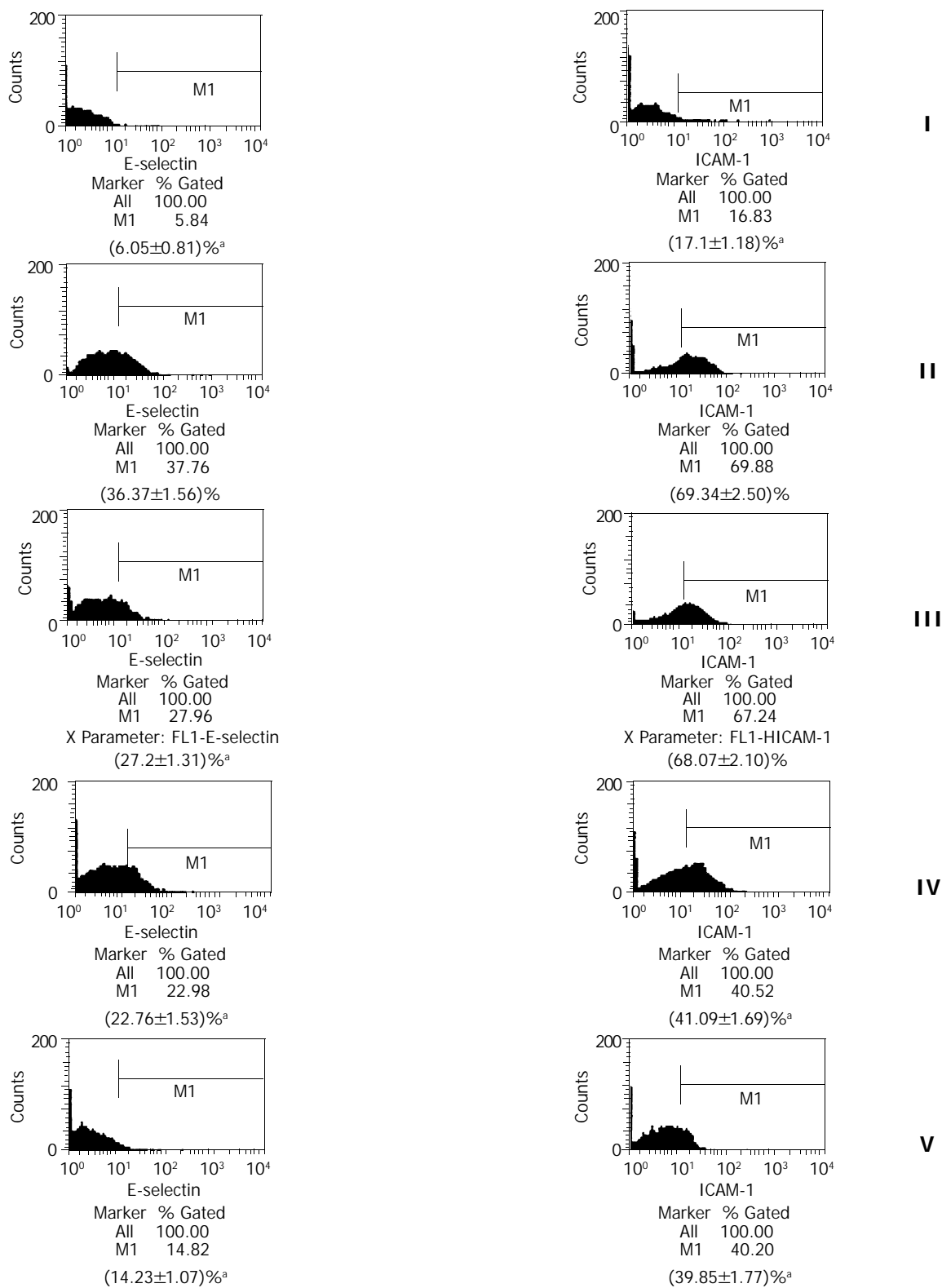


Figure 1 Effect of ASON on expression of E-selectin and ICAM-1 in endothelial cells (^a*P*<0.01, vs group II, *n*=5). I: Basal, II: TNF- α , III: cimetidine, IV: lipo-ASON, V: lipo-ASON/cimetidine.

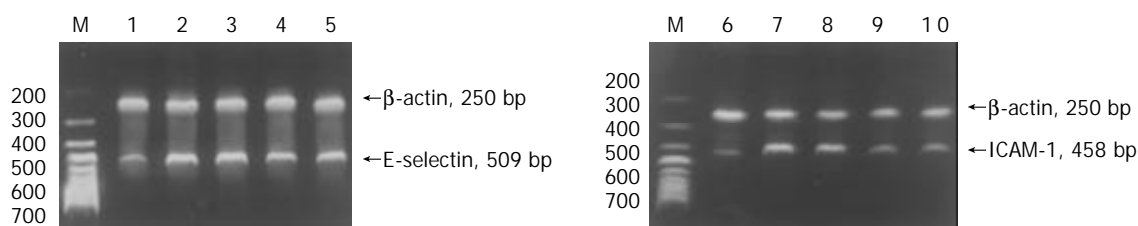


Figure 2 Agarose gel electrophoresis of RT-PCR products. M:Marker, 1: E/basal, 2: E/TNF- α , 3: E/cimetidine, 4: E/lipo-ASON, 5: E/lipo-ASON/cimetidine, 6: I/basal, 7: I/TNF- α , 8: I/cimetidine, 9: I/lipo-ASON, 10: I/cimetidine.

Agarose gel electrophoresis of RT-PCR products

To investigate the effects of lipo-ASON and/or cimetidine on the level of E-selectin and ICAM-1 mRNA, RT-PCR analysis was carried out. As shown in Figures 2 and 3, TNF- α could induce E-selectin and ICAM-1 gene expression. Lipo-ASON or lipo-ASON/cimetidine could significantly reduce the level of E-selectin and ICAM-1 mRNA, but cimetidine did not.

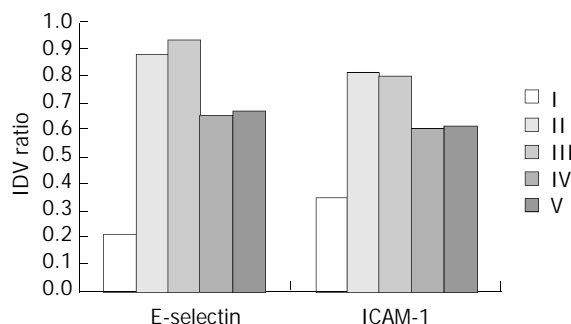


Figure 3 Relative expression value of ICAM-1 and E-selectin to β -actin by RT-PCR. I: Basal, II: TNF- α , III: Cimetidine, IV: Lipo-ASON, V: Lipo-ASON/Cimetidine.

Effect of ASON and/or cimetidine on adhesion

To examine the effects of lipo-ASON and/or cimetidine on the adhesion between tumor cells and ECV304 cells, a monolayer cell adhesion assay was carried out. As shown in Table 2, the adhesions of HepG2, BEL7404 and Ls-174-t cells to ECV304 cells were strongly induced by stimulation with TNF- α . Compared with TNF- α inducing group, the rate of adhesion was markedly decreased in lipo-E-selectin ASON and lipo-E-selectin ASON/cimetidine treated groups ($P < 0.05$), and lipo-E-selectin ASON/cimetidine worked better than lipo-E-selectin ASON alone except for HepG2/ECV304 group ($P < 0.05$). However, the decrease of adhesion was not significant in lipo-ICAM-1 ASON and lipo-ICAM-1 ASON/cimetidine treated groups except for HepG2/ECV304 group ($P > 0.05$).

Table 2 Adhesion rate of endothelial cells transfected by E-selectin and ICAM-1 ASON to tumor cells ($\bar{x} \pm s$)%

Group	I	II	III	IV	V
E-selectin/HepG2	17.7 \pm 0.9 ^a	80.4 \pm 6.2	58.9 \pm 2.7	38.0 \pm 5.0 ^a	24.1 \pm 1.5 ^a
E-selectin/BEL7404	8.1 \pm 1.0 ^a	75.9 \pm 0.6	52.2 \pm 2.4 ^a	26.7 \pm 1.6 ^a	17.4 \pm 1.1 ^{a,b}
E-selectin/Ls-174-t	16.0 \pm 1.6 ^a	77.9 \pm 5.7	53.9 \pm 2.6 ^a	43.1 \pm 1.7 ^a	29.5 \pm 2.6 ^{a,b}
ICAM-1/HepG2	5.0 \pm 1.3 ^a	71.0 \pm 2.4	68.6 \pm 1.8	69.0 \pm 1.4	67.3 \pm 2.2 ^a
ICAM-1/BEL7404	3.0 \pm 0.9 ^a	65.9 \pm 4.1	63.6 \pm 5.0	63.5 \pm 4.0	64.7 \pm 1.7
ICAM-1/Ls-174-t	5.8 \pm 0.8 ^a	63.0 \pm 2.0	63.4 \pm 1.2	64.5 \pm 1.8	62.8 \pm 1.3

(1) I: Basal, II: TNF- α , III: Cimetidine, IV: Lipo-ASON, V: Lipo-ASON/Cimetidine. (2) ^a $P < 0.05$, vs group II; ^b $P < 0.05$, group V vs group IV.

DISCUSSION

ICAM-1 cDNA with 2.98 Kb in length consists of 5' -untranslated region, 57 bp, a continuous open reading frame, 1 598 bp, and 3' -untranslated region, 1 330 bp. E-selectin cDNA with 3.85 Kb in length consists of 5' -untranslated region, 116 bp, a continuous open reading frame, 1 830 bp, and 3' -untranslated region, 1 898 bp. Bennett's research^[14] showed that among all the designed ASONs, ASONs hybridized to 3' -untranslated region were more potent than those hybridized to AUG transcription-initiation site or 5' -untranslated region. In our previous experiment, we found that each selected ASON of ICAM-1 and E-selectin hybridized to 3' -untranslated region

could reduce the expression of objective gene by nearly 40% respectively, demonstrating that their effects were sequence specific. This loss in mRNA might be due to the ASON targeted objective pre-mRNA in the nucleus, which resulted in activation of endogenous RNase H or a related enzyme and mediated hydrolysis of mRNA-ODN at the hybridization site^[17,18].

With the presence of cytokines such as IL-1 β and TNF- α secreted by tumor cells, vascular endothelial cells can produce different adhesive molecules at different times. After stimulation of cytokines, E-selectin shows its features in 4 to 5 hours, which mediate the early adhesion, and ICAM-1 shows its features in 12 to 48 hours, which mediate the late adhesion. In this article, through the treatment with E-selectin or ICAM-1 ASON before the induction by TNF- α , the expressions of objective molecules were blocked, but the adhesion between endothelial cells and tumor cells was only significantly inhibited by E-selectin ASON. The reasons were as follows: 1) Hepatic and colorectal cancer cells could highly express sle^x Ag^[19], the ligand of E-selectin. It is the major molecule that mediates the adhesion to endothelial cells directly. 2) ICAM-1 also appeared in the membrane of hepatic or colorectal cancer cells. The adhesion between cancer cells and vascular endothelial cells *in vitro* resorted to LFA-1^[20], the ligand of ICAM-1, which expresses on the membrane of white blood cells. However, there were no white blood cells to bridge *in vivo*. 3) Hepatic or colorectal cancer cells like HepG2 could also express affluent integrin $\alpha_2\beta_1$, which directly mediated the adhesion between tumor cells and endothelial cells^[19]. It is this kind of molecules that work in ICAM-1 ASON treated group.

Cimetidine, a kind of H2 receptor antagonist, has been used to inhibit the secretion of gastric acid in clinic. It has also been used to prolong the survival of patients with various forms of cancer in recent years^[21,22]. Even at the highest noncytotoxic concentration (10^{-4} M), cimetidine has been shown not to influence the expression of ICAM-1 protein, ICAM-1 mRNA and E-selectin mRNA, but could obviously reduce the expression of E-selectin protein^[22,23]. We proposed that cimetidine's inhibitory action on metastasis was due to blocking the adhesion between endothelial cells and tumor cells, especially colorectal cells with higher expression of sle^x Ag^[24]. Since other H2 receptor antagonists, such as ranitidine and famotidine, did not play the same role under the same experimental conditions^[22], it has become obvious that the mechanism of cimetidine's inhibiting function is involved in a step after transcription. p38 MAPK^[25], for instance, might be the regulatory molecule that activates the expression, of a number of genes at the level of posttranscription^[26-28].

Our research demonstrated that E-selectin played a primary role in initiating the adhesion of cancer cells to vascular endothelial cells through its interaction with its specific ligand, sialyl Lewis antigens^[29,30]. Lipo-E-selectin ASON in combination with cimetidine could inhibit the expression of E-selectin more effectively and reduce the adhesive rate of endothelial cells to tumor cells in early stage, reaching the goal of double benefits from outside and inside of cells. It not only guarantees the major aim of inhibiting adhesion, but also lowers the negative influence of cells subjected to drug *ab extra*. In short, this study provides some useful proofs for gene therapy of antiadhesion, which would become a new therapeutic alternative to inhibit high recurrence and metastasis of hepatic or colorectal cancer.

REFERENCES

- Giles RV. Antisense oligonucleotide technology: from EST to therapeutics. *Curr Opin Mol Ther* 2000; **2**: 238-252
- Capiati DA, Vazquez G, Tellez Inon MT, Boland RL. Antisense oligonucleotides targeted against protein kinase c alpha inhibit proliferation of cultured avian myoblasts. *Cell Prolif* 2000; **33**:

- 307-315
- 3 **Zhou S**, Wen SM, Zhang DF, Wang QL, Wang SQ, Ren H. Sequencing of PCR amplified HBV DNA pre-c and c regions in the 2.2.15 cells and antiviral action by targeted antisense oligonucleotide directed against sequence. *World J Gastroenterol* 1998; **4**: 434-436
 - 4 **Wang XW**, Yuan JH, Zhang RG, Guo LX, Xie Y, Xie H. Antihepatoma effect of alpha-fetoprotein antisense phosphorothioate oligodeoxyribonucleotides *in vitro* and in mice. *World J Gastroenterol* 2001; **7**: 345-351
 - 5 **Acosta R**, Montanez C, Gomez P, Cisneros B. Delivery of antisense oligonucleotides to PC12 cells. *Neurosci Res* 2002; **43**: 81-86
 - 6 **Agrawal S**, Kandimalla ER, Yu D, Hollister BA, Chen SF, Dexter DL, Alford TL, Hill B, Bailey KS, Bono CP, Knoerzer DL, Morton PA. Potentiation of antitumor activity of irinotecan by chemically modified oligonucleotides. *Int J Oncol* 2001; **18**: 1061-1069
 - 7 **Guo F**, Li Y, Wu S. Antisense IRAK-2 oligonucleotide blocks IL-1-stimulated NF-kappaB activation and ICAM-1 expression in cultured endothelial cells. *Inflammation* 1999; **23**: 535-543
 - 8 **Stepkowski SM**, Wang ME, Condon TP, Cheng-Flournoy S, Stecker K, Graham M, Qu X, Tian L, Chen W, Kahan BD, Bennett CF. Protection against allograft rejection with intercellular adhesion molecule-1 antisense oligodeoxynucleotides. *Transplantation* 1998; **66**: 699-707
 - 9 **Cheng Q**, Chen X, Ye Y. Antisense oligonucleotide attenuates renal tubulointerstitial injury in mice with unilateral ureteral obstruction. *Zhonghua Yixue Zazhi* 1999; **79**: 533-537
 - 10 **Lawson JA**, Adams WJ, Morris DL. Rantidine and cimetidine differ in their *in vitro* and *in vivo* effects on human colonic cancer growth. *Br J Cancer* 1996; **73**: 872-876
 - 11 **Hahm KB**, Kim WH, Lee SL, Kang JK, Park IS. Comparison of immunomodulative effects of the histamine-2 receptor antagonist cimetidine ranitidine, and famotidine on peripheral blood mononuclear cells in gastric cancer patients. *Scand J Gastroenterol* 1995; **30**: 265-271
 - 12 **Adams WJ**, Morris DL, Rose WR, Lubowski DZ, King DW. Cimetidine preserves non-specific immune function after colonic resection for cancer. *Aust N Z J Surg* 1994; **64**: 847-852
 - 13 **Adams WJ**, Lawson JA, Morris DL. Cimetidine inhibits *in vivo* growth of human colon cancer and reverses histamine stimulated *in vitro* and *in vivo* growth. *Gut* 1994; **35**: 1632-1636
 - 14 **Bennett CF**, Condon TP, Grimm S, Chan H, Chiang MY. Inhibition of endothelial cell adhesion molecule expression with antisense oligonucleotides. *J of Immunol* 1994; **152**: 3530-3540
 - 15 **Zhang XP**, Kelemen SE, Eisen HJ. Quantitative assessment of cell adhesion molecule gene expression in endomyocardial biopsy specimens from cardiac transplant recipients using competitive polymerase chain reaction. *Transplantation* 2000; **70**: 505-513
 - 16 **Gao X**, Huang L. Cationic liposome mediated gene transfer. *Gene Ther* 1995; **2**: 710-722
 - 17 **Condon TP**, Bennett CF. Altered mRNA splicing and inhibition of human E-selectin expression by an antisense oligonucleotide in human umbilical vein endothelial cells. *J Biol Chem* 1996; **271**: 30398-30403
 - 18 **Vickers TA**, Koo S, Bennett CF, Crooke ST, Dean NM, Baker BF. Efficient reduction of target RNAs by small interfering RNA and RNase H-dependent antisense agents. A comparative analysis. *J Biol Chem* 2003; **278**: 7108-7118
 - 19 **Kawakami-Kimura N**, Narita T, Ohmori K, Yoneda T, Matsumoto K, Nakamura T, Kannagi R. Involvement of hepatocyte growth factor in increased integrin expression on HepG2 cells triggered by adhesion to endothelial cells. *Br J Cancer* 1997; **75**: 47-53
 - 20 **Tanabe K**, Alexander JP, Steinbach F, Campbell S, Novick AC, Klein EA. Retroviral transduction of intercellular adhesion molecule-1 enhances endothelial attachment of bladder cancer. *Urol Res* 1997; **25**: 401-405
 - 21 **Matsumoto S**. Cimetidine and survival with colorectal cancer. *Lancet* 1995; **346**: 115
 - 22 **Kobayashi K**, Matsumoto S, Morishima T, Kawabe T, Okamoto T. Cimetidine inhibits cancer cell adhesion to endothelial cells and prevents metastasis by blocking E-selectin expression. *Cancer Res* 2000; **60**: 3978-3984
 - 23 **Leonardi A**, DeFranchis G, De Paoli M, Fregona I, Plebani M, Secchi A. Histamine-induced cytokine production and ICAM-1 expression in human conjunctival fibroblasts. *Curr Eye Res* 2002; **25**: 189-196
 - 24 **Matsumoto S**, Imaeda Y, Umemoto S, Kobayashi K, Suzuki H, Okamoto T. Cimetidine increases survival of colorectal cancer patients with high levels of sialyl Lewis-X and sialyl Lewis-A epitope expression on tumour cells. *Br J Cancer* 2002; **86**: 161-167
 - 25 **Read MA**, Whitley MZ, Gupta S, Pierce JW, Best J, Davis RJ, Collins T. Tumor necrosis factor α -induced E-selectin expression is activated by the nuclear factor- κ B and c-JUN N-terminal kinase/p38 mitogen-activated protein kinase pathways. *J Biol Chem* 1997; **272**: 2753-2761
 - 26 **Pietersma A**, Tilly BC, Gaestel M, de Jong N, Lee JC, Koster JF, Sluiter W. p38 mitogen activated protein kinase regulates endothelial VCAM-1 expression at the post-transcriptional level. *Biochem Biophys Res Commun* 1997; **230**: 44-48
 - 27 **Caivano M**. Role of MAP kinase cascades in inducing arginine transporters and nitric oxide synthetase in RAW264 macrophages. *FEBS Lett* 1998; **429**: 249-253
 - 28 **Miyazawa K**, Mori A, Miyata H, Akahane M, Ajisawa Y, Okudaira H. Regulation of interleukin-1 β -induced interleukin-6 gene expression in human fibroblast-like synoviocytes by p38 mitogen-activated protein kinase. *J Biol Chem* 1998; **273**: 24832-24838
 - 29 **Majuri ML**, Niemela R, Tiisala S, Renkonen O, Renkonen R. Expression and function of α 2,3-sialyl- and α 1,3/1,4-fucosyltransferases in colon adenocarcinoma cell lines: role in synthesis of E-selectin counter-receptors. *Int J Cancer* 1995; **63**: 551-559
 - 30 **Kunzendorf U**, Kruger-Krasagakes S, Notter M, Hock H, Walz G, Diamantstein T. A sialyl-Le(x)-negative melanoma cell line binds to E-selectin but not to P-selectin. *Cancer Res* 1994; **54**: 1109-1112

Edited by Zhu LH and Wang XL

Single-level dynamic spiral CT of hepatocellular carcinoma: Correlation between imaging features and density of tumor microvessels

Wei-Xia Chen, Peng-Qiu Min, Bin Song, Bong-Liang Xiao, Yan Liu, Ying-Hui Ge

Wei-Xia Chen, Peng-Qiu Min, Bin Song, Department of Radiology, West China Hospital, Sichuan University, Chengdu 610041, Sichuan Province, China

Bong-Liang Xiao, Department of Toxicology and Pathology, School of Public Health, Sichuan University, Chengdu 610041, Sichuan Province, China

Yan Liu, Department of Radiology, West China Hospital, Sichuan University, now working in Rijin Hospital, Shanghai, China

Ying-Hui Ge, Department of Radiology, West China Hospital, Sichuan University, now working in Henan Province Hospital, Henan Province, China

Correspondence to: Wei-Xia Chen, MD, Department of Radiology, West China Hospital, Sichuan University, Chengdu 610041, Sichuan Province, China. wxchen25@sohu.com

Telephone: +86-28-85422595 **Fax:** +86-28-85582944

Received: 2003-06-21 **Accepted:** 2003-07-30

Abstract

AIM: To investigate the correlation of enhancement features of hepatocellular carcinoma (HCC) revealed by single-level dynamic spiral CT scanning (DSCT) with tumor microvessel density (MVD), and to determine the validity of DSCT in assessing *in vivo* tumor angiogenic activity of HCC.

METHODS: Twenty six HCC patients were diagnosed histopathologically. DSCT was performed for all patients according to standard scanning protocol. Time-density curves were generated, relevant curve parameters were measured, and gross enhancement morphology was analyzed. Operation was performed to remove HCC lesions 1 to 2 weeks following CT scan. Histopathological slides were carefully prepared for the standard F₈RA immunohistochemical staining and tumor microvessel counting. Enhancement imaging features of HCC lesions were correlatively studied with tumor MVD and its intra-tumor distribution characteristics.

RESULTS: On DSCT images of HCC lesions, three patterns of time-density curve and three types of gross enhancement morphology were recognized. Histomorphologically, the distribution of positively stained tumor endothelial cells within tumor was categorized into 3 types. Curve parameters such as peak enhancement value and contrast enhancement ratio were significantly correlated with tumor tissue MVD ($r=0.508$ and $r=0.423$, $P<0.01$ and $P<0.05$ respectively). Both the pattern of time-density curve and the gross enhancement morphology of HCC lesions were also correlated with tumor MVD, and reflected the distributive features of tumor microvessels within HCC lesions. Correlation between the likelihood of intrahepatic metastasis of HCC lesions with densely enhanced pseudocapsules and rich pseudocapsular tumor MVD was found.

CONCLUSION: Enhancement imaging features of HCC lesions on DSCT scanning are correlated with tumor MVD, and reflect the intra-tumor distribution characteristics of

tumor microvessels. DSCT is valuable in assessing the angiogenic activity and tumor neovascularity of HCC patients *in vivo*.

Chen WX, Min PQ, Song B, Xiao BL, Liu Y, Ge YH. Single-level dynamic spiral CT of hepatocellular carcinoma: Correlation between imaging features and density of tumor microvessels. *World J Gastroenterol* 2004; 10(1): 67-72

<http://www.wjgnet.com/1007-9327/10/67.asp>

INTRODUCTION

Tumor angiogenesis plays a fundamental role in the pathogenesis of tumor growth and metastasis^[1-3], and significantly influences the biological behaviors of tumor and prognosis of patients^[3-6]. The inhibition or blockade of this angiogenic activity, on the other hand, can slow down the tumor growth rate and positively affect the outcome of patients^[7-9]. Although a single standardized and thoroughly validated method to evaluate the structure and function of tumor angiogenesis is not available, some histomorphological markers, such as microvessel density (MVD) and vascular endothelial growth factor, have been used as indicators of tumor angiogenic activity currently^[3,10-12]. However, these markers were studied immunohistochemically *in vitro* on biopsy or surgical tissues, and could not provide information of functional status of tumor angiogenesis, and were hardly to repeat for patients in follow-up. An ideal test should be non-invasive, fast, easy to perform, repeatable and reproducible, and most importantly, it should provide accurate and comprehensive information on the structure and biological characteristics of tumors *in vivo*.

Modern medical imaging modalities can depict the blood flow or reflect the hemodynamic changes. Recent studies using Doppler Sonography^[13-16] or MR^[17-28] or CT^[29,30] to assess tumor angiogenesis and neovascularity have yielded encouraging results in differential diagnosis and the correlation of aggressiveness and metastasis of tumor with the prognosis of patients. Correlation of enhanced imaging features of hepatocellular carcinoma (HCC) with tumor MVD was investigated to determine the validity of single-level dynamic spiral CT scanning (DSCT) *in vivo* for assessment of tumor angiogenic activity and neovascularity.

MATERIALS AND METHODS

Study subjects

From June 1997 to January 1999, 26 HCC patients were histopathologically proved and used for the study, and all the patients met the criteria for DSCT scanning and for histopathological specimen sampling and slides preparation. There were 23 males and 3 females with a mean age of 43.5 years (27 to 72 years). None of them had anti-tumor therapies prior to CT examination, and 1-2 weeks after CT, surgery was performed on all HCC patients to remove the lesions.

DSCT protocol

A Somatom Plus 4 VA spiral CT scanner (Siemens, Erlangen, Germany) was used for the study, 2 ml/kg of 65% angiografin or ultravist-300 (Schering, Germany) was used as intravenous contrast agent and injected via the antecubital route on the constant rate of 3 ml/sec. Before the start of CT scanning, the patients were educated and trained on how to cooperate for CT examination. The whole scanning procedure included 3 steps. First, all the liver was scanned without enhancement, then dynamic scanning at the selected target slice level (single-slice dynamic scanning) was followed, and finally the portal venous phase spiral CT acquisition of the entire liver was obtained. The target slice was selected based on the abnormal findings on the initial scanning. Only the central slice with the smallest area of tumor necrosis was chosen as the target for dynamic scanning. The dynamic scanning was performed 18 seconds after intravenous administration of contrast agent. For the dynamic scanning the sequence scan mode was employed with the cycle time of 2.3 seconds. A total of 18 slices were generated. The spiral scan mode was used for the initial scan and acquisition data on the final portal venous phase. Seven mm was used for calibration, table feed and slice thickness (pitch=1/1), and the scan delay time for the portal venous phase was 65 seconds.

Image data processing

Generation of time-density (T-D) curve Any visible blood vessel, necrotic foci and hypodense septum were avoided in selection of the region of interest (ROI) for HCC lesions. For the abdominal aorta, ROI was placed in its cross sectional center. The size of ROI was restricted to around 1 cm in diameter. With the built-in software program, the T-D curves of both HCC lesions and abdominal aorta were generated on the basis of the selected ROIs.

T-D curve parameters Several curve parameters were defined for the T-D curve of HCC lesions. (a) The peak enhancement value (PV) of the abdominal aorta was defined as the CT attenuation number at the junction between the up-slope portion with the steepest rise and the portion with gradual or flat rise. The corresponding time was referred to as the peak enhancement time (PT). (b) The PV for HCC lesion was the result of maximum enhancement CT attenuation number minus the baseline CT attenuation number on plain CT scan, and the time to reach the maximum CT attenuation number after enhancement was the PT. (c) The contrast enhancement ratio (CER) was defined as the percentage of the PV of HCC lesion divided by the PV of the abdominal aorta. Patterns of T-D curves were analyzed and the related curve parameters (PV, PT, and CER) were calculated.

Image interpretation All the CT images were jointly analyzed with standardized criteria by two senior radiologists experienced in liver imaging. Special attention was paid to the morphological enhancement patterns of HCC lesions and other associated imaging findings, such as pseudocapsules, daughter foci, and invasion of the portal venous system.

Histomorphological analysis of tissue specimen

Great care was taken to ensure that the matching of tissue sampling sites of surgically resected gross HCC tumor specimen with the correspondingly selected ROIs on DSCT images was on one-to-one basis. The obtained tissue specimens were processed by standard macro- and micro-slide techniques to verify the histomorphological tumor extension. Then slides of 5 μ m thickness were stained with the standard immunoperoxidase method using factor VIII-related antigen (F₈RA stain)^[2]. Criteria for positive stain and microvessel counting were those established by Weidner *et al*^[2-3]. Two

independent experienced pathologists counted each ROI separately, and consensus counting was done for dispute. The counting was first proceeded at 100 x magnification for "hot spot" representing the area of the highest microvessel density (MVD), then switched to 200 x magnification for clear depiction and better counting. For each slide three "hot spots" were counted, and the mean count represented the final MVD. The distribution of "hot spots" within tumor lesions was also recorded.

Statistical analysis

Pearson's correlation analysis and variance analysis were performed to test the strength of association between CT imaging features and the histomorphological marker, $P < 0.05$ was considered statistically significant.

RESULTS

Dynamic CT scan

Patterns of T-D curve Some distinctively different patterns of T-D curves of HCC lesions were observed and categorized into three types. Type I, the initial rise of T-D curve was very fast and steep, then abruptly changed to a more flat and steady gradual rise till the plateau phase. This curve pattern occurred in 7 patients. In type II curve, the up-rise of the curve slope was obvious, yet relatively smooth, no abrupt turn in the configuration of the curve up-slope. Thirteen patients demonstrated T-D curve pattern of type II. Type III curve in 6 patients was characterized by slow and flat rise of the initial curve up-slope with low amplitude. These three patterns of T-D curves of HCC lesions are depicted in Figure 1, and the calculated curve parameters are summarized in Table 1. PV and CER of type III patients were obviously lower than those of type I and type II patients, and the differences were statistically significant ($P < 0.05$). On the other hand, the differences of PV and CER between type I and type II patients were not statistically significant. There was a trend for PT to increase gradually from type I to type III, but the differences among the three types were not statistically significant.

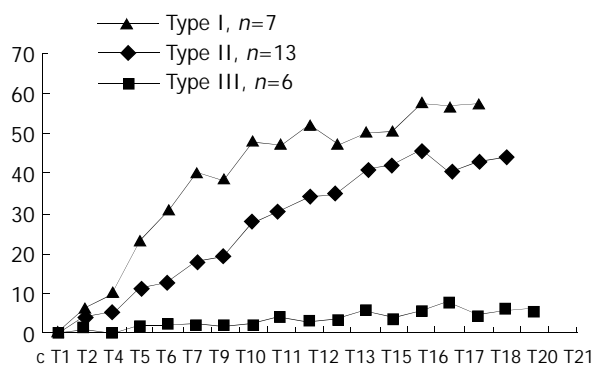


Figure 1 Three patterns (I, II, III) of time-density curve observed in HCC patients. The transverse axis represents the time and the Y-axis represents the peak enhancement value in Hounsfield units.

Table 1 HCC time-density curve patterns

Curve parameters	Type I	Type II	Type III
Number of patients	7	13	6
PV (Hu)	53.6 \pm 7.8	47.9 \pm 12.6	20.6 \pm 7.2 ^a
PT (Sec)	43.8 \pm 9.5	52.2 \pm 7.7	57.9 \pm 8.3
CER (%)	25.0 \pm 7.2	22.5 \pm 6.5	8.2 \pm 3.4 ^a

^aThe differences of PV and CER between type III and those of type I and II were statistically significant ($P < 0.05$).

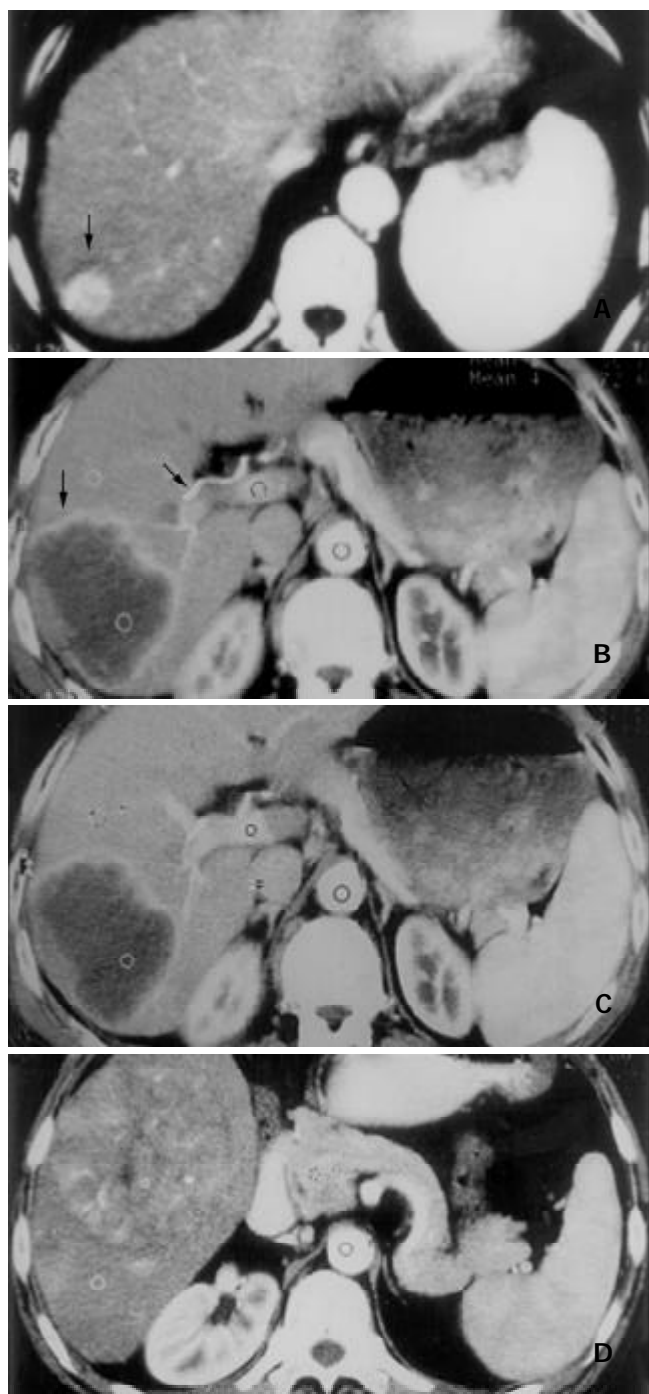


Figure 2 Three types of enhancement morphology depicted in HCC patients. A: Type A. Marked and homogeneous enhancement of the entire HCC lesion in the posterosuperior segment of right hepatic lobe (black arrow). B: Type B. Bright peripheral ring-like enhancement of HCC lesion on arterial phase image in the right posterosuperior segment (black arrow), and the dilated right hepatic artery (black arrow). C: Portal venous image at the same slice level as in (B). HCC lesion remained hypodense despite obvious enhancement of normal liver parenchyma elsewhere. D: Type C. Inhomogeneous patchy enhancement of HCC lesion in right lower hepatic lobe from arterial phase image. Bright dots and linear shadows represent enhanced tumor vessels within the lesion.

Morphological enhancement patterns of HCC The gross morphological enhancement manifestations of HCC lesions could also be grouped into 3 types (Figure 2). Type A was seen in 7 patients, the HCC lesions were densely enhanced in a homogeneous pattern (Figure 2A). The mean transverse diameter of lesions was 3.1 cm. Type B was in 5 patients, the

lesions demonstrated complete or partial rim-like peripheral enhancement, without or with only few dots of enhanced tumor vessels within the lesion center (Figure 2B, 2C). Mean diameter was 5.7 cm. Type C was seen in 14 patients, HCC lesions were inhomogeneously enhanced in a patchy fashion. Many small round-shaped, linear or reticular shadows representing enhanced tumor vessels were clearly visible, along with many hypodense necrotic foci and fibrous septa within the lesions (Figure 2D). The mean transverse diameter in this group of patients was 8.5 cm. The differences in the transverse diameter of tumor lesions among the three groups were statistically significant.

Immunohistochemical findings

F₈RA staining revealed a great variation in the distribution of positively stained tumor vascular endothelial cells within HCC lesions. Such a distribution variability in our patient could be roughly grouped into three patterns (Figure 3). (1) Twelve patients exhibited very rich blood sinusoids but scanty tumor microvessels in the interstitium. In 9 patients, positively stained sinusoidal endothelial cells were abundant and distributed inhomogeneously in a patchy fashion (Figure 3A). But in the rest 3 patients, sinusoidal endothelial cells had no positive staining. (2) Eleven patients had both rich sinusoids and interstitial microvessels, a large number of positively stained endothelial cells were distributed in both sinusoids and interstitium (Figure 3B). (3) Three patients had rich interstitium, with few interstitial microvessels and scanty sinusoids, and positively stained endothelial cells were very scarce (Figure 3C).

The MVD of HCC tumor tissue varied greatly from 6 to 91 among patients.

Correlation of DSCT features and tumor MVD

(1) T-D curve parameters and MVD A statistically significant positive correlation was demonstrated between tumor MVD and both PV and CER of corresponding HCC lesions. The correlation coefficients (r) were 0.508 ($P<0.01$) and 0.423 ($P<0.05$) respectively. However, MVD had no positive correlation with PT.

(2) Curve patterns, enhancement morphology and MVD The relationships between tumor MVD and T-D curve patterns and the three gross enhancement morphological types of HCC lesions are summarized in Table 2. The tumor MVDs of T-D curve type III and the gross enhancement morphology type B were significantly lower than those of curve type I and II ($P<0.05$), and gross morphology type A and C ($P<0.05$), respectively. The differences of MVDs between types I, II of T-D curve and the enhancement morphological patterns (type A, C) were not statistically significant.

Table 2 HCC time-density curve patterns, types of gross enhancement morphology and tumor MVD

	Type I	Type II	Type III	Type A	Type B	Type C
Patient No	7	13	6	7	5	14
MVD	41.8±16.7	48.0±18.2	23.0±7.4 ^a	49.7±14.2	15.6±5.7 ^b	44.0±19.7

^aThe differences of MVDs between type III and type I, type II were statistically significant ($P<0.05$). ^bThe differences of MVDs between types B, A, C were statistically significant ($P<0.05$).

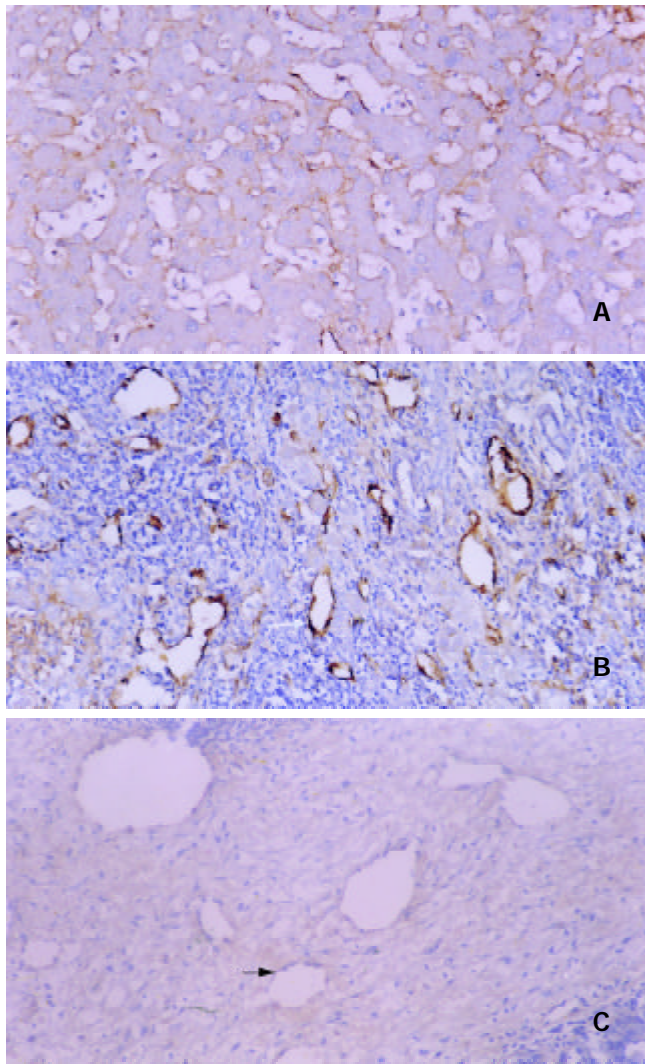
(3) Curve patterns, enhancement morphology and distribution of MVD The intratumoral distribution characteristics of tumor MVD and their relationships with T-D curve patterns and gross morphological enhancement types of HCC lesions are listed in Table 3.

Table 3 HCC time-density curve patterns, types of gross enhancement morphology and intratumoral MVD distribution

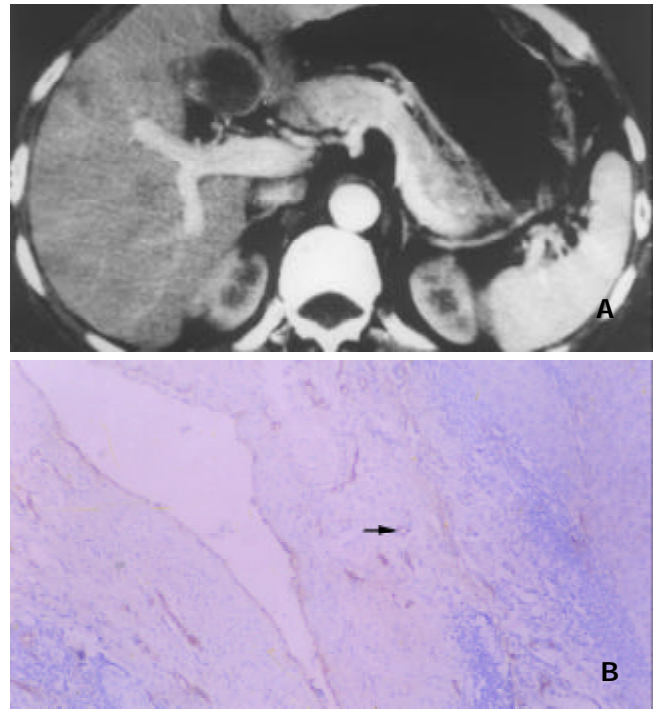
	Type I	Type II	Type III	Type A	Type B	Type C
Rich S	0	10	2	4	2	6
Rich S & I MVD	7	3	1	3	0	8
Scanty S & I MVD	0	0	3	0	3	0

S-tumor blood sinusoids, I-tumor interstitium.

(4) Other DSCT signs and related histomorphological changes Eleven patients demonstrated intrahepatic metastatic foci or daughter lesions. 7 of the 11 patients had prominent pseudocapsules that were hyperdense on DSCT images (Figure 4). In 1 patient the pseudocapsule remained to be hypodense throughout the entire scanning period, and no discrete pseudocapsule was discernible in the other 3 patients. Immunohistochemical F₈RA stain revealed abundant positively stained tumor endothelial cells in connective tissue of the tumor pseudocapsule in 8 patients. In the remaining 3 patients, judgement could not be made as whether or not the tumor pseudocapsule was present on the histopathological slides, due to improper tissue sampling, which missed the border region between HCC lesion and the neighboring normal liver tissue.

**Figure 3** Three patterns of intratumoral MVD distribution revealed by F₈RA immunohistochemical staining. A: Pattern I. Markedly dilated and abundant blood sinusoids with very rich positively stained sinusoidal endothelial cells and scanty tumor interstitium. B: Pattern II. Sinusoids and interstitium

abundant and rich in positively stained endothelial cells (black arrow). C: Pattern III. Rich tumor interstitium with few positively stained endothelial cells (white arrow) and scanty blood sinusoids.

**Figure 4** Enhancement of HCC pseudocapsules and pseudocapsular MVD. A: Marked enhancement of HCC pseudocapsule (hyperdensity) in the medial segment of left hepatic lobe shown by DSCT. Note the similar enhancement pattern of the satellite or daughter lesion in the anterior segment of right hepatic lobe. B: F₈RA staining Rich positively stained endothelial cells within tumor pseudocapsule (black arrow) revealed by F₈RA staining.

DISCUSSION

MVD, one of the histomorphological markers, is currently regarded as the best available means to represent tumor angiogenesis, and has been widely used to characterize tumor angiogenic activity *in vitro*. However, it may not be an ideal method for clinical purposes, as it is invasive and hard to perform and to repeat. Clearly, from the clinical perspective, it is of great clinical importance to look for a noninvasive method, which can provide *in vivo* overall functional information about tumor angiogenesis, besides accurate morphological information. We designed this dynamic spiral CT study to investigate the correlation of enhancement patterns of HCC lesions with the histomorphological marker of tumor angiogenesis – tumor MVD, and to determine the validity of DSCT in assessing angiogenic activity and neovascularity of HCC lesions.

Our study showed that the curve parameters generated from T-D curves of HCC lesions, such as PV and CER, were positively correlated to tumor MVD with statistical significance. As T-D curve parameters were representative of the hemodynamic characteristics of tumor microvasculature, this observation indicated that the degree of tumor enhancement on DSCT was affected by tumor MVD. The tumor enhancement degree could also truly reflect the distribution characteristics of tumor microvessels within a tumor mass, as the area with the greatest enhancement was often associated with the highest MVD. Higher tumor MVD was shown to be associated with worse degree of

malignancy and more potential of metastases^[4,10], thus it is possible to estimate the biological behaviors of HCC in terms of aggressiveness and metastasis by calculating the parameters of HCC T-D curve through dynamic spiral CT scanning.

The patterns of T-D curves of HCC lesions also provided *in vivo* clues to the histomorphological distribution characteristics of tumor microvessels within a tumor mass. Type I curve was often histologically associated with rich blood sinusoids and microvessels in the interstitium, both demonstrating abundant positively stained tumor vascular endothelial cells. Such a histomorphological feature of microvessel-rich tumor interstitium might well explain the early rapid rise of the up-slope and the high amplitude of this type of T-D curves observed in this subset of HCC patients. As more and more contrast agents reached the sinusoids where the rate of blood flow was sluggish, alteration of the rise pace resulted in an abrupt turn of the curve up-slope configuration. Abundant, often dilated and tortuous sinusoids with positively stained tumor endothelial cells resulted in type II curve. Sluggish blood flow with prolonged accumulation of contrast agent in sinusoids might cause the slow and steady rise of the up-slope of T-D curve in this group of HCC patients. However, in 3 patients with type II curve, both sinusoids and interstitium showed rich positively stained endothelial cells. Two reasons might be implicated for this discrepancy between T-D curve pattern and histomorphological marker. First, the hemodynamic effect of rich blood sinusoids might overrun that of microvessel-rich interstitium in these 3 HCC patients, causing the distribution of contrast-containing blood within the tumor mass to be relatively slower. Misrepresentation due to sampling error was another possible reason. As the selected area of ROI was 1 cm, much larger than what could be represented on a histological slide, it was possible that the selected ROIs might actually contain many more sinusoids than what was shown on the corresponding histological slides in these 3 HCC patients. Type III curve was histologically characterized either by rich interstitium but with scanty interstitial microvessels and scanty blood sinusoids, or by rich sinusoids which were devoid of positively stained endothelial cells. These tumor sinusoids had structural and functional resemblance to those of normal liver sinusoids, therefore, the rise of the up-slope in this type of T-D curve was quite slow and flat in the hepatic arterial phase. In the patient with type III curve, both rich sinusoids and interstitial microvessels with positively stained endothelial cells were observed. We speculated that the cause might be the mismatch of selected ROI with the sampling site for histomorphological measurement, and the variation in tumor angiogenic activity within a tumor lesion, which could lead to the misrepresentation by MVD.

The study also found that the gross enhancement morphology of HCC lesions was related to the distribution of tumor microvessels within a tumor mass. As shown in Table 3, type A enhancement morphology was mainly seen in relatively small HCC lesions, while type C enhancement morphology was found in larger lesions. However, both types were histomorphologically characterized by rich blood sinusoids or coexistence of microvessel-rich interstitium, both of which had abundant positively stained endothelial cells. Such findings might suggest that when a hypervascular HCC lesion was small, the distribution of tumor microvessels within it tended to be homogeneous, giving rise to the homogeneous enhancement appearance on DSCT scan. With the tumor became larger, intratumoral necrosis, fibrous septation and granulation formation occurred. The original homogeneity of tumor microvessels distribution was altered and distorted, so did the gross morphological enhancement patterns on CT images. Type B enhancement morphology showed that tumor interstitium was abundant in quantity, but either with scanty

interstitial microvessels and few sinusoids, or with rich sinusoids that were devoid of positively stained endothelial cells. In sharp contrast, tumor microvessels with positively stained endothelial cells were rich in pseudocapsules of this type of HCC patients. Thus the gross morphological enhancement pattern could well reflect the underlying histomorphological characteristics of tumor microvessels in this group of HCC patients. Therefore, by analyzing the enhancement morphology of HCC lesions on dynamic spiral CT scan, it was possible to estimate both the *in vivo* tumor angiogenic activity and the distribution characteristics of tumor neovascularity. Compared to the measurement of histomorphological markers, dynamic spiral CT was able to maximally avoid the possibility of sampling errors and offered a comprehensive overview of the gross enhancement morphology of HCC lesions.

Our another interesting finding was that most of HCC lesions with intrahepatic metastases or daughter foci demonstrated characteristic hyperdense pseudocapsules on dynamic CT images corresponding to hepatic arterial phase. These pseudocapsules were histomorphologically characterized by very rich positively stained endothelial cells diffusely distributed in the connective tissues of pseudocapsules. Such an association indicated that hypervascularized tumor pseudocapsules with abundant interstitial structurally defective tumor microvessels^[31] might facilitate intrahepatic metastasis or homogeneous spreading of HCC.

Though the close positive correlation of enhancement imaging features of HCC lesions revealed by DSCT with tumor MVD was demonstrated, several other factors, such as perfusion rate, microvessel permeability, and size or volume of extracellular space, might also influence the uptake rate of contrast agent by tumor tissue, thus affecting the configurations of T-D curve. Little has been known about major contributors for the difference in the contrast agent uptake rate^[11,32]. We suspect that the differences might depend on the type or even subtype of tumors, and further studies are required to clarify this issue.

In conclusion, the characteristics of T-D curve of HCC revealed by DSCT scanning are closely related to tumor MVD. The gross enhancement morphology of HCC lesions on DSCT images can reflect the features of histomorphological distribution of tumor microvessels within a tumor. DSCT is valid for the *in vivo* assessment of tumor angiogenic activity and neovascularity of HCC lesions, which is very important in making differential diagnosis, evaluating tumor malignancy and aggressiveness, monitoring therapeutic effects, and determining the final outcome of HCC patients.

ACKNOWLEDGEMENT

Our thanks go to Dr. Luinan Yan, MD, and Dr. Sheng He, MD, for their valuable assistance of this research work.

REFERENCES

- 1 **Folkman J, Shing Y.** Angiogenesis. *J Biol Chem* 1992; **267**: 10931-10934
- 2 **Weidner N, Semple J, Welch W, Folkman J.** Tumor angiogenesis and metastasis: correlation in invasive breast carcinoma. *N Engl J Med* 1991; **324**: 1-8
- 3 **Weidner N.** Intratumor microvessel density as a prognostic factor in cancer. *Am J Pathol* 1995; **147**: 9-19
- 4 **Jinno K, Tanimizu M, Hyodo I, Nishikawa Y, Hosokawa Y, Doi T, Endo H, Yamashita T, Okada Y.** Circulating vascular endothelial growth factor (VEGF) is a possible tumor marker for metastasis in human hepatocellular carcinoma. *J Gastroenterol* 1998; **33**: 376-382
- 5 **Weidner N, Carroll PR, Flax J, Blumenfeld W, Folkman J.** Tumor angiogenesis correlates with metastasis in invasive prostate carcinoma. *Am J Pathol* 1993; **143**: 401-409

- 6 **Poon RT**, Ng IO, Lau C, Yu WC, Yang ZF, Fan ST, Wong J. Tumor microvessel density as a predictor of recurrence after resection of hepatocellular carcinoma: a prospective study. *J Clin Oncol* 2002; **20**: 1775-1785
- 7 **Augustin HG**. Antiangiogenic tumor therapy: will it work? *Trends Pharmacol Sci* 1998; **19**: 216-222
- 8 **Hama Y**, Shimizu T, Hosaka S, Sugeno A, Usuda N. Therapeutic efficacy of the angiogenesis inhibitor O-(chloroacetyl-carbamoyl) fumagillol (TNP-470; AGM-1470) for human anaplastic thyroid carcinoma in nude mice. *Exp Toxicol Pathol* 1997; **49**: 239-247
- 9 **Kin M**, Torimura T, Ueno T, Nakamura T, Ogata R, Sakamoto M, Tamaki S, Sata M. Angiogenesis inhibitor TNP-470 suppresses the progression of experimentally-induced hepatocellular carcinoma in rats. *Int J Oncol* 2000; **16**: 375-382
- 10 **Tomisaki S**, Ohno S, Ichiyoshi Y, Kuwano H, Maehara Y, Sugimachi K. Microvessel quantification and its possible relation with liver metastasis in colorectal cancer. *Cancer* 1996; **77**(8 Suppl): 1722-1728
- 11 **Hawighorst H**, Knapstein PG, Knopp MV, Vaupel P, van Kaick G. Cervical carcinoma: standard and pharmacokinetic analysis of time-intensity curves for assessment of tumor angiogenesis and patient survival. *MAGMA* 1999; **8**: 55-62
- 12 **Wild R**, Ramakrishnan S, Sedgewick J, Griffioen AW. Quantitative assessment of angiogenesis and tumor vessel architecture by computer-assisted digital image analysis: effects of VEGF-toxin conjugate on tumor microvessel density. *Microvasc Res* 2000; **59**: 368-376
- 13 **Sahin Akyar G**, Sumer H. Color Doppler ultrasound and spectral analysis of tumor vessels in the differential diagnosis of solid breast masses. *Invest Radiol* 1996; **31**: 72-79
- 14 **Raza S**, Baum JK. Solid breast lesions: evaluation with power Doppler US. *Radiology* 1997; **203**: 164-168
- 15 **Louvar E**, Littrup PJ, Goldstein A, Yu L, Sakr W, Grignon D. Correlation of color Doppler flow in the prostate with tissue microvascularity. *Cancer* 1998; **83**: 135-140
- 16 **Peters-Engl G**, Medl M, Mirau M, Wanner C, Bilgi S, Sevelde P, Obermair A. Color-coded and spectral Doppler flow in breast carcinoma-relationship with the tumor microvasculature. *Breast Cancer Res Treat* 1998; **47**: 83-89
- 17 **Stomper PC**, Winston JS, Herman S, Klippenstein DL, Arredondo MA, Blumenson LE. Angiogenesis and dynamic MR imaging gadolinium enhancement of malignant and benign breast lesions. *Breast Cancer Res Treat* 1997; **45**: 39-46
- 18 **Hawighorst H**, Knapstein PG, Weikel W, Knopp MV, Zuna I, Knof A, Brix G, Schaeffer U, Wilkens C, Schoenberg SO, Essig M, Vaupel P, van Kaick G. Angiogenesis of uterine cervical carcinoma: characterization by pharmacokinetic magnetic resonance parameters and histological microvessel density with correlation to lymphatic involvement. *Cancer Res* 1997; **57**: 4777-4786
- 19 **Pham CD**, Roberts TP, van Bruggen N, Melnyk O, Mann J, Ferrara N, Cohen RL, Brasch RC. Magnetic resonance imaging detects suppression of tumor vascular permeability after administration of antibody to vascular endothelial growth factor. *Cancer Invest* 1998; **16**: 225-230
- 20 **Hawighorst H**, Knapstein PG, Knopp MV, Weikel W, Brix G, Zuna I, Schonberg SO, Essig M, Vaupel P, van Kaick G. Uterine cervical carcinoma: comparison of standard and pharmacokinetic analysis of time-intensity curves for assessment of tumor angiogenesis and patient survival. *Cancer Res* 1998; **58**: 3598-3602
- 21 **Hawighorst H**, Schaeffer U, Knapstein PG, Knopp MV, Weikel W, Schonberg SO, Essig M, van Kaick G. Detection of angiogenesis-dependent parameters by functional MRI: correlation with histomorphology and evaluation of clinical relevance as prognostic factor using cervix carcinoma as an example. *Rofu Fortschr Geb Rontgenstr Neuen Bildgeb Verfahr* 1998; **169**: 499-504
- 22 **Hawighorst H**, Weikel W, Knapstein PG, Knopp MV, Zuna I, Schonberg SO, Vaupel P, van Kaick G. Angiogenic activity of cervical carcinoma: assessment by functional magnetic resonance imaging-based parameters and a histomorphological approach in correlation with disease outcome. *Clin Cancer Res* 1998; **4**: 2305-2312
- 23 **Mayr NA**, Hawighorst H, Yuh WT, Essig M, Magnotta VA, Knopp MV. MR microcirculation assessment in cervical cancer: correlations with histomorphological tumor markers and clinical outcome. *J Magn Reson Imaging* 1999; **10**: 267-276
- 24 **Miles KA**, Charnsangavej C, Lee FT, Fishman EK, Horton K, Lee TY. Application of CT in the investigation of angiogenesis in oncology. *Acad Radiol* 2000; **7**: 840-850
- 25 **Gossmann A**, Helbich TH, Mesiano S, Shames DM, Wendland MF, Roberts TP, Ferrara N, Jaffe RB, Brasch RC. Magnetic resonance imaging in an experimental model of human ovarian cancer demonstrating altered microvascular permeability after inhibition of vascular endothelial growth factor. *Am J Obstet Gynecol* 2000; **183**: 956-963
- 26 **Okuhata Y**, Brasch RC, Pham CD, Daldrup H, Wendland MF, Shames DM, Roberts TP. Tumor blood volume assays using contrast-enhanced magnetic resonance imaging: regional heterogeneity and postmortem artifacts. *J Magn Reson Imaging* 1999; **9**: 685-690
- 27 **Padhani AR**, Neeman M. Challenges for imaging angiogenesis. *Br J Radiol* 2001; **74**: 886-890
- 28 **Roberts HC**, Roberts TP, Brasch RC, Dillon WP. Quantitative measurement of microvascular permeability in human brain tumors achieved using dynamic contrast-enhanced MR imaging: correlation with histologic grade. *Am J Neuroradiol* 2000; **21**: 891-899
- 29 **Miles KA**. Tumour angiogenesis and its relation to contrast enhancement on computed tomography: a review. *Eur J Radiol* 1999; **30**: 198-205
- 30 **Kwak BK**, Shim HJ, Park ES, Kim SA, Choi D, Lim HK, Park CK, Chung JW, Park JH. Hepatocellular carcinoma: correlation between vascular endothelial growth factor level and degree of enhancement by multiphase contrast-enhanced computed tomography. *Invest Radiol* 2001; **36**: 487-492
- 31 **Less JR**, Skalak TC, Sevic EM, Jain RK. Microvascular architecture in a mammary carcinoma: branching patterns and vessel dimensions. *Cancer Res* 1991; **51**: 265-273
- 32 **Degani H**, Gusic V, Weinstein D, Fields S, Strano S. Mapping pathophysiological features of breast tumors by MRI at high spatial resolution. *Nat Med* 1997; **3**: 780-782

Protective effect of nitric oxide induced by ischemic preconditioning on reperfusion injury of rat liver graft

Jian-Ping Gong, Bing Tu, Wei Wang, Yong Peng, Shou-Bai Li, Lu-Nan Yan

Jian-Ping Gong, Wei Wang, Lu-Nan Yan, Department of General Surgery, Huaxi Hospital, Sichuan University, Chengdu 610041, Sichuan Province, China

Jian-Ping Gong, Bing Tu, Yong Peng, Shou-Bai Li, Department of General Surgery, the Second Affiliated Hospital of Chongqing Medical University, Chongqing 400010, China

Supported by the National Natural Science Foundation of China, No. 30200278, and China Postdoctoral Science Foundation, No. 2001-5

Correspondence to: Dr. Jian-Ping Gong, Department of General Surgery, the Second Affiliated Hospital of Chongqing Medical University, 74 Linjiang Road, Chongqing 400010, China. gongjianping11@hotmail.com

Telephone: +86-23-63766701 **Fax:** +86-23-63829191

Received: 2003-03-04 **Accepted:** 2003-04-03

Abstract

AIM: Ischemic preconditioning (IP) is a brief ischemic episode, which confers a state of protection against the subsequent long-term ischemia-reperfusion injuries. However, little is known regarding the use of IP before the sustained cold storage and liver transplantation. The present study was designed to evaluate the protective effect of IP on the long-term preservation of liver graft and the prolonged anhepatic-phase injury.

METHODS: Male Sprague-Dawley rats were used as donors and recipients of orthotopic liver transplantation. All livers underwent 10 min of ischemia followed by 10 min of reperfusion before harvest. Rat liver transplantation was performed with the portal vein clamped for 25 min. Tolerance of transplanted liver to the reperfusion injury and liver damage were investigated. The changes in adenosine concentration in hepatic tissue and those of nitric oxide (NO) and tumor necrosis factor (TNF) in serum were also assessed.

RESULTS: Recipients with IP significantly improved their one-week survival rate and liver function, they had increased levels of circulating NO and hepatic adenosine, and a reduced level of serum TNF, as compared to controls. Histological changes indicating hepatic injuries appeared improved in the IP group compared with those in control group. The protective effect of IP was also obtained by administration of adenosine, while blockage of the NO pathway using N ω -nitro-L-arginine methyl ester abolished the protective effect of IP.

CONCLUSION: IP appears to have a protective effect on the long-term preservation of liver graft and the prolonged anhepatic-phase injuries. NO may be involved in this process.

Gong JP, Tu B, Wang W, Peng Y, Li SB, Yan LN. Protective effect of nitric oxide induced by ischemic preconditioning on reperfusion injury of rat liver graft. *World J Gastroenterol* 2004; 10(1): 73-76

<http://www.wjgnet.com/1007-9327/10/73.asp>

INTRODUCTION

Liver transplantation is an accepted therapy for patients with

end-stage liver diseases^[1]. Hepatic ischemia-reperfusion (I/R) injury associated with liver transplantation is an unresolved problem in the clinical practice. Primary non-function of liver graft remains one of the most severe complications of liver transplantation, and poor initial graft function also occurs in one third of cases after liver transplantation. To deal with these complications, no effective treatment can be used but retransplantation^[2,3]. Evidently, approaches need to be established to handle or even to avoid these complications.

The underlying mechanisms of cold I/R injuries are still poorly understood. Long-term ischemia of liver graft leads to impairment of liver function and reduction in survival rate of the recipients^[4]. On the other hand, anhepatic phase is the most important parameter for orthotopic rat liver transplantation (ORLT), because prolonged anhepatic phase can be associated with an endotoxin-like syndrome caused by the warm intestinal ischemia and is not related to the cold ischemia injuries of the liver^[5]. The hepatic reticulo-endothelial system plays a key role in the elimination of endotoxins. The detoxification system is usually deficient in recipients due to liver failure and is completely absent during the anhepatic phase of transplantation. The endotoxin content has been proven to increase markedly in the portal circulation of cirrhotic patients compared to that in the peripheral blood^[6]. The hypothermia may affect the ability of Kupffer cells to eliminate endotoxins and to release cytokines, such as tumor-necrosis factor (TNF). It has been shown that TNF is partly responsible for initiation of the lethal toxicity of endotoxins^[7].

Ischemic preconditioning (IP) is a process by which a brief ischemic episode confers a state of protection against the subsequent more sustained ischemic insult^[8]. Recent studies have demonstrated that a brief ischemia treatment, followed by an episode of reperfusion, can reduce the sustained I/R injury^[9,10]. These observations suggest a potential application of IP in liver transplantation. In this study, the protective effect of IP on the long-term preservation of liver grafts and the prolonged anhepatic phase was observed.

MATERIALS AND METHODS

Materials

Male *Sprague-Dawley* rats weighing 200 to 230 g supplied by the Center of Experimental Animal in Sichuan University, were used as donors and recipients. Animals were bred in a controlled environment with a 12 hour light/dark cycle. Donor rats were fasted for 12 hours with free access to water before surgery, while the recipients had free access to normal rat chow and water before surgery. This study was approved by Sichuan Bioethics Committee, and the procedures were carried out according to the routine animal-care guidelines.

ORLT

Liver transplantation was performed according to Kamada's cuff-technique^[11] under anesthesia with ether inhalation. Briefly, the abdomen was opened through a midline incision and the liver was freed from its ligaments with minimal manipulation. The donor bile duct was transected, and a 0.4 cm

length of tube was insert into the lumen of the bile duct and secured with a circumferential 5-0 silk suture. The animal was injected intravenously with 50 U of heparin. The liver was perfused through portal vein with an intravenous cannula connected with a syringe with 36 U of heparin in 6 ml of cold saline. The donor liver was placed in the saline bath at 4 °C for 100 min. The cuff preparation of portal vein and infrahepatic vena cava was performed also in the saline-ice bath. After the recipient liver was removed, the donor liver was implanted in the orthotopic position by connecting the suprahepatic vena cava with a running suture, inserting cuffs into the infrahepatic vena cava and the portal vein, and splint tube into the bile duct. The anhepatic phase was estimated to be 25 min for all recipients. ORLT was performed without artery reconstruction.

Experimental design

A total number of 128 rats were randomly divided into 4 groups, 32 for each. 1) Control group, the donor livers were flushed through the portal veins with physiological saline containing heparin only before harvested. 2) IP group, before the donor livers were harvested, the portal vein and hepatic artery were interrupted for 10 min, and the blood flow was restored for 10 min, then the liver was treated as control group. 3) Adenosine group, the donor livers were flushed through the portal vein with physiological saline containing heparin and adenosine (10 mmol/L) only before harvested. 4) N ω -nitro-L-arginine methyl ester (NAME) group, the donor livers were treated as IP group, but NAME (10 mmol/L), an NO synthesis inhibitor, was included in flushing solution. For each group, half of animals were used to investigate the one-week survival rate of recipients, and the remaining animals were for sample collection of blood from infrahepatic vena cava and hepatic tissue after 2 hours of reperfusion.

Determination of liver function and survival

Serum alanine transaminase (ALT) was measured using an automated analyzer (BECKMAN CX7, Beckman Instruments, Fullerton, CA). Survival of recipients was observed for 7 days after operation.

Determination of serum NO

Values of circulating nitrate and nitrite were determined to reflect serum NO level. Serum was separated by centrifugation and stored at -70 °C before use. Nitrite was measured after enzymatic conversion by nitrate reductase using the Griess reaction, as described by Schmidt^[12]. Values obtained represented the sum of serum nitrite and nitrate.

Determination of serum TNF

Serum was separated by centrifugation, and concentration of serum TNF was measured by radioimmunoassay. The TNF standard (100 μ l, Sigma, ST. Louis, MO. USA) and the serum samples (100 μ l) were added separately to appropriate tubes. Two hundred μ l of the 0 ng/ml TNF standard was added to each non-specific binding tube. All tubes were added 100 μ l of ¹²⁵I-TNF reagent (Sigma, ST. Louis, MO. USA). TNF antiserum (100 μ l) was also added to each tube, except the nonspecific binding tubes. Incubation was done at 4 °C for 24 hours following gentle agitation for 2-3 seconds. With 500 μ l of precipitating reagent added, the tubes were vortexed immediately, and incubated for 20 minutes at room temperature (-25 °C). All the tubes were centrifuged at 1500 \times g for 25 min, the suspension was dropped out. Radioactivity was read using a gamma counter (262 Factory, Xi' an, Shaanxi, China).

Assay for adenosine from hepatic tissue

Adenosine standard was purchased from Sigma (St. Louis, MO,

USA). High-performance liquid chromatography (HPLC) was performed using a Beckman Gold Nouveau system equipped with a 168 photo-diode-array detector (210 nm; 262 Factory, Xi' an, Shaanxi, China). Satisfactory separation of the marker substances was obtained with a reversed-phase column and eluted at a flow rate of 1 ml/min. Adenosine separation was allowed to precede in a phosphate-buffer solution (331 mmol/L KH₂PO₄, pH 6.24) containing 3.5% CH₃CN and 2.3 mmol/L *t*-butylamine (TBA). Lyophilized liver tissue was homogenized in 0.5 ml of 0.42 mol/L perchloric acid and incubated for 20 min at 4 °C. The supernatant was separated by centrifugation at 3 000 rpm for 10 min at 0.5 °C, and neutralized with 85 μ l/200 μ l NaOH. After 5 min of centrifugation at 3 000 rpm, 20 μ l of the supernatant was subjected to HPLC.

Histopathologic examination

Liver samples were fixed in 10% neutral buffered formalin, embedded in paraffin. Sections of 5 μ m in thickness were prepared, stained with hematoxylin and eosin, and observed under a light microscope.

Statistics

All statistical computations were performed using SPSS software (version 10.0 for Windows 98; SPSS, Inc., Chicago, Illinois). The *P* values less than 0.05 were considered statistically significant.

RESULTS

Animal survival

The survival rates of these four groups are shown in Figure 1. Most of the recipients died within 3 days after liver transplantation. The survival rate at day 7 was higher in IP group (87.5%, 7 of 8) and adenosine group (87.5%, 7 of 8) than that in control group (37.5%, 3 of 8) and NAME group (25%, 2 of 8, *P*<0.05, Figure 1).

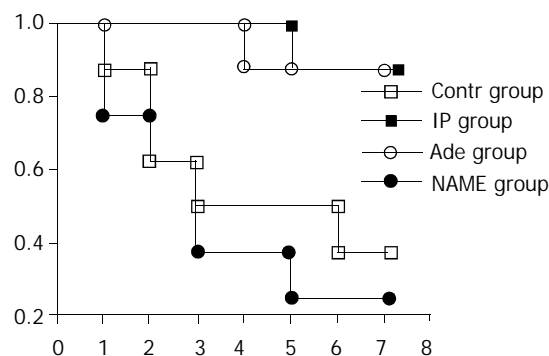


Figure 1 Survival of recipients in different groups. The donor livers were treated respectively as described in Materials and Methods, and the recipients were divided into control (Contr group), IP (IP group), adenosine (Ade group), and NAME-treated groups. The 7-day survival rate was 37.5% (3/8) and 25% (2/8), respectively, in the control group and NAME group, compared with 87.5% (7/8) in both the IP group and adenosine group (*P*<0.05). The survival curves were calculated using Kaplan-meier's methods.

Liver function

The serum ALT values in control group (588 \pm 58 U/L) were significantly higher as compared to those in IP group (287 \pm 82 U/L) (*P*<0.001). Meanwhile, administration of adenosine also reduced the level of serum ALT (357 \pm 93 U/L) as compared to that in control group (*P*<0.001). However, with administration of NAME, the response in ALT level to IP was abrogated (634 \pm 65 U/L, *P*>0.05, Figure 2).

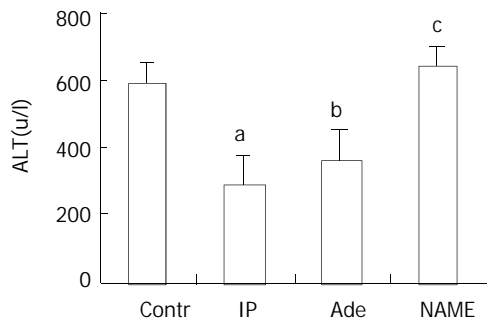


Figure 2 Values of serum ALT in different groups of recipients at 2 hours after ORLT. The ALT levels in control group and NAME group increased significantly compared with IP group and adenosine group. ^a*P* and ^b*P*<0.001, ^c*P*>0.05 vs. control group. The values were expressed as means \pm SD.

Serum TNF and NO level

TNF concentration in serum was measured 2 hours after ORLT as described previously^[5,6]. In IP group (1.15 \pm 0.23 ng/ml) and adenosine group (1.14 \pm 0.27 ng/ml), it was significantly lower compared to that in control group (1.59 \pm 0.35 ng/ml, *P*<0.01). The level in NAME group (1.71 \pm 0.23 ng/ml) was as high as that in control group (*P*>0.05, Figure 3).

Concentrations of NO were shown to be 32.96 \pm 6.10 μ mol/L, 29.14 \pm 6.49 μ mol/L in IP and adenosine groups, respectively, which were significantly higher than that in control group (15.44 \pm 2.99 μ mol/L, *P*<0.001). The value of the recipients in NAME group was 13.74 \pm 3.11 μ mol/L, which was similar to that in control group (*P*>0.05, Figure 4).

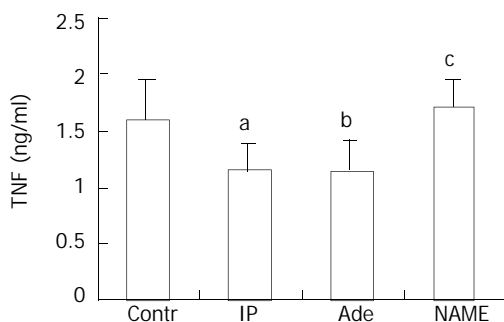


Figure 3 Serum TNF levels measured at 2 hours after ORLT in different recipient groups. In control and NAME groups, the concentrations of serum TNF were elevated significantly as compared to those in IP and adenosine groups. ^a*P* and ^b*P*<0.01, ^c*P*>0.05 vs. control group. Values were expressed as means \pm SD.

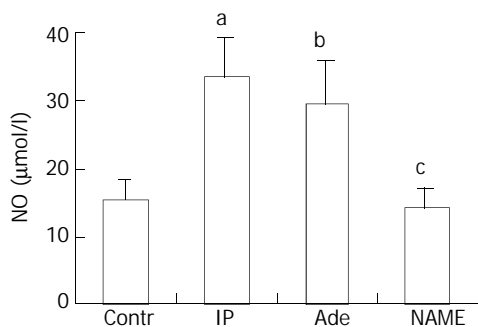


Figure 4 NO levels in serum at 2 hours after ORLT. When the donor livers were pretreated with IP or adenosine, the serum NO levels were elevated significantly. When IP-treatment followed by administration with NAME, the serum NO concentration was as low as that in control group. ^a*P* and ^b*P*<0.001, ^c*P*>0.05 vs. control group. Values were expressed as means \pm SD.

Adenosine in hepatic tissue

Figure 5 shows the levels of hepatic adenosine at 2 hours after ORLT in liver grafts. Concentrations of tissue adenosine were 7.22 \pm 1.83 mol/g, 5.68 \pm 1.32 mol/g, and 5.56 \pm 1.19 mol/g in liver grafts pretreated with IP, adenosine and IP+NAME, respectively, which were higher than that in the reference liver grafts (3.69 \pm 0.54 μ mol per gram of dry liver tissue, *P*<0.05). Animal survival and liver function were improved after adenosine administration. The protective effect of IP was abrogated in NAME group, though the content of adenosine in the tissue also increased.

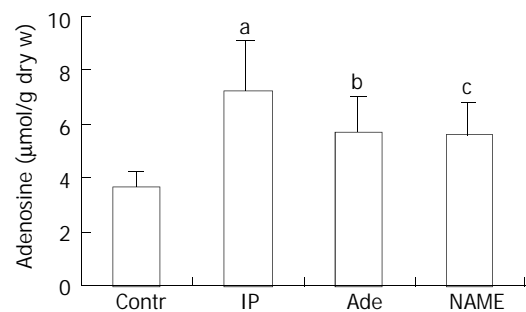


Figure 5 Adenosine concentrations in liver tissues at 2 hours after ORLT. When the donor livers were pretreated with IP or adenosine, or even the IP-treatment followed NAME, the adenosine levels in dry hepatic tissue were elevated as compared to that in control group. ^a*P*, ^b*P* and ^c*P*<0.05 vs. control group. Results were expressed as means \pm SD.

Histopathologic examination

Hepatocyte swelling and ballooning were observed in tissues from the control and NAME groups. No identifiable morphological alterations or only minor changes were found in IP and adenosine groups (data not shown).

DISCUSSION

The ORLT model, established in 1973 by Lee *et al.*^[13], has received wide acceptance in the study of liver transplantation. IP is a procedure originally described during heart transplantation. A brief ischemia treatment followed by reperfusion has been shown to be able to decrease infarct size after subsequent prolonged I/R^[8,14,15]. IP has been found to be protective during transplantation of several organs including brain, intestine and skeletal muscle^[16-18]. In liver, IP was found to reduce tissue damages and mortality after warm ischemia and cold ischemic storage^[5, 19].

In the present study, The harvested livers were preserved in saline for 100 min at 4 °C and the anhepatic phase was selected for 25 minutes, poor outcomes of recipients in control group were observed, and the survival rate 7 days after operation was 37.5% (3/8). In IP group, ALT level was reduced markedly and the survival rate was significantly elevated (87.5%, 7 of 8). The protective effect of IP was further indicated by the morphologic parameters presented.

The effects of a long anhepatic phase on the graft were associated with an endotoxin-like syndrome induced by the prolonged congestion of internal organs. Endotoxemia has been shown to be one of the processes causative for early graft dysfunction^[20,21]. This was most probably associated with Kupffer cell activation by splanchnic endotoxin accumulation and release during intestinal congestion/reperfusion^[22,23]. During the ORLT with a long anhepatic phase, Kupffer cells were shown to be directly responsible for overproduction of TNF, causing endotoxicosis-like syndrome^[24]. The cytotoxic effects of TNF are associated with activation of phospholipase

A₂, release of ceramide, formation of reactive oxygen intermediate (ROI) and promotion of cell apoptosis. However, it is not known whether the protective effect of IP in this study was associated with TNF.

The definite mechanism underlying IP is not clear, and there are several explanations about its protective effects. According to some authors, the protective effects were not attributed to blood flow alterations^[25,26]. However, the IP protective effect was associated to certain substances produced by ischemic tissue against injury^[4]. On the contrary, another study indicated that IP could improve blood flow, and decrease hepatic vascular resistance of liver grafts preserved in cold storage^[10], and this was probably related to some potential mediators such as NO and adenosine.

NO was reported to exert a protective effect through inhibiting endothelin synthesis^[27], and the upregulating effect of adenosine NO release in endothelial cells was also documented^[28]. During ischemia, adenosine is rapidly formed from adenosine triphosphate and reaches high concentrations. Enhanced adenosine level might in turn induce NO synthesis through the activation of adenosine A₂ receptors^[27]. The functions of the two mediators might lead to an improvement in graft blood flow and accordingly improve liver function. Since the ROIs are known to cause cell injury by promoting the peroxidation of lipids and proteins in cell membranes, it is possible that the antioxidant action of NO might also be involved in the protective effect of IP.

In the present study, the concentrations of NO in serum and adenosine in hepatic tissues of IP group were significantly higher than those in control group. In contrast, the level of serum TNF was greatly reduced after IP treatment. Furthermore, the protective effect of IP was also achieved by administration of adenosine before the donor livers were harvested. Our results showed NAME had negative effects on the protective effect of IP and suppressed NO synthesis, indicating that, in the absence of NO, adenosine was unable to develop protective effects. IP might exert its protective role by inducing the production of NO.

In summary, the data presented suggest that an elevated adenosine level can induce the generation of NO under IP, conferring protection to liver grafts and recipients. IP may be an important approach to reduce the transplantation risk resulted from preservation/reperfusion injuries. Further studies are needed for further understanding of the underlying mechanisms.

REFERENCES

- 1 **Lemasters JJ**, Thurman RG. Reperfusion injury after liver preservation for transplantation. *Annu Rev Pharmacol Toxicol* 1997; **37**: 327-338
- 2 **Ploeg RJ**, D' Alessandro AM, Knechtle SJ, Stegall MD, Pirsch JD, Hoffmann RM, Sasaki T, Sollinger HW, Belzer FO, Kalayoglu M. Risk factors for primary dysfunction after liver transplantation—a multivariate analysis. *Transplantation* 1993; **55**: 807-813
- 3 **Strasberg SM**, Howard TK, Molmenti EP, Hertl M. Selecting the donor liver: risk factors for poor function after orthotopic liver transplantation. *Hepatology* 1994; **20**(4Pt1): 829-838
- 4 **Yin DP**, Sankary HN, Chong AS, Ma LL, Shen J, Foster P, Williams JW. Protective effect of ischemic preconditioning on liver preservation-reperfusion injury in rats. *Transplantation* 1998; **66**: 152-157
- 5 **Urata K**, Nguyen B, Brault A, Lavoie J, Rocheleau B, Huet PM. Decreased survival in rat liver transplantation with extended cold preservation: role of portal vein clamping time. *Hepatology* 1998; **28**: 366-373
- 6 **Lumsden AB**, Henderson JM, Kutner MH. Endotoxin levels measured by a chromogenic assay in portal, hepatic and peripheral venous blood in patients with cirrhosis. *Hepatology* 1988; **8**: 232-236
- 7 **Fernandez ED**, Flohe S, Siemers F, Nau M, Ackermann M, Ruwe M, Schade FU. Endotoxin tolerance protects against local hepatic ischemia/reperfusion injury in the rat. *J Endotoxin Res* 2000; **6**: 321-328
- 8 **Murry CE**, Jennings RB, Reimer KA. Preconditioning with ischemia: a delay of lethal cell injury in ischemic myocardium. *Circulation* 1986; **74**: 1124-1136
- 9 **Arai M**, Thurman RG, Lemasters JJ. Contribution of adenosine A(2) receptors and cyclic adenosine monophosphate to protective ischemic preconditioning of sinusoidal endothelial cells against Storage/Reperfusion injury in rat livers. *Hepatology* 2000; **32**: 297-302
- 10 **Ricciardi R**, Schaffer BK, Kim RD, Shah SA, Donohue SE, Wheeler SM, Quarfordt SH, Callery MP, Meyers WC, Chari RS. Protective effects of ischemic preconditioning on the cold-preserved liver are tyrosine kinase dependent. *Transplantation* 2001; **72**: 406-412
- 11 **Kamada N**, Calne RY. A surgical experience with five hundred thirty liver transplants in the rat. *Surgery* 1983; **93**(1Pt1): 64-69
- 12 **Moshage H**, Kok B, Huizenga JR, Jansen PL. Nitrite and nitrate determinations in plasma: a critical evaluation. *Clin Chem* 1995; **41**(6Pt1): 892-896
- 13 **Lee S**, Charters AC, Chandler JG, Orloff MJ. A technique for orthotopic liver transplantation in the rat. *Transplantation* 1973; **16**: 664-669
- 14 **Martin HB**, Walter CL. Preconditioning: an endogenous defense against the insult of myocardial ischemia. *Anesth Analg* 1996; **83**: 639-645
- 15 **Schwarz ER**, Whyte WS, Kloner RA. Ischemic preconditioning. *Curr Opin Cardiol* 1997; **12**: 475-481
- 16 **Heurteaux C**, Lauritzen I, Widmann C, Lazdunski M. Essential role of adenosine, adenosine A1 receptors, and ATP-sensitive K⁺ channels in cerebral ischemic preconditioning. *Proc Natl Acad Sci U S A* 1995; **92**: 4666-4670
- 17 **Schroeder CA Jr**, Lee HT, Shah PM, Babu SC, Thompson CI, Belloni FL. Preconditioning with ischemia or adenosine protects skeletal muscle from ischemic tissue reperfusion injury. *J Surg Res* 1996; **63**: 29-34
- 18 **Hotter G**, Closa D, Prados M, Fernandez-Cruz L, Prats N, Gelpi E, Rosello-Catafau J. Intestinal preconditioning is mediated by a transient increase in nitric oxide. *Biochem Biophys Res Commun* 1996; **222**: 27-32
- 19 **Arai M**, Thurman RG, Lemasters JJ. Ischemic preconditioning of rat livers against cold storage-reperfusion injury: role of nonparenchymal cells and the phenomenon of heterologous preconditioning. *Liver Transpl* 2001; **7**: 292-299
- 20 **Clavien PA**, Harvey PR, Strasberg SM. Preservation and reperfusion injuries in liver allografts. An overview and synthesis of current studies. *Transplantation* 1992; **53**: 957-978
- 21 **Zipfel A**, Schenk M, You MS, Lauchart W, Bode C, Viebahn R. Endotoxemia in organ donors: graft function following liver transplantation. *Transpl Int* 2000; **13**(Suppl 1): S286-287
- 22 **Maring JK**, Klompaker IJ, Zwaveling JH, van Der Meer J, Limburg PC, Slooff MJ. Endotoxins and cytokines during liver transplantation: changes in plasma levels and effects on clinical outcome. *Liver Transpl* 2000; **6**: 480-488
- 23 **Miyata T**, Yokoyama I, Todo S, Tzakis A, Selby R, Starzl TE. Endotoxaemia, pulmonary complications, and thrombocytopenia in liver transplantation. *Lancet* 1989; **2**: 189-191
- 24 **Urata K**, Brault A, Rocheleau B, Huet PM. Role of Kupffer cells in the survival after rat liver transplantation with long portal vein clamping times. *Transpl Int* 2000; **13**: 420-427
- 25 **Cohen MV**, Liu GS, Downey JM. Preconditioning causes improved wall motion as well as smaller infarcts after transient coronary occlusion in rabbits. *Circulation* 1991; **84**: 341-349
- 26 **Peralta C**, Hotter G, Closa D, Gelpi E, Bulbena O, Rosello-Catafau J. Protective effect of preconditioning on the injury associated to hepatic ischemia-reperfusion in the rat: role of nitric oxide and adenosine. *Hepatology* 1997; **25**: 934-937
- 27 **Peralta C**, Hotter G, Closa D, Prats N, Xaus C, Gelpi E, Rosello-Catafau J. The protective role of adenosine in inducing nitric oxide synthesis in rat liver ischemia preconditioning is mediated by activation of adenosine A2 receptors. *Hepatology* 1999; **29**: 126-132
- 28 **Smits P**, Williams SB, Lipson DE, Banitt P, Rongen GA, Creager MA. Endothelial release of nitric oxide contributes to the vasodilator effect of adenosine in humans. *Circulation* 1995; **92**: 2135-2141

Effects of cytokines on carbon tetrachloride-induced hepatic fibrogenesis in rats

Li-Juan Zhang, Jie-Ping Yu, Dan Li, Yue-Hong Huang, Zhi-Xin Chen, Xiao-Zhong Wang

Li-Juan Zhang, Jie-Ping Yu, Department of Gastroenterology, Renmin Hospital, Wuhan University Medical School, Wuhan 430060, Hubei Province, China

Dan Li, Yue-Hong Huang, Zhi-Xin Chen, Xiao-Zhong Wang, Department of Gastroenterology, Union Hospital of Fujian Medical University, Fuzhou 350001, Fujian Province, China

Supported by Science and Technology fund of Fujian Province, No. 2003D05

Correspondence to: Xiao-Zhong Wang, Department of Gastroenterology, Union Hospital of Fujian Medical University, Fuzhou 350001, Fujian Province, China. drwangxz@pub6.fz.fj.cn

Telephone: +86-591-3357896-8482

Received: 2003-06-16 **Accepted:** 2003-07-24

Abstract

AIM: To observe the possible effects of transforming growth factor (TGF) β_1 , interleukin (IL)-6, tumor-necrosis factor (TNF) α and IL-10 on experimental rat hepatic fibrosis.

METHODS: One hundred SD rats were divided randomly into the three groups. Control group received intraperitoneal injection of saline (2 ml·kg⁻¹), twice a week. Fibrogenesis group was injected intraperitoneally with 50% carbon tetrachloride (CCl₄) (2 ml·kg⁻¹) twice a week. Fibrosis-intervention group was given IL-10 at a dose of 4 μ g·kg⁻¹ 20 minutes before CCl₄ administration from the third week. At the fifth, seventh, and ninth weeks, 7 to 10 rats in each group were sacrificed to collect serum. Levels of TGF- β_1 , TNF- α , IL-6 and IL-10 were determined by enzyme-linked immunosorbent assay (ELISA). The liver tissues were taken for routine histological examination.

RESULTS: Hepatic fibrosis was developed with the injection of CCl₄. Values of the circulating TGF β_1 , TNF α , IL-6 and IL-10 in the control group were 25.49±5.56 ng·L⁻¹, 15.18±3.83 ng·L⁻¹, 63.64±13.03 ng·L⁻¹ and 132.90±12.13 ng·L⁻¹, respectively. Their levels in the CCl₄-intoxication group were 31.13±6.41 ng·L⁻¹, 18.91±5.31 ng·L⁻¹, 89.08±25.39 ng·L⁻¹ and 57.63±18.88 ng·L⁻¹, respectively, and those in the IL-10-intervention group were 26.11±5.32 ng·L⁻¹, 13.99±1.86 ng·L⁻¹, 74.71±21.15 ng·L⁻¹ and 88.19±20.81 ng·L⁻¹, respectively. A gradual increase was observed in the levels of TGF β_1 , TNF α and IL-6 during hepatic fibrogenesis. These changes were partially reversed by simultaneous administration of IL-10. The histological parameters, characterized by CCl₄-intoxification, also seemed to be improved with IL-10 treatment, the collagen production was reduced at the ninth week and the histological activity index was decreased from 7.9±1.2 to 4.7±0.9.

CONCLUSION: TGF β_1 , TNF α and IL-6 may play important roles during CCl₄-induced hepatic fibrogenesis, and IL-10 may counterbalance their effects.

Zhang LJ, Yu JP, Li D, Huang YH, Chen ZX, Wang XZ. Effects of cytokines on carbon tetrachloride-induced hepatic fibrogenesis in rats. *World J Gastroenterol* 2004; 10(1): 77-81
<http://www.wjgnet.com/1007-9327/10/77.asp>

INTRODUCTION

Hepatic fibrosis is a common process of chronic liver injuries, characterized by increased deposition and altered composition of extracellular matrix (ECM)^[1-3]. Its final stage is cirrhosis, with the liver architecture distorted by collagen bands and formation of islands of regenerating parenchymal cells^[4,5]. Advanced fibrosis and cirrhosis are generally considered irreversible conditions. Many of the cellular mechanisms have been associated to hepatic fibrosis. Cytokines are soluble autocrine and paracrine mediators^[6]. Expression of several cytokines has been described in human liver diseases and experimental liver injuries. Carbon tetrachloride (CCl₄) is a hepatotoxin, causing liver necrosis, fibrosis and cirrhosis when administered sequentially. Hepatotoxicity is thought to involve two phases^[7]. First, CCl₄ is metabolized by cytochrome P450 in hepatocytes, giving rise to highly reactive trichloromethyl radicals. Second, inflammatory responses caused by CCl₄ play an important role. In the latter process, some hepatic cells, including Kupffer cells (KCs), hepatic stellate cells (HSCs) and sinusoidal endothelial cells (SECs), are activated to secrete cytokines which mediate the liver fibrogenesis. Several functions have been attributed to cytokines, including activation of HSCs, modulating expression and deposition of matrix proteins and regulating the regeneration of hepatocytes. Therefore, resolution of liver fibrosis could be associated with the downregulation of inflammatory responses mediated by cytokines^[8,9]. Among the cytokines, transforming growth factor (TGF) β_1 is associated to the activation of HSC and the following production of ECM^[10]. Tumor-necrosis factor (TNF) α and interleukin (IL)-6 are considered major hepatotoxicity mediators in several experimental models of liver injuries^[11]. IL-10 can modulate the inflammatory response and alleviate hepatotoxicity^[12]. In the present study, levels of circulating TGF β_1 , TNF- α , IL-6 and IL-10 were measured to investigate their possible roles during CCl₄-induced hepatic fibrogenesis in rats.

MATERIALS AND METHODS

Animals

One hundred SD rats, weighing 140 to 180 g, were divided randomly into control ($n=24$), fibrogenesis ($n=40$) and fibrosis-intervention groups ($n=36$). All rats were bred under routine conditions (room temperature, 22 °C±2 °C; humidity, 55%±5%; light, 12 hrs per day; drinking tap water and eating in any time; animal feed was provided by BK Company in Shanghai, China). The control rats were injected intraperitoneally with saline at a dose of 2 ml·kg⁻¹, twice a week. The rats in the other groups received intraperitoneal injection of 50% CCl₄ (2 ml·kg⁻¹), twice a week, as described previously^[13]. From the third week, the rats in intervention group were given intraperitoneally IL-10 (4 μ g·kg⁻¹, dissolved in saline) 20 minutes before CCl₄ administration, as proposed by Nelson *et al*^[14]. All injections were performed at Monday and Thursday, with their body weights determined before each injection. In the fifth week, 3 rats in the fibrogenesis group and 2 in the intervention group died. In the seventh week, 8 and 4 animals

in these two groups died. In the ninth week, 10 and 6 died. At this time point, 3 rats in the control group also died. In the fifth, seventh and ninth weeks, 7 to 10 rats in each group were sacrificed to collect plasma from the common carotid artery and their liver samples.

Histological examination

The formalin-fixed liver tissues were embedded in paraffin. Sections were stained with hematoxylin and eosin (HE) and examined under a light microscope independently by two pathologists. Stages of fibrosis were assessed using a semi-quantitative score method as described previously. Histological activity index (HAI) was evaluated using a numerical system proposed by Knodell *et al*^[15].

Enzyme-linked immunosorbent assay (ELISA)

Serum was collected by centrifugation at 4 °C and frozen till use. The levels of TGF- β_1 , TNF- α , IL-6 and IL-10 were measured by ELISA using the kits following the manufacture's instructions (Endogen Company, USA). Briefly, diluted serum samples were added in duplicate to 96-well plates coated with antibody and incubated at 37 °C for 2 hours. After each well was washed five times with washing buffer, peroxidase-labeled secondary antibody was added to each well and the plate was incubated at 37 °C for 1 hour. After each well was washed in a similar manner, the plate was incubated with tetramethylbenzidine at room temperature for 20 minutes. The reaction was stopped by adding 1 N sulfuric acid. Optical density was measured at 450 nm using a spectrophotometric reader. Sample concentration was accessed by a standard curve.

Statistical analysis

All data were expressed as $\bar{x} \pm s$, *t* test was used for comparison between groups. *P* values less than 0.05 were regarded as statistically significance.

RESULTS

Animal model

Liver fibrosis, as shown histologically, became remarkable during the treatment with CCl₄. In the fifth week, steatosis and ballooning degeneration were obvious. In the seventh week, the collagen fibers increased and began to extend to the parenchyma. In the ninth week, complete fibrous septa were seen and psedolobular structures were also present occasionally. In the IL-10-intervention group, the CCl₄-caused alterations as described above seemed to be markedly alleviated, with no evident changes observed in the fifth week, less profound steatosis and necrosis noted in the seventh week, and only early-stage fibrosis found in the ninth week. HAI decreased from 7.9 ± 1.2 in the fibrogenesis group to 4.7 ± 0.9 in the IL-10-intervention group ($P < 0.05$) (Figures 1-5).

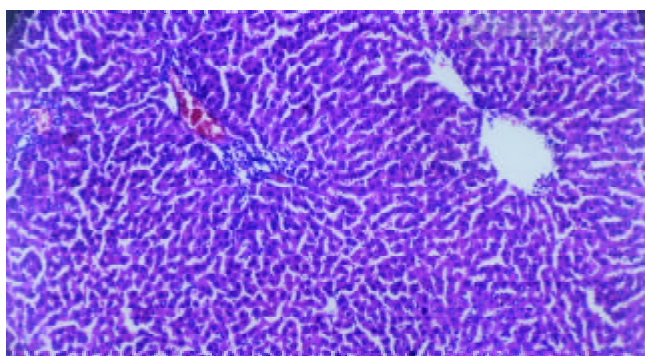


Figure 1 Liver of normal rat (H-E staining, $\times 100$).

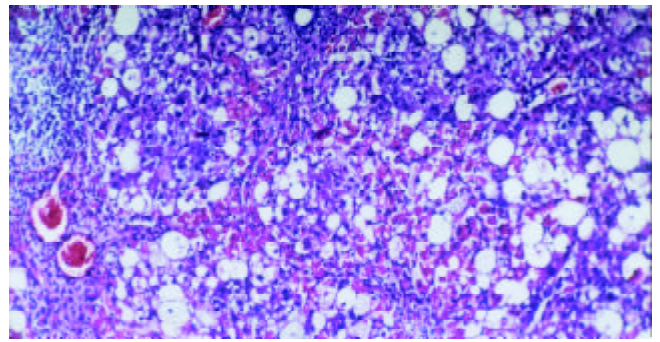


Figure 2 Liver of rats in group C (the fifth week, H-E staining, $\times 100$).

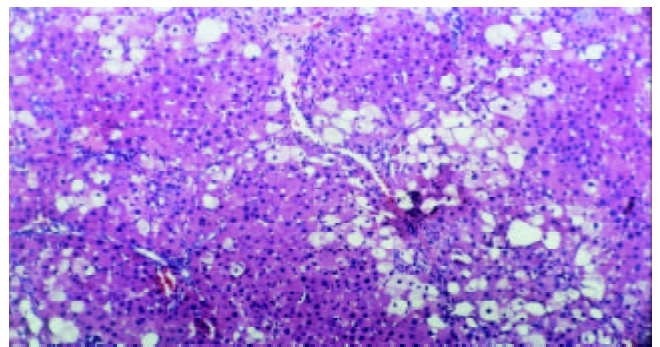


Figure 3 Liver of rats in group C (the seventh week, H-E staining, $\times 100$).

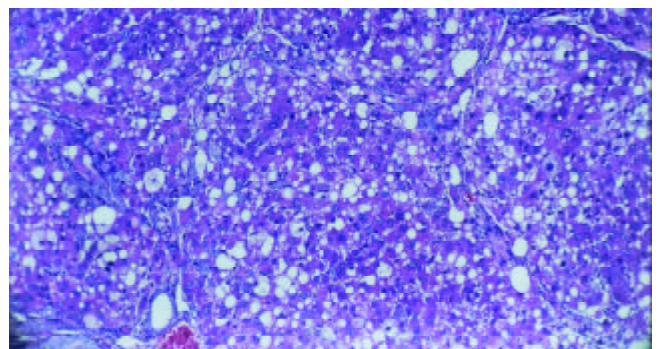


Figure 4 Liver of rats in group C (the ninth week, H-E staining, $\times 100$).

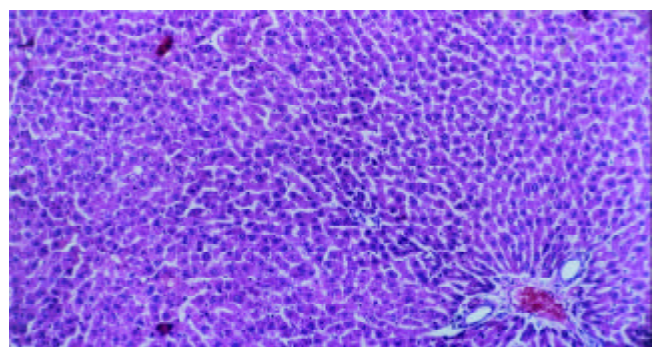


Figure 5 Liver of rats in group E (the ninth week, H-E staining, $\times 100$).

Serum levels of TGF β_1 , TNF- α , IL-6 and IL-10

As shown in Figure 6, the level of circulating IL-10 was lower in fibrogenesis group than in the control group ($P < 0.05$). The levels of TGF- β_1 , TNF- α and IL-6 in were higher in

fibrogenesis group than in the control group ($P < 0.05$). However, values of these three cytokines were significantly reduced after the intervention treatment with IL-10 ($P < 0.05$), being similar to the levels in the control group ($P > 0.05$). Therefore, serum concentrations of TGF- β_1 , IL-6 and TNF- α were increased during CCl₄-caused hepatic fibrogenesis.

Table 1 Concentrations of TGF- β_1 , TNF- α , IL-6 and IL-10 in sera from different groups (ng·L⁻¹)

Groups	Numbers of rats	TGF- β_1	TNF- α	IL-6	IL-10
Control (N)	21	25.49±5.56	15.18±3.83	63.64±13.03	132.90±12.13 ^{a,b}
Fibrogenesis (C)	30	31.13±6.41	18.91±5.31	89.08±25.39	57.63±18.88
IL-10-intervention (E)	30	26.11±5.32	13.99±1.86	74.71±21.15	88.19±20.81 ^c

^a $P < 0.05$ vs. C, ^b $P < 0.05$ vs. E, ^c $P > 0.05$ vs. C.

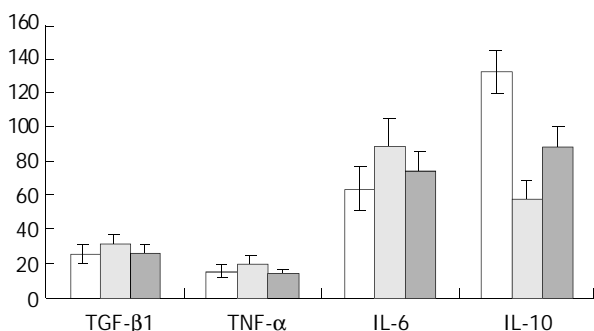


Figure 6 Levels of TGF- β_1 , TNF- α , IL-6 and IL-10 in serum from control, fibrogenesis and IL-10-intervention groups.

As shown in Figures 7-10, concentrations of TGF- β_1 , TNF- α and IL-6 were gradually increased along with CCl₄-intoxication ($P < 0.05$). These changes were partially reversed by the treatment with IL-10, particularly in the ninth week ($P < 0.05$).

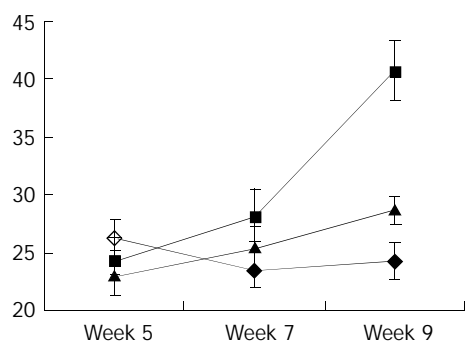


Figure 7 Levels of TGF- β_1 in serum from control (◆-), fibrogenesis (■-) and IL-10-intervention groups (▲-).

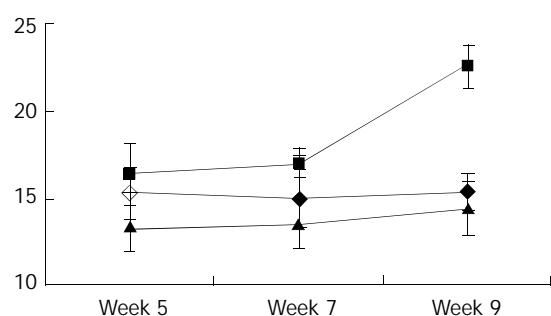


Figure 8 Levels of TNF- α in serum from control (◆-), fibrogenesis (■-) and IL-10-intervention groups (▲-).

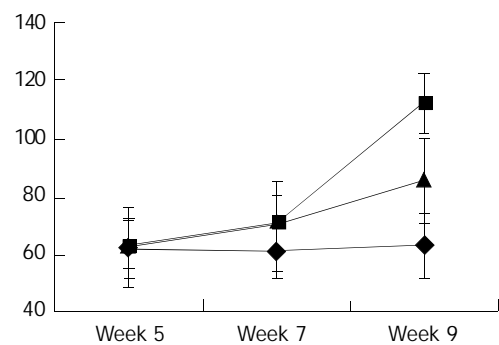


Figure 9 Levels of IL-6 in serum from control (◆-), fibrogenesis (■-) and IL-10-intervention groups (▲-).

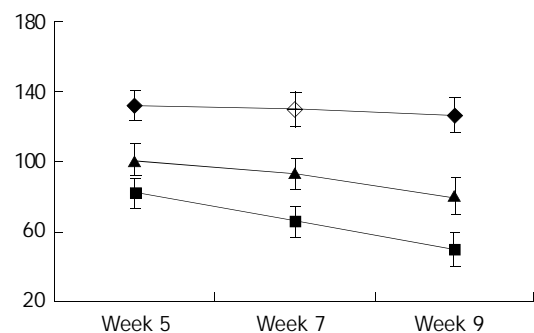


Figure 10 Levels of IL-10 in serum from control (◆-), fibrogenesis (■-) and IL-10-intervention groups (▲-).

DISCUSSION

Previous data have shown that rats chronically exposed to CCl₄ were resistant to cirrhosis. In rats, exposed to CCl₄ for 8 to 12 weeks could result in localized fibrosis^[16]. In the present study, fully developed hepatic fibrosis was observed in the rats after 9 weeks of CCl₄ intoxication. The contents of cytokines in serum were found to vary during the process. Cytokines constitute a complex network involved in the regulation of inflammatory responses and homeostasis of organ functions. Following liver injury, a wound healing process evolves, including proliferation of surrounding hepatocytes, proliferation and differentiation of stem cells, and conversion of parasinusoidal cells into activated HSCs capable of driving the accumulation of ECM. If the injuries were persistent or the wound healing process was aberrant, the final phenotype might be a fibrotic, dysfunctional liver^[8]. A number of cytokines and growth factors could augment or inhibit the fibrotic response to injuries^[18]. Accumulating data indicate that HSCs are the major source of fibrillar and non-fibrillar matrix proteins during hepatic fibrogenesis. When activated, HSCs could proliferate and transform to a myofibroblast-like phenotype, expressing α -smooth muscle actin (α -SMA) and collagen types I, III and IV, fibronectin and proteoglycan^[19]. It has been found several cytokines play roles by acting on HSC, and among them, TGF- β_1 is one of the most important cytokines involved in the fibrotic and cirrhotic transformation of the liver^[20-23]. After a fibrogenic injury, expression of three forms of TGF- β is greatly upregulated in HSCs. It was reported that administration of TGF- β_1 *in vivo* induced an inflammatory reaction, and knock-out of TGF- β_1 gene resulted in widespread inflammatory diseases. Therefore, TGF- β_1 may have a pro-inflammatory effect.

TNF- α was originally identified as a circulating factor that resulted in remarkable hemorrhage and necrosis of tumors when administered to tumor-bearing mice. It has been implicated in a number of liver diseases and is an important mediator of

many physiological conditions. Several evidences suggest that TNF- α is among the most crucial components in the early signaling pathways leading to regeneration. However, there has been evidence that TNF- α is a primary endogenous factor mediating acute inflammatory conditions such as endotoxic shock. It appears that inhibition of the TNF- α effect might have a broader clinical application value than expected previously^[26]. In several animal models of immune-mediated liver injury or hepatotoxin sensitization, TNF- α administration could lead to hepatocyte apoptosis and liver failure^[27]. Besides its modulation effect on ECM production, TNF- α has been considered a mediator of cell injuries in liver caused by alcoholism, reperfusion, primary graft nonfunctional, graft rejection and endotoxic insult^[28,29]. TNF- α is expressed by both infiltrating inflammatory cells and hepatocytes in chronic liver injuries, and it has been proposed to play an important role during tissue damage^[30]. Our data provide a further evidence for the role during hepatic fibrosis.

The role of IL-6 during chronic liver injuries and fibrogenesis remains to be clarified. Some reports provided evidences for an important role of IL-6 in reducing CCl₄-induced acute and chronic liver injury and fibrosis^[31-33]. However, some other data showed that the serum level of IL-6 was associated with hepatic necroinflammatory activity in patients with chronic hepatitis and cirrhosis^[34,35]. Our results support the latter view. Animal experiments showed that IL-6 was associated to activated HSCs during acute and chronic injuries, indicating that IL-6 is a responsive element to liver injuries. Moreover, CCl₄-induced expression of TGF- β ₁ and hepatocyte growth factor in liver was shown to be associated with the serum level of IL-6. Thus, IL-6 might be vitally involved in fibrotic changes, partly by modulating intrahepatic expression of other cytokines^[36,37].

Recent studies have suggested a protective role of IL-10 during liver transplantation and experimental liver injuries induced by galactosamine and lipopolysaccharide^[38]. However, the mechanism of the protective effects is not fully understood. IL-10 is a potent anti-inflammatory cytokine that inhibits the synthesis of pro-inflammatory cytokines by T helper type 1 cells. It is produced locally in the liver and acts in an autocrine or a paracrine manner. Previous reports indicated that IL-10 had some role in remodeling ECM^[39,40]. IL-10 was shown to downregulate the synthesis of collagen type I and to upregulate expression of metalloproteinase. It could also play an antifibrogenic role by downregulating the profibrogenic cytokines including TGF- β ₁ and TNF- α ^[11,41]. Nelson *et al* treated 24 patients with chronic hepatitis C using IL-10, and found that IL-10 administration resulted in reduction of the serum ALT level, partial resolution of the hepatic inflammation and alleviation of the fibrosis^[14]. IL-10 may be useful in the treatment of chronic liver diseases regarding the prevention of advanced fibrosis and cirrhosis^[42].

REFERENCES

- Friedman SL.** Molecular mechanisms of hepatic fibrosis and principles of therapy. *J Gastroenterol* 1997; **32**: 424-430
- Du WD, Zhang YE, Zhai WR, Zhou XM.** Dynamic changes of type I, III and IV collagen synthesis and distribution of collagen-producing cells in carbon tetrachloride-induced rat liver fibrosis. *World J Gastroenterol* 1999; **5**: 397-403
- Wang JY, Guo JS, Yang CQ.** Expression of exogenous rat collagenase *in vitro* and in a rat model of liver fibrosis. *World J Gastroenterol* 2002; **8**: 901-907
- Friedman SL.** Seminars in medicine of the Beth Israel Hospital, Boston. The cellular basis of hepatic fibrosis: Mechanisms and treatment strategies. *N Engl J Med* 1993; **328**: 1828-1835
- Abdel-Aziz G, Lebeau G, Rescan PY, Clement B, Rissel M, Deugnier Y, Campion JP, Guillouzo A.** Reversibility of hepatic fibrosis in experimentally induced cholestasis in rat. *Am J Pathol* 1990; **137**: 1333-1342
- Nakamura T, Sakata R, Ueno T, Sata M, Ueno H.** Inhibition of transforming growth factor β prevents progression of liver fibrosis and enhances hepatocyte regeneration in dimethylnitrosamine-treated rats. *Hepatology* 2000; **32**: 247-255
- Shi J, Aisaki K, Ikawa Y, Wake K.** Evidence of hepatocyte apoptosis in rat liver after the administration of carbon tetrachloride. *Am J Pathol* 1998; **153**: 515-525
- Friedman SL.** Cytokines and fibrogenesis. *Semin Liver Dis* 1999; **19**: 129-140
- Koziel JK.** Cytokines in viral hepatitis. *Semin Liver Dis* 1999; **19**: 157-169
- Bissell DM, Roulot D, George J.** Transforming growth factor β and the liver. *Hepatology* 2001; **34**: 859-867
- Kovalovich K, DeAngelis RA, Li W, Furth EE, Ciliberto G, Taub R.** Increased toxin-induced liver injury and fibrosis in interleukin-6-deficient mice. *Hepatology* 2000; **31**: 149-159
- Yoshidome H, Kato A, Edwards MJ, Lentsch AB.** Interleukin-10 suppresses hepatic ischemia/reperfusion injury in mice: implications of a central role for nuclear factor κ B. *Hepatology* 1999; **30**: 203-208
- Morrow JD, Awad JA, Kato T, Takahashi K, Badr KF, Robert LJ 2nd, Burk KF.** Formation of novel non-cyclooxygenase-derived prostanoids (F2-isoprostanines) in carbon tetrachloride hepatotoxicity. An animal model of lipid peroxidation. *J Clin Invest* 1992; **90**: 2502-2507
- Nelson DR, Lauwers GY, Lau JY, Davis G.** Interleukin 10 treatment reduces fibrosis in patients with chronic hepatitis C: a pilot trial of interferon nonresponders. *Gastroenterology* 2000; **118**: 655-660
- Knodell RG, Ishak KG, Black WC, Chen TS, Craig R, Kaplowitz N, Kiernan TW, Wollman J.** Formulation and application of a numerical scoring system for assessing histological activity in asymptomatic chronic active hepatitis. *Hepatology* 1981; **1**: 431-435
- Tsukamoto H, Matsuoka M, French SW.** Experimental models of hepatic fibrosis: a review. *Semin Liver Dis* 1990; **10**: 56-65
- Missale G, Ferrari C, Fiaccadori F.** Cytokine mediators in acute inflammation and chronic course of viral hepatitis. *Ann Ital Med Int* 1995; **10**: 14-18
- Davis BH, Kresina TF.** Hepatic fibrogenesis. *Clin Lab Med* 1996; **16**: 361-375
- Iredale JP, Benyon RC, Pickering J, McCullen M, Northrop M, Pawley S, Hovell C, Arthur MJ.** Mechanisms of spontaneous resolution of rat liver fibrosis. Hepatic stellate cell apoptosis and reduced hepatic expression of metalloproteinase inhibitors. *J Clin Invest* 1998; **102**: 538-549
- Nakamura T, Sakata R, Ueno T, Sata M, Ueno H.** Inhibition of transforming growth factor β prevents progression of liver fibrosis and enhances hepatocyte regeneration in dimethylnitrosamine-treated rats. *Hepatology* 2000; **32**: 247-255
- Dooley S, Delvoux B, Lahme B, Mangasser-Stephan K, Gressner AM.** Modulation of transforming growth factor β response and signaling during transdifferentiation of rat hepatic stellate cells to myofibroblasts. *Hepatology* 2000; **31**: 1094-1106
- Garcia-Trevijano ER, Iraburu MJ, Fontana L, Dominguez-Rosales JA, Auster A, Covarrubias-Pinedo A, Rojkind M.** Transforming growth factor β 1 induces the expression of α 1 (I) procollagen mRNA by a hydrogen peroxide-C/EBP β -dependent mechanism in rat hepatic stellate cells. *Hepatology* 1999; **29**: 960-970
- Si XH, Yang LJ.** Extraction and purification of TGF β and its effect on the induction of apoptosis of hepatocytes. *World J Gastroenterol* 2001; **7**: 527-531
- Bissell DM, Wang SS, Jarnagin WR, Roll FJ.** Cell-specific expression of transforming growth factor-beta in rat liver. Evidence for autocrine regulation of hepatocyte proliferation. *J Clin Invest* 1995; **96**: 447-455
- Knittel T, Janneck T, Muller T, Fellmer P, Ramadori G.** Transforming growth factor beta 1-regulated gene expression of Ito cells. *Hepatology* 1996; **24**: 352-360
- Llorent L, Richaud-Patin Y, Alcocer-Castillejos N, Ruiz-soto R, Mercado MA, Orozco H, Gamboa-Dominguez A, Alcocer-Varela J.** Cytokine gene expression in cirrhotic and non-cirrhotic human liver. *J Hepatol* 1996; **24**: 555-563
- Zhang GL, Wang YH, Teng HL, Lin ZB.** Effects of aminoguanidine

- on nitric oxide production induced by inflammatory cytokines and endotoxin in cultured rat hepatocytes. *World J Gastroenterol* 2001; **7**: 331-334
- 28 **Roberts RA**, James NH, Cosulich SC. The role of protein kinase B and mitogen-activated protein kinase in epidermal growth factor and tumor necrosis factor α -mediated rat hepatocyte survival and apoptosis. *Hepatology* 2000; **31**: 420-427
- 29 **Crespo J**, Cayon A, Fernandez-Gil P, Hernandez-Guerra M, Mayorga M, Dominguez-Diez A, Fernandez-Escalante JC, Pons-Romero F. Gene expression of tumor necrosis factor α and TNF-receptors, p55 and p75, in nonalcoholic steatohepatitis patients. *Hepatology* 2001; **34**: 1158-1163
- 30 **Hernandez-munoz I**, de La Torre P, Sanchez-Alcazar JA, Garcia I, Santiago E, Munoz-Yague MT, Solis-Herruzo JA. Tumor necrosis factor α inhibits collagen $\alpha 1$ (I) gene expression in rat hepatic stellate cells through a G protein. *Gastroenterology* 1997; **113**: 625-640
- 31 **Selzner M**, Camargo CA, Clavien PA. Ischemia impairs liver regeneration after major tissue loss in rodents: protective effects of interleukin-6. *Hepatology* 1999; **30**: 469-475
- 32 **Sakamoto T**, Liu Z, Murase N, Ezure T, Yokomuro S, Poli V, Demetris AJ. Mitosis and apoptosis in the liver of interleukin-6-deficient mice after partial hepatectomy. *Hepatology* 1999; **29**: 403-411
- 33 **Peters M**, Blinn G, Jostock T, Schirmacher P, Meyer zum Buschenfelde KH, Galle PR, Rose-John S. Combined interleukin-6 and soluble interleukin-6 receptor accelerates murine liver regeneration. *Gastroenterol* 2000; **119**: 1663-1671
- 34 **Wang JY**, Wang XL, Lin P. Detection of serum TNF- α , IFN- γ , IL-6 and IL-8 in patients with hepatitis B. *World J Gastroenterol* 1999; **5**: 38-40
- 35 **Zhen Z**, Zhou JY, Liu JX, Hong ZJ, Pei X. Relationship between IL-6 and IL-6R and their pathogenicity in viral hepatitis. *Shijie Huaren Xiaohua Zazhi* 2000; **8**: 1434-1435
- 36 **Cressman DE**, Greenbaum LE, DeAngelis RA, Ciliberto G, Furth EE, Poli V, Taub R. Liver failure and defective hepatocyte regeneration in interleukin-6-deficient mice. *Science* 1996; **274**: 1379-1383
- 37 **Natsume M**, Tsuji H, Harada A, Akiyama M, Yano T, Ishikura H, Nakanishi I, Matsushima K, Kaneko S, Mukaid N. Attenuated liver fibrosis and depressed serum albumin levels in carbon tetrachloride-treated IL-6-deficient mice. *J Leukoc Biol* 1999; **66**: 601-608
- 38 **Louis H**, Le Moine O, Peny MO, Gulbis B, Nisol F, Goldman M, Deviere J. Hepatoprotective role of interleukin 10 in galactosamine/lipopolysaccharide mouse liver injury. *Gastroenterology* 1997; **112**: 935-942
- 39 **Reitamo S**, Remitz A, Tamai K, Uitto J. Interleukin-10 modulates type 1 collagen and matrix metalloprotease gene expression in cultured human skin fibroblasts. *J Clin Invest* 1994; **94**: 2489-2492
- 40 **Thompson K**, Maltby J, Fallowfield J, McAulay M, Millward-Sadler H, Sheron N. Interleukin-10 expression and function in experimental murine liver inflammation and fibrosis. *Hepatology* 1998; **28**: 1597-1606
- 41 **Louis H**, Van Laethem JL, Wu W, Quertinmont E, Degraef C, Van den Berg K, Demols A, Goldman M, Le Moine O, Geerts A, Deviere J. Interleukin-10 controls neutrophilic infiltration, hepatocyte proliferation, and liver fibrosis induced by carbon tetrachloride in mice. *Hepatology* 1998; **28**: 1607-1615
- 42 **Wang XZ**, Zhang LJ, Li D, Huang YH, Chen ZX, Li B. Effects of transmitters and interleukin-10 on rat hepatic fibrosis induced by CCl₄. *World J Gastroenterol* 2003; **9**: 539-543

Edited by Su Q and Wang XL

HBV cccDNA in patients' sera as an indicator for HBV reactivation and an early signal of liver damage

Ying Chen, Johnny Sze, Ming-Liang He

Ying Chen, Johnny Sze, Ming-Liang He, The Institute of Molecular Biology, The University of Hong Kong, Hong Kong, China

Supported by CRCG grant from the University of Hong Kong, CERG grant from University Grant Council of Hong Kong, and Research Fund from Science and Technology Commission of Shanghai, China

Correspondence to: Dr. Ming-Liang He, The Institute of Molecular Biology, The University of Hong Kong, Hong Kong, China. mlhe@hkucc.hku.hk

Telephone: +852-2299-0758 **Fax:** +852-2817-1006

Received: 2003-08-02 **Accepted:** 2003-10-22

Abstract

AIM: To evaluate the covalently closed circle DNA (cccDNA) level of hepatitis B virus (HBV) in patients' liver and sera.

METHODS: HBV DNA was isolated from patients' liver biopsies and sera. A sensitive real-time PCR method, which is capable of differentiation of HBV viral genomic DNA and cccDNA, was used to quantify the total HBV cccDNA. The total HBV viral DNA was quantitated by real-time PCR using a HBV diagnostic kit (PG Biotech, LTD, Shenzhen, China) described previously.

RESULTS: For the first time, we measured the level of HBV DNA and cccDNA isolated from ten HBV patients' liver biopsies and sera. In the liver biopsies, cccDNA was detected from all the biopsy samples. The copy number of cccDNA ranged from 0.03 to 173.1 per cell, the copy number of total HBV DNA ranged from 0.08 to 3 717 per cell. The ratio of total HBV DNA to cccDNA ranged from 1 to 3 406. In the sera, cccDNA was only detected from six samples whereas HBV viral DNA was detected from all ten samples. The ratio of cccDNA to total HBV DNA ranged from 0 to 1.77%. To further investigate the reason why cccDNA could only be detected in some patients' sera, we performed longitudinal studies. The cccDNA was detected from the patients' sera with HBV reactivation but not from the patients' sera without HBV reactivation. The level of cccDNA in the sera was correlated with ALT and viral load in the HBV reactivation patients.

CONCLUSION: HBV cccDNA is actively transcribed and replicated in some patients' hepatocytes, which is reflected by a high ratio of HBV total DNA vs cccDNA. Detection of cccDNA in the liver biopsy will provide an end-point for the anti-HBV therapy. The occurrence of cccDNA in the sera is an early signal of liver damage, which may be another important clinical parameter.

Chen Y, Sze J, He ML. HBV cccDNA in patients' sera as an indicator for HBV reactivation and an early signal of liver damage. *World J Gastroenterol* 2004; 10(1): 82-85

<http://www.wjgnet.com/1007-9327/10/82.asp>

INTRODUCTION

Chronic hepatitis B Virus (HBV) infection is one of the most

common diseases leading to a high morbidity and mortality due to the development of liver failure, liver cirrhosis (LC) and hepatocellular carcinomas (HCC)^[3-28]. There are over 300 million people suffering from HBV infection worldwide, and more than 10% of Chinese are HBV carriers^[3,5,14]. Infection by hepatitis B virus causes complicated biochemical, immunological and histological changes in host^[7-9,11,16,18,23,24,27]. Viral kinetic studies have shown that the viral load goes through a complex series of stages during anti-HBV chemotherapy^[21,22,29-31]. The HBV reactivation often occurs after cessation of anti-HBV treatment^[22,24,32], which is reflected by the increases of hepatitis B e antigen (HBeAg) and DNA levels in serum. Clinically, this may manifest as hepatitis, hepatic failure, and even death. Despite its clinical importance, there are few data on the incidence and risk factors of hepatitis due to HBV reactivation after chemotherapy. In particular, the relationship of various HBV virological parameters and HBV reactivation is unclear.

HBV covalently closed circular (ccc) DNA is a critical intracellular replicative intermediate, which acts as the template for transcription of viral RNAs serving either as viral pregenome RNAs, or as mRNAs coding for the multifunctional polymerase, core, X and envelope (S) proteins^[25,26]. All the HBV proteins play crucial roles in HBV gene transcription, replication, viral packaging and recycling. Due to lack of proofreading functions of polymerase, HBV goes through a fast mutagenesis and creates drug resistant strains^[13,17,19,24,26,29,32], which contributes to the viral cccDNA pool. Because cccDNA of HBV is resource of new HBV viruses and resistance to drug treatment, it is believed that cccDNA is the major reason for HBV reactivation after stopping the anti-HBV therapy^[21,24,25]. Monitoring of HBV viral load, antigens, mutations and cccDNA levels will therefore provide a direct indication of HBV activity in the body^[12,13,15,17-21, 28-32].

We previously developed a sensitive method to quantify HBV cccDNA, which has been successfully used to determine the amount of HBV cccDNA isolated from liver biopsy^[1]. Here we report that HBV cccDNA can be detected both in liver biopsy and in patients' sera. The sera cccDNA level is correlated with ALT and viral load in HBV reactivation patients, but cannot be detected in patients' sera without HBV reactivation. Our results indicate that the occurrence of cccDNA is an early signal of liver damage, which may be another important clinical parameter.

MATERIALS AND METHODS

cccDNA standard^[1,2]

A plasmid containing Chinese HBV genome (pHBV-adr) was a gift from Professor Yuan Wang. The supercoiled plasmid (cccDNA) was isolated by CsCl purification. The cccDNA concentration was determined by measurement of OD260 and verified by agarose gel electrophoresis. The copy number was determined by its molecular weight.

HBV viral DNA preparation^[1]

HBV viral DNA was extracted from either 200 ul of patients' sera or weighed liver biopsies using a QIAamp DNA blood or

tissue mini kit (QIAGEN, Hilden, Germany) according to the manufacturer's instructions.

Quantification of HBV cccDNA using real-time PCR

HBV cccDNA quantification was performed as described previously^[1,2], with minor modifications. Briefly, a pair of primers (forward primer: 5'-ACTCTTGGACTCBCAGCAATG-3', reverse primer: 5'-CTTTATACGGGTCAATGTCCA-3'), which can specifically amplify a DNA fragment from HBV cccDNA but not viral genomic DNA by PCR, were used for real-time PCR. In a typical real-time PCR reaction, 250 nM of the probe (5'-FAM-CTTTTTCACCTCTGCCTAATCATCTCWTGTTCA-TAMRA-3') and 900 nM of the two PCR primers were used. For total HBV quantification, PCR amplification was performed with an HBV DNA diagnostic kit (PG Biotech. Ltd, China) using ABI 7900HT sequence detection system. The PCR program consisted of an initial denaturing step at 95 °C for 10 min, followed by 40 amplification cycles at 95 °C for 15 sec and at 61.5 °C for 1 min.

Patient samples

The patients were treated with chemotherapy at Queen Mary Hospital, Hong Kong, from January 2000 to May 2002. In accordance with the standard protocols, all the patients who received chemotherapy were screened for HBsAg, HBsAb, human immunodeficiency virus antibody (HIV Ab), and HBV DNA by PCR and hepatitis C antibody (anti-HCV), with commercially-available enzyme immunoassays (Abbott Laboratories, Chicago, IL, USA). HBcAb was tested by RIA (Corab; Abbott). For all HBsAg positive patients, further serological testing for hepatitis B e antigen (HBeAg), hepatitis B e antibody (HBeAb) and serum HBV DNA was performed by PCR, and chemotherapy was administered with lamivudine. All HbsAg-positive recipients were tested at 2-week intervals for liver function (including serum alanine aminotransferase, serum albumin and bilirubin) and serum HBV DNA during chemotherapy. Hepatitis serology (HBsAg, HBeAg, HBeAb, HBV DNA by PCR, and HCV RNA by RT-PCR) was performed on the serum collected preceding and during the events whenever there was any clinical suspicion of liver damage due to hepatitis B infection. The occurrences of hepatic events (acute hepatitis, chronic hepatitis, anicteric and icteric hepatitis, hepatic failure) were recorded. Hepatitis was defined as a more than three-fold elevation of serum aminotransferase above the upper limit of normal, on two consecutive determinations at least five days apart. HBV reactivation was defined to occur when preceded or accompanied by an elevation of serum HBV DNA to more

than ten times that of the pre-exacerbation baseline, or when the serum HBV DNA turned from negative to positive, or when the HBsAg became positive and remained so for two consecutive readings five days apart.

All serum and biopsy samples were stored at -70 °C. All patients who developed post-chemotherapy hepatitis due to HBV reactivation were treated with lamivudine 100 mg once daily.

RESULTS

HBV cccDNA existed in all patients' hepatocytes but only in a subset of patients' sera

To elucidate the cccDNA status in HBV patients, we quantified the cccDNA and total HBV DNA level in the liver biopsies. The total DNA was isolated from weighed liver biopsies and quantified with an HBV diagnostic kit by real-time PCR. The HBV cccDNA was also measured by real-time PCR. HBV cccDNA was detected in all the HBV patients' liver biopsies. The copy number of cccDNA in patients' hepatocytes ranged from 0.05 to 168 copies per cell, which is consistent with the estimates from Southern blot data^[10]. The copy number of total HBV DNA in patients' hepatocytes ranged from 0.08 to over 3 000 copies per cell. The ratio of cccDNA to total HBV DNA ranged from 1 to 3 406 (Table 1), indicating that cccDNA in patients' hepatocytes had active replication and relative silent status.

To investigate whether cccDNA could be released into sera due to liver inflammation and necrosis, viral DNA was isolated from patients' sera and quantified by real-time PCR. Interestingly, cccDNA could only be detected in a subset of patients' sera, while HBV DNA was detected in all the patients' sera. The copy number of viral load ranged from 5.4×10^5 to 1.8×10^{11} per ml while the copy number of cccDNA ranged from undetectable level (less than 1 000 copies/ml^[11]) to 3.1×10^7 per ml. The ratio of cccDNA to total viral DNA ranged from 0 to 1.77%. There was no correlation between the copy number of cccDNA and total viral DNA in the randomized patients (Table 1).

cccDNA is an early signal of liver damage

To investigate the medical significance of cccDNA in sera, longitudinal studies were performed. Patients with or without HBV reactivation during lamivudine treatment were chosen for this study. The patients' sera were collected every two weeks and HBV DNA was isolated for quantification of HBV cccDNA and total HBV DNA. According to our results, HBV cccDNA was not detectable by sensitive real-time PCR in patients without HBV reactivation (data not shown), but was detectable in patients with HBV reactivation (Figures

Table 1 HBV cccDNA in patients' hepatocytes and sera

Patients	HBV DNA in the Biopsies (copy/cell)			HBV DNA in the sera (copy/ml)		
	cccDNA	HBV DNA ^a	HBV/ccc ^b	cccDNA	HBV DNA ^c	ccc/HBV ^d
1	2.05	195.5	98.7	3.4×10^6	4.8×10^{10}	0.01%
2	0.03	0.17	5.8	UN	6.6×10^7	--
3	173.1	799.5	4.6	3.1×10^5	6.0×10^{10}	0.001%
4	0.16	8.13	51.7	UN	1.9×10^7	--
5	0.03	0.08	2.8	UN	5.4×10^5	--
6	16.02	17.4	1.1	2.4×10^6	5.3×10^8	0.46%
7	18.03	3717	206	3.1×10^7	1.8×10^{11}	0.02%
8	0.79	13.1	16.5	UN	2.4×10^{10}	--
9	0.05	153.3	3406	2.8×10^5	3.0×10^9	0.01%
10	2.06	16.4	8	2.7×10^6	7.5×10^8	1.77%

^aThe total HBV copies per cell in the patients' liver biopsies; ^bThe ratio of total HBV DNA to cccDNA in the patients' liver biopsy; ^cThe total HBV copies per ml of the patients' sera; ^dThe ratio of cccDNA to total HBV DNA in the patients' sera. UN, undetectable.

1A and 1B). The cccDNA level was correlated with viral load (Figures 1A and 1B), which occurred earlier than ALT. Before the ALT value increased, both the cccDNA level and viral load rose to a high level. Once the ALT value increased, the cccDNA level dropped rapidly. These results suggest that patients whose sera contain cccDNA are at a high risk of HBV reactivation, and that HBV cccDNA develops in the sera earlier than ALT elevation.

Our results suggest that serum cccDNA level may be an important parameter for anti-HBV treatment, and that a low level of cccDNA in hepatocytes should be an end point of anti-HBV treatment.

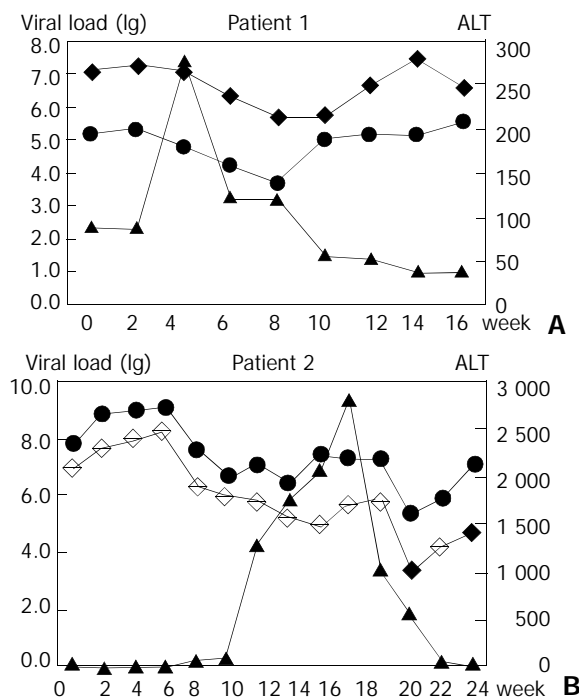


Figure 1 Kinetics of cccDNA in HBV reactivation patients. The copy numbers of total HBV and cccDNA were determined by real-time PCR. The cccDNA level was parallel to the total viral load both in the patients 1 and 2; the cccDNA level increased before ALT rose. Diamond: HBV viral load, dot: cccDNA, triangle: ALT.

DISCUSSION

Little information is available about HBV cccDNA and its activities *in vivo* due to the difficulty of differentiation of HBV cccDNA and viral genomic DNA, although a lot of work has been done on the HBV viral kinetics^[21,22,29-31]. In the hepatitis B virus life cycle, cccDNA serves as templates for viral gene transcription and replication in hepatocytes^[25,26]. It has been shown that cccDNA is the major reason for HBV reactivation after cessation of anti-HBV treatment^[24,25]. Therefore, quantification of HBV cccDNA will provide useful information for the end-point of anti-HBV therapy.

In this paper, we first report the quantitative data on HBV cccDNA in patients' liver biopsy and sera. We previously established a quantitative real-time PCR method which can specifically differentiate HBV viral genomic DNA and cccDNA^[1]. This sensitive method provided us an opportunity to investigate HBV cccDNA status in the liver biopsy and patients' sera. Our data indicated that cccDNA in the patients' liver might have two status: active and relative silent status. This was reflected by the ratio of viral total DNA to cccDNA. To our surprising, HBV cccDNA was also detected in a part of patients' sera. The release of cccDNA of hepatitis B virus to the sera might be the consequence of liver damages, such as

liver inflammation, necrosis. Longitudinal studies revealed that the release of cccDNA to the sera was an early signal of liver damage, which is correlated with ALT and viral load in HBV reactivated patients. Therefore, measurement of the cccDNA level in the liver may provide an end-point of anti-HBV therapy, and detection of the cccDNA level in the sera may provide a better guidance to protect patients from HBV reactivation.

Because this is the first time to provide the quantitative data on HBV cccDNA status, and the limitation of patient samples, more clinic studies on the cccDNA kinetics are required to better understand HBV biology and provide a better guidance for the anti-HBV treatment.

ACKNOWLEDGMENTS

We wish to thank Prof. Y. Wang (Inst. Of Biochemistry, Shanghai, China) for providing HBV genomic clone pHBV, and Dr. G. Lau (Queen Mary Hospital, Hong Kong) for the liver biopsies and sera.

REFERENCES

- 1 He ML, Wu J, Chen Y, Lin MC, Lau GK, Kung HF. A new and sensitive method for the quantification of HBV cccDNA by real-time PCR. *Biochem Biophys Res Commun* 2002; **295**: 1102-1107
- 2 Chen Y, Du Y, Wu Y, Chan CP, Tan YQ, Kung HF, He ML. Inhibition of hepatitis B virus (HBV) replication by stably-expressed shRNA. *Biochem Biophys Res Commun* 2003; **311**: 398-404
- 3 Wang FS. Current status and prospects of studies on human genetic alleles associated with hepatitis B virus infection. *World J Gastroenterol* 2003; **9**: 641-644
- 4 Tang ZY. Hepatocellular carcinoma-cause, treatment and metastasis. *World J Gastroenterol* 2001; **7**: 445-454
- 5 Cai RL, Meng W, Lu HY, Lin WY, Jiang F, Shen FM. Segregation analysis of hepatocellular carcinoma in a moderately high-incidence area of East China. *World J Gastroenterol* 2003; **9**: 2428-2432
- 6 Cao ZX, Chen XP, Wu ZD. Effects of splenectomy in patients with cirrhosis undergoing hepatic resection for hepatocellular carcinoma. *World J Gastroenterol* 2003; **9**: 2460-2463
- 7 Wang NS, Wu ZL, Zhang YE, Guo MY, Liao LT. Role of hepatitis B virus infection in pathogenesis of IgA nephropathy. *World J Gastroenterol* 2003; **9**: 2004-2008
- 8 Wang JY, Liu P. Abnormal immunity and gene mutation in patients with severe hepatitis-B. *World J Gastroenterol* 2003; **9**: 2009-2011
- 9 Wang KX, Peng JL, Wang XF, Tian Y, Wang J, Li CP. Detection of T lymphocyte subsets and mIL-2R on surface of PBMC in patients with hepatitis B. *World J Gastroenterol* 2003; **9**: 2017-2020
- 10 Li XM, Yang YB, Hou HY, Shi ZJ, Shen HM, Teng BQ, Li AM, Shi MF, Zou L. Interruption of HBV intrauterine transmission: A clinical study. *World J Gastroenterol* 2003; **9**: 1501-1503
- 11 Wu CH, Ouyang EC, Walton C, Promrat K, Forouhar F, Wu GY. Hepatitis B virus infection of transplanted human hepatocytes causes a biochemical and histological hepatitis in immunocompetent rats. *World J Gastroenterol* 2003; **9**: 978-983
- 12 Jaboli MF, Fabbri C, Liva S, Azzaroli F, Nigro G, Giovanelli S, Ferrara F, Miracolo A, Marchetto S, Montagnani M, Colecchia A, Festi D, Reggiani LB, Roda E, Mazzella G. Long-term alpha interferon and lamivudine combination therapy in non-responder patients with anti-HBe-positive chronic hepatitis B: Results of an open, controlled trial. *World J Gastroenterol* 2003; **9**: 1491-1495
- 13 Wang Y, Liu H, Zhou Q, Li X. Analysis of point mutation in site 1896 of HBV precore and its detection in the tissues and serum of HCC patients. *World J Gastroenterol* 2000; **6**: 395-397
- 14 Roussos A, Goritsas C, Pappas T, Spanaki M, Papadaki P, Ferti A. Prevalence of hepatitis B and C markers among refugees in Athens. *World J Gastroenterol* 2003; **9**: 993-995
- 15 Peng XM, Chen XJ, Li JG, Gu L, Huang YS, Gao ZL. Novel assay of competitively differentiated polymerase chain reaction for screening point mutation of hepatitis B virus. *World J Gastroenterol* 2003; **9**: 1743-1746
- 16 Song CZ, Bai ZL, Song CC, Wang QW. Aggregate formation of hepatitis B virus X protein affects cell cycle and apoptosis. *World*

- J Gastroenterol* 2003; **9**: 1521-1524
- 17 **Yang X**, Tang XP, Lei JH, Luo HY, Zhang YH. A novel stop codon mutation in HBsAg gene identified in a hepatitis B virus strain associated with cryptogenic cirrhosis. *World J Gastroenterol* 2003; **9**: 1516-1520
- 18 **Shen LJ**, Zhang HX, Zhang ZJ, Li JY, Chen MQ, Yang WB, Huang R. Detection of HBV, PCNA and GST-pi in hepatocellular carcinoma and chronic liver diseases. *World J Gastroenterol* 2003; **9**: 459-462
- 19 **Yang SS**, Hsu CT, Hu JT, Lai YC, Wu CH. Lamivudine does not increase the efficacy of interferon in the treatment of mutant type chronic viral hepatitis B. *World J Gastroenterol* 2002; **8**: 868-871
- 20 **Zhuang L**, You J, Tang BZ, Ding SY, Yan KH, Peng D, Zhang YM, Zhang L. Preliminary results of Thymosin- α 1 versus interferon- α -treatment in patients with HBeAg negative and serum HBV DNA positive chronic hepatitis B. *World J Gastroenterol* 2001; **7**: 407-410
- 21 **Lewin SR**, Ribeiro RM, Walters T, Lau GK, Bowden S, Locarnini S, Perelson AS. Analysis of hepatitis B viral load decline under potent therapy: complex decay profiles observed. *Hepatology* 2001; **34**: 1012-1020
- 22 **Lau GK**, He ML, Fong DY, Bartholomeusz A, Au WY, Lie AK, Locarnini S, Liang R. Preemptive use of lamivudine reduces hepatitis B exacerbation after allogeneic hematopoietic cell transplantation. *Hepatology* 2002; **36**: 702-709
- 23 **Hou CS**, Wang GQ, Lu SL, Yue B, Li MR, Wang XY, Yu JW. Role of activation-induced cell death in pathogenesis of patients with chronic hepatitis B. *World J Gastroenterol* 2003; **9**: 2356-2358
- 24 **Yokosuka O**, Omata M, Imazeki F, Okuda K, Summers J. Changes of hepatitis B virus DNA in liver and serum caused by recombinant leukocyte interferon treatment: analysis of intrahepatic replicative hepatitis B virus DNA. *Hepatology* 1985; **5**: 728-734
- 25 **Seeger C**, Mason WS. Hepatitis B Virus Biology. *Microb Molec Biol Review* 2000; **64**: 51-58
- 26 **Summers J**, Mason WS. Replication of the genome of a hepatitis B-like virus by reverse transcription of an RNA intermediate. *Cell* 1982; **29**: 403-415
- 27 **Jiang YG**, Wang YM, Liu TH, Liu J. Association between HLA class II gene and susceptibility or resistance to chronic hepatitis B. *World J Gastroenterol* 2003; **9**: 2221-2225
- 28 **Fan CL**, Wei L, Jiang D, Chen HS, Gao Y, Li RB, Wang Y. Spontaneous viral clearance after 6-21 years of hepatitis B and C viruses coinfection in high HBV endemic area. *World J Gastroenterol* 2003; **9**: 2012-2016
- 29 **Gaillard RK**, Barnard J, Lopez V, Hodges P, Bourne E, Johnson L, Allen MI, Condreay P, Miller WH, Condreay LD. Kinetic analysis of wild-type and YMDD mutant hepatitis B virus polymerases and effects of deoxyribonucleotide concentrations on polymerase activity. *Antimicrob Agents Chemother* 2002; **46**: 1005-1013
- 30 **Tsiang M**, Rooney JF, Toole JJ, Gibbs CS. Biphasic clearance kinetics of hepatitis B virus from patients during adefovir dipivoxil therapy. *Hepatology* 1999; **29**: 1863-1869
- 31 **Zeuzem S**, de Man RA, Honkoop P, Roth WK, Schalm SW, Schmidt JM. Dynamics of hepatitis B virus infection *in vivo*. *J Hepatol* 1997; **27**: 431-436
- 32 **Ni YH**, Chang MH, Hsu HY, Chen HL. Long-term follow-up study of core gene deletion mutants in children with chronic hepatitis B virus infection. *Hepatology* 2000; **32**: 124-128

Edited by Wang XL

Expression of TIMP-1 and TIMP-2 in rats with hepatic fibrosis

Qing-He Nie, Guo-Rong Duan, Xin-Dong Luo, Yu-Mei Xie, Hong Luo, Yong-Xing Zhou, Bo-Rong Pan

Qing-He Nie, Guo-Rong Duan, Xin-Dong Luo, Yu-Mei Xie, Hong Luo, Yong-Xing Zhou, Chinese PLA Centre of Diagnosis and Treatment for Infectious Diseases, Tangdu Hospital, Fourth Military Medical University, Xi'an 710038, Shaanxi Province, China
Bo-Rong Pan, Department of Oncology, Xijing Hospital, Fourth Military Medical University, Xi'an 710032, Shaanxi Province, China
Supported by the Postdoctoral Science Foundation of China, No. 1999-10

Correspondence to: Dr. Qing-He Nie, Chinese PLA Centre of Diagnosis and Treatment for Infectious Diseases, Tangdu Hospital, Fourth Military Medical University, Xi'an 710038, Shaanxi Province, China. nieqinghe@hotmail.com

Telephone: +86-29-3377852 **Fax:** +86-29-3537377

Received: 2003-05-13 **Accepted:** 2003-06-02

Abstract

AIM: To investigate the location and expression of TIMP-1 and TIMP-2 in the liver of normal and experimental hepatic fibrosis in rats.

METHODS: The rat models of experimental immunity hepatic fibrosis ($n=20$) were prepared by the means of immunologic attacking with human serum albumin (HSA), and normal rats ($n=10$) served as control group. Both immunohistochemistry and *in situ* hybridization methods were respectively used to detect the TIMP-1 and TIMP-2 mRNA and related antigens in liver. The liver tissue was detected to find out the gene expression of TIMP-1 and TIMP-2 with RT-PCR.

RESULTS: The TIMP-1 and TIMP-2 related antigens in livers of experimental group were expressed in myofibroblasts and fibroblasts (TIMP-1: 482 ± 65 vs 60 ± 20 ; TIMP-2: 336 ± 48 vs 50 ± 19 , $P<0.001$). This was the most obvious in portal area and fibrous septum. The positive signals were located in cytoplasm, not in nucleus. Such distribution and location were confirmed by *situ* hybridization (TIMP-1/*b-actin*: 1.86 ± 0.47 vs 0.36 ± 0.08 ; TIMP-2/*b-actin*: 1.06 ± 0.22 vs 0.36 ± 0.08 , $P<0.001$). The expression of TIMP-1 and TIMP-2 was seen in the liver of normal rats, but the expression level was very low. However, the expression of TIMP-1 and TIMP-2 in the liver of experimental group was obviously high.

CONCLUSION: In the process of hepatic fibrosis, fibroblasts and myofibroblasts are the major cells that express TIMPs. The more serious the hepatic fibrosis is in the injured liver, the higher the level of TIMP-1 and TIMP-2 gene expression.

Nie QH, Duan GR, Luo XD, Xie YM, Luo H, Zhou YX, Pan BR. Expression of TIMP-1 and TIMP-2 in rats with hepatic fibrosis. *World J Gastroenterol* 2004; 10(1): 86-90

<http://www.wjgnet.com/1007-9327/10/86.asp>

INTRODUCTION

Chronic viral hepatitis, alcoholism and schistosomiasis are the most common diseases in China^[1-9]. At present, two main strategies for the treatment of chronic liver diseases are anti-

viral therapies and anti-fibrotic therapies^[10-14]. Hepatic fibrosis is a main pathologic basis of chronic liver diseases, particularly caused by viral hepatitis, and cirrhosis as a severe outcome is the end stage of various chronic liver diseases with increased synthesis and/or inhibition of matrix degradation. Although important progress in hepatic fibrosis has been achieved in the last decades, its mechanism is still debated at present. The formation of hepatic fibrosis is a response to inflammation, but it is interesting that hepatic fibrosis is not found in acute liver injury. It has been proved by the experiment *in vitro* that apoptosis could not be found in inactive hepatic stellate cells (HSC). This may imply that the mechanism of hepatic fibrosis is complicated, and many questions are being explored^[15-23].

Hepatic fibrosis is a pathological process with the overlapped extracellular matrix (ECM) protein. The latest evidence suggests that the change of ECM mainly is regulated by metalloproteinases (MMPs). Hepatic fibrosis is formed because the specific tissue inhibitors of metalloproteinases (TIMPs) inhibit ECM degradation^[24-28]. Which cells can express and produce TIMPs? Until now, there still are different views on the involvement of TIMPs in normal liver tissue and experimental hepatic fibrosis rats. The expression and location of TIMPs antigens and TIMP mRNA are measured in rat livers with mAb and cDNA probes of TIMP-1 and TIMP-2 by immunohistochemical staining, and gene expression of TIMP-1 and TIMP-2 is observed by PCR technique.

MATERIALS AND METHODS

Animal experiments

Forty adult female Wistar rats, weighing 120-150 g (provided by Experimental Animal Centre of Fourth Military Medical University) were employed in the study. The rats were randomly divided into 2 groups. A rat model of hepatic fibrosis was produced by immunological attacking with human serum albumin (HSA), using the method introduced by Wang *et al*^[29]. Anti-mouse monoclonal antibody IgG was purchased from Coulter Co.(France). Twenty healthy female Wistar rats were regarded as control group. Animals survived from the experimental attack were randomly allocated as follows. All rats were injected with 0.5 mL HSA diluted with normal saline (0.5 mL equals to 4 mg HSA) and same quantity of an incomplete Freund's adjuvant (Sigma), once every 14 days for the first two times, then once every 10 days, 2 times. Ten days after the last injection, serum antibody was measured. Positive rats were chosen for experiment through coccygeal vein injection of HSA, twice a week, 2.5 mg for each at the first week, and then gradually 0.5 mg- increase once for each to 4.5 mg, and this dose was maintained for 2 months. All animals were sacrificed under narcosis, and their livers were immediately excised. Part of liver specimen was frozen in liquid nitrogen, part fixed in 40 g/L formaldehyde, the rest was fixed with glutaraldehyde, and investigated with electron microscope.

Immunohistochemical staining of TIMP-1 and TIMP-2

According to the methods previously described^[30-33], the serial paraffin sections of liver samples at 4 μ m thickness were performed for SP immune staining described by streptomycin

Table 1 Sequences of TIMP-1, TIMP-2 and β -actin primers

	Primer	Nucleic acid sections	Position (bp)
TIMP-1	Positive strand	5'-TTCGTGGGGACACCAGAAGTC-3'	482
	Antisense strand	5'-TATCTGGGACCGCAGGGACTG-3'	
β -actin	Positive strand	5'-GGAGAAGATGACCCAGATCA-3'	234
	Antisense strand	5'-GATCTTCATGAGGTAGTCAG-3'	
TIMP-2	Positive strand	5'-GTTTTGCAATGCAGATGTAG-3'	540
	Antisense strand	5'-ATGTCGAGAAACTCCTGCTT-3'	
β -actin	Positive strand	5'-ACCCCACTGAAAAA-3'	120
	Antisense strand	5'-ATCTTCAAACCTCCATGATG-3'	

avidin-peroxidase immunohistochemical kit (Maxim Biological Technology Company, USA). Anti-mouse monoclonal antibodies of TIMP-1 and TIMP-2 were also obtained from Maxim. The sections were deparaffinized and rehydrated. After retrieval of the antigens, nonspecific binding sites were blocked with 100 mL/L normal serum for 20 min. The sections were incubated with monoclonal antibody against TIMP-1 or TIMP-2 at 4 °C overnight, and then with secondary antibody at 37 °C for 30-40 min, avidin-peroxidase at 37 °C for 20 min, and finally with DAB to be colorated for 10 min, and counterstained with hematoxylin, dehydrated with ethanol, rinsed in xylene, and mounted with gum for microscopic examination and photography. To ensure the reliability of the experiment, rabbit serum and phosphate buffer were used instead of monoclonal antibody and secondary antibody, respectively. In addition, 10 healthy liver tissues were selected for control group. The background density of positive cells from 5 microscopic fields at random was measured, and its mean value was used for statistical analysis with SPSS 10.0.

In situ hybridization

The experiment was performed as previously described^[33,34] using *in situ* hybridization kit (Boshide Biological Technology Limited Company, Wuhan, China, No MK1549). Briefly, the serial paraffin sections (thickness 4 μ m) were dried at 80 °C, then deparaffinized by xylene and rehydrated in graded ethanol, acidified in 1 mol/L HCl for 30 min, and blocked in 30 ml/L H₂O₂ 3 mL for 10 min before digestion with proteinase K for 30 min, and then dehydrated with graded ethanol. After prehybridization at 37-40 °C for 2 h, the labeled cDNA probes were denatured at 95 °C for 10 min, then at -20 °C for 10 min, added onto liver tissue sections which had been prehybridized at 37 °C overnight. The sections were washed with 2 \times SSC, 1 \times SSC, and 0.2 \times SSC respectively. Buffer I was added, and then blocking solution was added at room temperature for 20 min, and then rabbit anti-digoxin at 37 °C for 60 min, biotinylated goat anti-rabbit at 37 °C for 30 min, SABC at 37 °C for 30 min, finally DAB was added to develop color. After several washings, the sections were counter-stained with hematoxylin, dehydrated with ethanol, rinsed in xylene, and mounted with gum for microscopic examination and photography. Blank control: TIMP-1 and TIMP-2 cDNA probes for positive hepatic tissues were replaced by prehybridization solution. Negative control: *in situ* hybridization was performed in 10 normal liver tissues. Semi-quantitative results were determined by *in situ* hybridization. (-) as no positive cells, (+) as positive cells <1/3 of all hepatic cells, (++) as positive cells between 1/3-2/3 of all hepatic cells, (+++) as positive cells >2/3 of all hepatic cells in a lobule.

PCR amplification

PCR primers of TIMP-1 were designed according to the whole TIMP-1 cDNA sequence of rats^[35]. The PCR primers of TIMP-1 and TIMP-2 are listed in Table 1.

Total RNA of the liver was extracted with an isolation system (Promega). PCR was performed in 20 μ L reaction volume containing 2 μ L cDNA, 2 μ L 10 \times buffer, 2 μ L (2 mmol/L) 4 \times dNTP, 10 mmol/L primer (2 μ L TIMP-1, 2 μ L β -actin and 2 μ L TIMP-1, 2 μ L β -actin, respectively) and 1U *Taq* DNA polymerase. The samples were subjected to 30 thermal cycles, each consisting of 2 min at 97 °C for pre-denaturation, 30 s at 94 °C for denaturing, 30 s at 56 °C for annealing, 50 s at 72 °C for extension and 7 min at 72 °C for final extension after the last cycle. Ten μ L sample of PCR product was subjected to electrophoresis in 20 g/L agarose gel with TAE buffer at 50 V for 1 h. After stained with ethidium bromide, quantitative analysis was performed. The ratios of TIMP-1/*b-actin* and TIMP-2/*b-actin* were regarded as the expression levels of TIMP-1 and TIMP-2.

Pathologic observation

Some liver sections were stained with hematoxylin and eosin, while other sections for Von Gieson and Masson special staining. The liver samples were also fixed with glutaraldehyde, and examined with electron microscope.

Statistical analysis

Was performed with SPSS 10.0.

RESULTS

Pathologic findings

In liver tissues from rats with hepatic fibrosis, hyperplasia of the lattice fibers and collagenous fibers was observed in portal area and extended outwards. Hyperplasia surrounding the central vein observed was distributed along hepatic sinus and connected each other. The hepatic lobules were encysted and separated by collagen bundles. The normal structure of lobules was destroyed, and pseudolobules formed. Infiltration of inflammatory cells was found around the portal area and central vein. The structure of liver tissues was normal in control.

Under electron microscopy, proliferation of activated hepatic stellate cells (HSC) surrounded by collagen fibers was found in early stage, in which abundant rough endoplasmic reticulum and lipids were present. Eventually, with the deposition of collagen bundles, myofibroblasts formed in portal area, and the deposition of collagens produced a wide compartment. Lots of collagen fibrils resided within the space of Disse. A vast amount of swelling mitochondria and some lipids were detectable in degenerative hepatocytes.

TIMP-1 and TIMP-2 expression and localization

TIMP-1 and TIMP-2 antigens in the liver from experimental rats were detected in myofibroblasts, fibroblasts and vascular endothelial cells predominantly in the portal area and fibrous septum. Expression of TIMP-1 and TIMP-2 exhibited as brown particles in cytoplasm. No positive expression was found in nucleus. There was only a mild positive expression in vascular

endothelial cells of the normal rat liver. Image pattern analysis showed that the expression in the experimental group was much stronger than that in the control group (Table 2, Figure 1), so did the *in situ* hybridization (Figure 2). In order to confirm the specificity of immunohistochemical experiment, the first antibody and second antibody were replaced by at serum and buffer, respectively. Negative results were found in controls, with specific confirming experiment *for in situ* hybridization, and no positive result was found.

Table 2 Expression of TIMP-1 and TIMP-2 related antigens in rat liver

Group	n	TIMP-1	TIMP-2
Experimental group	20	482.50±65.00	336.50±48.32
Normal group	10	59.8±20.31	49.86±18.54

$P < 0.001$.

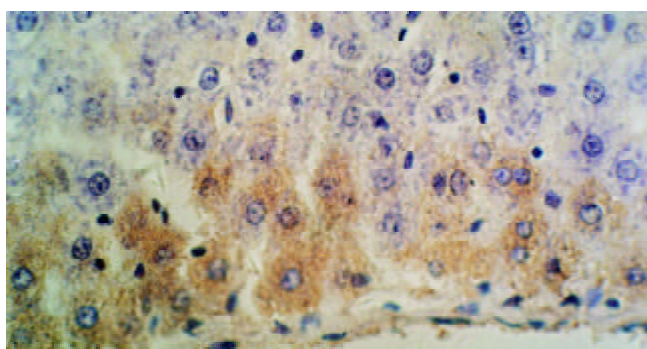


Figure 1 Expression of TIMP-1-related antigens in liver tissue from rats with experimental fibrosis (Immunohistochemical staining ×400).

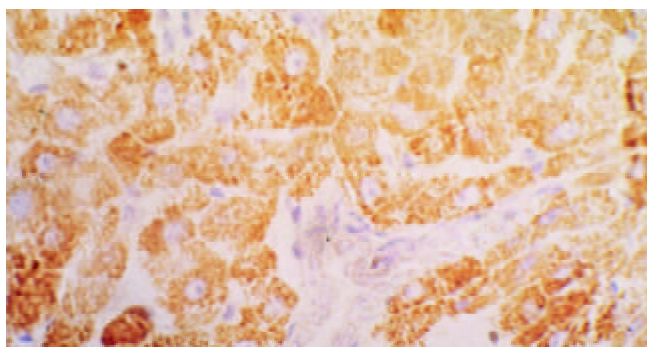


Figure 2 Expression of TIMP-1 mRNA in liver tissue from rats with experimental fibrosis (*in situ* hybridization ×400).

TIMP-1 and TIMP-2 gene expression

The expression of TIMP-1 in the liver of normal rats was strikingly low, while its expression in experimental group was significantly higher than that in the normal group (Table 3).

Table 3 Gene expression of TIMP-1 and TIMP-2 in rat liver

Group	n	TIMP-1/β-actin	TIMP-2/β-actin
Experimental group	20	1.86±0.47	1.06±0.22
Normal group	10	0.36±0.08	0.36±0.08

$P < 0.001$.

DISCUSSION

It is necessary to establish and develop an ideal animal model

of hepatic fibrosis, so as to investigate the etiology or pathogenesis, to explore the effective diagnosis or treatment and to select or evaluate anti-fibrotic medicines. An ideal animal model should be very similar to the characteristics of human disease, with distinct stages of disease and a low mortality. The model should be economically and easily established without difficulty to get the animals.

Researchers began to establish the hepatic fibrosis model of rats with carbon tetrachloride (CCL₄) in 1936, which was an early study on animal model of hepatic fibrosis and cirrhosis. Since it was repeatedly improved, the experimental model has been widely employed. People gradually established various models, such as rat model by bile duct ligation (Zimmermann, 1992), rabbit model with schistosomiasis (Dunn, 1994), rat model by thioacetamide (Okanoue, 1954), *etc.* However, these models with various characteristics are not very ideal to the animal experiment because of their common shortcomings that the hepatic fibrosis lasted shortly and was absorbed spontaneously soon.

In 1966, Paronetto and Popper^[36] have proved that an immune response could induce liver injury. The animals injected repeatedly with the globulin or swine albumin or the serum from swine, bovine or horse developed hepatic fibrosis after 5 weeks, and cirrhosis after 10 weeks. However, the model had a high mortality because of allergic reaction. We studied various models and improved the model developed by Wang *et al*^[29]. The survival rate of rats obviously increased and the fibrosis lasted for more than 363 days when the rats were injected with a small quantity of dexamethasone through its caudal vein soon after the first or secondary attack. The fibrosis was proved pathologically and the formation of fibrosis belonged to the type III allergic reaction induced by the immunocomplex of albumin. Under electron microscopy it was proved that the pathological process stimulated the proliferation of hepatic stellate cells (HSC), which would transform to the myofibroblasts and secrete a large amount of collagens.

At present, it was found that TIMP-1 in the injured liver increased early and obviously, and many researchers thought that TIMP-1 was a very important promoting factor in the process of hepatic fibrosis^[27,32,37], and that it could inhibit MMPs (such as MMP-1) to deposit ECM. Up to now, only TIMP-1 and TIMP-2 were found in liver and TIMP-1 increased more obviously than TIMP-2, and strong expression of TIMP-1 reflected the severity of hepatic fibrosis. With the method of immunohistochemistry, we found that TIMP-1 and TIMP-2 were expressed obviously only in myofibroblasts or fibroblasts of livers from experimental group, mostly in portal area and fibrous septum, while very mildly in vascular endothelial cells of livers from control group. Such a distribution was also shown in the results of *in situ* hybridization.

The results of *in situ* hybridization demonstrated that TIMP-1 mRNA was expressed in hepatocytes and in almost all mesenchymal cells, especially strong in lipocytes of inflammation area of the liver induced by CCL₄ or bile duct ligation model^[38]. Our results indicated that it was strongly expressed only in myofibroblasts, fibroblasts and vascular endothelial cells, mainly in portal area and fibrous septum. The results of immunohistochemistry were similar. Whether the expression difference is due to various models or other causes is still unknown.

From the gene expression levels of TIMP-1 and TIMP-2 we suggested that the more severe the hepatic fibrosis was, the higher the gene expression levels of TIMP-1 and TIMP-2 were, and that the strong expression of TIMP-1 inhibited the degeneration of collagen by MMP-1 and pro MMP-9, and that the expression of TIMP-2 inhibited MMP-2, MMP-9, *etc.* to promote the deposition of ECM. The continuous deposition of collagen fibers in the liver finally resulted in hepatic fibrosis.

The concentrations of TIMP-1 and TIMP-2 in peripheral blood indicated their gene expression levels. Iredale *et al.*^[39] isolated hepatocytes, HSC and Kupffer cells from the liver of experimental hepatic fibrosis model, but failed to find TIMP-1 mRNA in hepatocytes with Northern hybridization in 1997. We detected the expression of TIMP-1 in hepatocytes, HSC and Kupffer cells with PCR technique, and the expression of TIMP-1 was mild in normal rat liver, but strong in fibrotic rat liver. Therefore, further experiments might prove no expression of TIMP-1 in hepatocytes. The strong expression of TIMP-1 in fibroblasts and myofibroblasts of fibrotic liver probably resulted from the activation of HSC. In fact, hepatic fibrosis was essentially a “repair” reaction to chronic liver damage because of the cell-cell interaction mediated by cytokines and the activation of HSC induced by the interaction of mesenchymal cells. The persistence of HSC activation was induced by repeated liver damage. Thus, the activation of HSC was mainly in the pathologic process of hepatic fibrosis^[19,21].

Although TIMP-1 and TIMP-2 were closely related to hepatic fibrosis, study on TIMPs has just begun. Thus far, the mechanism of strong expression of TIMP-1 and TIMP-2 in fibrotic liver is still unknown, and other characteristics of TIMPs are being studied^[40-43]. To enhance the study on TIMPs has become very important for the diagnosis, treatment and pathogenesis of hepatic fibrosis^[44-47].

ACKNOWLEDGEMENT

We acknowledge the advice and help of Prof. Meng-Dong Li.

REFERENCES

- Nie QH, Li MD, Hu DR, Chen GZ. Study on the cause of human protective immunodeficiency after HCV infection. *Shijie Huaren Xiaohua Zazhi* 2000; **8**: 28-30
- Dai YM, Shou ZP, Ni CR, Wang NJ, Zhang SP. Localization of HCV RNA and capsid protein in human hepatocellular carcinoma. *World J Gastroenterol* 2000; **6**: 136-137
- Wang Y, Liu H, Zhou Q, Li X. Analysis of point mutation in site 1896 of HBV precore and its detection in the tissues and serum of HCC patients. *World J Gastroenterol* 2000; **6**: 395-397
- Hu YP, Yao YC, Li JX, Wang XM, Li H, Wang ZH, Lei ZH. The cloning of 3' truncated preS/2S gene from HBV genomic DNA and its expression in transgenic mice. *World J Gastroenterol* 2000; **6**: 734-737
- Wen SJ, Xiang KJ, Huang ZH, Zhou R, Qi XZ. Construction of HBV specific ribozyme and its recombinant with HDV and their cleavage activity *in vitro*. *World J Gastroenterol* 2000; **6**: 377-380
- Nie QH, Li L, Li MD, Hu DR, Zhu YH, Chen GZ. Clinical and immunopathological studies in GBV-B infection. *Shijie Huaren Xiaohua Zazhi* 2000; **8**: 775-781
- Wang FS, Wu ZZ. Current situation in studies of gene therapy for liver cirrhosis and liver fibrosis. *Shijie Huaren Xiaohua Zazhi* 2000; **8**: 371-373
- Wang GQ, Kong XT. Action of cell factor and Decorin in tissue fibrosis. *Shijie Huaren Xiaohua Zazhi* 2000; **8**: 458-460
- Liu F, Wang XM, Liu JX, Wei MX. Relationship between serum TGFβ1 of chronic hepatitis B and hepatic tissue pathology and hepatic fibrosis quantity. *Shijie Huaren Xiaohua Zazhi* 2000; **8**: 528-531
- Yao XX. Diagnosis and treatment of liver fibrosis. *Shijie Huaren Xiaohua Zazhi* 2000; **8**: 681-689
- Albanis E, Friedman SL. Hepatic fibrosis. Pathogenesis and principles of therapy. *Clin Liver Dis* 2001; **5**: 315-334
- Sherker AH, Senosier M, Kermack D. Treatment of transfusion-dependent thalassemic patients infected with hepatitis C virus with interferon alpha-2b and ribavirin. *Hepatology* 2003; **37**: 223
- Han HL, Lang ZW. Changes in serum and histology of patients with chronic hepatitis B after interferon alpha-2b treatment. *World J Gastroenterol* 2003; **9**: 117-121
- Wang XZ, Zhang LJ, Li D, Huang YH, Chen ZX, Li B. Effects of transmitters and interleukin-10 on rat hepatic fibrosis induced by CCl₄. *World J Gastroenterol* 2003; **9**: 539-543
- Jiang HQ, Zhang XL. Mechanism of liver fibrosis. *Shijie Huaren Xiaohua Zazhi* 2000; **8**: 687-689
- Schuppan D, Ruehl M, Somasundaram R, Hahn EG. Matrix as a modulator of hepatic fibrogenesis. *Semin Liver Dis* 2001; **21**: 351-372
- Vaillant B, Chiaramonte MG, Cheever AW, Soloway PD, Wynn TA. Regulation of hepatic fibrosis and extracellular matrix genes by the th response: new insight into the role of tissue inhibitors of matrix metalloproteinases. *J Immunol* 2001; **167**: 7017-7026
- Wei HS, Lu HM, Li DG, Zhan YT, Wang ZR, Huang X, Cheng JL, Xu QF. The regulatory role of AT 1 receptor on activated HSCs in hepatic fibrogenesis: effects of RAS inhibitors on hepatic fibrosis induced by CCl₄. *World J Gastroenterol* 2000; **6**: 824-828
- Schuppan D, Ruehl M, Somasundaram R, Hahn EG. Matrix as a modulator of hepatic fibrogenesis. *Semin Liver Dis* 2001; **21**: 351-372
- Lewindon PJ, Pereira TN, Hoskins AC, Bridle KR, Williamson RM, Shepherd RW, Ramm GA. The role of hepatic stellate cells and transforming growth factor-beta (1) in cystic fibrosis liver disease. *Am J Pathol* 2002; **160**: 1705-1715
- Benyon RC, Arthur MJ. Extracellular matrix degradation and the role of hepatic stellate cells. *Semin Liver Dis* 2001; **21**: 373-384
- Liu YK, Shen W. Effect of Cordyceps sinensis on hepatocytic proliferation of experimental hepatic fibrosis in rats. *Shijie Huaren Xiaohua Zazhi* 2002; **10**: 388-391
- Qin JP, Jiang MD. Phenotype and regulation of hepatic stellate cells and liver fibrosis. *Shijie Huaren Xiaohua Zazhi* 2001; **9**: 801-804
- Yoshiji H, Kuriyama S, Miyamoto Y, Thorgeirsson UP, Gomez DE, Kawata M, Yoshii J, Ikenaka Y, Noguchi R, Tsujinoue H, Nakatani T, Thorgeirsson SS, Fukui H. Tissue inhibitor of metalloproteinases-1 promotes liver fibrosis development in a transgenic mouse model. *Hepatology* 2000; **32**: 1248-1254
- Murphy FR, Issa R, Zhou X, Ratnarajah S, Nagase H, Arthur MJ, Benyon C, Iredale JP. Inhibition of apoptosis of activated hepatic stellate cells by tissue inhibitor of metalloproteinase-1 is mediated *via* effects on matrix metalloproteinase inhibition: implications for reversibility of liver fibrosis. *J Biol Chem* 2002; **277**: 11069-11076
- Dudas J, Kovalszky I, Gallai M, Nagy JO, Schaff Z, Knittel T, Mehde M, Neubauer K, Szalay F, Ramadori G. Expression of decorin, transforming growth factor-beta 1, tissue inhibitor metalloproteinase 1 and 2, and type IV collagenases in chronic hepatitis. *Am J Clin Pathol* 2001; **115**: 725-735
- Nie QH, Cheng YQ, Xie YM, Zhou YX, Bai XG, Cao YZ. Methodologic research on TIMP-1, TIMP-2 detection as a new diagnostic index for hepatic fibrosis and its significance. *World J Gastroenterol* 2002; **8**: 282-287
- Nie QH, Cheng YQ, Xie YM, Zhou YX, Cao YZ. Inhibiting effect of antisense oligonucleotides phosphorothioate on gene expression of TIMP-1 in rat liver fibrosis. *World J Gastroenterol* 2001; **7**: 363-369
- Wang BE, Wang ZF, Ying WY, Huang SF, Li JJ. The study on animal model of experimental liver fibrosis. *Zhonghua Yixue Zazhi* 1989; **69**: 503-505
- Nie QH, Hu DR, Li MD, Xie Q. The expression of HGV/GBV-C or HCV related antigens in the liver tissue of patients coinfecting with hepatitis C and G viruses. *Shijie Huaren Xiaohua Zazhi* 2000; **8**: 114-115
- Nie QH, Li MD, Hu DR, Li L. The expression of hepatitis G virus-related antigens in the liver tissues of with hepatitis patients. *Zhonghua Chuanranbing Zazhi* 2000; **18**: 173-175
- Nie QH, Zhou YX, Xie YM. Expression and significance of tissue inhibitors of metalloproteinase-1 and -2 in serum and liver tissue of patients with liver cirrhosis. *Zhonghua Yixue Zazhi* 2001; **81**: 805-807
- Xie YM, Nie QH, Zhou YX, Cheng YQ, Kang WZ, Zhao YL. Tissue inhibitors of metalloproteinase-1 and -2 (TIMP-1 and TIMP-2) mRNA and antigens location in the liver of patients with cirrhosis. *Zhonghua Chuanranbing Zazhi* 2001; **19**: 352-354
- Nie QH, Hu DR, Li MD, Li L, Zhu YH. Detection of hepatitis G virus RNA in liver tissue using digoxigenin labelled probe *in situ* hybridization. *Shijie Huaren Xiaohua Zazhi* 2000; **8**: 771-774
- Okada A, Garnier JM, Vicaire S, Basset P. Cloning of the cDNA encoding rat tissue inhibitor of metalloproteinase 1 (TIMP-1),

- amino acid comparison with other TIMPs, and gene expression in rat tissues. *Gene* 1994; **147**: 301-302
- 36 **Paronetto F**, Popper H. Chronic liver injury induced by immunologic reactions. Cirrhosis following immunization with heterologous sera. *Am J Pathol* 1966; **49**: 1087-1101
- 37 **Flisiak R**, Maxwell P, Prokopowicz D. Plasma tissue inhibitor of metalloproteinases-1 and transforming growth factor beta 1—possible non-invasive biomarkers of hepatic fibrosis in patients with chronic B and C hepatitis. *Hepatology* 2002; **49**: 1369-1372
- 38 **Roeb E**, Purucker E, Breuer B, Nguyen H, Heinrich PC, Rose-John S, Matern S. TIMP expression in toxic and cholestatic liver injury in rat. *J Hepatol* 1997; **27**: 535-544
- 39 **Iredale JP**, Benyon RC, Arthur MJ, Ferris WF, Alcolado R, Winwood PJ, Clark N, Murphy G. Tissue inhibitor of metalloproteinase-1 messenger RNA expression is enhanced relative to interstitial collagenase messenger RNA in experimental liver injury and fibrosis. *Hepatology* 1996; **24**: 176-184
- 40 **Benyon RC**, Arthur MJ. Extracellular matrix degradation and the role of hepatic stellate cells. *Semin Liver Dis* 2001; **21**: 373-384
- 41 **Lewindon PJ**, Pereira TN, Hoskins AC, Bridle KR, Williamson RM, Shepherd RW, Ramm GA. The role of hepatic stellate cells and transforming growth factor-beta (1) in cystic fibrosis liver disease. *Am J Pathol* 2002; **160**: 1705-1715
- 42 **Schnabl B**, Purbeck CA, Choi YH, Hagedorn CH, Brenner D. Replicative senescence of activated human hepatic stellate cells is accompanied by a pronounced inflammatory but less fibrogenic phenotype. *Hepatology* 2003; **37**: 653-664
- 43 **Liu YK**, Shen W. Inhibitive effect of cordyceps sinensis on experimental hepatic fibrosis and its possible mechanism. *World J Gastroenterol* 2003; **9**: 529-533
- 44 **Lamireau T**, Desmouliere A, Bioulac-Sage P, Rosenbaum J. Mechanisms of hepatic fibrogenesis. *Arch Pediatr* 2002; **9**: 392-405
- 45 **Brenner DA**, Waterboer T, Sung Kyu Choi, Lindquist JN, Stefanovic B, Burchardt E, Yamauchi M, Gillan A, Rippe RA. New aspects of hepatic fibrosis. *J Hepatol* 2000; **32**(Suppl 1): 32-38
- 46 **de Lorenzo MS**, Ripoll GV, Yoshiji H, Yamazaki M, Thorgeirsson UP, Alonso DF, Gomez DE. Altered tumor angiogenesis and metastasis of B16 melanoma in transgenic mice overexpressing tissue inhibitor of metalloproteinases-1. *In Vivo* 2003; **17**: 45-50
- 47 **Liu WB**, Yang CQ, Jiang W, Wang YQ, Guo JS, He BM, Wang JY. Inhibition on the production of collagen type I,III of activated hepatic stellate cells by antisense TIMP-1 recombinant plasmid. *World J Gastroenterol* 2003; **9**: 316-319

Edited by Zhang JZ and Wang XL

Protective role of metallothionein (I/II) against pathological damage and apoptosis induced by dimethylarsinic acid

Guang Jia, Yi-Qun Gu, Kung-Tung Chen, You-Yong Lu, Lei Yan, Jian-Ling Wang, Ya-Ping Su, J. C. Gaston Wu

Guang Jia, Lei Yan, Jian-Ling Wang, Department of Occupational and Environmental Health Sciences, School of Public Health, Peking University, Beijing 100083, China

Yi-Qun Gu, Department of Pathology, Hepingli Hospital, Beijing 100013, China

Kung-Tung Chen, Department of General Education, Ming-hsin University of Science and Technology, Taiwan, China

You-Yong Lu, School of Oncology, Peking University, Beijing 100034, China

Ya-Ping Su, J. C. Gaston Wu, Department of Chemistry, National Taiwan Normal University, Taiwan, China

Correspondence to: Dr. Guang Jia, Department of Occupational and Environmental Health Sciences, School of Public Health, Peking University, 38 Xue Yuan Road, Beijing 100083, China. jiaguangjia@yahoo.com.cn

Telephone: +86-10-82801523 **Fax:** +86-10-62015583

Received: 2003-07-04 **Accepted:** 2003-07-24

Abstract

AIM: To better clarify the main target organs of dimethylarsinic acid toxicity and the role of metallothionein (MTs) in modifying dimethylarsinic acid (DMAA) toxicity.

METHODS: MT-I/II null (MT^{-/-}) mice and the corresponding wild-type mice (MT^{+/+}), six in each group, were exposed to DMAA (0-750 mg/kg body weight) by a single oral injection. Twenty four hours later, the lungs, livers and kidneys were collected and undergone pathological analysis, induction of apoptotic cells as determined by TUNEL and MT concentration was detected by radio-immunoassay.

RESULTS: Remarkable pathological lesions were observed at the doses ranging from 350 to 750 mg/kg body weight in the lungs, livers and kidneys and MT^{+/+} mice exhibited a relatively slight destruction when compared with that in dose matched MT^{-/-} mice. The number of apoptotic cells was increased in a dose dependent manner in the lungs and livers in both types of mice. DMAA produced more necrotic cells rather than apoptotic cells at the highest dose of 750 mg/kg, however, no significant increase was observed in the kidney. Hepatic MT level in MT^{+/+} mice was significantly increased by DMAA in a dose-dependent manner and there was no detectable amount of hepatic MT in untreated MT^{-/-} mice.

CONCLUSION: DMAA treatment can lead to the induction of apoptosis and pathological damage in both types of mice. MT exhibits a protective effect against DMAA toxicity.

Jia G, Gu YQ, Chen KT, Lu YY, Yan L, Wang JL, Su YP, Wu JCG. Protective role of metallothionein (I/II) against pathological damage and apoptosis induced by dimethylarsinic acid. *World J Gastroenterol* 2003; 10(1): 91-95

<http://www.wjgnet.com/1007-9327/10/91.asp>

INTRODUCTION

Arsenic is a metalloid that naturally occurs in soil, water, and

air. Arsenicals are also non-biodegradable by-products during production of copper, lead, and other ores and coal consumption. Exposure to arsenic by food, drinking water, soil and air containing arsenic is widely existed in the world. Inorganic arsenicals are well known human carcinogens, specifically for the lung, liver, kidney, skin, bladder and other internal organs^[1,2]. Dimethylarsinic acid (DMAA) is a major form of organic arsenic in the environment and the main metabolite of ingested inorganic arsenicals in most mammals, including humans^[2-4]. DMAA itself can be used as herbicide and pesticide and also naturally exists in some seafood. Recent studies have revealed that DMAA is a genotoxic, multi-site promoter of carcinogenesis as well as a complete carcinogen in rodents^[5-7], which provides a novel clue to investigate the mechanism of arsenicals in carcinogenesis.

Arsenicals, including DMAA, are moderately effective inducers of MT in mice and rats^[8,9]. MTs, thiol-rich metal binding proteins, have been shown to be easily induced by oxidative stress and heavy metals and play an important role in homeostasis of essential metals, detoxication of heavy metals, scavenging reactive oxygen intermediates and preventing carcinogenesis as an endogenous defensive factor^[10-15]. Especially to be mentioned, its capacity of scavenging hydroxyl and superoxide radicals is much more efficient than GSH, an established antioxidant^[15]. Among the four major isoforms of identified MTs, MT-I and MT-II existing in all tissues examined, are the predominant forms in the livers. Recently Liu *et al*^[16] reported that MT-I/II null mice were more sensitive than wild type mice to hepatotoxic and nephrotoxic effects of oral or injected inorganic arsenicals. Sakurai *et al*^[17] reported that DMAA could induce apoptosis by reducing glutathione (GSH) *in vitro*. However, the effect of MT on induction of apoptosis and the main organic toxicity by DMAA *in vivo* remain elusive.

MT-I/II null (MT^{-/-}) mice have been proved to be a good tool for studying MT's normal function and the consequences of its deficiency^[18]. In the present study, MT-I/II null (MT^{-/-}) mice and the corresponding wild-type mice (MT^{+/+}) were exposed to DMAA by oral injection, we investigated the pathological lesions and apoptosis in main target organs including the liver, lung and kidney of the mice, to elucidate the toxicity of DMAA and the ability of MT to modify DMAA toxicity.

MATERIALS AND METHODS

Chemicals

Dimethylarsinic acid (purity 100 %) was purchased from Wako Pure Chemical Co. (Osaka, Japan). An *in situ* apoptosis detection kit (ApopTagTM) was purchased from Intergen Co. NY, USA.

Animals and treatment

MT null (MT^{-/-}) mice whose MT-I and II genes had null mutation and wild type (MT^{+/+}) mice provided kindly by Dr. A. Choo (Murdoch Institute for Research into Birth Defects, Royal Children's Hospital, Australia), were of a mixed genetic background of 129 Ola and C57BL/6 strains. F1

hybrid mice were mated with C57BL/6 mice, and their offsprings were back-crossed to C57BL/6 for six generations. MT^{-/-} and MT^{+/+} mice were obtained by mating of those heterozygous (MT^{+/-}) mice.

MT^{-/-} and MT^{+/+} mice were routinely bred in the vivarium of the National Institute for Environmental Studies (NIES, Japan). Microbiological and viral examinations were performed with regular quarantine procedures for more than one year, and we did not find either pathogenic infections or significant phenotypical abnormalities. Both strains of mice were housed in cages in ventilated animal rooms with a controlled temperature of 23±1 °C, a relative humidity of 55±10%, and a 12 h light/dark cycle. They were maintained on standard laboratory chow and tap water *ad lib*, and received humane care throughout the experiment according to the guidelines of the NIES. Eight-week-old female MT^{-/-} and MT^{+/+} mice were assigned randomly in equal numbers to all groups (six mice for each treatment group). Fresh DMAA solution was prepared by dissolving it in sterilized water. The mice were administered DMAA (0-750 mg/kg) by oral gavage.

Sample collection

At 24 h after administration of DMAA, the lung, liver and kidney were collected from each mouse under diethyl ether anesthesia. Portions of tissues were fixed in 10% neutral formalin, processed by the standard histological techniques, and stained with hematoxylin and eosin for light microscopic examination. For TUNEL staining, sections (5 µm) were placed on poly-L-lysine precoated slides.

TUNEL for apoptosis

Apoptotic cells were detected with an apoptosis detection kit according to the manufacturer's instructions. Briefly, the samples were incubated with digoxigenin-labeled dNTP in the presence of terminal deoxynucleotidyl transferase followed by peroxidase-conjugated anti-digoxigenin antibody. Nuclear staining of apoptotic cells was detected with 3', 3'-diaminobenzidine followed by counterstaining of nuclei with methyl green. An apoptosis index (AI) was obtained by dividing the number of positive cells in the area observed^[19].

MT Concentration

MT (MT-I and MT-II isoforms) concentration in the liver was measured by radioimmunoassay using sheep anti-rat MT-I antiserum^[20]. The detection limit of this method was 0.2 µg MT/g of tissue.

Statistical analysis

ANOVA with subsequent *post hoc*'s test was used as appropriate. All values were expressed as $\bar{x}\pm s$. Differences were considered significant at $P<0.05$.

RESULTS

Histopathological observation

In untreated MT^{-/-} mice and the corresponding MT^{+/+} mice, the lung, liver and kidney showed normal morphology. Significant lesions were observed at doses of DMAA ranging from 375 to 750 mg/kg body weight in both types of mice. However, the pathological lesions in MT^{-/-} mice were more severely widespread when compared to that in dose matched MT^{+/+} mice.

Changes including congestion, atelectasis and mild to moderate hemorrhages in the alveoli of the lungs were observed in MT^{-/-} mice. Adequate air space in the alveoli was observed more frequent in MT^{+/+} mice compared to that of MT^{-/-} mice. Pulmonary capillary congestion could affect alveolar space, resulting in severe acute impairment of respiratory function.

Capillary rupture led to leakage of red blood cells into the interstitium, as well as into the alveoli (Figure 1).

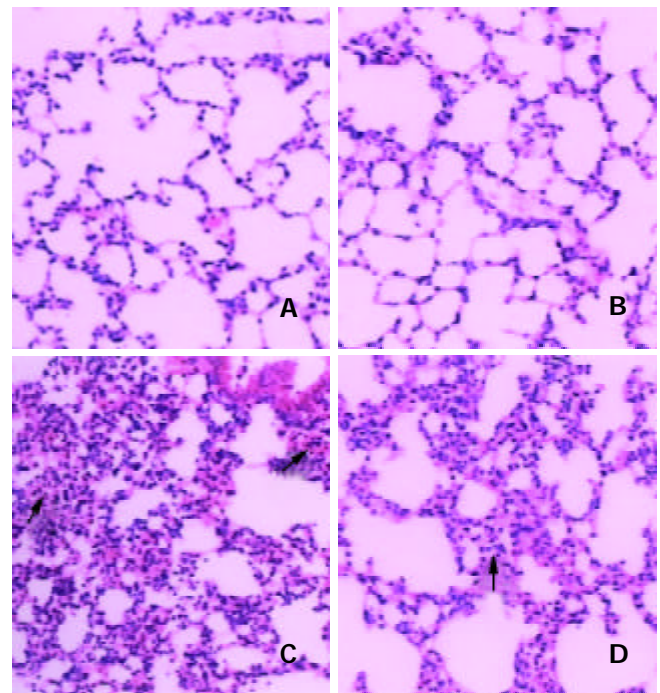


Figure 1 Typical HE staining. The bar is 100 µm. A, B: the lungs from control of MT^{-/-} and MT^{+/+} mice; C, D: the lungs from 750 mg/kg DMAA group of MT^{-/-} and MT^{+/+} mice. Arrows indicate atelectasis and hemorrhage.

At 24 h after DMAA treatment, severe liver damages characterized by cellular cloudy swelling, paleness of cell cytoplasm, vacuolization of hepatocytes and a few areas of focal necrosis were found in MT^{-/-} mice while a limited degree of changes was observed in dose matched MT^{+/+} mice livers (Figure 2).

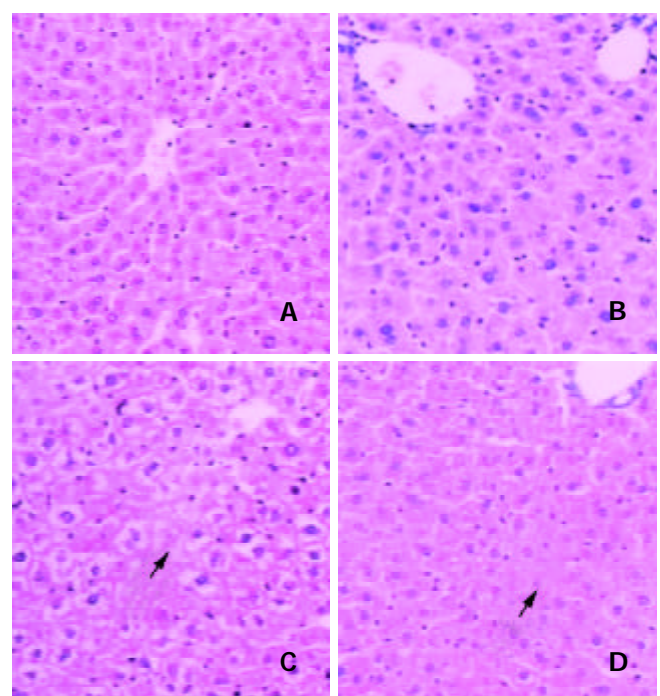


Figure 2 Typical HE staining. The bar is 100 µm. A, B: the livers from control of MT^{-/-} and MT^{+/+} mice; C, D: the livers from 750 mg/kg DMAA group of MT^{-/-} and MT^{+/+} mice. The arrows indicate necrosis.

Histological changes in the kidney are shown in Figure 3. Treatment with DMAA produced swelling of glomerulus and its surrounding tubular tissue and urinary space compression in both types of mice.

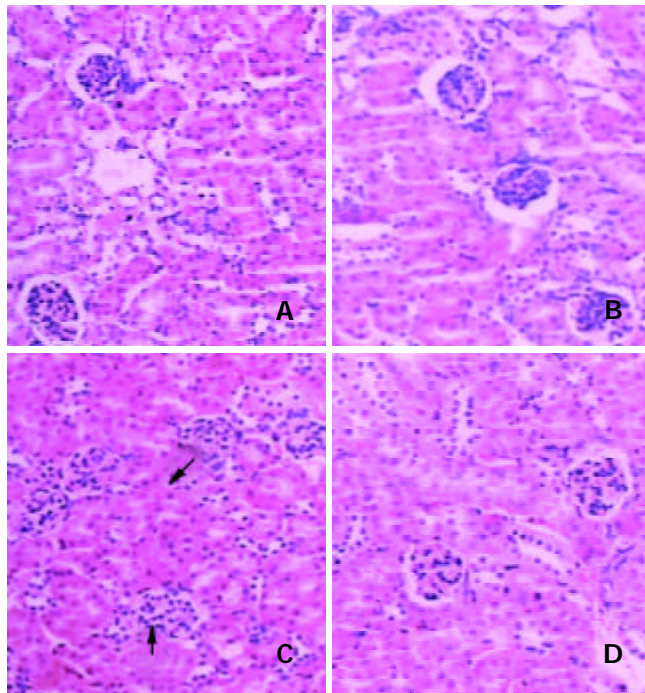


Figure 3 Typical HE staining. The bar is 100 μ m. A, B: the kidneys from control of MT^{-/-} and MT^{+/+} mice; C, D: the kidneys from 750 mg/kg DMAA group of MT^{-/-} and MT^{+/+} mice. The arrows indicate the swelling of glomerulus and the surrounding tubular tissue and urinary space compression.

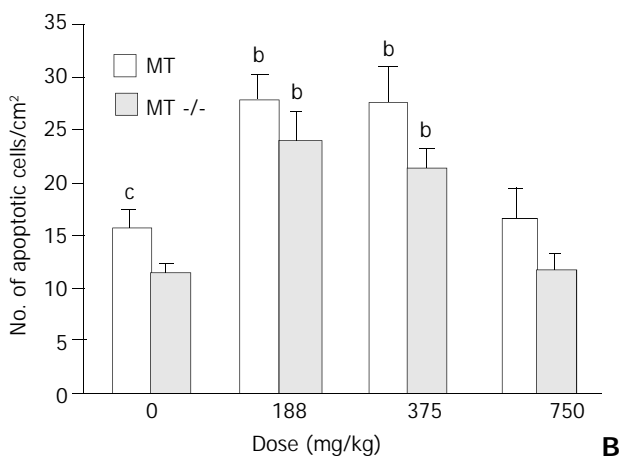
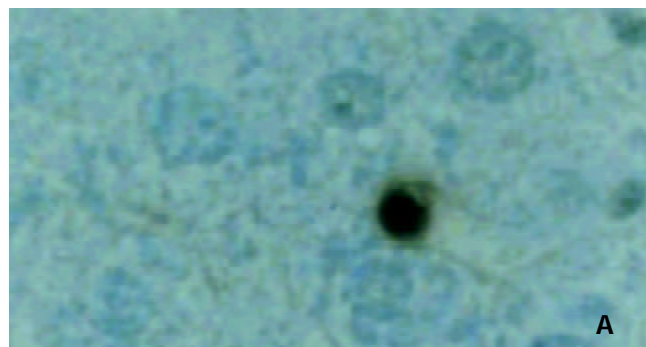


Figure 5 Apoptosis in livers of MT^{+/+} and MT^{-/-} mice detected by TUNEL twenty-four hours after oral DMAA treatment. A: Typical apoptotic cells in the liver of MT^{-/-} mice at a dose of

188 mg/kg body weight. Brown staining indicates apoptotic cells. The bar is 20 μ m. B: AI in the livers. All values were expressed as $\bar{x} \pm s$. ANOVA with subsequent *post hoc*'s test was performed for comparison of AI. ^{a,b}Significant difference at $P < 0.05$, $P < 0.01$ when compared with the corresponding control group. ^{c,d}Significant difference at $P < 0.05$, $P < 0.01$ when compared with the dose-matched MT^{-/-} mice group.

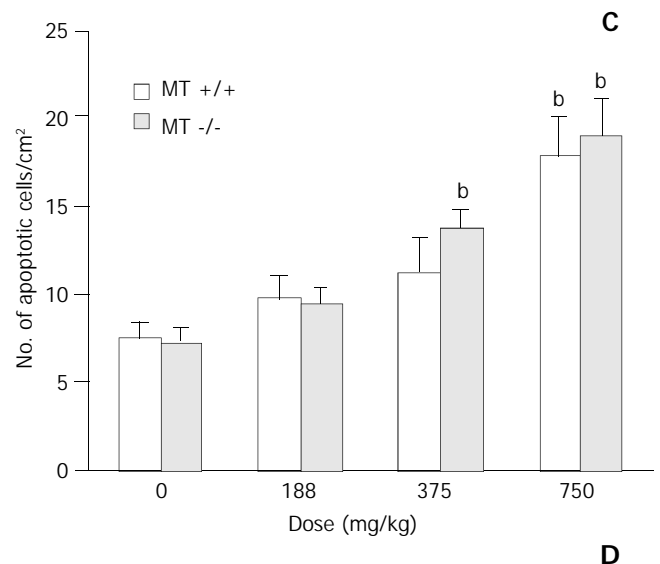
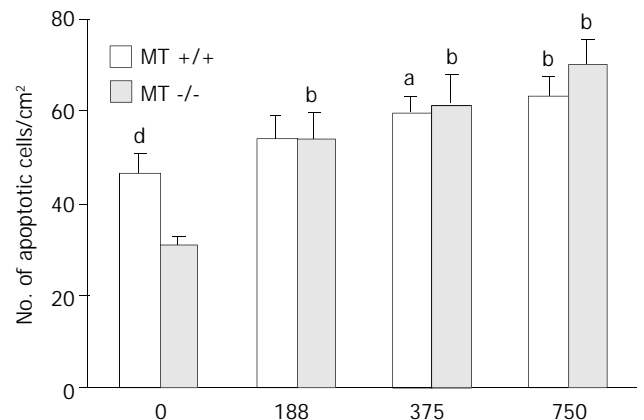
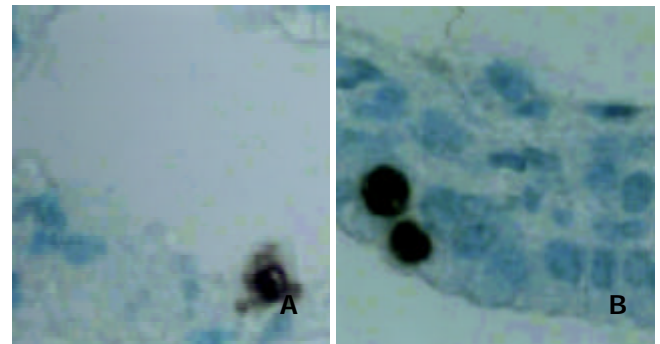


Figure 4 Apoptosis in lungs of MT^{+/+} and MT^{-/-} mice detected by TUNEL twenty-four hours after oral DMAA treatment. A: Typical apoptotic cells in alveolar area of MT^{-/-} mice at a dose of 188 mg/kg body weight. Brown staining indicates the apoptotic cells. The bar is 20 μ m. B: Typical apoptotic cells in bronchial area of MT^{-/-} mice at a dose of 188 mg/kg body weight. Brown staining indicates apoptotic cells. The bar is 20 μ m. C: AI in alveolar area. D: AI in bronchial area. All the values were expressed as $\bar{x} \pm s$. ANOVA with subsequent *post hoc*'s test was performed for comparison of AI. ^{a,b}Significant difference at $P < 0.05$, $P < 0.01$ when compared with the corresponding control group. ^{c,d}Significant difference at $P < 0.05$, $P < 0.01$ when compared with the dose-matched MT^{-/-} mice group.

Induction of apoptotic cells detected in lungs, livers and kidneys of $MT^{-/-}$ and $MT^{+/+}$ mice

High induction of apoptotic cells in bronchial epithelial cells was observed in $MT^{-/-}$ mice treated with DMAA at 375 mg/kg body weight, however, the same changes were not observed in dose matched $MT^{+/+}$ mice. At a high dose of 750 mg/kg body weight, the coincident increase of apoptotic cells was observed in both types of mice and no significant difference was observed between them.

In control group, the incidence of apoptotic cells in alveolar epithelial cells in $MT^{+/+}$ mice was significantly higher than that in $MT^{-/-}$ mice, implying that $MT^{+/+}$ mice might have a stronger ability to induce apoptosis than $MT^{-/-}$ mice. A significant increase of apoptotic cells occurred in $MT^{-/-}$ mice treated by 188 mg/kg DMAA, a relative low dose when compared with that in bronchial epithelial cells. However, no significant increase was observed in $MT^{+/+}$ mice at the same dose of 188 mg/kg DMAA. With the increase of dose, high induction of apoptotic cells was observed in both types of mice (Figure 4).

Figure 5 shows that in control group, the incidence of apoptotic cells in $MT^{+/+}$ mice was $156.33 \pm 41.041/\text{cm}^2$, significantly higher than that in $MT^{-/-}$ mice. The incidence of apoptotic cells in the livers rose with the increase of dose in both types of mice. However, at the highest dose of 750 mg/kg, DMAA produced more necrotic cells rather than apoptotic cells observed by HE staining (Figure 2).

DMAA failed to induce remarkable apoptotic cells in the kidneys from both types of mice (data not shown).

MT concentration in liver of $MT^{+/+}$ mice

MT concentration was determined in the liver of $MT^{+/+}$ mice and $MT^{-/-}$ mice treated with DMAA (Figure 6). Hepatic MT level in $MT^{+/+}$ mice was significantly increased by DMAA in a dose-dependent manner. However, there was no detectable amount of hepatic MT in untreated $MT^{-/-}$ mice, and it could not be induced by DMAA.

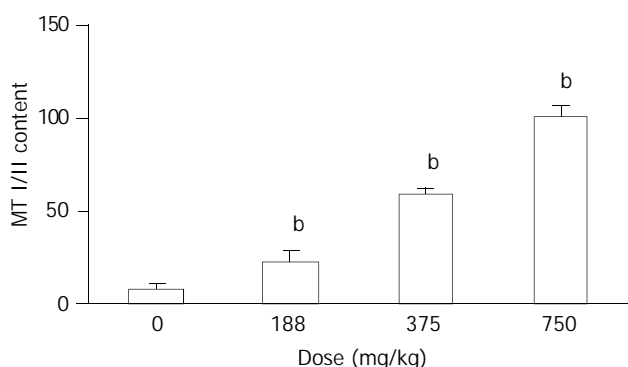


Figure 6 MT concentration in livers of $MT^{+/+}$ mice detected by radio-immunoassay. All the values were expressed as $\bar{x} \pm s$. ANOVA with subsequent *post hoc* 's test was performed for comparison of AI. ^bSignificant difference at $P < 0.01$ when compared with the corresponding control group.

DISCUSSION

The present study demonstrated that DMAA could produce pathological lesions in the lungs, livers and kidneys, and induce apoptosis in the lungs and livers. Most importantly, it is the first report to show that inability to produce MT-I/II in $MT^{-/-}$ mice caused an increased sensitivity to toxicity induced by DMAA.

Treatment with DMAA caused severe and wide spread lesions in $MT^{-/-}$ mice, whereas, these changes were much less severe in $MT^{+/+}$ mice. It indicates that $MT^{-/-}$ mice were more

sensitive to DMAA and MT played a protective role against the toxicities to main organs. Yamanaka^[7] reported that DMAA in mice could be further metabolized and converted into dimethylarsine radicals and dimethyl arsenic peroxy radicals. Marked formation of 8-oxod G was observed in the lung and liver, which are the target organs for arsenic carcinogenesis. No increase in 8-oxod G levels was observed in the kidney. Meanwhile, MT was capable of scavenging hydroxyl and superoxide radicals and its capability of scavenging them was much more efficient^[11,12,15]. In our study, the expression of MT (I/II) was induced by DMAA in a dose dependent manner in the livers of $MT^{+/+}$ mice, no MT(I/II) was observed in $MT^{-/-}$ mice. Thus the reduction of lesions induced by DMAA in the main target organs of $MT^{+/+}$ mice could be explained at least partly by MT reduction induced by DMAA, and the toxicity induced by DMAA could be explained partly by way of oxidative stress participation.

After a lethal damaging stimulation, two main structural routes of cell death might occur: apoptosis and necrosis. It has become apparent that the magnitude and type of injurious stimuli could determine whether a cell underwent death through apoptosis or necrosis. Severe damaging stimuli tended to result in necrosis, and lower grade damaged stimuli tended to cause apoptosis^[21-30].

Recently, Sakurai *et al* reported that DMAA could induce apoptosis by reducing glutathione (GSH) *in vitro*^[17]. However, the effect of MT on the induction of apoptosis by DMAA *in vivo* remains elusive. Furthermore, the perturbation of apoptosis has been thought to contribute to carcinogenesis either through enhanced initiation or progression^[29-38]. In this study, the induction of apoptosis was detected by TUNEL in the lungs, livers and kidneys from both types of mice. In the lungs, a significant increase of apoptosis was observed in alveolar cells of $MT^{-/-}$ mice at a relative low level compared with that in bronchial cells, suggesting that alveolar cells were more sensitive than bronchial cells and MT had some protective role against the induction of apoptosis induced by DMAA at a relative low level. With the increase of dose, DMAA induced high levels of apoptosis in both types of mice and at the highest dose of 750 mg/kg, necrotic cells predominated over apoptosis in the livers, revealing the serious toxicity of DMAA at this dose. Since the kidney is the major organ for arsenic elimination and most of arsenicals could be rapidly eliminated through the kidney^[1-3], renal cells are thus exposed to a major portion of the absorbed arsenical dose. However, the induction of apoptosis was not affected by DMAA, the underlying mechanism needs further investigations.

In conclusion, the present studies demonstrate that oral administration of DMAA can produce toxic response of the respiratory system, liver and kidney in both $MT^{-/-}$ and $MT^{+/+}$ mice. The pathological effects are clearly pronounced in $MT^{-/-}$ mice. Intracellular MT appears to play an important role in preventing the toxic effects of DMAA.

ACKNOWLEDGEMENT

We thank Dr. Sone Hideko and Masahiko Satoh (National Institute for Environmental Studies, Japan) for kindly providing the experiment materials. This work was supported in part by a Grant-in-aid for Scientific Research from the Ministry of Education, China and a grant from the Japan Science and Technology Agency, Japan.

REFERENCES

- Huff J, Chan P, Nyska A. Is the human carcinogen arsenic carcinogenic to laboratory animals? *Toxicol Sci* 2000; **55**: 17-23
- Kitchin KT. Recent advances in arsenic carcinogenesis: modes

- of action, animal model systems, and methylated arsenic metabolites. *Toxicol Appl Pharmacol* 2001; **172**: 249-261
- 3 **Goering PL**, Aposhian HV, Mass MJ, Cebrian M, Beck BD, Waalkes MP. The enigma of arsenic carcinogenesis: role of metabolism. *Toxicol Sci* 1999; **49**: 5-14
- 4 **Braman RS**, Foreback CC. Methylated forms of arsenic in the environment. *Science* 1973; **182**: 1247-1249
- 5 **Yamamoto S**, Wanibuchi H, Hori T, Yano Y, Matsui-Yuasa I, Otani S, Chen H, Yoshida K, Kuroda K, Endo G, Fukushima S. Possible carcinogenic potential of dimethylarsinic acid as assessed in rat *in vivo* models: a review. *Mutat Res* 1997; **386**: 353-361
- 6 **Kenyon EM**, Hughes MF. A concise review of the toxicity and carcinogenicity of dimethylarsinic acid. *Toxicology* 2001; **160**: 227-236
- 7 **Yamanaka K**, Takabayashi F, Mizoi M, An Y, Hasegawa A, Okada S. Oral exposure of dimethylarsinic acid, a main metabolite of inorganic arsenics, in mice leads to an increase in 8-Oxo-2'-deoxyguanosine level, specifically in the target organs for arsenic carcinogenesis. *Biochem Biophys Res Commun* 2001; **287**: 66-70
- 8 **Kreppel H**, Bauman JW, Liu J, McKim JM Jr, Klaassen CD. Induction of metallothionein by arsenicals in mice. *Fundam Appl Toxicol* 1993; **20**: 184-189
- 9 **Albores A**, Koropatnick J, Cherian MG, Zelazowski AJ. Arsenic induces and enhances rat hepatic metallothionein production *in vivo*. *Chem Biol Interact* 1992; **85**: 127-140
- 10 **Cherian MG**, Howell SB, Imura N, Klaassen CD, Koropatnick J, Lazo JS, Waalkes MP. Role of metallothionein in carcinogenesis. *Toxicol Appl Pharmacol* 1994; **126**: 1-5
- 11 **Andrews GK**. Regulation of metallothionein gene expression by oxidative stress and metal ions. *Biochem Pharmacol* 2000; **59**: 95-104
- 12 **Viarengo A**, Burlando B, Ceratto N, Panfoli I. Antioxidant role of metallothioneins: a comparative overview. *Cell Mol Biol* 2000; **46**: 407-417
- 13 **Cheng ML**, Wu J, Wang HQ, Xue LM, Tan YZ, Ping L, Li CX, Huang NH, Yao YM, Ren LZ, Ye L, Li L, Jia ML. Effect of Maotai liquor in inducing metallothioneins and on hepatic stellate cells. *World J Gastroenterol* 2002; **8**: 520-523
- 14 **Huang GW**, Yang LY. Metallothionein expression in hepatocellular carcinoma. *World J Gastroenterol* 2002; **8**: 650-653
- 15 **Deneke SM**. Thiol-based antioxidants. *Curr Top Cell Regul* 2000; **36**: 151-180
- 16 **Liu J**, Liu Y, Goyer RA, Achanzar W, Waalkes MP. Metallothionein-I/II null mice are more sensitive than wild-type mice to the hepatotoxic and nephrotoxic effects of chronic oral or injected inorganic arsenicals. *Toxicol Sci* 2000; **55**: 460-467
- 17 **Sakurai T**, Qu W, Sakurai MH, Waalkes MP. A major human arsenic metabolite, dimethylarsinic acid, requires reduced glutathione to induce apoptosis. *Chem Res Toxicol* 2002; **15**: 629-637
- 18 **Michalska AE**, Choo KH. Targeting and germ-line transmission of a null mutation at the metallothionein I and II loci in mouse. *Proc Natl Acad Sci U S A* 1993; **90**: 8088-8092
- 19 **Jia G**, Tohyama C, Sone H. DNA damage triggers imbalance of proliferation and apoptosis during development of preneoplastic foci in the liver of Long-Evans Cinnamon rats. *Int J Oncol* 2002; **21**: 755-761
- 20 **Tohyama C**, Shaikh ZA. Metallothionein in plasma and urine of cadmium-exposed rats determined by a single-antibody radioimmunoassay. *Fundam Appl Toxicol* 1981; **1**: 1-7
- 21 **Wu K**, Zhao Y, Liu BH, Li Y, Liu F, Guo J, Yu WP. RRR- α -tocopheryl succinate inhibits human gastric cancer SGC-7901 cell growth by inducing apoptosis and DNA synthesis arrest. *World J Gastroenterol* 2002; **8**: 26-30
- 22 **Gao F**, Yi J, Shi GY, Li H, Shi XG, Tang XM. The sensitivity of digestive tract tumor cells to As₂O₃ is associated with the inherent cellular level of reactive oxygen species. *World J Gastroenterol* 2002; **8**: 36-39
- 23 **Shen ZY**, Shen WY, Chen MH, Shen J, Cai WJ, Yi Z. Nitric oxide and calcium ions in apoptotic esophageal carcinoma cells induced by arsenite. *World J Gastroenterol* 2002; **8**: 40-43
- 24 **Shan CM**, Li J. Study of apoptosis in human liver cancers. *World J Gastroenterol* 2002; **8**: 247-252
- 25 **Liu JW**, Tang Y, Shen Y, Zhong XY. Synergistic effect of cell differential agent-II and arsenic trioxide on induction of cell cycle arrest and apoptosis in hepatoma cells. *World J Gastroenterol* 2003; **9**: 65-68
- 26 **Gu QL**, Li NL, Zhu ZG, Yin HR, Lin YZ. A study on arsenic trioxide inducing *in vitro* apoptosis of gastric cancer cell lines. *World J Gastroenterol* 2000; **6**: 435-437
- 27 **Tu SP**, Zhong J, Tan JH, Jiang XH, Qiao MM, Wu YX, Jiang SH. Induction of apoptosis by arsenic trioxide and hydroxy-camptothecin in gastric cancer cells *in vitro*. *World J Gastroenterol* 2000; **6**: 532-539
- 28 **Shen ZY**, Shen J, Li QS, Chen CY, Chen JY, Yi Z. Morphological and functional changes of mitochondria in apoptotic esophageal carcinoma cells induced by arsenic trioxide. *World J Gastroenterol* 2002; **8**: 31-35
- 29 **Evan GI**, Vousden KH. Proliferation, cell cycle and apoptosis in cancer. *Nature* 2001; **411**: 342-348
- 30 **Waalkes MP**, Fox DA, States JC, Patierno SR, McCabe MJ Jr. Metals and disorders of cell accumulation: modulation of apoptosis and cell proliferation. *Toxicol Sci* 2000; **56**: 255-261
- 31 **Manning FC**, Patierno SR. Apoptosis: Inhibitor or instigator of carcinogenesis? *Cancer Invest* 1996; **14**: 455-465
- 32 **Chen YX**, Zhong XY, Qin YF, Bing W, He LZ. 15d-PGJ(2) inhibits cell growth and induces apoptosis of MCG-803 human gastric cancer cell line. *World J Gastroenterol* 2003; **9**: 2149-2153
- 33 **Wang L**, Li J, Li Q, Zhang J, Duan XL. Morphological changes of cell proliferation and apoptosis in rat jejunal mucosa at different ages. *World J Gastroenterol* 2003; **9**: 2060-2064
- 34 **Jiang YA**, Luo HS, Zhang YY, Fan LF, Jiang CQ, Chen WJ. Telomerase activity and cell apoptosis in colon cancer cell by human telomerase reverse transcriptase gene antisense oligodeoxynucleotide. *World J Gastroenterol* 2003; **9**: 1981-1984
- 35 **Liu ZS**, Tang SL, Ai ZL. Effects of hydroxyapatite nanoparticles on proliferation and apoptosis of human hepatoma BEL-7402 cells. *World J Gastroenterol* 2003; **9**: 1968-1971
- 36 **Li MY**, Deng H, Zhao JM, Dai D, Tan XY. Peroxisome proliferator-activated receptor gamma ligands inhibit cell growth and induce apoptosis in human liver cancer BEL-7402 cells. *World J Gastroenterol* 2003; **9**: 1683-1688
- 37 **Li JY**, Wang XZ, Chen FL, Yu JP, Luo HS. Nimesulide inhibits proliferation via induction of apoptosis and cell cycle arrest in human gastric adenocarcinoma cell line. *World J Gastroenterol* 2003; **9**: 915-920
- 38 **Cheng ML**, Wu J, Wang HQ, Xue LM, Tan YZ, Ping L, Li CX, Huang NH, Yao YM, Ren LZ, Ye L, Li L, Jia ML. Effect of Maotai liquor in inducing metallothioneins and on hepatic stellate cells. *World J Gastroenterol* 2002; **8**: 520-523

Edited by Zhu LH and Wang XL

Effect of Qingyitang on activity of intracellular Ca^{2+} - Mg^{2+} -ATPase in rats with acute pancreatitis

Ying Qiu, Yong-Yu Li, Shu-Guang Li, Bo-Gen Song, Gui-Fen Zhao

Ying Qiu, Bo-Gen Song, Gui-Fen Zhao, Department of Pathology, Medical School of Tongji University, Shanghai 200331, China

Yong-Yu Li, Department of Pathophysiology, Medical School of Tongji University, Shanghai 200331, China

Shu-Guang Li, Department of Prevention Medicine, Medical School of Tongji University, Shanghai 200331, China

Supported by National Natural Science Foundation of China, No. 30060031

Correspondence to: Yong-Yu Li, Department of Pathophysiology, Medical School of Tongji University, 500 Zhennan Road, Shanghai 200331, China. liyyu@163.net

Telephone: +86-21-68537254 **Fax:** +86-21-62846993

Received: 2003-03-03 **Accepted:** 2003-05-21

Abstract

AIM: To study the change of intracellular calcium-magnesium ATPase (Ca^{2+} - Mg^{2+} -ATPase) activity in pancreas, liver and kidney tissues of rats with acute pancreatitis (AP), and to investigate the effects of Qingyitang (QYT) (Decoction for clearing the pancreas) and tetrandrine (Tet) and vitamin E (VitE) on the activity of Ca^{2+} - Mg^{2+} -ATPase.

METHODS: One hundred and five Sprague-Dawley rats were randomly divided into: normal control group, AP group, treatment group with QYT (1 ml/100 g) or Tet (0.4 ml/100 g) or VitE (100 mg/kg). AP model was prepared by a retrograde injection of sodium taurocholate into the pancreatic duct. Tissues of pancreas, liver and kidney of the animals were taken at 1 h, 5 h, 10 h respectively after AP induction, and the activity of Ca^{2+} - Mg^{2+} -ATPase was studied using enzyme-histochemistry staining. Meanwhile, the expression of Ca^{2+} - Mg^{2+} -ATPase of the tissues was studied by RT-PCR.

RESULTS: The results showed that the positive rate of Ca^{2+} - Mg^{2+} -ATPase in AP group (8.3%, 25%, 29.2%) was lower than that in normal control group (100%) in all tissues ($P < 0.01$), the positive rate of Ca^{2+} - Mg^{2+} -ATPase in treatment group with QYT (58.3%, 83.3%, 83.3%), Tet (50.0%, 70.8%, 75.0%) and VitE (54.2%, 75.0%, 79.2%) was higher than that in AP group (8.3%, 25.0%, 29.2%) in all tissues ($P < 0.01$). RT-PCR results demonstrated that in treatment groups Ca^{2+} - Mg^{2+} -ATPase gene expression in pancreas tissue was higher than that in AP group at the observing time points, and the expression at 5 h was higher than that at 1 h. The expression of Ca^{2+} - Mg^{2+} -ATPase in liver tissue was positive, but without significant difference between different groups.

CONCLUSION: The activity and expression of intracellular Ca^{2+} - Mg^{2+} -ATPase decreased in rats with AP, suggesting that Ca^{2+} - Mg^{2+} -ATPase may contribute to the occurrence and development of cellular calcium overload in AP. QYT, Tet and VitE can increase the activity and expression of Ca^{2+} - Mg^{2+} -ATPase and may relieve intracellular calcium overload to protect the tissue and cells from injuries.

Qiu Y, Li YY, Li SG, Song BG, Zhao GF. Effect of Qingyitang on

activity of intracellular Ca^{2+} - Mg^{2+} -ATPase in rats with acute pancreatitis. *World J Gastroenterol* 2004; 10(1): 100-104
<http://www.wjgnet.com/1007-9327/10/100.asp>

INTRODUCTION

The pathogenesis of acute pancreatitis (AP) is complicated. A number of theories have been proposed. It is generally accepted that "calcium overload" plays a key role in the occurrence and progression of AP^[1-3]. However, the exact mechanism of intracellular calcium overload in acute pancreatitis is not clear yet. This study was designed to explore the mechanism of intracellular calcium overload by determining the activity of intracellular Ca^{2+} - Mg^{2+} ATPase in AP rats. The experiment also investigated the therapeutic mechanisms of some medicines, such as Chinese medicines Qingyitang (QYT) and tetrandrine (Tet), and Vitamin E (VitE) on AP in rats.

MATERIALS AND METHODS

Animals

One hundred and five Sprague-Dawley (SD) rats including male and female (1:1) were used. The animals, weighing 220-250 g, were provided by the Animal Center of Chinese Academy of Sciences, Shanghai, China.

Reagents

Sodium taurocholate from Sigma Co. was diluted with distilled water to make a 4% solution for use. QYT was from Zunyi Medical College, Tet from the Pharmaceutical Institute of the Second Military Medical University, VitE (emulsion, 2 ml/kg) from Xinan Pharmaceutical Factory, ATP disodium salt from Shanghai Institute of Biochemistry, Chinese Academy of Sciences. Trizol, reverse transcriptase Superscript II RNase H- were from Gib Co. (USA), hexamer from Promega (USA), and Taq DNA polymerase, dNTP, RNAase inhibitor from Takara Co. (Japan), diethyl pyrocarbonate (DEPC) from Serva Co. (USA). Primers for Ca^{2+} - Mg^{2+} -ATPase (upstream primer -5' GAACATCCTGCAGACGGACA-3', downstream primer -5' CAAAGCTATGGGAGTGGTGG-3') (790-1 241 bp) and primers for GAPDH (upper -5' ACCACAGTCCATGCCATCAC-3', lower -5' TCCACCACCCTGTTGCTGTA-3') were purchased from Takara Co. (Japan).

Animal model preparation and grouping

The rats were randomly divided into normal control group ($n=9$), AP+ normal saline (NS) group ($n=24$), AP+QYT group ($n=24$), AP+Tet group ($n=24$), AP+VitE group ($n=24$). In normal control group the pancreas of rats were exposed. In the other groups, the pancreas of rats was exposed and sodium taurocholate was injected into the pancreatic duct to induce AP^[4]. In AP+NS group, rats were injected with NS (0.4 ml/100 g, ip) after AP induction. In AP+QYT group, rats were infused with QYT (1 ml/100 g) by a nose-gastric catheter, in AP+Tet group, rats were injected peritoneally

with Tet (0.4 ml/100 g), and in AP+VitE group, rats were given VitE (100 mg/kg) intravenously through mesenteric vein.

HE staining

At 1 h, 5 h or 10 h after operation, the tissue samples of pancreas, liver and kidney were taken and fixed with formalin solution. Some sections of the specimens were stained with HE, and then observed under a light microscope.

Enzyme histochemistry

Some of the tissue blocks were used for enzyme histochemistry staining. Four μm thick tissue slices were mounted to polylysine-coated slides with a cryotome. Wachstein-Meisid lead nitrate method^[5] was used to conduct enzyme histochemistry stain for intracellular Ca²⁺-Mg²⁺-ATPase. The slides were examined under a light microscope.

RT-PCR

Primers for Ca²⁺-Mg²⁺-ATPase gene were designed based on mRNA sequence of intracellular Ca²⁺-Mg²⁺-ATPase^[6]. GAPDH gene was used as internal housekeeping gene. Total RNA of pancreas and liver were taken for RT-PCR at 1 h and 5 h after AP was induced. Total RNA was extracted with Trizol reagents. Quantity and purity of RNA were determined with an ultraviolet spectrophotometer. RNA integrity was confirmed by agar gel electrophoresis. The reverse transcription system was 20 μl in volume, containing 2 μg total RNA, 1 μl reverse transcriptase, 1 μl dNTP (10 mmol/L), 2 μl (100 ng/1 μl) hexamer, 4 μl 5×buffer, 2 μl 0.1M DTT, 8 μl water. The mixture was incubated at 37 °C for 1 hour and then at 70 °C for 15 minutes to inactivate reverse transcriptase. cDNA was used as a template for subsequent PCR. PCR reaction was performed in a thermal cycler (PE480). PCR reaction solution contained 1 μl cDNA, 2 μl dNTP (2 mmol/L), 1 μl primers, 2.5 μl 10×buffer, 2U Taq polymerase, 18 μl water. PCR process was at 94 °C for 5 minutes, followed by 35 cycles at 94 °C for 1 min, at 57 °C for 1 min, and at 72 °C for 1 min. Final extension was at 72 °C for 10 minutes, 8 μl of PCR products was examined on 1% agar gel electrophoresis. The bands were observed and photographed under Ultraviolet light.

Statistical analysis

Data were analyzed by χ² test and P<0.01 was considered significant.

RESULTS

Pathological findings in pancreas, liver and kidney tissues of AP rats

Pancreas Large areas of hemorrhage were found in pancreatic tissue of AP+NS group. Acinar structure was obscure. There were large areas of necrosis. Some nuclei were lysed and disappeared. Apparently saponified spots were seen. A

number of inflammatory cell infiltrations were observed in the peri-necrotic tissues. In AP+QYT, AP+Tet or AP+VitE groups, the pancreas only slightly swelled with sporadic bleeding and necrosis, and mild inflammatory infiltration in the pancreatic tissue.

Liver In AP+NS group, degeneration and necrosis of the liver cells were found, and hepatocytes were disordered and some hepatic cords disappeared. In AP+QYT, AP+Tet or AP+VitE groups, hepatocytes were only degenerated and swelled with slight focal hemorrhagic necrosis.

Kidney In AP+NS group, epithelial cells in the proximal convoluted renal tubule were observed with degeneration and necrosis. Hyperemia, swelling and inflammatory cell infiltration were seen in renal glomeruli. Only edema was found in proximal convoluted renal tubular epithelial cells in AP+QYT, AP+Tet and AP+VitE groups (Figure 1).

Activity of intracellular Ca²⁺-Mg²⁺-ATPase in pancreas, liver and kidney tissues of AP rats

Positive stains were diffusely distributed in cellular membrane and cytoplasm of pancreatic acinar cells, hepatocytes, and proximal renal tubule epithelial cells. Positive rate of Ca²⁺-Mg²⁺-ATPase stain in tissues of normal group was significantly higher than that of other groups. The lowest positive rate was found in AP+NS group (P<0.01). There was no significant difference between groups of AP+QYT, AP+Tet, and AP+VitE (P>0.05) (Table 1, Figure 2).

Positive cells were defined as cells with uneven chocolate brown particles in cytoplasm under light microscope. The darker the staining color was, the higher the activity was. The cells were classified into 4 levels based on color intensity and number of positive cells. No staining or only a small number of light brown particles in cellular membrane and cytoplasm, and more than 25% of stained cells were negative (-); with a medium number of brown particles, and 25%-50% of stained cells were positive (+); with a large number of brown particles and more than 50% of stained cells were positive (++); more than 75% of stained cells were positive (+++).

Expression of Ca²⁺-Mg²⁺-ATPase in pancreas and liver tissues of AP rats

By RT-PCR technique, the expression of Ca²⁺-Mg²⁺-ATPase in pancreas and liver of all groups was measured respectively. The gene fragment of Ca²⁺-Mg²⁺-ATPase was 451 bp. The amplified fragment of internal housekeeping gene GAPDH was 450 bp. The results showed that the highest expression of Ca²⁺-Mg²⁺-ATPase was in normal group, the lowest was in AP+NS group, and moderate in AP+QYT, AP+Tet and AP+VitE groups. The expression decreased with time in AP+NS group, While in AP+QYT, AP+Tet and AP+VitE groups, the expression increased with time. The expression of Ca²⁺-Mg²⁺-ATPase in liver had no significant difference between groups (Figure 3).

Table 1 Positive rate of activity of intracellular Ca²⁺-Mg²⁺-ATPase in tissues of AP rats

Group	n	Pancreatic acinar cells				Hepatocytes				Renal epithelial cells			
		-	+	++~+++	Positive (%)	-	+	++~+++	Positive (%)	-	+	++~+++	Positive (%)
Normal group	9	0	5	4	100 ^a	0	3	6	100 ^a	0	5	6	100 ^a
AP+NS	24	22	2	0	8.3	18	5	1	25.0	17	5	2	29.2
AP+QYT	24	10	7	7	58.3 ^a	4	11	9	83.3 ^a	4	12	8	83.3 ^a
AP+Tet	24	12	9	3	50.0 ^a	7	9	8	70.8 ^a	6	10	8	75.0 ^a
AP+VitE	24	11	7	6	54.2 ^a	6	11	7	75.0 ^a	5	11	8	79.2 ^a

^aP<0.01 vs AP+NS.

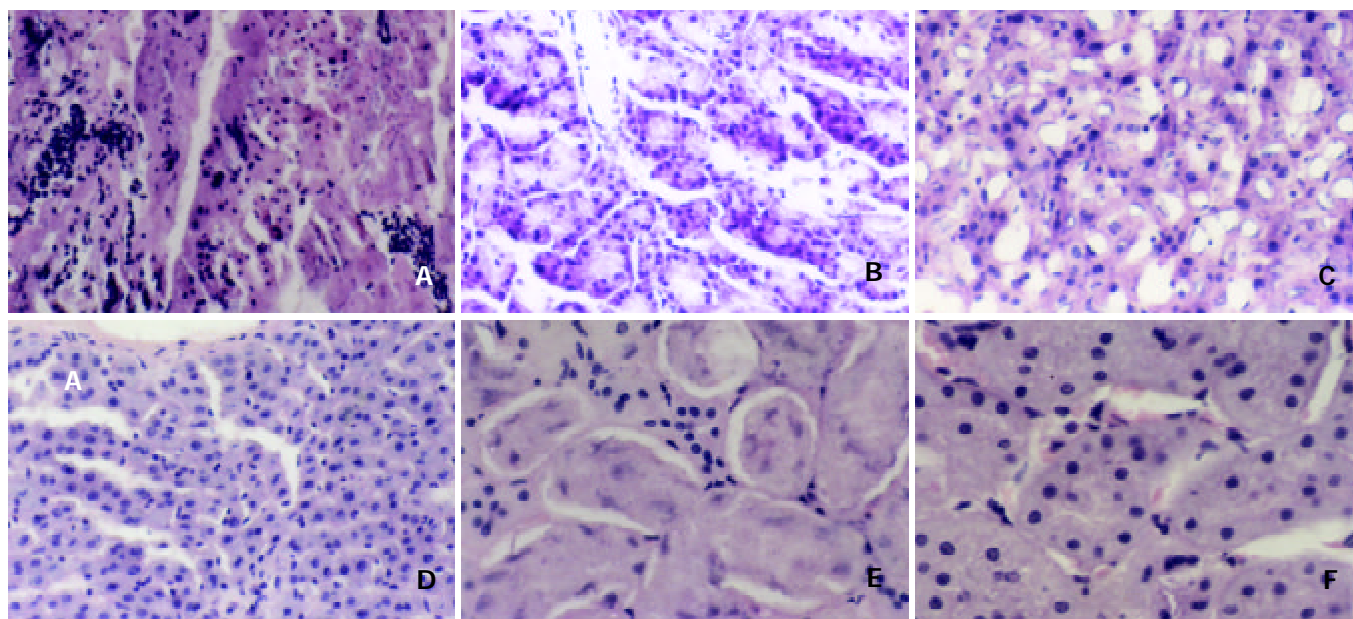


Figure 1 Histopathological findings in AP rats before and after treatment, HE stains. A: Morphological changes in pancreatic tissue of AP rats before treatment, $\times 200$. B: Morphological changes in pancreatic tissue of AP rats after treatment with QYT, $\times 200$. C: Morphological changes in hepatic tissue of AP rats before treatment, $\times 200$. D: Morphological changes in hepatic tissue of AP rats after treatment with VitE, $\times 200$. E: Morphological changes in renal tissue of AP rats before treatment, $\times 400$. F: Morphological changes in hepatic tissue of AP rats after treatment with Tet, $\times 400$.

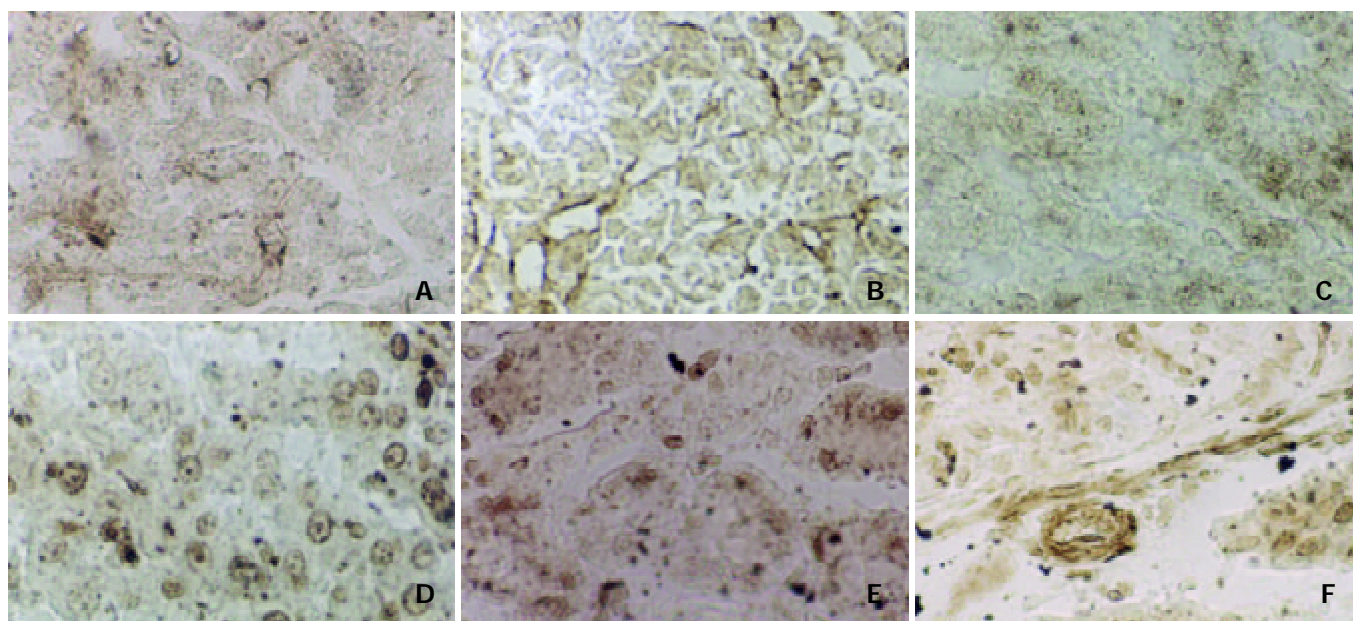


Figure 2 Enzyme histochemistry staining for intracellular Ca^{2+} - Mg^{2+} -ATPase in AP rats before and after treatment. A: Pancreatic tissue in AP rats before treatment, $\times 400$. B: Pancreatic tissue in AP rats after treatment with QYT, $\times 400$. C: Hepatic tissue in AP rats before treatment, $\times 200$. D: Hepatic tissue in AP rats after treatment with VitE, $\times 200$. E: Renal tissue in AP rats before treatment, $\times 400$. F: Renal tissue in AP rats after treatment with Tet, $\times 400$.

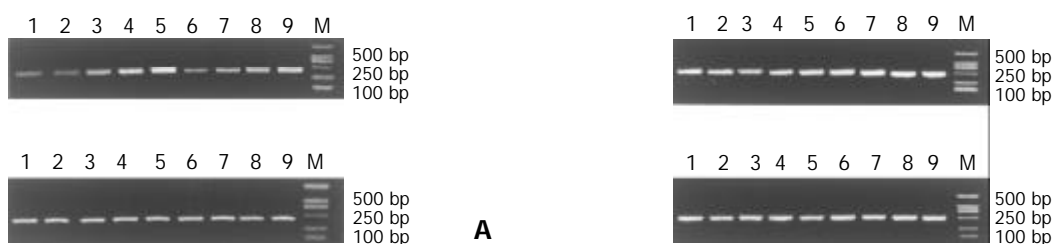


Figure 3 Expression of Ca^{2+} - Mg^{2+} -ATPase in AP rats before and after treatment analyzed by RT-PCR. A: Expression of Ca^{2+} - Mg^{2+} -ATPase mRNA in pancreatic tissue of different groups. B: Expression of Ca^{2+} - Mg^{2+} -ATPase mRNA in hepatic tissue of different groups. C: amplification product of GAPDH gene in pancreatic tissue of different groups. D: amplification product of GAPDH gene in hepatic tissue of different groups. Note: 1: AP 1 h, 2: AP 5 h, 3: QYT+AP 1 h, 4: QYT+AP 5 h, 5: Normal control group, 6: Tet+AP 1 h, 7: Tet+AP 5 h, 8: VitE+AP 1 h, 9: VitE+AP 5 h, M: PCR marker.

DISCUSSION

The level of intracellular free calcium (Ca²⁺) is not only dependent on the inflow of extracellular calcium through cell membrane and release from calcium reservoir inside the cell, but also on the function of Ca²⁺-Mg²⁺-ATPase on cell membrane and membrane of endoplasmic reticulum and mitochondria. By Ca²⁺-Mg²⁺-ATPase, Ca²⁺ could be pumped out of cell or into calcium reservoir. Thus Ca²⁺-Mg²⁺-ATPase could play an important role in intracellular calcium homeostasis^[7-9].

Activity and expression of intracellular Ca²⁺-Mg²⁺-ATPase in AP and its implication

Our experimental results showed that, in AP rats, the activity of Ca²⁺-Mg²⁺-ATPase in pancreatic, hepatic and renal tissues was decreased in AP rats. At the same time the pathological findings were aggravated. These results suggested that alteration of Ca²⁺-Mg²⁺-ATPase activity in AP might take part in the occurrence and progression of AP. It was reported that permeability of cell membrane was increased in AP. Ca²⁺ inflow might increase and lead to intracellular calcium overload. In the meantime, some stimulating factors could activate corresponding receptors on the surface of membrane to activate guanylate cyclation (GC). As a result, energy was released to cascade effector phospholipase C intracellular phosphatidylinositol diphosphate (PIP₂) into inositol triphosphate (IP₃) and diacylglycerol (DG). The IP₃ subsequently activated IP₃ receptors on endoplasmic reticulum to stimulate Ca²⁺ release from calcium reservoir. Consequently intracellular Ca²⁺ level increased abruptly. If the intracellular Ca²⁺-Mg²⁺-ATPase activity was decreased, Ca²⁺ could not be effectively pumped back into the reservoir or out of cells, which further aggravated intracellular calcium overload^[10,11]. Intracellular calcium overload further facilitated the release of pro-inflammatory mediators, which would cause strong contraction and thrombosis of microcirculation. Thus energy metabolism in tissues was disordered and ATP production was reduced^[12-16]. In addition, large quantities of free radicals produced during acute pancreatitis would cause phospholipids re-distribution in cell membrane. All of these factors might contribute to the inhibition of ATPase activity, which in turn would aggravate intracellular calcium overload. The vicious cycle occurred. Therefore, decrease of intracellular Ca²⁺-Mg²⁺-ATPase activity plays a key role in the development and aggravation of calcium overload.

In the present study, we found that activity of intracellular Ca²⁺-Mg²⁺-ATPase was decreased in hepatocyte of AP rat, but the expression of Ca²⁺-Mg²⁺-ATPase in the tissues did not change greatly. This finding suggested that intracellular Ca²⁺-Mg²⁺-ATPase activity was not only dependent on the level of its gene expression but also was affected by many other factors^[17-19].

Therapeutic effect and mechanism of QYT, Tet and VitE

Chinese medicine QYT is an effective compound in the treatment of AP. It has been proved to have bacteriostatic and anti-inflammatory effects, and to promote intestinal movement^[20,21]. Tet is a kind of bisbenzylisoquinoline alkaloid extracted from root tuber of *Stephania tetrandran*, a Chinese herbal medicine. It has been proved to be a natural non-selective calcium channel blocker^[22,23], and VitE has also been proved to be a scavenging agent of free radicals and blocker for lipid peroxidation^[24-27]. The present study found that in AP rats, intracellular Ca²⁺-Mg²⁺-ATPase activity in pancreatic, hepatic and renal tissues was increased after treatment with the above three medicines, and in pancreas the expression of Ca²⁺-Mg²⁺-ATPase was enhanced. Furthermore, pathological changes of hemorrhage and necrosis in the tissues were relieved. The complicating ascites and pleural effusion were improved^[28-34].

In summary, QYT, Tet and VitE have certain protecting effects on tissues and cells in AP, and the mechanisms are related with improved blood supply, increased intracellular Ca²⁺-Mg²⁺-ATPase activity and reduced intracellular calcium overload.

REFERENCES

- Weber H**, Roesner JP, Nebe B, Rychly J, Werner A, Schroder H, Jonas L, Leitzmann P, Schneider KP, Dummler W. Increased cytosolic Ca²⁺ amplifies oxygen radical induced alterations of the ultrastructure and the energy metabolism of isolated rat pancreatic acinar cells. *Digestion* 1998; **59**: 175-185
- Pu Q**, Yan L, Shen J. Effects of calcium overload in the conversion of acute edematous pancreatitis to necrotizing pancreatitis in rats. *Zhonghua Yixue Zazhi* 1999; **79**: 143-145
- Redondo Valdeolmillos M**, del Olmo Martinez ML, Almaraz Gomez A, Belmonte A, Coca MC, Caro-Paton Gomez A. The effects of an oral calcium overload on the rat exocrine pancreas. *Gastroenterol Hepatol* 1999; **22**: 211-217
- Rueda Chimento JC**, Ortega Medina L, Arguello de Andres JM, Landa Garcia JJ, Balibrea Cantero JL. Experimental acute pancreatitis in the rat. The quantification of pancreatic necrosis after the retrograde ductal injection of sodium taurocholate. *Rev Esp Enferm Dig* 1991; **80**: 178-182
- Tachibana T**, Nawa T. Ultrastructural localization of Ca(++)-ATPases in Meissner's corpuscle of the Mongolian gerbil. *Arch Histol Cytol* 1992; **55**: 375-379
- Gunteski-Hamblin AM**, Greeb J, Shull GE. A novel Ca²⁺ pump expressed in brain, kidney, and stomach is encoded by an alternative transcript of the slow-twitch muscle sarcoplasmic reticulum Ca-ATPase gene. Identification of cDNAs encoding Ca²⁺ and other cation-transporting ATPases using an oligonucleotide probe derived from the ATP-binding site. *J Biol Chem* 1988; **263**: 15032-15040
- Pariente JA**, Lajas AI, Pozo MJ, Camello PJ, Salido GM. Oxidizing effects of vanadate on calcium mobilization and amylase release in rat pancreatic acinar cells. *Biochem Pharmacol* 1999; **58**: 77-84
- Gorini A**, Villa RF. Effect of *in vivo* treatment of clonidine on ATP-ase's enzyme systems of synaptic plasma membranes from rat cerebral cortex. *Neurochem Res* 2001; **26**: 821-827
- Fu Y**, Wang S, Lu Z, Li H, Li S. Erythrocyte and plasma Ca²⁺, Mg²⁺ and cell membrane adenosine triphosphatase activity in patients with essential hypertension. *Chin Med J* 1998; **111**: 147-149
- Weber H**, Roesner JP, Nebe B, Rychly J, Werner A, Schroder H, Jonas L, Leitzmann P, Schneider KP, Dummler W. Increased cytosolic Ca²⁺ amplifies oxygen radical-induced alterations of the ultrastructure and the energy metabolism of isolated rat pancreatic acinar cells. *Digestion* 1998; **59**: 175-185
- Parkinson NA**, James AF, Hendry BM. Actions of endothelin-1 on calcium homeostasis in Madin-Darby canine kidney tubule cells. *Nephrol Dial Transplant* 1996; **11**: 1532-1537
- van Ooijen B**, Ouwendijk RJ, Kort WJ, Zijlstra FJ, Vincent JE, Wilson JH, Westbroek DL. Raised plasma thromboxane B₂ levels in experimental acute necrotizing pancreatitis in rats. The effects of flunarizine, dazoxiben, and indomethacin. *Scand J Gastroenterol* 1988; **23**: 188-192
- Xu H**, Shi AY. Effect of magnesium on postischemic reperfusion myocardial mitochondria. *Shengli Xuebao* 1996; **48**: 303-306
- Bassani RA**, Bassani JW, Lipsius SL, Bers DM. Diastolic SR Ca efflux in atrial pacemaker cells and Ca-overloaded myocytes. *Am J Physiol* 1997; **273**(2 Pt 2): H886-892
- He ZJ**, Matikainen MP, Alho H, Harmoinen A, Ahola T, Nordback I. Extraprostatic organ impairment in caerulein induced pancreatitis. *Ann Chir Gynaecol* 1999; **88**: 112-117
- Jiang XC**, D' Armiento J, Mallampalli RK, Mar J, Yan SF, Lin M. Expression of plasma phospholipid transfer protein mRNA in normal and emphysematous lungs and regulation by hypoxia. *J Biol Chem* 1998; **273**: 15714-15718
- Yokomori H**, Oda M, Kamegaya Y, Ogi M, Tsukada N, Ishii H. Bile canalicular contraction and dilatation in primary culture of rat hepatocytes-possible involvement of two different types of plasma membrane Ca (2+)-Mg(2+)-ATPase and Ca(2+)-pump-

- ATPase. *Med Electron Microsc* 2001; **34**: 115-122
- 18 **Ding J**, Wu Z, Crider BP, Ma Y, Li X, Slaughter C, Gong L, Xie XS. Identification and functional expression of four isoforms of ATPase II, the putative aminophospholipid translocase. Effect of isoform variation on the ATPase activity and phospholipid specificity. *J Biol Chem* 2000; **275**: 23378-23386
- 19 **Hansson A**, Willows RD, Roberts TH, Hansson M. Three semi-dominant barley mutants with single amino acid substitutions in the smallest magnesium chelatase subunit form defective AAA+ hexamers. *Proc Natl Acad Sci U S A* 2002; **99**: 13944-13949
- 20 **Wu C**, Li Z, Xiong D. An experimental study on curative effect of Chinese medicine Qingyitang in acute necrotizing pancreatitis. *Zhongguo Zhongxiyi Jiehe Zazhi* 1998; **18**: 236-238
- 21 **Deng Q**, Wu C, Li Z, Xiong D, Liang Y, Lu L, Sun X. The prevention of infection complicating acute necrotizing pancreatitis: an experimental study. *Zhonghua Waikexue* 2000; **38**: 625-629
- 22 **Xie QM**, Tang HF, Chen JQ, Bian RL. Pharmacological actions of tetrandrine in inflammatory pulmonary diseases. *Acta Pharmacol Sin* 2002; **23**: 1107-1113
- 23 **Wang B**, Xiao JG. Effect of tetrandrine on free intracellular calcium in cultured calf basilar artery smooth muscle cells. *Acta Pharmacol Sin* 2002; **23**: 1121-1126
- 24 **Christman JW**, Holden EP, Blackwell TS. Strategies for blocking the systemic effects of cytokines in the sepsis syndrome. *Crit Care Med* 1995; **23**: 955-963
- 25 **Jiang XC**, Tall AR, Qin S, Lin M, Schneider M, Lalanne F, Deckert V, Desrumaux C, Athias A, Witztum JL, Lagrost L. Phospholipid transfer protein deficiency protects circulating lipoproteins from oxidation due to the enhanced accumulation of vitamin E. *J Biol Chem* 2002; **277**: 31850-31856
- 26 **Prokop'eva NV**, Gulyaeva LF, Kolosova NG. Time course of malonic dialdehyde and alpha-tocopherol in rat pancreas during the first hours of acute pancreatitis. *Bull Exp Biol Med* 2000; **129**: 452-454
- 27 **Antosiewicz J**, Popinigis J, Ishiguro H, Hayakawa T, Wakabayashi T. Cerulein-induced acute pancreatitis diminished vitamin E concentration in plasma and increased in the pancreas. *Int J Pancreatol* 1995; **17**: 231-236
- 28 **Kempainen E**, Hietaranta A, Puolakkainen P, Sainio V, Halttunen J, Haapiainen R, Kivilaakso E, Nevalainen T. Bactericidal/permeability-increasing protein and group I and II phospholipase A2 during the induction phase of human acute pancreatitis. *Pancreas* 1999; **18**: 21-27
- 29 **Nevalainen TJ**, Gronroos JM, Kortesoja PT. Pancreatic and synovial type phospholipases A2 in serum samples from patients with severe acute pancreatitis. *Gut* 1993; **34**: 1133-1136
- 30 **Smirnov DA**. Acute pancreatitis and biological antioxidants. *Khirurgiia* 1994; **3**: 30-32
- 31 **Li ZL**, Wu CT, Lu LR, Zhu XF, Xiong DX. Traditional Chinese medicine Qingyitang alleviates oxygen free radical injury in acute necrotizing pancreatitis. *World J Gastroenterol* 1998; **4**: 357-359
- 32 **Wu CT**, Li ZL, Xiong DX. Relationship between enteric microecologic dysbiosis and bacterial translocation in acute necrotizing pancreatitis. *World J Gastroenterol* 1998; **4**: 242-245
- 33 **Ai J**, Gao HH, He SZ, Wang L, Luo DL, Yang BF. Effects of matrine, artemisinin, tetrandrine on cytosolic [Ca²⁺]_i in guinea pig ventricular myocytes. *Acta Pharmacol Sin* 2001; **22**: 512-515
- 34 **Lai JH**. Immunomodulatory effects and mechanisms of plant alkaloid tetrandrine in autoimmune diseases. *Acta Pharmacol Sin* 2002; **23**: 1093-1101

Edited by Zhu LH and Wang XL

Red oil A5 inhibits proliferation and induces apoptosis in pancreatic cancer cells

Mi-Lian Dong, Xian-Zhong Ding, Thomas E. Adrian

Mi-Lian Dong, Affiliated Taizhou Hospital, Wenzhou Medical College, Linhai 317000, Zhejiang Province, China

Xian-Zhong Ding, Thomas E. Adrian, Northwestern University Medical School, Chicago, IL60611-3008, U.S.A

Supported by the National Cancer Institute of USA, No. CA72712, and Special Funds for Zhejiang 151 Talent Project of China, No. 98-2095

Correspondence to: Mi-Lian Dong, Taizhou Hospital of Wenzhou Medical College, 150 Ximen Street, Linhai 317000, Zhejiang Province, China. mdong2@hotmail.com

Telephone: +86-576-5315829 **Fax:** +86-576-5315829

Received: 2003-06-04 **Accepted:** 2003-08-16

Abstract

AIM: To study the effect of red oil A5 on pancreatic cancer cells and its possible mechanisms.

METHODS: Effect of different concentrations of red oil A5 on proliferation of three pancreatic cancer cell lines, AsPC-1, MiaPaCa-2 and S2013, was measured by ³H-methyl thymidine incorporation. Time-dependent effects of 1:32 000 red oil A5 on proliferation of three pancreatic cancer cell lines, were also measured by ³H-methyl thymidine incorporation, and Time-course effects of 1:32 000 red oil A5 on cell number. The cells were counted by Z1-Coulter Counter. Flow-cytometric analysis of cellular DNA content in the control and red oil A5 treated AsPC-1, MiaPaCa-2 and S2013 cells, were stained with propidium iodide. TUNEL assay of red oil A5-induced pancreatic cancer cell apoptosis was performed. Western blotting of the cytochrome c protein in AsPC-1, MiaPaCa-2 and S2013 cells treated 24 hours with 1:32 000 red oil A5 was performed. Proteins in cytosolic fraction and in mitochondria fraction were extracted. Proteins extracted from each sample were electrophoresed on SDS-PAGE gels and then were transferred to nitrocellulose membranes. Cytochrome c was identified using a monoclonal cytochrome c antibody. Western blotting of the caspase-3 protein in AsPC-1, MiaPaCa-2 and S2013 cells treated with 1:32 000 red oil A5 for 24 hours was carried out. Proteins in whole cellular lysates were electrophoresed on SDS-PAGE gels and then transferred to nitrocellulose membranes. Caspase-3 was identified using a specific antibody. Western blotting of poly-ADP ribose polymerase (PARP) protein in AsPC-1, MiaPaCa-2 and S2013 cells treated with 1:32 000 red oil A5 for 24 hours was performed. Proteins in whole cellular lysates were separated by electrophoresis on SDS-PAGE gels and then transferred to nitrocellulose membranes. PARP was identified by using a monoclonal antibody.

RESULTS: Red oil A5 caused dose- and time-dependent inhibition of pancreatic cancer cell proliferation. Propidium iodide DNA staining showed an increase of the sub-G0/G1 cell population. The DNA fragmentation induced by red oil A5 in these three cell lines was confirmed by the TUNEL assay. Furthermore, Western blotting analysis indicated that cytochrome c was released from mitochondria to cytosol during apoptosis, and caspase-3 was activated following red oil A5 treatment which was measured by procaspase-3 cleavage and PARP cleavage.

CONCLUSION: These findings show that red oil A5 has potent anti-proliferative effects on human pancreatic cancer cells with induction of apoptosis *in vitro*.

Dong ML, Ding XZ, Adrian TE. Red oil A5 inhibits proliferation and induces apoptosis in pancreatic cancer cells. *World J Gastroenterol* 2004; 10(1): 105-111

<http://www.wjgnet.com/1007-9327/10/105.asp>

INTRODUCTION

Pancreatic cancer is one of the most enigmatic and aggressive malignant diseases^[1-4]. It is now the fourth leading cause of cancer death in both men and women in the USA and the incidence of this disease shows no sign of decline^[1-3,5]. Pancreatic cancer is characterized by a poor prognosis and lack of effective response to conventional therapy^[6]. The 5-year survival rate is less than 4% and the median survival period after diagnosis is less than 6 months^[7,8]. At present, surgical resection is still the only effective treatment option, but only about 15% of carcinomas of the head of pancreas are resectable and there are few long-term survivors even after apparent curative resection^[7,8]. On the other hand, chemotherapy or radiation therapy provide only limited palliation, without meaningful improvement of survival in patients with non-resectable pancreatic cancer^[7-9]. Only new therapeutic strategies can improve this dismal situation^[10,11].

A series of prospective and case-control studies have shown an association between higher fish intake and reduced cancer incidence, and other benefits including inhibition of cancer cell proliferation, induction of apoptosis^[12-22]. Recent studies indicate that diets containing a high proportion of long-chain n-3 polyunsaturated fatty acids was associated with inhibition of growth and metastasis of human cancer including pancreatic cancer^[12,14,23,24]. Diets rich in linoleic acid (LA), an n-6 fatty acid, stimulate the progression of human cancer cell in athymic nude mice, whereas supplement of fish oil components, docosahexaenoic acid (DHA) and eicosapentaenoic acid (EPA) exerts suppressive effects. Fish oil has been shown to reduce the induction of different cancer in animal models by a mechanism which may involve suppression of mitosis, increase apoptosis through long-chain n-3 polyunsaturated fatty acid EPA^[12,14,25-27]. In parallel, dietary supplementation with DHA is accompanied by reduced levels of 12- and 15-hydroxyeicosatetraenoic acids (12- and 15-HETE), suggesting that changes in eicosanoid biosynthesis may have been responsible for the observed decrease in tumor growth^[14,16,28,29]. Previous studies also have shown that the anti-cancer effect of fish oil is accompanied by a decreased production of cyclooxygenase and lipoyxygenase metabolites^[10,30,31]. The efficacy of fish oil which we have found exhibits particularly potent anticancer effects that appear to be related to its content of lipoyxygenase inhibitors rather than its EPA or DHA contents. Red oil A5 is lipid isolates from the epithelial layer of the echinoderm. This oil is non-toxic and exerts a marked anti-inflammatory effect in laboratory animals. Red oil A5 almost totally inhibits pancreatic cancer cell proliferation at dilutions

of up to 1:32 000. The inhibition of proliferation induced by this fish oil is accompanied by marked induction of apoptosis. To date, no information is available regarding the effects of red oil A5 in pancreatic cancer. In the present study, the effects of red oil A5 on proliferation, apoptosis and cell cycle distribution were investigated in pancreatic cancer cells.

MATERIALS AND METHODS

Pancreatic cancer cell lines

The human pancreatic cancer cell lines (AsPC-1, MiaPaCa-2 and S2013) were purchased from the American Type Culture Collection (Rockville, MD, USA). These cell lines span the types of differentiation in human pancreatic adenocarcinomas. AsPC-1 and MiaPaCa-2 are poorly-differentiated, whereas S2013 is well-differentiated but heterogenous.

The cells were cultured in Dulbecco's Modified Eagle's Medium (DMEM) (obtained from Sigma, St. Louis, MO) supplemented with penicillin G (100 U/mL), streptomycin (100 U/mL) and 10% Fetal Bovine Serum (FBS) (purchased from Atlanta Biologicals, Atlanta, GA) in humidified air with 5% CO₂ at 37 °C. The cells were harvested by incubation in trypsin-EDTA (obtained from Sigma, St. Louis, MO) solution for 10-15 minutes. Then the cells were centrifuged at ×300 g for 5 minutes and the cell pellets suspended in fresh culture medium prior to seeding into culture flasks or plates.

Red oil A5

Red oil A5 (Coastside Research Chemical Co.) was dissolved in 1:2 DMEM as a stock solution. The stock solution was diluted to the appropriate concentrations with serum-free medium prior to the experiments.

Cell proliferation assay

Cell proliferation was analyzed by the ³H-methyl thymidine (from Amersham Inc., Arlington Heights, IL) incorporation and cell counting. Following treatment of pancreatic cancer cells with a series of concentrations of red oil A5 from 1:64 000 to 1:4 000 for 24 hours, and following treatment of pancreatic cancer cells with 1:32 000 red oil A5 for 6, 12 and 24 hours, cellular DNA synthesis was assayed by adding ³H-methyl thymidine 0.5 μCi/well. After a 2 hour incubation, the cells were washed twice with PBS, precipitated with 10% TCA for two hours and solubilized from each well with 0.5 ml of 0.4 N sodium hydroxide. Incorporation of ³H-methyl thymidine into DNA was measured by adding scintillation cocktail and counting in a scintillation counter (LSC1414 WinSpectral, Wallac, Turku, Finland). For cell counting, the cells were seeded in 12-well plates and cultured in serum-free medium for 24 hours prior to red oil A5 treatment and then switched to serum-free medium with or without 1:32 000 red oil A5 for the respective treatment times (24, 48, 72 and 96 hours). The cells were removed from the plates by trypsinization to produce a single cell suspension for cell counting. The cells were counted using Z1-Coulter Counter (Luton, UK).

Analysis of cellular DNA content by flow cytometry

The cells were grown at 50%-60% confluence in T75 flasks, serum-starved for 24 hours and then treated with 1:32 000 red oil A5 for 24 hours. At the end of the treatment, the cells were harvested with trypsin-EDTA solution to produce a single cell suspension. The cells were then pelleted by centrifugation and washed twice with PBS. Then the cell pellets were suspended in 0.5 ml PBS and fixed in 5 mL ice-cold 70 % ethanol at 4 °C. The fixed cells were centrifuged at 300×g for 10 minutes and the pellets were washed with PBS. After resuspension with 1 ml PBS, the cells were incubated with 10 μL of RNase I (10 mg/mL) and 100 μL of propidium iodide (400 μg/mL; Sigma) and

shaken for 1 hour at 37 °C in the dark. Samples were analyzed by flow cytometry. The red fluorescence of single events was recorded using a laser beam at 488 nm excitation λ with 610 nm as emission λ, to measure the DNA index.

Terminal deoxynucleotidyl transferase-mediated deoxyuridine triphosphate nick-end labeling (TUNEL) assay

TUNEL assay kits were purchased from Pharmingen and PARP antibody from BioMol. The assay was carried out for terminal incorporation of fluorescein 12-dUTP by terminal deoxynucleotidyl transferase into fragmented DNA, in pancreatic cells. Cells grown in T75 flasks were cultured in serum-free conditions for 24 hours and then treated with or without 1:32 000 red oil A5 for 24 hours. The cells were then trypsinized and fixed in 1% ethanol-free formaldehyde-PBS for 15 minutes. The cells were incubated with the enzyme substrate mixture with the addition of 20 mM EDTA and then counterstained with 5 μg/mL propidium iodide in PBS containing 0.5 mg/mL DNase-free RNase A, in the dark for 30 minutes. Laser flow cytometry was used to quantify the green fluorescence of fluorescein-12-dUDP incorporated against the red fluorescence of propidium iodide.

Preparation of cytosolic and mitochondrial extraction

Mitochondria/Cytosol Fractionation Kit was purchased from BioVision (Mountain View, CA94043, USA). Cells (5×10⁷) were collected by centrifugation at 600×g for 5 minutes at 4 °C from control and red oil A5-treated AsPC-1, MiaPaCa-2 and S2013 cells. Wash the cells with ice-cold PBS twice. Centrifuge at 600×g for 5 minutes at 4 °C. Remove the supernatant and resuspend the cells with 1.0 mL of 1×Cytosol Extraction Buffer Mix containing DTT and Protease Inhibitors. Incubate on ice for 10 minutes. Homogenize the cells in an ice-cold dounce tissue grinder (45 strokes) until 70-80% of the nuclei do not have the shiny ring. Transfer the homogenate to a 1.5 mL microcentrifuge tube, and centrifuge at 700×g for 10 minutes at 4 °C. Transfer the supernatant to a fresh 1.5 mL tube, and centrifuge at 10 000×g for 30 minutes at 4 °C. Collect the supernatant as cytosolic fraction. Resuspend the pellet in 0.1 mL Mitochondrial Extraction Buffer Mix containing DTT and Protease inhibitors, vortex for 10 seconds and save as Mitochondrial Fraction. Both cytosolic fraction and mitochondrial fraction were stored at -80 °C until ready for Western blot.

Western blot

Cells were seeded into flasks and grown to 50% to 60% confluence for 24 hours. The cells were then placed in serum-free medium with or without 1:32 000 red oil A5 for a period of 24 hours. In the end, the attached cells and floating cells were extracted in lysis buffer [20 mM Tris-HCl (pH 7.4), 2 mM sodium vanadate, 1.0 mM sodium fluoride, 100 mM NaCl, 2.0 mM phosphate substrate, 1% NP40, 0.5% sodium deoxycholate, 20 μg/mL each aprotinin and leupeptin, 25.0 μg/mL pepstatin, and 2.0 mM each EDTA and EGTA] for further analysis. Protein concentrations were determined using the bicinchoninic acid assay with BSA as standard. Western blot was carried out using standard techniques. Briefly, equal amounts of proteins in each sample were resolved in 10% sodium dodecyl sulfate polyacrylamide gel electrophoresis (SDS-PAGE) and the proteins transferred onto nitrocellulose membranes. After blocking with non-fat dried milk, the membranes were incubated with the appropriate dilution of primary antibody (Santa Cruz Biotech, Santa Cruz, CA, USA). The membranes were then incubated with a horseradish peroxidase-conjugated secondary antibody. The proteins were detected by an enhanced chemiluminescence detection system (Santa Cruz Biotech), and light emission was captured on

Kodak X-ray films (Eastman Kodak Company, Rochester, NY). The rabbit polyclonal antibody against cytochrome c and caspase-3, and the mouse monoclonal antibody against PARP were also purchased from Santa Cruz Biotech.

Statistical analysis

The data was analyzed by analysis of variance (ANOVA) with Bonferonni's or Dunnet's multiple comparison post-test for significance between each two groups. This analysis was performed with the Prism software package (GraphPad, San Diego, CA, USA). The data were expressed as mean \pm SEM and represented at least 3 different experiments.

RESULTS

Effect of red oil A5 on thymidine incorporation in pancreatic cancer cells

Red oil A5 caused marked, concentration-dependent inhibition of thymidine incorporation in AsPC-1, MiaPaCa-2 and S2013 cells, at concentrations ranging from 1:64 000 to 1:4 000 (ANOVA, AsPC-1: $F(5,23)=86.99$, $P<0.0001$; MiaPaCa-2: $F(5,23)=92.63$, $P<0.0001$; S2013: $F(5,23)=94.94$, $P<0.0001$ (Figure 1). The red oil A5-induced inhibition of proliferation was also time-dependent (ANOVA, AsPC-1: $F(3,11)=89.88$, $P<0.0001$; MiaPaCa-2: $F(3,11)=53.64$, $P<0.0001$; S2013: $F(3,11)=80.06$, $P<0.0001$ (Figure 2).

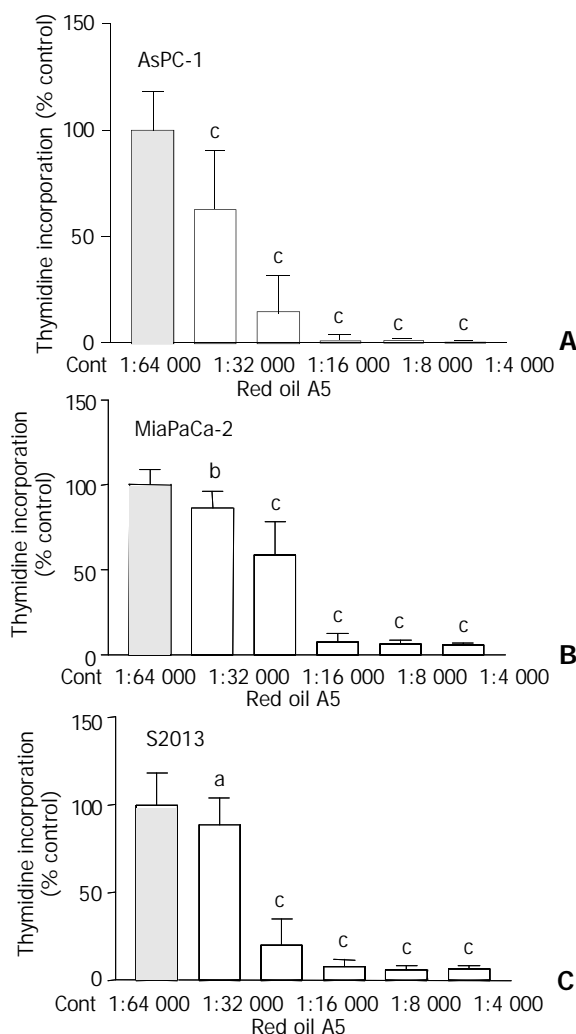


Figure 1 (A,B,C) Effect of different concentrations of red oil A5 on proliferation of three pancreatic cancer cell lines, AsPC-1, MiaPaCa-2 and S2013, as measured by ^3H -methyl thymidine incorporation. Results are expressed as % of control from three separate experiments. ^a $P<0.05$, ^b $P<0.01$, ^c $P<0.001$ vs control.

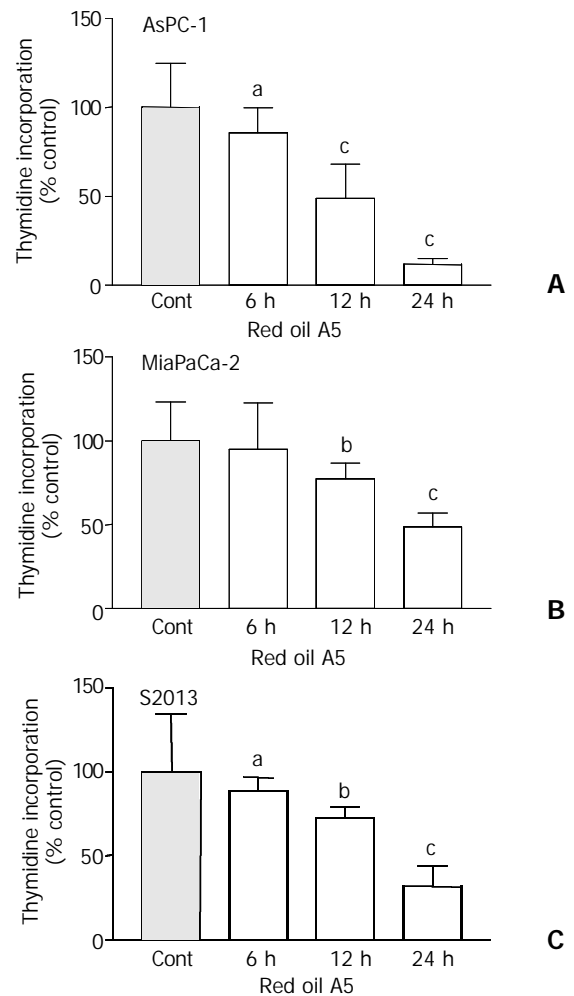


Figure 2 (A,B,C) Time-dependent effects of 1:32 000 red oil A5 on proliferation of three pancreatic cancer cell lines, AsPC-1, MiaPaCa-2 and S2013, as measured by ^3H -methyl thymidine incorporation at 6, 12 and 24 hours. The results are expressed as % of control from three separate experiments. ^a $P<0.05$, ^b $P<0.01$, ^c $P<0.001$ vs control.

Effect of red oil A5 on pancreatic cancer cell proliferation measured by cell counting

Red oil A5 induced significant time dependent inhibition of pancreatic cancer cell growth, as measured by the cell number in AsPC-1, MiaPaCa-2 and S2013 cells (two-way ANOVA, AsPC-1: $F(4,29)=49.54$, $P<0.0001$; MiaPaCa-2: $F(4,29)=43.48$, $P<0.0001$; S2013: $F(4,29)=39.25$, $P<0.0001$). During the first 24 hours, no obvious effects were seen compared to controls. At 48, 72, and 96 hours, red oil A5 resulted in a marked and progressive decrease in cell number compared to control (Figure 3).

Effect of red oil A5 on cell cycle phase distribution

To understand the mechanism of inhibition of cell proliferation, the distribution of cell cycle phases was analyzed following treatment with 1:32 000 red oil A5 for 24 hours. The cells were accumulated in the G2/M-phase in AsPC-1, MiaPaCa-2 and S2013 cell lines. The number of the cells in S-phase was increased also in all three cell lines when compared to control. A peak of the sub-G0/G1 cell population, a hallmark of apoptosis, was seen following 24 hours, exposure in all three cell lines (Figure 4).

Apoptosis of pancreatic cancer cells induced by red oil A5

To characterize the observed apoptosis, analysis of DNA fragmentation was carried out using the TUNEL assay. TUNEL staining of pancreatic cancer cells was markedly increased by 1:32 000 red oil A5 treatment for 24 hours (Figure 5).

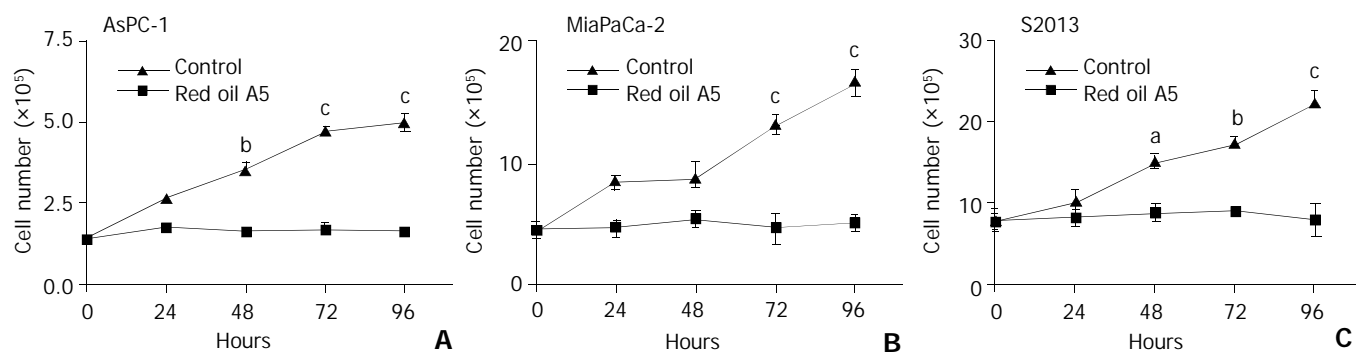


Figure 3 (A,B,C) Time-course effects of 1:32 000 red oil A5 on cell number in AsPC-1, MiaPaCa-2 and S2013 cells from 24 to 96 hours. The data represent mean \pm SEM of three separate experiments. ^a $P < 0.05$, ^b $P < 0.01$, ^c $P < 0.001$ vs control.

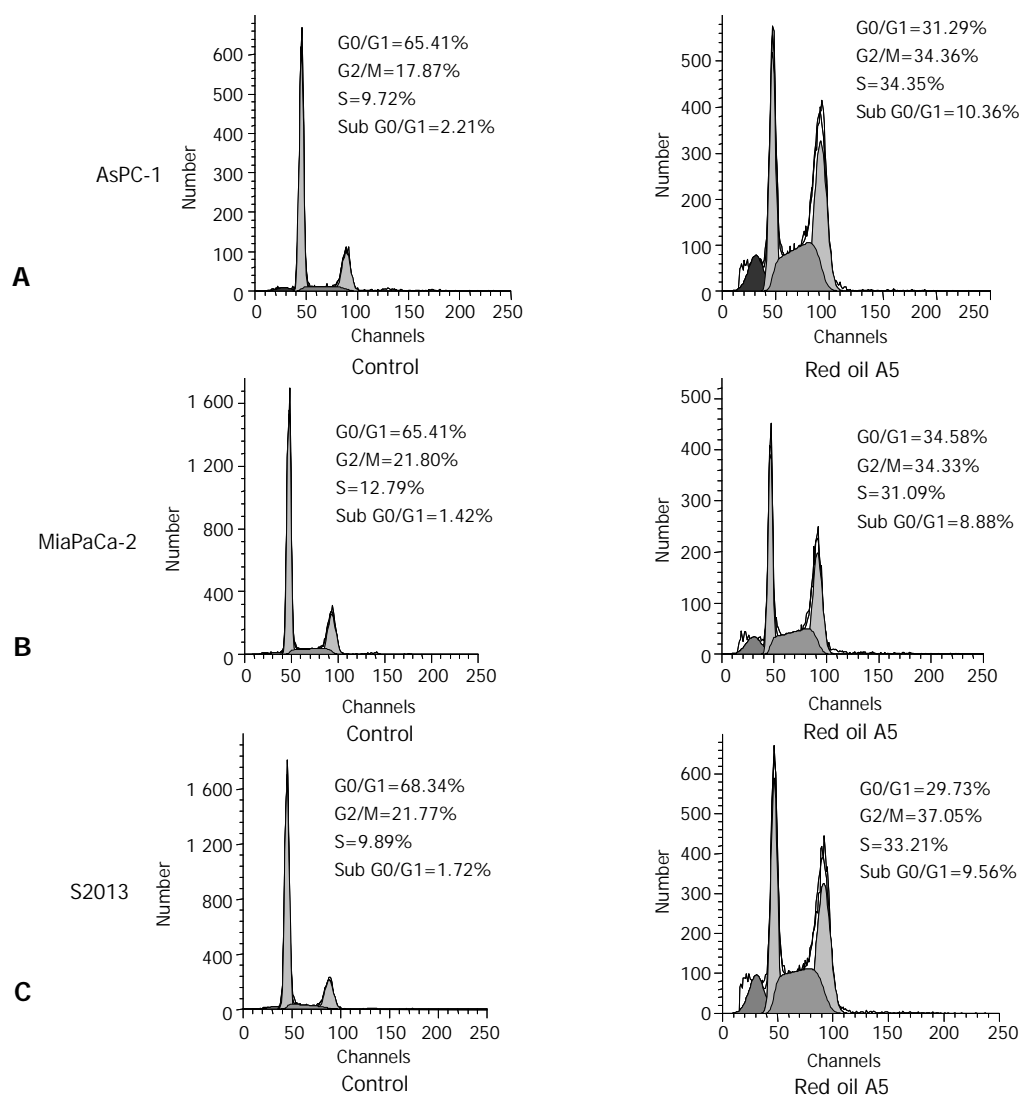


Figure 4 (A,B,C) Flow-cytometric analysis of cellular DNA content in control and red oil A5 treated AsPC-1, MiaPaCa-2 and S2013 cells, stained with propidium iodide. The cells were treated with 1:32000 red oil A5 in serum-free conditions for 24 hours. The distribution of cell cycle phases is expressed as % of total cells. Results were representative of three separate experiments.

Red oil A5 induced cytochrome C release

Cytochrome c is a mitochondrial protein that is released from the mitochondria to cytosol during apoptosis when mitochondrial membrane permeability is disrupted. An increase in the amount of cytochrome c in the cytosolic fraction was seen in all three cell lines, AsPC-1, MiaPaCa-2 and S2013 after red oil A5 treatment. Meanwhile, a decrease in the amount of cytochrome c in the mitochondrial fraction was seen in all three cell lines after red oil A5 treatment (Figure 6).

Effect of red oil A5 on activation of caspase-3 and cleavage of PARP

The expression and activation of caspase-3 by cleavage as well as the specific cleavage of its downstream substrate, PARP during apoptosis were observed by Western blotting. The 32 kDa procaspase-3 was cleaved into products of lower molecular weight, including a band corresponding to the 17 kDa active form. The uncleaved 116 kDa proform of PARP and its active 85 kDa cleaved fragment were detected. Both caspase-3

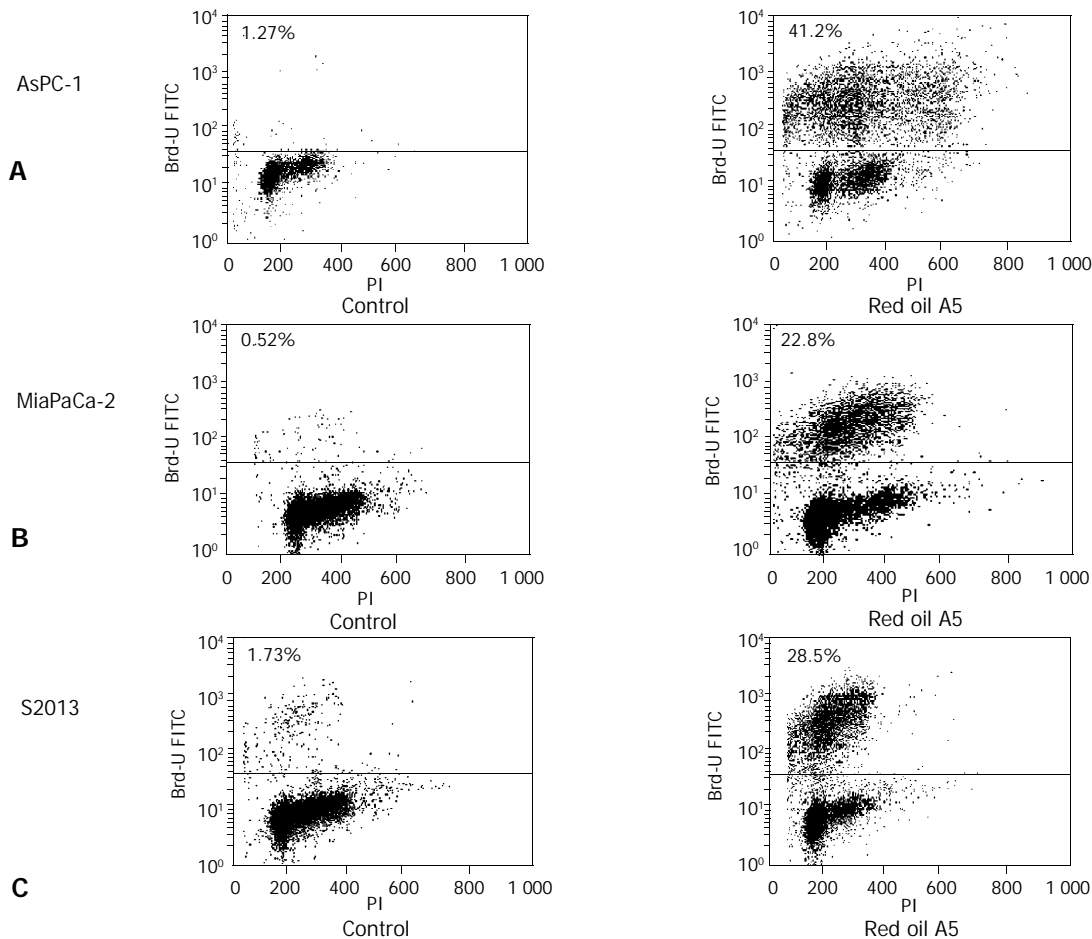


Figure 5 (A,B,C) TUNEL assay of red oil A5-induced pancreatic cancer cell apoptosis. Dot plot shows TdT-mediated dUTP nick-end labeling of control cells and cells treated with 1:32 000 red oil A5 which is expressed as % of total cells. The increases in fluorescence events in the upper panels are due to UTP labeling of fragmented DNA. The results are representative of three different experiments.

activation and PARP cleavage were induced and coincident with the induction of apoptosis (Figures 7, 8).

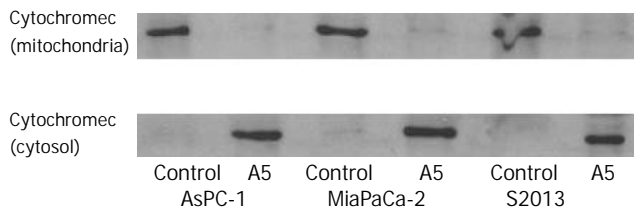


Figure 6 Western blot of the cytochrome c protein in AsPC-1, MiaPaCa-2 and S2013 cells treated with 1:32 000 red oil A5 for 24 hours. Proteins in cytosolic fraction and in mitochondrial fraction are extracted. Proteins extracted from each sample are electrophoresed on an SDS-PAGE gel and then are transferred to nitrocellulose membranes. Cytochrome c is identified using a monoclonal cytochrome c antibody. The results are representative of three different experiments.

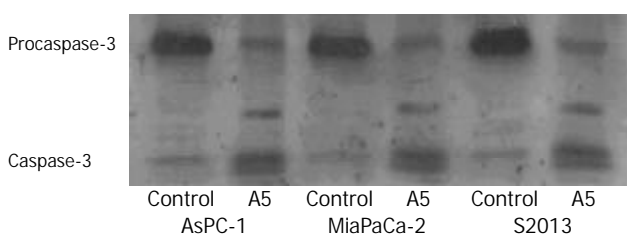


Figure 7 Western blot of the caspase-3 protein in AsPC-1, MiaPaCa-2 and S2013 cells are treated with 1:32 000 red oil A5

for 24 hours. Proteins in the whole cellular lysates are electrophoresed on an SDS-PAGE gel and then transferred to nitrocellulose membranes. Caspase-3 is identified using a specific antibody. The results are representative of three different experiments.

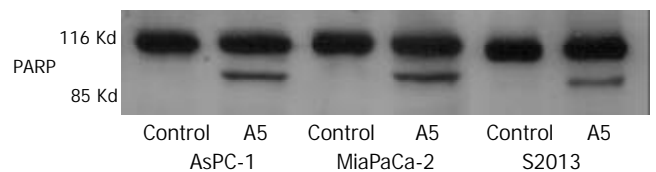


Figure 8 Western blot of poly-ADP ribose polymerase (PARP) protein in AsPC-1, MiaPaCa-2 and S2013 cells are treated with 1:32 000 red oil A5 for 24 hours. Proteins in whole cellular lysates are separated by electrophoresis on SDS-PAGE gels and then are transferred to nitrocellulose membranes. PARP is identified using a monoclonal antibody. The results are representative of three different experiments.

DISCUSSION

Because of its significant medical properties, fish oil has been used for many years. The experimental results in the present study indicate that red oil A5 inhibits proliferation and induces apoptosis in pancreatic cancer cells.

In preliminary experiments, we tested a series of concentrations of red oil A5 ranging from 1:64 000 to 1:4 000. At low concentrations, red oil A5 inhibited growth and induced apoptosis in a concentration-dependent and time-dependent manner in all three cell lines tested. Because 1:32 000 red oil

A5 inhibited ^3H -methyl thymidine incorporation into DNA by about 30%-50% in 24 hours, we tested this concentration on cell proliferation by cell counting over a longer time period (24 to 96 hours). The results revealed profound inhibition that was time-dependent.

To better understand the effect of red oil A5 on the proliferation of pancreatic cancer cells, flow cytometric analysis of propidium iodide-stained cells and TUNEL assay were carried out. Cytometric analysis showed that cells were accumulated in the G2/M-phase and S-phase in all three cell lines at 24 hours, compared to control. These cell cycle changes suggested that pancreatic cancer cells underwent an oxidative stress response to red oil A5, with DNA damage leading to apoptosis. Because the effects of red oil A5 persisted throughout the course of cell proliferation, cells with DNA damage increased progressively and developed apoptosis successively. Therefore, the sub-G0/G1 cell population typical of apoptosis was observed after 24-hour treatment with red oil A5. At the late stages of apoptosis, genomic DNA was cleaved in fragments following activation of endonucleases. The TUNEL assay used attachment of a fluorescent indicator to identify DNA fragments in apoptotic cells. The TUNEL assay results showed marked apoptosis in all the cell lines tested.

Red oil A5 induces cytochrome c release from the mitochondria to cytosol. Caspases are cysteine proteases produced as inactive forms and activated during apoptosis. Apoptosis in pancreatic cancer cells is mitochondria dependent as evidenced by release of cytochrome c into the cytosol^[32]. Caspases induce cytochrome c release from mitochondria by activating cytosolic factors^[33]. Once cytochrome c is released from the mitochondria, it complexes with apoptosis, apoptotic protease-activating factor 1 to activate caspase-3^[34-37]. Caspase-3 is the most important executor in the apoptotic process. Caspase-3 plays an important role in the apoptotic program of cells^[38-44]. The present experiment shows that caspase-3 is activated by cleavage of procaspase during apoptosis of pancreatic cancer cells induced by red oil A5. Furthermore red oil A5 also causes specific activation by cleavage of the caspase-3 substrate, PARP provides further evidence of apoptosis. PARP, a nuclear protein implicated in DNA repair, is one of the earliest proteins targeted for a specific cleavage to the signature 85-kDa fragment during apoptosis. PARP cleavage can serve as a sensitive parameter for identification of early apoptosis^[45,46].

Induction of cancer cell apoptosis, without affecting healthy cells or producing side-effects, is a major goal for development of new therapeutic agents. Our findings indicate that red oil A5 has a potent anti-proliferative effect on human pancreatic cancer cells with induction of apoptosis.

REFERENCES

- 1 **Blackstock AW**, Cox AD, Tepper JE. Treatment of pancreatic cancer: current limitations, future possibilities. *Oncology* 1996; **10**: 301-307
- 2 **Cameron JL**, Pitt HA, Yeo CJ, Lillemoe KD, Kaufman HS. One hundred and forty-five consecutive pancreaticoduodenotomies without mortality. *Ann Surg* 1993; **217**: 430-435
- 3 **Doll R**, Peto R. Mortality in relation to smoking: 20 years observations on male British doctors. *Br Med J* 1976; **2**: 1525-1536
- 4 **Abbruzzese JL**. Past and present treatment of pancreatic adenocarcinoma: chemotherapy as a standard treatment modality. *Semin Oncol* 2002; **29**(6 Suppl 20): 2-8
- 5 **Ozawa F**, Friess H, Tempia-Caliera A, Kleeff J, Buchler MW. Growth factors and their receptors in pancreatic cancer. *Teratog Carcinog Mutagen* 2001; **21**: 27-44
- 6 **Kleeff J**, Friess H, Berberat PO, Martignoni ME, Z' graggen K, Buchler MW. Pancreatic cancer—new aspects of molecular biology research. *Swiss Surg* 2000; **6**: 231-234
- 7 **Silverberg E**. Boring CC, Squires TS. Cancer Statistics, 1990. *CA Cancer J Clin* 1990; **40**: 9-26
- 8 **Hunstad DA**, Norton JA. Management of pancreatic carcinoma. *Surg Oncol* 1995; **4**: 61-74
- 9 **Neri B**, Cini G, Doni L, Fulignati C, Turrini M, Pantalone D, Mini E, De Luca Cardillo C, Fioreto LM, Ribocco AS, Moretti R, Scatizzi M, Zocchi G, Quattrone A. Weekly gemcitabine plus Epirubicin as effective chemotherapy for advanced pancreatic cancer: a multicenter phase II study. *Br J Cancer* 2002; **87**: 497-501
- 10 **Ding XZ**, Tong WG, Adrian TE. Cyclooxygenases and lipoxygenases as potential targets for treatment of pancreatic cancer. *Pancreatol* 2001; **1**: 291-299
- 11 **Su Z**, Lebedeva IV, Gopalkrishnan RV, Goldstein NI, Stein CA, Reed JC, Dent P, Fisher PB. A combinatorial approach for selectively inducing programmed cell death in human pancreatic cancer cells. *Proc Natl Acad Sci U S A* 2001; **98**: 10332-10337
- 12 **Fay MP**, Freedman LS, Clifford CK, Midthune DN. Effect of different types and amounts of fat on the development of mammary tumors in rodents: a review. *Cancer Res* 1997; **57**: 3979-3988
- 13 **Ravichandran D**, Cooper A, Johnson CD. Effect of lithium gamma-linolenate on the growth of experimental human pancreatic carcinoma. *Br J Surg* 1998; **85**: 1201-1205
- 14 **Hawkins RA**, Sangster K, Arends MJ. Apoptotic death of pancreatic cancer cells induced by polyunsaturated fatty acids varies with double bond number and involves an oxidative mechanism. *J Pathol* 1998; **185**: 61-70
- 15 **Ravichandran D**, Cooper A, Johnson CD. Growth inhibitory effect of lithium gammalinolenate on pancreatic cancer cell lines: the influence of albumin and iron. *Eur J Cancer* 1998; **34**: 188-192
- 16 **Falconer JS**, Ross JA, Fearon KC, Hankins RA, O' Riordain MG, Carter DC. Effect of eicosapentaenoic acid and other fatty acids on the growth *in vitro* of human pancreatic cancer cell lines. *Br J Cancer* 1994; **69**: 826-832
- 17 **Clerc P**, Bensaadi N, Pradel P, Estival A, Clemente F, Vaysse N. Lipid-dependent proliferation of pancreatic cancer cell lines. *Cancer Res* 1991; **51**: 3633-3638
- 18 **Tisdale MJ**. Inhibition of lipolysis and muscle protein degradation by EPA in cancer cachexia. *Nutrition* 1996; **12**(1 Suppl): S31-33
- 19 **Barber MD**, Ross JA, Voss AC, Tisdale MJ, Fearon KC. The effect of an oral nutritional supplement enriched with fish oil on weight-loss in patients with pancreatic cancer. *Br J Cancer* 1999; **81**: 80-86
- 20 **Von Hoff DD**, Bearss D. New drugs for patients with pancreatic cancer. *Curr Opin Oncol* 2002; **14**: 621-627
- 21 **Barber MD**, Fearon KC, Tisdale MJ, McMillan DC, Ross JA. Effect of a fish oil-enriched nutritional supplement on metabolic mediators in patients with pancreatic cancer cachexia. *Nutr Cancer* 2001; **40**: 118-124
- 22 **Tang DG**, La E, Kern J, Kehrer JP. Fatty acid oxidation and signaling in apoptosis. *Biol Chem* 2002; **383**: 425-442
- 23 **Hawkins RA**, Sangster K, Arends MJ. Apoptotic death of pancreatic cancer cells induced by polyunsaturated fatty acids varies with double bond number and involves an oxidative mechanism. *J Pathol* 1998; **185**: 61-70
- 24 **Huang PL**, Zhu SN, Lu SL, Dai ZS, Jin YL. Inhibitor of fatty acid synthase induced apoptosis in human colonic cancer cells. *World J Gastroenterol* 2000; **6**: 295-297
- 25 **Calviello G**, Palozza P, Franceschelli P, Frattucci A, Piccioni E, Tessitore L, Bartoli GM. Eicosapentaenoic acid inhibits the growth of liver preneoplastic lesions and alters membrane phospholipid composition and peroxisomal beta-oxidation. *Nutr Cancer* 1999; **34**: 206-212
- 26 **Bartsch H**, Nair J, Owen RW. Dietary polyunsaturated fatty acids and cancers of the breast and colorectum: emerging evidence for their role as risk modifiers. *Carcinogenesis* 1999; **20**: 2209-2218
- 27 **Lai PB**, Ross JA, Fearon KC, Anderson JD, Carter DC. Cell cycle arrest and induction of apoptosis in pancreatic cancer cells exposed to eicosapentaenoic acid *in vitro*. *Br J Cancer* 1996; **74**: 1375-1383
- 28 **Karmali RA**, Donner A, Gobel S, Shimamura T. Effect of n-3 and n-6 fatty acids on 7, 12 dimethylbenz anthracene-induced mammary tumorigenesis. *Anticancer Res* 1989; **9**: 1161-1167
- 29 **Rose DP**, Connolly JM. Antiangiogenicity of docosahexaenoic acid and its role in the suppression of breast cancer cell growth in nude mice. *Int J Oncol* 1999; **15**: 1011-1015
- 30 **Larsen LN**, Hovik K, Bremer J, Holm KH, Myhren F, Borretzen B. Heneicosapentaenoate (21: 5n-3): its incorporation into lipids

- and its effects on arachidonic acid and eicosanoid synthesis. *Lipids* 1997; **32**: 707-714
- 31 **Noguchi M**, Earashi M, Minami M, Kinoshita K, Miyazaki I. Effects of eicosapentaenoic and docosahexaenoic acid on cell growth and prostaglandin E and Leukotriene B production by a human breast cancer cell line (MDA-MB-231). *Oncology* 1995; **52**: 458-464
- 32 **Qanungo S**, Basu A, Das M, Haldar S. 2-Methoxyestradiol induces mitochondria dependent apoptotic signaling in pancreatic cancer cells. *Oncogene* 2002; **21**: 4149-4157
- 33 **Bossy-Wetzel E**, Green DR. Caspases induce cytochrome c release from mitochondria by activating cytosolic factors. *J Biol Chem* 1999; **274**: 17484-17490
- 34 **Tong WG**, Ding XZ, Witt RC, Adrian TE. Lipoxygenase inhibitors attenuate growth of human pancreatic cancer xenografts and induce apoptosis through the mitochondrial pathway. *Mol Cancer Ther* 2002; **1**: 929-935
- 35 **Gerhard MC**, Schmid RM, Hacker G. Analysis of the cytochrome c-dependent apoptosis apparatus in cells from human pancreatic carcinoma. *Br J Cancer* 2002; **86**: 893-898
- 36 **Mouria M**, Gukovskaya AS, Jung Y, Buechler P, Hines OJ, Reber HA, Pandol SJ. Food-derived polyphenols inhibit pancreatic cancer growth through mitochondrial cytochrome C release and apoptosis. *Int J Cancer* 2002; **10**: 761-769
- 37 **Kluck RM**, Bossy-Wetzel E, Green DR, Newmeyer DD. The release of cytochrome c from mitochondria: a primary site for Bcl-2 regulation of apoptosis. *Science* 1997; **275**: 1132-1136
- 38 **Thornberry NA**, Lazebnik Y. Caspase: enemies within. *Science* 1998; **281**: 1312-1316
- 39 **Mancini M**, Nicholson DW, Roy S, Thornberry NA, Peterson EP, Casciola-Rosen LA, Rosen A. The caspase-3 precursor has a cytosolic and mitochondrial distribution: implications for apoptotic signaling. *J Cell Biol* 1998; **140**: 1485-1495
- 40 **Kothakota S**, Azuma T, Reinhard C, Klippel A, Tang J, Chu K, McGarry TJ, Kirschner MW, Kohts K, Kwiatkowski DJ, Williams LT. Caspase-3-generated fragment of gelsolin: effector of morphological change in apoptosis. *Science* 1997; **278**: 294-298
- 41 **Kobayashi D**, Sasaki M, Watanabe N. Caspase-3 activation downstream from reactive oxygen species in heat-induced apoptosis of pancreatic carcinoma cells carrying a mutant p53 gene. *Pancreas* 2001; **22**: 255-260
- 42 **Virkajarvi N**, Paakko P, Soini Y. Apoptotic index and apoptosis influencing proteins bcl-2, mcl-1, bax and caspases 3, 6 and 8 in pancreatic carcinoma. *Histopathology* 1998; **33**: 432-439
- 43 **Pirocanac EC**, Nassirpour R, Yang M, Wang J, Nardin SR, Gu J, Fang B, Moossa AR, Hoffman RM, Bouvet M. Bax-induction gene therapy of pancreatic cancer. *J Surg Res* 2002; **106**: 346-351
- 44 **Kirsch DG**, Doseff A, Chau BN, Lim DS, de Souza-Pinto NC, Hansford R, Kastan MB, Lazebnik YA, Hardwick JM. Caspase-3-dependent cleavage of Bcl-2 promotes release of cytochrome c. *J Biol Chem* 1999; **274**: 21155-21161
- 45 **Decker P**, Isenberg D, Muller S. Inhibition of caspase-3-mediated poly (ADP-ribose) polymerase (PARP) apoptotic cleavage by human PARP autoantibodies and effect on cells undergoing apoptosis. *J Biol Chem* 2000; **275**: 9043-9046
- 46 **Sellers WR**, Fisher DE. Apoptosis and cancer drug targeting. *J Clin Invest* 1999; **104**: 1655-1661

Edited by Wu XN

Transfection of mEpo gene to intestinal epithelium *in vivo* mediated by oral delivery of chitosan-DNA nanoparticles

Jing Chen, Wu-Li Yang, Ge Li, Ji Qian, Jing-Lun Xue, Shou-Kuan Fu, Da-Ru Lu

Jing Chen, Ge Li, Ji Qian, Jing-Lun Xue, Da-Ru Lu, State Key Laboratory of Genetic Engineering, Institute of Genetics, School of Life sciences, Fudan University, Shanghai 200433, China

Wu-Li Yang, Shou-Kuan Fu, The Key Laboratory of Molecular Engineering of Polymers under Ministry of Education, Department of Macromolecular Science, Fudan University, Shanghai, 200433, China
Supported by the State High Technology Development Program 863 (2001AA217181), the National Natural Science Foundation of China (No.50233030), Foundation of Doctor Degree Thesis from Ministry of Education (199925), Encourage Project of Teaching and Research of University Excellent Youth Teacher, and the Youth Foundation of Fudan University

Correspondence to: Dr. Da-Ru Lu, State Key Laboratory of Genetic Engineering, Institute of Genetics, School of Life Sciences, Fudan University, Shanghai 200433, China. drlu@fudan.edu.cn

Telephone: +86-21-65642424 **Fax:** +86-21-65642799

Received: 2003-05-12 **Accepted:** 2003-06-19

Abstract

AIM: To prepare the chitosan-pmEpo nanoparticles and to study their ability for transcellular and paracellular transport across intestinal epithelia by oral administration.

METHODS: ICR mice were fed with recombinant plasmid AAV-tetO-CMV-mEpo (containing mEpo gene) or pCMV β (containing LacZ gene), whether it was wrapped by chitosan or no. Its size and shape were observed by transmission electron microscopy. Agarose gel electrophoresis was used to assess the efficiency of encapsulation and stability against nuclease digestion. Before and after oral treatment, blood samples were collected by retro-orbital puncture, and hematocrits were used to show the physiological effect of mEpo.

RESULTS: Chitosan was able to successfully wrap the plasmid and to protect it from DNase degradation. Transmission electron microscopy showed that freshly prepared particles were approximately 70-150 nm in size and fairly spherical. Three days after fed the chitosan-pCMV β complex was fed, the mice were killed and most of the stomach and 30% of the small intestine were stained. Hematocrit was not modified in naive and 'naked' mEpo-fed mice, a rapid increase of hematocrit was observed during the first 4 days of treatment in chitosan-mEpo-fed animals, reaching $60.9 \pm 1.2\%$ ($P < 0.01$), and sustained for a week. The second feed (6 days after the first feed) was still able to promote a second hematocrit increase in chitosan-mEpo-fed animals, reaching $65.9 \pm 1.4\%$ ($P < 0.01$), while the second hematocrit increase did not appear in the 'naked' mEpo-second-fed mice.

CONCLUSION: Oral chitosan-DNA nanoparticles can efficiently deliver genes to enterocytes, and may be used as a useful tool for gene transfer.

Chen J, Yang WL, Li G, Qian J, Xue JL, Fu SK, Lu DR. Transfection of mEpo gene to intestinal epithelium *in vivo* mediated by oral delivery of chitosan-DNA nanoparticles. *World J Gastroenterol* 2004; 10(1): 112-116

<http://www.wjgnet.com/1007-9327/10/112.asp>

INTRODUCTION

The oral delivery of peptide, protein, vaccine and nucleic acid-based biotechnology products is the greatest challenge facing the drug delivery industry. Oral delivery is most attractive due to easy administration, leading to improved convenience and compliance to patients, thereby reducing the overall healthcare cost. Gene therapy will provide a huge new therapeutic opportunity, and has stimulated an interest in oral gene delivery. To date, various methods have been used for oral gene therapy, such as cationic lipids, recombinant viruses, recombinant live bacteria, polymers, and particle bombardment to buccal mucosa^[1-3].

Chitosan is a natural biodegradable mucoadhesive polysaccharide derived from crustacean shells, and a biocompatible polymer that has been widely used in controlled drug delivery^[4-9], and it may provide a less immunogenic and non-toxic carrier for successful oral delivery of plasmid DNA. Complex coacervates of DNA and chitosan could be used as a delivery vehicle in gene therapy and vaccine design^[10-12], and have been shown to increase transcellular and paracellular transport of macromolecules across intestinal epithelial monolayers^[13-15], further indicative of its potential in oral gene delivery.

Erythropoietin is a glycoprotein, which stimulates red blood cell production. It is produced in the kidney and stimulates the division and differentiation of committed erythroid progenitors in the bone marrow. When the kidney function decreases, anemia or low red blood cells are developed. Erythropoietin is used in patients with anemia associated with chronic renal failure, and in cancer patients for stimulation of erythropoiesis during autologous transfusion. Erythropoietin is also a good reporter gene in gene therapy study *in vivo*, because obvious biological effect can be observed even in a low dose of it. Hormones of therapeutic interest like growth hormone and erythropoietin require a tight adjustment of dose delivery to prevent adverse effects. Since most of the physiological regulatory processes are difficult to transfer to engineered cells, transgene expression must rely on artificial regulatory systems. Artificial inducible expression systems use transcriptional stimulation by chimeric transactivating factors, the activity of which can be controlled by drugs such as tetracycline derivatives^[16], mifepristone^[17], ecdysone^[18], or rapamycin^[19]. Heard observed that retrovirus-engineered myoblasts expressing rtTA and the chimeric transactivator conferring doxycycline-inducible gene expression, could be stably engrafted in mice, thus allowing the long-term control of Epo secretion *in vivo*^[20]. Here we reported the oral gene therapy using chitosan-DNA nanoparticles carrying murine Epo (mEpo driven by tetO-CMV and rtTA) and LacZ, and demonstrated their efficacy in delivering genes to enterocytes.

MATERIALS AND METHODS

Materials

Chitosan (molecular weight, about 300 000Da) was supplied by Shandong Luneng Chemical Company. Plasmid pCMV β was purchased from Clontech. mEpo was a gift from Jean

Michel Heard (MD, Laboratoire Re´trovirus et Transfert Ge´ne´tique, Institut Pasteur, Paris, France). A 630 bp DNA fragment containing the murine Epo coding sequence was inserted between tetO-CMV promoter and 5' end of the SV40 polyadenylation signal puHD10.3^[21]. An expression cassette for the reverse transactivator (rtTA) chimeric protein^[16] was inserted into the SV40 polyadenylation signal in reverse orientation. This cassette contains a 1 858 bp fragment of the MFG retroviral vector^[22] encompassing the 5' LTR and *gag* intronic sequences, followed by an 1 020 bp of the rtTA coding sequence.

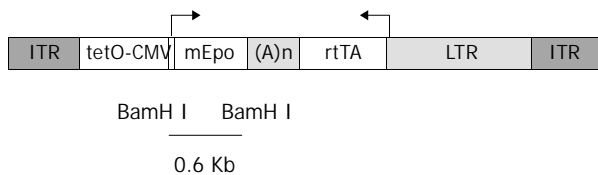


Figure 1 Structure of rAAV-ET vector. ITR: AAV-2 inverted terminal repeats, tetO-CMV: tetracycline-inducible promoter including seven repeats of the tetracycline operator inserted upstream of the CMV minimal promoter, mEpo: murine erythropoietin cDNA, (A)n: SV40 bidirectional polyadenylation signal, rtTA: coding sequences for the tetracycline reverse transactivator, LTR: long terminal repeat of the MFG retrovirus construct. The BamHI fragment used as an Epo-specific probe is indicated.

The construction was then constructed into the pSUB-201 AAV vector plasmid, giving rise to pAAV-ET, with a total length of 5 017 bp (Figure 1). Plasmid was purified by CsCl super centrifugation.

Nanoparticle formulation

Nanoparticles were made by complex coacervation of chitosan and DNA as reported^[12]. Plasmid (10 µg) was added to 100 µl of 50 mM sodium sulfate and heated to 55 °C. Chitosan (pH 5.7, 0.02% in a 25 mM sodium acetate-acetic acid buffer) was also heated to 55 °C and 100 µl of chitosan was added to the DNA–sodium sulfate solution while samples were vortexed at a high speed for 20 s. Complex particles were examined immediately and stored at room temperature.

Measurement of nanoparticle size and morphology

Transmission electron microscopy (TEM, Hitachi HU-11B) was used to determine the particle size and morphology. A drop of particle dispersion was placed on a carbon-coated copper grid, and the particle size was determined from the micrographs.

DNase degradation test

Agarose gel electrophoresis was performed in a 1% (w:v) gel, ethidium bromide included for visualization, for 2 h at 60V. To assess the efficiency of encapsulation and stability against nuclease digestion, uncomplexed plasmid DNA (1 µg) and chitosan-DNA complex (containing 1 µg plasmid) were incubated with 1 mU DNaseI per µg of DNA for 1 h at 37 °C. Adding EDTA stopped the reaction. Then the undegraded (1 µg) and degraded plasmid, undegraded and degraded chitosan-DNA complex, were subjected to agarose gel electrophoresis as described above.

Gene expression and animal experiments

ICR mice (4-week-old, purchased from BK Company, Shanghai) were fed with either chitosan–DNA nanoparticles containing the LacZ gene (pCMVβ, 50 µg/mice) or ‘naked’ plasmid DNA (pCMVβ), using animal feeding needles. Three

days later, the mice were killed, with their stomachs and small intestines surgically removed. The whole tissues were stained with 4-chloro-5-bromo-3-indolyl-β-galactoside (X-Gal) according to standard protocols. After stained overnight in a humidified chamber, the tissues were photographed by a digital camera (Nikon CoolPIX995). The pictures were transferred into a computer and adjusted for equal brightness and contrast using Adobe Photoshop.

ICR mice were fed every week with either chitosan–DNA nanoparticles containing the mEpo gene (50 µg/mice) or ‘naked’ plasmid DNA using animal feeding needles. Doxycycline-HCl (Sigma, Saint-Quentin Fallavier, France) was dissolved in drinking water to a final concentration of 200 µg/mL with 5% sucrose. No obvious side effect was observed in animals. Hematocrit was measured every two days by collecting 40 µL of blood via retro-orbital puncture before and after feeding.

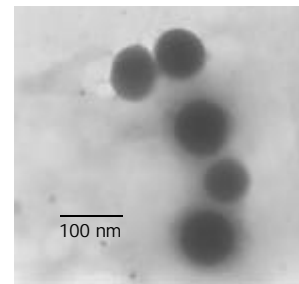


Figure 2 Measurement of microsphere size and morphology. Transmission electron micrographs of chitosan–DNA nanoparticles, and scale bar represents 100 nm.

Statistical analysis

Results of quantitative data in hematocrit analysis were expressed as mean ±SD, statistical differences between groups were tested with F-test, and the significant level was defined as a $P < 0.01$. The data were analyzed by SPSS statistical software.

RESULTS

Nanoparticle synthesis and characterization

We synthesized nanoparticles by complexing high-molecular-weight (about 300 000Da) chitosan with plasmid DNA, and obtained the particles by adding 0.02% chitosan, pH 5.7, at 55 °C to plasmid DNA (50 µg/ml in 50 mM sodium sulfate) during high-speed vortexing. Transmission electron microscopy showed that freshly prepared particles were approximately 70–150 nm in size and fairly spherical (Figure 2). The encapsulation efficiency was higher than 98 %, and the complex could efficiently protect the plasmid from DNase degradation (Figure 3).

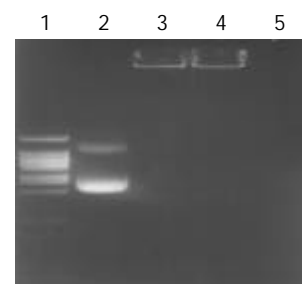


Figure 3 Determination of encapsulation efficiency, and DNase degradation test. Line 1. DNA ladder, Line 2. undegraded pCMVβ (1 µg), Line 3. undegraded chitosan-DNA complex (containing plasmid 1 µg), Line 4. degraded chitosan-DNA complex (containing plasmid 1 µg), Line 5. degraded plasmid (1 µg).

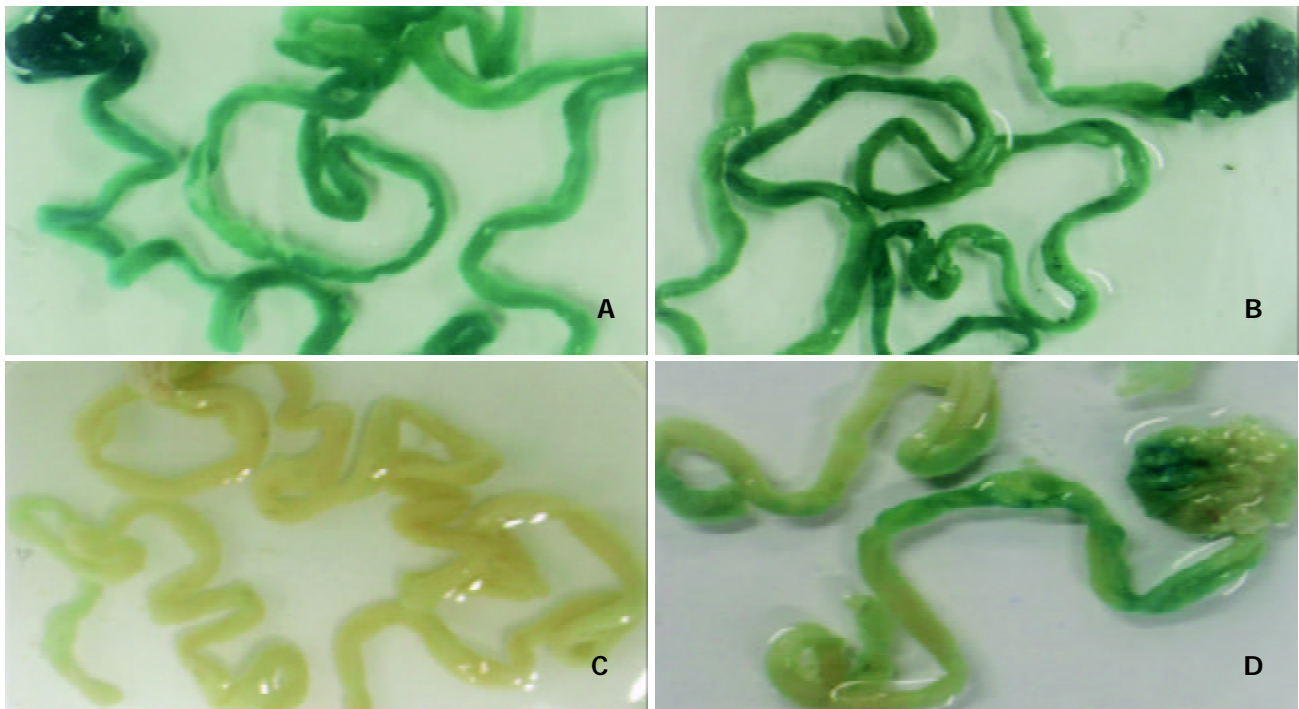


Figure 4 β -galactosidase expression in mouse stomach and small intestine 3 days after oral delivery of DNA nanoparticles. A-D: Whole tissue staining for LacZ, only stained sections are shown. The mice were fed with high-molecular-weight chitosan-pCMV β nanospheres at a dose of 50 μ g (A) or 100 μ g (B) per mouse, PBS (C) or 'naked' DNA (pCMV β , D).

Gene expression studies

To assess the expression and distribution of transduced genes after oral DNA delivery, we fed ICR mice with either chitosan-DNA nanoparticles containing the LacZ gene (pCMV β) or 'naked' plasmid DNA (pCMV β), and then determined the expression of bacterial β -galactosidase (LacZ) in the stomach and small intestine 3 days after oral administration of DNA (Figures 4A-D). Most of the whole small intestines and stomachs were stained. Although naive mice and those fed with 'naked' DNA showed some background staining, mice fed nanoparticles showed a higher level of gene expression both in stomachs and in small intestines.

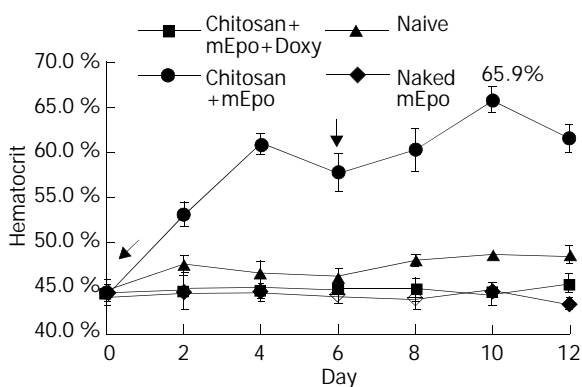


Figure 5 mEpo expression and its physiological effect test. Hematocrit was measured every two days in mice fed with (●) chitosan-mEpo and doxycycline (200 μ g/mL), $n=9$; (▲) chitosan-mEpo alone, $n=3$; (◆) doxycycline (200 μ g/mL) alone, $n=4$; (■) naked mEpo and doxycycline (200 μ g/mL), $n=5$. ↓ indicating the mice fed with 'naked' mEpo DNA or chitosan-Epo.

mEpo expression and its physiological effect

Hematocrit was measured every two days in mice that were fed with 'naked' mEpo DNA, chitosan-mEpo and doxycycline-HCl or not (Figure 5). To assess the basal Epo secretion level, three animals were fed with chitosan-mEpo and not treated

with doxycycline, and their hematocrit remained 45%-48%. Doxycycline (200 μ g/mL) was added to drinking water for naive ($n=4$), 'naked' mEpo-fed mice ($n=5$), and chitosan-mEpo-fed mice ($n=9$). Though hematocrit was not modified in naive and 'naked' mEpo-fed mice, a rapid increase was observed during the first 4 days of treatment in chitosan-mEpo-dox-fed animals, reaching $60.9 \pm 1.2\%$, and sustained for a week. The second feed (6 days after the first feed) seemed to promote a second hematocrit increase in chitosan-mEpo-dox-fed animals, reaching $65.9 \pm 1.4\%$, while the second hematocrit increase did not appear in the 'naked' mEpo-second-fed mice (Figure 5). Statistical analysis showed the hematocrit level in chitosan-mEpo-dox-fed group was significantly higher than that in other groups ($F=184.1$, $P<0.01$), while there were no significant difference between the 'naked' mEpo-fed group and naïve group ($F=0.3$, $P>0.01$). These results indicated that oral administration of chitosan-mEpo induced repetitively robust Epo secretion in doxycycline-treated mice.

DISCUSSION

In 1998, Heard *et al* transfected erythropoietin in mice by intramuscular injection of an adeno-associated vector, and they observed the long-term, high-level and controlled expression of erythropoietin in mice^[23]. Although viral gene delivery vectors yielded a high transfection efficiency over a wide range of cell targets^[24-26], they presented major drawbacks, such as virally induced inflammatory responses and oncogenic effects. To circumvent these obstacles, gene delivery research also aimed at the development of non-viral gene delivery vectors. To date, there have been many available methods that are able to deliver plasmids to cells *in vitro* and *in vivo*, such as liposomes^[27], cationic polymers^[28], electro-gene-transfer^[29], ultrasound^[30] and hydrodynamic^[31], but they have also many disadvantages, such as toxicity, relatively low transfection efficiency as compared to viral gene delivery vectors, tissue damage and difficulties of application in humans.

However, chitosan is a useful oral gene carrier because of its adhesive and transport properties in the gut, and has already

been available in a pill form as an alternative therapy to reduce dietary fat and cholesterol absorption^[32]. Recently, chitosan has been successfully used to deliver a reporter gene (encoding chloram-phenicol acetyl transferase) orally to enterocytes, Peyer's patches and mesenteric lymph nodes^[33]. Chitosan, when complexed with plasmid DNA, can form stable nanoparticles that are endocytosed by cells in the gastrointestinal tract. Further more, its safety and non-toxicity have been shown in animal models and humans^[12,34,35], indication that chitosan-DNA nanoparticles may be a useful tool for gene therapy by oral administration.

Ion concentration, temperature, pH and the ratio of chitosan to DNA (or N/P) were the four main factors that influenced the formulation of chitosan-DNA complex^[36]. The conditions we used above, could make the complex smaller, more stable, and easier to be absorbed. The zeta potential was approximately +10 mV at pH 5.7 and close to neutral at pH 7. Thus, the particles might be positively charged at gastric and early duodenal pH but neutral thereafter at more physiological or alkaline pH. Since pH influences the formulation and stability of the complex, the buffer that dilutes the complex is crucial in the test. The 25 mM sodium acetate-acetic acid buffer (pH 5.7) is able to partially neutralize the alkaline condition in small intestine, making the complex infect more enterocytes than other buffers (PBS, Ringer's, buffer saline). The long-term expression and the expression level still need to be improved, such as to increase the complex's absorptivity and to resist expression silence *etc.*

Further more, as chitosan is a mucoadhesive polymer^[37-39], such DNA nanoparticles might adhere to gastrointestinal epithelia, be transported across the mucosal boundary by M cells and transfect epithelial and/or immune cells in the gut associated lymphoid tissues either directly or through 'antigen transfer', indicating that it may generate protective mucosal immune responses.

ACKNOWLEDGEMENTS

We thank Dr. Jihua Yao, Dr. Huanzhang Zhu, Mrs. Qi Shen and Dr. Bin Lu for their help in this work.

REFERENCES

- 1 **Page DT**, Cudmore S. Innovations in oral gene delivery: challenges and potentials. *Drug Discov Today* 2001; **6**: 92-101
- 2 **Jung T**, Kamm W, Breitenbach A, Kaiserling E, Xiao JX, Kissel T. Biodegradable nanoparticles for oral delivery of peptides: is there a role for polymers to affect mucosal uptake? *Eur J Pharm Biopharm* 2000; **50**: 147-160
- 3 **Ren JM**, Zou QM, Wang FK, He Q, Chen W, Zen WK. PELA microspheres loaded *H pylori* lysates and their mucosal immune response. *World J Gastroenterol* 2002; **8**: 1098-1102
- 4 **Ko JA**, Park HJ, Hwang SJ, Park JB, Lee JS. Preparation and characterization of chitosan microparticles intended for controlled drug delivery. *Int J Pharm* 2002; **249**: 165-174
- 5 **Shimono N**, Takatori T, Ueda M, Mori M, Higashi Y, Nakamura Y. Chitosan dispersed system for colon-specific drug delivery. *Int J Pharm* 2002; **245**: 45-54
- 6 **Tozaki H**, Odoriba T, Okada N, Fujita T, Terabe A, Suzuki T, Okabe S, Muranishi S, Yamamoto A. Chitosan capsules for colon-specific drug delivery: enhanced localization of 5-aminosalicylic acid in the large intestine accelerates healing of TNBS-induced colitis in rats. *J Control Release* 2002; **82**: 51-61
- 7 **Lee JY**, Nam SH, Im SY, Park YJ, Lee YM, Seol YJ, Chung CP, Lee SJ. Enhanced bone formation by controlled growth factor delivery from chitosan-based biomaterials. *J Control Release* 2002; **78**: 187-197
- 8 **Vila A**, Sanchez A, Tobio M, Calvo P, Alonso MJ. Design of biodegradable particles for protein delivery. *J Control Release* 2002; **78**: 15-24
- 9 **Tozaki H**, Komoike J, Tada C, Maruyama T, Terabe A, Suzuki T, Yamamoto A, Muranishi S. Chitosan capsules for colon-specific drug delivery: improvement of insulin absorption from the rat colon. *J Pharm Sci* 1997; **86**: 1016-1021
- 10 **Leong KW**, Mao HQ, Truong-Le VL, Roy K, Walsh SM, August JT. DNA-polycation nanospheres as non-viral gene delivery vehicles. *J Control Release* 1998; **53**: 183-193
- 11 **Kumar M**, Behera AK, Lockey RF, Zhang J, Bhullar G, De La Cruz CP, Chen LC, Leong KW, Huang SK, Mohapatra SS. Intranasal gene transfer by chitosan-DNA nanospheres protects BALB/c mice against acute respiratory syncytial virus infection. *Hum Gene Ther* 2002; **13**: 1415-1425
- 12 **Roy K**, Mao HQ, Huang SK, Leong KW. Oral gene delivery with chitosan-DNA nanoparticles generates immunologic protection in a murine model of peanut allergy. *Nat Med* 1999; **5**: 387-391
- 13 **Artursson P**, Lindmark T, Davis SS, Illum L. Effect of chitosan on the permeability of monolayers of intestinal epithelial cells (Caco-2). *Pharm Res* 1994; **11**: 1358-1361
- 14 **Ranaldi G**, Marigliano I, Vespignani I, Perozzi G, Sambuy Y. The effect of chitosan and other polycations on tight junction permeability in the human intestinal Caco-2 cell line(1). *J Nutr Biochem* 2002; **13**: 157-167
- 15 **Dodane V**, Amin Khan M, Merwin JR. Effect of chitosan on epithelial permeability and structure. *Int J Pharm* 1999; **182**: 21-32
- 16 **Gossen M**, Freundlieb S, Bender G, Muller G, Hillen W, Bujard H. Transcriptional activation by tetracyclines in mammalian cells. *Science* 1995; **268**: 1766-1769
- 17 **Wang Y**, O' Malley BW Jr, Tasai SY, O' Malley BW. A regulatory system for use in gene transfer. *Proc Natl Acad Sci U S A* 1994; **91**: 8180-8184
- 18 **No D**, Yao TP, Evans RM. Ecdysone- inducible gene expression in mammalian cells and transgenic mice. *Proc Natl Acad Sci U S A* 1996; **93**: 3346-3351
- 19 **Rivera VM**, Clackson T, Natesan S, Pollock R, Amara JF, Keenan T, Magari SR, Phillips T, Courage NL, Cerasoli F Jr, Holt DA, Gilman M. A humanized system for pharmacologic control of gene expression. *Nat Med* 1996; **2**: 1028-1032
- 20 **Bohl D**, Naffakh N, Heard JM. Long-term control of erythropoietin secretion by doxycycline in mice transplanted with engineered primary myoblasts. *Nat Med* 1997; **3**: 299-305
- 21 **Gossen M**, Bujard H. Tight control of gene expression in mammalian cells by tetracycline-responsive promoters. *Proc Natl Acad Sci U S A* 1992; **89**: 5547-5551
- 22 **Dranoff G**, Jaffee E, Lazenby A, Golumbek P, Levitsky H, Brose K, Jackson V, Hamada H, Pardoll D, Mulligan RC. Vaccination with irradiated tumor cells engineered to secrete murine granulocyte-macrophage colony-stimulating factor stimulates potent, specific, and long-lasting anti-tumor immunity. *Proc Natl Acad Sci U S A* 1993; **90**: 3539-3543
- 23 **Bohl D**, Salvetti A, Moullier P, Heard JM. Control of erythropoietin delivery by doxycycline in mice after intramuscular injection of adeno-associated vector. *Blood* 1998; **92**: 1512-1517
- 24 **Ghazizadeh S**, Taichman LB. Virus-mediated gene transfer for cutaneous gene therapy. *Hum Gene Ther* 2000; **11**: 2247-2251
- 25 **May C**, Rivella S, Callegari J, Heller G, Gaensler KM, Luzzatto L, Sadelain M. Therapeutic haemoglobin synthesis in beta-thalassaemic mice expressing lentivirus-encoded human beta-globin. *Nature* 2000; **406**: 82-86
- 26 **Lee HC**, Kim SJ, Kim KS, Shin HC, Yoon JW. Remission in models of type 1 diabetes by gene therapy using a single-chain insulin analogue. *Nature* 2000; **408**: 483-488
- 27 **Cao YJ**, Shibata T, Rainov NG. Liposome-mediated transfer of the bcl-2 gene results in neuroprotection after *in vivo* transient focal cerebral ischemia in an animal model. *Gene Ther* 2002; **9**: 415-419
- 28 **Bragonzi A**, Boletta A, Biffi A, Muggia A, Sersale G, Cheng SH, Bordignon C, Assael BM, Conese M. Comparison between cationic polymers and lipids in mediating systemic gene delivery to the lungs. *Gene Ther* 1999; **6**: 1995-2004
- 29 **Lu QL**, Bou-Gharios G, Partridge TA. Non-viral gene delivery in skeletal muscle: a protein factory. *Gene Ther* 2003; **10**: 131-142
- 30 **Taniyama Y**, Tachibana K, Hiraoka K, Aoki M, Yamamoto S, Matsumoto K, Nakamura T, Ogihara T, Kaneda Y, Morishita R. Development of safe and efficient novel nonviral gene transfer

- using ultrasound: enhancement of transfection efficiency of naked plasmid DNA in skeletal muscle. *Gene Ther* 2002; **9**: 372-380
- 31 **Niidome T**, Huang L. Gene therapy progress and prospects: nonviral vectors. *Gene Ther* 2002; **9**: 1647-1652
- 32 **Gallaher CM**, Munion J, Hesslink R Jr, Wise J, Gallaher DD. Cholesterol reduction by glucomannan and chitosan is mediated by changes in cholesterol absorption and bile acid and fat excretion in rats. *J Nutr* 2000; **130**: 2753-2759
- 33 **MacLaughlin FC**, Mumper RJ, Wang J, Tagliaferri JM, Gill I, Hinchcliffe M, Rolland AP. Chitosan and depolymerized chitosan oligomers as condensing carriers for *in vivo* plasmid delivery. *J Control Release* 1998; **56**: 259-272
- 34 **Koping-Hoggard M**, Tubulekas I, Guan H, Edwards K, Nilsson M, Varum KM, Artursson P. Chitosan as a nonviral gene delivery system. Structure-property relationships and characteristics compared with polyethylenimine *in vitro* and after lung administration *in vivo*. *Gene Ther* 2001; **8**: 1108-1121
- 35 **Bokura H**, Kobayashi S. Chitosan decreases total cholesterol in women: a randomized, double-blind, placebo-controlled trial. *Eur J Clin Nutr* 2003; **57**: 721-725
- 36 **Borchard G**. Chitosans for gene delivery. *Adv Drug Deliv Rev* 2001; **52**: 145-150
- 37 **Takeuchi H**, Yamamoto H, Niwa T, Hino T, Kawashima Y. Mucoadhesion of polymer-coated liposomes to rat intestine *in vitro*. *Chem Pharm Bull* 1994; **42**: 1954-1956
- 38 **Bernkop-Schnurch A**, Krajicek ME. Mucoadhesive polymers as platforms for peroral peptide delivery and absorption: synthesis and evaluation of different chitosan- EDTA conjugates. *J Control Release* 1998; **50**: 215-223
- 39 **Ferrari F**, Rossi S, Bonferoni MC, Caramella C, Karlsen J. Characterization of rheological and mucoadhesive properties of three grades of chitosan hydrochloride. *Farmaco* 1997; **52**: 493-497

Edited by Zhang JZ and Wang XL

Ultrastructure of junction areas between neurons and astrocytes in rat supraoptic nuclei

Li Duan, Hua Yuan, Chang-Jun Su, Ying-Ying Liu, Zhi-Ren Rao

Li Duan, Hua Yuan, Ying-Ying Liu, Zhi-Ren Rao, Institute of Neurosciences, Fourth Military Medical University, Xi'an 710032, Shaanxi Province, China

Chang-Jun Su, Tangdu Hospital, Fourth Military Medical University, Xi'an 710032, Shaanxi Province, China

Supported by National Natural Science Foundation of China, No. 39770251 and The Fourth Military Medical University Foundation (CX01A024)

Correspondence to: Dr. Zhi-Ren Rao, Institute of Neurosciences, Fourth Military Medical University, Xi'an 710032, Shaanxi Province, China. zrrao@fmmu.edu.cn

Telephone: +86-29-83374505 **Fax:** +86-29-83246270

Received: 2003-05-11 **Accepted:** 2003-06-12

Abstract

AIM: To determine the ultrastructure of junction areas between neurons and astrocytes of supraoptic nuclei in rats orally administered 30 g/L NaCl solution for 5 days.

METHODS: The anti-connexin (CX) 43 and anti-CX32 double immunoelectromicroscopic labeled method, and anti-Fos or anti-glial fibrillary acidic protein (GFAP) immunohistochemistry were used to detect changes in the junctional area between neurons and astrocytes in supraoptic nuclei of 5 rats after 30 g/L NaCl solution was given for 5 days.

RESULTS: A heterotypic connexin32/connexin43 gap junction (HGJ) between neurons and astrocytes (AS) in rat supraoptic nuclei was observed, which was characterized by the thickening and dark staining of cytomembranes with a narrow cleft between them. The number of HGJs and Fos like immunoreactive (-LI) cells was significantly increased following hyperosmotic stimuli, that is, the rats were administered 30 g/L NaCl solution orally or 90 g/L NaCl solution intravenously. HGJs could be blocked with carbenoxolone (CBX), a gap junction blocker, and the number of Fos-LI neurons was significantly decreased compared with that in rats without CBX injection, while Fos-LI ASs were not affected.

CONCLUSION: HGJ may be a rapid adaptive signal structure between neurons and ASs in response to stimulation.

Duan L, Yuan H, Su CJ, Liu YY, Rao ZR. Ultrastructure of junction areas between neurons and astrocytes in rat supraoptic nuclei. *World J Gastroenterol* 2004; 10(1): 117-121

<http://www.wjgnet.com/1007-9327/10/117.asp>

INTRODUCTION

Human and animals normally maintain homeostasis of ion concentration, pH, body fluid and osmotic pressure. Homeostasis would markedly change, if human and animals drink excessive hypernatric fluids. Variations in osmotic pressure of extracellular fluid induce changes in cell volume that result in profound alteration of cell function and signal transduction between cells by modifying both extracellular and intercellular spatial arrangement and solute concentrations. Osmotic stimuli are

resulted from the integration of multiple sensory inputs including peripheral and central osmoreceptors^[1,2]. Peripheral osmoreceptors are mainly localized in mesenteric vasculature of the upper small intestine and hepatic portal vein^[3]. The osmotic, immune, and noxious information from these peripheral receptors would transmit to medullary nuclei (the medullary visceral zone-MVZ that includes nucleus of the tractus solitarius and ventrolateral medulla) via vagus^[4-8]. The effects of infusions of salt and water on the stomach can be mostly prevented by damage of the splanchnic or hepatic vagal nerves^[3]. The neurons in medullary nucleus relay information and reach the supraoptic nucleus (SON) and paraventricular nucleus (PVN) of hypothalamic neurosecretory cells^[4-6].

It is well known that the supraoptic nucleus (SON) plays a key role in regulation of osmotic pressure regulation. Increased Cx32 mRNA levels in rat supraoptic nuclei have been found in late pregnancy and during lactation^[2]. But the ultrastructural characteristics of the gap junctions (GJs) between neurons and astrocytes in SON following osmotic stimulation are unknown. In the present study, the characteristics of ultrastructure at junction areas between the neurons and astrocytes were examined in rat SON following hyperosmotic stimulation by using an immuno-electron-microscopic technique, and a heterotypic Cx32/Cx43 GJs at junction areas between neurons and astrocytes was observed.

It is well known that carbenoxolone (CBX), a drug to treat gastric ulcer, could block information transmitting *via* GJs, but whether CBX affects action of GJs between the neurons and astrocytes in SON is not clear. Thus, we studied the effect of CBX on GJs and found that CBX inhibited the activity of neurons in SON rather than the activity of astrocytes.

MATERIALS AND METHODS

Animal model

Ten adult male Sprague-Dawley rats (250-300 g) were provided by the Laboratory Animal Center, Fourth Military Medical University (FMMU, Xi'an, China) and divided into experimental group and control group. The protocols used in animal study were approved by the FMMU Committee of Animal Use for Research and Education. Adequate measures were taken to minimize pains or discomforts for all experimental animals. The experimental animals were fed with 30 g/L NaCl solution, the control animals with fresh water. After 5 days, the animals were anesthetized (ip) and transcardially perfused with 500 mL solution of 0.1 mol/L PB (pH 7.4) containing 40 g/L paraformaldehyde and 2 g/L saturated picric acid for 0.5 hour. Hypothalamus including SON was then removed immediately and placed in 0.05 mol/L PB containing 200 g/L sucrose at 4 °C overnight.

Tissue preparation

Hypothalamus including SON was cut into 50 µm thick frontal sections on a vibratome (Microslicer DTK-100; Dosaka, Kyoto, Japan) and placed into 0.01 mol/L KPBS for 60 minutes. Subsequently, the sections were frozen in liquid nitrogen for enhancement of penetration of antibody. Then the sections were placed in 0.01 mol/L KPBS and divided randomly into three groups.

The sections in the first group were incubated in rabbit polyclonal antibody against GFAP (1:3 000, Dako) for 48 hours at 4 °C, and then in secondary goat anti-rabbit IgG (1:500, Sigma) and in ABC complex (1:500, Sigma) at room temperature for 2 hours. Finally, the sections were visualized with glucose oxidase-DAB-nikel as a chromogen.

The sections in the second group were incubated in rabbit anti-Cx43 antibody (Chemicon, CA) for 48 hours at 4 °C, and then processed according to the methods mentioned above. After washed, the sections were again incubated with monoclonal antibody against Cx32 (Chemicon, CA) and labeled with 5nm gold particles.

The sections in the third group were used as control.

After washed with 0.01 mol/L PBS, the sections were post-fixed with 10 g/L OsO₄ in PB for 45 minutes, dehydrated through a graded ethanol and propylene oxide, flat-embedded with Epon 812. The sections were examined with a light microscope and the regions containing GFAP-like immunoreactive (-LI) cells or Cx-32- and Cx43- LI cells were investigated under an electron microscope. Small pieces from tissue were sampled from SON and re-embedded in beam capsules. Tissue samples from the selected regions were cut into sections on an ultramicrotome (Reichert – Nissei S; Leica, Vienna, Austria), and prepared for the study with electron microscope (H-7100; Hitachi, Tokyo, Japan).

CBX blockade

Twenty-one adult male SD rats were divided into three groups. The rats in control group ($n=5$) were intravenously injected with 9 g/L NaCl (1 mL). The rats in hyperosmotic group ($n=10$) were intravenously injected with 90 g/L NaCl (1 mL). The rats in the third group rats ($n=6$) were pre-injected with CBX (1.5 µg/g, 10 g/L) into the lateral ventricle and 2 hours latter, injected with 90g /L NaCl (1 mL) into the femoral vein. One hour after NaCl injection, all the rats in three groups were transcardially perfused. The brains were removed with the methods mentioned above. Then the hypothalamus including SON was cut into 30 µm thick frontal sections on a cryostat (Cryostal; Leitz, Wetzal, Germany).

The sections from each rat were randomly divided into three sets. Two sets were processed for anti-Fos and anti-glial fibrillary acidic protein (GFAP) immunohistochemical staining respectively. Briefly, the sections were incubated with rabbit polyclonal antibodies anti-Fos (1:3 000; Santa Cruz), and GFAP (1:3 000; Dako) at 4 °C for 48 hours, and then in goat anti-rabbit IgG (1:500, Sigma) and ABC complex (1:500, Sigma) at room temperature for 2 hours. Nickel-intensified DAB reaction was used to detect peroxidase. The other set group of sections was treated as control, and processed without primary antibodies and therefore no immunoreactivity was found.

RESULTS

The behaviors of control animals were normal, while experimental animals looked languid and emaciated.

Puncta electron dense areas at the membrane of junction areas between neurons and astrocytes within SON were found on control sections. This structure consisted of astrocytic process on one side and neurons (cell body or dendrite) on the other side. It was characterized by thickened and dark stained membrane with a 2nm-cleft between them (Figure1A).

We also observed anti-GFAP-like immunoreactive (-LI) processes located within astrocyte side of the junction area between neurons and astrocytes (Figure1B).

The results of anti-Cx32 and anti-Cx43 double immunoelectron-microscopic reaction indicated that Cx32-LI and Cx43-LI appeared in the neuron side and astrocyte side of the junction areas respectively (Figure1C). We concluded that

puncta electron dense areas at the junction areas might be the heterotypic Cx32/Cx43 gap junction that was called heterotypic gap junction (HGJ) in our study.

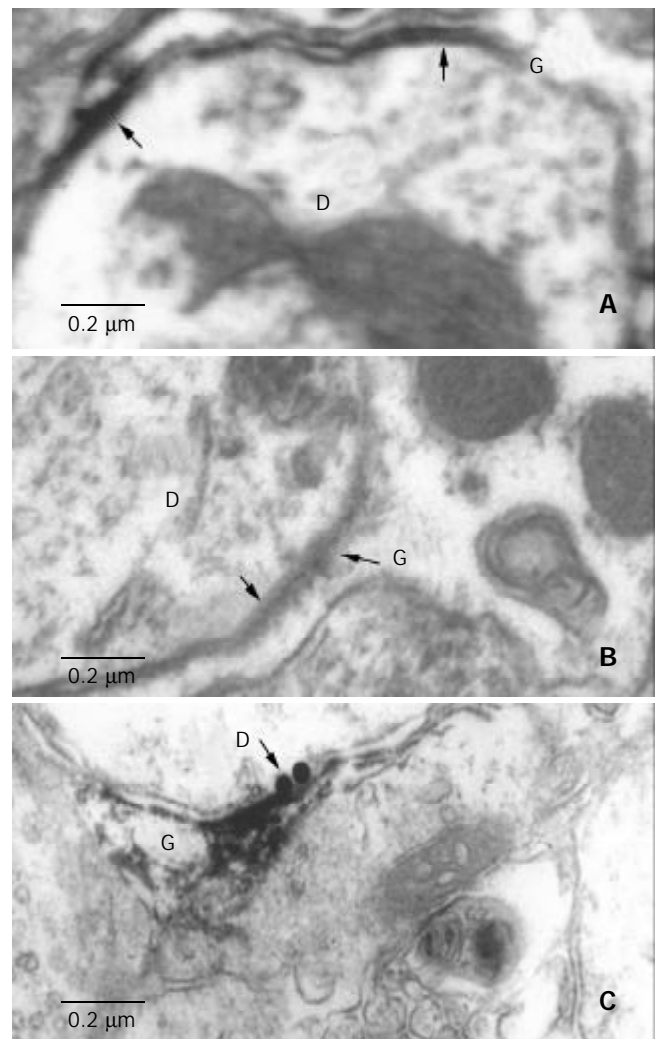


Figure 1 Electron microscopic observation of HGJ. A: A dendrite (D) contacts with the process of ASs (G), the arrow indicates the thickened and dark stained cell membrane, and there is a narrow cleft between them. B: Peroxidase labeling shows a dendrite (D) and a process of astrocyte (G). C: Located between the Cx32-LI dendrites (D) (5 nm black gold particles labeling, black arrow) and astrocytic process (G) (peroxidase labeling).

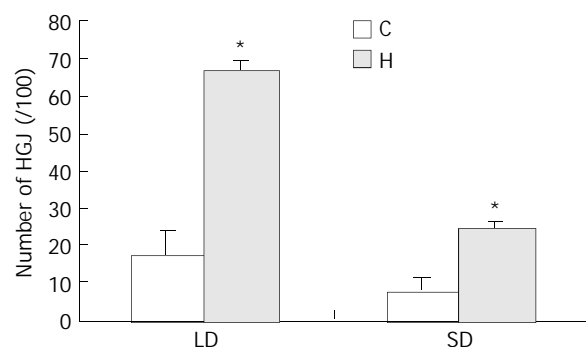


Figure 2 Histogram comparison between hyperosmotic group (H) and control group (C) demonstrating percentages of HGJ formed by processes of astrocytes with neuronal dendrites (LD: large dendrites, SD: small dendrites). The percentage indicated the ratio of positive LD or SD bearing HGJ in the total number of LD or SD, respectively. Significant difference was seen between the experimental group and control group ($P<0.001$).

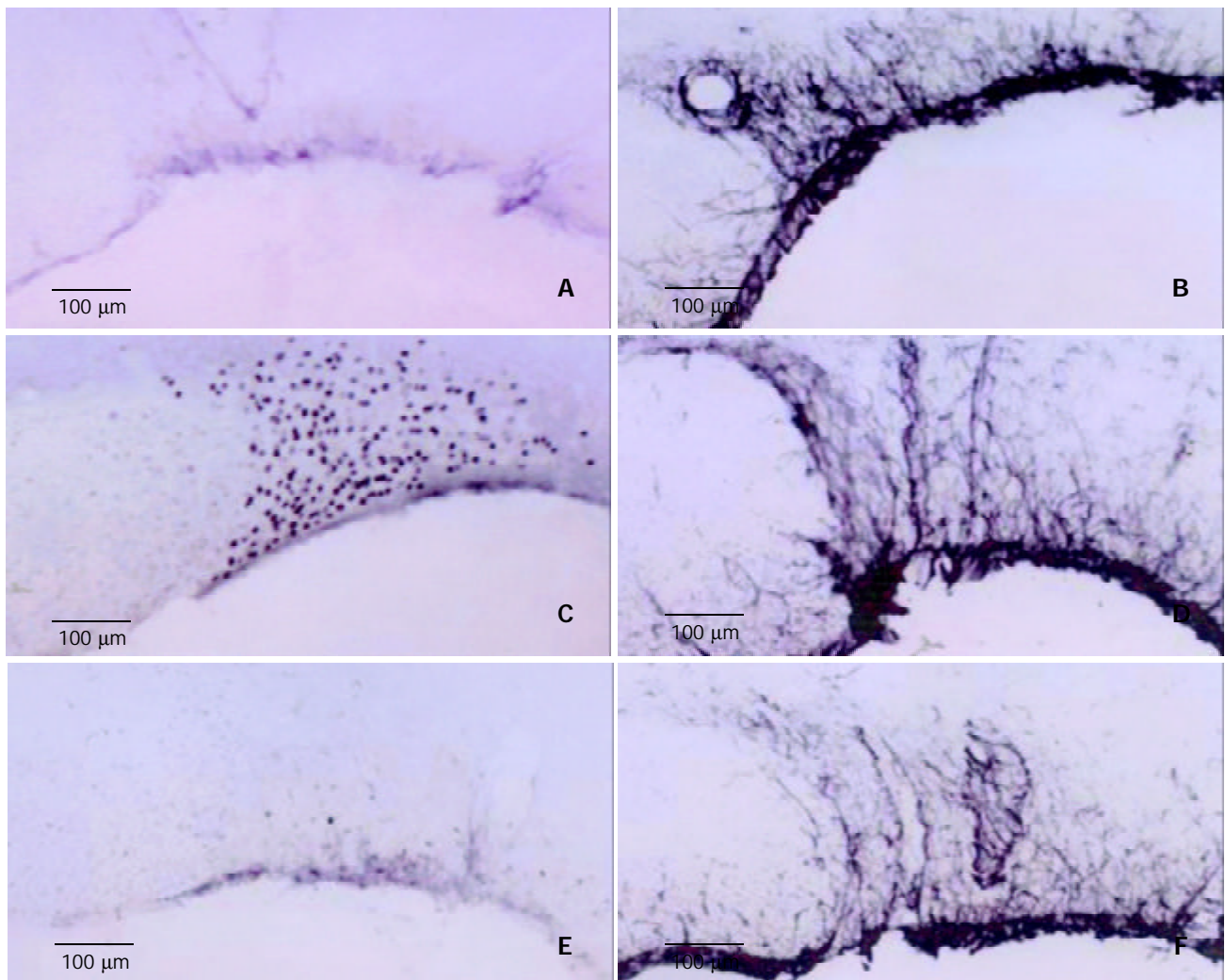


Figure 3 A,B: Expression of Fos-LI neurons and GFAP-LI ASs in SON of control group rats. C, D: Number of Fos-LI neurons and GFAP-LI ASs in hyperosmotic stimulation group compared to that of control group. E, F: Inhibited expression of Fos-LI neurons in CBX-injected rats, and uninhibited GFAP-LI ASs.

It is of interest to note that the number of HGJ in SON of the experimental group rats was significantly increased compared with that in control. We found that 17.43 per 100 large dendrites ($\geq 1 \mu\text{m}$) and 7.43 per 100 smaller dendrites ($< 1 \mu\text{m}$) had specialized areas in SON of normal control rats, while in SON of experimental group rats, 66.75 per 100 large dendrites ($\geq 1 \mu\text{m}$) and 24.35 per 100 smaller dendrites ($< 1 \mu\text{m}$) were found to bear HGJs. Statistical analysis suggested that there was a significant difference in the number of dendrites and axons bearing specialized areas between the control and experimental rats (Figure 2). It indicated that HGJs could sensitively respond to stimulation.

CBX inhibited expression of Fos-LI neurons. In control group, Fos-LI neurons in SON were not found and a few GFAP-LI astrocytes were observed. In hyperosmotic group, the number of Fos-LI neurons was significantly increased compared with that in control group. The number of GFAP-LI astrocytes was also slightly increased, and activated GFAP-LI astrocytes became hypertrophied and their processes became thickened. In the third group, the number of Fos-LI neurons in SON was decreased more significantly than that in hyperosmotic group, while GFAP-LI ASs did not differ remarkably (Figure 3).

DISCUSSION

It is well known that peripheral osmoreceptors are mainly localized in the mesenteric vasculature of the upper small

intestine and the hepatic portal vein^[3]. The osmotic, immune, and noxious information from these peripheral receptors could transmit to medullary nuclei (medullary visceral zone-MVZ that include nucleus of the tractus solitarius and ventrolateral medulla) *via* vagal nerve^[4-8]. The neurons in medullary nuclei could relay information and reach hypothalamic neurosecretory cells of the supraoptic nucleus (SON) and paraventricular nucleus (PVN)^[4-6].

Our study indicated that astrocytes, as well as neurons, could sensitively respond to hyperosmotic stimuli induced by administration of 30 g/L NaCl solution orally or 90 g/L NaCl solution intravenously. Activated astrocytes appeared to be GFAP-LI positive, and activated neurons exhibited Fos-LI nuclei. The activated astrocytes have been found to be generally marked with GFAP, and neurons with Fos^[9-12].

The discovery of intercommunication between neurons and astrocytes was an important advance in neurobiology in recent twenty years^[13]. It has been that gap junction is an important channel of intercellular communication and also a direct link of the interiors of cells^[14-16], and consists of connexins of the protein family^[17,18]. However, about 15 types of Cx (followed by molecular mass designation) have been identified in mammals including the nervous and non-nervous systems^[19,20]. At least 9 of the 15 types of Cx identified so far were expressed in CNS^[21]. The same Cx types could be expressed in different cells and more than one Cx type could be expressed by the same cell. Nagy and Rash^[18] reported that Cx30 was labeled by 5nm

gold particles and Cx43 was labeled with immunoperoxidase, which was observed at the same astrocytic GJ in rat brain. Neurons and oligodendrocytes expressed Cx32, astrocytes expressed Cx43, and ependyma and leptomeningeal cells expressed both Cx26 and Cx43.

It is well known that GJs may occur between the same cell types such as neurons and glia, they may also occur between different cell types such as neuron and astrocyte, neuron and oligodendrocyte, and astrocyte and oligodendrocyte. GJs consisting of the same Cx protein have been termed as homotypic GJs^[14-16], while that consisting of different Cxs at two sides of GJs in culture as heterotypic Cxs GJ^[17, 21]. It was reported that heterotypic Cx45/Cx43 GJs were observed in culture HeLa cells^[11, 22, 23] and the oligo-astrocyte GJs in white matter arose by pairing astrocytic Cx43 with oligodendrocytic Cx45^[24]. Whether there were GJs between the neurons and astrocytes, some studies suggested that astrocytes might play a direct role in neuromodulation through GJs-mediated interaction between astrocytes and neurons^[15, 17]; Meanwhile, on the basis of fracture replica immunogold labeling, no evidence has been found for GJs between glial cells and neurons in the adult brain^[19].

This study demonstrated that Cx32 and Cx43 appeared simultaneously at the neuronal side and astrocyte side, respectively, and formed the heterotypic Cx32/Cx43 gap junction. The special heterotypic Cx32/Cx43 gap junctions observed in this study had a narrow cleft (diameter: 2nm) between the neuronal and astrocytic membranes. This structure differed from the conventional gap junction, which has a seven-layer structure. It is of interest to note that the number of HGJs in SON of experimental group rats was significantly increased compared with that in control rats. In this study we also observed other types of ultrastructures, for example, synapses between neurons and astrocytes, tripartite synaptic structures and the gap junction between glial cells, but their number and structure did not show any significant change following stimulation (data not shown). It indicated that HGJs might be involved in signal communication of osmotic pressure regulation.

Results from this study indicated that the expression of Fos-LI neurons in experimental animals, which were injected CBX into the lateral ventricular, was markedly decreased compared with control animals. CBX, a glycyrrhetic acid, is used to treat gastric ulcer by blocking information transmitting via gap junction. It was reported that CX cloud block GJs between neurons, and delay induction of epileptiform activity and reduces established epileptiform activity^[25-27], and significantly decrease the spread of cell death induced by ischemia^[28]. CX could also blocks GJs between glia^[29, 30] or between neurons and glia^[15, 31].

There has been debate on direction of intercommunication between the neurons and astrocytes coupling. Nedergaard^[32] and Robinson *et al.*^[33] described that unidirectional dye coupling from astrocytes to neurons and from astrocytes to oligodendrocytes occurred in intact neural tissues. Alvarez-Maubecin *et al.*^[15] also suggested the existence of functional coupling between brainstem glia and noradrenergic neurons in slices taken from postnatal animals. But Rozental *et al.* and Carmignoto^[15, 34] considered that there was bidirectional signaling through gap junction between neurons and astrocytes. The results from the present research indicated that the expression of Fos-LI SON neurons induced by hyperosmotic stimulation could be inhibited with CBX, while the response of astrocytes to stimulation was not affected. It is suggested that the signaling via HGJs is unidirectional from astrocytes to neurons.

REFERENCES

- Bourque CW**, Oliet SH. Osmoreceptors in the central nervous system. *Annu Rev Physiol* 1997; **59**: 601-619
- Hussy N**, Deleuze C, Desarmenien MD, Moos FC. Osmotic regulation of neuronal activity: a new role for taurine and glial cells in a hypothalamic neuroendocrine structure. *Prog Neurobiol* 2000; **62**: 113-134
- Baertschi AJ**, Pence RA. Gut-brain signaling of water absorption inhibits vasopressin in rats. *Am J Physiol* 1995; **268**: R236-R247
- Bourque CW**, Oliet SH, Richard D. Osmoreceptors, osmoreception, and osmoregulation. *Front Neuroendocrinol* 1994; **15**: 231-274
- Dong YX**, Xiong KH, Rao ZR, Shi JW. Fos expression in catecholaminergic medullary neurons induced by chemical stimulation of stomach projecting to the paraventricular nucleus of hypothalamus in rats. *China Natl J New Gastroenterol* 1997; **3**: 72-74
- Yang ZJ**, Rao ZR, Ju G. Evidence for the medullary visceral zone as a neuronal station of neuroimmunomodulation. *Neurosci Res* 2000; **38**: 237-247
- Ge X**, Yang ZJ, Duan L, Rao ZR. Evidence for involvement of the neuronal pathway containing the peripheral vagus nerve, medullary visceral zone and central amygdaloid nucleus in neuroimmunomodulation. *Brain Res* 2001; **914**: 149-158
- Wang X**, Wang BR, Zhang XJ, Xu Z, Ding YQ, Ju G. Evidences for vagus nerve in maintenance of immune balance and transmission of immune information from gut to brain in STM-infected rats. *World J Gastroenterol* 2002; **8**: 540-545
- Colburn RW**, DeLeo JA. The effect of perineural colchicine on nerve injury-induced spinal glial activation and neuropathic pain behavior. *Brain Res Bull* 1999; **49**: 419-427
- Coyle DE**. Partial peripheral nerve injury leads to activation of astroglia and microglia which parallels the development of allodynic behavior. *Glia* 1998; **23**: 75-83
- Eliasson C**, Sahlgren C, Berthold CH, Stakeberg J, Celis JE, Betsholtz C, Eriksson JE, Pekny M. Intermediate filament protein partnership in astrocytes. *J Biol Chem* 1999; **274**: 3996-4006
- Hashizume H**, DeLeo JA, Colburn RW, Weinstein JN. Signal glial activation and cytokine expression after lumbar root injury in the rat. *Spine* 2000; **25**: 1206-1217
- Hermanson O**, Blomqvist A. Differential expression of the AP-1/CRE-binding proteins FOS and CREB in preproenkephalin mRNA-expressing neurons of the rat parabrachial nucleus after nociceptive stimulation. *Brain Res Mol Brain Res* 1997; **51**: 188-196
- Bezzi P**, Volterra A. A neuron-glia signalling network in the active brain. *Curr Opin Neurobiol* 2001; **11**: 387-394
- Alvarez-Maubecin V**, Garc á-Hern ández F, Williams JT, Van Nockstaele EJ. Functional coupling between neurons and glia. *J Neurosci* 2000; **20**: 4091-4098
- Rozental R**, Andrade-Rozental AF, Zheng X, Urban M, Spray DC, Chiu FC. Gap junction-mediated bidirectional signaling between human fetal hippocampal neurons and astrocytes. *Dev Neurosci* 2001; **23**: 420-431
- Froes MM**, Correia AH, Garcia-Abreu J, Spray DC, Campos de Carvalho AC, Neto MV. Gap-junctional coupling between neurons and astrocytes in primary central nervous system cultures. *Proc Natl Acad Sci U S A* 1999; **96**: 7541-7546
- Nagy JI**, Rash JE. Connexin and gap junctions of astrocytes and oligodendrocytes in the CNS. *Brain Res* 2000; **32**: 29-44
- Rash JE**, Yasumura T, Dudek FE, Nagy JI. Cell-specific expression of connexins and evidence of restricted gap junctional coupling between glial cells and between neurons. *J Neurosci* 2001; **21**: 1983-2000
- Ma XD**, Sui YF, Wang WL. Expression of gap junction genes connexin 32, connexin 43 and their proteins in hepatocellular carcinoma and normal liver tissues. *World J Gastroenterol* 2000; **6**: 66-69
- Rozental R**, Giaume C, Spray DC. Gap junctions in the nervous system. *Brain Res* 2000; **32**: 11-15
- Bukauskas FF**, Angele AB, Verselis VK, Bennett MV. Coupling asymmetry of heterotypic connexin 45/connexin43-EGFP gap junctions: properties of fast and slow gating mechanisms. *Proc Natl Acad Sci U S A* 2002; **99**: 7113-7118
- Bittman K**, Becker DL, Cicirata F, Parnavelas JG. Connexin expression in homotypic and heterotypic cell coupling in the developing cerebral cortex. *J Comp Neurol* 2002; **443**: 201-212
- Kunzelmann P**, Blumcke I, Traub O, Dermietzel R, Willecke K.

- Coexpression of connexin45 and -32 in oligodendrocytes of rat brain. *J Neurocytol* 1997; **26**: 17-22
- 25 **Jahromi SS**, Wentlandt K, Piran S, Carlen PL. Anticonvulsant actions of gap junctional blockers in an *in vitro* seizure model. *J Neurophysiol* 2002; **88**: 1893-1902
- 26 **Schmitz D**, Schuchmann S, Fisahn A, Draguhn A, Buhl EH, Petrasch-Parwez E, Dermietzel R, Heinemann U, Traub RD. Axo-axonal coupling. A novel mechanism for ultrafast neuronal communication. *Neuron* 2001; **31**: 831-840
- 27 **Traub RD**, Draguhn A, Whittington MA, Baldeweg T, Bibbig A, Buhl EH, Schmitz D. Axonal gap junctions between principal neurons: a novel source of network oscillations, and perhaps epileptogenesis. *Rev Neurosci* 2002; **13**: 1-30
- 28 **Frantseva MV**, Kokarotseva L, Perez Velazquez JL. Ischemia-induced brain damage depends on a specific gap-junctional coupling. *J Cereb Blood Flow Metab* 2002; **22**: 453-462
- 29 **Bani-Yaghoob M**, Underhill TM, Naus CC. Gap junction blockage interferes with neuronal and astroglial differentiation of mouse P19 embryonal carcinoma cells. *Dev Genet* 1999; **24**: 69-81
- 30 **Menezes JR**, Froes MM, Moura Neto V, Lent R. Gap junction-mediated coupling in the postnatal anterior subventricular zone. *Dev Neurosci* 2000; **22**: 34-43
- 31 **Ozog MA**, Siushansian R, Naus CC. Blocked gap junctional coupling increases glutamate-induced neurotoxicity in neuron-astrocyte co-cultures. *J Neuropathol Exp Neurol* 2002; **61**: 132-141
- 32 **Nedergaard M**. Direct signaling from astrocytes to neurons in cultures of mammalian brain cells. *Science* 1994; **263**: 1768-1771
- 33 **Robinson SR**, Hampson EC, Munro MN, Vancy DI. Unidirectional coupling of gap junctions between neuroglia. *Science* 1993; **262**: 1072-1074
- 34 **Carmignoto G**. Reciprocal communication systems between astrocytes and neurons. *Progr Neurobiol* 2000; **62**: 561-581

Edited by Ren SY and Wang XL

Effects of exercise on lipid metabolism and musculoskeletal fitness in female athletes

Kung-Tung Chen, Rong-Sen Yang

Kung-Tung Chen, Department of General Education, Ming Hsin University of Science and Technology, Hsinchu 304, Taiwan, China
Rong-Sen Yang, Department of Orthopaedics, College of Medicine, National Taiwan University, Taipei 10043, Taiwan, China
Supported by the National Science Council of Taiwan, NSC91-2413-H-159-001

Correspondence to: Dr. Rong-Sen Yang, Department of Orthopaedics, National Taiwan University Hospital, No.7 Chung-Shan South Road, Taipei 10043, Taiwan, China. yang@ha.mc.ntu.edu.tw
Telephone: +886-2-2312-3456 Ext 3958 **Fax:** +886-2-23936577
Received: 2003-10-16 **Accepted:** 2003-11-20

Abstract

AIM: This study investigated the effects of intense training on lipid metabolism, bone metabolism and bone mineral density (BMD) in female athletes.

METHODS: Sixty-six female subjects participated in this study, age ranging from 18 to 55 years. The sample group included thirty-six athletic subjects and the control group comprised thirty non-athletic individuals. Five athletes competed with national level (5/36) and nine non-athletic subjects (9/30) were postmenopausal women. The assessment items included body composition, radius BMD, calcaneus BMD, lung function, muscular endurance, renal and liver function, bone marker assay and hormone status. All data were analysed, using SPSS 10.0 software, and were presented as mean rank statistical difference, using the Kurskal-Wallis (K-W) test. After that the non-parameter statistics were used. Either *K* value or *P* value below 0.05 was considered significant.

RESULTS: Urine deoxyypyridinoline/creatinine (Dpd/Cre) levels increased significantly (5.93 ± 2.31 vs 6.85 ± 1.43 , $K < 0.01$), sit-reach (29.30 ± 9.48 cm vs 41.31 ± 9.43 cm, $K < 0.001$, $P < 0.001$), 1 minute sit-ups with bended knees (1 min sit-ups) (17.60 ± 9.34 count vs 30.00 ± 10.38 count, $K < 0.001$, $P < 0.001$), and vertical jump (25.27 ± 6.63 cm vs 34.69 ± 7.99 cm, $K < 0.001$, $P < 0.001$) improved significantly in the athletes group. The athletes group also had a significantly increased level of estriol (E_3) (0.14 ± 0.13 pg/mL vs 0.07 ± 0.04 pg/mL, $K < 0.01$, $P < 0.01$), radius BMD (1.37 ± 0.49 gm/cm² vs 1.19 ± 0.40 gm/cm², $K < 0.05$) and calcaneus BMD (0.57 ± 0.17 gm/cm² vs -0.20 ± 0.17 gm/cm², $K < 0.01$, $P < 0.05$) compared with those of the controls. The high density lipoprotein (HDL) (65.00 ± 14.02 mg/dL vs 52.26 ± 4.84 mg/dL, $K < 0.05$, $P < 0.05$) was significantly lower in postmenopausal inactive athletes (5/36) than premenopausal active athletes (31/36). On the other hand, low-density lipoprotein (LDL) (98.35 ± 23.84 mg/dL vs 131.00 ± 21.63 mg/dL, $K < 0.05$, $P < 0.01$), cholesterol (CHO) (164.03 ± 27.01 mg/dL vs 193.00 ± 23.48 mg/dL, $K < 0.05$, $P < 0.05$), triglyceride (TG) (63.00 ± 26.39 mg/dL vs 147.00 ± 87.21 mg/dL, $K < 0.01$), body fat % (BF%) ($28.16 \pm 4.90\%$ vs $34.84 \pm 4.44\%$, $K < 0.05$, $P < 0.001$) and body mass index (BMI) (21.98 ± 2.98 kg/m² vs 26.42 ± 5.01 kg/m², $K < 0.05$, $P < 0.001$) were significantly higher in postmenopausal inactive athletes (5/36) than premenopausal active athletes (31/36). TG (90.22 ± 39.82 mg/dL vs 147.00 ± 87.21 mg/dL), CHO

(186.44 ± 24.90 mg/dL vs 193.00 ± 23.48 mg/dL) were higher, but the HDL was significantly lower (62.18 ± 10.68 mg/dL vs 52.26 ± 4.84 mg/dL, $P < 0.05$) in postmenopausal athletes (5/36) group than in postmenopausal control group (9/30).

CONCLUSION: Postmenopausal athletes (5/36) who no longer took competing exercises had reduced levels of physical activity, faced increased risk of cardiovascular disease compared to active athletes (31/36) and the postmenopausal controls (9/30). We may thus concluded that long term exercise effectively improves musculoskeletal fitness and prevents BMD loss in female athletes.

Chen KT, Yang RS. Effects of exercise on lipid metabolism and musculoskeletal fitness in female athletes. *World J Gastroenterol* 2004; 10(1): 122-126

<http://www.wjgnet.com/1007-9327/10/122.asp>

INTRODUCTION

Weightlessness or immobilization, as experienced by astronauts in space, is a well known cause of significant and rapid bone mineral loss^[1-24]. Furthermore sedentary individuals generally have a lower bone mass than physically active individuals, moderate exercise is known to increase skeletal mass^[3]. The above effect is most obvious in sports that place a significant stress on the skeleton. Investigations of athletes have identified physical activity as a major determinant of bone mass in the general population.

Physical fitness significantly influences quality of life. In Taiwan, medical care quality and public health environment have improved markedly over recent decades. The incidence of fatal infectious diseases thus has reduced significantly and the life span of Taiwanese has elongated. Simultaneously, the incidence of chronic diseases has increased, yet people remain ignorant of the importance of exercise^[1-5].

Exercising for 20-60 min per day, three days per week, at moderate intensity level of 3-6 Metabolic Equivalent units (METs) for most individuals derives at least some health-related benefits, including improved cardiorespiratory fitness, muscle strength and endurance, flexibility and body composition, as well as associated psychological benefits. Consequently, lifelong physical exercise is recommended to optimize health-related benefits^[2-8]. And the influence of physical activity and exercise training on BMD in females previously has been assessed in cross-sectional, retrospective longitudinal and controlled trial studies^[3-13].

Even though no relationship about growth hormone and BMD was found. But the effect of E_3 significantly improved BMD by inhibiting bone resorption, female athletes with low estradiol (E_2) level take a risk for increased lipid peroxidation following exercise^[11-15]. Thus hormone status and lipid metabolism may play an important role in the protection against cardiovascular disease, this physiological response has implications for risks of heart disease. Longitudinal information on associations between life style factors and age-related bone loss remains quite controversial. Some studies have found no relationship between bone loss and body composition or body weight, while others

have shown them to predict bone mass changes^[3-16].

Therefore, the purpose of this study was to explore the physiological function of female athletes, including BMD, renal function, liver function, hormone status, bone marker assay, lipid metabolism and muscle biology related to the effectiveness of exercise intervention for the health status of female athletes compared with controls.

MATERIALS AND METHODS

Subjects

Sixty-six female subjects participated in this investigation, with ages ranging between 18 and 55 yrs. The sample group was the athlete group ($n=36$), while the control group comprised non-athletic individuals ($n=30$). Inclusion criteria were that the female athletes had participated in high-intensity resistance or impact activities (e.g., basketball, dancing). Exclusion criteria for both the subjects and the controls were that the subjects had no major medical illnesses, including coronary artery disease which could influence lipid metabolism, and were free of other risk factors that are associated with influencing lipid metabolism, such as smoking or ethanol intake or treatment within the last two years with systemic glucocorticoids, anticonvulsants, bisphosphonates, oestrogen, or raloxifene. Five athletes competed with national level (5/36) and nine non-athletic subjects (9/30) were included in the analysis of postmenopausal women. The parameters to be measured included body composition, radius BMD and calcaneus BMD, lung function, muscular endurance, renal function, liver function and hormone status.

Anthropometric measurement of body composition

Anthropometric measurements were taken based on conventional criteria. The measurement procedures of body weight (Wt) and body height (Ht) were estimated to the nearest 0.1 kg and 0.5 cm, respectively. Finally BMI was calculated using the formula: $BMI (kg/m^2) = Wt (kg) / Ht (m^2)$.

Health related fitness

They were tested using a modified Guthrie R test^[6]. Health related fitness tests included vertical jump, 3 min steps, sit-reach, hand grip and 1 min sit-ups items.

Lung function

Respiratory muscle strength and pulmonary function were assessed by spirometry. The flow volume and respiratory muscle forces were measured using a Fukuda, microspiro HI-501 model spirometer.

Renal and liver function

Sixty-six blood samples per subject were drawn from an antecubital vein with the subjects in the seated position. Routine complete blood counts (CBC) were taken using a Sysmex-E9000 (TOA Electronic, Inc., Tokyo, Japan) and renal and liver function tests were performed using a Hitachi 7170 instrument (Hitachi Electronic, Inc., Tokyo, Japan) by clinical chemistry laboratory staff at Li-Shin Hospital, Taoyuan County, Taiwan.

Hormone status

E_2 , E_3 , triiodothyronine (T_3), thyroxine (T_4), thyroid stimulating hormone (TSH), parathyroid hormone (PTH), cortisol and human growth hormone (HGH) were assayed in basal conditions, using commercial radioimmunoassay (RIA) and enzymeimmunoassay (EIA) Kits.

Bone marker assay

Serum bone specific alkaline phosphatase (BAP) activity was

measured using an EIA kit obtained from Metra Biosystems (Monuntain View, CA, USA). Urine Dpd level was measured using enzyme immunoassay (Ciba-Corning ACS-180) kits purchased from Bayer international (Bayer Diagnostics, Tarrytown, NY, USA).

BMD determination

Calcaneus site BMD was measured via speed of sound (SOS) equipped for a bone mineral densitometry (Aloka Medical Ltd, modelAOS-100, Tokyo, Japan) and all BMD values were also expressed as a T-score, accurately reflecting the BMD. Distal site BMD was measured using the osmometer DTX-100 (SPA, Single Photon Absorptiometry, Osmometer, Rodovre, Denmark). The scanners were calibrated daily against the standard calibration block supplied by the manufacturer to control baseline drift.

Statistical analysis

All data were analysed, using SPSS 10.0 software, and were presented as mean rank statistical difference, using the Kurskal-Wallis (K-W) test. After that the non-parameter statistics were be used. The confidence interval was set at 95% and the significance level used was $K < 0.05$ (two sides). All statistical analyses were carried out with SPSS statistical package. The Kruskal-Wallis test does not use any information on the relative magnitude of each observation when compared with every other observation in the combined sample. This comparison is replaced in each observation by its rank in the pool sample. The smallest observation is replaced by its rank 1, the next smallest by rank 2, and so on, the largest by its rank n . Since the test is an extension of the Mann-Whitney-Wilcoxon (M-W-W) test. Either K value or P value below 0.05 is considered significant.

RESULTS

No difference in body composition

The thirty-six female athletes enrolled in this cross-sectional study did not differ significantly in terms of BF, BF%, BMI and resistance compared with the control group (Table 1).

Table 1 Body composition of two groups

Variables	66 females		K-Value
	Control group $n=30$	Athlete group $n=36$	
	mean rank		
Body fat	31.68	35.01	0.483
BF%	33.83	33.22	0.898
BMI	32.45	34.38	0.685
Resistance	34.95	32.29	0.575

Exercise improvements muscular endurance in female athletes

These two different groups did not differ significantly in muscular endurance. The hand grip (28.06 ± 6.14 kg vs 26.85 ± 5.73 kg), 3 min steps (55.32 ± 6.90 count/min vs 57.82 ± 7.21 count/min) and vital capacity (86.86 ± 15.98 L vs 88.23 ± 12.05 L) in athlete group were better than those in control group, but did differ significantly in terms of sit-reach (29.3 ± 9.48 cm vs 41.31 ± 9.43 cm, $K < 0.001$, $P < 0.001$), 1 min sit-ups (17.60 ± 9.34 count vs 30.00 ± 10.38 count, $K < 0.001$, $P < 0.001$) and vertical jump (25.27 ± 6.63 cm vs 34.69 ± 7.99 cm, $K < 0.001$, $P < 0.001$) as listed in Table 2.

Lipid metabolism

Table 3 shows that the results were not significantly different between both groups. But lipid metabolism including HDL (59.36 ± 12.23 mg/dL vs 63.23 ± 13.83 mg/dL) and Hb (12.95 ± 1.22 g/dL vs 13.43 ± 1.09 g/dL) in the athlete group was higher than

in the control group. However, LDL (105.93±30.76 mg/dL vs 102.89±25.92 mg/dL), TG (81.53±49.53 mg/dL vs 74.60±48.31 mg/dL) and CHO (170.20±32.20 mg/dL vs 168.06±28.13 mg/dL) were lower in the athlete group than those of the control group. Thus exercise could improve the lipid metabolism, and it is good for health.

Table 3 No significant differences in blood CHO and lipid variables between both groups

Group	n	HDL	LDL	CHO	TG	Hb
Control group (mean rank)	30	31.92	34.65	34.92	35.02	28.75
Athlete group (mean rank)	36	34.82	32.54	32.32	32.24	37.46

Table 2 Muscular strength and endurance assessment among controls and athlete groups

Group	n	Sit-reach	1 min sit-ups	Vertical jump	Hand grip	3 min steps	Vital capacity
Control group (mean rank)	30	22.18	22.05	22.23	31.27	29.60	30.58
Athlete group (mean rank)	36	42.93 ^{ab}	43.04 ^{ab}	42.89 ^{ab}	35.36	36.75	35.93

^aK<0.001 vs statistically significant when compared with control group. ^bP<0.001 vs statistically significant when compared with control group.

Table 5 BMD, urine electrolytes, blood electrolytes in two groups

Group	n	Urine-Cre	Blood-Ca	BMD/radius	BMD /calcaneus	Blood-Cl
Control group (mean rank)	30	26.87	42.42	28.38	26.23	45.90
Athletes group (mean rank)	36	39.03 ^{ad}	26.07 ^b	37.76 ^a	39.56 ^{bd}	23.17 ^c

^aK<0.05 vs statistically significant when compared with control group. ^bK<0.01 vs statistically significant when compared with control group. ^cK<0.001 vs statistically significant when compared with control group. ^dP<0.05 vs statistically significant when compared with control group.

Table 6 Hormonal findings in athletes with significance by non-parameter statistics test compared with controls

Group	n	Cortisol	E ₃	T ₃	T ₄	PTH	HGH
Control group (mean rank)	30	32.28	25.78	31.77	36.43	31.37	35.65
Athletes group (mean rank)	36	34.51	39.93 ^{ab}	34.94	31.06	35.28	31.71

^aK<0.01 vs statistically significant when compared with control group. ^bP<0.01 vs statistically significant when compared with control group.

Table 7 Biochemical bone turnover markers and BMD in athletes with significance by non-parameter statistics test as compared with controls

Group	n	Dpd	Urine-Cre (24 hrs)	Dpd/Cre	BAP	BMD/radius	BMD/Calcaneus
Control group (mean rank)	30	25.87	27.23	25.72	20.10	28.38	26.23
Athletes group (mean rank)	36	39.86 ^{be}	38.72 ^{ad}	39.99 ^b	43.83 ^{ef}	37.76 ^a	39.56 ^b

^aK<0.05 vs statistically significant when compared with control group. ^bK<0.01 vs statistically significant when compared with control group. ^cK<0.001 vs statistically significant when compared with control group. ^dP<0.05 vs statistically significant when compared with control group. ^eP<0.01 vs statistically significant when compared with control group. ^fP<0.001 vs statistically significant when compared with control group.

Table 8 Postmenopausal female athlete lipid metabolism compared to premenopausal active athletes

Athletes group	n	BF%	BMI	HDL	LDL	CHO	TG	Hb
Premenopausal (mean rank)	31	16.84	17.08	20.15	16.74	16.98	16.55	18.79
Postmenopausal (mean rank)	5	28.60 ^{ac}	27.30 ^{be}	8.30 ^{ac}	29.40 ^{ad}	27.90 ^{ac}	30.60 ^b	16.70

^aK<0.05 vs statistically significant when compared with premenopausal group. ^bK<0.01 vs statistically significant when compared with premenopausal group. ^cP<0.05 vs statistically significant when compared with premenopausal group. ^dP<0.01 vs statistically significant when compared with premenopausal group. ^eP<0.001 vs statistically significant when compared with premenopausal group.

Table 4 Serum enzyme activities related to renal and liver metabolism

Group	n	ALP	Cre	ALB	DBIL
Control group (mean rank)	30	27.07	27.88	27.77	27.65
Athlete group (mean rank)	36	38.86 ^{ac}	38.18 ^{ab}	38.28 ^a	38.38 ^a

^aK<0.05 vs statistically significant when compared with control group. ^bP<0.05 vs statistically significant when compared with control group. ^cP<0.01 vs statistically significant when compared with control group.

Renal and liver function

Table 4 shows that no difference between the data (data not shown here) of the two groups in terms of blood enzymes such

as glutamic oxalocetic transaminase (GOT), glutamic pyruvic transaminase (GPT), blood urea nitrogen (BUN), uric acid (UA), total protein (TP), globulin (GLO) and bilirubin (BIL). But the control group displayed significantly lower alkaline phosphatase (ALP) (61.03 ± 13.99 U/L vs 70.81 ± 15.23 U/L, $K < 0.05$, $P < 0.01$), ALB (4.52 ± 0.18 g/dL vs 4.62 ± 0.27 g/dL, $K < 0.05$), Cre (0.75 ± 0.09 mg/dL vs 0.81 ± 0.10 mg/dL, $P < 0.05$, $K < 0.05$) and direct bilirubin (DBIL) (0.25 ± 1.11 mg/dL vs 0.29 ± 0.8 mg/dL, $K < 0.05$) than the athlete group.

Electrolytes and BMD

According to non-parameter statistical tests, both the radius BMD (1.37 ± 0.49 gm/cm² vs 1.19 ± 0.40 gm/cm², $K < 0.05$) and calcaneus BMD (0.57 ± 0.17 gm/cm² vs -0.20 ± 0.17 gm/cm², $K < 0.01$, $P < 0.05$), increased significantly in the athlete group compared with those of the control group. Moreover, the athlete group's body electrolytes such as urine-Cre (132.22 ± 72.30 mg/dL vs 166.83 ± 62.52 mg/dL, $K < 0.05$, $P < 0.05$), blood calcium (Ca) (8.76 ± 0.32 mg/dL vs 8.43 ± 0.37 mg/dL, $K < 0.01$) and chloride (Cl) (99.94 ± 2.41 meq/L vs 102.83 ± 1.97 meq/L, $K < 0.001$) significantly decreased compared to the control group.

Hormone status

HGH and T₄ were lower in the athlete group than in the control group (8.95 ± 1.51 µg/dL vs 9.38 ± 1.51 µg/dL), but cortisol (11.39 ± 4.03 µg/dL vs 10.75 ± 3.42 µg/dL), E₂ (88.82 ± 66.42 pg/mL vs 80.56 ± 63.10 pg/mL), T₃ (112.07 ± 13.52 ng/dL vs 114.78 ± 17.16 ng/dL) and PTH (39.07 ± 16.97 pg/mL vs 34.70 ± 11.66 pg/mL) levels were higher. Notably, E₃ level (0.14 ± 0.13 pg/mL vs 0.07 ± 0.04 pg/mL, $K < 0.01$, $P < 0.01$) significantly increased in the athlete group compared to those of the control group.

Bone marker assay and BMD

All biochemical and bone turnover markers, for example, (67.97 ± 39.67 nmol/mmol vs 102.63 ± 46.97 nmol/mmol, $K < 0.01$, $P < 0.01$), Dpd/Cre ratio (5.93 ± 2.31 vs 6.85 ± 1.43 , $K < 0.01$), and BAP (14.04 ± 3.31 µg/L vs 20.93 ± 6.17 µg/L, $K < 0.001$, $P < 0.001$) significantly increased in the female athlete group compared to those of the control group. The athletes displayed positive correlation of regional radius BMD ($K < 0.05$) and calcaneus BMD ($K < 0.01$, $P < 0.05$) with these results (Table 7).

Lipid metabolism in postmenopausal athletes

Table 8 displays levels of LDL (98.35 ± 23.84 mg/dL vs 131.00 ± 21.63 mg/dL, $K < 0.05$, $P < 0.01$), CHO (164.03 ± 27.01 mg/dL vs 193.00 ± 23.48 mg/dL, $K < 0.05$, $P < 0.05$), TG (63.00 ± 26.39 mg/dL vs 147.00 ± 87.21 mg/dL, $K < 0.01$), BF% ($28.16 \pm 4.90\%$ vs $34.84 \pm 4.44\%$, $K < 0.05$, $P < 0.001$) and BMI (21.98 ± 2.98 kg/m² vs 26.42 ± 5.01 kg/m², $K < 0.05$, $P < 0.001$) increased in the postmenopausal (5/36) inactive athletes group compared to the premenopausal (31/36) active athletes. Then the level of HDL (65.00 ± 14.02 mg/dL vs 52.26 ± 4.84 mg/dL, $K < 0.05$, $P < 0.05$) markedly decreased in the postmenopausal (5/36) inactive athletes.

Table 9 Lipid metabolism of postmenopausal female athletes

Postmenopausal group	n	BMI	HDL	LDL	CHO	TG	Hb
Control group (mean rank)	9	6.56	9.00	7.11	7.06	6.44	7.61
Athletes group (mean rank)	5	9.20	4.80*	8.20	8.30	9.40	7.30

* $P < 0.05$ vs statistically significant when compared with postmenopausal control group.

Lipid metabolism in postmenopausal females

Results from this study show higher levels of TG (90.22 ± 39.82 mg/dL vs 147.00 ± 87.21 mg/dL), CHO (186.44 ± 24.90 mg/dL vs 193.00 ± 23.48 mg/dL), but lower levels of HDL (62.18 ± 10.68 mg/dL vs 52.26 ± 4.84 mg/dL, $P < 0.05$), Hb (13.82 ± 0.88 g/dL vs 13.52 ± 0.21 g/dL) in postmenopausal athletes (5/36) group compared with the postmenopausal control group (9/30). This implies that the effect is a cardiovascular disease risk for postmenopausal retired female athletes (Table 9).

DISCUSSION

The data in this study were expressed as mean $\bar{x} \pm s$. Statistical significance in the mean values was evaluated by the Student's *t* test. But in our study, only sixty-six female subjects participated in this investigation. Therefore, we use K-W test to analyze the results of all tests. The Kruskal-Wallis test does not use any information on the relative magnitude of each observation when compared with every other observation in the combined sample. This comparison is replaced in observation by its rank in the pool sample. The smallest observation is replaced by its rank 1, the next smallest by rank 2, and so on, the largest by its rank *n*. Since the test is an extension of the M-W-W test. Either *K* value or *P* value below 0.05 was considered significant.

Exercise is important for maintaining skeletal health. However, the ability of exercise to influence bone might not be entirely related to hormone status. This study has shown that hormones and exercise interact to influence bone adaptations, and thus raise E₃ level related to increased BMD following exercise in female athletes. For example, serum E₂, cortisol, PTH and T₃ levels in the athlete group were higher than those of the controls, and the major finding of this study was that increased radius BMD ($K < 0.05$) and calcaneus BMD ($K < 0.01$, $P < 0.05$) were significantly and positively related to serum E₃ ($K < 0.01$, $P < 0.01$) concentrations^[10-12]. Therefore, a clear understanding the interaction suggested by the present data between E₃ concentration and the adaptation of bone to exercise is important, and provides an interaction through which the estrogen receptors involved in the early response of bone cells might increase their responsiveness to loading^[11,12].

These results indicate that physical exercise positively affects the maintenance of radius BMD ($K < 0.05$), calcaneus BMD ($K < 0.01$, $P < 0.05$) in female athletes, thus increased E₃ level can prevent BMD loss and possible risk of osteoporosis^[12]. The athletes have higher levels of all the biomarkers than the controls, including Dpd ($K < 0.01$, $P < 0.01$), urine-Cre ($K < 0.05$, $P < 0.05$), Dpd/Cre ratio ($K < 0.005$), BAP ($K < 0.001$, $P < 0.001$) and lower levels of blood-Ca ($K < 0.01$), blood-Cl ($K < 0.001$) these results were associated with markedly increased radius BMD and calcaneus BMD^[13-22].

Further studies are required to examine a larger population, and also to consider the effects of BMD marker assay (for example insulin-like growth factors).

Physical inactivity has been designated by the American Heart Association as a major modifiable risk factor for cardiovascular disease. Numerous studies have examined individual morbidity and mortality from cardiovascular disease. The results presented here indicate that exercise can improve physiological characteristics, such the lowering levels of serum CHO and TG in female athletes, all of which may improve cardiovascular fitness and reduce morbidity and mortality from cardiovascular disease^[12-16,23-26].

But the findings regarding the renal function, liver function and lipid metabolism of retired female athletes were surprising. Enzyme activity indicates that this group (5/36) may not have the same health benefits from physical exercise as the control subjects. Specifically, this group displayed decreased HDL ($K < 0.05$, $P < 0.05$), Hb and increased LDL ($K < 0.05$, $P < 0.01$),

CHO ($K < 0.05$, $P < 0.05$), TG ($K < 0.01$) compared to the premenopausal active athletes (31/36). Postmenopausal retired female athletes (5/36) engaged in less physical activity than previously, displayed increase rates of liver and renal dysfunction, which require further investigation^[17,23-28].

An understanding of the dyslipidemia and ensuing atherosclerosis has implications for the pathophysiology of coronary heart disease (CHD). Risk of cardiac morbidity and mortality is directly related to concentration of plasma total CHO or LDL. Lipid lowering therapy has been shown to reduce the risk of cardiovascular events in both high risk individuals and patients with manifest CHD^[17-22,24-28]. The present study has found that postmenopausal retired female athletes (5/36) who were no longer engaged in strenuous physical activity, they had a significantly higher BF% ($K < 0.05$, $P < 0.001$) and BMI ($K < 0.05$, $P < 0.001$) compared to the active female athletes (31/36) group, specifically, in lipid dysfunction marker with the postmenopausal retired female athletes. Results from this study show higher levels of TG, CHO, but lower levels of HDL, Hb in athletes (5/36) group compared with the control group (9/30). Then, five postmenopausal athletes (5/36), who had retired from competition, and were engaged in less physical activity than previously, had significantly higher BF%, BMI and lipid dysfunction markers had a significantly decreased level of HDL ($P < 0.05$) compared to the controls (9/30). This suggest that the effect is a cardiovascular disease risk for postmenopausal retired female athletes.

Future studies should recruit more numbers of female athletes, who have retired from competition but still maintained high levels of physical activity, and then compare this group with the low physical activity group that serves as the control group. Lipid metabolism related apolipoprotein E (*ApoE*) genotypes with an allele specific oligonucleotide (ASO) based microarray system may interact with exercise training to affect their plasma lipid profiles. To clarify the atherogenic risk of different lipoprotein phenotypes, the relations among total CHO, LDL, HDL and CHD risk in older female athletes should be investigated.

ACKNOWLEDGEMENTS

We are grateful to Li-Shin Hospital in Taoyuan County, Taiwan that provided all laboratory tests in this study, which helped us to complete the research subjects.

REFERENCES

- 1 **Huuskonen J**, Vaisanen SB, Kroger H, Jurvelin JS, Alhava E, Rauramaa R. Regular physical exercise and bone mineral density: a four-year controlled randomized trial in middle-aged men. The DNASCO study. *Osteoporos Int* 2001; **12**: 349-355
- 2 **Humphries B**, Newton RU, Bronks R, Marshall S, McBride J, Triplett MT, Hakkinen K, Kraemer WJ, Humphries N. Effect of exercise intensity on bone density, strength, and calcium turnover in older women. *Med Sci Sports Exerc* 2000; **32**: 1043-1050
- 3 **Wolff I**, van Croonenborg JJ, Kemper HC, Kostense PJ, Twisk JW. The effect of exercise training programs on bone mass: a meta-analysis of published controlled trials in pre- and postmenopausal women. *Osteoporos Int* 1999; **9**: 1-12
- 4 **Karlsson MK**. Skeletal effects of exercise in men. *Calcif Tissue Int* 2001; **69**: 196-199
- 5 **Pettersson U**, Nordstrom P, Lorentzon R. A comparison of bone mineral density and muscle strength in young male adults with different exercise level. *Calcif Tissue Int* 1999; **64**: 490-498
- 6 **Guthrie R**. The use of medical examinations for employment purposes. *J Law Med* 2003; **11**: 93-102
- 7 **Kraemer WJ**, Ratamess NA, French DN. Resistance training for health and performance. *Curr Sports Med Rep* 2002; **1**: 165-171

- 8 **Hendriksen JJ**, Meeuwse T. The effect of intermittent training in hypobaric hypoxia on sea-level exercise: a cross-over study in humans. *Eur J Appl Physiol* 2003; **88**: 396-403
- 9 **Williams CD**, Dobridge JD, Meyer WR, Hackney AC. Effects of the route of estrogen administration and exercise on hormonal levels in postmenopausal women. *Fertil Steril* 2002; **77**: 1118-1124
- 10 **Leelawattana R**, Ziambaras K, Roodman WJ, Lyss C, Wagner D, Klug T, Armamento VR, Civitelli R. The oxidative metabolism of estradiol conditions postmenopausal bone density and bone loss. *J Bone Miner Res* 2000; **15**: 2513-2520
- 11 **Deschenes MR**, Kraemer WJ. Performance and physiologic adaptations to resistance training. *Am J Phys Med Rehabil* 2002; **81**: S3-16
- 12 **Hayashi T**, Ito I, Kano H, Endo H, Iguchi A. Estriol (E_3) replacement improves endothelial function and bone mineral density in very elderly women. *J Gerontol A Biol Sci Med Sci* 2000; **55**: 183-190
- 13 **Hou MF**, Lin SB, Yuan SS, Tsai LY, Tsai SM, Hsieh JS, Huang TJ. Diagnostic value of urine deoxyypyridinoline for detecting bone metastases in breast cancer patients. *Ann Clin Lab Sci* 2003; **33**: 55-61
- 14 **Miller CJ**, Dunn EV, Thomas EJ, Sankarankutty M. Urinary free deoxyypyridinoline excretion in lactating and non-lactating Arabic women of the United Arab Emirates. *Ann Clin Biochem* 2003; **40**: 394-397
- 15 **Ormarsdottir S**, Ljunggren O, Mallmin H, Olofsson H, Blum WF, Loof L. Circulating levels of insulin-like growth factors and their binding proteins in patients with chronic liver disease: Lack of correlation with bone mineral density. *Liver* 2001; **21**: 123-128
- 16 **Wu LY**, Yang TC, Kuo SW, Hsiao CF, Hung YJ, Hsieh CH, Tseng HC, Hsieh AT, Chen TW, Chang JB, Pei D. Correlation between bone mineral density and plasma lipids in Taiwan. *Endocrine Res* 2003; **29**: 317-319
- 17 **Huang TH**, Lin SC, Chang FL, Hsieh SS, Liu SH, Yang RS. Effects of different exercise modes on mineralization, structure, and biomechanical properties of growing bone. *J Appl Physiol* 2003; **95**: 300-307
- 18 **Tsauo JY**, Chien MY, Yang RS. Spinal performance and functional impairment in postmenopausal women with osteoporosis and osteopenia without vertebral fracture. *Osteoporos Int* 2002; **13**: 456-460
- 19 **Huang TH**, Yang RS, Hsieh SS, Liu SH. Effects of caffeine and exercise on the development of bone: a densitometric and histomorphometric study in young Wistar rats. *Bone* 2002; **30**: 293-299
- 20 **Hui SL**, Perkins AJ, Zhou L, Longcope C, Econs MJ, Peacock M, McClintock C, Johnston CC Jr. Bone loss at the femoral neck in premenopausal white women: effects of weight change and sex-hormone levels. *J Clin Endocrinol Metab* 2002; **87**: 1539-1543
- 21 **Prestwood KM**, Kenny AM, Kleppinger A, Kulldorff M. Ultralow-dose micronized 17beta-estradiol and bone density and bone metabolism in older women: a randomized controlled trial. *JAMA* 2003; **290**: 1042-1048
- 22 **van den Beld AW**, de Jong FH, Grobbee DE, Pols HA, Lamberts SW. Measures of bioavailable serum testosterone and estradiol and their relationships with muscle strength, bone density, and body composition in elderly men. *J Clin Endocrinol Metab* 2000; **85**: 3276-3282
- 23 **Guichelaar MM**, Malinchoc M, Sibonga J, Clarke BL, Hay JE. Bone metabolism in advanced cholestatic liver disease: analysis by bone histomorphometry. *Hepatology* 2002; **36**: 895-903
- 24 **Fan JG**, Zhong L, Xu ZJ, Tia LY, Ding XD, Li MS, Wang GL. Effects of low-calorie diet on steatohepatitis in rats with obesity and hyperlipidemia. *World J Gastroenterol* 2003; **9**: 2045-2049
- 25 **Lu LG**, Zeng MD, Li JQ, Hua J, Fan JG, Fan ZP, Qiu DK. Effects of lipid on proliferation and activation of rat hepatic stellate cells (I). *World J Gastroenterol* 1998; **4**: 497-499
- 26 **Wakatsuki A**, Okatani Y, Ikenoue N, Shinohara K, Watanabe K, Fukaya T. Effect of lower dose of oral conjugated equine estrogen on size and oxidative susceptibility of low-density lipoprotein particles in postmenopausal women. *Circulation* 2003; **108**: 808-813
- 27 **Tanko LB**, Bagger YZ, Nielsen SB, Christiansen C. Does serum cholesterol contribute to vertebral bone loss in postmenopausal women? *Bone* 2003; **32**: 8-14
- 28 **Chen BY**, Wei JG, Wang YC, Wang CM, Yu J, Yang XX. Effects of cholesterol on the phenotype of rabbit bile duct fibroblasts. *World J Gastroenterol* 2003; **9**: 351-355

Acute diarrhea during army field exercise in southern China

Yang Bai, Ying-Chun Dai, Jian-Dong Li, Jun Nie, Qing Chen, Hong Wang, Yong-Yu Rui, Ya-Li Zhang, Shou-Yi Yu

Yang Bai, Ya-Li Zhang, Nan Fang Hospital, The First Military Medical University, Guangzhou 510515, Guangdong Province, China
Ying-Chun Dai, Jian-Dong Li, Jun Nie, Qing Chen, Hong Wang, Yong-Yu Rui, Shou-Yi Yu, Department of Epidemiology, The First Military Medical University, Guangzhou 510515, Guangdong Province, China

Supported by the Key Program of Military Medical Science and Technique Foundation during the 9th-Five Year Plan Period

Correspondence to: Yang Bai, Department of Digestive Diseases, Nan Fang Hospital, The First Military Medical University, Guangzhou 510515, Guangdong Province, China. baiyang1030@hotmail.com

Telephone: +86-20-61641531

Received: 2003-03-05 **Accepted:** 2003-06-02

Abstract

AIM: During emergency period, infectious diseases can be a major threat to military forces. During field training in southern China, diarrhea is the main cause of nonbattle injury. To evaluate the causes of and risk factors for diarrhea in emergency period, we collected clinical and epidemiological data from the People's Liberation Army (PLA) during field training in southern China.

METHODS: From September 25 to October 2 1997, 2636 military personnel were investigated. Fecal sample cultures for lapactic pathogens were obtained from 103 military personnel with diarrhea. In addition, a questionnaire was administered to 103 cases and 206 controls to evaluate the association between illness and potential risk factors. At the same time, another questionnaire of 1:4 case-case control was administered to 22 severe cases (each severe case paired 4 mild cases).

RESULTS: The training troop's diarrhea incidence rate was significantly higher than that of garrison. The diarrhea incidence rate of officers was significantly lower than that of soldiers. A lapactic pathogen was identified in 63.1% (65/103) of the troops with diarrhea. *Enterotoxigenic Escherichia coli* (35.0%) and *pleiomona shigelloides* (16.5%) were the most common bacterial pathogens. All bacterial isolates were sensitive to norfloxacin and ceftazidime. However, almost all of them were resistant to sulfamethoxazole, trimethoprim-sulfamethoxazole, oxytetracycline, doxycycline, furazolidone, ampicillin and cloromycetin to a different degree. Risk factors associated with diarrhea included drinking raw water, eating outside, contacting diarrhea patients, lacking sanitation, depression, lacking sleep, which were established by multiple-factor logistic regression analysis. In addition, the unit incidence rate was associated with the density of flies and the average daily boiled water available by regression and discriminate analysis.

CONCLUSION: A series of risk factors are associated with the incidence rate of diarrhea. Our results may provide a useful basis for prevention and cure of diarrhea in emergency period of PLA.

Bai Y, Dai YC, Li JD, Nie J, Chen Q, Wang H, Rui YY, Zhang YL, Yu SY. Acute diarrhea during army field exercise in southern China. *World J Gastroenterol* 2004; 10(1): 127-131
<http://www.wjgnet.com/1007-9327/10/127.asp>

INTRODUCTION

Acute diarrhea (abbreviated diarrhea) is a common disease during peace and war period in the army^[1-4]. It has been shown that the year incidence rate of diarrhea varied from 49.5% to 64.0% in the stationed army in southern China and the main pathogens were *enterotoxigenic Escherichia coli* (ETEC) and *enteropathogenic Escherichia coli* (EPEC)^[5]. Diarrhea is also a serious problem for military forces during an emergency period usually including war, military maneuver, dealing with emergency and providing disaster relief, field training, *etc.* In addition, diarrhea is the major cause of nonbattle injury^[6,7]. The life style, sanitary system, and appliance of foreign armies are quite different from our army, therefore, the results from their study cannot be applied to our army^[8-13]. To probe into the epidemic features, pathogen spectrum and the main risk factors of diarrhea during an emergency period and to provide the basis for taking preventive and therapeutic measures, we carried out an initial study during an army exercising in a coastal training field in southern China.

At the training base in the west of Leizhou Peninsula, weeds and bushes are overgrown and tall trees are rare. There is no other inhabitant except the garrison. The weather is harsh, with constant high temperature, high humidity, and plenty of rain. Insects, such as flies and midges, are present everywhere. Along the coastline, camps, kitchens, reservoirs, simple toilets, garbage disposal facilities, and other life support facilities have been established. At the base, the whole sanitary standard is low and the living condition is hard. During exercises, villagers nearby provide fried dishes, cold dishes, fruits, and other seafood products. None of the food has hygiene certificates. The source of drinking water is from the wells with self-prepared covers. The water supply is limited, and no laboratory test has been carried out to check the quality of the water.

MATERIALS AND METHODS

Concerned definition

As was recommended by WHO, the definition of diarrhea is attacking acutely, having three or more motions with properties changed. Those whose interval between two diarrheas exceeded 7 days were recorded twice. According to the clinical manifestations, cases were divided into group of severe cases and group of mild cases. Severe cases were defined as those with diarrhea of more than 5 stools or accompanied by fever ($\geq 38^{\circ}\text{C}$).

Surveillance of disease

Our study lasted for 20 days, and was divided into transporting and assembling stage (8 days) and field training stage (12 days). At the first stage, diarrhea patients were investigated retrospectively by battalion medical officers because the army was on the move. We began formal surveillance at the second stage. Battalion medical officers and investigators registered all training soldiers and collected information about diarrhea attack twice a day (morning and evening). They also delivered fecal samples to laboratory for detection of pathogens before antibiotics were used.

Pathogen detection

The samples on LB were incubated in alkaline peptone solution

for 24 hours at 37 °C. Next day 1 ml of culture medium was taken out and put into glycerin and paraffin oil separately. Detection of pathogens was based on the diarrhea detection rules of WHO^[14]. ETEC was detected by a DNA probe, which was prepared by our department. The micro-biochemical tubes used to detect the germs of enterobacteriaceae, vibrio and serum of Shigella, Salmonella, EPEC and EIEC were bought from Lanzhou Institute of Biological Products.

The antibiotic susceptibility was performed by K-B method recommended by WHO^[15]. The antibiotics included norfloxacin, ceftazidime sulfamethoxazole, trimethoprim-sulfamethoxazole, oxytetracycline, doxycycline, furazolidone, ampicillin and cloromycetin. Standard strain coliform bacillus ATCC25923 and staphylococcus aureus ATCC25923 and pseudomonas ATCC27853 were used for quality control.

Epidemiologic survey

The diarrhea patients identified by surveillance were investigated using "The army acute diarrhea epidemiological case survey form" and "System distress checklist (SCL-90)" in 48 hours by 1:2 case-control study. Controls were chosen from soldiers without diarrhea within 7 days in the same company, with the same sex, the same rank. The differences of age and time of military service were within 1 year. The 129 investigated factors in 15 categories in these two survey forms were analyzed with conditional one-way and multiple logistic regression analysis. To explore the relationship between environmental hygiene and the unit diarrhea incidence, unit environmental hygiene questionnaire of field training troop was filled by surveillance group. In addition, 1:4 case-case control was administered to 22 severe cases (each severe case paired 4 mild cases) to study the main factors of severe clinical manifestations.

Quality control

(1) In order to reduce the failure of report and to increase the collection rate of specimens, we strengthened propaganda and organization and tried to make officers and soldiers fully understand the meaning and purpose of our study. (2) All investigators were trained. (3) To ensure the quality of survey, the screening results from one or two companies were checked randomly and about 10% of the forms in the same day were reinvestigated to identify potential mistakes. (4) The collected fecal specimens were sent in iceboxes and examined by a full-time laboratory technician.

Statistic methods

The data were recorded and checked using SPSS10.0/PC statistical package (SPSS, Chicago). Proportions were compared using the chi-square test with Fisher's exact test. Conditional multiple logistic regression analysis was performed using SAS. Logistic models were established by the maximum-likelihood method. Confidence intervals were calculated by the method of Woolf for univariate analysis and logistic-regression parameter estimates and their standard errors were used for multivariate analysis^[16]. A two-tailed *P* value of 0.05 was considered as statistically significant.

RESULTS

Diarrhea incidence rate

The personnel investigated consisted of 320 officers and 2 316 soldiers in the training troop, and 24 officers and 180 soldiers in the garrison. They were all males, with a mean age of 22 years (SD of 4 years, ranging from 18 to 48 years). There was no difference in constituent ratio in these two troops by statistic analysis ($\chi^2=0.025$, $P=0.874$). During the whole training

period, the diarrhea incidence rate was 7.32% (193/2 636). The diarrhea incidence rate at the second training stage was 4.10% (108/2 636), which was significantly higher than that of the permanent garrison in corresponding time (0.98%, 2/204). The incidence rate of each training company varied from 0.84% to 12.38%. There was also a significant difference among different companies in the same battalion ($\chi^2=11.105$, $P<0.001$), but no difference was found in the same company. The severe cases who could not work due to diarrhea accounted for 20.4% of the patients with diarrhea.

Pathogen detection

We surveyed 108 diarrhea patients and collected 103 samples (including 37 cotton swabs of anus). The collection rate was 95.4%. Most of the samples were watery and loose stools; few were mucus or pus and bloody stool.

The pathogens found in our study included 72 strains of 6 types of lapactic bacteria (Table 1). The positive detection rate was 63.1% (65/103). The most common pathogen was ETEC, followed by plesiomonas shigelloides. The rate of Shigella and Samonella infection was relatively high. There were 7 samples in which two types of pathogens were detected at the same time. Campylobacter and Yersinia were not found because of the limited conditions on the spot.

Table 1 Pathogen detection rate

Pathogen	Number of patients	Detection rate (%)
ETEC	36	35%
Plesiomonas shigelloides	17	16.5%
Salmonella	6	5.8%
Shigella	5	4.9%
EIEC	3	2.9%
Aeromonas schubertii	2	1.9%
Aeromonas hydrophila	1	1%
Vibrio metschnikovi	1	1%
Vibrio vulnificus	1	1%

The susceptibility of seventy-two strains of lapactic bacteria to nine types of antibiotics was examined. It showed that all these bacteria were sensitive to norfloxacin (95.8%) and ceftazidime (100%). All the lapactic bacteria were resistant to sulfamethoxazole, trimethoprim-sulfamethoxazole, oxytetracycline, doxycycline, furazolidone, ampicillin and cloromycetin to a different degree (Table 2)^[17,18].

Table 2 Resistance rate of pathogens to antibiotics

Antibiotics	ETEC <i>n</i> [*] =36	Vibrio <i>n</i> =22	Salmonnlla <i>n</i> =6	Shigella <i>n</i> =5	EIEC <i>n</i> =3	Overall <i>n</i> =72
Sulfamethoxazole	91.7	68.2	83.3	100.0	66.7	83.3
Trimethoprim-Sulfamethoxazole	91.7	59.1	83.3	80.0	66.7	79.2
Oxytetracycline	69.4	77.3	100.0	100.0	100.0	75.0
Doxycycline	61.1	72.7	100.0	100.0	100.0	69.4
Furazolidone	16.7	90.9	50.5	100.0	33.3	52.0
Ampicillin	30.6	36.4	50.0	40.0	33.3	34.7
Cloromycetin	25.0	4.5	0.0	40.0	33.3	18.1
Norfloxacin	5.6	0.0	0.0	20.0	0.0	4.2
Ceftazidime	0.0	0.0	0.0	0.0	0.0	0.0

**n* was the number of strains.

Sixty-eight environmental specimens (drinking water, flies, seafood, cooking utensils of the training troops and local vendors) were examined for lapactic pathogens^[19-22]. Forty-two strains of 10 types of lapactic pathogens were detected, including 14 strains of lapactic vibrio, 12 strains of aerobacter

cloacae, 8 strains of *Plesiomonas shigelloides*, 8 strains of *Aeromonas*, 7 strains of ETEC, 3 strains of *Shigella*, 2 strains of *Salmonella* and 1 strain of EIEC (Table 3). All the environmental specimens had lapactic pathogens to some extent, especially flies, seafood, and cooking utensils of the local vendors, which reached 87.5%, 80.0%, and 73.3%, respectively^[23].

Table 3 Detection rate of lapactic pathogens from environmental specimens

Source of specimen	Number	Detection rate (%)
Flies	8	87.5
Seafood	10	80.0
Cooking utensils of vendors	15	73.3
Drinking water	15	66.7
Cooking utensils of troops	10	40.0
Camping appliances	10	20.0
Total	68	61.8

Risk factors analysis

Analysis of individual risk factors of diarrhea Unconditional single factor logistic regression analysis was performed, and the result showed that 25 factors were in association with individual diarrhea. In order to control interactions and confounding factors, and to make the studied factors more actually significant in theory, the above-mentioned 25 factors were entered to the equation of conditional multivariate logistic regression following the significant level <0.05 , seven statistical significant variables were screened in the end (Table 4).

Analysis of unit risk factors of diarrhea Thirty-seven environmental sanitary questionnaires, which were checked to satisfy statistic requirements, were analyzed. Linear stepping regression was performed to determine the relationship between the 23 environmental factors with the incidence of field training troops. The result indicated that the density of flies in toilets, garbage disposal methods and daily average boiled water supply per person were the main factors. The regression equation was $\text{incidence} = -3.107 + 2.051 * \text{density of flies in toilets} + 1.601 * \text{garbage disposal methods} - 0.743 * \text{daily average boiled water supply per person}$. The standard regression coefficient was 0.544, 0.264, and 0.201, respectively. The R square was 0.784. The variance analysis showed that F value of the regression equation was 40.34 ($P < 0.001$).

To simplify the equation and improve the goodness of fit, ten curves estimation (quadratic, compound, growth, logarithmic, cubic, s, exponential, power, inverse and logistic) was used to fit the relation between the density of flies in toilets

and the diarrhea incidence. R square of 5 curves estimation (power, compound, growth, exponential and logistic) was larger than that of linear regression equation, of which power's R square reached 0.816 and the left four's R square was 0.798.

The diarrhea incidence rates were further divided into 3 groups: $\leq 3\%$, 3-6%, $\geq 6\%$. According to the field environmental sanitary questionnaire and the incidence, stepping discriminate function was used to establish the discriminate function. The discriminate function was composed of six variables (density of flies in toilets, toilet disinfection, density of flies in garbage dump, disposal method of garbage, density of flies near waste water and use of anti-fly cover) (Table 5). The false discriminate rate was 0%, 13.3% and 11.1%, respectively. The total false discriminate rate was 91.9%.

Table 5 Linear discriminant function coefficients

Factor	Linear discriminant	Function coefficient		
		$<3\%$	3%-6%	$\geq 6\%$
Disinfection of toilets	29.354	46.645	45.882	
Garbage disposal methods	-14.564	-34.839	-25.324	
Density of flies in toilets	9.127	7.143	19.911	
Density of flies in garbage dumps	8.753	16.595	16.056	
Density of flies near waste-water	15.855	38.361	27.858	
Use of anti-fly cover	21.243	34.128	32.386	
Constant	-46.378	-117.197	-133.264	

Analysis of case-case control study Twenty-two case-case control study questionnaires were collected, 20 of them had no missing data and were analyzed by single factor conditional logistic regression. The result showed that 30 possible risk factors had a relationship with severe symptoms. Drinking raw water within seven days, eating outside, not washing hand before eating, were then analyzed by conditional logistic multiple-regression (Table 6).

DISCUSSION

The diarrhea incidence rate during the training stage was 4.10%, which was significantly higher than that of the garrison at the corresponding time (0.98%) and much higher than the 10 day incidence rate (1.35%) of a stationed army in the same season^[5]. Because of the differences in duration, location and diagnostic standard in an emergency period, the rates could not be directly compared, however, the increase of diarrhea incidence rate was a common phenomenon during emergency. There must be some factors that contribute to the increased diarrhea incidence, and

Table 4 Multiple-factor conditional logistic- regression results of case-control study

Factor	Regression coefficient	Standard error	Odds ratio	95% Confidence interval	P value
Drinking raw water	3.1460	0.4638	23.2148	9.3641-57.6862	0.0000
Eating outside	3.1365	0.6055	23.0229	7.0273-75.4280	0.0000
Contacting with patients	2.9447	0.5707	19.0055	6.2104-58.1625	0.0000
Lack of hygiene knowledge	1.7776	0.5071	5.9155	2.1893-15.9833	0.0005
Depression	1.1654	0.3633	3.2071	1.5735-6.5364	0.0013
Not frequently cutting fingernails	1.0504	0.3888	2.8588	1.3341-6.1258	0.0069
Lack of sleep	0.6555	0.21264	1.9261	1.2360-3.0016	0.0038

Table 6 Multiple-factor conditional logistic regression results of case-case control study

Factors	Regression coefficient	Standard error	Odd ratio (OR)	95% confidence interval	P value
Drinking raw water	3.8610	1.1724	47.5119	4.7738-472.8718	0.0010
Eating outside	2.5711	0.7506	13.0802	3.0040-56.9537	0.0006
Not washing hand before eating	1.3445	0.6142	2.7487	1.1519-12.7877	0.0286

if we can find these factors and control them, we should be able to strengthen the fighting capacity of the army.

The incidence rate of officers was clearly lower than that of soldiers, which was not in accordance with the results from stationed army and other related researches^[24]. For example, a research of Hyams in "desert shield action" suggested the incidence rate was not affected by age and rank, while another study showed that the risk of officers was a little higher than that of soldiers. More data are still needed to confirm the real features of our army^[25]. According to our study, the possible explanation was that the training and working of soldiers were more intensive, meanwhile their hygiene habits were worse than officers. In addition, they drank raw water and eating outside more often than officers^[26].

From our research, the time distribution of diarrhea can be concluded as follow. The number of patients increased obviously in the early days of an action, then became stable after three or four days, and sustained at a certain rate^[27]. During this period the incidence rate in each unit of the army was different and small outbreak could be seen occasionally, which was similar to some conclusions from foreign armies. The possible reasons of the increased rate during the early time were as follows. Normal living pattern of soldiers was disrupted and physically weakened. During training, soldiers increased significantly their contact with environments and the chances of infection were also increased. Failure to adapt to a new environment and lack of immunity, and no sanitary and anti-epidemic measures were taken. These possible reasons still need to be further explored. To control the incidence peak at early stages, we should strengthen propaganda on hygiene and enhance soldiers' abilities to self-guard against diarrhea. In addition, antibiotics should be used to prevent special diarrheas (such as tourist diarrhea, soldier diarrhea with special task), but attention should be paid to selection and time limit of antibiotics^[28,29]. With the army's adapting to the environment and the perfection of preventive measures, the incidence rate maintained at a lower degree. However, because of the existence of many unhygienic temporary food stalls outside the camps and soldiers often eating outside, outbreak of different scales did take place^[30,31]. Apart from propaganda, we should strengthen the discipline and forbid soldiers to eat outside the camps.

In spite of the failure to detect *Campylobacter* and *Yersinia* due to limited condition on spot, 61.3% detection rate indicated that bacterial diarrhea was a main cause in Summer and Autumn during field training in coastal area in southern China. It was reported ETEC was the most common pathogen in stationed army^[32] and so was in our study, which was in accordance with some reports from American army^[8]. It suggested that ETEC was one of the focal points in diarrhea prevention in army, no matter Chinese or foreign^[8,33-35], stationed or training in field. We should enhance the basic clinical and preventive researches on diarrhea to guarantee fighting capacity. Moreover, we detected a relatively high rate of vibrio, especially that of *Vibrio cholerae* which was 16.5%, at the second place^[36]. This may be correlated with training at coastal area as water, food, and articles for daily use contain high counts of such pathogens (results not shown). Many studies showed that this germ had a relatively high detection rate in southeast coastal area.

It is important to evaluate hygiene standards of our army and develop related education to analyze individual risk factors of diarrhea. The incidence rate will decrease markedly if we can efficiently control these risk factors. As shown in Table 4, after multi variable analysis seven variables emerged as significant risk factors, which were drinking raw water, eating outside, lack of hygiene knowledge, not frequently trimming nails, contacting with diarrhea patients, having no enough sleep

and depression. Of these factors the first two were consistent with the results from stationed army, which indicates that the two risk factors are common in our military officers and soldiers. So it is necessary to strengthen sanitary education, to enforce administration, and to change unhealthy habits. During the survey, we found that none of the patients was separated from others and all the patients ate, slept and trained with the healthy personnel, which made contact transmission more easily.

For a long time, mental factors of diarrhea in an emergency period have been ignored. To explore the relationship between mental factors and diarrhea in an emergency period, we used "SCL-90" widely used in foreign countries, especially in mental health field. In a study, the mental condition of new recruits and the influence of each mental factor on injury in military training were analyzed by "SCL-90" in our army, and evaluation of the results was excellent. It indicated that using "SCL-90" to analyze the mental factors was feasible^[37-40]. In an emergency period, especially in modern warfare, intense danger and cruelty would cause a great pressure on servicemen's mentality. Therefore, mental factor may be a risk factor of diarrhea in an emergency period. In our study, 1:2 case-control study was performed to evaluate the relation between mental factor and diarrhea. The result of single-factor analysis suggested that the gross score and 9 factors (except paranoiac factor) were associated with diarrhea. In addition, the result of multiple-factor analysis suggested that depression was a risk factor of diarrhea, as only depression was entered to the aggressive equation. Whether this relation exists or not is still a problem worth further studying. The possible explanation is that mental factor, acting through the neuroendocrine system, can lead to enterocinesia and gastroenteric secretion disorder or weaken the immune functions, so the body is more susceptible to pathogens, resulting in diarrhea^[41,42].

Case-case control study has been used to analyze the risk factors of chronic infant diarrhea^[40] but not used to analyze that of diarrhea in a military emergency period. For the first time, we used it to analyze the risk factors of diarrhea in an emergency period. During the emergency period, it was critical to deal with the problems which influenced the fighting capacity due to limited human and material resources. Our study demonstrated that 20.4% of diarrhea patients could not work, because of the severe clinical manifestations. If these patients can be prevented from diarrhea, the fighting capacity will be greatly increased. In our study, the result indicated that three risk factors (drinking raw water 7 days before diarrhea, eating outside, not washing hand before eating) had a relation with severe clinical manifestations. Overall, the result indicated that preventive measures should be taken to control the three risk factors.

No report has been published on using unit incidence as risk factors to prevent diarrhea. In our study, the unit diarrhea incidence rate was different. To maintain the fighting capacity, decreasing the unit incidence rate is important. If we can find out the unit risk factors, measures can be taken to control them. The result of linear stepping regression showed that three (density of flies in toilets, garbage disposal methods and daily average boiled-water supply) out of 23 potential factors might be the cause of the increased unit incidence. From the standard regression coefficient, the density of flies in toilets had the major influence on diarrhea incidence rate. The higher the density of flies in toilets, the higher the diarrhea incidence rate. Fly is an important route of transmission, which has been confirmed before. The study of the Gulf War also demonstrated that persistent existence of flies was an important reason of low-epidemic diarrhea. Meanwhile, we thought the garbage disposal methods have a relation with the density of flies. Some troops buried garbage by the sanitary unit strictly, thus preventing the reproduction of flies.

ACKNOWLEDGEMENTS

We would like to thank all the military personnel participated in this study. We are also grateful to Professor Chen Pingyan in Department of Statistics, Professor Xie Yaning in Department of Psychology of the First Military Medical University, and Professor Wang Nengping in CDC of Nanfang Hospital, Professor Liu Qing in Department of Statistics of Sun yet-sen Medical University for their generous help in this study.

REFERENCES

- Sanchez JL**, Gelnett J, Petrucci BP, Defraites RF, Taylor DN. Diarrheal disease incidence and morbidity among United States military personnel during short-term missions overseas. *Am J Trop Med Hyg* 1998; **58**: 299-304
- Heggors JP**. Microbial invasion—the major ally of war (natural biological warfare). *Mil Med* 1978; **143**: 390-394
- Quin NE**. The impact of diseases on military operations in the Persian Gulf. *Mil Med* 1978; **147**: 728-734
- Pazzaglia Walker RI**. A retrospective survey of enteric infections in active duty Navy and Marine Corps personnel. *Mil Med* 1982; **147**: 27-33
- Nie J**, Yu SY, Chen YZ, Chen Q, Wu M, Meng FH. The epidemiological investigation on acute diarrhea in a certain unit of PLA in South China. *Zhongguo Gonggong Weisheng Zazhi* 1996; **12**: 249-250
- Hyams KC**, Riddle J, Trump DH, Graham JT. Endemic infectious diseases and biological warfare during the Gulf War: a decade of analysis and final concerns. *Am J Trop Med Hyg* 2001; **65**: 664-670
- Connor P**, Farthing MJ. Travellers' diarrhoea: a military problem? *J R Army Med Corps* 1999; **145**: 95-101
- Haberberger RL Jr**, Mikhail IA, Burans JP, Hyams KC, Glenn JC, Diniega BM, Sorgen S, Mansour N, Blacklow NR, Woody JN. Travelers' diarrhea among United States military personnel during joint American-Egyptian armed forces exercises in Cairo Egypt. *Mil Med* 1991; **156**: 27-30
- Pazzaglia G**, Walker RI. A retrospective survey of enteric infections in active duty Navy and Marine Corps personnel. *Mil Med* 1982; **147**: 27-33
- Echeverria P**, Ramirez G, Blacklow NR, Ksiazek T, Cukor G, Cross JH. Travelers' diarrhea among U.S. Army troops in South Korea. *J Infect Dis* 1979; **139**: 215-219
- Barrett KE**. New insights into the pathogenesis of intestinal dysfunction: secretory diarrhea and cystic fibrosis. *World J Gastroenterol* 2000; **6**: 470-474
- Oyfo BA**, el-Gendy A, Wasfy MO, el-Etr SH, Churilla A, Murphy J. A survey of enteropathogens among United States military personnel during Operation Bright Star '94, in Cairo, Egypt. *Mil Med* 1995; **160**: 331-334
- Oyfo BA**, Peruski LF, Ismail TF, el Etr SH, Churilla AM, Wasfy MO, Petrucci BP, Gabriel ME. Enteropathogens associated with diarrhea among military personnel during Operation Bright Star 96, in Alexandria, Egypt. *Mil Med* 1997; **162**: 396-400
- Oyfo BA**, Lesmana M, Subekti D, Tjaniadi P, Larasati W, Putri M, Simanjuntak CH, Punjabi NH, Santoso W, Muzahar, Sukarma, Sriwati, Sarumpaet S, Abdi M, Tjindi R, Ma'ani H, Sumardiati A, Handayani H, Campbell JR, Alexander WK, Beecham HJ 3rd, Corwin AL. Surveillance of bacterial pathogens of diarrhea disease in Indonesia. *Dia Microbiol Infect Dis* 2002; **44**: 227-234
- Tan TY**. Use of molecular techniques for the detection of antibiotic resistance in bacteria. *Exp Rev Mol Dia* 2003; **3**: 93-103
- Song J**, Swekla M, Colorado P, Reddy R, Hoffmann S, Fine S. Liver abscess and diarrhea as initial manifestations of ulcerative colitis: case report and review of the literature. *Dig Dis Sci* 2003; **48**: 417-421
- Ruskone-Fourmestraux A**, Attar A, Chassard D, Coffin B, Bornet F, Bouhnik Y. A digestive tolerance study of maltitol after occasional and regular consumption in healthy humans. *Eur J Clin Nutr* 2003; **57**: 26-30
- Bhattacharya SK**. Therapeutic methods for diarrhoea in children. *World J Gastroenterol* 2000; **6**: 497-500
- Taylor WR**, Schell WL, Wells JG, Choi K, Kinnunen DE, Heiser PT, Helstad AG. A foodborne outbreak of enterotoxigenic *Escherichia coli* diarrhea. *N Engl J Med* 1982; **306**: 1093-1095
- Davis H**, Taylor JP, Perdue JN, Stelma GN Jr, Humphreys JM Jr, Rowntree R 3rd, Greene KD. A shigellosis outbreak traced to commercially distributed shredded lettuce. *Am J Epidemiol* 1988; **128**: 1312-1314
- Martin DL**, Gustafson TL, Pelosi JW, Suarez L, Pierce GV. Contaminated produce—a common source for two outbreaks of *Shigella* gastroenteritis. *Am J Epidemiol* 1986; **124**: 299-305
- Griffin MR**, Surowiec JJ, McCloskey DI, Capuano B, Pierzynski B, Quinn M, Wojnarski R, Parkin WE, Greenberg H, Gary GW. Foodborne Norwalk virus. *Am J Epidemiol* 1982; **115**: 178-184
- Binder HJ**. Pathophysiology of diarrhea. *Shijie Huaren Xiaohua Zazhi* 1997; **5**: 62
- Haberberger RL**, Scott DA, Thornton SA, Hyams KC. Diarrheal disease aboard a U.S. Navy ship after a brief port visit to a high risk area. *Mil Med* 1994; **159**: 445-448
- Hyams KC**, Bourgeois AL, Merrell BR, Rozmajzl P, Escamilla J, Thornton SA, Wasserman GM, Burke A, Echeverria P, Green KY. Diarrheal disease during Operation Desert Shield. *N Engl J Med* 1991; **325**: 1423-1428
- Wolfe M**. Acute diarrhea associated with travel. *Am J Med* 1990; **88**: 345-375
- Sharp TW**, Thornton SA, Wallace MR, Defraites RF, Sanchez JL, Batchelor RA, Rozmajzl PJ, Hanson RK, Echeverria P, Kapikian AZ. Diarrhea disease among military personnel during operation Restore Hope, Somalia, 1992-1993. *Am J Trop Med Hyg* 1995; **52**: 188-193
- Dupont H**. Prevention and treatment of traveler's diarrhea. *N Engl J Med* 1993; **328**: 1821-1827
- Xiong Q**. Microbial sensitivity tests result of Dysenteric Bacillus. *Shijie Huaren Xiaohua Zazhi* 1996; **4**: 536
- DeMaio J**, Bailey L, Hall K, Boyd R. A major outbreak of foodborne gastroenteritis among Air Force personnel during Operation Desert Storm. *Mil Med* 1993; **158**: 161-164
- Bruins J**, Bwire R, Slooman EJ, van Leusden AJ. Diarrhea morbidity among Dutch military service men in Goma, Zaire. *Mil Med* 1995; **160**: 446-448
- Huerta M**, Grotto I, Gdalevich M, Mimouni D, Gavrieli B, Yavzori M, Cohen D, Shpilberg O. A waterborne outbreak of gastroenteritis in the Golan Heights due to enterotoxigenic *Escherichia coli*. *Infection* 2000; **28**: 267-271
- Sack DA**, Kaminsky DC, Sack RB, Wamola IA, Orskov F, Orskov I, Slack RC, Arthur RR, Kapikian AZ. Enterotoxigenic *Escherichia coli* diarrhea of travelers: a prospective study of American Peace Corps volunteers. *Johns Hopkins Med J* 1977; **141**: 63-70
- Echeverria P**, Blacklow NR, Zipkin C, Vollet JJ, Olson JA, DuPont HL, Cross JH. Etiology of gastroenteritis among Americans living in the Philippines. *Am J Epidemiol* 1979; **109**: 493-501
- Steffen R**, Mathewson JJ, Ericsson CD, DuPont HL, Helminger A, Balm TK, Wolff K, Witassek F. Travelers' diarrhea in West Africa and Mexico: fecal transport systems and liquid bismuth subsalicylate for self-therapy. *J Infect Dis* 1988; **157**: 1008-1013
- Cohen D**, Sela T, Slepion R, Yavzori M, Ambar R, Orr N, Robin G, Shpilberg O, Eldad A, Green M. Prospective cohort studies of shigellosis during military field training. *Eur J Clin Microbiol Infect Dis* 2001; **20**: 123-126
- Zhang LX**. An investigation on new recruits' mental condition of army. *Jiefangjun Yufang Yixue Zazhi* 1997; **15**: 374-375
- Zhou H**, Li F, Zhang YG, Lei ZJ, Yang Y. Recruit training injure and psychology factors. *Renmin Junyi* 2000; **43**: 64-65
- Chui SF**, Liu XH, Yang XG, Liu YL, Jin BA, Zhang ZY. An investigation of singletons of new recruit's mental health. *Renmin Junyi* 1998; **41**: 64-65
- Xu NF**, Wu B, Yuan JA, Chen SQ. The case-control study on infant chronic diarrhea's risk factors. *Zhongguo Gonggong Weishen Xuebai* 1999; **14**: 41-43
- Ivashkin VT**, Lapina TL, Bondarenko OY, Sklanskaya OA, Grigoriev PY, Vasiliev YV, Yakovenko EP, Gulyaev PV, Fedchenko VI. Azithromycin in a triple therapy for *H pylori* eradication in active duodenal ulcer. *World J Gastroenterol* 2002; **8**: 879-882
- Qin XY**, Shen KT, Zhang X, Cheng ZH, Xu XR, Han ZG. Establishment of an artificial beta-cell line expressing insulin under the control of doxycycline. *World J Gastroenterol* 2002; **8**: 367-370

Alteration of somatostatin receptor subtype 2 gene expression in pancreatic tumor angiogenesis

Ren-Yi Qin, Ru-Liang Fang, Manoj Kumar Gupta, Zheng-Ren Liu, Da-Yu Wang, Qing Chang, Yi-Bei Chen

Ren-Yi Qin, Ru-Liang Fang, Manoj Kumar Gupta, Zheng-Ren Liu, Da-Yu Wang, Qing Chang, Yi-Bei Chen, Department of Surgery, Tongji Hospital, Tongji Medical College, Huazhong University of Science and Technology, Wuhan 430030, Hubei Province, China

Supported by National Natural Science Foundation of China, No. 30271473

Correspondence to: Professor Ren-Yi Qin, Department of Surgery, Tongji Hospital, Tongji Medical College, Huazhong University of Science and Technology, Wuhan 430030, Hubei, Province, China. ryqin@tjh.tjmu.edu.cn

Telephone: +86-27-83662389 **Fax:** +86-27-83662389

Received: 2003-06-04 **Accepted:** 2003-07-30

Abstract

AIM: To explore the difference of somatostatin receptor subtype 2 (SST2R) gene expression in pancreatic cancerous tissue and its adjacent tissue, and the relationship between the change of SST2R gene expression and pancreatic tumor angiogenesis related genes.

METHODS: The expressions of SST2R, DPC4, p53 and ras genes in cancer tissues of 40 patients with primary pancreatic cancer, and the expression of SST2R gene in its adjacent tissue were determined by immunohistochemical LSAB method and EnVision™ method. Chi-square test was used to analyze the difference in expression of SST2R in pancreatic cancer tissue and its adjacent tissue, and the correlation of SST2R gene expression with the expression of p53, ras and DPC4 genes.

RESULTS: Of the tissue specimens from 40 patients with primary pancreatic cancer, 35 (87.5%) cancer tissues showed a negative expression of SST2R gene, whereas 34 (85%) a positive expression of SST2R gene in its adjacent tissues. Five (12.5%) cancer tissues and its adjacent tissues simultaneously expressed SST2R. The expression of SST2R gene was markedly higher in pancreatic tissues adjacent to cancer than in pancreatic cancer tissues ($P < 0.05$). The expression rates of p53, ras and DPC4 genes were 50%, 60% and 72.5%, respectively. There was a significant negative correlation of SST2R with p53 and ras genes ($\chi^2 = 9.33$, $P < 0.01$), but no significant correlation with DPC4 gene ($\chi^2 = 2.08$, $P > 0.05$).

CONCLUSION: There was a significant difference of SST2R gene expression in pancreatic cancer tissues and its adjacent tissues, which might be one cause for the different therapeutic effects of somatostatin and its analogs on pancreatic cancer patients. There were abnormal expressions of SST2R, DPC4, p53 and ras genes in pancreatic carcinogenesis, and moreover, the loss or decrease of SST2R gene expression was significantly negatively correlated with the overexpression of tumor angiogenesis correlated p53 and ras genes, suggesting that SST2R gene together with p53 and ras genes may participate in pancreatic cancerous angiogenesis.

Qin RY, Fang RL, Gupta MK, Liu ZR, Wang DY, Chang Q, Chen YB. Alteration of somatostatin receptor subtype 2 gene expression in pancreatic tumor angiogenesis. *World J Gastroenterol* 2004; 10(1): 132-135

<http://www.wjgnet.com/1007-9327/10/132.asp>

INTRODUCTION

Recent studies have indicated that somatostatin and its analogs have obviously antiproliferative effects on various solid tumors, such as colon cancer, liver cancer, which are mediated through somatostatin receptors^[1-7], but a large number of clinical researches indicate that the therapeutic effects of somatostatin and its analogs on pancreatic cancer are different, the reason is not known^[8,9]. Moreover, studies have already reported that the change of SST2R gene expression in human pancreatic cancerous cells is related with tumor angiogenesis factors such as transforming growth factor beta (TGF- β), but the relationship between SST2R and tumor angiogenesis related genes such as DPC4, ras and p53 is still not clear^[10]. Our study aimed at exploring the cause for the different therapeutic effects of somatostatin and its analogs on human pancreatic cancer, and the relationship between the changes of SST2R gene expression and pancreatic tumor angiogenesis correlated genes.

MATERIALS AND METHODS

Tissue specimens

Tissue samples from 40 primary pancreatic cancer patients were obtained from the Department of Pathology in Tongji Hospital. The patients consisted of 26 males and 14 females aged from 33 to 71 years (means: 55.65 years). All lesions were diagnosed pathologically as pancreatic ductal adenocarcinoma, consisting of 23 pancreatic cancers in the head, and 17 pancreatic cancers in the body and tail of pancreas. All patients were staged according to UICC TNM classification, I-II in 14 patients, and III-IV in 26 patients. All the specimens of pancreatic cancer tissues and its adjacent tissues were fixed and dehydrated in 10% formalin, embedded in paraffin and cut into 4 μ m serial sections.

Reagents

Goat SST2R and DPC4 polyclonal antibodies were from Santa Cruz (USA). p53, ras monoclonal antibody and mouse anti-human ras monoclonal antibody were from Maixin Biotech Kaifa Company (Fuzhou, China). Secondary biotinylated rabbit anti-sheep IgG (ZB-2050) was from ZYMED (USA). EnVision™ mouse-anti reagent kit, EnVision™ rabbit-anti reagent kit and peroxidase conjugated streptavidin were from DAKO (Denmark).

Immunohistochemical staining

Three-step methods (LSAB) were used for DPC4 and SST2R staining, and two-step methods (EnVision™ system) were used for p53 and ras genes. Formalin-fixed, paraffin-embedded sections were dewaxed, rehydrated, and boiled in 0.01M-citrate buffer, pH 6.0 in a microwave oven for 10 minutes. Then primary antibody was added and incubated at 4 °C overnight. Biotinylated rabbit anti-sheep IgG (1:300 dilution) was added

and incubated at 37 °C for 1 hour, followed by incubation with peroxidase conjugated streptavidin (1:400 dilution) at 37 °C for 30 minutes. For p53 and ras staining, peroxidase conjugated streptavidin was replaced by EnVision. DAB chromogen was applied for 10 to 20 minutes and rinsed for visualization under microscope, followed by slight counterstaining with haematoxylin, dehydration, and finally cover slips were sealed with permount. Negative control was obtained by replacing the primary antibody with PBS.

Evaluation of immunohistochemical staining

Positive staining was located in cell membrane/cytoplasm for SST2R, and the cytoplasm for DPC4 and ras, and the nucleus for p53. At least 1000 cells were counted per 40 X 10 field. The expressions were graded, as follows. Negative (-) if <10% of the cancerous cells in a given specimen were positively stained. Weak positive (+) if 10% to 20% of the cancerous cells in a given specimen were positively stained. Positive (++) if 20% to 50% of the cancer cells in a given specimen were positively stained, and strongly positive (+++) if 75% of the cancer cells in a given specimen were positively stained.

Statistical analysis

Chi-square test was used to analyze the results. $P < 0.05$ was considered statistically significant.

RESULTS

Expression of SST2R gene in pancreatic cancer tissue and its adjacent tissue

The expression rate of SST2R gene was markedly higher in the adjacent non-cancerous tissue (85%) than in cancer tissue (12.5%) ($P < 0.05$). Twenty-nine patients (72.5%) expressed SST2R gene only in the adjacent non-cancerous tissue. For SST2R gene expression in pancreatic cancer tissue, strong positive was only 10%, weak positive 2.5%, and negative 87.5%, 12.5% pancreatic cancer tissue and its adjacent non-cancerous tissue expressed SST2R simultaneously (Table 1 and Figures 1, 2).

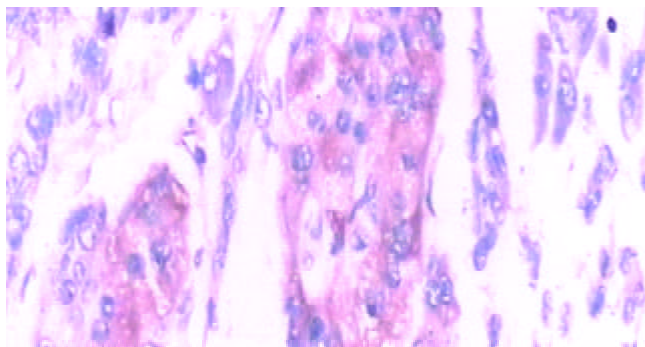


Figure 1 Ductal adenocarcinoma in pancreatic head (Immunohisto-chemistry LSAB method, ×400). Brown yellow staining of SST2R gene expression in cell membrane/cytoplasm.

Expression of p53 gene in pancreatic cancer tissue

For p53 gene in pancreatic cancerous tissue, 19 patients (47.5%) had strong positive expression, 20 patients (50%) negative expression, and 1 patient (2.5%) weak positive expression. The SST2R gene expression in 17 patients with strong positive expression of p53 was negative. Three patients with strong positive expression of SST2R were negative for p53 gene expression. The SST2R and p53 gene expressions in 1 patient were strong positive. One patient with weak positive expression of p53 gene was negative for SST2R gene expression. The SST2R gene expression of 1 patient with strong positive expression of p53 gene was weak positive (Table 1 and Figure 3).

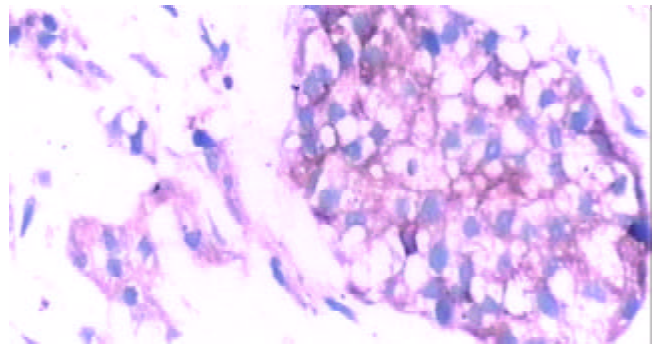


Figure 2 Pancreatic ductal adenocarcinoma in pancreatic body and tail (Immunohistochemistry LSAB method, ×400). Brown yellow staining of SST2R gene expression in cell membrane/cytoplasm.

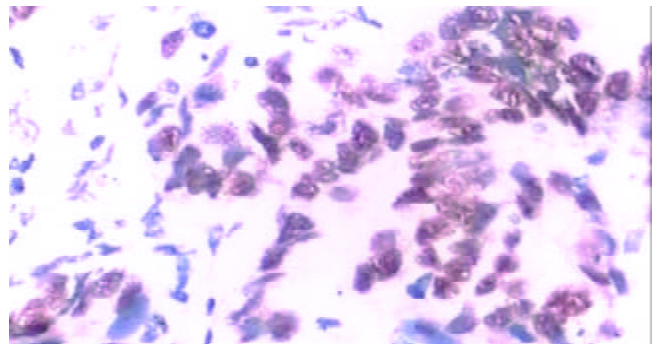


Figure 3 Ductal adenocarcinoma in pancreatic head (EnVision™ method, ×400). Brown yellow staining of p53 gene expression in cell nucleus.

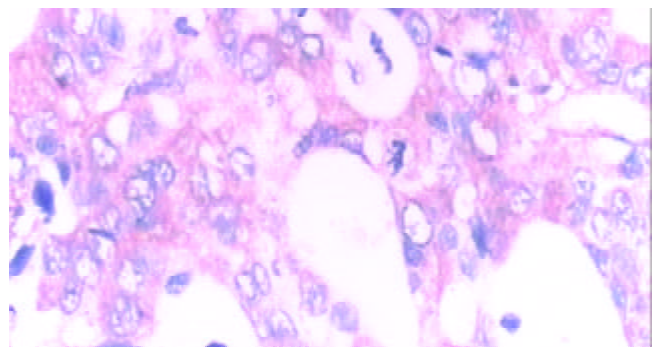


Figure 4 Ductal adenocarcinoma in pancreatic body and tail (EnVision™ method, ×400). Brown yellow staining of ras gene expression located in cytoplasm.

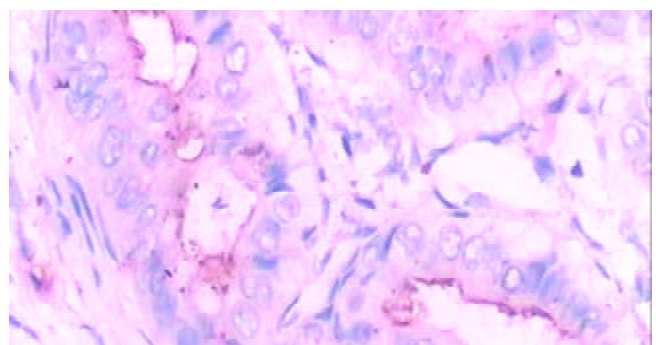


Figure 5 Ductal adenocarcinoma in pancreatic body and tail (EnVision™ method, ×400). Brown yellow staining of DPC4 gene expression located in cytoplasm.

Expression of ras gene in pancreatic cancer tissue

For expression of ras gene, 14 patients (35%) were strong positive, 10 patients (25%) weak positive, and 16 patients (40%) negative. Eleven patients with strong positive expression of ras gene showed negative expression of SST2R gene, 1 patient with negative expression of ras gene showed strong positive expression of SST2R gene. The SST2R and ras genes in 4 patients showed positive expression of different grades correspondingly. The SST2R and ras gene expressions in 15 patients were negative. Nine patients with weak positive expression of ras gene were negative for SST2R gene expression (Table 1 and Figure 4).

Expression of DPC4 gene in pancreatic cancer tissue

Seven patients (17.5%) were positive, 4 patients (10%) weak positive, and 29 patients (72.5%) negative for DPC4 gene expression. Twenty-six patients (65%) had negative expression of both DPC4 and SST2R gene. Of the 9 patients with negative expression of SST2R gene, 5 patients were strong positive, and 4 patients weak positive for DPC4 gene expression. Both SST2R and DPC4 genes expression of 2 patients were strong positive. One patient with negative expression of DPC4 gene was weak positive for SST2R gene expression (Table 1 and Figure 5).

Statistical analysis indicated that SST2R was significantly negatively correlated with the expression of p53 or ras genes ($P < 0.01$), whereas not distinctly correlated with DPC4 gene ($P > 0.05$).

Table 1 Expressions of SST2R and ras, DPC4 and p53 genes in 40 primary pancreatic cancerous tissues

	Strong positive (+++ to +++) n (%)	Weak positive (+) n (%)	Negative (-) n (%)
SST2R	4.0 (10)	1.0 (2.5)	35.0 (87.5)
ras	14.0 (35)	10.0 (25)	16.0 (4)
DPC4	7.0 (17.5)	4.0 (10)	19.0 (47.5)
P53	19.0 (47.5)	1.0 (2.5)	20.0 (50)
Cancer adjacent SST2R	34.0 (85)	0.0	6.0 (15)

DISCUSSION

Somatostatin and its analogs can inhibit the growth of benign and malignant tumors, and it has been found that the inhibitory effects are directly correlated with the expression of SST2R on tumor tissues^[11-15]. The mechanisms of the inhibition are the combined interaction of somatostatin and its analogs with SST2R in tumor tissues, either directly inhibiting division and proliferation of tumor cells or inhibiting the activities of growth factors such as vascular endothelial growth factor (VEGF), insulin-like growth factor (IGF)^[16-21], and moreover, counteracting tumorigenesis and tissue proliferation^[22,23]. In addition, somatostatin and its analogs could arrest pancreatic cancer cell cycle at G₀-S₁ phase by up-regulating p27, and thus induced apoptosis^[24,25].

The expression of SST2R was decreased or lost in primary pancreatic cancerous tissue^[26-29], but there is no report on the expression of SST2R in pancreatic cancerous adjacent tissue. Our study showed that 5 of 40 primary pancreatic cancer tissues showed positive expression of SST2R gene, suggesting that most of pancreatic cancerous tissues lack the expression of SST2R, which may be the major reason why somatostatin and its analogs had no marked therapeutic effects on pancreatic cancer. Interestingly, expression of SST2R was higher in most of the pancreatic cancerous adjacent tissues, which may be beneficial for somatostatin and its analogs to inhibit fast outward infiltration and growth of tumor cells. Our study

indicated that if SST2R decreased in pancreatic cancerous tissue and its adjacent tissue, somatostatin and its analogs might not have therapeutic effect on pancreatic cancer. But when pancreatic cancerous tissue and its adjacent tissue obviously expressed SST2R, they had a definite therapeutic effect on patients with pancreatic cancer. Hence the differences in the expression of SST2R in pancreatic cancerous tissue and its adjacent tissue would certainly lead to different therapeutic effects. At present, this is the main possible cause for the different therapeutic effects of somatostatin and its analogs on pancreatic cancer. We consider that it is important to define the expression of SST2R in pancreatic cancerous tissue and its adjacent tissue before using somatostatin and its analogs. This will be beneficial to the ultimate definition of the exact therapeutic effects of somatostatin and its analogs on pancreatic cancer.

Mutations of DPC4, ras and p53 genes have been found to play crucial roles in tumor angiogenesis^[30-32]. The mutation rates of these genes are higher in pancreatic cancerous tissue, indicating that the similar mechanism of pancreatic tumorigenesis with other tumorigenesis involving mutation and abnormal expression of multiple genes. Our study indicated that the expression of SST2R gene was significantly negatively correlated with p53 and ras genes, suggesting that the decrease or loss of SST2R gene expression in pancreatic cancerous tissue participates in tumor angiogenesis through certain pathway, further investigation is required to probe into its the mechanism.

REFERENCES

- O'Byrne KJ, Schally AV, Thomas A, Carney DN, Steward WP. Somatostatin, its receptors and analogs, in lung cancer. *Chemotherapy* 2001; **47**(Suppl): 78-108
- Kouroumalis E, Skordilis P, Thermos K, Vasilaki A, Moschandrea J, Manousos ON. Treatment of hepatocellular carcinoma with octreotide: a randomised controlled study. *Gut* 1998; **42**: 442-447
- Wolff RA. Chemoprevention for pancreatic cancer. *Int J Gastrointest Cancer* 2003; **33**: 27-41
- Samonakis DN, Moschandreas J, Arnaoutis T, Skordilis P, Leontidis C, Vafiades I, Kouroumalis E. Treatment of hepatocellular carcinoma with long acting somatostatin analogues. *Oncol Rep* 2002; **9**: 903-907
- Hejna M, Schmidinger M, Raderer M. The clinical role of somatostatin analogues as antineoplastic agents: much ado about nothing? *Ann Oncol* 2002; **13**: 653-668
- Hofslie E. The somatostatin receptor family—a window against new diagnosis and therapy of cancer. *Tidsskr Nor Laegeforen* 2002; **122**: 487-491
- Vainas IG. Octreotide in the management of hormone-refractory prostate cancer. *Chemotherapy* 2001; **47**(Suppl 2): 109-126
- Raderer M, Kurtaran A, Scheithauer W, Fiebigler W, Weinlaender G, Oberhuber G. Different response to the long-acting somatostatin analogues lanreotide and octreotide in a patient with a malignant carcinoid. *Oncology* 2001; **60**: 141-145
- Raderer M, Hamilton G, Kurtaran A, Valencak J, Haberl I, Hoffmann O, Kornek GV, Vorbeck F, Hejna MH, Virgolini I, Scheithauer W. Treatment of advanced pancreatic cancer with the long-acting somatostatin analogue lanreotide: *in vitro* and *in vivo* results. *Br J Cancer* 1999; **79**: 535-537
- Gupta MK, Qin RY. Mechanism and its regulation of tumor-induced angiogenesis. *World J Gastroenterol* 2003; **9**: 1144-1155
- Rochaix P, Delesque N, Esteve JP, Saint-Laurent N, Voight JJ, Vaysse N, Susini C, Buscail L. Gene therapy for pancreatic carcinoma: local and distant antitumor effects after somatostatin receptor sst2R gene transfer. *Hum Gene Ther* 1999; **10**: 995-1008
- Buscail L, Saint-Laurent N, Chastre E, Vaillant JC, Gest Capella G, Kalthoff H, Lluís F, Vaysse N, Susini C. Loss of sst2 Somatostatin receptor gene expression in human pancreatic and colorectal cancer. *Cancer Res* 1996; **56**: 1823-1827
- Guillemet J, Saint-Laurent N, Rochaix P, Cuvillier O, Levade T, Schally AV, Pradayrol L, Buscail L, Susini C, Bousquet C. Soma-

- tostatin receptor subtype 2 sensitizes human pancreatic cancer cells to death ligand-induced apoptosis. *Proc Natl Acad Sci U S A* 2003; **100**: 155-160
- 14 **Vernejoul F**, Faure P, Benali N, Calise D, Tiraby G, Pradayrol L, Susini C, Buscail L. Antitumor effect of *in vivo* somatostatin receptor subtype 2 gene transfer in primary and metastatic pancreatic cancer models. *Cancer Res* 2002; **62**: 6124-6131
- 15 **Faiss S**, Pape UF, Bohmig M, Dorffel Y, Mansmann U, Golder W, Riecken EO, Wiedenmann B. Prospective, randomized, multicenter trial on the antiproliferative effect of lanreotide, interferon alfa, and their combination for therapy of metastatic neuroendocrine gastroenteropancreatic tumors—the International Lanreotide and Interferon Alfa Study Group. *J Clin Oncol* 2003; **21**: 2689-2696
- 16 **Hortala M**, Ferjoux G, Estival A, Bertrand C, Schulz S, Pradayrol L, Susini C, Clemente F. Inhibitory role of the somatostatin receptor SST2 on the intracrine-regulated cell proliferation induced by the 210-amino acid fibroblast growth factor-2 isoform: implication of JAK2. *J Biol Chem* 2003; **278**: 20574-20581
- 17 **Pollak MN**, Schally AV. Mechanisms of antineoplastic action of somatostatin analogs. *Proc Soc Exp Biol Med* 1998; **217**: 143-152
- 18 **Buscail L**, Vernejoul F, Faure P, Torrisani J, Susini C. Regulation of cell proliferation by somatostatin. *Ann Endocrinol* 2002; **63**(2 Pt 3): 2S13-2S18
- 19 **Puente E**, Saint-Laurent N, Torrisani J, Furet C, Schally AV, Vaysse N, Buscail L, Susini C. Transcriptional activation of mouse sst2 somatostatin receptor promoter by transforming growth factor-beta. Involvement of Smad4. *J Biol Chem* 2001; **276**: 13461-13468
- 20 **Pages P**, Benali N, Saint-Laurent N, Esteve JP, Schally AV, Tkaczuk J, Vaysse N, Susini C, Buscail L. Sst2 somatostatin receptor mediates cell cycle arrest and induction of p27(Kip1). Evidence for the role of SHP-1. *J Biol Chem* 1999; **274**: 15186-15193
- 21 **Kikutsuji T**, Harada M, Tashiro S, Ii S, Moritani M, Yamaoka T, Itakura M. Expression of somatostatin receptor subtypes and growth inhibition in human exocrine pancreatic cancers. *J Hepatobiliary Pancreat Surg* 2000; **7**: 496-503
- 22 **Bousquet C**, Puente E, Buscail L, Vaysse N, Susini C. Antiproliferative effect of somatostatin and analogs. *Chemotherapy* 2001; **47**(Suppl 2): 30-39
- 23 **Ferjoux G**, Bousquet C, Cordelier P, Benali N, Lopez F, Rochaix P, Buscail L, Susini C. Signal transduction of somatostatin receptors negatively controlling cell proliferation. *J Physiol Paris* 2000; **94**: 205-210
- 24 **Benali N**, Cordelier P, Calise D, Pages P, Rochaix P, Nagy A, Esteve JP, Pour PM, Schally AV, Vaysse N, Susini C, Buscail L. Inhibition of growth and metastatic progression of pancreatic carcinoma in hamster after somatostatin receptor subtype 2 (sst2) gene expression and administration of cytotoxic somatostatin analog AN-238. *Proc Natl Acad Sci U S A* 2000; **97**: 9180-9185
- 25 **Fisher WE**, Wu Y, Amaya F, Berger DH. Somatostatin receptor subtype 2 gene therapy inhibits pancreatic cancer *in vitro*. *J Surg Res* 2002; **105**: 58-64
- 26 **Buscail L**, Saint-Laurent N, Chastre E, Vaillant JC, Gespach C, Capella G, Kalthoff H, Lluís F, Vaysse N, Susini C. Loss of sst2 somatostatin receptor gene expression in human pancreatic and colorectal cancer. *Cancer Res* 1996; **56**: 1823-1827
- 27 **Benali N**, Ferjoux G, Puente E, Buscail L, Susini C. Somatostatin receptors. *Digestion* 2000; **621**(Suppl 1): 27-32
- 28 **Fueger BJ**, Hamilton G, Raderer M, Pangerl T, Traub T, Angelberger P, Baumgartner G, Dudczak R, Virgolini I. Effects of chemotherapeutic agents on expression of somatostatin receptors in pancreatic tumor cells. *J Nucl Med* 2001; **42**: 1856-1862
- 29 **Qin RY**, Qiu FZ. SST2R and SST2R mRNA expression in rats with pancreatic cancer and the effect of octreotide. *Yixian Bingxue* 2002; **2**: 41-44
- 30 **Schwarte-Waldhoff I**, Volpert OV, Bouck NP, Sipos B, Hahn SA, Klein-Scory S, Luttes J, Kloppel G, Graeven U, Eilert-Micus C, Hintelmann A, Schmiegel W. Smad4/DPC4-mediated tumor suppression through suppression of angiogenesis. *Proc Natl Acad Sci U S A* 2000; **97**: 9624-9629
- 31 **Shu X**, Wu W, Mosteller RD, Broek D. Sphingosine kinase mediates vascular endothelial growth factor-induced activation of ras and mitogen-activated protein kinases. *Mol Cell Biol* 2002; **22**: 7758-7768
- 32 **Bacher M**, Schrader J, Thompson N, Kuschela K, Gemsa D, Waeber G, Schlegel J. Up-regulation of macrophage migration inhibitory factor gene and protein expression in glial tumor cells during hypoxic and hypoglycemic stress indicates a critical role for angiogenesis in glioblastoma multiforme. *Am J Pathol* 2003; **162**: 11-17

Edited by Ren SY and Wang XL

Perioperative cimetidine administration promotes peripheral blood lymphocytes and tumor infiltrating lymphocytes in patients with gastrointestinal cancer: Results of a randomized controlled clinical trial

Cong-Yao Lin, De-Jiao Bai, Hong-Yin Yuan, Kun Wang, Guo-Liang Yang, Ming-Bai Hu, Zhou-Qing Wu, Yan Li

Cong-Yao Lin, De-Jiao Bai, Hong-Yin Yuan, Kun Wang, Guo-Liang Yang, Ming-Bai Hu, Zhou-Qing Wu, Yan Li, Department of Oncology, Zhongnan Hospital of Wuhan University, Wuhan 430071, Hubei Province, China

Supported by the Science Progress Project of Hubei Province, No. 2001AA301C35

Co-correspondents: Cong-Yao Lin and Yan Li

Correspondence to: Professor Cong-Yao Lin, Department of Oncology, Zhongnan Hospital of Wuhan University, 169 Dong Hu Rd, Wuhan 430073, Hubei Province, China. liyansd@hotmail.com

Telephone: +86-27-87335585 **Fax:** +86-27-87307622

Received: 2003-06-16 **Accepted:** 2003-07-24

Abstract

AIM: To study the effects of perioperative administration of cimetidine (CIM) on peripheral blood lymphocytes, natural killer (NK) cells and tumor infiltrating lymphocytes (TIL) in patients with gastrointestinal (GI) cancer.

METHODS: Forty-nine GI cancer patients were randomized into treatment group, who took CIM in perioperative period, and control group, who did not take the drug. The treatment was initiated 7 days before operation and continued for 10 days after surgery. At baseline examination before operation, on the 2nd and 10th postoperative days, total T lymphocytes, T helper cells, T suppressor cells, and NK cells in peripheral blood were measured respectively by immunocytochemical method using mouse-anti human CD₃, CD₄, CD₈ and CD₅₇ monoclonal antibodies. Blood samples from 20 healthy volunteers were treated in the same way as normal controls. Surgical specimens were examined during routine histopathological evaluation for the presence of TIL in tumor margin. Immunohistochemical study was performed to measure the proportion of T and B lymphocytes in TIL population. T and B lymphocytes were detected respectively using mouse-anti-human CD₃ and CD₂₀ monoclonal antibodies.

RESULTS: In comparison with normal controls, both the treatment and control groups had decreased T cells, T helper cells and NK cells at baseline. In control group, total T cells, T helper cells and NK cells declined continuously with the disease progression and the decrease became more obvious after operation. From baseline to the 2nd postoperative day, the proportion of total T cells, T helper cells, and NK cells went down from 60.5±4.6% to 56.2±3.8%, 33.4±3.7% to 28.1±3.4%, and 15.0±2.8% to 14.2±2.2%, respectively. On the other hand, there were significant improvements in these parameters after CIM treatment. On the 10th postoperative day, the treatment group had significantly higher percentages of total T cells, T helper cells and NK cells than control group. Moreover, CIM treatment also boosted TIL response, as was reflected by findings that 68%

(17/25) of the patients in treatment group had significant TIL responses and only 25% (6/24) of the cases had discernible TIL responses ($P<0.01$).

CONCLUSION: Perioperative application of CIM to GI cancer patients could help restore the diminished cellular immunity induced by tumor burden and surgical maneuver. The drug could also boost TIL responses to tumor. These effects suggest that the drug be used as an immunomodulator for GI cancer patients.

Lin CY, Bai DJ, Yuan HY, Wang K, Yang GL, Hu MB, Wu ZQ, Li Y. Perioperative cimetidine administration promotes peripheral blood lymphocytes and tumor infiltrating lymphocytes in patients with gastrointestinal cancer: Results of a randomized controlled clinical trial. *World J Gastroenterol* 2004; 10(1): 136-142
<http://www.wjgnet.com/1007-9327/10/136.asp>

INTRODUCTION

Gastric and colorectal cancers are the most common cancers in China, with their incidence ranking number one and number four respectively. Although surgery, chemotherapy and radiotherapy are major treatment options for GI cancer, the long-term survival is low. Treatment failure is mainly due to recurrence and metastasis. One major cause for such an adverse outcome is the patients' diminished immunity against residual tumor cells after surgery. Therefore, how to restore and improve the patients' immunity against cancer has been an area of active study.

There has been much progress in understanding the relationship between the immune system and GI cancer, which has led to the use of immunomodulatory therapy as an adjuvant and palliative treatment. Many non-specific immunomodulatory agents such as levamisole, CIM, alpha interferon, *n*-3 fatty acids, polysaccharide K (PSK), supplementary diet with glutamine, arginine and omega-3-fatty acids, and Bacillus Calmette-Guerin (BCG) have been tried^[1-4]. CIM is a type 2 histamine receptor antagonist widely used for the treatment of peptic ulcers. It also has important effects on immune system. Administration of CIM has been found to preserve, to some degree, the patients' perioperative immunity^[5,6], to improve the survival of patients with colorectal cancer, melanoma, and renal cell cancer^[7-15]. Although it is not clear whether this effect of CIM on cancer is direct or indirect, it has been proposed that CIM may act by enhancing the host immune response to tumor cells^[16,17] or by blocking the cell growth-promoting activity of histamine in cancer cell lines^[14,16-20].

In this study, we used CIM in the perioperative period as an adjuvant immunomodulatory agent, and studied its effects on peripheral blood lymphocytes, NK cells and TIL in a randomized controlled clinical trial in patients with GI cancer.

MATERIALS AND METHODS

Study design

This was a prospective, randomized clinical trial. The subjects included in this study were selected from patients with pathologically confirmed GI cancer who were admitted to the Department of Oncology, Zhongnan Hospital of Wuhan University, from Sept.1997 to May 1998. The entry criteria were: primary GI cancers indicative of surgery, no preoperative evidence of distant metastasis, no history of previous immunity-impairing chronic diseases such as diabetes mellitus, and no history of preoperative chemotherapy, radiotherapy or immunotherapy. From a total of 125 patients admitted during this period, 49 eligible patients were recruited and staged according to the International Union against Cancer Classification. After signing informed consent forms, the patients were randomized into treatment group ($n=25$) and control group ($n=24$). The clinico-pathological characteristics of the two groups were comparable and balanced. The patients in treatment group started oral CIM treatment (Tagamet, Tianjin Smith Kline and French Laboratories Ltd.) at the dose of 400 mg, tid, 7 days before operation until the operation day. During and after operation, they were given CIM at 600 mg, i.v. drip, bid, until the 10th postoperative day. The patients in control group received similar routine treatment except for perioperative CIM intervention. All the patients in both groups underwent curative resection of cancer.

Separation of peripheral blood mononuclear cells (PBMCs) and immunocytochemical staining

From all the patients in both groups, 2 ml of venous blood was taken and heparinized at admission, before operation, on the 2nd and the 10th postoperative days, respectively. PBMCs were obtained immediately by standard Ficoll-Hypaque gradient centrifugation at 2 000 rpm for 20 min at 4 °C and smeared onto slides, dried and fixed for immunocytochemical staining. The primary antibodies were mouse-anti-human CD₃, CD₄, CD₈ and CD₅₇ monoclonal antibodies (Sigma Chemical Company, St Louis, MO, USA) for the detection of total T lymphocytes, helper T lymphocytes, inhibitor T lymphocytes and natural killer (NK) cells, respectively. The primary antibody was visualized with avidin-biotin-peroxidase supersensitive kit (Wuhan Boster Bioengineering Co. Ltd., Wuhan, China). The slides were counterstained with methyl green. PBMCs from 20 healthy controls were processed in the same way as normal controls.

The slides were mounted and viewed under binocular microscope (Olympus, Japan) by an independent viewer. Positive cells were stained green in nuclei and yellow-brown in cytoplasm and cell membrane (Figure 1). A total of 200 cells were counted on each slide and positive cells were recorded. The immunocytochemical staining procedure was repeated 3 times and the percentage of each cell subpopulation was calculated and expressed as mean \pm standard deviation ($\bar{x}\pm s$).

Immunohistochemical study on TIL in surgical specimens

Immediately after resection, the specimens were cut open and washed clean. For each patient, three pieces of tumor samples were taken at different sites from the peripheral margin of the tumor, fixed in 10% neutral formalin and processed in standard histopathology procedure. For observation of TIL responses, conventional HE staining was performed on the 4 μ m thick tissue sections. Immunohistochemical staining on the sections was conducted for subpopulation study of TIL, with anti-CD₃ monoclonal antibody to recognize T lymphocytes and anti-CD₂₀ monoclonal antibody to recognize B lymphocytes (both from Sigma). The immunohistochemical staining procedure followed a standard protocol. The sections were

counterstained by hematoxylin, mounted and interpreted under microscope. The number of TIL was recorded in five high power (HP, 200 \times) view fields randomly chosen at the tumor border. The degree of TIL response was determined based on a modified grading system by Jass^[21]. Grade I (\pm): no TIL response, in which there were less than 10 infiltrating lymphocytes per HP view field; grade II (+): mild TIL response, in which there were 10-100 infiltrating lymphocytes per HP view field; grade III (++) : intermediate TIL response, in which there were 101-200 infiltrating lymphocytes per HP view field; and grade IV (+++) : prominent TIL response in which there were over 201 infiltrating lymphocytes per HP view field. Grades I and II TIL responses were defined as poor responses and grades III and IV lymphocyte responses as significant responses.

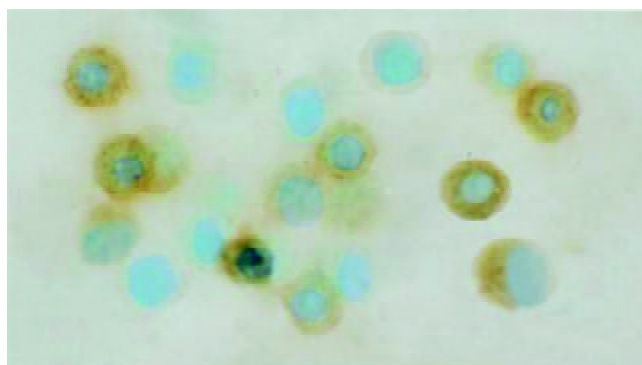


Figure 1 Immunocytochemical staining of PBMCs with monoclonal antibodies to CD₃, CD₄, CD₈ and CD₅₇. Positive cells were stained green in the nuclei and yellow-brown in cytoplasm and cell membrane. The microphoto showed CD₃ positive cells.

Statistical analysis

All data were expressed as mean \pm standard deviation ($\bar{x}\pm s$). Analysis of variance (ANOVA) was used to process the data within groups. Student's *t* test and *chi*-square test were used to evaluate the differences between groups. For the comparison in TIL response among different tumor TNM stages, Fisher's exact test was used. All the tests were two-tailed with a level of significance $P=0.05$.

RESULTS

Clinico-pathological characteristics of patients

A total of 49 eligible patients were enrolled in this study, 25 of whom were randomized into treatment group and 24 into control group. Their clinico-pathological characteristics are detailed in Table 1. There were no statistically significant differences in demographic and histopathologic variables between the two groups ($P>0.05$) (Table 1).

Percentages of lymphocyte subpopulations at baseline

At randomization, the percentages of CD₃⁺, CD₄⁺, CD₅₇⁺ cells and the CD₄⁺/CD₈⁺ ratio in both treatment and control groups were lower than those in normal control ($P<0.001$), and the percentage of CD₈⁺ cells was higher in treatment and control groups than in normal control ($P<0.05$) (Table 2). There were no statistically significant differences between the treatment and control groups in the percentages of the above parameters, implying that the patients were well balanced with regard to peripheral lymphocyte subpopulations at randomization. The results indicated that the cellular immunity was significantly decreased in patients with GI cancer in this study population.

Table 1 Clinico-pathological characteristics of 49 GI cancer patients

Parameters	Treatment group (n=25)	Control group (n=24)
Age (y)		
Mean (range)	50 (25-73)	53 (27-78)
Gender		
Male	13	16
Female	12	8
Tumor sites		
Stomach	6	5
Colon	3	3
Rectum	16	16
Pathological types		
Tubular adenocarcinoma	14	12
Papillary adenocarcinoma	3	3
Villous adenocarcinoma	2	1
Signet-ring-cell carcinoma	2	3
Mucous adenocarcinoma	4	5
TNM stages		
I	3	5
II	7	9
III	9	6
IV	6	4
Tumor differentiation		
Well differentiated	5	6
Moderately differentiated	8	7
Poorly differentiated	12	11

All the variables showed no statistically significant differences between the two groups ($P>0.05$).

Table 2 Baseline values of lymphocyte subpopulations in peripheral blood mononuclear cells of normal control, treatment and control groups (%; $\bar{x}\pm s$)

Groups	n	CD ₃ ⁺	CD ₄ ⁺	CD ₈ ⁺	CD ₅₇ ⁺	CD ₄ ⁺ /CD ₈ ⁺
Normal control	20	67.1±6.3	40.2±5.1	27.7±5.0	18.5±2.31	1.49/0.24
Treatment	25	60.8±6.3 ^b	33.6±4.2 ^b	30.6±5.2	14.8±4.4 ^a	1.15±0.34 ^b
Control	24	60.5±4.6 ^b	33.4±3.7 ^b	31.0±3.9 ^a	15.0±2.8 ^a	1.11±0.25 ^b

^a $P<0.05$ vs normal control, ^b $P<0.01$ vs normal control.

Changes in lymphocyte subpopulations in PBMCs during CIM treatment

During the perioperative period, dynamic changes in the percentages of peripheral blood lymphocyte subpopulations were observed in both treatment and control groups. Preoperative treatment with CIM for 1 wk had positive effects on the percentages of CD₃⁺, CD₄⁺ lymphocytes, and CD₄⁺/CD₈⁺ ratio. CD₃⁺ cells were increased from 60.8±6.3% at randomization to 63.0±4.9% after CIM treatment for 1 wk. After operation, CD₃⁺ cells were decreased to 60.3±5.4% on the 2nd postoperative day, and recovered gradually thereafter until it reached 64.2±3.9% on the 10th postoperative day, which was higher than the pretreatment level. In contrast, the percentage of CD₃⁺ cells in control group continued declining during the perioperative period, and became significantly lower than that in the treatment group on both the 2nd and 10th postoperative days. The changes in CD₄⁺ and CD₅₇⁺ cells followed a similar pattern (Table 3, Figures 2, 3, 4).

Effects of CIM treatment on TIL

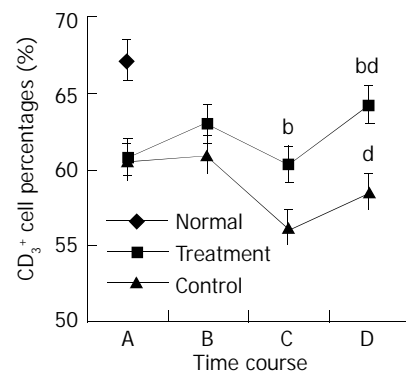
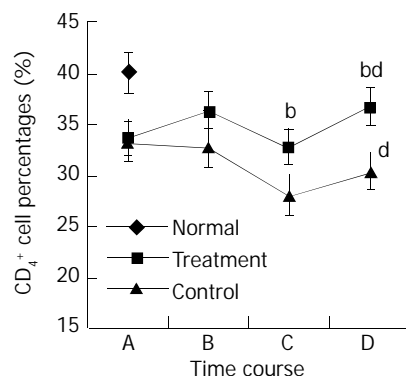
In addition to routine histopathological examinations of

resected specimens, all the tumor sections were reviewed for the presence of peritumor lymphocytes and TIL responses. Six out of 24 patients (25%) in control group had discernible lymphocyte infiltration in the peritumor area, whereas 17 out of 25 cases (68%) in CIM treatment group had obvious TIL responses ($P<0.01$) (Table 4).

Table 3 Changes of lymphocytes and NK cells in perioperative period (%; $\bar{x}\pm s$)

Items	Groups	Perioperative period			
		A	B	C	D
CD ₃ ⁺	Treatment	60.8±6.3	63.0±4.9 ^d	60.3±5.4 ^a	64.2±3.9 ^d
	Control	60.5±4.6	61.0±2.7	56.2±3.8 ^{bd}	58.6±4.0 ^{ab}
CD ₄ ⁺	Treatment	33.6±4.2	36.3±3.4 ^a	32.8±4.0 ^d	36.6±6.2 ^d
	Control	33.4±3.7	32.8±3.3 ^b	28.1±3.4 ^{bd}	30.4±3.3 ^{ab}
CD ₈ ⁺	Treatment	30.6±5.2	29.6±4.3	31.1±4.3	29.4±3.6
	Control	31.0±3.9	31.2±4.8	32.9±4.4 ^a	32.1±5.3
CD ₅₇ ⁺	Treatment	14.8±4.4	15.7±3.8	17.2±3.7	21.1±4.5 ^b
	Control	15.0±2.8	13.1±2.5	14.2±2.2 ^b	15.6±1.7 ^b
CD ₄ ⁺ / CD ₈ ⁺	Treatment	1.15±0.34	1.25±0.23 ^a	1.08±0.21 ^d	1.27±0.30 ^d
	Control	1.11±0.25	1.08±0.22 ^b	0.87±0.17 ^{bd}	0.98±0.24 ^{ab}

A: at admission, B: before operation, C: on the 2nd postoperative day, D: on the 10th postoperative day. ^a $P<0.05$, ^d $P<0.01$, B vs A, C vs B, D vs C; ^b $P<0.01$ vs treatment group.

**Figure 2** Changes in CD₃⁺ cell percentages in perioperative period. A: at randomization; B: before operation; C: on the 2nd postoperative day; and D: on the 10th postoperative day. The difference in CD₃⁺ percentages between treatment and control groups at time points C and D was statistically significant, ^b $P<0.01$. The difference in CD₃⁺ percentages on the 10th postoperative day and the randomization day was statistically significant for both treatment and control groups, ^d $P<0.01$.**Figure 3** Changes in CD₄⁺ cell percentages in perioperative period. A: at randomization; B: before operation; C: on the 2nd postoperative day; and D: on the 10th postoperative day. The difference in CD₄⁺ percentages between treatment and control

groups at time points C and D was statistically significant, ^b*P*<0.01. The differences in CD₄⁺ percentages on the 10th postoperative day and the randomization day was statistically significant for both treatment and control groups, ^d*P*<0.01.

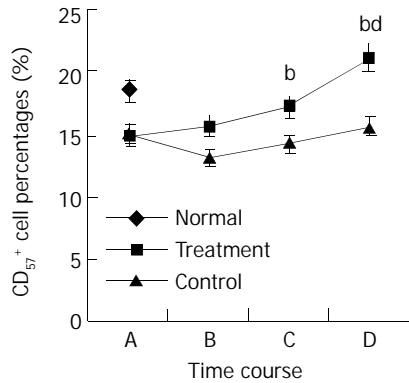


Figure 4 Changes in CD₅₇⁺ cell percentages in perioperative period. A: at randomization; B: before operation; C: on the 2nd postoperative day; and D: on the 10th postoperative day. The difference in CD₅₇⁺ percentages between treatment and control groups at time points C and D was statistically significant, ^b*P*<0.01. The differences in CD₅₇⁺ percentages between treatment group and normal control on the 10th postoperative day was statistically significant, ^d*P*<0.01.

Table 4 TIL responses in treatment and control groups

Groups	SR		PR		Total	Rate (%)
	+++	++	+	+		
Treatment	9	8	6	2	25	68 ^b
Control	2	4	9	9	24	25
Total	23		26		49	

SR=significant response, PR=poor response. ^b*P*<0.01 vs control group, *chi-square* test.

There was a negative correlation between TIL response and the clinico-pathological stages of the tumor (Table 5). In control group, TIL responses were mainly observed in TNM stages I and II cases, and there were very few peritumor lymphocyte responses in stages III and IV cases. In contrast, there were obvious TIL responses in 78% (7/9) of TNM stage III cases and 83% (5/6) of stage IV cases in CIM treatment group, both of which were significantly higher than those in control group (*P*<0.05 and *P*<0.01, respectively, Fisher's exact test) (Figure 4). Immunohistochemical studies of the specimens revealed that most of the TILs were CD₃⁺ T lymphocytes clustered around tumor tissues. There were few CD₂₀⁺ cells in TIL population.

Table 5 Comparison in TIL responses by TNM stages between control and treatment groups

TNM stages	Groups	Poor response	Significant response	Response rate (%)
I	Treatment	2	1	33
	Control	3	2	40
II	Treatment	3	4	57
	Control	6	3	33
III	Treatment	2	7	78 ^a
	Control	5	1	17
IV	Treatment	1	5	83 ^b
	Control	4	0	0

^a*P*<0.05, ^b*P*<0.01, vs control (Fisher's exact test).

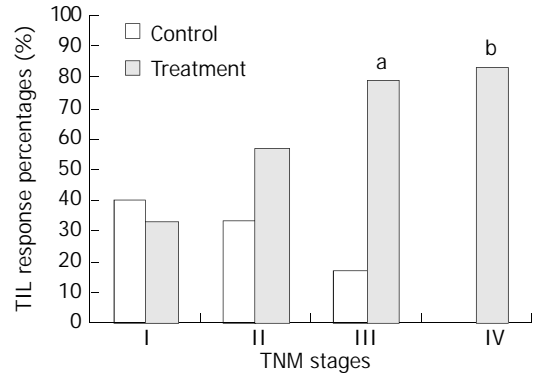


Figure 5 TIL responses in surgical specimens in treatment and control groups. In control group, there was a progressive decrease in TIL responses with increase of TNM staging. On the other hand, the treatment group showed a steady increase in TIL responses after CIM treatment for 1 wk. The differences in TIL response rates were statistically significant between treatment and control groups for TNM stages III and IV diseases (^a*P*<0.05 and ^b*P*<0.01, respectively, Fisher's exact test).

DISCUSSION

To date, surgical resection remains the only approach that can offer possible cure for GI cancer patients. However, operation itself is a double-edged sword to cancer patients in terms of tumor immunology. On the one hand, a successful operation can remove tumor burden which is immuno-suppressive. This will help bring about an improved clinical outcome for most patients. On the other hand, the operation itself is a major blow to the immune system. Lines of evidence suggest that surgical patients undergo a period of immunodepression immediately after operation, the length of which depends on many factors such as the general status of the patients, extent of the operation itself, pre-operative treatment. Previous studies demonstrated that T helper cells decreased and T suppressor cells increased significantly as early as 1 day after surgery.^[22-24] Many subsequent studies also confirmed that surgery for patients with lung cancer^[25], esophageal cancer^[26], gastric cancer^[27,28] and colorectal cancer^[29,30] induced immediate severe immunosuppression. For cancer patients, an important function adversely affected by this immunosuppression is the anti-tumor response itself. This immunosuppression might increase the chance of accelerated growth of residual tumors or micro-metastases already present at the time of surgical resection. As a result, postoperative immunosuppression maybe one of the major contributing factors for post-operative recurrence and metastases. Indeed our previous study found a local recurrent rate as high as 34.27% for rectal cancer 5 years after curative resection, most of which (89.04%) occurred 3 years after operation^[31]. Other studies also revealed that 7% to 65% of rectal cancer patients would develop local recurrence after curative surgery^[32-34]. Therefore, how to effectively improve peri-operative immunity of GI cancer patients remains a major challenge of significant clinical importance.

Many researches have been conducted to tackle this problem, and one approach is to use small molecular immunomodulator drugs such as CIM, a histamine H₂ receptor antagonist. It has long been observed that histamine was a growth factor for certain cancers and could, by itself, stimulate tumor cell proliferation^[18-20]. As one of the many important chemo-mediators involved in immune responses, histamine had inhibitory effects on immune response^[35-38] via its H₂ receptors^[39]. It was discovered that T suppressor cells, which are part of the regulatory arm of the immune system, could express histamine receptors on their surface^[40-42], and histamine was capable of suppressing the immune response by activating

these T suppressor cells^[43]. Many tumors, particularly colorectal cancer, secrete histamine resulting in elevated histamine levels within the tumor. Histamine is also often secreted in response to surgical resection of colorectal cancers. All these factors working together will create an immuno-suppressive environment both in the area of tumor growth and in the whole body, facilitating tumor growth.

Several clinical studies have shown that administration of CIM could help reduce the immuno-suppression due to increased histamine level in the tumor environment^[15,16,44-46]. *In vitro* studies also demonstrated that CIM could inhibit the adhesion of some breast cancer cells^[47], and the adhesion of human colon cancer cells to human umbilical cord cells^[48], a very important step in tumor growth and progression. *In vivo* experimental studies also showed that daily administration of CIM to a mouse model of colon cancer significantly retarded tumor growth by up-regulating the expression of tumor-suppressive cytokines^[49], and the use of CIM also retarded the growth of human melanoma in a nude mouse model and prolonged the survival of tumor bearing SCID mice by directly inhibiting the proliferation of tumor cells and indirectly promoting the infiltration of activated macrophages to tumor site^[50,51].

In line with previous findings, our study discovered the diminished cellular immunity in GI cancer patients. Compared with normal controls, the total T lymphocytes (CD₃⁺), T helper lymphocytes (CD₄⁺), and NK cells (CD₅₇⁺) were significantly decreased in GI cancer patients. This reflects the nature that GI tumor burden exerts inhibitory effects on immune system. Moreover, the percentages of these immune cells showed a continuously declining trend with the progression of the disease, as reflected by the finding that patients with advanced TNM stage tumors had a more profound decrease in these immune cells than those with early stage tumors. Surgery itself, while removing the tumor burden, did have a temporary negative impact on host cellular immunity, as reflected by the marked decline in total T lymphocytes, T helper cells and NK cells in the immediate post-operative period. This decline continued with a downhill course in control group, in which no immunity-boosting therapies were given besides conventional surgical treatment. It is noteworthy that total T cells, T helper cells and NK cells did not return to baseline level 10 days after curative resection. This again highlighted the fact that while most patients in control group were physically recovered from operation at this time, they were far from immunologically recovered, and some interventional measures should be warranted to facilitate the recovery of cellular immune functions.

In contrast to control group, patients in treatment group showed favorable responses to CIM therapy in terms of cellular immunity parameters. After CIM treatment for 1 wk, total T cells, T helper cells and NK cells showed a slow but steady increase, although the increments did not reach statistical significance for NK cells, they did reach statistical significance for both total T cells and T helper cells. However, their levels were still lower than those found in normal controls, implying that while GI cancer patients have reduced their cellular immunity, they were nevertheless responsive to immunity-boosting measures, although such measures alone could not efficiently restore the hosts' cellular immunity to the level of normal controls. The data demonstrated again that surgery itself reduced cellular immunity, but to a much less degree, as a result of CIM treatment. Moreover, such reductions were quickly addressed and a positive balance was reached 10 days after CIM treatment, as reflected by the fact that the total T cells, T helper cells and NK cells on the 10th postoperative day were significantly higher than the baseline level (at randomization). Although total T cells, T helper cells were not up to the level of normal controls, NK cells did exceed the

level of normal controls. If the cellular immunity parameters for both treatment and control groups on the 10th postoperative day were analyzed, it would be obvious that CIM treatment did exert remarkable boosting effects on cellular immunity parameters.

The current study also demonstrated that immunity-enhancing effects of CIM treatment were not limited to peripheral blood immune cells alone, it also enhanced TIL response at the tumor site, as was revealed by the findings that while 25% of the patients in the control group had discernible TIL responses in the peri-tumor area, as high as 68% of cases in the treatment group showed obvious TIL responses. As demonstrated by immunohistochemical studies, most of the TILs were T lymphocytes. TILs have been found to be the highly effective tumoricidal lymphocytes^[52-54], and TIL treatment could decrease the relapse rate and prolong the survival of stage III melanoma patients with one positive lymph node^[55,56], and the overall survival of stage IV gastric and colorectal cancers^[57,58], and induce regression of metastatic tumors in the lung, liver and lymph nodes in patients with advanced melanoma after lymphodepletion^[59]. The enhanced TIL response at the tumor site induced by CIM treatment, therefore, might help reduce tumor aggressiveness and promote local control.

In summary, the current randomized clinical trial demonstrated that perioperative administration of CIM to GI cancer patients helped accelerate the recovery of cellular immunity and boost TIL responses at the tumor sites. This has potential therapeutic implications. Since circulating T lymphocytes and NK cells are major defense mechanisms against tumor cells released into the circulation, and TIL is one of the most crucial factors restricting local tumor growth and progression, it is desirable to use it as an immunomodulator in the perioperative period. Moreover, since CIM has many other favorable effects besides immunomodulation on lymphocytes, such as activating macrophages, increasing tumor inhibitory cytokines^[49], enhancing the antigen presenting capacity of dendritic cells^[60], reducing tumor cell proliferation, inhibiting tumor cell metastasis via anti-adhesion mechanisms^[49] and increasing the overall survival of colorectal cancer patients with high levels of sialyl Lewis-X and sialyl Lewis-A epitope expression on tumor cells^[61], it is therefore advisable to use this low cost, convenient and almost nontoxic drug as a practical immunity-enhancing measure for GI cancer patients.

REFERENCES

- 1 **Yip D**, Strickland AH, Karapetis CS, Hawkins CA, Harper PG. Immunomodulation therapy in colorectal carcinoma. *Cancer Treat Rev* 2000; **26**: 169-190
- 2 **Weiss G**, Meyer F, Matthies B, Pross M, Koenig W, Lippert H. Immunomodulation by perioperative administration of n-3 fatty acids. *Br J Nutr* 2002; **87** (Suppl 1): S89-94
- 3 **Shibata M**, Nezu T, Kanou H, Nagata Y, Kimura T, Takekawa M, Ando K, Fukuzawa M. Immunomodulatory effects of low dose cis-Diaminedichloroplatinum (cisplatin) combined with UFT and PSK in patients with advanced colorectal cancer. *Cancer Invest* 2002; **20**: 166-173
- 4 **Wu GH**, Zhang YW, Wu ZH. Modulation of postoperative immune and inflammatory response by immune-enhancing enteral diet in gastrointestinal cancer patients. *World J Gastroenterol* 2001; **7**: 357-362
- 5 **Tayama E**, Hayashida N, Fukunaga S, Tayama K, Takaseya T, Hiratsuka R, Aoyagi S. High-dose cimetidine reduces proinflammatory reaction after cardiac surgery with cardiopulmonary bypass. *Ann Thorac Surg* 2001; **72**: 1945-1949
- 6 **Bai DJ**, Yang GL, Yuan HY, Li Y, Wang K. Effects of cimetidine on T lymphocyte subsets in perioperative gastrointestinal cancer patients. *Shijie Huaren Xiaohua Zazhi* 2000; **8**: 147-149
- 7 **Adams WJ**, Morris DL. Short-course cimetidine and survival with

- colorectal cancer. *Lancet* 1994; **344**: 1768-1769
- 8 **Matsumoto S.** Cimetidine and survival with colorectal cancer. *Lancet* 1995; **346**: 115
- 9 **Svendson LB,** Ross C, Knigge U, Frederiksen HJ, Graversen P, Kjaergard J, Luke M, Stimpel H, Sparso BH. Cimetidine as an adjuvant treatment in colorectal cancer. A double-blind, randomized pilot study. *Dis Colon Rectum* 1995; **38**: 514-518
- 10 **Hellstrand K,** Naredi P, Lindner P, Lundholm K, Rudenstam CM, Hermodsson S, Asztely M, Hafstrom L. Histamine in immunotherapy of advanced melanoma: a pilot study. *Cancer Immunol Immunother* 1994; **39**: 416-419
- 11 **Creagan ET,** Ahmann DL, Green SJ, Long HJ, Frytak S, Itri LM. Phase II study of recombinant leukocyte A interferon (IFN- α) plus cimetidine in disseminated malignant melanoma. *J Clin Oncol* 1985; **3**: 977-981
- 12 **Sagaster P,** Micksche M, Flamm J, Ludwig H. Randomised study using IFN- α versus IFN- α plus coumarin and cimetidine for treatment of advanced renal cell cancer. *Ann Oncol* 1995; **6**: 999-1003
- 13 **Morris DL,** Adams WJ. Cimetidine and colorectal cancer-old drug, new use? *Nat Med* 1995; **1**: 1243-1244
- 14 **Sasson AR,** Gamagami R, An Z, Wang X, Moossa AR, Hoffman RM. Cimetidine: an inhibitor or promoter of tumor growth? *Int J Cancer* 1999; **81**: 835-838
- 15 **Kelly MD,** King J, Cherian M, Dwerryhouse SJ, Finlay IG, Adams WJ, King DW, Lubowski DZ, Morris DL. Randomized trial of preoperative cimetidine in patients with colorectal carcinoma with quantitative assessment of tumor-associated lymphocytes. *Cancer* 1999; **85**: 1658-1663
- 16 **Hansbrough JF,** Zapata-Sirvent RL, Bender EM. Prevention of alterations in postoperative lymphocyte subpopulations by cimetidine and ibuprofen. *Am J Surg* 1986; **151**: 249-255
- 17 **Adams WJ,** Morris DL, Ross WR, Lubowski DZ, King DW, Peters L. Cimetidine preserves non-specific immune function after colonic resection for cancer. *Aust N Z J Surg* 1994; **64**: 847-852
- 18 **Adams WJ,** Lawson JA, Morris DL. Cimetidine inhibits *in vivo* growth of human colon cancer and reverses histamine stimulated *in vitro* and *in vivo* growth. *Gut* 1994; **35**: 1632-1636
- 19 **Lawson JA,** Adams WJ, Morris DL. Ranitidine and cimetidine differ in their *in vitro* and *in vivo* effects on human colonic cancer growth. *Br J Cancer* 1996; **73**: 872-876
- 20 **Reynolds JL,** Akhter J, Morris DL. *In vitro* effect of histamine and histamine H1 and H2 receptor antagonists on cellular proliferation of human malignant melanoma cell lines. *Melanoma Res* 1996; **6**: 95-99
- 21 **Jass JR,** Ajioka Y, Allen JP, Chan YF, Cohen RJ, Nixon JM, Radojkovic M, Restall AP, Stables SR, Zwi LJ. Assessment of invasive growth pattern and lymphocytic infiltration in colorectal cancer. *Histopathology* 1996; **28**: 543-548
- 22 **Hansbrough JF,** Bender EM, Zapata-Sirvent R, Anderson J. Altered helper and suppressor lymphocyte populations in surgical patients. A measure of postoperative immunosuppression. *Am J Surg* 1984; **148**: 303-307
- 23 **Nichols PH,** Ramsden CW, Ward U, Sedman PC, Primrose JN. Perioperative immunotherapy with recombinant interleukin 2 in patients undergoing surgery for colorectal cancer. *Cancer Res* 1992; **52**: 5765-5769
- 24 **Espi A,** Arenas J, Garcia-Granero E, Marti E, Lledo S. Relationship of curative surgery on natural killer cell activity in colorectal cancer. *Dis Colon Rectum* 1996; **39**: 429-434
- 25 **Leaver HA,** Craig SR, Yap PL, Walker WS. Lymphocyte responses following open and minimally invasive thoracic surgery. *Eur J Clin Invest* 2000; **30**: 230-238
- 26 **van Sandick JW,** Gisbertz SS, ten Berge JJ, Boermeester MA, van der Pouw Kraan TC, Out TA, Obertop H, van Lanschot JJ. Immune responses and prediction of major infection in patients undergoing transhiatal or transthoracic esophagectomy for cancer. *Ann Surg* 2003; **237**: 35-43
- 27 **Sato N,** Endo S, Kimura Y, Ikeda K, Aoki K, Iwaya T, Akiyama Y, Noda Y, Saito K. Influence of a human protease inhibitor on surgical stress induced immunosuppression. *Dig Surg* 2002; **19**: 300-305
- 28 **Yao XX,** Yin L, Sun ZC. The expression of hTERT mRNA and cellular immunity in gastric cancer and precancerosis. *World J Gastroenterol* 2002; **8**: 586-590
- 29 **Braga M,** Vignali A, Zuliani W, Radaelli G, Gianotti L, Martani C, Toussoun G, Di Carlo V. Metabolic and functional results after laparoscopic colorectal surgery: a randomized, controlled trial. *Dis Colon Rectum* 2002; **45**: 1070-1077
- 30 **Wang YX,** Ruan CP, Li L, Shi JH, Kong XT. Clinical significance of changes of perioperative T cell and expression of its activated antigen in colorectal cancer patients. *World J Gastroenterol* 1999; **5**: 181-182
- 31 **Yuan HY,** Li Y, Yang GL, Bei DJ, Wang K. Study on the causes of local recurrence of rectal cancer after curative resection: analysis of 213 cases. *World J Gastroenterol* 1998; **4**: 527-529
- 32 **Ballantyne GH,** Quin J. Surgical treatment of liver metastases in patients with colorectal cancer. *Cancer* 1993; **71**(12 Suppl): 4252-4266
- 33 **Vaughn D,** Haller DG. Nonsurgical management of recurrent colorectal cancer. *Cancer* 1993; **71**: 4278-4292
- 34 **Turk PS,** Wanebo HJ. Results of surgical treatment of nonhepatic recurrence of colorectal carcinoma. *Cancer* 1993; **71**(12 Suppl): 4267-4277
- 35 **Beer DJ,** Rocklin RE. Histamine-induced suppressor-cell activity. *J Allergy Clin Immunol* 1984; **73**: 439-452
- 36 **Lima M,** Rocklin RE. Histamine modulates *in vitro* IgG production by pokeweed mitogen-stimulated human mononuclear cells. *Cell Immunol* 1981; **64**: 324-336
- 37 **Rocklin RE,** Blidy A, Kamal M. Physicochemical characterization of human histamine-induced suppressor factor. *Cell Immunol* 1983; **76**: 243-252
- 38 **Uotila P.** Inhibition of prostaglandin E2 formation and histamine action in cancer immunotherapy. *Cancer Immunol Immunother* 1993; **37**: 251-254
- 39 **Black JW,** Duncan WA, Durant CJ, Ganellin CR, Parsons EM. Definition and antagonism of histamine H2-receptors. *Nature* 1972; **236**: 385-390
- 40 **Melmon KL,** Bourne HR, Weinstein J, Sela M. Receptors for histamine can be detected on the surface of selected leukocytes. *Science* 1972; **177**: 707-709
- 41 **Osband M,** McCaffrey R. Solubilization, separation, and partial characterization of histamine H₁ and H₂ receptors from calf thymocyte membranes. *J Biol Chem* 1979; **254**: 9970-9972
- 42 **Burtin C,** Scheinmann P, Salomon JC, Lespinats G, Canu P. Decrease in tumour growth by injections of histamine or serotonin in fibrosarcoma-bearing mice: Influence of H₁ and H₂ histamine receptors. *Br J Cancer* 1982; **45**: 54-60
- 43 **Rocklin RE,** Greineder DK, Melmon KL. Histamine-induced suppressor factor (HSF): Further studies on the nature of the stimulus and the cell which produces it. *Cell Immunol* 1979; **44**: 404-415
- 44 **Adams WJ,** Lawson JA, Nicholson SE, Cook TA, Morris DL. The growth of carcinogen-induced colon cancer in rats is inhibited by cimetidine. *Eur J Surg Oncol* 1993; **19**: 332-335
- 45 **Nishiguchi S,** Tamori A, Shioimi S, Enomoto M, Tatsumi N, Koh N, Habu D, Sakaguchi H, Takeda T, Seki S, Nakamura K, Kubo S, Kinoshita H. Cimetidine reduces impairment of cellular immunity after transcatheter arterial embolization in patients with hepatocellular carcinoma. *Hepatogastroenterology* 2003; **50**: 460-462
- 46 **Zhu Q,** Si F, Xu JY, Wu YL. Effect of Cimetidine against digestive tract tumors. *Huaren Xiaohua Zazhi* 1998; **6**: 68-69
- 47 **Bobek V,** Boubelik M, Kovarik J, Taltyonov O. Inhibition of adhesion breast cancer cells by anticoagulant drugs and cimetidine. *Neoplasma* 2003; **50**: 148-151
- 48 **Kobayashi K,** Matsumoto S, Morishima T, Kawabe T, Okamoto T. Cimetidine inhibits cancer cell adhesion to endothelial cells and prevents metastasis by blocking E-selectin expression. *Cancer Res* 2000; **60**: 3978-3984
- 49 **Takahashi K,** Tanaka S, Ichikawa A. Effect of cimetidine on intratumoral cytokine expression in an experimental tumor. *Biochem Biophys Res Commun* 2001; **281**: 1113-1119
- 50 **Szincsak N,** Hegyesi H, Hunyadi J, Falus A, Juhasz I. Different h2 receptor antihistamines dissimilarly retard the growth of xenografted human melanoma cells in immunodeficient mice. *Cell Biol Int* 2002; **26**: 833-836
- 51 **Szincsak N,** Hegyesi H, Hunyadi J, Martin G, Lazar-Molnar E, Kovacs P, Rivera E, Falus A, Juhasz I. Cimetidine and a tamoxifen derivative reduce tumour formation in SCID mice xenotransplanted with a human melanoma cell line. *Melanoma Res* 2002; **12**: 231-240

- 52 **Rosenberg SA**, Spiess P, Lafreniere R. A new approach to the adoptive immunotherapy of cancer with tumor-infiltrating lymphocytes. *Science* 1986; **233**: 1318-1321
- 53 **Rosenberg SA**. Progress in human tumour immunology and immunotherapy. *Nature* 2001; **411**: 380-384
- 54 **Wang XZ**, Li B, Zheng XX, Qu YZ, Lin GZ, Tang NH, Chen ZX. Experimental and clinical study on tumor infiltrating lymphocytes in solid tumor. *Xin Xiaohuabingxue Zazhi* 1997; **5**: 481-482
- 55 **Dreno B**, Nguyen JM, Khammari A, Pandolfino MC, Tessier MH, Bercegeay S, Cassidanius A, Lemarre P, Billaudel S, Labarriere N, Jotereau F. Randomized trial of adoptive transfer of melanoma tumor-infiltrating lymphocytes as adjuvant therapy for stage III melanoma. *Cancer Immunol Immunother* 2002; **51**: 539-546
- 56 **Labarriere N**, Pandolfino MC, Gervois N, Khammari A, Tessier MH, Dreno B, Jotereau F. Therapeutic efficacy of melanoma-reactive TIL injected in stage III melanoma patients. *Cancer Immunol Immunother* 2002; **51**: 532-538
- 57 **Kono K**, Takahashi A, Ichihara F, Amemiya H, Iizuka H, Fujii H, Sekikawa T, Matsumoto Y. Prognostic significance of adoptive immunotherapy with tumor-associated lymphocytes in patients with advanced gastric cancer: a randomized trial. *Clin Cancer Res* 2002; **8**: 1767-1771
- 58 **Liu SC**, Yuan SZ. Relationship between infiltration of dendritic cells, pericancerous lymphocytic reaction and prognosis in colorectal carcinomas. *Xin Xiaohuabingxue Zazhi* 1997; **5**: 156-157
- 59 **Dudley ME**, Wunderlich JR, Robbins PF, Yang JC, Hwu P, Schwartzentruber DJ, Topalian SL, Sherry R, Restifo NP, Hubicki AM, Robinson MR, Raffeld M, Duray P, Seipp CA, Rogers-Freezer L, Morton KE, Mavroukakis SA, White DE, Rosenberg SA. Cancer regression and autoimmunity in patients after clonal repopulation with antitumor lymphocytes. *Science* 2002; **298**: 850-854
- 60 **Kubota T**, Fujiwara H, Ueda Y, Itoh T, Yamashita T, Yoshimura T, Okugawa K, Yamamoto Y, Yano Y, Yamagishi H. Cimetidine modulates the antigen presenting capacity of dendritic cells from colorectal cancer patients. *Br J Cancer* 2002; **86**: 1257-1261
- 61 **Matsumoto S**, Imaeda Y, Umemoto S, Kobayashi K, Suzuki H, Okamoto T. Cimetidine increases survival of colorectal cancer patients with high levels of sialyl Lewis-X and sialyl Lewis-A epitope expression on tumour cells. *Br J Cancer* 2002; **86**: 161-167

Edited by Zhu LH and Wang XL

Response of TT virus to IFN plus ribavirin treatment in patients with chronic hepatitis C

Javier Moreno, Gloria Moraleda, Rafael Barcena, Mluisa Mateos, Santos del Campo

Javier Moreno, Rafael Barcena, Santos del Campo, Gloria Moraleda, Department of Gastroenterology, Hospital Ramon y Cajal, Facultad de Medicina, Universidad de Alcala, Madrid, Spain
Mluisa Mateos, Department of Microbiology, Hospital Ramon y Cajal, Madrid, Spain

Supported by Fundacion Manchega de Investigacion y Docencia en Gastroenterologia and partially by Red Nacional en Investigación de Hepatología y Gastroenterología (RNIHG)

Javier Moreno and Gloria Moraleda contributed equally to this work

Correspondence to: Dr. Rafael Barcena Marugan, Department of Gastroenterology, Hospital Ramon y Cajal, Ctra. Colmenar, Km 9.1, 28034 Madrid, Spain. rbarcena@hrc.insalud.es

Telephone: +34-91-3368093 **Fax:** +34-91-7291456

Received: 2003-08-11 **Accepted:** 2003-10-22

Abstract

AIM: TT virus (TTV) is a newly described DNA virus related to posttransfusion hepatitis that produces persistent viremia in the absence of clinical manifestations. PEG-IFN plus ribavirin have been useful in the treatment of chronic hepatitis C infection. This study investigated the responses of TT virus (TTV) and hepatitis C virus (HCV) to PEG-IFN plus ribavirin therapy.

METHODS: Fifteen patients infected with HCV were treated with PEG-IFN (0.5 µg/body weight/week) and ribavirin (1 000 mg-1 200 mg/daily) for 48 weeks. Blood samples were drawn at the beginning and the end of the therapy. Serum TTV DNA and HCV RNA were quantified by real time PCR.

RESULTS: At the beginning of treatment, TTV infection was detected in 10/15 (66.6%) of HCV-infected patients. Loss of serum TTV DNA at the end of therapy occurred in 6/10 (60%) patients. Out of these 6 patients, 4 (67%) became positive for TTV DNA after 6 months of therapy. Regarding HCV viremia, 11/15 (73%) patients were negative for serum HCV RNA after 48 weeks of therapy, 7/11 (64%) of these cases also became negative for TTV DNA following the combined treatment. In the 3/4 (75%) patients who were positive for HCV RNA at the end of therapy, TTV DNA was detected as well. Sustained HCV response at 6 months after treatment was 53% (8/15).

CONCLUSION: No TTV sustained response can be achieved in any patient after PEG-IFN plus ribavirin administration.

Moreno J, Moraleda G, Barcena R, Mateos M, del Campo S. Response of TT virus to IFN plus ribavirin treatment in patients with chronic hepatitis C. *World J Gastroenterol* 2004; 10(1): 143-146
<http://www.wjgnet.com/1007-9327/10/143.asp>

INTRODUCTION

TT virus (TTV) has been recently identified in patients with elevated alanine aminotransferase (ALT) levels following transfusions^[1]. TTV presents an extreme diffusion of active

infection throughout the world^[2]. It is known that TTV may be highly contagious although its way of spread is poorly understood. However, its high prevalence rate among the people receiving or being in contact with blood products could indicate that TTV can be parenterally transmitted^[3]. Although it has been proposed that TT virus be responsible for the small proportion of acute and chronic forms of hepatitis that still remain unsolved, no other illness has yet been attributed to the virus. The TTV genome is a circular, single-stranded DNA of negative polarity, which shares similarities with members of the Circoviridae family and, in contrast to DNA viruses, TTV isolates exhibit a high level of genetic heterogeneity^[4,5].

Hepatitis C virus (HCV) is the major cause of chronic liver infection which may progress to cirrhosis and eventually to hepatocellular carcinoma (HCC)^[6]. Recently, pegylated interferon (PEG-IFN), initially alone and later in combination with ribavirin, a nucleoside analogue with a broad antiviral activity against a variety of DNA and RNA viruses, has provided new perspectives for the treatment of most patients with chronic HCV infection^[7,8]. Co-infection of TTV and HCV is commonly seen maybe because both viruses share the same transmission routes such as blood transfusion^[9]. In previous studies, IFN therapy was reported to be effective against TTV^[10,11], but the possible susceptibility of the virus to the combination of PEG-IFN plus ribavirin treatment has not yet been investigated. Thus, we investigated the response of TTV infection to PEG-IFN plus ribavirin therapy in patients with chronic hepatitis C and evaluated whether PEG-IFN plus ribavirin combined therapy on chronic hepatitis C was influenced by a TTV co-infection.

MATERIALS AND METHODS

Patients

We enrolled randomly in the study 15 patients (11 males and 4 females, mean age: 41.6 years, range: 30 to 57 years) with chronic HCV infection who had undergone PEG-IFN plus ribavirin therapy. The diagnosis of chronic hepatitis was made on histological (stage of fibrosis and grade of activity) and biochemical liver function tests. Five patients had a history of blood transfusion, 6 acquired HCV infection by parenteral route (intravenous drug abusers, tattoos..) and in 4 patients the transmission route was unknown. Biochemical and virological features of the patients are shown in Table 1.

PEG-IFN was administered intramuscularly at a dose of 0.5 µg/body weight/week, ribavirin was given orally at a dose of 1 000-1 200 mg/daily (weight adjusted) for 48 weeks. Blood samples were taken at the baseline time and when therapy was stopped. To evaluate the effects of PEG-IFN plus ribavirin, levels of ALT, TTV DNA and HCV RNA were evaluated at each time. TTV and HCV clearance was defined as the disappearance of serum TTV DNA and HCV RNA after 48 weeks of combined treatment. All patients gave written informed consent before enrollment in the study, which was approved by the Ethics Committee of the hospital.

Detection and quantification of TTV DNA

Total DNA was purified from 200 µl of serum using the high

pure viral nucleic acid kit (Roche Diagnostic, Mannheim, Germany) and eluted in 50 μ l distilled water. TTV DNA was subjected to nested PCR for qualitative analysis. First PCR was performed with primer pair NG054/NG132^[12] and nested PCR with primer pair T801/T935^[13]. In those positive samples for viral DNA, TTV DNA quantification was carried out with real time PCR by the SYBR Green approach using primers targeting a fragment of the untranslated region (UTR) of the viral genome as previously described by Garcia *et al*^[14].

HCV markers

HCV antibodies (anti-HCV) were determined by immunoassay (Ortho Diagnostic System, Raritan, NJ). Serum HCV RNA levels were measured using the Amplicor HCV monitor test (Roche). HCV genotyping was carried out using the Inno-Lipa HCV test (Innogenetics).

Statistical analysis

Statistical analyses were performed using Student's *t* test. Data were analyzed with the computer program SPSS (SPSS Inc., Chicago, IL, USA). A probability (*P*) value less than 0.05 was considered statistically significant.

RESULTS

Detection and response of TTV to PEG-IFN plus ribavirin therapy

Fifteen patients infected with HCV were monitored randomly for levels of TTV and HCV in serum, at the beginning and end of PEG-IFN plus ribavirin combined treatment. Of the 15 patients, serum TTV DNA could be detected in 10/15 (67%) by real time PCR at the beginning of therapy, with a TTV value that ranged from 1.3×10^3 to 1.7×10^5 genomes/ml of serum (mean: 3.4×10^4 genomes/ml). After 48 weeks of PEG-

IFN plus ribavirin therapy, 6/10 patients (60%) lost serum TTV DNA. Regarding the 4 patients who still had detectable serum TTV DNA, TTV value ranged from 10^3 to 4×10^4 genomes/ml of serum (mean: 1.4×10^4 genomes/ml). In 3/4 patients (75%) positive for TTV, circulating HCV RNA was detected simultaneously after completion of the combined therapy. With respect to these 4 positive TTV DNA patients, at the end of treatment and relative to baseline levels, 3 patients (75%) had a reduction of serum TTV load and 1 case (25%) presented an increase in the levels of serum TTV DNA. The latter patient presented a grade III fibrosis while the remaining 3 individuals presented a grade I fibrosis (Table 1).

When TTV DNA was analyzed at 6 months after stopping PEG-IFN plus ribavirin administration, four responders (67%) had a relapse of TTV viremia, in the 2 remaining cases no serum samples were available (Table 1). The 4 patients, who did not eliminate TTV DNA at the end of treatment, still maintained DNA during the follow-up period. With respect to the 5 TTV DNA negative patients at the beginning of therapy, 1 (20%) became positive for TTV after stopping combined therapy, 2 (40%) cases remained negative for TTV and in 2 individuals viral marker was not determined (Table 1).

Serum TTV DNA level with respect to HCV in non-responder and responder patients to PEG-IFN plus ribavirin treatment was also analyzed and no statistically significant differences were found when pretreatment serum samples were compared between both groups ($P=0.281$). However, we observed that those patients eliminating TTV at the end of therapy presented a lower basal HCV load when compared with the non-responder TTV patients (1.1×10^6 vs 2.1×10^6 genomes/ml, respectively $P=0.03$). Regarding the changes of ALT levels, no statistical differences were observed when they were analyzed between TTV responder and non-responder (Table 2). In contrast, serum ALT level was persistently maintained

Table 1 Features of patients in the study

Patient No.	HCV Genotype	Fibrosis	Before treatment			End of treatment			6 months after treatment		
			ALT	TTV	HCV	ALT	TTV	HCV	ALT	TTV	HCV
1	1a	I	51	1.7×10^5	5×10^5	26	-	-	83	+	ND
2	1a	III	139	1.5×10^3	9.4×10^5	35	-	-	19	ND	-
3	1a	III	102	1.7×10^3	8×10^5	30	-	-	11	+	-
4	1b	III	225	1.1×10^4	1.1×10^6	29	4×10^4	-	27	+	-
5	1a	II	82	1.4×10^3	9×10^5	30	-	-	168	+	1.9×10^6
6	1b	III	92	1.3×10^3	1.5×10^6	42	-	-	48	+	-
7	3a	II	117	1.8×10^4	2.4×10^6	9	-	-	23	ND	-
8	1b	III	102	-	1.5×10^6	59	-	-	39	-	-
9	1b	I	86	5.7×10^4	7×10^5	30	1.3×10^4	6×10^5	44	+	9.9×10^5
10	1b	I	183	-	9×10^4	26	-	-	17	+	-
11	1a	I	77	-	2.5×10^6	16	-	-	27	ND	-
12	1b	I	72	4.6×10^4	2×10^5	36	10^3	3.5×10^5	76	+	5×10^5
13	1a	III	101	-	2.3×10^5	47	-	3×10^4	153	ND	+
14	1b	I	68	-	5×10^5	29	-	-	56	-	2×10^5
15	1a	I	29	3.1×10^4	6.3×10^6	13	2.5×10^3	2.1×10^6	30	+	+

ALT level was expressed as IU/L. TTV and HCV loads were expressed as viral genomes/ml of serum.

Table 2 Changes of ALT levels in TTV and HCV responder and non-responder patients to PEG-IFN plus ribavirin therapy

	TTV		<i>P</i> ^a	HCV		<i>P</i> ^a
	Responders (<i>n</i> =6)	Non-responders (<i>n</i> =4)		Responders (<i>n</i> =11)	Non-responders (<i>n</i> =4)	
Before therapy	97.16 \pm 30.18	103.0 \pm 84.87	0.09	112.54 \pm 51.90	72.00 \pm 31.01	0.33
End of therapy	28.66 \pm 11.09	27.00 \pm 9.83	0.92	30.09 \pm 12.96	31.50 \pm 14.20	0.76

ALT level was expressed as IU/L. ^aStudent's *t*-test.

in the normal range before and after the combined therapy in one patient who did not eliminate TTV and HCV (Table 2, patient No. 15).

HCV response to PEG-IFN plus ribavirin treatment

Pretreatment serum HCV RNA values ranged between 9×10^4 and 6.3×10^6 genomes/ml of serum (mean: 1.36×10^6 genomes/ml). The decline of HCV viremia was clearly evident after therapy and the response rate was 73% (11/15). When serum HCV RNA pretreatment levels were compared between non-responder and responder patients, the difference was statistically significant (1.85×10^6 vs 1.15×10^6 genomes/ml, respectively; $P=0.005$). Sustained HCV response after 6 months of treatment was found in 8/15 (53%) patients, 2 patients (13%) became HCV RNA positive during the follow-up period and in one case no serum sample was available for the detection of HCV RNA (Table 1). Following combined therapy, baseline and final ALT levels between responder and non-responder patients were compared but the differences between both groups were not statistically significant (Table 2).

DISCUSSION

Many studies have been done trying to assess whether TTV could cause liver disease, but its molecular properties and its pathogenic potential are still poorly understood. Different epidemiological studies have clearly indicated that TTV is a transmissible blood-borne virus sharing common transmission routes with hepatitis viruses. Then, coinfection of TTV was frequently observed in patients with chronic hepatitis C^[9]. We found that 66.6% of our patients infected with HCV were TTV DNA-positive, which confirms previous studies showing that the prevalence of TTV infection varied between 30%-88%^[15,16].

It has been reported that TTV infection treated with IFN alone had a response rate of 62%-83% after monotherapy^[11,17]. Our data showed that 60% of the TTV-infected patients could eliminate TT virus at the end of PEG-IFN plus ribavirin combination treatment. By comparing our results with earlier published studies, the novel and interesting information obtained from our work is that the treatment of TTV infection with PEG-IFN plus ribavirin, for a period of 48 weeks, did not promote an additional and increased response to therapy. Then, ribavirin did not produce any effect on TTV replication because of the similar sensitivity of TTV to combined treatment or to standard IFN monotherapy. Moreover, in these published studies the sustained TTV response after 6 months of therapy was decreased to 32%-50%^[18]. In contrast, in our series no sustained clearance of TTV was achieved in any patient after 6 months of combined therapy. It is well known that TTV tended to last many years^[19] although spontaneously resolved viremias after short periods of time were described in the literature^[20]. That the majority of our TTV responder patients relapsed during the follow-up period could suggest the possibility that TTV could become temporarily latent, as a result of the sensitivity of TTV to PEG-IFN during its administration, and that a new reinfection of the virus occurred. In other words, it was possible that TTV could persist in other type cells such as peripheral blood mononuclear cells where TTV persistence could occur^[10]. Among other explanations, it could be possible that because of TTV high level of genetic diversity, viral genomes with different PEG-IFN sensitivities could arise over time. Finally, we suggest that TTV response to PEG-IFN may be affected by a combination of virus and host factors as observed in other viruses^[21].

With respect to the effect of PEG-IFN plus ribavirin administration for the treatment of chronic hepatitis C, this study confirms earlier reports in which HCV infection responded positively to the combined therapy with a high rate

of viral clearance and normalization of ALT levels during the treatment period. Both factors occurred in HCV/TTV-coinfected patients as well as in non-coinfected ones, so it could be suggested that the response of HCV to IFN-PEG plus ribavirin treatment was not affected by TTV coinfection. Moreover, in those patients without sustained TTV response ALT levels were normal in contrast with those who had a HCV relapse. Then, in agreement with other published studies, TTV might not have any clinical association with producing HCV hepatitis^[16,22]. Furthermore, another interesting result from our study was that PEG-IFN plus ribavirin therapy seemed to be specially efficacious in patients with more advanced liver diseases such as grade III fibrosis. Thus, in 45.5% of HCV responder patients with advanced fibrosis, only 25% of non-responder ones presented a minor grade fibrosis, which supported the beneficial effect of PEG-IFN on patients with difficult-to-treat diseases reported in previous studies^[23,24].

In conclusion, TTV has a similar response rate to PEG-IFN plus ribavirin combined treatment or to IFN monotherapy, suggesting that neither PEG-IFN nor ribavirin has any additional effect on TTV replication. Furthermore, TTV relapse was found in most of the responder patients after the combined therapy was stopped for 6 months, so it seems likely that TTV is not as sensitive to PEG-IFN as HCV.

REFERENCES

- 1 **Nishizawa T**, Okamoto H, Konishi K, Yoshizawa H, Miyakawa Y, Mayumi M. A novel DNA virus (TTV) associated with elevated transaminase levels in posttransfusion hepatitis of unknown etiology. *Biochem Biophys Res Commun* 1997; **241**: 92-97
- 2 **Abe K**, Inami T, Asano K, Miyoshi C, Masaki N, Hayashi S, Ishikawa K, Takebe Y, Win KM, El Zayadi AR, Han KH, Zhang DY. TT virus infection is widespread in the general populations from different geographic regions. *J Clin Microbiol* 1999; **37**: 2703-2705
- 3 **Matsumoto A**, Yeo AE, Shih JW, Tanaka E, Kiyosawa K, Alter HJ. Transfusion-associated TT virus infection and its relationship to liver disease. *Hepatology* 1999; **30**: 283-288
- 4 **Miyata H**, Tsunoda H, Kazi A, Yamada A, Khan MA, Murakami J, Kamahora T, Shiraki K, Hino S. Identification of a novel GC-rich 113-nucleotide region to complete the circular, single-stranded DNA genome of TT virus, the first human circovirus. *J Virol* 1999; **73**: 3582-3586
- 5 **Hijikata M**, Takahashi K, Mishiro S. Complete circular DNA genome of a TT virus variant (isolate name SANBAN) and 44 partial ORF2 sequences implicating a great degree of diversity beyond genotypes. *Virology* 1999; **260**: 17-22
- 6 **Levero M**, Tagger A, Balsano C, De Marzio E, Avantaggiati ML, Natoli G, Diop D, Villa E, Diodati G, Alberti A. Antibodies to hepatitis C virus in patients with hepatocellular carcinoma. *J Hepatol* 1991; **12**: 60-63
- 7 **Brillanti S**, Garson J, Foli M, Whitby K, Deaville R, Masci C, Miglioli M, Barbara L. A pilot study of combination therapy with ribavirin plus interferon alfa for interferon alfa-resistant chronic hepatitis C. *Gastroenterology* 1994; **107**: 812-817
- 8 **Hoofnagle JH**, Di Bisceglie AM. The treatment of chronic viral hepatitis. *N Engl J Med* 1997; **336**: 347-356
- 9 **Irving WL**, Ball JK, Berridge S, Curran R, Grabowska AM, Jameson CL, Neal KR, Ryder SD, Thomson BJ. TT virus infection in patients with hepatitis C: frequency, persistence, and sequence heterogeneity. *J Infect Dis* 1999; **180**: 27-34
- 10 **Maggi F**, Pistello M, Vatteroni M, Presciuttini S, Marchi S, Isola P, Fornai C, Fagnani S, Andreoli E, Antonelli G, Bendinelli M. Dynamics of persistent TT virus infection, as determined in patients treated with alpha interferon for concomitant hepatitis C virus infection. *J Virol* 2001; **75**: 11999-12004
- 11 **Nishizawa Y**, Tanaka E, Orii K, Rokuhara A, Ichijo T, Yoshizawa K, Kiyosawa K. Clinical impact of genotype 1 TT virus infection in patients with chronic hepatitis C and response of TT virus to alpha-interferon. *J Gastroenterol Hepatol* 2000; **15**: 1292-1297

- 12 **Okamoto H**, Takahashi M, Nishizawa T, Ukita M, Fukuda M, Tsuda F, Miyakawa Y, Mayumi M. Marked genomic heterogeneity and frequent mixed infection of TT virus demonstrated by PCR with primers from coding and noncoding regions. *Virology* 1999; **259**: 428-436
- 13 **Takahashi K**, Hoshino H, Ohta Y, Yoshida N, Mishiro S. Very high prevalence of TT virus (TTV) infection in general population of Japan revealed by a new set of PCR primers. *Hepatol Res* 1998; **12**: 233-239
- 14 **Garcia JM**, Marugan RB, Garcia GM, Lindeman MLM, Abete JF, del Terron SC. TT virus infection in patients with chronic hepatitis B and response of TTV to lamivudine. *World J Gastroenterol* 2003; **9**: 1261-1264
- 15 **Lai YC**, Hu RT, Yang SS, Wu CH. Coinfection of TT virus and response to interferon therapy in patients with chronic hepatitis B or C. *World J Gastroenterol* 2002; **8**: 567-570
- 16 **Meng XW**, Komatsu M, Goto T, Nakane K, Ohshima S, Yoneyama K, Lin JG, Watanabe S. Clinical significance of TT virus in chronic hepatitis C. *J Gastroenterol Hepatol* 2001; **16**: 202-208
- 17 **Dai CY**, Yu ML, Chuang WL, Hou NJ, Hou C, Chen SC, Lin ZY, Hsieh MY, Wang LY, Chang WY. The response of hepatitis C virus and TT virus to high dose and long duration interferon-alpha therapy in naive chronic hepatitis C patients. *Antiviral Res* 2002; **53**: 9-18
- 18 **Kawanaka M**, Niiyama G, Mahmood S, Ifukube S, Yoshida N, Onishi H, Hanano S, Ito T, Yamada G. Effect of TT virus co-infection on interferon response in chronic hepatitis C patients. *Liver* 2002; **22**: 351-355
- 19 **Matsumoto A**, Yeo AE, Shih JW, Tanaka E, Kiyosawa K, Alter HJ. Transfusion-associated TT virus infection and its relationship to liver disease. *Hepatology* 1999; **30**: 283-288
- 20 **Lefrere JJ**, Roudot-Thoraval F, Lefrere F, Kanfer A, Mariotti M, Lerable J, Thauvin M, Lefevre G, Rouger P, Girot R. Natural history of the TT virus infection through follow-up of TTV DNA-positive multiple-transfused patients. *Blood* 2000; **95**: 347-351
- 21 **Booth JC**, Foster GR, Kumar U, Galassini R, Goldin RD, Brown JL, Thomas HC. Chronic hepatitis C virus infections: predictive value of genotype and level of viraemia on disease progression and response to interferon alpha. *Gut* 1995; **36**: 427-432
- 22 **Watanabe H**, Saito T, Kawamata O, Shao L, Aoki M, Terui Y, Mitsuhashi H, Matsuo T, Takeda Y, Saito K, Togashi H, Shinzawa H, Takahashi T. Clinical implications of TT virus superinfection in patients with chronic hepatitis C. *Am J Gastroenterol* 2000; **95**: 1776-1780
- 23 **Pockros PJ**. Developments in the treatment of chronic hepatitis C. *Expert Opin Investig Drugs* 2002; **11**: 515-528
- 24 **Heathcote EJ**, Shiffman ML, Cooksley WG, Dusheiko GM, Lee SS, Balart L, Reindollar R, Reddy RK, Wright TL, Lin A, Hoffman J, De Pamphilis J. Peginterferon alfa-2a in patients with chronic hepatitis C and cirrhosis. *N Engl J Med* 2000; **343**: 1673-1680

Edited by Wang XL

Do there exist synergistic antitumor effects by coexpression of herpes simplex virus thymidine kinase with cytokine genes on human gastric cancer cell line SGC7901?

Jian-Hua Zhang, Ming-Xi Wan, Jia-Ying Yuan, Bo-Rong Pan

Jian-Hua Zhang, Ming-Xi Wan, Department of Biomedical Engineering, School of Life Science and Technology, Xi'an Jiaotong University, 28 West Xianning Road, Xi'an 710049, Shaanxi Province, China

Jia-Ying Yuan, Department of Ultrasonic Diagnosis, Xijing Hospital, Fourth Military Medical University, 127 West Changle Road, Xi'an 710033, Shaanxi Province, China

Bo-Rong Pan, Department of Oncology, Xijing Hospital, Fourth Military Medical University, 127 West Changle Road, Xi'an 710033, Shaanxi Province, China

Supported by Doctoral Foundation of Xi'an Jiaotong University, No.69925101 and National Natural Science Foundation of China, No.30270404

Correspondence to: Dr. Ming-Xi Wan, Department of Biomedical Engineering, School of Life Science and Technology, Xi'an Jiaotong University, 28 West Xianning Road, Xi'an 710049, Shaanxi Province, China. wanmingxi@yahoo.com.cn

Telephone: +86-29-2667924

Received: 2003-03-03 **Accepted:** 2003-04-01

Abstract

AIM: To evaluate the synergistic antitumor effects of herpes simplex virus thymidine kinase (HSV-TK) together with tumor necrosis factor alpha (TNF- α) or interleukin-2 (IL-2) gene expression on gastric cancer cell line SGC7901.

METHODS: Recombinant vectors pL(TT)SN and pL(TI)SN, which express TK-IRES-TNF- α and TK-IRES-IL-2 genes separately, as well as the control plasmids pL(TK)SN and pLXSN were employed to transfect PA317 cells respectively to generate the viruses that can stably express the objective genes through G418 selection. The gastric cancer cells were then transfected by the retroviral serum from the package cells and maintained in culture to determine the cell growth and apoptosis. The cytotoxic effects of HSV-TK together with TNF- α or IL-2 gene expression on the transfected cancer cells were evaluated by the cell viability and bystander effects in the presence of GCV supplemented in the cultural medium.

RESULTS: Expression of recombinant proteins including TNF- α and IL-2 by stable transfectants was confirmed by Western blotting. The percentage of cell apoptosis in the SGC/0, SGC/TK-TNF- α , SGC/TK-IL-2 and SGC/TK clone was 2.3%, 12.3%, 11.1% and 10.9% respectively at 24 h post-transfection. Cell growth status among all the experimental groups as judged by cell absorbance (A) at 570nm did not exhibit any significant difference ($P>0.05$); although it was noted to be slightly lower in the SGC/TT group. Cell survival rate in SGC/TI, SGC/TT and SGC/TK group was significantly decreased in a dose-dependent manner of GCV compared with that of the SGC/0 group ($P<0.05-0.01$). Among all studied cells, the SGC/TT was shown most sensitive to GCV with a half lethal dose of 0.5 mg·L⁻¹. In contrast, the survival rate of SGC/0 cells was not affected by the presence of GCV with the doses less than 10 mg·L⁻¹. The half lethal dose of

GCV for SGC/0 cells was more than 100 mg·L⁻¹. Marked bystander effect induced by SGC/TI, SGC/TT and SGC/TK cells was confirmed by the fact that 20% of these stable transfectants could kill 50% of the co-cultured cells, in which the most prominent bystander effect was found in the circumstance of SGC/TT presence. However, no significant difference of these variables was found among SGC/TI, SGC/TT and SGC/TK cells ($P>0.05$).

CONCLUSION: The synergistic antitumor effects produced by the co-expression of HSV-TK with TNF- α or IL-2 genes were not present in the transfected SGC7901 cells. The mechanism underlying these phenomena was not known.

Zhang JH, Wan MX, Yuan JY, Pan BR. Do there exist synergistic antitumor effects by coexpression of herpes simplex virus thymidine kinase with cytokine genes on human gastric cancer cell line SGC7901? *World J Gastroenterol* 2004; 10(1): 147-151 <http://www.wjgnet.com/1007-9327/10/147.asp>

INTRODUCTION

Gastric cancer is one of the most prevalent malignancies in China^[1]. Despite the recent progress in early diagnosis and treatment of the disease, aggressive surgical or chemotherapeutic interventions have not sufficiently prolonged the survival time of patients with distant metastases^[2]. Thus, searching for more effective therapeutic modalities, especially for the stage IV gastric cancer patients, has become an urgent task in our daily medical practice.

The transfer of suicide genes into tumor cells that is currently being studied as a method of treatment for various cancers has made the target cells become sensitive to the pharmacological agents. Suicide gene therapy with the herpes simplex virus thymidine kinase (HSV-TK) fragment, the most widely used strategy for the cancer therapeutic study^[3], has been shown to exert antitumor efficacy in various cancer models^[4-7]. However, its efficacy seems not to be fully developed to eliminate tumor cells in some of the investigations^[8-12]. Gene therapy with HSV-TK and cytokine genes together may produce a complementary effect, and has become a new insight for the treatment of malignancies^[13, 14].

Previously, we constructed two retroviral vectors, pL(TT)SN and pL(TI)SN, which have been confirmed to express TK-IRES-TNF- α and TK-IRES-IL-2 genes respectively in the gastric cancer cell line SGC7901^[15]. In the present study, the synergistic antitumor effects of these vectors on human gastric cancer cells were investigated in the presence of GCV to confirm their efficiency.

MATERIALS AND METHODS

Cell lines and vectors

The mouse fibroblast cell line NIH3T3 and the amphotropic retroviral packaging cells PA317 were the generous gifts from

Dr. Yu Bing (Fourth Military Medical University, Xi' an, China). The human gastric carcinoma cell lines SGC7901 were obtained from Shanghai Institute of Biochemistry. All of the cells were maintained in RPMI 1640 medium, supplemented with 10% FBS (Hangzhou, Sijiqing Biotech Company), 2 mM L-glutamine, 100 units/ml penicillin and 100 µg/ml streptomycin. The PA317 was used as the packaging cell and the NIH 3T3 cells were employed to assay the virus titre. The cell cultures were maintained at 37 °C in a humidified atmosphere with 5% CO₂.

The recombinant vectors pL(TT)SN and pL(TI)SN, which express TK-IRES-TNF-α and TK-IRES-IL-2 genes respectively, as well as the control plasmid pL(TK)SN carrying only TK fragment were constructed and identified in our previous study^[15]. The empty plasmid PLXSN used as another control vector was provided by Dr. Yu Bing (Fourth Military Medical University, Xi' an, China).

Establishment of stable transfectants

The retrovirus plasmids pL(TT)SN, pL(TI)SN, pL(TK)SN and pLXSN were transferred into PA317 cells respectively by lipofectamine (Gibco) according to the manual instructions^[16, 17]. After 48 h of transfection, G418 (Promega) was added to the culture medium at a concentration of 500 mg · L⁻¹ to select G418-resistant colonies. After 2-weeks' culture with the changing of the G418-containing medium every 3 days, the supernatant of G418-resistant colonies was collected and diluted to different concentrations to infect NIH3T3 cells, which were further undergone the G418 selection for 2w, then the G418-resistant NIH3T3 colonies were counted for the determination of viral titre^[18]. The viral titers of pL(TT)SN, pL(TI)SN, pL(TK)SN and empty plasmid pLXSN were 5×10⁸ CFU/L, 6×10⁸ CFU/L, 1×10⁹ CFU/L and 1×10⁹ CFU/L respectively.

A total number of 5×10⁵ SGC7901 cells were incubated in a 6-well plate for 24 h, then rinsed with serum-free RPMI 1640 medium twice and incubated with 100 µl supernatant of G418-resistant PA317 colony for 3 h. After 4-weeks' cultivation, the G418-resistant colonies designated as SGC/TK-TNF-α, SGC/TK-IL-2, SGC/TK and SGC/0 respectively according to the transfected vectors were collected and used both to confirm the objective gene expression by Western blot and to perform other determinations.

For Western blotting, the SGC/TT and SGC/TI cells were incubated respectively in the six-well plates at a density of 2.5×10⁵ cells/well for 24 h, followed by a further cultivation of 48 h with the culture medium replaced with 1 ml of serum-free RPMI 1640. Then the serum-free medium was totally collected, concentrated in a microconcentrator to 20 µl and subjected to electrophoresis on a 120 g · L⁻¹ SDS/PAGE gel. Proteins were transferred to a nitrocellulose membrane and incubated overnight in 50 ml · L⁻¹ fat free milk in PBS at 4 °C. After washed in 10 ml · L⁻¹ fat free milk, the membrane was incubated with monoclonal antibody of mouse anti-rhIL-2 or anti-TNF-α, followed by incubation with horseradish peroxidase-conjugated antimouse immunoglobulin. Proteins were detected by using the ECL kit according to the manufacturer's instruction (Amersham)^[19].

Determination of cell apoptosis

Cell apoptosis was quantitated by the protocol of flow cytometry. Briefly, 100 µl of the observed cells (2×10⁵) in binding buffer and 5 µl of FITC-conjugated annexin V/PI dual staining reagents (Annexin V-FITC kit, Pharmingen, USA) were transferred in turn into a 5 ml culture tube and incubated for 15 min at room temperature in the dark. After 400 µl of binding buffer was added into the culture tube, the flow cytometric analysis for apoptosis was performed as soon as possible within 12 h (FACScaliber; Becton, Dickinson, USA).

Cell growth assay

Cell growth was scaled in SGC/TI, SGC/TT, SGC/TK and SGC/0 cells as described in the references^[20, 21]. Cells were cultured in 24-well plate (Nuc, Co) at 37 °C in a humidified atmosphere with 5% CO₂ and adjusted to a density of 1.5×10⁴ cells/well at the time of determination. Cell absorbance (A) at 570nm was determined each day for 6 days. The figures obtained were used to draw a cell growth curve.

MTT assay

An MTT assay was conducted to determine the cell survival rate^[22, 23]. Following 24 h incubation, cells cultured in 96-well plates were treated with different concentrations of GCV (Roche Co.) and continued to be cultured for 6 d, when the MTT mixture was added to medium and the cells were incubated further for another 4 h. The absorbance of the cells was measured at a wavelength of 525nm with a microtiter plate reader. The survival rate was expressed as A/B×100%, where A was the absorbance value from the experimental cells and B was that from the control by SGC7901 cells.

Bystander effect observation

Twenty-four hours after tumor cells were infected with recombinant retrovirus, different proportions of transfected and untransfected cells that were adjusted to a density of 1×10⁵ cells/well were co-cultured on 4-well flat-bottom plates at 37 °C for 5 d in the presence of 5 mg · L⁻¹ GCV. The cell survival rate was measured by MTT method^[24].

Statistical analysis

Quantitative variables are described as mean ± standard error of the mean. Categorical variables are expressed as percentages. Comparisons between means were done with the Student's *t*-test. Comparison between percentages was performed with the χ^2 test. A *P* value <0.05 was taken as the criterion of statistical significance.

RESULTS

Expressions of stable transfectants

The stable expression of recombinant proteins in target cells was confirmed by Western blot, in which two distinct bands of 15ku and 17ku were observed on the nitrocellulose membrane, corresponding to the fragment sizes of IL-2 and TNF-α respectively (Figure 1).

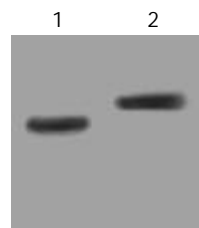


Figure 1 Stably expressed recombinant protein in transduced SGC7901 cells confirmed by Western blot. Lane 1: IL-2 (15ku) expressed in SGC/TI cells; Lane 2: TNF-α (17ku) expressed in SGC/TT cells.

Cell apoptosis

Cells in the early phase of apoptosis were labeled by single annexin V fluorescence. The percentage of cell apoptosis in the SGC/0, SGC/TK-TNF-α, SGC/TK-IL-2 and SGC/TK clone was 2.3%, 12.3%, 11.1% and 10.9% respectively at 24 h post-transfection, indicating a slightly higher percentage of apoptosis appeared in the SGC/TK-TNF-α, SGC/TNF-α

and SGC/TK clones compared with that in the SGC/0 clone ($P>0.05$, Figure 2).

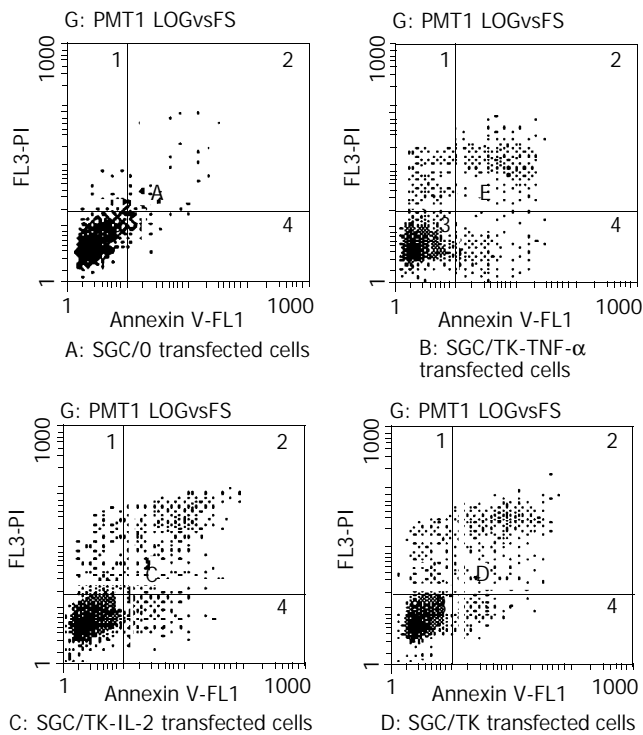


Figure 2 Percentage of early apoptotic cells in different groups of transfectants.

Cell growth status

The A value of cells among all experimental groups did not exhibit any significant difference ($P>0.05$), although it was slightly lower in the SGC/TT group (Figure 3). The result showed that the cell growth status was not severely influenced by the vector's variety used for the transfection in the present study.

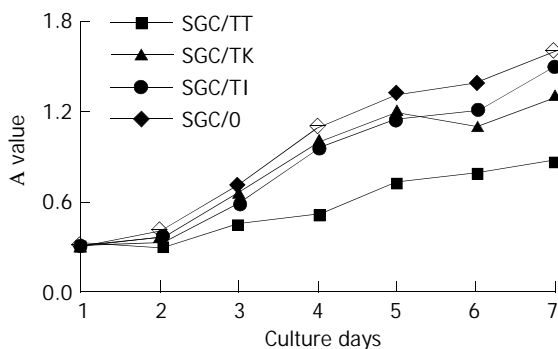


Figure 3 Cell growth status of the different transfectants.

Cell viability

Cell survival rate in SGC/TT, SGC/TK and SGC/TK group was significantly decreased in a dose-dependent manner of GCV compared with that of the SGC/0 group ($P<0.05-0.01$). Among all studied cells, the SGC/TT was shown most sensitive to GCV with a half lethal dose of $0.5 \text{ mg} \cdot \text{L}^{-1}$. In contrast, the survival rate of SGC/0 cells was not affected by the presence of GCV with the doses less than $10 \text{ mg} \cdot \text{L}^{-1}$. The half lethal dose of GCV for SGC/0 cells was more than $100 \text{ mg} \cdot \text{L}^{-1}$ (Figure 4).

Bystander effect

Marked bystander effect was shown by SGC/TT, SGC/TK and SGC/TK cells as manifested by the fact that 20% of these stable

transfectants could kill 50% of the co-cultured cells (Figure 5). However, the most prominent bystander effect was found in the circumstance of SGC/TT presence.

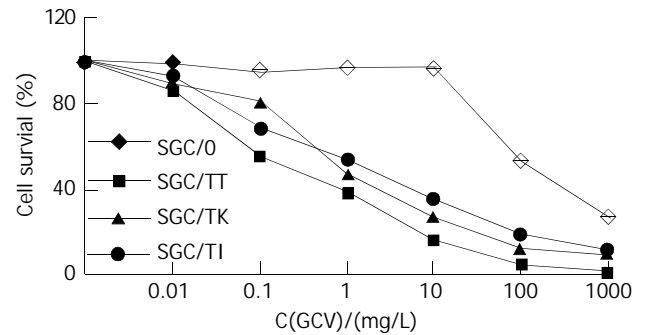


Figure 4 Cell survival rate in different experimental group treated with $5 \text{ mg} \cdot \text{L}^{-1}$ GCV for 6 d.

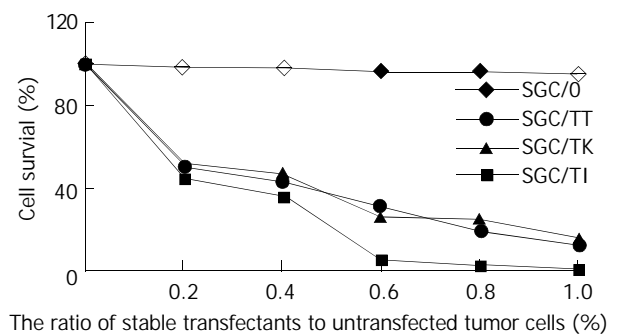


Figure 5 Bystander effect of different transfectants.

DISCUSSION

Transfer of suicide gene into tumor cells has emerged as an attractive strategy of gene therapy for the selective elimination of cancer cells, in which the suicide gene system alone or in combination with other immunological genes have been considered to be the favorable modalities for the treatment of malignancies^[25-27]. The suicide genes encode non-mammalian enzymes that can convert nontoxic prodrugs into cellular toxic metabolites. The most widely used suicide gene is the HSV-TK/GCV system that can convert prodrug GCV into phosphorylated GCV. The latter is further phosphorylated by the cellular kinase to form GCV triphosphate, a toxic substance that can inhibit cellular DNA synthesis and lead cell to death. Besides, the "bystander effect" induced by TK gene can also enhance the tumor-killing capacity of the HSV-TK/GCV system^[28-30]. However, it was found in some investigations that the antitumor efficiency of this system was limited by the lower rate of gene transfection and their insufficient induction of host immunity^[31-33].

Cytokine therapy is another strategy for the treatment of malignancies. It can not only directly kill tumor cells, inhibit tumorigenesis and tumor metastasis, but can also enhance these effects by the induction of antitumor immunity. Based on the antitumor properties of certain cytokines such as IL-2 and TNF- α , it is believed that the gene therapy combining cytokine with TK suicide gene would produce more beneficial and effective effects for the treatment of cancers, which has received strong supports from some of the recently published literatures. Majumdar and his associates^[33] have compared the therapeutic effect of IL-2 expression alone with that by the co-expression of IL-2 and TK genes on squamous cell carcinoma in nude mice, and found that the combined gene expression was most efficient for the gene therapy. In another study, Chen *et al.*^[34]

reported that cytokine gene IL-2 could act synergistically with the suicide gene to induce a systemic antitumor immunity. Unfortunately, there have been few reports up to the present about this therapeutic strategy in the antitumor study of gastric malignancy.

In the present study, we tried to observe the antitumor effects by the co-expression of suicide gene HSV-TK and cytokine gene TNF- α or IL-2 on gastric carcinoma cell lines SGC7901. It was found that the percentage of cell apoptosis in the SGC/0, SGC/TK-TNF- α , SGC/TK-IL-2 and SGC/TK clone was 2.3%, 12.3%, 11.1% and 10.9% respectively at 24 h post-transfection, and the cell growth status as judged by cell absorbance (A) at 570nm among all the experimental groups did not exhibit any significant difference ($P>0.05$), although they were noted to be slightly varied in the SGC/TT group. This indicated that the apoptosis and growth status of SGC7901 cells were not severely influenced by the vector's variety used in the study. Whereas the cell survival rate in SGC/0, SGC/TT and SGC/TK group was significantly decreased in a dose-dependent manner of GCV compared with that of the SGC/0 group ($P<0.05-0.01$) in the presence of GCV, in which the SGC/TT cells were shown to be most sensitive to GCV with a half lethal dose of 0.5 mg·L⁻¹. In contrast, the survival rate of SGC/0 cells was not affected by the presence of GCV with the doses less than 10 mg·L⁻¹. The half lethal dose of GCV for SGC/0 cells was more than 100 mg·L⁻¹. Marked bystander effect induced by SGC/0, SGC/TT and SGC/TK cells was also confirmed by the fact that 20% of these stable transfectants could kill 50% of the co-cultured cells and the most prominent bystander effect was found in the presence of SGC/TT. However, no significant difference of these variables was found among SGC/0, SGC/TT and SGC/TK cells, which meant that the synergistic antitumor effects produced by the co-expression of HSV-TK and TNF- α or IL-2 genes were not present in the transfected SGC7901 cells. Whether this was due to the speciality of the gastric cancer cell line is unknown. Further studies, therefore, are needed to elucidate the mechanisms underlying these phenomena in order to search for more efficient therapeutic modalities for the treatment of gastric malignancies.

REFERENCES

- Xu CT**, Huang LT, Pan BR. Current gene therapy for stomach carcinoma. *World J Gastroenterol* 2001; **7**: 752-759
- Ikeda Y**, Mori M, Adachi Y, Matsushima T, Sugimachi K, Saku M. Carcinoembryonic antigen (CEA) in stage IV gastric cancer as a risk factor for liver metastasis: a univariate and multivariate analysis. *J Surg Oncol* 1993; **53**: 235-238
- van der Eb MM**, Cramer SJ, Vergouwe Y, Schagen FH, van Krieken JH, van der Eb AJ, Rinkes IH, van de Velde CJ, Hoeben RC. Severe hepatic dysfunction after adenovirus-mediated transfer of the herpes simplex virus thymidine kinase gene and ganciclovir administration. *Gene Ther* 1998; **5**: 451-458
- Narita M**, Bahar R, Hatano M, Kang MM, Tokuhisa T, Goto S, Saisho H, Sakiyama S, Tagawa M. Tissue-specific expression of a suicide gene for selective killing of neuroblastoma cells using a promoter region of the NCX gene. *Cancer Gene Ther* 2001; **8**: 997-1002
- Van Dillen JJ**, Mulder NH, Vaalburg W, de Vries EF, Hospers GA. Influence of the bystander effect on HSV-tk/GCV gene therapy. A review. *Curr Gene Ther* 2002; **2**: 307-322
- Nowak AK**, Lake RA, Kindler HL, Robinson BW. New approaches for mesothelioma: biologics, vaccines, gene therapy, and other novel agents. *Semin Oncol* 2002; **29**: 82-96
- Qiao J**, Doubrovina M, Sauter BV, Huang Y, Guo ZS, Balatoni J, Akhurst T, Blasberg RG, Tjuvahev JG, Chen SH, Woo SL. Tumor-specific transcriptional targeting of suicide gene therapy. *Gene Ther* 2002; **9**: 168-175
- Engelmann C**, Heslan JM, Fabre M, Lagarde JP, Klatzmann D, Panis Y. Importance, mechanisms and limitations of the distant bystander effect in cancer gene therapy of experimental liver tumors. *Cancer Lett* 2002; **179**: 59-69
- Adachi Y**, Matsubara S, Muramatsu T, Curiel DT, Reynolds PN. Midkine promoter-based adenoviral suicide gene therapy to midkine-positive pediatric tumor. *J Pediatr Surg* 2002; **37**: 588-592
- Pulkkanen KJ**, Laukkanen JM, Fuxe J, Kettunen MI, Rehn M, Kannasto JM, Parkkinen JJ, Kauppinen RA, Pettersson RF, Yla-Herttuala S. The combination of HSV-tk and endostatin gene therapy eradicates orthotopic human renal cell carcinomas in nude mice. *Cancer Gene Ther* 2002; **9**: 908-916
- Floeth FW**, Shand N, Bohar H, Prissack HB, Felsberg J, Neuen-Jacob E, Aulich A, Burger KJ, Bock WJ, Weber F. Local inflammation and devascularization-*in vivo* mechanisms of the "bystander effect" in VPC-mediated HSV-Tk/GCV gene therapy for human malignant glioma. *Cancer Gene Ther* 2001; **8**: 843-851
- Warren P**, Song W, Holle E, Holmes L, Wei Y, Li J, Wagner T, Yu X. Combined HSV-TK/GCV and secondary lymphoid tissue chemokine gene therapy inhibits tumor growth and elicits potent antitumor CTL response in tumor-bearing mice. *Anticancer Res* 2002; **22**: 599-604
- Niranjan A**, Moriuchi S, Lunsford LD, Kondziolka D, Flickinger JC, Fellows W, Rajendiran S, Tamura M, Cohen JB, Glorioso JC. Effective treatment of experimental glioblastoma by HSV vector-mediated TNF alpha and HSV-tk gene transfer in combination with radiosurgery and ganciclovir administration. *Mol Ther* 2000; **2**: 114-120
- Zhang R**, DeGroot LJ. An adenoviral vector expressing functional heterogeneous proteins herpes simplex viral thymidine kinase and human interleukin-2 has enhanced *in vivo* antitumor activity against medullary thyroid carcinoma. *Endocr Relat Cancer* 2001; **8**: 315-325
- Zhang JH**, Wan MX, Yuan JY, Pan BR. Construction and identification of the recombinant vectors carrying herpes simplex virus thymidine kinase and cytokine genes expressed in gastric carcinoma cell line SGC7901. *World J Gastroenterol* 2003; **9** (data to be published)
- Chen Y**, Wu Q, Song SY, Su WJ. Activation of JNK by TPA promotes apoptosis via PKC pathway in gastric cancer cells. *World J Gastroenterol* 2002; **8**: 1014-1018
- Shen ZY**, Xu LY, Chen MH, Shen J, Cai WJ, Zeng Y. Progressive transformation of immortalized esophageal epithelial cells. *World J Gastroenterol* 2002; **8**: 976-981
- Zhao LS**, Qin S, Zhou TY, Tang H, Liu L, Lei BJ. DNA-based vaccination induces humoral and cellular immune responses against hepatitis B virus surface antigen in mice without activation of C-myc. *World J Gastroenterol* 2000; **6**: 239-243
- Khurana VG**, Katusic ZS. Gene transfer for cerebrovascular disease. *Curr Cardiol Rep* 2001; **3**: 10-16
- Akyurek LM**, Nallamshetty S, Aoki K, San H, Yang ZY, Nabel GJ, Nabel EG. Coexpression of guanylate kinase with thymidine kinase enhances prodrug cell killing *in vitro* and suppresses vascular smooth muscle cell proliferation *in vivo*. *Mol Ther* 2001; **3**: 779-786
- Pulkkanen KJ**, Parkkinen JJ, Laukkanen JM, Kettunen MI, Tyynela K, Kauppinen RA, Ala-Opas MY, Yla-Herttuala S. HSV-tk gene therapy for human renal cell carcinoma in nude mice. *Cancer Gene Ther* 2001; **8**: 529-536
- Cao WX**, Ou JM, Fei XF, Zhu ZG, Yin HR, Yan M, Lin YZ. Methionine-dependence and combination chemotherapy on human gastric cancer cells *in vitro*. *World J Gastroenterol* 2002; **8**: 230-232
- Wei XC**, Wang XJ, Chen K, Zhang L, Liang Y, Lin XL. Killing effect of TNF-related apoptosis inducing ligand regulated by tetracycline on gastric cancer cell line NCI-N87. *World J Gastroenterol* 2001; **7**: 559-562
- Guo SY**, Gu QL, Liu BY, Zhu ZG, Yin HR, Lin YZ. Experimental study on the treatment of gastric cancer by TK gene combined with mL-2 gene. *Shijie Huaren Xiaohua Zazhi* 2000; **8**: 974-978
- Guan J**, Ma L, Wei L. Characteristics of ovarian cancer cells transduced by the bicistronic retroviral vector containing GM-CSF and HSV-tk genes. *Chin Med J* 2001; **114**: 147-151
- Balzarini J**, Ostrowski T, Goslinski T, De Clercq E, Golankiewicz

- B. Pronounced cytostatic activity and bystander effect of a novel series of fluorescent tricyclic acyclovir and ganciclovir derivatives in herpes simplex virus thymidine kinase gene-transduced tumor cell lines. *Gene Ther* 2002; **9**: 1173-1182
- 27 **Burrows FJ**, Gore M, Smiley WR, Kanemitsu MY, Jolly DJ, Read SB, Nicholas T, Kruse CA. Purified herpes simplex virus thymidine kinase retroviral particles: III. Characterization of bystander killing mechanisms in transfected tumor cells. *Cancer Gene Ther* 2002; **9**: 87-95
- 28 **Hall SJ**, Canfield SE, Yan Y, Hassen W, Selleck WA, Chen SH. A novel bystander effect involving tumor cell-derived Fas and FasL interactions following Ad.HSV-tk and Ad.mIL-12 gene therapies in experimental prostate cancer. *Gene Ther* 2002; **9**: 511-517
- 29 **Boucher PD**, Ostruszka LJ, Murphy PJ, Shewach DS. Hydroxyurea significantly enhances tumor growth delay *in vivo* with herpes simplex virus thymidine kinase/ganciclovir gene therapy. *Gene Ther* 2002; **9**: 1023-1030
- 30 **Hayashi K**, Hayashi T, Sun HD, Takeda Y. Contribution of a combination of ponocidin and acyclovir/ganciclovir to the anti-tumor efficacy of the herpes simplex virus thymidine kinase gene therapy system. *Hum Gene Ther* 2002; **10**: 415-423
- 31 **Huang H**, Wang A. The adenovirus-mediated HSV-tk/GCV suicide gene system in the treatment of tongue carcinoma cell line. *Zhonghua Kouqiang Yixue Zazhi* 2001; **36**: 457-460
- 32 **Gao G**, Huang T, Chen S. *In vitro* and *in vivo* bystander effect of adenovirus-mediated transfer of the herpes simplex virus thymidine kinase gene. *Zhonghua Waikexue Zazhi* 2002; **40**: 301-303
- 33 **Majumdar AS**, Zolotorey A, Samuel S, Tran K, Vertin B, Hall-Meier M, Antoni BA, Adeline E, Philip M, Philip R. Efficacy of herpes simplex virus thymidine kinase in combination with cytokine gene therapy in an experimental metastatic breast cancer model. *Cancer Gene Ther* 2000; **7**: 1086-1099
- 34 **Chen SH**, Kosai K, Xu B, Khiem PN, Contant C, Finegold MJ, Woo SL. Combined suicide and cytokine gene therapy for hepatic metastasis of colon carcinoma: sustained antitumor immunity prolongs animal survival. *Cancer Res* 1996; **56**: 3758-3762

Edited by Zhu LH

Rising plasma nociceptin level during development of HCC: A case report

Andrea Horvath, Aniko Folhoffer, Peter Laszlo Lakatos, Judit Halász, Gyorgy Illyés, Zsuzsa Schaff, Monika Beatrix Hantos, Kornelia Tekes, Ferenc Szalay

Andrea Horvath, Aniko Folhoffer, Peter Laszlo Lakatos, Ferenc Szalay, 1st Department of Medicine of Semmelweis University, Budapest, Hungary

Judit Halász, Gyorgy Illyés, Zsuzsa Schaff, 2nd Department of Pathology of Semmelweis University, Budapest, Hungary

Kornelia Tekes, Department of Pharmacodynamics of Semmelweis University, Budapest, Hungary

Monika Beatrix Hantos, Neurochemical Research Unit of Hungarian Academy of Sciences, Budapest, Hungary

Correspondence to: Szalay Ferenc, MD, PhD, 1st Department of Medicine, Semmelweis University, Korányi St. 2/A, H-1083 Budapest, Hungary. szalay@bell.sote.hu

Telephone: +36-1-210-1007 **Fax:** +36-1-210-1007

Received: 2003-09-23 **Accepted:** 2003-11-16

Abstract

AIM: Although liver cirrhosis is a predisposing factor for hepatocellular carcinoma (HCC), relatively few reports are available on HCC in primary biliary cirrhosis. High plasma nociceptin (N/OFQ) level has been shown in Wilson disease and in patients with acute and chronic pain.

METHODS: We report a follow-up case of HCC, which developed in a patient with primary biliary cirrhosis. The tumor appeared 18 years after the diagnosis of PBC and led to death within two years. Alfa fetoprotein and serum nociceptin levels were monitored before and during the development of HCC. Nociceptin content was also measured in the tumor tissue.

RESULTS: The importance and the curiosity of the presented case was the novel finding of the progressive elevation of plasma nociceptin level up to 17-fold (172 pg/mL) above the baseline (9.2 ± 1.8 pg/mL), parallel with the elevation of alpha fetoprotein (from 13 ng/mL up to 3 480 ng/mL) during tumor development. Nociceptin content was more than 15-fold higher in the neoplastic tissue (0.16 pg/mg) than that in the tumor-free liver tissue samples (0.01 pg/mg) taken during the autopsy.

CONCLUSION: Results are in concordance with our previous observation that a very high plasma nociceptin level may be considered as an indicator for hepatocellular carcinoma.

Horvath A, Folhoffer A, Lakatos PL, Halász J, Illyés G, Schaff Z, Hantos MB, Tekes K, Szalay F. Rising plasma nociceptin level during development of HCC: A case report. *World J Gastroenterol* 2004; 10(1): 152-154

<http://www.wjgnet.com/1007-9327/10/152.asp>

INTRODUCTION

The incidence of hepatocellular carcinoma (HCC) in primary biliary cirrhosis (PBC) is reported to range from 0.5% to 4.2%, which is somewhat less frequent than that in liver cirrhosis from other etiologies^[1,2]. However, recent reports have shown an increasing trend. The incidence of HCC was found higher

in stage III/IV than in stage I/II patients^[1,3,4].

Relatively few prospective and comprehensive studies are available on HCC in PBC, and the number of case reports is also limited. Summarizing the data of the literature, 126 of 6 188 PBC patients (2.0%) were found to have HCC. Since HCC usually develops many years after the diagnosis of PBC, screening of HCC has clinical importance and offers best with hope for early detection. Serum AFP is a widely accepted marker of HCC^[5]; however, using the conventional cut-off value of 500 ng/mL, it has a sensitivity of about 50% and a specificity of more than 90% in detecting HCC in a patient with coexisting liver disease^[6]. The average survival of patients with HCC improved in the last decades^[7]. Female HCC patients often have a better prognosis than male patients^[8]. Because of the lack of sensitive markers of malignant hepatic tumors, HCC is usually recognized in the advanced stage.

We reported a follow-up case of HCC in a PBC patient. The importance of this case is the novel finding of progressive elevation in plasma nociceptin (N/OFQ, formerly named as orphanin FQ) up to 17-fold above the baseline, parallel with the elevation of alpha fetoprotein (AFP) during tumor development. Moreover, high nociceptin content was found in the tumor tissue as well.

Nociceptin, a newly discovered neuropeptide of 17 aminoacids, is the natural agonist of NOP receptor, earlier named opioid receptor-like 1 (ORL1) receptor. N/OFQ is a neuropeptide that is endowed with pronociceptive activity *in vivo*. Both the long and the short splice variants of the OP4 receptor mRNA were isolated in rat liver^[9]; however, there are no data about its physiological or pathophysiological role in liver function. To date only few clinical studies on nociceptin were reported, and only one of them dealt with liver disease.

Findings of the presented case are in concordance with our previous observation that a high plasma NC level may be an indicator of HCC.

CASE REPORT

A 47-year-old woman was admitted for fatigue, itching, hepatomegaly, high alkaline phosphatase and gamma-GT levels. Primary biliary cirrhosis was diagnosed based on the clinical symptoms, laboratory findings, AMA M2 positivity, normal US and ERCP pictures. Liver biopsy revealed stage II/III. There was no family history of liver disease or autoimmune disease, and all other confounding risk factors including alcohol, HBV and HCV infections were excluded. The patient was a heavy smoker. The past surgical history was significant only for an appendectomy and two caesarean sections. Her menopause started at the age of 38. Bone mineral density was slightly below the normal range at the time of diagnosis of PBC. Ursodeoxycholic acid (Ursofalk) treatment, calcium and vitamin D supplementation were introduced.

Severe progression of osteoporosis was observed during the following years. Five years after the diagnosis of PBC significantly decreased bone mineral density was shown both on the femoral neck (T-score: -5.12, Z score: -3.38) and on the lumbar vertebrae (T-score: -5.44, Z-score: -3.9). At the age of

57 despite the calcium, vitamin-D supplementation, calcitonin and bisphosphonate (Fosamax) treatment, the severe osteoporosis led to hip fracture and multiple vertebral collapses, which made the patient lifelong disabled.

Progression of PBC to stage IV occurred. She was monitored by yearly US, by regular laboratory tests and AFP every 3–4 months. For different reasons we collected blood samples for plasma nociceptin level determination as well. Sampling was done in conformity to accepted ethical standards and was approved by the regional ethical committee.

Hepatocellular carcinoma developed 18 years after the diagnosis of PBC. Regular follow-up US investigations revealed a focal lesion of 2.5 cm in diameter, which increased rapidly in segment V of the liver. Fine needle biopsy findings proved hepatocellular carcinoma. After the HCC diagnosis a continuous and rapid increase in the size of the tumor, an elevation of ALP, GGT, plasma nociceptin and AFP levels and clinical deterioration were observed.

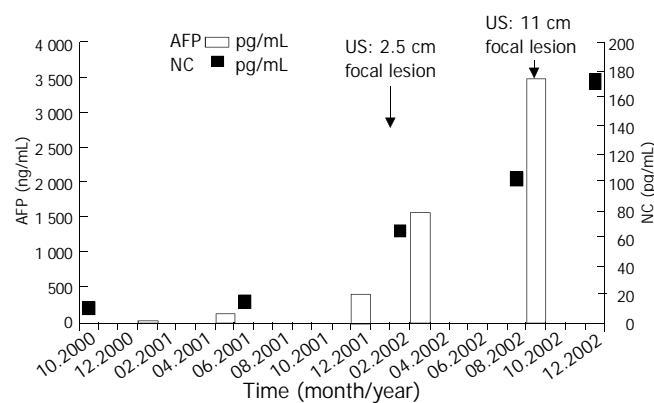


Figure 1 Serum alpha fetoprotein and plasma nociceptin levels before and during the development of hepatocellular carcinoma in the presented patient with primary biliary cirrhosis.

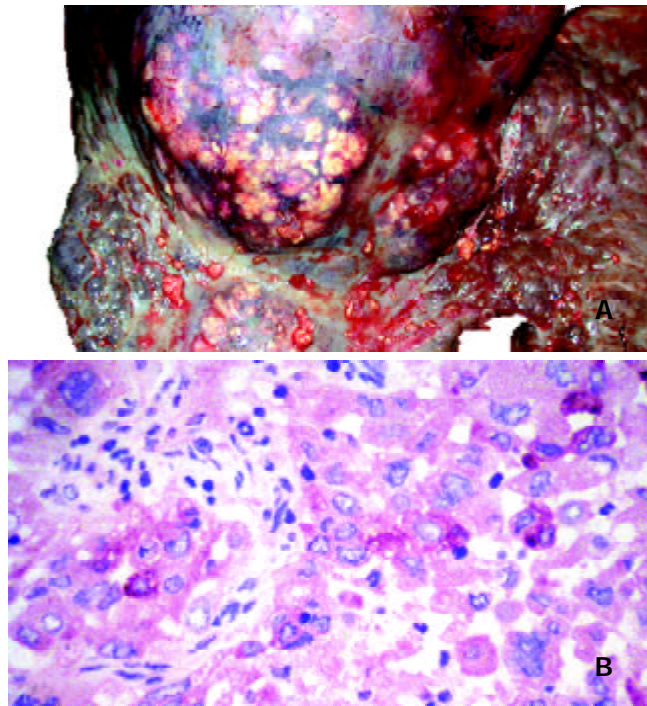


Figure 2 Hepatocellular carcinoma in the presented patient with primary biliary cirrhosis. A: Gross view of liver at autopsy. Grayish nodules of carcinoma protrude on the surface of the cirrhotic liver. Bar=1 cm. B: The focal red staining on the histologic picture of the hepatocellular carcinoma shows the immunohistochemical reaction of AFP. Original magnification 400 \times .

The AFP value had been within the normal range one year before the tumor was detected (13 ng/mL), but it was elevated at the time of the diagnosis of HCC (426 ng/mL) and rose up to 3480 ng/mL. The plasma nociceptin measured by radioimmunoassay ^{125}I -Nociceptin-kit, Phoenix Pharmaceuticals, Phoenix, CA, USA (10.6 pg/mL) was within the normal range (9.2 ± 1.8 pg/mL) in the tumor-free stage, while progressive elevation was detected during the tumor development (15.8, 65.8, 103.7, 128.0, 172.2 pg/mL), reaching the highest value before death (Figure 1). Higher nociceptin content was measured in the tumor tissue (0.16 pg/mg) compared to the tumor-free liver tissue sample (0.01 pg/mg) taken during the autopsy. The patient refused any surgical or other systemic or local tumor treatment. The size of the tumor increased up to 12 cm in diameter and involved segments V, VII, VIII and partly IV. No metastasis was detected, but necrosis developed in the central region of the tumor. The patient received supportive treatment, analgetics, and died of tumorous cachexia 19 months after the discovery of HCC. The autopsy confirmed both PBC stage IV and HCC. Focal presence of AFP was shown in the tumor by immunohistochemistry (Figures 2 A and B).

A nociceptin content in the HCC tissue (0.16 pg/mg) was 15-fold higher than that in the tumor free liver tissue sample (0.01 pg/mg) taken during the autopsy.

DISCUSSION

The presented case is a further example of the occurrence of HCC in PBC, and it supports previous observations that HCC usually develops in stage III/IV patients^[3]. The tumor developed 18 years after the diagnosis of PBC and led to the death of the patient within two years. Furthermore, severe osteoporosis is a common disorder in PBC, although recently it is considered as a non-specific complication^[10,11]. In our patient the early menopause together with PBC resulted in many bone fractures causing lifelong disability. The low serum osteocalcin level indicated a low turnover osteoporosis. High serum osteoprotegerin and low RANKL have been reported in PBC^[12], and we found the same alteration in this patient. Progression of bone loss was detected despite the serum osteoprotegerin was two-fold higher than normal, which suggested that inflammatory process in the liver could also contribute to the elevation of osteoprotegerin.

This is the first follow-up case in which progressive elevation of plasma nociceptin level was detected in parallel with the elevation of AFP during tumor development, and high N/OFQ content was found in the tumor tissue.

Nociceptin is the endogenous agonist of a G-protein coupled, naloxon insensitive opioid-like 1 receptor (ORL1) recently named as OP4. Although nociceptin is structurally related to opioid peptides, especially to dynorphin A, it does not interact with μ , δ and κ receptors. N/OFQ/OP4 system is a newly discovered peptide-based signalling pathway, involved in the modulation of pain and cognition. Opioid antagonists were successfully used for the treatment of pruritus in patients with PBC^[13]. These results together with the data that high plasma N/OFQ level has been reported in Wilson disease and in patients with chronic pain, led us to measure plasma nociceptin level in primary biliary cirrhosis^[14]. Our motivation was reinforced by an accidental observation that we found extremely high N/OFQ in a Wilson patient with advanced HCC.

The nociceptin levels in blood samples collected in the pre-tumor stage and during the tumor development period clearly showed that the elevation of N/OFQ was parallel with that of AFP and the clinical deterioration. When the tumor was first detected the N/OFQ level was 6-fold higher than that in healthy controls (65.8 versus 9.2 ± 1.8 pg/mL, $n=29$) and in other PBC patients without HCC (12.1 ± 3.2 pg/mL, $n=21$). When the tumor reached 11 cm the N/OFQ level was 17-fold

higher than normal. Since N/OFQ content was 15-fold higher in tumor tissue than in tumor free parts of the liver, the question arose whether nociceptin was produced by HCC tissue or it accumulated in the tumor by passive binding or via increased nociceptin receptor expression.

Further research is needed to clarify the mechanism and clinical significance of the highly elevated N/OFQ level in HCC. Since N/OFQ transcripts are expressed in immune cells^[15], the high N/OFQ level may also be an indicator of altered reaction of the body including immunological, cytokine and other mechanisms.

Elevated N/OFQ level might represent a compensatory mechanism in the N/OFQ/OP4 system to modulate pain perception in the central nervous system. This mechanism could explain why some patients with a very high plasma N/OFQ level did not have pain despite advanced stage of malignant liver tumor. It is remarkable that the N/OFQ was 3-fold higher in our patient than the highest values reported in patients with chronic pain without malignant disease^[16].

In conclusion, the novel finding of this study is that progressive elevation of plasma nociceptin was detected in parallel with the elevation of AFP during tumor development, as well as high N/OFQ content was found in the tumor tissue in a PBC patient with hepatocellular carcinoma. This is in concordance with our previous observation that high plasma N/OFQ level might be considered as an indicator of HCC.

REFERENCES

- 1 **Nakanuma Y**, Terada T, Doishita K, Miwa A. Hepatocellular carcinoma in primary biliary cirrhosis: an autopsy study. *Hepatology* 1990; **11**: 1010-1016
- 2 **Krasner N**, Johnson PJ, Portmann B, Watkinson G, Macsween RNM, Williams R. Hepatocellular carcinoma in primary biliary cirrhosis. *Gut* 1979; **20**: 255-258
- 3 **Jones D**, Metcalf J, Collier J, Bassendine M, James O. Hepatocellular carcinoma in primary biliary cirrhosis and its impact on outcomes. *Hepatology* 1997; **26**: 1138-1142
- 4 **Caballeria L**, Pares A, Castells A, Gines A, Bru C, Rodes J. Hepatocellular carcinoma in primary biliary cirrhosis: similar incidence to that in hepatitis C virus-related cirrhosis. *Am J Gastroenterol* 2001; **96**: 1160-1163
- 5 **Nguyen MH**, Keefe EB. Screening for hepatocellular carcinoma. *J Clin Gastroenterol* 2002; **35**(5 Suppl 2): S86-91
- 6 **Johnson PJ**. The role of serum alpha-fetoprotein estimation in the diagnosis and management of hepatocellular carcinoma. *Clin Liver Dis* 2001; **5**: 145-159
- 7 **Tang ZY**. Clinical research of hepatocellular carcinoma in the 21st century. *China Natl J Gastroenterol* 1995; **1**: 2-3
- 8 **Qin LX**, Tang ZY. The prognostic significance of clinical and pathological features in hepatocellular carcinoma. *World J Gastroenterol* 2002; **8**: 193-199
- 9 **Wang JB**, Johnson PS, Imai Y, Persico AM, Ozenberger BA, Eppler CM, Uhl GR. cDNA cloning of an orphan opiate receptor gene family member and its splice variant. *FEBS Lett* 1994; **348**: 75-79
- 10 **Newton J**, Francis R, Prince M, James O, Bassendine M, Rawlings D, Jones D. Osteoporosis in primary biliary cirrhosis revisited. *Gut* 2001; **49**: 282-287
- 11 **Floreani A**. Osteoporosis is not a specific complication of primary biliary cirrhosis (PBC). *Gut* 2002; **50**: 898; author reply 898-899
- 12 **Szalay F**, Hegedus D, Lakatos PL, Tornai I, Bajnok E, Dunkel K, Lakatos P. High serum osteoprotegerin and low RANKL in primary biliary cirrhosis. *J Hepatol* 2003; **38**: 395-400
- 13 **Neuberger J**, Jones EA. Liver transplantation for intractable pruritus is contraindicated before an adequate trial of opiate antagonist therapy. *Eur J Gastroenterol Hepatol* 2001; **13**: 1393-1394
- 14 **Hantos MB**, Szalay F, Lakatos PL, Hegedus D, Firneisz G, Reiczigel J, Torok T, Tekes K. Elevated plasma nociceptin level in patients with Wilson disease. *Brain Res Bull* 2002; **58**: 311-313
- 15 **Arjomand J**, Cole S, Evans C. Novel orphanin FQ/nociceptin transcripts are expressed in human immune cells. *J Neuroimmunol* 2002; **13**: 1631-1633
- 16 **Ko MH**, Kim YH, Woo RS, Kim KW. Quantitative analysis of nociceptin in blood of patients with acute and chronic pain. *Neuroreport* 2002; **13**: 1361-1363

Edited by Zhang JZ